In this Issue

Highlights from this issue of *A&R* | By Lara C. Pullen, PhD

Reappearance of Antibodies May Be Associated With Relapse in Patients With ANCA-associated Vasculitis

Previous research has shown that 40–100% of patients with antineutrophil cytoplasmic antibody (ANCA)–associated vasculitis (AAV) convert from being positive for myeloperoxidase (MPO)–ANCA to negative following induction treatment. Some researchers have suggested that disease classification may underlie the difference in conversion between patients. In this issue, Watanabe et al (p. 1626) report the results of their evaluation of the clinical link between levels of MPO-ANCA antibodies and relapse in patients with AAV. They analyzed data from 2 nationwide prospective cohort studies and report that the reappearance of MPO-ANCA may be a clinically useful biomarker for predicting relapse in remitted patients with MPO-ANCA–positive AAV.

p. 1626

The analysis included 271 MPO-ANCA–positive patients, 183 of whom had microscopic polyangiitis, 34 of whom had granulomatosis with polyangiitis, 15 of whom had eosinophilic granulomatosis with polyangiitis, and 39 of whom were unclassifiable. All the patients had achieved remission during the 6 months of remission induction therapy. The median age of the patients was 73 years, and 61% of them were female.

The investigators measured MPO-ANCA levels at months 0, 3, 6, 12, 18, and 24 and at time of relapse (the primary outcome measure). Most patients (72%) experienced a decrease in MPO-ANCA to normal levels after 6 months of remission induction therapy. MPO-ANCA then reappeared in 40% of patients with complete follow-up data. When the investigators performed a nested case–control analysis and a multivariable analysis to investigate the relationship between the reappearance of ANCA and relapse, they found that the reappearance of MPO-ANCA was more common in patients with relapse than in 75 age- and sex-matched control patients without relapse (odds ratio 26.2). They conclude their report by suggesting that patients with AAV who are MPO-ANCA positive and in remittance be routinely monitored for reappearance of MPO-ANCA.

Stopping TNFi Treatment May Make Solid Economic Sense for Some Patients With Rheumatoid Arthritis

Multiple studies have addressed the effects of discontinuing tumor necrosis factor inhibitor (TNFi) treatment on clinical outcomes in patients with rheumatoid arthritis (RA). In this issue, Tran-Duy et al (p. 1557) report the results of their analysis, which takes a societal perspective, on the incremental cost-effectiveness of withdrawal of TNFi treatment compared to continuation of these drugs. They focused their analysis on patients with RA who had longstanding, stable disease activity or remission.

p. 1557

The analysis of 1-year data included 531 patients who were randomized to the stop group and 286 patients who were randomized to the continuation group. The investigators found that withdrawal of TNFi treatment was associated with a 60% reduction of the total drug cost and an increase of 30% in other health care expenditures. When they compared the stop group to the continuation group, they found that stopping TNFi treatment translated into a mean yearly cost savings of €7,133 ($8,272).

The researchers then calculated a mean saved cost of €368,269 ($427,060) per quality-adjusted life year (QALY) lost when these patients stopped TNFi treatment. In other words, for these patients, stopping TNFi treatment resulted in considerable cost savings and only a small QALY loss. Although the investigators acknowledge that an official willingness-to-accept threshold (WTA) has not been defined, they proposed a WTA of €98,438 ($127,593) per QALY lost, noting that such a figure seemed realistic in The Netherlands within the context of the existing data on willingness to pay. When the investigators applied that WTA to their analysis, they calculated a 100% probability that stopping TNFi treatment for these patients would be cost-effective.

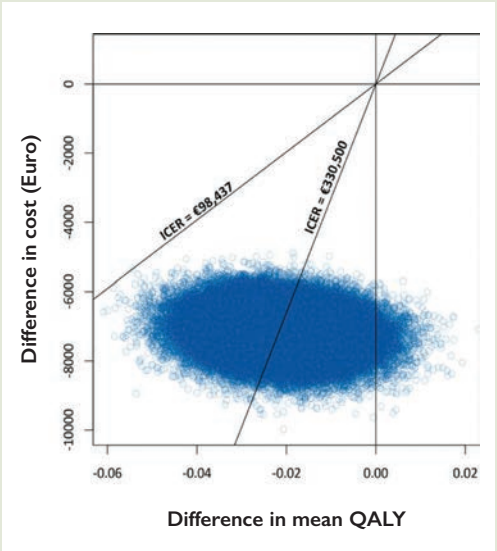

Figure 1. Scatter plot of incremental mean cost against incremental mean QALYs with the stop strategy compared to the continuation strategy. Each data point was obtained from 1 bootstrap replication. ICER = incremental cost-effectiveness ratio.

Risk Factors and Biomarkers for Uveitis in Patients With Juvenile Idiopathic Arthritis

Some patients with juvenile idiopathic arthritis (JIA) develop uveitis, which is often asymptomatic initially but can lead to irreversible vision impairment. In this issue, Tappeiner et al (p. 1685) report the results of their analysis of the value of demographic, clinical, and therapeutic factors, as well as laboratory biomarkers, in predicting the occurrence of uveitis in patients with JIA. The investigators evaluated data from 954 patients with JIA. These children were enrolled within the first year after diagnosis of JIA. In addition to demographic and clinical parameters, the investigators collected serum samples at study enrollment, at 3-month follow-up visits during the first year, and every 6 months thereafter.

p. 1685

The investigators found that uveitis occurred in 133 patients (13.9%) over the 44.5 months of observation. This incidence is consistent with results reported in previous publications, which have reported an overall prevalence of uveitis in JIA of 9–13%. They also found that children who received conventional synthetic or biologic disease-modifying antirheumatic drugs (DMARDs) had a significantly lower risk of uveitis onset.

When the researchers performed a multivariable Cox regression analysis to evaluate the impact of demographic, clinical, laboratory, and therapeutic parameters on uveitis onset, they found that both young age at onset of JIA and antinuclear antibody positivity were significantly associated with the onset of uveitis. Other predictors of uveitis included elevated erythrocyte sedimentation rate at baseline and continuing moderate or high disease activity during follow-up, as measured by the 10-joint clinical Juvenile Arthritis Disease Activity Score. The researchers also found that S100A12 levels of ≥250 ng/ml at baseline were significantly associated with the risk of uveitis. The investigators conclude by suggesting that JIA disease activity scores and laboratory biomarkers could be used to better define which patients with JIA are most likely to develop uveitis. They propose that such factors be combined with demographic risk factors and treatment modalities when assessing patient risk for uveitis.

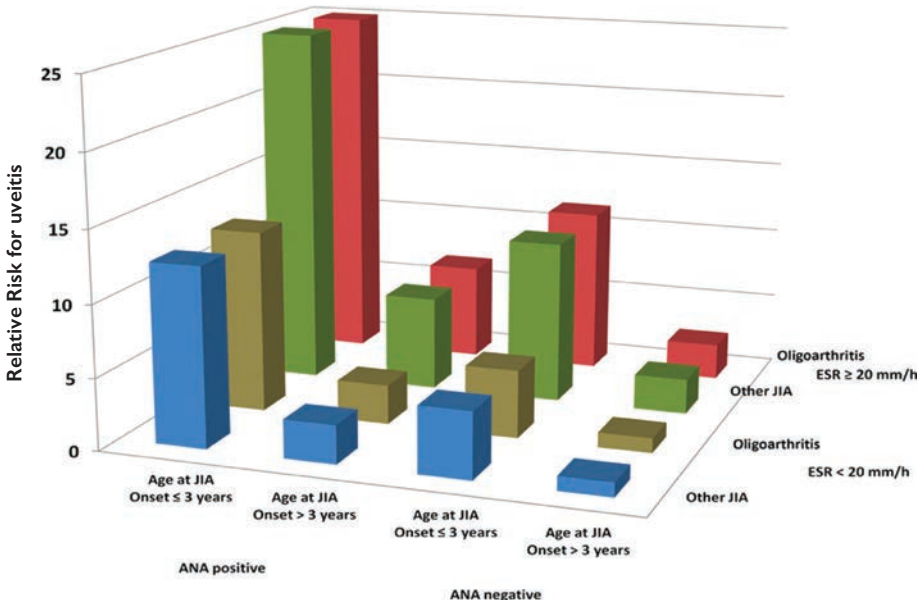

Figure 1. Relative risk of uveitis onset based on age at onset of JIA, antinuclear antibody (ANA) positivity, and erythrocyte sedimentation rate (ESR) at follow-up, adjusted for the 10-joint clinical Juvenile Arthritis Disease Activity Score and treatment with methotrexate (MTX) and MTX/biologic disease-modifying antirheumatic drugs.

Novel Autoantibody in Patients With Sjögren's Syndrome

Autoantibodies are a useful tool for phenotyping patients across the spectrum of autoimmune rheumatic diseases. In this issue, Birnbaum et al (p. 1610) report that they were able to use immunoblotting to detect a new autoantibody in patients with Sjögren's syndrome (SS). Specifically, they report that 11% of the SS patients studied have antibodies against the protein calponin 3, and these antibodies associate with the subset of patients who experienced neuropathies.

p. 1610

The investigators examined 209 patients with SS, 138 patients with systemic lupus erythematosus (SLE), 138 patients with myositis, 44 patients with multiple sclerosis (MS), and 46 healthy controls. They documented anti–calponin 3 antibodies in 8.7% of patients with SLE, 5.1% of patients with myositis, 6.8% of patients with MS, and 1 healthy control (2.2%). When the researchers looked more closely at patients with SS, they found that the frequency of anti–calponin 3 antibodies was highest in those with neuropathies (17.9% of 39), a frequency that differed significantly from healthy controls. They also report that calponin 3 is expressed in rat dorsal root ganglia perineuronal satellite cells (as opposed to neurons) and propose that these cells may be a target in SS.

ACR ANNOUNCEMENTS

AMERICAN COLLEGE OF RHEUMATOLOGY
2200 Lake Boulevard NE, Atlanta, Georgia 30319-5312
www.rheumatology.org

ACR Meetings

Annual Meetings
October 19–24, 2018, Chicago
November 8–13, 2019, Atlanta

Winter Rheumatology Symposium
January 26–February 1, 2019, Snowmass

State-of-the-Art Clinical Symposium
April 5–7, 2019, Chicago

For additional information, contact the ACR office.

ACR Open Rheumatology Accepting Submissions and Publishing Soon

The American College of Rheumatology will be publishing the first issue of its third official journal, *ACR Open Rheumatology* (*ACROR*), in early 2019. Editors-in-Chief Drs. Patricia P. Katz and Edward H. Yelin, and Clinical and Basic Science Deputy Editors Drs. David I. Daikh and Bruce N. Cronstein, will be heading *ACROR*'s editorial team.

ACROR will publish manuscripts describing potentially important findings of rigorously conducted studies in all aspects of rheumatology. As an open access journal, immediate access to full content of *ACROR* will be available to all readers. The electronic-only format of the journal, as well as other aspects of the review and production processes, will allow for faster review and publication, and liberal sharing of articles. The projected article publication fee (APC) for *ACROR* will be $2,500 with a discounted rate of $2,000 for articles in which the first or corresponding author is an ACR/ARHP member. In addition, there will be waivers of the APC for all articles submitted in the first 6 months from the time submission opens.

For additional information, visit https://www.rheumatology.org/Learning-Center/Publications-Communications/Journals/ACR-Open-Rheumatology.

ACR 2019 Winter Rheumatology Symposium

The 2019 Winter Rheumatology Symposium boasts a carefully crafted program that provides a unique blend of world-class lectures and interactive sessions in an intimate setting, allowing for quality interactions with peers and experts in the field. The symposium will provide attendees with a well-rounded view of the latest advances in the discipline. Highlights for this annual event include the interactive panel discussion on arthritis, with Jon Giles, MD, MPH, Vivien Bykerk, MD, FRCPC, Joel Kremer, MD, Christopher Ritchlin, MD, MPH, Douglas Veale, MD, FRCPI, and Michael Weinblatt, MD. The program also includes a second panel discussion on systemic lupus erythematosus, with Maria Dall'Era, MD, David Wofsy, MD, Joseph McCune, MD, and David Pisetsky, MD, PhD. Back by popular demand will be the Points-on-Joints session, presented in the "thieves' market" format and providing a series of interesting, difficult, or puzzling rheumatologic cases via 10-minute summaries followed by audience discussion. Registration and housing for the 2019 Winter Rheumatology Symposium are limited, so be sure to register by the early-bird deadline of November 28, 2018, and book your hotel room by December 19, 2018. For additional information and to register, visit www.rheumatology.org/Learning-Center/Educational-Activities.

Clinical Connections

Toll-Like Receptor 9 Deficiency Breaks Tolerance to RNA-Associated Antigens and Up-Regulates Toll-Like Receptor 7 Protein in *Sle1* Mice

Celhar et al, *Arthritis Rheumatol* 2018;70:1597–1609.

CORRESPONDENCE
Anna-Marie Fairhurst, PhD: annamarie_fairhurst@immunol.a-star.edu.sg

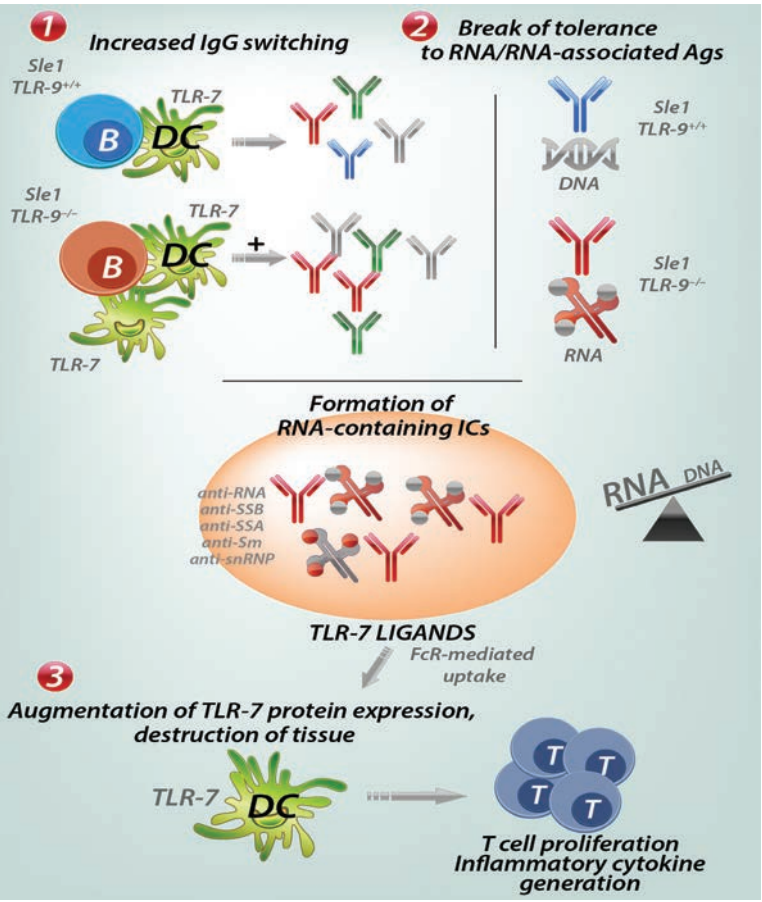

SUMMARY

Toll-like receptor 7 (TLR-7) and TLR-9 are innate pathogen-recognition receptors for single-stranded RNA and double-stranded DNA (dsDNA), respectively. They are important for host defense against viruses and bacteria; however, in systemic lupus erythematosus, self-reactive anti-RNA and anti-dsDNA autoantibody–containing immune complexes (ICs) can act as their ligands. Evidence supports a role for TLR-7 in the initial loss of self-tolerance and increased expression resulting in severe disease. In contrast, despite similar signaling pathways, elimination of TLR-9 across murine models results in aggressive lupus nephritis. This is due to the protective effect of TLR-9 on excessive antibody switching to IgG and RNA specificity and the regulation of TLR-7 expression. As reported in the study by Celhar et al, in the absence of TLR-9, both the TLR-7 protein and its ligands are increased, leading essentially to a TLR-7–driven autoimmune disease phenotype.

KEY POINTS

- Severe disease in TLR-9$^{-/-}$ *Sle1* mice is associated with increased TLR-7 protein expression.
- Increased TLR-7 in renal dendritic cells (DCs) precedes disease, implying their causative role.
- TLR-9 deficiency drives B cell antibody specificity toward RNA-associated antigens.
- Increased TLR-7–reactive ICs and TLR-7 protein combine to drive severe disease in murine lupus models.

Functional Characterization of the Osteoarthritis Genetic Risk Residing at *ALDH1A2* Identifies rs12915901 as a Key Target Variant

Shepherd et al, *Arthritis Rheumatol* 2018;70:1577–1587.

CORRESPONDENCE
Colin Shepherd, PhD: colin.shepherd@ncl.ac.uk
John Loughlin, PhD: john.loughlin@ncl.ac.uk

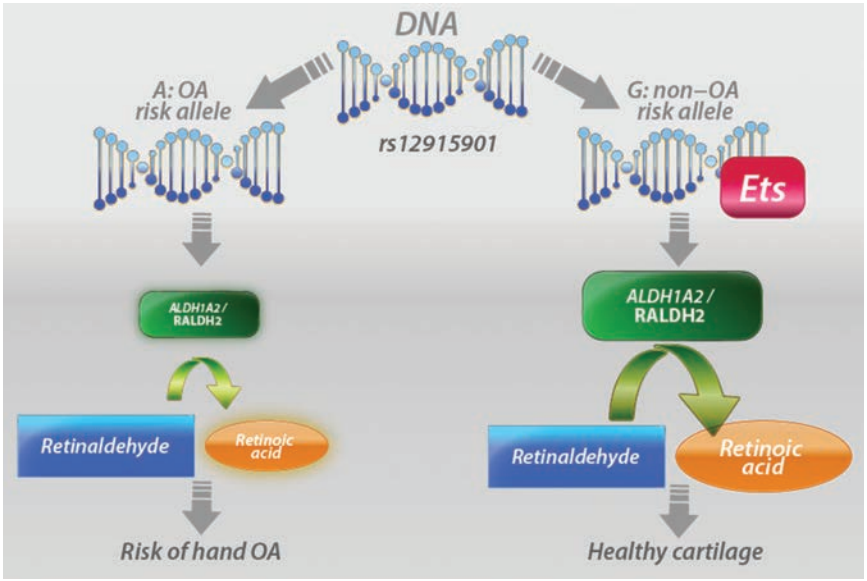

KEY POINTS

- Hand OA risk correlates with a decrease in expression of *ALDH1A2*, which is the gene encoding the retinoic acid–synthesizing enzyme RALDH2.
- Several genes associated with the retinoic acid pathway, including *ALDH1A2*, are differentially expressed between OA and control cartilage tissues.
- The chondrocyte transcriptional profile is altered when *ALDH1A2* expression is manipulated in vitro.
- Differential binding of the Ets transcription factors to the rs12915901 SNP likely mediates this disease-associated process.

SUMMARY

Retinoic acid has long been known as a critical regulator of skeletal formation during fetal and embryonic development. The results of a genome-wide association scan implicated genetic variation in the *ALDH1A2* gene in hand osteoarthritis (OA) disease risk. *ALDH1A2* encodes the RALDH2 enzyme, which converts retinaldehyde to retinoic acid. Genetic risk correlated with a decrease in *ALDH1A2* gene expression in cartilage tissue samples from OA patients.

Shepherd et al functionally characterized the *ALDH1A2* genetic risk locus in greater detail. RNA sequencing in cartilage from OA patients and controls revealed that *ALDH1A2* and several additional genes within the retinoic acid pathway were differentially expressed in OA samples. The decrease in *ALDH1A2* expression, which correlated with disease risk, was confirmed in cartilage and for the first time the correlation was observed in additional joint tissues and in trapezium tissue taken from patients with hand OA. By reducing *ALDH1A2* expression in chondrocytes in vitro, the expression of key chondrocyte genes decreased in response. Further in vitro analysis identified a target single-nucleotide polymorphism (SNP), rs12915901, which recapitulated the decrease in gene expression. The Ets family of transcription factors were identified as potential regulators of this effect, with strong Ets binding to the non-risk allele of rs12915901 (G), while no binding to the risk allele (A) was observed.

These data further implicate retinoic acid and the wider retinoic acid pathway in OA. As a consequence of perturbation of the retinoic acid pathway, expression of key cartilage genes is altered, which may cause pathologic changes to cartilage integrity over time. This work suggests that the retinoic acid pathway may be exploited for therapeutic benefit in hand OA patients.

Arthritis & Rheumatology

An Official Journal of the American College of Rheumatology
www.arthritisrheum.org and wileyonlinelibrary.com

Arthritis & Rheumatology
An Official Journal of the American College of Rheumatology
www.arthritisrheum.org and wileyonlinelibrary.com

VOLUME 70 OCTOBER 2018 NO. 10

Cover image: The figure on the cover (from Karmouty-Quintana et al, page 1681) illustrates a skin biopsy specimen from a patient with systemic sclerosis who was positive for antibodies to α-smooth muscle actin (green) and for a hyaluronan binding protein (white). The section was counterstained with DAPI (blue).

ARTHRITIS & RHEUMATOLOGY
Vol. 70, No. 10, October 2018, pp 1533–1543
DOI 10.1002/art.40568

Arthritis & Rheumatology
An Official Journal of the American College of Rheumatology
www.arthritisrheum.org and wileyonlinelibrary.com

REVIEW

The Eyes Have it

A Rheumatologist's View of Uveitis

James T. Rosenbaum[1] and Andrew D. Dick[2]

Uveitis is defined as intraocular inflammation. It is an extraarticular manifestation of many forms of joint disease, which include spondyloarthritis, juvenile idiopathic arthritis, and Behçet's disease. Rheumatologists may be asked to consult on the ophthalmologic care of patients with uveitis in order to identify an associated systemic illness. Diagnoses such as spondyloarthritis, sarcoidosis, and interstitial nephritis with uveitis are frequently overlooked by referring ophthalmologists. Alternatively, rheumatologists may be asked to help manage the patient's immunosuppression, including biologic therapy, which can be required to treat a subset of patients with uveitis. This review is intended to provide rheumatologists with the necessary information to facilitate collaboration in the comanagement of patients with uveitis.

Imagine a symphony orchestra in which the conductor cannot coordinate the play of the wind instruments with the strings or percussion. Imagine a basketball or soccer team that has not mastered the concept of passing the ball. Imagine an epidemiologic study in which the statisticians and those who conceptualized the study each had a different understanding of the study's purpose. Many endeavors represent a gestalt for which the anticipated goal requires multiple parts, and the whole is greater than the sum of those parts. Since rheumatologists see patients with multisystem disease, they are well aware of this need for collaboration.

Uveitis, also known as intraocular inflammation, is a prototypical illness that begs for collaboration. Uveitis is often best assessed and optimally treated by an interdisciplinary team. In this review, we seek to prepare rheumatologists with the information necessary to help facilitate the success of this collaborative effort.

Background

The term uvea derives from the Latin word for grape. The Roman anatomists felt that peeling away the outer layer of the eye, the cornea and sclera, left a grape-like structure: the iris, ciliary body, and choroid (Figure 1). Any portion of the uvea can be inflamed,

Dr. Rosenbaum's work was supported by the William and Mary Bauman Foundation, the Stan and Madelle Rosenfeld Family Trust, the Spondylitis Association of America, Research to Prevent Blindness, the NIH (National Eye Institute grant R01-EY-026572), the Rheumatology Research Foundation, and the Alcon Research Institute. Dr. Dick's work was supported in part by the National Institute for Health Research Biomedical Research Centre (Moorfields Eye Hospital), National Health Service Foundation Trust, and University College London Institute of Ophthalmology.

[1]James Rosenbaum, MD: Oregon Health & Science University and Legacy Devers Eye Institute, Portland, Oregon; [2]Andrew Dick, MD, FMedSci: University College London, National Institute for Health Research Biomedical Research Centre at Moorfields Eye Hospital, London, UK, and University of Bristol, Bristol Eye Hospital, Bristol, UK.

Dr. Rosenbaum has received speaking fees and/or honoraria from Regeneron, Topivert, Cavtherx, Mallinckrodt, UCB, and Eyevensys (less than $10,000 each) and AbbVie, Gilead, and Novartis (more than $10,000 each), royalties from UpToDate, and research support from Pfizer and owns stock in Novartis. Dr. Dick has received speaking fees and/or honoraria from AbbVie, Astellas, Sanofi, and Quark Pharmaceuticals (less than $10,000 each).

Address correspondence to James T. Rosenbaum, MD, Departments of Ophthalmology, Medicine, and Cell Biology, Oregon Health & Science University, 3181 Southwest Sam Jackson Park Road, L467Ad, Portland, OR 97239. E-mail: rosenbaj@ohsu.edu.

Submitted for publication February 11, 2018; accepted in revised form May 17, 2018.

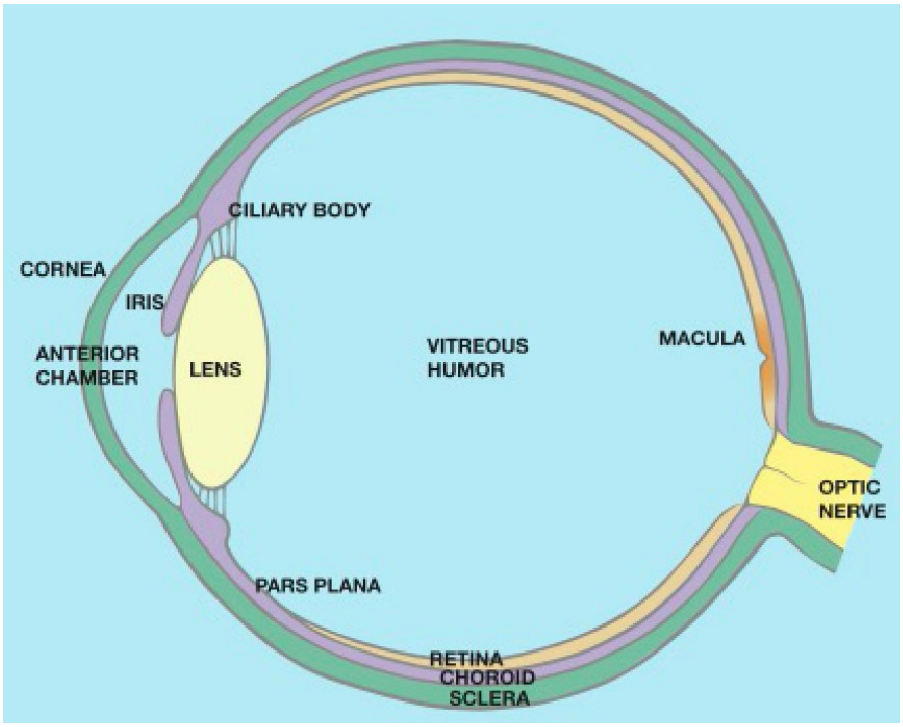

Figure 1. Anatomy of the eye. The uveal tract includes the iris, ciliary body, and choroid.

and often the inflammation involves adjacent structures (Figure 2). Anatomic subsets of uveitis include iritis (synonymous with anterior uveitis), iridocyclitis, intermediate uveitis, posterior uveitis (such as choroiditis, retinochoroiditis, and chorioretinitis), and panuveitis. Just as an increased number of leukocytes in the synovial fluid is indicative of synovitis, so is an increase in leukocytes in either the aqueous humor or vitreous humor taken as evidence of uveitis, even though neither the anterior chamber, which is filled with aqueous humor, nor the vitreous cavity is technically a part of the uveal tract.

Uveitis has a prevalence of roughly 1 per 1,000 individuals (1). Several forms of uveitis are episodic, and the prevalence is usually stated as a point prevalence, meaning that active disease was present at the time of the survey. Despite its relative rarity, uveitis accounts for approximately the same amount of visual morbidity as either macular degeneration or diabetic retinopathy (2), although the latter 2 diseases are generally more commonly recognized by the public as major causes of visual loss. The duration of some subsets of uveitis probably accounts for this paradox. Both macular degeneration and diabetic retinopathy are diseases that occur toward the end of life. In contrast, uveitis might start in childhood or early adulthood and persist through decades.

The uveitis–rheumatology interface

Patients with uveitis often do need a rheumatologist. As shown in Table 1, many systemic rheumatic diseases can involve both the joints and the uveal tract. Furthermore, most forms of uveitis are immune-mediated and respond to immunosuppression, a type of therapy that is outside the expertise of most ophthalmologists.

Just as arthritis has multiple causes, several etiologic factors have been identified in uveitis. Broad etiologic categories are provided in Table 2. The majority of patients with uveitis have an immune-mediated process. This is supported by observations of leukocytes in the eye, and by the known ability to produce uveitis in laboratory animals by stimulating the immune response. However, just as the preferred approach to therapy differs between systemic lupus and rheumatoid arthritis, even though both are immune-mediated, so it is likely that the preferred treatment for a form of uveitis, such as that secondary to juvenile idiopathic arthritis (JIA), will differ from the optimal therapy for another form of uveitis, such as that secondary to sarcoidosis. Currently, however, most therapy for noninfectious uveitis is determined more by the severity and anatomic location of the uveitis, rather than its etiology, although some notable exceptions are slowly emerging.

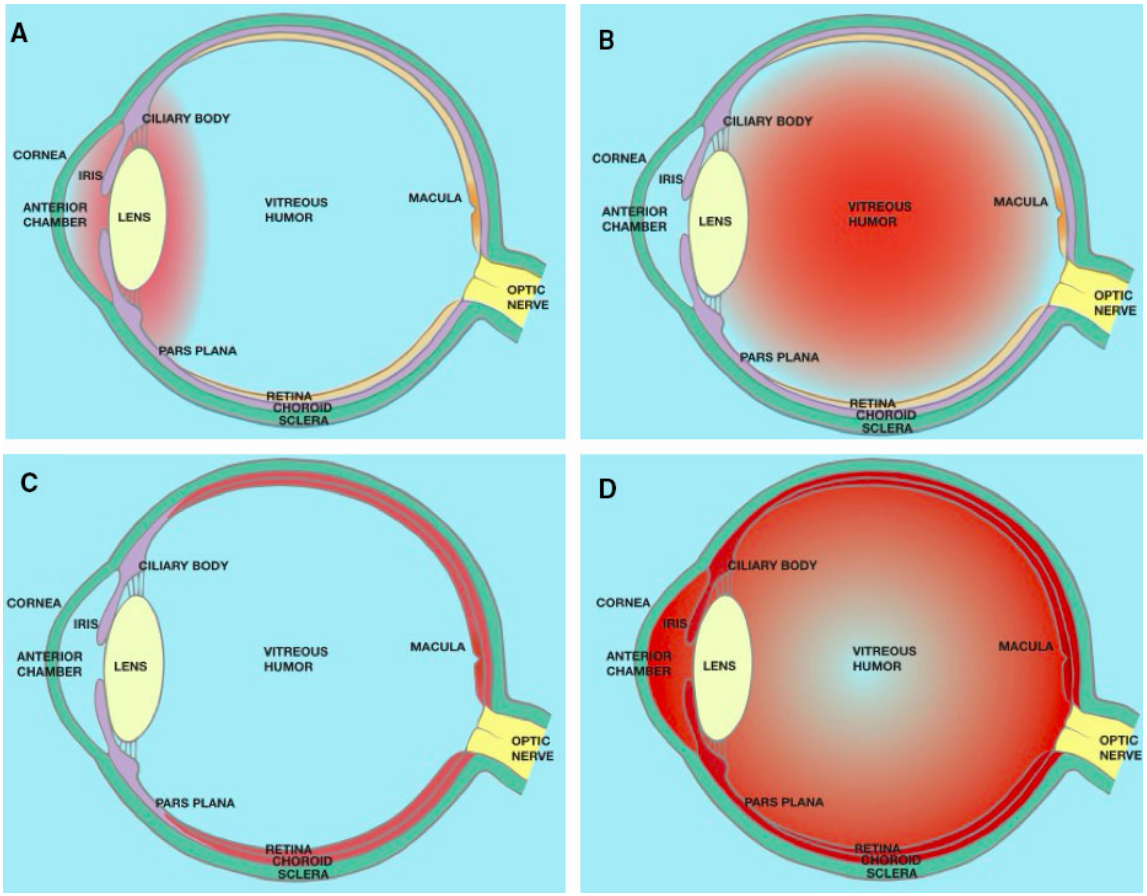

Figure 2. **A,** Anterior uveitis is defined as inflammation of the iris and/or ciliary body. **B,** Intermediate uveitis is diagnosed when inflammatory cells in the vitreous humor are the predominant finding. **C,** Posterior uveitis is diagnosed if the retina and/or choroid are inflamed. **D,** Panuveitis is diagnosed if inflammation is present in the anterior uvea, the vitreous humor, and the retina or choroid. It is also possible to have anterior and intermediate uveitis if the retina and choroid are not involved, or to have intermediate and posterior uveitis if inflammation in the anterior chamber is minimal or nonexistent.

Although case reports rarely elucidate pathogenesis, the disease course documented in a physician who survived Ebola infection may reveal clues about the intersection between uveitis and rheumatic diseases (3). The patient contracted Ebola in Africa and was flown to Atlanta for care. Although he experienced multiorgan failure, he survived. Fourteen weeks after presentation, this patient exhibited a severe uveitis, and the treating physicians were able to recover the Ebola virus from his eye, presumably because the eye is an immune-privileged site. The virus was no longer detectable in the blood. At the time that the uveitis developed, he also had low back pain and enthesitis, symptoms suggestive of a spondyloarthropathy, although the uveitis was intermediate and posterior, locations which are not typically inflamed with ankylosing spondylitis.

When joint swelling is present, we narrow the differential diagnosis on the basis of relevant parameters, such as determination of which joints are involved, whether the disease is symmetric or asymmetric, whether the onset was acute or insidious, and the patient's age and sex. Similarly, subsets of uveitis are recognized by such variables as the specific anatomic portion of the uveal tract that is inflamed, whether the disease is unilateral or bilateral, whether the inflammation is chronic or episodic, whether onset began suddenly or insidiously, and, of course, the patient's age and sex.

Both Behçet's disease and ankylosing spondylitis, for example, are associated with uveitis. In patients with Behçet's disease or ankylosing spondylitis, low back pain, peripheral arthritis, and diarrhea have been observed. Oral sores are often present in patients with HLA–B27–associated reactive arthritis, just as they are present in Behçet's disease. However, the uveitis associated with ankylosing spondylitis almost always affects only one eye

Table 1. Differential diagnosis of uveitis in association with arthritis*

Diagnosis	Comments
Adverse reaction to medication	Drugs include TNF inhibitors, intravenous bisphosphonates, and checkpoint inhibitors.
Ankylosing spondylitis	Affects ~40% of patients; usually unilateral, sudden onset, anterior, and recurrent.
Behçet's syndrome	Affects ~60–80% of patients; usually bilateral, recurrent, and often severe, with associated retinal vasculitis.
Blau syndrome and other autoinflammatory syndromes	In Blau syndrome, uveitis is a common manifestation of an uncommon disease, and usually occurs bilaterally with chorioretinitis; optic nerve edema or uveitis are also reported in NOMID or other autoinflammatory syndromes.
Crohn's disease	Uveitis and scleritis can be associated, often along with skin and joint disease; phenotype of uveitis resembles PsA with uveitis phenotype.
Juvenile idiopathic arthritis	In the pauciarticular, early-onset, ANA-positive subset, usually occurs as a bilateral, insidious-onset chronic anterior uveitis; uveitis is also associated with juvenile ankylosing spondylitis or juvenile-onset PsA.
Kawasaki disease and, in rare cases, other forms of vasculitis	Bilateral, mild anterior uveitis in association with conjunctivitis. Other forms include PAN, GPA, LCV, or GCA, but they very rarely cause uveitis.
Lyme disease	Rare, but is a reported cause of uveitis.
Psoriatic arthritis	Affects ~7% of patients with PsA; can be bilateral, chronic, anterior, intermediate, and insidious in onset.
Reactive arthritis	Conjunctivitis is a classic eye manifestation, but a sudden-onset, unilateral, anterior uveitis has been well described.
Relapsing polychondritis	Can cause iritis, episcleritis, or scleritis.
Rheumatic fever	Very rarely associated with uveitis.
Sweet's syndrome	Rarely reported with uveitis.
Systemic lupus erythematosus	Rarely causes uveitis or optic neuritis; often causes lacrimal gland disease; can cause cotton wool spots or choroidal vasculopathy.
Ulcerative colitis	Uveitis or scleritis is less common than with Crohn's disease, but is clearly associated.
Whipple's disease	Vitreous humor inflammation can be associated.

* Although this list includes rare causes of arthritis and uveitis, such as Blau syndrome or Whipple's disease, it does not include everything within the differential diagnosis. For example, tuberculosis could cause uveitis and arthritis simultaneously, and some patients with arthritis of unknown cause also develop uveitis. TNF = tumor necrosis factor; NOMID = neonatal-onset multisystem inflammatory disease; PsA = psoriatic arthritis; ANA = antinuclear antibody; PAN = polyarteritis nodosa; GPA = granulomatosis with polyangiitis; LCV = leukocytoclastic vasculitis; GCA = giant cell arteritis.

at a time, lasts no longer than 3 months, predominantly affects the anterior uveal tract, may cause hypopyon (pus in the anterior chamber of the eye; see Table 3 for a glossary of relevant terms), and tends to be recurrent (4). The uveitis associated with Behçet's disease is also recurrent, but rarely does the eye remain completely uninflamed between attacks. The uveitis associated with Behçet's disease is usually bilateral. Moreover, it tends to manifest as both an anterior and an intermediate uveitis (intermediate uveitis being recognized by leukocytes in the vitreous humor) or a panuveitis, often with retinal vasculitis.

Table 2. Broad categories of disease associated with uveitis*

Disease category	Comments
Infections	Includes viruses such as HSV, VZV, and CMV; also includes syphilis, toxoplasmosis, and tuberculosis, among other infections.
Masquerade syndromes	Includes B cell lymphoma, leukemia, and retinal detachments.
Medication reactions	See Table 1.
Ocular syndromes	Includes birdshot retinochoroidopathy, pars planitis, acute multifocal placoid pigmentary epitheliopathy, and multifocal choroiditis with panuveitis.
Systemic immune-mediated diseases	In addition to those listed in Table 1, also includes multiple sclerosis, tubulointerstitial nephritis with uveitis, and Vogt-Koyanagi-Harada syndrome.
Trauma	Penetrating trauma can cause sympathetic ophthalmia; surgical trauma, as in cataract surgery, usually causes some self-limited inflammation.
"Idiopathic"	Also called primary or undifferentiated uveitis; probably the most common diagnosis in a uveitis clinic.

* HSV = herpes simplex virus; VZV = varicella zoster virus; CMV = cytomegalovirus.

While both Behçet's disease and ankylosing spondylitis may cause hypopyon, the eye of a patient with ankylosing spondylitis and hypopyon is red, tender, and sensitive to light; fibrin is frequently present in the anterior chamber. In contrast, hypopyon in association with Behçet's disease does not necessarily cause pain or redness, and fibrin is rarely present. In some instances, the medical history alone can help distinguish the 2 entities, since review of a patient's history will usually help determine whether one or both eyes are affected or will help ascertain the duration of the eye inflammation. However, other subtleties, such as the presence of retinal vasculitis, require examination by an eye specialist for detection. Thus, the ophthalmologist potentially can help the rheumatologist make a diagnosis, and the rheumatologist can assist the

Table 3. Glossary of terms often used by a uveitis specialist

Anterior uveitis:
Inflammation predominantly anterior to the lens of the eye.
Band keratopathy:
Deposition of calcium in the corneal epithelium. It is a common finding in the uveitis associated with juvenile idiopathic arthritis.
Cystoid macular edema:
A common complication of uveitis that affects central vision and is often treated by a local injection of corticosteroid.
Flare:
The diffraction of the slit lamp beam caused by the increased protein in the anterior chamber that results when the blood aqueous barrier is disrupted, as in anterior uveitis.
Intermediate uveitis:
Inflammation predominantly in the vitreous humor. Technically, neither the vitreous humor nor the anterior chamber is a part of the uveal tract, but leukocytes in either usually indicate a uveitis, just as cells in the synovial fluid usually indicate a synovitis.
Keratic precipitates:
The concretions of cells adherent to the endothelium of the cornea, as seen with a slit lamp examination. Large concretions are called "granulomatous" and are seen in such diseases as sarcoidosis, tuberculosis, and herpes zoster infection.
Panuveitis:
Inflammation simultaneously in the anterior chamber, the vitreous humor, and the retina and/or choroid.
Posterior synechiae:
The adherence of the iris to the lens. This is a nonspecific finding that is nonetheless much more common in some forms of uveitis (such as that associated with HLA–B27 or in sarcoidosis) than in others.
Posterior uveitis:
Inflammation that involves the choroid and often adjacent structures, such as the retina.
Retinal vasculitis:
An abnormality of retinal vessels, such as increased vascular permeability. Retinal vasculitis is a common feature of many forms of uveitis and does not correlate well with the occurrence of a systemic vasculitis.
SUN criteria:
An acronym for the Standardization of Uveitis Nomenclature, an international consortium that helped to define terms related to uveitis.

ophthalmologist in differential diagnosis of the systemic disease and collaborate with the management of immunosuppression.

The coexistence of uveitis and arthritis is not well understood, despite how frequently it occurs, as is shown in Table 1. Some specific forms of uveitis are discussed in Table 4. Both the eye and the joint share some biochemical similarities, such as the presence of hyaluronic acid, type II collagen, and aggrecan. Uveitis and arthritis also occur together in several animal models, such as in the SKG mouse model of arthritis (5), adjuvant arthritis in rats (6), and aggrecan-induced arthritis in BALB/c mice (7). Their coexistence suggests a shared pathogenesis, but in the aggrecan-induced arthritis model, the mice, which do not produce interferon-γ, develop a far more severe uveitis, whereas arthritis in these mice is dramatically ameliorated (7). Similarly, characterizing the genetics of the uveitis associated with HLA–B27 shows that ankylosing spondylitis and acute anterior uveitis share a variety of predisposing genes, such as HLA–B27 itself, the interleukin-23 receptor (IL-23R), and endoplasmic reticulum aminopeptidase 1. At the same time, there are identifiable genes, such as IL-6R and IL-18R1 (and probably IL-10), that seem to influence solely the susceptibility to acute anterior uveitis (8).

Differential diagnosis and laboratory testing

The heterogeneity of uveitis has multiple implications. In terms of differential diagnosis, it is obviously critical to distinguish an infection from an immune-mediated cause of uveitis. Some infections, such as syphilis and tuberculosis, can be quite variable in terms of their presentation within the eye, and these types of infections are frequently entered into the differential diagnosis. Some of the more common infectious causes of uveitis include herpes simplex, herpes zoster, toxoplasmosis, and cytomegalovirus (the latter usually occuring in an immunocompromised host). Most infections of the uveal tract cause characteristic changes that can be recognized with a slit lamp examination or with indirect ophthalmoscopy. The "partnership" between a rheumatologist and ophthalmologist is, in our opinion, such that the rheumatologist must trust that the ophthalmologist has excluded infection as a potential etiologic factor; both specialists must be aware that a patient who fails to respond to immunosuppression could have an overlooked infectious cause for his or her disease.

Likewise, 2 other etiologic factors, masquerade syndromes and drug-induced disease, are relatively rare, but each has a distinct therapeutic implication. The most common uveitis "masquerade" is probably a B cell lymphoma that is usually confined to the brain and the eye (9,10). It typically occurs bilaterally in patients who are older than age 45 years. This diagnosis can be easily missed. Medications do not usually cause uveitis, but possible culprits may include intravenous bisphosphonates (11), tumor necrosis factor (TNF) inhibitors (12), checkpoint inhibitors (13), and several antibiotics (14).

In rheumatology, distinguishing gout from rheumatoid arthritis as a cause of joint swelling will markedly change the therapeutic strategy. Most forms of noninfectious uveitis are approached with the use of a treatment algorithm that is not impacted by the cause of the uveitis. Two prominent exceptions are Behçet's disease and the anterior uveitis associated with JIA.

Table 4. Forms of uveitis of potential special interest to rheumatologists*

Diagnosis	Comment	Laboratory testing
Behçet's disease	Typically a bilateral, recurrent, potentially blinding panuveitis associated with retinal vasculitis.	No definitive test; strictly a clinical diagnosis.
Birdshot retinochoroidopathy	A chronic, bilateral intermediate and posterior uveitis very strongly associated with HLA–A29 and frequently treated by long-term immunosuppression.	Almost all patients are HLA–A29 positive.
Blau syndrome	A very rare autosomal-dominant form of uveitis associated with mutations in the nucleotide binding domain of *NOD2*, a gene that codes for an important component of the innate immune system which recognizes the bacterial cell wall.	Genotyping identifies the mutations known to be associated with this syndrome.
HLA–B27 related uveitis	Typically, a sudden-onset, self-limited (resolves within 3 months), anterior, recurrent, unilateral uveitis. Most uveitis from any cause is anterior, and 50% of those with a sudden onset of anterior uveitis are HLA–B27 positive, most of whom have some form of spondyloarthropathy. Usually can be managed by topical corticosteroids.	HLA–B27 typing; sacroiliac imaging to help diagnose associated spondyloarthritis.
Idiopathic uveitis	The most common diagnosis made in most series of patients from a uveitis clinic. The term is used to mean a form of uveitis that does not fit a diagnostic niche. Other suggested terms include nonclassifiable, undifferentiated, or primary (as opposed to secondary to another condition, such as ankylosing spondylitis).	A diagnosis made when all other diagnoses have been excluded.
JIA-associated uveitis	Characteristically, a bilateral, insidious-onset, chronic (lasting longer than 3 months), anterior uveitis, especially likely to occur in patients with JIA who have a pauciarticular, early-onset, ANA-positive form of arthritis.	A positive ANA finding is supportive of the diagnosis, but is neither sensitive nor specific.
Pars planitis	A relatively common form of uveitis that usually begins insidiously and causes inflammation in the vitreous humor, resulting in prominent floaters (however, the majority of patients with floaters do not have pars planitis). The disease is named for the pars plana, an anatomic area immediately posterior to the ciliary body and a site where leukocyte concretions are found in this disease.	A clinical diagnosis based on the location of inflammation; occasionally associated with multiple sclerosis, for which a brain MRI is sometimes obtained.
Primary intraocular lymphoma	A very rare form of uveitis, usually occurring in individuals older than age 45 years, and presenting as bilateral cells in the vitreous humor, sometimes with subretinal infiltrates, and often in association with central nervous system lymphoma.	Definitive diagnosis is made by characterization of malignant cells in the vitreous humor or on retinal biopsy.
Sarcoidosis	A form of uveitis with "promiscuous" or highly varied presentations, ranging from anterior uveitis to retinal vasculitis with or without chorioretinal lesions. Ocular inflammation and pulmonary disease are the 2 most common initial manifestations of sarcoidosis, and it accounts for a relatively common systemic illness among patients in a uveitis clinic.	Chest computed tomography is the most sensitive test. Biopsy is rarely required if symmetric hilar or mediastinal adenopathy is present. Testing for levels of ACE, lysozyme, and interleukin-2 receptor has questionable specificity and limited sensitivity.
Syphilis	Late secondary or tertiary syphilis are in the differential diagnosis for any patient labeled as having "idiopathic" uveitis.	FTA or comparable test is preferred. RPR can be negative in up to 40% of patients with uveitis secondary to syphilis.
Tubulointerstitial nephritis with uveitis	A form of uveitis that is typically sudden in onset, bilateral, and mostly anterior with a variable amount of vitreous humor inflammation. The disease has an extremely strong association with HLA–DRB1*0102. Patients are typically systemically ill with fever, myalgias, and arthralgias as well as a markedly elevated sedimentation rate.	Elevation of urine β_2-microglobulin levels is a sensitive way to support the diagnosis. Renal biopsy is definitive but often not required. Serum blood urea nitrogen or serum creatinine levels have limited sensitivity.

Table 4. *(Cont'd)*

Diagnosis	Comment	Laboratory testing
Tuberculosis	A rare form of uveitis in the US, but a very common form of uveitis in countries such as India or Saudi Arabia. Also a very difficult diagnosis to confirm, as the organism is rarely cultured from the eye. The diagnosis should be considered if the patient has a risk factor for tuberculosis (such as being born outside the US or a history of incarceration) or if the illness does not respond to immunosuppression such as oral corticosteroids.	Culture is the ideal confirmatory test, but it is often negative. PCR, when available, is a good alternative. Interferon-γ release assays and skin test responses are useful in confirming exposure to tuberculosis, but neither establishes whether active infection is present.
Vogt-Koyanagi-Harada syndrome	An autoimmune form of uveitis with the triggering antigen putatively being tyrosinase. Patients are almost always either Asian or native American or are Spanish speaking. The uveitis is a bilateral, severe panuveitis with serous retinal elevation. Additional symptoms may include headache, meningismus, eight nerve abnormalities, and vitiligo.	Fluorescein angiography and/or optical coherence tomography should show characteristic serous elevation of the retina.
Whipple's disease	A rare but treatable cause of uveitis in association with arthritis. The presentation in the eye is generally cells in the vitreous humor.	Identification of the causative organism, *Tropheryma whippeli*, in the vitreous humor or elsewhere.

* JIA = juvenile idiopathic arthritis; ANA = antinuclear antibody; MRI = magnetic resonance imaging; ACE = angiotensin-converting enzyme; FTA = fluorescent treponemal antibody; RPR = rapid plasma reagin; PCR = polymerase chain reaction.

For Behçet's disease, a monoclonal antibody that inhibits TNF is used frequently, because of its dramatic efficacy (15). For the anterior uveitis associated with JIA, the more frequent use of methotrexate and/or a TNF inhibitor such as adalimumab has improved the prognosis markedly for this disease (16).

The above considerations regarding differential diagnosis obviously could impact the search for an etiology. The rheumatologist is often tasked with finding a systemic immune-mediated cause, but should not be the practitioner who diagnoses an infection or masquerading malignancy as the cause. As is true of differential diagnosis in general, the history is key, and pattern recognition aids greatly in the goal. Some forms of uveitis, such as Behçet's disease or Vogt-Koyanagi-Harada (VKH) syndrome, are clinical diagnoses that lack a definitive diagnostic laboratory test. Other diagnoses, like Crohn's disease, ulcerative colitis, or sarcoidosis, can be established or supported by biopsy or imaging, but the procedure may be too costly, too toxic (radiation from a computed tomography [CT] scan of a young person), too unlikely to yield positive results, or too uncomfortable (colonoscopy) to recommend on a routine basis. Our practice is to choose tests selectively based on clues gained from the examination or history. For example, multiple areas of serous elevation of the retina can be detected on examination and confirmed by testing with such techniques as optical coherence tomography or fluorescein angiography. The finding is suggestive of a diagnosis of VKH.

The most common systemic disease associated with uveitis is spondyloarthritis. Approximately one-half of all patients with sudden-onset, noninfectious, anterior uveitis in Europe or North America are HLA–B27 positive (17). Recent studies, one from an emergency room in Dublin, Ireland (18) and another from Spain involving 798 subjects and a collaboration between rheumatologists and ophthalmologists (19), concluded that roughly 80% of patients with B27-associated acute anterior uveitis have axial spondyloarthritis based on the Assessment of SpondyloArthritis international Society criteria. This observation was attained even though both studies excluded any patient with uveitis who had a known spondyloarthropathy. Spondyloarthritis is less common among those who have anterior uveitis and are HLA–B27 negative, but the diagnosis remains surprisingly frequent (19). Older studies using more stringent criteria to diagnose spondyloarthritis had also concluded that spondyloarthropathy was endemic among patients with anterior uveitis (4,20). Rheumatologists who are unaware of this association will frequently fail to recognize the clinical significance of the chronic inflammatory back pain that afflicts many individuals with anterior uveitis.

Another critical cause of uveitis to appreciate is sarcoidosis. In a study from the Cleveland Clinic, 57% of women older than age 61 years with idiopathic uveitis had normal findings on chest radiography but had chest CT evidence of sarcoidosis (21). We recently found a similar, slightly lower yield by performing chest CT on patients older than age 40 years with idiopathic

uveitis (22). In addition, we noted that 21% of those discovered to have sarcoidosis on chest CT also had cardiac sarcoidosis with associated ventricular tachycardia (22). Thus, recognition of the systemic illness had potentially life-saving implications. A study from Japan reached a similar conclusion about uveitis and cardiac sarcoidosis (23).

While most systemic rheumatic diseases associated with uveitis, such as Behçet's disease, are diagnosed on the basis of the clinical presentation, tubulointerstitial nephritis with uveitis (TINU) is another of those easily overlooked entities. Rheumatologists might be asked to see a patient with TINU because the patient has redness in both eyes and photophobia from the anterior uveitis, and the patient is typically systemically ill with fever, myalgias, a markedly elevated erythrocyte sedimentation rate, mild anemia, and mildly abnormal liver enzyme levels (24,25). Unless one is cognizant of the diagnosis and requests a measurement of β_2-microglobulin levels in the urine, the diagnosis is frequently overlooked.

In virtually every series of patients with uveitis, a diagnosis of "idiopathic" disease is the most common etiology noted (26). Other terms to describe idiopathic uveitis include nonclassifiable disease, primary uveitis, or undifferentiated disease (27).

Despite the breadth of the differential diagnosis for uveitis, the rheumatologist should be able to take a relatively targeted approach to laboratory testing (28). The initial examination by the ophthalmologist should reveal any suspicion of a masquerade syndrome or an infectious cause. The detailed history should point to most of the possible associated systemic immune-mediated diseases. If the history and clinical examination have failed to point to a probable cause, we screen for syphilis, since this infection can be latent for many years and its uveal manifestations are protean.

In addition, we obtain a chest radiograph, as sarcoidosis might be asymptomatic in the lungs and this is also useful as a screen for tuberculosis. The sensitivity of chest radiography for either ocular tuberculosis or sarcoidosis is probably 50% or lower. Because of the potential exposure to extensive radiation, we usually do not obtain a chest CT scan to search for sarcoid, unless the patient is more than 40 years of age (22). In the US, we also do not screen for tuberculosis exposure, unless the patient has a specific risk factor for tuberculosis, such as birth outside the US or a history of incarceration (29). Additional tests might be useful to monitor therapy, such as a complete blood cell count and metabolic panel. Targeted testing is also useful if the presentation suggests a specific entity. For example, we often test for HLA–B27 if the patient presents with unilateral, acute, anterior uveitis. We check urine for the levels of β_2-microglobulin in patients who present with a bilateral, sudden-onset, anterior uveitis. We consider a diagnosis of multiple sclerosis if the patient relates the presence of neurologic symptoms that might be explained by this diagnosis.

Therapy

The heterogeneity of uveitis has impacted the ability to design clinical trials. The relative rarity of vision-threatening uveitis is such that different etiologies are usually combined into a single clinical trial. However, the manifestations of a disease such as birdshot retinochoroidopathy are such that the end point for treatment differs greatly from the end point for treatment of an inflammation-related entity such as Behçet's disease. This challenge in trial design may have contributed to the failure of promising therapies, such as voclosporine (a congener of cyclosporine), secukinumab (anti–IL-17A) (30,31), gevokizumab (anti–IL-1β) (32), or intravitreal rapamycin (33), to show consistent benefit in clinical uveitis trials.

Most practitioners treat uveitis, especially anterior uveitis, initially with topical corticosteroids. Although these are frequently effective, their penetration posterior to the lens is limited. In addition, use of topical corticosteroids can be complicated by cataractogenesis or elevated intraocular pressure. One formulation, difluprednate, has greater ability to treat inflammation posterior to the lens, but it also has a greater tendency to cause a cataract or glaucoma. If topical corticosteroids fail, a locally injected corticosteroid such as triamcinolone can be useful. However, in addition to being an uncomfortable injection, risks include cataract, glaucoma, lid ptosis, and, in rare instances, retinal detachment. Triamcinolone can be injected directly into the vitreous humor, where it has increased benefit and increased risk of intraocular infection or hemorrhage. Oral corticosteroids represent an additional option, but long-term use has toxic effects that are well known to rheumatologists (34). Antimetabolites, including mycophenolate mofetil, methotrexate, and azathioprine, are popular corticosteroid-sparing drugs that are often utilized by uveitis experts (35). Additional options include calcineurin antagonists such as cyclosporine or tacrolimus (36), alkylators like cyclophosphamide, or long-lasting corticosteroid implants delivered either by surgery or injection.

The rheumatologist has a major role to play in managing the therapy in a subset of patients with ocular inflammatory disease. Many ophthalmologists are

comfortable prescribing oral corticosteroids but rarely resort to steroid-sparing medications (37). The dosage of prednisone or its equivalent is often such that the treatment has considerable morbidity. A National Institutes of Health–sponsored trial known as MUST (Multicenter Uveitis Steroid Treatment) for patients with noninfectious, intermediate posterior uveitis or panuveitis recently showed the superior efficacy of systemic immunosuppression, as with antimetabolites, compared to a sustained release of fluocinolone into the vitreous humor of the eye. This conclusion was based on findings of visual acuity testing after 7 years of follow-up (38).

Progress in the approval of new therapies for uveitis is hampered by the relative rarity of specific forms of uveitis, by the variety of presumed causes, and by the heterogeneity of outcomes that might define successful therapy. In 2 time-to–treatment failure trials reported in 2016, adalimumab showed a clear-cut benefit in the treatment of noninfectious intermediate, posterior uveitis or panuveitis (39,40). In most instances, adalimumab is indicated for patients whose previous treatment with oral corticosteroids was unsuccessful, as well as for patients who have failed treatment with another oral immunosuppressant, such as methotrexate or mycophenolate mofetil. The responsiveness of Behçet's disease to adalimumab or infliximab is such that physicians sometimes consider the use of such therapy without conducting a trial of an antimetabolite (41). Multiple sclerosis (MS) can be associated with intermediate uveitis (42). Since a diagnosis of MS is a relative contraindication to TNF inhibitor therapy, this diagnosis may need to be excluded prior to the initiation of adalimumab therapy for uveitis.

It is rare to prescribe a biologic agent for anterior uveitis, since in most patients with anterior uveitis, the disease can be controlled with topical medication alone. An exception is the uveitis characteristically associated with a subset of patients with JIA. The typical JIA patient with chronic uveitis develops the disease between ages 2 years and 8 years, and it affects a few joints. The majority of JIA patients are antinuclear antibody positive and are female. The SYCAMORE study tested the efficacy of adalimumab for patients with JIA whose uveitis was active despite treatment with methotrexate and topical corticosteroids (43). The trial was halted early, since the evidence of benefit was apparent. Another randomized controlled trial used a different outcome measure, quantification of protein in the anterior chamber of the eye, and also concluded that adalimumab was useful for the chronic anterior uveitis associated with JIA (44).

These successes have encouraged additional uveitis trials, such as one assessing the benefit of the JAK inhibitor filgotinib for indications similar to those supporting the use of adalimumab. Many emerging biologics, however, have not been studied rigorously for possible benefit in the treatment of uveitis. Moreover, although uveitis is increasingly targeted in therapeutic trials, a search of the ClinicalTrials.gov website (http://www.clinicaltrials.gov) in February 2018 identified only 7 current or prior randomized controlled trials involving patients with uveitis. A similar search for clinical trials in patients with rheumatoid arthritis identified 54 trials. Finally, although some ophthalmologists are comfortable prescribing immunosuppression without close physician collaboration, virtually all ophthalmologists lack an infrastructure that is prepared to deal with the systemic infectious complications, which are rare but unavoidable when one suppresses the immune system.

To aid physicians who care for patients with uveitis, several international groups have recently offered guidelines to assist in the care of patients with ocular inflammatory diseases (45,46). The FOCUS (Fundamentals of Care for Uveitis) group consisted of 146 international experts who graded the strength of the evidence and who used consensus methodology (45).

Patients with spondyloarthritis tend to have recurrent episodes of uveitis. As most of these episodes are anterior, last for no more than 3 months, and can be managed with topical corticosteroids alone, the issue of prophylaxis often does not arise. Several medications do reduce the frequency of uveitis. The use of sulfasalazine to prevent attacks of uveitis in patients with spondyloarthritis is supported by the results of randomized controlled trials (47,48). Monoclonal antibodies that neutralize TNF, especially adalimumab or infliximab, also prevent attacks of uveitis (49), but these treatments are generally not prescribed if the sole reason is to prevent attacks of anterior uveitis. At this time, extensive data on how treatments such as secukinumab or tofacitinib affect recurrent uveitis in patients with spondylitis have not been published.

In the future, therapies delivered locally to the eye might become the treatment of choice for ocular inflammation. Locally injected corticosteroid into the eye itself can be very effective, but the therapy is limited, in part because the medication frequently causes cataract and glaucoma. Gene therapy for inherited retinal degeneration has now been approved by the US Food and Drug Administration and is successful, in part, because the injected gene enters a confined space with minimal worries about expression in other tissues (50). In contrast to that in polyarticular rheumatoid arthritis, successful

gene therapy for ocular inflammation needs to target no more than 2 locations. In the decades ahead, 1 or more locally delivered inhibitors of inflammation might become the standard of care for uveitis.

Conclusions

We recognize the challenges in attempting to familiarize oneself with a group of diseases that one cannot fully assess by using the tools in a conventional rheumatology clinic. Moreover, we empathize with the time requirements that impair optimal management of a patient whose illness requires at least 2 subspecialists to confer. Mechanisms that facilitate communication with an ophthalmologist include interdisciplinary clinics and case conferences to discuss patients whose illness lies in the interstices between these 2 disciplines. The gratification of practicing medicine derives primarily from the opportunity to improve the welfare of our patients. That welfare is best served if we as rheumatologists share our knowledge and experience, while welcoming the collaboration of ophthalmologists who, quite literally, have a different view of our patients and their disease. Just as a conductor of a symphony orchestra coordinates multiple musicians, physicians can and should achieve a similar collaboration.

AUTHOR CONTRIBUTIONS

Both authors drafted the article, revised it critically for important intellectual content, and approved the final version to be published.

REFERENCES

1. Thorne JE, Suhler E, Skup M, Tari S, Macaulay D, Chao J, et al. Prevalence of noninfectious uveitis in the United States: a claims-based analysis. JAMA Ophthalmol 2016;134:1237–45.
2. Nussenblatt RB. The natural history of uveitis. Int Ophthalmol 1990;14:303–8.
3. Varkey JB, Shantha JG, Crozier I, Kraft CS, Lyon GM, Mehta AK, et al. Persistence of Ebola virus in ocular fluid during convalescence. N Engl J Med 2015;372:2423–7.
4. Rosenbaum JT. Characterization of uveitis associated with spondyloarthritis. J Rheumatol 1989;16:792–6.
5. Ruutu M, Thomas G, Steck R, Degli-Esposti MA, Zinkernagel MS, Alexander K, et al. β-glucan triggers spondylarthritis and Crohn's disease-like ileitis in SKG mice. Arthritis Rheum 2012; 64:2211–22.
6. Petty RE, Johnston W, McCormick AQ, Hunt DW, Rootman J, Rollins DF. Uveitis and arthritis induced by adjuvant: clinical, immunologic and histologic characteristics. J Rheumatol 1989;16: 499–505.
7. Kezic JM, Davey MP, Glant TT, Rosenbaum JT, Rosenzweig HL. IFN-γ regulates discordant mechanisms of uveitis versus joint and axial disease in a murine model resembling spondyloarthritis. Arthritis Rheum 2012;64:762–71.
8. Robinson PC, Claushuis TA, Cortes A, Martin TM, Evans DM, Leo P, et al. Genetic dissection of acute anterior uveitis reveals similarities and differences in associations observed with ankylosing spondylitis. Arthritis Rheumatol 2015;67:140–51.
9. Smith JR, Braziel RM, Paoletti S, Lipp M, Uguccioni M, Rosenbaum JT. Expression of B-cell-attracting chemokine 1 (CXCL13) by malignant lymphocytes and vascular endothelium in primary central nervous system lymphoma. Blood 2003;101:815–21.
10. Smith JR, Rosenbaum JT, Wilson DJ, Doolittle ND, Siegal T, Neuwelt EA, et al. Role of intravitreal methotrexate in the management of primary central nervous system lymphoma with ocular involvement. Ophthalmology 2002;109:1709–16.
11. Patel DV, Horne A, House M, Reid IR, McGhee CN. The incidence of acute anterior uveitis after intravenous zoledronate. Ophthalmology 2013;120:773–6.
12. Lim LL, Fraunfelder FW, Rosenbaum JT. Do tumor necrosis factor inhibitors cause uveitis? A registry-based study. Arthritis Rheum 2007;56:3248–52.
13. Conrady CD, Larochelle M, Pecen P, Palestine A, Shakoor A, Singh A. Checkpoint inhibitor-induced uveitis: a case series. Graefes Arch Clin Exp Ophthalmol 2017;256:187–91.
14. Eadie B, Etminan M, Mikelberg FS. Risk for uveitis with oral moxifloxacin: a comparative safety study. JAMA Ophthalmol 2014;133:81–4.
15. Ohno S, Nakamura S, Hori S, Shimakawa M, Kawashima H, Mochizuki M, et al. Efficacy, safety, and pharmacokinetics of multiple administration of infliximab in Behçet's disease with refractory uveoretinitis. J Rheumatol 2004;31:1362–8.
16. Ramanan AV, Dick AD, Benton D, Compeyrot-Lacassagne S, Dawoud D, Hardwick B, et al. A randomised controlled trial of the clinical effectiveness, safety and cost-effectiveness of adalimumab in combination with methotrexate for the treatment of juvenile idiopathic arthritis associated uveitis (SYCAMORE Trial). Trials 2014;15:14.
17. Brewerton DA, Caffrey M, Nicholls A, Walters D, James DC. Acute anterior uveitis and HL-A 27. Lancet 1973;302:994–6.
18. Haroon M, O'Rourke M, Ramasamy P, Murphy CC, FitzGerald O. A novel evidence-based detection of undiagnosed spondyloarthritis in patients presenting with acute anterior uveitis: the DUET (Dublin Uveitis Evaluation Tool). Ann Rheum Dis 2015;74:1990–5.
19. Juanola X, Loza Santamaria E, Cordero-Coma M, Group SW. Description and prevalence of spondyloarthritis in patients with anterior uveitis: the SENTINEL interdisciplinary collaborative project. Ophthalmology 2016;123:1632–6.
20. Monnet D, Breban M, Hudry C, Dougados M, Brezin AP. Ophthalmic findings and frequency of extraocular manifestations in patients with HLA-B27 uveitis: a study of 175 cases. Ophthalmology 2004;111:802–9.
21. Kaiser PK, Lowder CY, Sullivan P, Sanislo SR, Kosmorsky GS, Meziano MA, et al. Chest computerized tomography in the evaluation of uveitis in elderly women. Am J Ophthalmol 2002;133: 499–505.
22. Han YS, Rivera-Grana E, Salek S, Rosenbaum JT. Distinguishing uveitis secondary to sarcoidosis from idiopathic disease: cardiac implications. JAMA Ophthalmol 2018;136:109–115.
23. Umazume A, Kezuka T, Okunuki Y, Ooshita M, Usui Y, Hirano M, et al. Prediction of severe cardiac involvement by fundus lesion in sarcoidosis. Jpn J Ophthalmol 2014;58:81–5.
24. Mandeville JT, Levinson RD, Holland GN. The tubulointerstitial nephritis and uveitis syndrome. Surv Ophthalmol 2001;46:195–208.
25. Mackensen F, Smith J, Rosenbaum JT. Enhanced recognition, treatment, and prognosis of tubulointerstitial nephritis and uveitis syndrome. Ophthalmology 2007;114:995–9.
26. Rosenbaum JT. Nibbling away at the diagnosis of idiopathic uveitis. JAMA Ophthalmol 2015;133:146–7.

27. Jabs DA, Busingye J. Approach to the diagnosis of the uveitides. Am J Ophthalmol 2013;156:228–36.
28. Rosenbaum JT, Wernick R. Selection and interpretation of laboratory tests for patients with uveitis. Int Ophthalmol Clin 1990;30:238–43.
29. Rosenbaum JT, Wernick R. The utility of routine screening of patients with uveitis for systemic lupus erythematosus or tuberculosis: a Bayesian analysis. Arch Ophthalmol 1990;108: 1291–3.
30. Dick AD, Tugal-Tutkun I, Foster S, Zierhut M, Melissa Liew SH, Bezlyak V, et al. Secukinumab in the treatment of noninfectious uveitis: results of three randomized, controlled clinical trials. Ophthalmology 2013;120:777–87.
31. Letko E, Yeh S, Foster CS, Pleyer U, Brigell M, Grosskreutz CL, et al. Efficacy and safety of intravenous secukinumab in noninfectious uveitis requiring steroid-sparing immunosuppressive therapy. Ophthalmology 2015;122:939–48.
32. Tugal-Tutkun IM, Kadayifcilar SM, Khairallah MM, Lee SC, Ozdal P, Ozyazgan Y, et al. Safety and efficacy of gevokizumab in patients with Behçet's disease uveitis: results of an exploratory phase 2 study. Ocul Immunol Inflamm 2017;25:62–70.
33. Nguyen QD, Sadiq MA, Soliman MK, Agarwal A, Do DV, Sepah YJ. The effect of different dosing schedules of intravitreal sirolimus, a mammalian target of rapamycin (mTOR) inhibitor, in the treatment of non-infectious uveitis (an American Ophthalmological Society thesis). Trans Am Ophthalmol Soc 2016;114:T3.
34. Miloslavsky EM, Naden RP, Bijlsma JW, Brogan PA, Brown ES, Brunetta P, et al. Development of a Glucocorticoid Toxicity Index (GTI) using multicriteria decision analysis. Ann Rheum Dis 2017;76:543–6.
35. Esterberg E, Acharya NR. Corticosteroid-sparing therapy: practice patterns among uveitis specialists. J Ophthalmic Inflamm Infect 2012;2:21–8.
36. Lee RW, Greenwood R, Taylor H, Amer R, Biester S, Heissigerova J, et al. A randomized trial of tacrolimus versus tacrolimus and prednisone for the maintenance of disease remission in noninfectious uveitis. Ophthalmology 2012;119:1223–30.
37. Nguyen QD, Hatef E, Kayen B, Macahilig CP, Ibrahim M, Wang J, et al. A cross-sectional study of the current treatment patterns in noninfectious uveitis among specialists in the United States. Ophthalmology 2011;118:184–90.
38. Writing Committee for the Multicenter Uveitis Steroid Treatment Trial and Follow-up Study Research Group, Kempen JH, Altaweel MM, Holbrook JT, Sugar EA, Thorne JE, et al. Association between long-lasting intravitreous fluocinolone acetonide implant vs systemic anti-inflammatory therapy and visual acuity at 7 years among patients with intermediate, posterior, or panuveitis. JAMA 2017;317:1993–2005.
39. Jaffe GJ, Dick AD, Brezin AP, Nguyen QD, Thorne JE, Kestelyn P, et al. Adalimumab in patients with active noninfectious uveitis. N Engl J Med 2016;375:932–43.
40. Nguyen QD, Merrill PT, Jaffe GJ, Dick AD, Kurup SK, Sheppard J, et al. Adalimumab for prevention of uveitic flare in patients with inactive non-infectious uveitis controlled by corticosteroids (VISUAL II): a multicentre, double-masked, randomised, placebo-controlled phase 3 trial. Lancet 2016;388:1183–92.
41. Rosenbaum JT. Blind insight: eyeing anti-tumor necrosis factor treatment in uveitis associated with Behçet's disease. J Rheumatol 2004;31:1241–3.
42. Messenger W, Hildebrandt L, Mackensen F, Suhler E, Becker M, Rosenbaum JT. Characterisation of uveitis in association with multiple sclerosis. Br J Ophthalmol 2015;99:205–9.
43. Ramanan AV, Dick AD, Jones AP, McKay A, Williamson PR, Compeyrot-Lacassagne S, et al. Adalimumab plus methotrexate for uveitis in juvenile idiopathic arthritis. N Engl J Med 2017;376:1637–46.
44. Quartier P, Baptiste A, Despert V, Allain-Launay E, Kone-Paut I, Belot A, et al. ADJUVITE: a double-blind, randomised, placebo-controlled trial of adalimumab in early onset, chronic, juvenile idiopathic arthritis-associated anterior uveitis. Ann Rheum Dis 2018;77:1003–11.
45. Dick AD, Rosenbaum JT, Al-Dhibi HA, Belfort R Jr, Brezin AP, Chee SP, et al. Guidance on noncorticosteroid systemic immunomodulatory therapy in noninfectious uveitis: fundamentals of care for uveitis (FOCUS) initiative. Ophthalmology 2018;125:757–73.
46. Wakefield D, McCluskey P, Wildner G, Thurau S, Carr G, Chee SP, et al. Inflammatory eye disease: pre-treatment assessment of patients prior to commencing immunosuppressive and biologic therapy: recommendations from an expert committee. Autoimmun Rev 2017;16:213–22.
47. Munoz-Fernandez S, Hidalgo V, Fernandez-Melon J, Schlincker A, Bonilla G, Ruiz-Sancho D, et al. Sulfasalazine reduces the number of flares of acute anterior uveitis over a one-year period. J Rheumatol 2003;30:1277–9.
48. Dougados M, Berenbaum F, Maetzel A, Amor B. Prevention of acute anterior uveitis associated with spondyloarthropathy induced by salazosulfapyridine. Rev Rhum 1993;60:81–3.
49. Lie E, Lindstrom U, Zverkova-Sandstrom T, Olsen IC, Forsblad-d'Elia H, Askling J, et al. Tumour necrosis factor inhibitor treatment and occurrence of anterior uveitis in ankylosing spondylitis: results from the Swedish biologics register. Ann Rheum Dis 2017;76:1515–21.
50. Trapani I, Banfi S, Simonelli F, Surace EM, Auricchio A. Gene therapy of inherited retinal degenerations: prospects and challenges. Hum Gene Ther 2015;26:193–200.

ARTHRITIS & RHEUMATOLOGY
Vol. 70, No. 10, October 2018, pp 1544–1554
DOI 10.1002/art.40574

REVIEW

The Lung in Rheumatoid Arthritis

Focus on Interstitial Lung Disease

Paolo Spagnolo,[1] Joyce S. Lee,[2] Nicola Sverzellati,[3] Giulio Rossi,[4] and Vincent Cottin[5]

Interstitial lung disease (ILD) is an increasingly recognized complication of rheumatoid arthritis (RA) and is associated with significant morbidity and mortality. In addition, approximately one-third of patients have subclinical disease with varying degrees of functional impairment. Although risk factors for RA-related ILD are well established (e.g., older age, male sex, ever smoking, and seropositivity for rheumatoid factor and anti–cyclic citrullinated peptide), little is known about optimal disease assessment, treatment, and monitoring, particularly in patients with progressive disease. Patients with RA-related ILD are also at high risk of infection and drug toxicity, which, along with comorbidities, complicates further treatment decision-making. There are distinct histopathologic patterns of RA-related ILD with different clinical phenotypes, natural histories, and prognoses. Of these, the usual interstitial pneumonia (UIP) subtype of RA-related ILD shares a number of clinical and histopathologic features with idiopathic pulmonary fibrosis, the most common and severe of the idiopathic interstitial pneumonias, suggesting the existence of common mechanistic pathways and possibly therapeutic targets. There remain substantial gaps in our knowledge of RA-related ILD. Concerted multinational efforts by expert centers has the potential to elucidate the basic mechanisms underlying RA-related UIP and other subtypes of RA-related ILD and facilitate the development of more efficacious and safer drugs.

Introduction

Pulmonary involvement is a common extraarticular manifestation of rheumatoid arthritis (RA) and occurs, to some extent, in 60–80% of patients with RA (1,2). The pulmonary disease associated with RA can affect any of the lung compartments and can be either secondary to the underlying RA or a complication of RA therapy, such as opportunistic infection and drug toxicity. One particular type of pulmonary involvement in RA is interstitial lung disease (ILD), which is associated with significant morbidity and mortality (3–5) and is the focus of this review.

Epidemiology and risk factors

The precise prevalence and incidence of RA-related ILD are unknown but range from 1% to 58% depending on the methodology used (1,4,6–10). Population-based studies in the US suggest that the cumulative incidence of clinically significant RA-related ILD (defined as abnormal high-resolution computed tomography [HRCT] and lung function tests with clinical manifestations of ILD) is 5% at 10 years (11), 6.3% at 15 years (12), and 6.8% over 30 years of follow-up (1). Another study that reviewed US death certificates in decedents with RA identified clinically significant ILD in 6.8% of women and 9.8% of men (4). However, studies that rely on medical records review and medical coding are subject to reporting bias and generally

Supported by the Department of Cardiac, Thoracic and Vascular Sciences, University of Padova (grant BIRD163522 to Dr. Spagnolo).

[1]Paolo Spagnolo, MD, PhD: University of Padova, Padua, Italy; [2]Joyce S. Lee, MD: University of Colorado Denver, Aurora; [3]Nicola Sverzellati, MD: University of Parma, Parma, Italy; [4]Giulio Rossi, MD: Azienda USL Valle d'Aosta, Regional Hospital, Aosta, Italy; [5]Vincent Cottin, MD: Hospices Civils de Lyon, Louis Pradel Hospital, National Reference Center for Rare Pulmonary Diseases, Lyon, France.

Dr. Spagnolo has received consulting fees, speaking fees, and/or honoraria from Roche, Boehringer Ingelheim, Zambon, Galapagos, and PPM Services (less than $10,000 each). Dr. Lee has received consulting fees from Genentech, Boehringer Ingelheim, and Celgene (less than $10,000 each). Dr. Sverzellati has received speaking fees from Roche and Boehringer Ingelheim (less than $10,000 each). Dr. Cottin has received consulting fees, speaking fees, and/or honoraria from Actelion, Bayer, Gilead, GlaxoSmithKline, Merck Sharp & Dohme, Novartis, Sanofi, Promedior, Celgene, and Galapagos (less than $10,000 each) as well as from Boehringer Ingelheim and Roche (more than $10,000 each) and research grants from Boehringer Ingelheim and Roche.

Address correspondence to Paolo Spagnolo, MD, PhD, Section of Respiratory Diseases, Department of Cardiac, Thoracic and Vascular Sciences, University of Padova, Via Giustiniani 3, 35128 Padua, Italy. E-mail: paolo.spagnolo@unipd.it.

Submitted for publication July 16, 2017; accepted in revised form May 22, 2018.

include only patients with clinically significant disease. Another factor that complicates determining the prevalence and incidence of RA-related ILD is that the ILD is often underrecognized (13). Patients with RA who undergo screening, regardless of the presence of symptoms, often have radiologic abnormalities on HRCT, referred to as subclinical ILD and/or interstitial lung abnormalities. The prevalence of subclinical ILD is variable and ranges from 19% to 57% (10,14). These radiographic findings are reported to be progressive in ~50% of cases (6) and are associated with increased respiratory symptoms and impaired lung function (15). Nonetheless, tools are lacking to predict the individual risk of progression to clinically significant RA-related ILD.

There are several recognized risk factors for the development of ILD in patients with RA. The most consistently reproduced associations across studies include older age (3,12,16), male sex (3,10,14), a history of ever smoking (6,14,17), and seropositivity for rheumatoid factor (RF) or anti–cyclic citrullinated peptide (anti-CCP) antibodies (6,13,17). Interestingly, smoking is associated with both an increased risk of RA (18) and a greater risk of developing RA-related ILD (13,18). RA disease activity has also been associated with the development of RA-related ILD, although these associations are less clear (3,12).

Hypothetical mechanisms behind the concomitance of joint and lung involvement

The mechanisms of ILD in RA are poorly understood, but genetic and environmental factors are believed to play a role (19,20). HLA–B54, HLA–DQ1B*0601, HLA–B40, and the site encoding α-1 protease inhibitor are associated with an increased risk of ILD in patients with RA (19). In addition, a conserved amino acid sequence at position 70–74 (QKRAA, RRRAA, or QRRAA) in the HLA–DRβ chain, referred to as the shared epitope (SE), is shared between the RA-associated HLA–DR alleles (21–23). Notably, the SE confers susceptibility to the development of RA and is highly associated with the presence of anti-CCP antibodies. Citrullination is the posttranslational enzymatic conversion of arginine to citrulline. In patients who also possess the SE, citrullinated residues may act as neoepitopes that break immunologic tolerance and become a target for autoimmunity (24,25). The site where this initial event occurs is unknown, but evidence points toward mucosal sites (26).

Two potential pathways linking joint and lung involvement have been proposed (27). In one of the pathways, RA-related ILD would begin in the synovial tissue following an immune response against citrullinated proteins that subsequently cross-react with similar antigens in the lung. The plausibility of this hypothesis stems from the observation that the majority of patients with RA-related ILD develop articular disease prior to lung involvement. In such cases, lung histology would exhibit an inflammatory non–usual interstitial pneumonia (non-UIP) pattern of disease. In the second pathogenetic paradigm, immune tolerance breakdown takes place in the lung, and ILD (including UIP) triggers an immune response against citrullinated proteins that secondarily spreads to the joints. The observations that ILD might precede extrapulmonary manifestations of RA by years (6,10), that an increased number of citrullinated peptides may be seen in the lung parenchyma of patients with RA-related ILD, and that the lung might locally produce RA-related autoimmunity lend support to this latter hypothesis (28,29).

Smoking is believed to play a major role in the pathogenesis of RA-related ILD. Lung injury from cigarette smoking and other sources of oxidative stress may contribute to citrullination of proteins and the creation of new epitopes that trigger SE-restricted autoimmune responses characterized by cellular infiltration and release of profibrotic cytokines (e.g., interleukin-4 [IL-4], IL-13, and transforming growth factor β [TGFβ]), chemokines, and growth factors such as vascular endothelial growth factor (VEGF) and platelet-derived growth factor (PDGF) that promote fibroblast proliferation and differentiation to myofibroblasts. However, smoking may also induce the activation of profibrotic pathways through repetitive injury to the alveolar epithelium. In turn, matrix metalloproteinases released from damaged epithelia may promote further cellular recruitment and activation of cytokines and profibrotic mediators, thereby amplifying the cross-talk between inflammatory and tissue-remodeling pathways.

Clinical features

The clinical manifestations of RA-related ILD resemble those of idiopathic interstitial pneumonias, although, in contrast to patients with idiopathic interstitial pneumonias, patients with RA-related ILD may remain asymptomatic despite significant radiographic abnormalities. The most common presenting symptoms include exertional dyspnea, which, in patients with debilitating arthritis pain may be masked by limited mobility and nonproductive cough. Physical signs of respiratory involvement may be minimal or absent despite the presence of radiographic abnormalities, but tachypnea and bibasilar inspiratory crackles are common (30). Pleural rubs may also be heard, and, in advanced disease, cyanosis, edema, and signs of pulmonary hypertension (PH) may occur. As with other connective tissue diseases (CTDs), in RA patients, PH

should be suspected in the presence of symptoms or exercise-induced arterial oxygen desaturation disproportionate to the severity of lung involvement. Clubbing has been reported in as many as 75% of patients with RA-associated UIP but occurs significantly less frequently in those with other patterns of RA-related ILD (31). The temporal relationship between articular disease and ILD is variable. One study showed a median duration of 4.9 years from the diagnosis of RA to the diagnosis of ILD (32), but lung disease may also precede the joint manifestations (33). The severity and extent of lung involvement do not necessarily correlate with the severity of RA, although high titers of RF are a known risk factor for the development of ILD.

Disease phenotypes

There are well-recognized phenotypes among patients with RA-related ILD. One of the more notable distinctions that often is made is the relationship to the UIP pattern of disease. Indeed, in contrast to patients with other CTD-related ILDs (e.g., systemic sclerosis [SSc], idiopathic inflammatory myositis, and mixed connective tissue disease), in which a nonspecific interstitial pneumonia (NSIP) pattern is most frequently seen, patients with RA have the highest prevalence of a UIP pattern (34), both pathologically and radiologically (Table 1). Patients with RA-related ILD with a histologic UIP pattern tend to be older, more frequently are male, and more frequently are active or former smokers compared with patients with RA-related ILD with a non-UIP pattern (5,6,32,33). Other data suggest that patients with RA-related ILD with a UIP pattern experience more respiratory system–related hospitalizations (35) and worse survival compared with those with a non-UIP pattern, although some of the data are mixed (5,36,37).

Similar to idiopathic UIP (e.g., idiopathic pulmonary fibrosis [IPF]), the clinical course of RA-related UIP is highly variable and can be punctuated by episodes of acute decompensation termed "acute exacerbations." In IPF, acute exacerbation is defined as a clinically significant worsening (or development) of dyspnea and lung function typically of <1 month duration, accompanied by new widespread pulmonary infiltrates on chest radiography or HRCT in the absence of cardiac failure and fluid overload (38). There are no studies comparing the prevalence of acute exacerbation across the spectrum of CTD-related ILD, but patients with a UIP pattern appear to be at higher risk for this complication irrespective of the underlying disease (39). In a retrospective study of 51 patients with RA-related ILD, acute exacerbation occurred in as many as 22% (11 of 51 patients) during a median follow-up period of 8.5 years, with a mortality rate of 64% (7 of 11 patients) (40). As expected, patients who experienced acute exacerbation had significantly worse survival compared with those who did not have acute exacerbation ($P = 0.001$). The overall 1-year incidence of acute exacerbation was 2.8% (6.5% in the UIP group and 1.7% in the non-UIP group). Older age at diagnosis, UIP pattern on HRCT, and methotrexate (MTX) treatment were associated with the development of acute exacerbation on univariate analysis, whereas the study was too small to perform multivariate analysis (40).

Given the phenotype of UIP in RA-related ILD, comparisons with IPF have been made. Patients with RA-related ILD with a UIP pattern on HRCT have similar age, sex distribution, and smoking history compared with patients with IPF (5,27). The radiologic pattern of UIP in RA-related ILD is also predictive of UIP on surgical lung biopsy, similar to what has been demonstrated in IPF (41). Finally, clinical predictors of mortality appear to be similar between RA-related UIP and IPF (40). NSIP occurs in approximately one-third of patients with RA-related ILD (33) and is generally associated with a longer duration of articular manifestations, a lower risk of disease progression, a better response to treatment, and better overall outcomes compared with UIP (5,6,36,42). The most common presenting symptoms are dyspnea and cough that have developed over weeks to months. Occasionally, patients initially diagnosed as having idiopathic NSIP may develop RA over time (43). The clinical course of RA-related NSIP is heterogeneous, with some patients remaining relatively stable and others (a minority) experiencing rapid deterioration (40). In addition, less frequent patterns of RA-related ILD include organizing pneumonia, lymphocytic interstitial pneumonia, diffuse alveolar damage, and desquamative interstitial pneumonia.

Imaging

Radiographic surveys for the presence of ILD are insensitive and imprecise in patients with RA. In a prospective study of asymptomatic patients with early disease, chest radiograph showed features of ILD in 6% of patients, and HRCT showed such features in 33% of patients (10). Abnormal chest radiographs can show bibasilar ground-glass opacities, reticular and nodular changes, and honeycombing. In advanced disease, enlargement of central pulmonary arteries and attenuation of peripheral vessels may suggest PH. On HRCT, ILD abnormalities are more extensive in males, patients with severe deforming joint disease, and those with high RF titers (9,10). However, in a study of 84 patients with longstanding RA, HRCT abnormalities were present in as many as 11 of 38

Table 1. Clinical, radiologic, and pathologic features across the spectrum of connective tissue disease–associated interstitial lung disease*

Disease	Epidemiology	Clinical manifestations	HRCT	Histologic findings
RA	Most cases occur at age 50–60 years. Male sex, longstanding disease, high RF titers, and history of cigarette smoking increase the risk of ILD.	Dyspnea at rest or with exertion and dry cough.	Bibasilar reticulation with or without honeycombing, ground-glass opacity, centrilobular branching lines with or without airway dilatation and consolidation.	UIP (predominantly), NSIP, LIP, OP.
SSc	The prevalence of ILD is significantly higher in patients with more extensive skin involvement and ranges from 10% to 50%. Anti-topo antibodies are a risk factor for the development of ILD, while ACAs are protective.	Fatigue, dyspnea and cough, either dry or productive.	Ground-glass attenuation, irregular linear opacities, small nodules, traction bronchiectasis, bilateral pleural thickening, honeycombing. Centrilobular nodules and fibrosis suggest recurrent aspiration.	NSIP (predominantly) and UIP. RB-ILD and OP are rare.
SS	More common in patients with more severe and extraglandular manifestations.	Exertional dyspnea and dry cough.	Ground-glass attenuation, centrilobular and subpleural nodules, linear opacities, interlobular septal thickening, bronchial wall thickening, bronchiectasis, and thin-walled cysts. Honeycombing is rare.	NSIP, OP, LIP, UIP, amyloidosis, constrictive bronchiolitis.
SLE	Uncommon (<5% of cases). Mean age at presentation is ~50 years.	Dry cough, dyspnea, pleuritic chest pain.	Intralobular and interlobular septal thickening, traction bronchiectasis, ground-glass opacity, consolidation. Honeycombing is rare.	NSIP (predominantly), UIP, LIP, OP, DAD in acute lupus pneumonitis. DAH, chronic thromboembolic disease and vasculitis can also be seen.
PM/DM	Prevalence of ILD 30–80% and higher in DM. Presence of an antisynthetase antibody is highly predictive of the development of ILD.	Acute/subacute onset of cough and dyspnea frequently accompanied by fever in acute ILD (more common in DM). Progressive dyspnea on exertion and dry cough in chronic ILD.	Bilateral lower-lobe irregular linear opacities, consolidation, ground-glass opacity, micronodules. Honeycombing is rare.	NSIP (predominantly), OP, UIP, DAD.
MCTD	ILD occurs in ~50–66% of patients.	Dry cough, dyspnea, and pleuritic chest pain.	Ground-glass attenuation and linear opacities with a peripheral and lower lobe predominance.	All histologic features of PM/DM, SLE, or SSc can be found.
AS	Rare (<5%). Male preponderance (M:F ratio 50:1).	Often asymptomatic. Cough, sputum, and dyspnea.	Apical fibrosis (usually bilateral), interlobular septal thickening, pleural thickening, parenchymal bands.	Early changes consist of a patchy pneumonic process. In advanced cases, dense pleural and pulmonary fibrosis (with or without bronchiectasis) predominates.

* HRCT = high-resolution computed tomography; RA = rheumatoid arthritis; RF = rheumatoid factor; UIP = usual interstitial pneumonia; LIP = lymphycytic interstitial pheumonia; OP = organizing pneumonia; SSc = systemic sclerosis; anti-topo = antitopoisomerase; ACAs = anticentromere antibodies; NSIP = nonspecific interstitial pneumonia; RB-ILD = respiratory bronchiolitis–associated interstitial lung disease; SS = Sjögren's syndrome; SLE = systemic lupus erythematosus; DAD = diffuse alveolar damage; DAH = diffuse alveolar hemorrhage; PM/DM = polymyositis/dermatomyositis; MCTD = mixed connective tissue disease; AS = ankylosing spondylitis.

(29%) asymptomatic patients and 27 of 39 (69%) symptomatic patients (44).

The spectrum of parenchymal changes that can be observed include ground-glass opacity, bronchiectasis/bronchiolectasis, linear opacities, and honeycombing (Figures 1A and B). Reticular changes, traction bronchiectasis/bronchiolectasis, and honeycombing are consistent with UIP; extensive ground-glass attenuation suggests NSIP, acute interstitial pneumonia, or desquamative interstitial pneumonia; and areas of subpleural consolidation suggest organizing pneumonia. In a large study of patients with RA-related lung disease, 4 major HRCT patterns of disease were identified, namely UIP (37%), NSIP (30%), obliterative bronchiolitis (17%), and organizing pneumonia (8%). Notably, in patients who underwent lung biopsy, the CT findings correlated with the pathologic findings in the majority of cases (45). A recent study showed that in patients with RA-related ILD, a *definite* UIP pattern on HRCT (characterized by basal, subpleural reticular opacities, traction bronchiectasis, and honeycombing) has a specificity of 96% and a sensitivity of 45% for histopathologic UIP, indicating that radiologic RA-related UIP may display features that mimic other patterns of disease (e.g., NSIP) (41). This point is not trivial, because patients with RA-related ILD rarely undergo surgical lung biopsy.

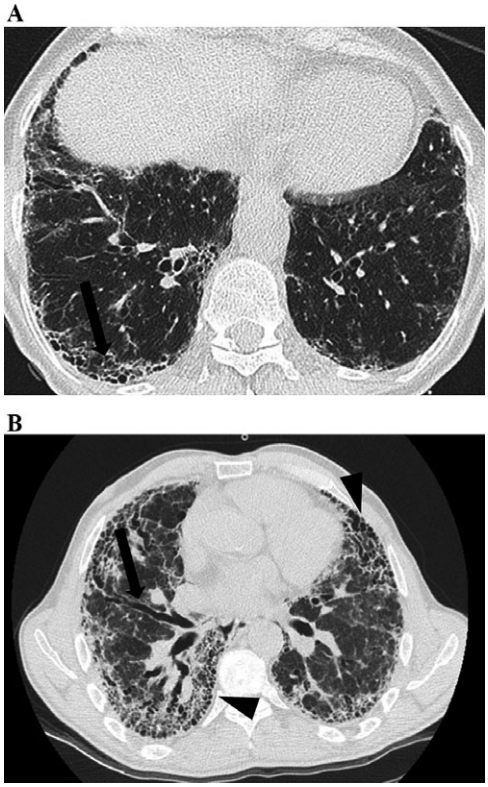

Figure 1. A, Interstitial lung disease in a 57-year-old man with rheumatoid arthritis (RA). Subpleural reticular opacities, cystic changes (**arrow**), and traction bronchiectasis in the lower lobes are shown. **B,** Advanced pulmonary fibrosis in a 62-year-old man with RA who was listed for lung transplantation. Bilateral predominantly subpleural reticular changes, traction bronchiectasis (**arrow**), and honeycombing (**arrowheads**) consistent with the usual interstitial pneumonia pattern are shown.

Diffuse ground-glass opacity on CT may be difficult to differentiate from desquamative interstitial pneumonia, particularly in smokers with RA. However, the diagnosis of desquamative interstitial pneumonia requires histologic confirmation. Conversely, features of desquamative interstitial pneumonia often overlap with those of NSIP and UIP in patients with RA-related ILD. Similarly, although lymphocytic interstitial pneumonia may be present in histologic specimens from RA patients, its distinguishing CT features (ground-glass opacity and/or reticular changes with lung cysts) are uncommon in patients with RA-related ILD and are far less frequent than in patients with primary Sjögren's syndrome.

Several non-ILD pulmonary features can be seen on imaging that are important to consider when evaluating patients with new-onset or established RA-related ILD. Airway involvement encompasses a number of abnormalities, including follicular bronchiolitis, bronchiectasis, and obliterative bronchiolitis. Follicular bronchiolitis is characterized on HRCT by centrilobular nodules measuring 1–12 mm in diameter, variably associated with peribronchial nodules and patchy areas of ground-glass opacity, while the CT appearance of obliterative bronchiolitis typically consists of a mosaic attenuation pattern with areas of air trapping on expiratory CT scan. Mild bronchial dilatation and wall thickening are common accompanying features. Rheumatoid nodules are generally associated with the presence of subcutaneous nodules and may wax and wane. Rheumatoid nodules may be single or multiple, of varying size (from a few millimeters to several centimeters), well circumscribed, and with the tendency to cavitate. Subpleural rheumatoid nodules may cause bronchopleural fistula or pneumothorax. Rheumatoid nodules should be closely monitored clinically and radiologically, because differentiating them from pulmonary neoplasm (e.g., carcinoma or lymphoma) or amyloidosis may be challenging.

Pulmonary function tests

In patients with RA-related ILD, pulmonary function tests may reveal a restrictive ventilatory defect with decreased diffusing capacity of the lung for carbon monoxide (DLCO) even in the absence of symptoms. In a study of patients with early RA, 33% had a DLCO of <80% of that predicted, while only 14% had symptoms (10). The DLCO is highly sensitive for predicting the

presence of ILD, whereas lung volumes may be more useful than DLCO for assessing disease extent (46,47). Similar to IPF, changes over time that are considered clinically relevant include a decrease in forced vital capacity (FVC) of ≥10% or a decrease in the DLCO of ≥15% over 6–12 months (47).

Bronchoalveolar lavage (BAL)

Findings in BAL fluid obtained from patients with RA-related ILD are frequently abnormal but are nonspecific, although an increase in the neutrophil count is more common in patients with UIP, and a lymphocytic cytology is more frequent in patients with NSIP or organizing pneumonia. In addition, BAL lymphocytosis is more common in RA patients without ILD (48). However, abnormalities in the cellular constituents of BAL fluid are not useful for predicting outcome or response to treatment. As a result, BAL is not routinely performed in the diagnostic work-up of patients with RA-related ILD. In RA patients with an acute onset or worsening of respiratory symptoms and radiographic abnormalities, BAL is useful for excluding ILDs other than RA-related ILD, malignancy, or infection (47).

Pathology

RA may be associated with a variety of pleural and pulmonary pathologies, including ILD, pleuritis, bronchiolitis, vascular abnormalities, and rheumatoid nodules (49,50). However, with the exception of rheumatoid nodules, very few of the histologic lesions observed in patients with RA are unique, while the majority of them display features that overlap with those of other entities (e.g., UIP/IPF).

In autopsy studies, pleural involvement has been reported in up to 70% of RA patients (51); however, most cases are asymptomatic and of no clinical relevance (52). Typically, pleural effusion has features of a sterile exudate with low pH (<7.3), a low glucose level (<60 mg/dl), and an elevated lactate dehydrogenase level (>700 IU/liter) (53). Chronic pleuritis is characterized by thickening of the visceral pleura by fibrous connective tissue and a chronic infiltration of lymphocytes and plasma cells. In the early phases of rheumatoid pleuritis, fibrin deposition with neutrophilic exudate is a common finding (49,54), while late phases are characterized by chronic inflammatory infiltrates accompanied by mesothelial hyperplasia with fibroblasts and elongated histiocytes perpendicularly oriented to the pleural surface (49,54). Cellular interstitial pneumonia with aggregates of lymphoid tissue (Figure 2) and follicular bronchitis/bronchiolitis, which consists of peribronchial/peribronchiolar lymphoid follicles with secondary germinal centers, are additional common findings (30,55,56).

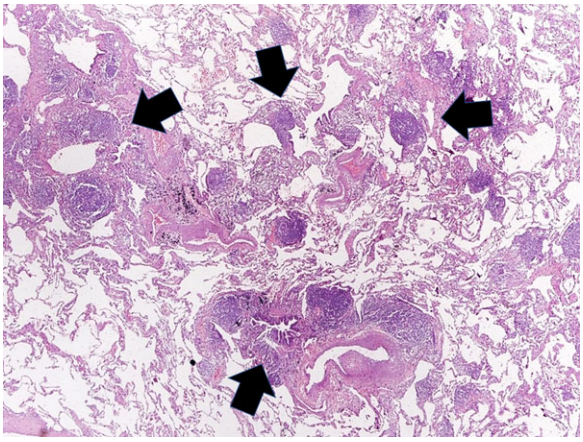

Figure 2. Photomicrograph showing highly cellulated interstitial pneumonia with several aggregates of nodular lymphoid tissue (**arrows**) around bronchi and bronchioles in a patient with rheumatoid arthritis. Hematoxylin and eosin stained; original magnification × 40.

RA may be complicated by a spectrum of ILD patterns, and UIP is more prevalent than NSIP (33,34,55,57) (Figure 3). A UIP pattern, which is characterized by patchy heterogeneous fibrosis with honeycomb changes, and actively fibrogenic "fibroblastic foci" (56) can be seen in 28–61% of patients with RA-related ILD (41,58). Compared with IPF, RA-related UIP is characterized by the concurrent presence of chronic pleuritis, follicular bronchiolitis, or cellular bronchiolitis with interstitial chronic infiltrates. In addition, lung biopsy specimens obtained from patients with RA-related UIP have an increased number of CD4+ lymphocytes compared with those from IPF patients (59).

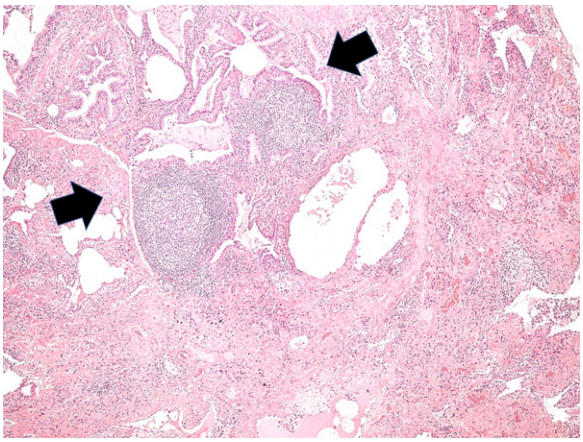

Figure 3. Photomicrograph showing interstitial lung disease with a usual interstitial pneumonia pattern and scattered follicular bronchiolitis (**arrows**) secondary to rheumatoid arthritis. Hematoxylin and eosin stained; original magnification × 100.

Surgical lung biopsy is generally not required in patients with RA-related ILD, unless the diagnosis of CTD is unclear or not established (e.g., when ILD precedes the onset of articular manifestations of RA). Bronchiolar chronic inflammatory infiltrates, interlobular lymphoid hyperplasia, cellular interstitial pneumonia, desquamative interstitial pneumonia, and bronchiolitis obliterans with organizing pneumonia, which may lead to constrictive bronchiolitis, are additional histologic manifestations of RA-related ILD. Lung abnormalities in RA patients may also be secondary to drug toxicity (e.g., MTX) or superimposed opportunistic infections. Therefore, pathologists should be familiar with drug-induced lung injury in patients with RA who are receiving immunosuppressive therapy, because virtually all drugs used to treat RA can cause lung toxicity with patterns identical to those observed in RA-related ILD, such as cellular NSIP with or without granulomas (MTX), organizing pneumonia and cellular interstitial pneumonia (rituximab), and diffuse alveolar damage (leflunomide) (www.pneumotox.com) (Table 2). A small proportion of patients with RA have rheumatoid nodules (54,57), which may be single or multiple and are typically located in the interlobular septa or on the pleural surface. The occurrence of potentially life-threatening infections should also be considered in patients with RA-related ILD. In suspected cases, special stains (e.g., methenamine–silver, periodic acid–Schiff, and Ziehl-Neelsen) should be performed when examining BAL fluid or lung tissue.

Management

The optimal treatment of RA-related ILD has not been determined and is largely based on data derived from other CTD-related ILDs, primarily SSc-associated ILD. Therefore, careful attention should be paid to the baseline assessment of disease severity, presentation (acute, subacute, and chronic), and the risks and benefits of therapy for each patient. In general, treatment should be considered in patients with clinical, functional, or radiologic deterioration and histopathologic patterns other than UIP (e.g., NSIP, organizing pneumonia, and lymphocytic interstitial pneumonia). However, in a retrospective study of 84 patients with RA-related UIP, 29 of whom were treated due to poor lung function or ILD progression, glucocorticoids alone or in combination with immunosuppressive agents improved or stabilized the disease in 50% of the patients (37). In IPF, however, the combination of glucocorticoids and immunosuppressive therapy is contraindicated (60).

Table 2. Potential noninfective pulmonary complications associated with drugs used to treat RA*

Complication	Drug
Fibrosis	Azathioprine, cyclophosphamide, gold, methotrexate, sulfasalazine
Obliterative bronchiolitis	Gold, sulfasalazine
Drug-induced lupus	Sulfasalazine, TNF inhibitors
Noncardiogenic pulmonary edema	Aspirin (high-dose), colchicine (overdose), cyclophosphamide, methotrexate, NSAIDs, rituximab, tocilizumab
Pneumonia	Anakinra, azathioprine, cyclophosphamide, gold, leflunomide, methotrexate, NSAIDs, rituximab, sulfasalazine, TNF inhibitors, tocilizumab

* RA = rheumatoid arthritis; TNF = tumor necrosis factor; NSAIDs = nonsteroidal antiinflammatory drugs.

Glucocorticoids are the mainstay of clinical management, and therapy is generally initiated with oral prednisone at a daily dose of 0.5 mg/kg, with gradual tapering over weeks to months based on the clinical response (47). An immunosuppressive agent such as mycophenolate mofetil (MMF) or azathioprine may be added to treatment in patients who fail to respond to or experience intolerable side effects of glucocorticoid treatment, although MTX is generally avoided in patients with RA-related ILD due to the risk of lung toxicity (see below). The safety and efficacy of MMF have been examined in a large cohort of patients with CTD-associated ILD (n = 125), including 18 patients with RA-related ILD (61), treated with MMF for a median of 897 days. Overall, the drug was well tolerated, with a discontinuation rate due to adverse events of less than 10%. In addition, MMF treatment was associated with improvement in the FVC and the DL_{CO} in the subgroup of patients without UIP and with stability of these same parameters in patients with UIP. Among patients with RA-related ILD, the FVC trended downward prior to MMF initiation and upward following MMF treatment. In a large observational study of rituximab-treated patients with RA (n = 700), including 56 patients with RA-related ILD, most patients remained stable or improved after treatment over a prolonged follow-up period (62). Notably, patients who deteriorated or died had the most severe ILD prior to rituximab initiation.

In severe and progressive forms of RA-related ILD, lung transplantation is a reasonable option, although extrapulmonary disease manifestations may complicate transplantation, while side effects of long-term treatment of RA (e.g., osteoporosis) may be a contraindication. However, in a retrospective review of patients with RA-related ILD (n = 10) who underwent lung transplantation, 1-year survival was comparable with that in lung transplant recipients with IPF (67% and 69%, respectively)

(63). Another study with a broader population of patients with non-SSc CTD-related lung disease, including RA, demonstrated similar findings (64).

Pulmonary toxicity of drugs used to treat RA. Several drugs used to treat RA may induce lung toxicity (Table 2). MTX, one of the most effective and commonly used agents for the treatment of articular manifestations of RA, is one such drug. A meta-analysis of randomized controlled trials demonstrated an increased risk of pulmonary complications in RA patients treated with MTX (65). Another study suggested that MTX may be a risk factor for progression of preclinical ILD (6). However, in a large prospective study of patients starting low-dose MTX treatment (n = 223, 154 of whom had RA) only ~1% developed pneumonitis, suggesting that this complication is not as common as previously thought (66). Similarly, a systematic literature search including 21 prospective studies of MTX monotherapy identified only 15 cases of pneumonitis among 3,463 patients receiving low-dose MTX (0.43%) for up to 36.5 months (67). Conversely, MTX treatment is associated with an increased risk of developing pulmonary toxicity in patients with preexisting ILD and should be avoided in this setting (68,69). Controversy also exists for tumor necrosis factor inhibitors (TNFi) and rituximab, with some studies showing improvement and others demonstrating worsening or development of ILD (70,71). However, recent reviews and meta-analyses suggest that serious respiratory adverse events in patients receiving TNFi have probably been overestimated (72). The risks and benefits of these drugs must be weighed carefully, but in patients with extensive or progressive pulmonary disease, the potential benefits often outweigh the risks of drug toxicity (30).

RA-related ILD and risk of infection. Patients with RA-related ILD are at increased risk of serious infections due to a combination of lung disease, immunosuppressive treatment, and abnormality of the immune system. This concern has been confirmed by a recent meta-analysis showing that the risk of infection increases with an increasing immunosuppressant burden (73). In addition, in a large cohort of patients with RA-related ILD, the risk of serious infections (i.e., those requiring antibiotic treatment or hospitalization) was higher in those receiving daily prednisone doses of >10 mg during the first year after ILD diagnosis and in patients with an organizing pneumonia pattern (compared with UIP and NSIP) (74). Fifty-four serious infections were identified (for an infection rate of 7.4 per 100 person-years), with pneumonia, septicemia, and opportunistic infections representing the most common types of infection. Notably, 15 of 72 deaths (21%) were directly attributable to infection.

Prognosis

ILD is second only to cardiac disease as a cause of mortality in patients with RA (3,4,30). In a large UK inception cohort of patients with RA, pulmonary fibrosis was the primary cause of death in 3.9% of cases (18 of 459) and contributed to or was a comorbid condition in another 17 deaths (17 of 459 [3.7%]) (75). In addition, ILD-associated PH may contribute to the high incidence of cardiovascular disease–related deaths in patients with RA. Indeed, although cases of isolated PH have also been described, particularly in older patients and those with a longer disease duration (76), PH generally occurs in the context of RA-related ILD.

Several predictors of mortality have been identified in RA-related ILD (5,17,34,77–79). Major limitations to these prior studies, however, have been the methodology and sample size. Age is the most consistent variable that has been identified as a significant predictor of a poor prognosis across multiple studies. Other variables associated with RA-related ILD mortality include male sex, disease severity as assessed by the DLco and FVC, the extent of fibrosis on HRCT, a UIP pattern, acute exacerbation, and RA disease activity (5,12,56,77–82). More

Table 3. Ongoing clinical trials of pharmacologic interventions in RA-related ILD*

Trial identifier	Trial characteristics				
	Intervention	Condition	Phase	Primary end point	Status
NCT02808871	Pirfenidone vs. placebo	RA-related ILD	II	Progression-free survival	Not yet recruiting
EudraCT no. 2014-000861-32	Pirfenidone vs. placebo	Progressive non-IPF lung fibrosis†	II	Change in FVC	Recruiting
NCT02999178	Nintedanib vs. placebo	Progressive fibrosing ILD†	III	Annual rate of decline in FVC	Recruiting
NCT03084419	Abatacept	RA-related ILD	II (open-label)	Change in FVC	Not yet recruiting

* RA = rheumatoid arthritis; ILD = interstitial lung disease; IPF = idiopathic pulmonary fibrosis; FVC = forced vital capacity.
† The study population may include patients with RA-related ILD.

recently, women with seropositive RA have been shown to have a nearly 3-fold increased risk of mortality due to respiratory disease (including chronic obstructive pulmonary disease, asthma, pleurisy, lung abscess, bronchiectasis, and pulmonary fibrosis) compared with women without RA (83).

The potential of IPF-specific antifibrotic drugs in RA-related ILD

RA-related ILD, particularly in patients with a UIP pattern, shares a number of phenotypic features with IPF, suggesting that RA-related ILD and IPF might also overlap biologically and therapeutically (27,31). However, although treatment of RA-related ILD generally consists of anti-inflammatory and/or immunosuppressive agents, in IPF, immunosuppression (e.g., combination therapy with azathioprine, prednisone, and *N*-acetylcysteine) is associated with increased all-cause mortality, hospitalization rate, and serious adverse events (84). Because a large proportion of patients with RA-related ILD have a histologic UIP pattern, it is expected, albeit not demonstrated, that they also may not benefit from immunosuppressive therapy.

Pirfenidone, a compound with antifibrotic, antiinflammatory, and antioxidant properties, and nintedanib, an intracellular inhibitor of multiple tyrosine kinases, including fibroblast growth factor receptor 1, VEGF receptor 2, and PDGF receptor α (PDGFRα) and PDGFRβ, have recently been approved for the treatment of IPF, based on their ability to reduce functional decline and disease progression (85,86). Given the mechanistic similarities between RA-related UIP and IPF, patients with RA-related UIP may potentially benefit from antifibrotic treatment, and a number of studies are currently evaluating the safety, tolerability, and efficacy of antifibrotic drugs in RA-related ILD (Table 3). Despite the plausible rationale of antifibrotic therapy in RA-related ILD, there are no published data for antifibrotic therapy in RA-related ILD. There is also some concern that TGFβ inhibitors, such as pirfenidone and, to a lesser extent, nintedanib, may increase joint inflammation, although joint pain was an uncommon adverse event in clinical trials of pirfenidone in patients with IPF (87).

Conclusions

ILD is a frequent complication of RA and is associated with increased morbidity and mortality. Despite extensive research in this field, there remain substantial gaps in knowledge, particularly with regard to 1) identification, clinical significance, and management of subclinical ILD in patients with RA; 2) assessment, staging, and monitoring of RA-related ILD; 3) identification of patients at higher risk of disease progression and mortality; 4) management of progressive disease; 5) potential utility of antifibrotic therapies in RA-related UIP; and 6) role of mechanisms involved in the pathogenesis of IPF (e.g., alterations in telomere biology and genetics) in RA-related ILD. A collaborative effort by expert centers has the potential to answer some of these questions.

AUTHOR CONTRIBUTIONS

All authors were involved in drafting the article or revising it critically for important intellectual content, and all authors approved the final version to be published.

REFERENCES

1. Turesson C, O'Fallon WM, Crowson CS, Gabriel SE, Matteson EL. Extra-articular disease manifestations in rheumatoid arthritis: incidence trends and risk factors over 46 years. Ann Rheum Dis 2003;62:722–7.
2. Cortet B, Perez T, Roux N, Flipo RM, Duquesnoy B, Delcambre B, et al. Pulmonary function tests and high resolution computed tomography of the lungs in patients with rheumatoid arthritis. Ann Rheum Dis 1997;56:596–600.
3. Bongartz T, Nannini C, Medina-Velasquez YF, Achenbach SJ, Crowson CS, Ryu JH, et al. Incidence and mortality of interstitial lung disease in rheumatoid arthritis: a population-based study. Arthritis Rheum 2010;62:1583–91.
4. Olson AL, Swigris JJ, Sprunger DB, Fischer A, Fernandez-Perez ER, Solomon J, et al. Rheumatoid arthritis-interstitial lung disease-associated mortality. Am J Respir Crit Care Med 2011;183:372–8.
5. Kim EJ, Elicker BM, Maldonado F, Webb WR, Ryu JH, Van Uden JH, et al. Usual interstitial pneumonia in rheumatoid arthritis-associated interstitial lung disease. Eur Respir J 2010;35:1322–8.
6. Gochuico BR, Avila NA, Chow CK, Novero LJ, Wu HP, MacDonald SD, et al. Progressive preclinical interstitial lung disease in rheumatoid arthritis. Arch Intern Med 2008;168:159–66.
7. Norton S, Koduri G, Nikiphorou E, Dixey J, Williams P, Young A. A study of baseline prevalence and cumulative incidence of comorbidity and extra-articular manifestations in RA and their impact on outcome. Rheumatology (Oxford) 2013;52:99–110.
8. Carmona L, Gonzalez-Alvaro I, Balsa A, Angel Belmonte M, Tena X, Sanmarti R. Rheumatoid arthritis in Spain: occurrence of extra-articular manifestations and estimates of disease severity. Ann Rheum Dis 2003;62:897–900.
9. Mori S, Cho I, Koga Y, Sugimoto M. Comparison of pulmonary abnormalities on high-resolution computed tomography in patients with early versus longstanding rheumatoid arthritis. J Rheumatol 2008;35:1513–21.
10. Gabbay E, Tarala R, Will R, Carroll G, Adler B, Cameron D, et al. Interstitial lung disease in recent onset rheumatoid arthritis. Am J Respir Crit Care Med 1997;156:528–35.
11. Myasoedova E, Crowson CS, Turesson C, Gabriel SE, Matteson EL. Incidence of extraarticular rheumatoid arthritis in Olmsted County, Minnesota, in 1995-2007 versus 1985-1994: a population-based study. J Rheumatol 2011;38:983–9.
12. Koduri G, Norton S, Young A, Cox N, Davies P, Devlin J, et al. Interstitial lung disease has a poor prognosis in rheumatoid arthritis: results from an inception cohort. Rheumatology (Oxford) 2010;49:1483–9.

13. Doyle TJ, Patel AS, Hatabu H, Nishino M, Wu G, Osorio JC, et al. Detection of rheumatoid arthritis-interstitial lung disease is enhanced by serum biomarkers. Am J Respir Crit Care Med 2015;191:1403–12.
14. Saag KG, Kolluri S, Koehnke RK, Georgou TA, Rachow JW, Hunninghake GW, et al. Rheumatoid arthritis lung disease: determinants of radiographic and physiologic abnormalities. Arthritis Rheum 1996;39:1711–9.
15. Doyle TJ, Dellaripa PF, Batra K, Frits ML, Iannaccone CK, Hatabu H, et al. Functional impact of a spectrum of interstitial lung abnormalities in rheumatoid arthritis. Chest 2014;146:41–50.
16. Mori S, Koga Y, Sugimoto M. Different risk factors between interstitial lung disease and airway disease in rheumatoid arthritis. Respir Med 2012;106:1591–9.
17. Kelly CA, Saravanan V, Nisar M, Arthanari S, Woodhead FA, Price-Forbes AN, et al. Rheumatoid arthritis-related interstitial lung disease: associations, prognostic factors and physiological and radiological characteristics: a large multicentre UK study. Rheumatology (Oxford) 2014;53:1676–82.
18. Saag KG, Cerhan JR, Kolluri S, Ohashi K, Hunninghake GW, Schwartz DA. Cigarette smoking and rheumatoid arthritis severity. Ann Rheum Dis 1997;56:463–9.
19. Spagnolo P, Grunewald J, du Bois RM. Genetic determinants of pulmonary fibrosis: evolving concepts. Lancet Respir Med 2014;2: 416–28.
20. Juge PA, Borie R, Kannengiesser C, Gazal S, Revy P, Wemeau-Stervinou L, et al. Shared genetic predisposition in rheumatoid arthritis-interstitial lung disease and familial pulmonary fibrosis. Eur Respir J 2017;49:1602314.
21. Williams RC, Jacobsson LT, Knowler WC, del Puente A, Kostyu D, McAuley JE, et al. Meta-analysis reveals association between most common class II haplotype in full-heritage Native Americans and rheumatoid arthritis. Hum Immunol 1995;42:90–4.
22. Laivoranta-Nyman S, Möttönen T, Hermann R, Tuokko J, Luukkainen R, Hakala M, et al. HLA-DR-DQ haplotypes and genotypes in Finnish patients with rheumatoid arthritis. Ann Rheum Dis 2004;63:1406–12.
23. Irigoyen P, Lee AT, Wener MH, Li W, Kern M, Batliwalla F, et al. Regulation of anti-cyclic citrullinated peptide antibodies in rheumatoid arthritis: contrasting effects of HLA–DR3 and the shared epitope alleles. Arthritis Rheum 2005;52:3813–8.
24. Scally SW, Petersen J, Law SC, Dudek NL, Nel HJ, Loh KL, et al. A molecular basis for the association of the HLA-DRB1 locus, citrullination, and rheumatoid arthritis. J Exp Med 2013; 210:2569–82.
25. Giles JT, Danoff SK, Sokolove J, Wagner CA, Winchester R, Pappas DA, et al. Association of fine specificity and repertoire expansion of anticitrullinated peptide antibodies with rheumatoid arthritis associated interstitial lung disease. Ann Rheum Dis 2014;73:1487–94.
26. Demoruelle MK, Deane KD, Holers VM. When and where does inflammation begin in rheumatoid arthritis? Curr Opin Rheumatol 2014;26:64–71.
27. Paulin F, Doyle TJ, Fletcher EA, Ascherman DP, Rosas IO. Rheumatoid arthritis-associated interstitial lung disease and idiopathic pulmonary fibrosis: shared mechanistic and phenotypic traits suggest overlapping disease mechanisms. Rev Invest Clin 2015;67:280–6.
28. Bongartz T, Cantaert T, Atkins SR, Harle P, Myers JL, Turesson C, et al. Citrullination in extra-articular manifestations of rheumatoid arthritis. Rheumatology (Oxford) 2007;46:70–5.
29. Klareskog L, Stolt P, Lundberg K, Källberg H, Bengtsson C, Grunewald J, et al. A new model for an etiology of rheumatoid arthritis: smoking may trigger HLA–DR (shared epitope)–restricted immune reactions to autoantigens modified by citrullination. Arthritis Rheum 2006;54:38–46.
30. Shaw M, Collins BF, Ho LA, Raghu G. Rheumatoid arthritis-associated lung disease. Eur Respir Rev 2015;24:1–16.
31. Rajasekaran BA, Shovlin D, Lord P, Kelly CA. Interstitial lung disease in patients with rheumatoid arthritis: a comparison with cryptogenic fibrosing alveolitis over 5 years. Rheumatology (Oxford) 2001;40:1022–5.
32. Zamora-Legoff JA, Krause ML, Crowson CS, Ryu JH, Matteson EL. Patterns of interstitial lung disease and mortality in rheumatoid arthritis. Rheumatology (Oxford) 2017;56:344–50.
33. Lee HK, Kim DS, Yoo B, Seo JB, Rho JY, Colby TV, et al. Histopathologic pattern and clinical features of rheumatoid arthritis-associated interstitial lung disease. Chest 2005;127:2019–27.
34. Kim EJ, Collard HR, King TE Jr. Rheumatoid arthritis-associated interstitial lung disease: the relevance of histopathologic and radiographic pattern. Chest 2009;136:1397–405.
35. Nurmi HM, Purokivi MK, Karkkainen MS, Kettunen HP, Selander TA, Kaarteenaho RL. Variable course of disease of rheumatoid arthritis-associated usual interstitial pneumonia compared with other subtypes. BMC Pulm Med 2016;16:107.
36. Tsuchiya Y, Takayanagi N, Sugiura H, Miyahara Y, Tokunaga D, Kawabata Y, et al. Lung diseases directly associated with rheumatoid arthritis and their relationship to outcome. Eur Respir J 2011;37:1411–7.
37. Song JW, Lee HK, Lee CK, Chae EJ, Jang SJ, Colby TV, et al. Clinical course and outcome of rheumatoid arthritis-related usual interstitial pneumonia. Sarcoidosis Vasc Diffuse Lung Dis 2013;30: 103–12.
38. Collard HR, Ryerson CJ, Corte TJ, Jenkins G, Kondoh Y, Lederer DJ, et al. Acute exacerbation of idiopathic pulmonary fibrosis: an international working group report. Am J Respir Crit Care Med 2016;194:265–75.
39. Spagnolo P, Wuyts W. Acute exacerbations of interstitial lung disease: lessons from idiopathic pulmonary fibrosis. Curr Opin Pulm Med 2017;23:411–7.
40. Hozumi H, Nakamura Y, Johkoh T, Sumikawa H, Colby TV, Kono M, et al. Acute exacerbation in rheumatoid arthritis-associated interstitial lung disease: a retrospective case control study. BMJ Open 2013;3:e003132.
41. Assayag D, Elicker BM, Urbania TH, Colby TV, Kang BH, Ryu JH, et al. Rheumatoid arthritis-associated interstitial lung disease: radiologic identification of usual interstitial pneumonia pattern. Radiology 2014;270:583–8.
42. Yunt ZX, Chung JH, Hobbs S, Fernandez-Perez ER, Olson AL, Huie TJ, et al. High resolution computed tomography pattern of usual interstitial pneumonia in rheumatoid arthritis-associated interstitial lung disease: relationship to survival. Respir Med 2017;126:100–4.
43. Kono M, Nakamura Y, Yoshimura K, Enomoto Y, Oyama Y, Hozumi H, et al. Nonspecific interstitial pneumonia preceding diagnosis of collagen vascular disease. Respir Med 2016;117:40–7.
44. Remy-Jardin M, Remy J, Cortet B, Mauri F, Delcambre B. Lung changes in rheumatoid arthritis: CT findings. Radiology 1994; 193:375–82.
45. Tanaka N, Kim JS, Newell JD, Brown KK, Cool CD, Meehan R, et al. Rheumatoid arthritis-related lung diseases: CT findings. Radiology 2004;232:81–91.
46. Dawson JK, Fewins HE, Desmond J, Lynch MP, Graham DR. Fibrosing alveolitis in patients with rheumatoid arthritis as assessed by high resolution computed tomography, chest radiography, and pulmonary function tests. Thorax 2001;56:622–7.
47. Bradley B, Branley HM, Egan JJ, Greaves MS, Hansell DM, Harrison NK, et al. Interstitial lung disease guideline: the British Thoracic Society in collaboration with the Thoracic Society of Australia and New Zealand and the Irish Thoracic Society. Thorax 2008;63:58.
48. Garcia JG, Parhami N, Killam D, Garcia PL, Keogh BA. Bronchoalveolar lavage fluid evaluation in rheumatoid arthritis. Am Rev Respir Dis 1986;133:450–4.
49. Yousem SA, Colby TV, Carrington CB. Lung biopsy in rheumatoid arthritis. Am Rev Respir Dis 1985;131:770–7.
50. Olson AL, Brown KK, Fischer A. Connective tissue disease-associated lung disease. Immunol Allergy Clin North Am 2012;32:513–36.

51. Corcoran JP, Ahmad M, Mukherjee R, Redmond KC. Pleuro-pulmonary complications of rheumatoid arthritis. Respir Care 2014; 59:e55–9.
52. Biederer J, Schnabel A, Muhle C, Gross WL, Heller M, Reuter M. Correlation between HRCT findings, pulmonary function tests and bronchoalveolar lavage cytology in interstitial lung disease associated with rheumatoid arthritis. Eur Radiol 2004;14:272–80.
53. Balbir-Gurman A, Yigla M, Nahir AM, Braun-Moscovici Y. Rheumatoid pleural effusion. Semin Arthritis Rheum 2006;35:368–78.
54. Colby TV. Pulmonary pathology in patients with systemic autoimmune diseases. Clin Chest Med 1998;19:587–612.
55. Tansey D, Wells AU, Colby TV, Ip S, Nikolakoupolou A, du Bois RM, et al. Variations in histological patterns of interstitial pneumonia between connective tissue disorders and their relationship to prognosis. Histopathology 2004;44:585–96.
56. Solomon JJ, Ryu JH, Tazelaar HD, Myers JL, Tuder R, Cool CD, et al. Fibrosing interstitial pneumonia predicts survival in patients with rheumatoid arthritis-associated interstitial lung disease (RA-ILD). Respir Med 2013;107:1247–52.
57. Nakamura Y, Suda T, Kaida Y, Kono M, Hozumi H, Hashimoto D, et al. Rheumatoid lung disease: prognostic analysis of 54 biopsy-proven cases. Respir Med 2012;106:1164–9.
58. Lamblin C, Bergoin C, Saelens T, Wallaert B. Interstitial lung diseases in collagen vascular diseases. Eur Respir J 2001;18:69s–80s.
59. Turesson C, Matteson EL, Colby TV, Vuk-Pavlovic Z, Vassallo R, Weyand CM, et al. Increased CD4+ T cell infiltrates in rheumatoid arthritis–associated interstitial pneumonitis compared with idiopathic interstitial pneumonitis. Arthritis Rheum 2005;52:73–9.
60. Raghu G, Collard HR, Egan JJ, Martinez FJ, Behr J, Brown KK, et al. An official ATS/ERS/JRS/ALAT statement: idiopathic pulmonary fibrosis: evidence-based guidelines for diagnosis and management. Am J Respir Crit Care Med 2011;183:788–824.
61. Fischer A, Brown KK, Du Bois RM, Frankel SK, Cosgrove GP, Fernandez-Perez ER, et al. Mycophenolate mofetil improves lung function in connective tissue disease-associated interstitial lung disease. J Rheumatol 2013;40:640–6.
62. Md Yusof MY, Kabia A, Darby M, Lettieri G, Beirne P, Vital EM, et al. Effect of rituximab on the progression of rheumatoid arthritis-related interstitial lung disease: 10 years' experience at a single centre. Rheumatology (Oxford) 2017;56:1348–57.
63. Yazdani A, Singer LG, Strand V, Gelber AC, Williams L, Mittoo S. Survival and quality of life in rheumatoid arthritis-associated interstitial lung disease after lung transplantation. J Heart Lung Transplant 2014;33:514–20.
64. Courtwright AM, El-Chemaly S, Dellaripa PF, Goldberg HJ. Survival and outcomes after lung transplantation for non-scleroderma connective tissue-related interstitial lung disease. J Heart Lung Transplant 2017;36:763–9.
65. Conway R, Low C, Coughlan RJ, O'Donnell MJ, Carey JJ. Methotrexate and lung disease in rheumatoid arthritis: a meta-analysis of randomized controlled trials. Arthritis Rheumatol 2014;66:803–12.
66. Sathi N, Chikura B, Kaushik VV, Wiswell R, Dawson JK. How common is methotrexate pneumonitis? A large prospective study investigates. Clin Rheumatol 2012;31:79–83.
67. Salliot C, van der Heijde D. Long-term safety of methotrexate monotherapy in patients with rheumatoid arthritis: a systematic literature research. Ann Rheum Dis 2009;68:1100–4.
68. Roubille C, Haraoui B. Interstitial lung diseases induced or exacerbated by DMARDS and biologic agents in rheumatoid arthritis: a systematic literature review. Semin Arthritis Rheum 2014;43: 613–26.
69. Alarcón GS, Kremer JM, Macaluso M, Weinblatt ME, Cannon GW, Palmer WR, et al. Risk factors for methotrexate-induced lung injury in patients with rheumatoid arthritis: a multicenter, case-control study. Ann Intern Med 1997;127:356–64.
70. Keir GJ, Maher TM, Ming D, Abdullah R, de Lauretis A, Wickremasinghe M, et al. Rituximab in severe, treatment-refractory interstitial lung disease. Respirology 2014;19:353–9.
71. Perez-Alvarez R, Perez-de-Lis M, Diaz-Lagares C, Pego-Reigosa JM, Retamozo S, Bove A, et al. Interstitial lung disease induced or exacerbated by TNF-targeted therapies: analysis of 122 cases. Semin Arthritis Rheum 2011;41:256–64.
72. Jani M, Hirani N, Matteson EL, Dixon WG. The safety of biologic therapies in RA-associated interstitial lung disease. Nat Rev Rheumatol 2014;10:284–94.
73. Singh JA, Cameron C, Noorbaloochi S, Cullis T, Tucker M, Christensen R, et al. Risk of serious infection in biological treatment of patients with rheumatoid arthritis: a systematic review and meta-analysis. Lancet 2015;386:258–65.
74. Zamora-Legoff JA, Krause ML, Crowson CS, Ryu HJ, Matteson EL. Risk of serious infection in patients with rheumatoid arthritis-associated interstitial lung disease. Clin Rheumatol 2016;35: 2585–9.
75. Young A, Koduri G, Batley M, Kulinskaya E, Gough A, Norton S, et al. Mortality in rheumatoid arthritis. Increased in the early course of disease, in ischaemic heart disease and in pulmonary fibrosis. Rheumatology (Oxford) 2007;46:350–7.
76. Dawson JK, Goodson NG, Graham DR, Lynch MP. Raised pulmonary artery pressures measured with Doppler echocardiography in rheumatoid arthritis patients. Rheumatology (Oxford) 2000;39:1320–5.
77. Wolfe F, Michaud K, Gefeller O, Choi HK. Predicting mortality in patients with rheumatoid arthritis. Arthritis Rheum 2003;48: 1530–42.
78. Solomon JJ, Chung JH, Cosgrove GP, Demoruelle MK, Fernandez-Perez ER, Fischer A, et al. Predictors of mortality in rheumatoid arthritis-associated interstitial lung disease. Eur Respir J 2016;47: 588–96.
79. Assayag D, Lubin M, Lee JS, King TE, Collard HR, Ryerson CJ. Predictors of mortality in rheumatoid arthritis-related interstitial lung disease. Respirology 2014;19:493–500.
80. Zamora-Legoff JA, Krause ML, Crowson CS, Ryu JH, Matteson EL. Progressive decline of lung function in rheumatoid arthritis–associated interstitial lung disease. Arthritis Rheumatol 2017;69:542–9.
81. Walsh SL, Sverzellati N, Devaraj A, Keir GJ, Wells AU, Hansell DM. Connective tissue disease related fibrotic lung disease: high resolution computed tomographic and pulmonary function indices as prognostic determinants. Thorax 2014;69:216–22.
82. Listing J, Kekow J, Manger B, Burmester GR, Pattloch D, Zink A, et al. Mortality in rheumatoid arthritis: the impact of disease activity, treatment with glucocorticoids, TNFα inhibitors and rituximab. Ann Rheum Dis 2015;74:415–21.
83. Sparks JA, Chang SC, Liao KP, Lu B, Fine AR, Solomon DH, et al. Rheumatoid arthritis and mortality among women during 36 years of prospective follow-up: results from the Nurses' Health Study. Arthritis Care Res (Hoboken) 2016;68:753–62.
84. Raghu G, Anstrom KJ, King TE Jr, Lasky JA, Martinez FJ. Idiopathic Pulmonary Fibrosis Clinical Research Network. Prednisone, azathioprine, and N-acetylcysteine for pulmonary fibrosis. N Engl J Med 2012;366:1968–77.
85. King TE Jr, Bradford WZ, Castro-Bernardini S, Fagan EA, Glaspole I, Glassberg MK, et al. A phase 3 trial of pirfenidone in patients with idiopathic pulmonary fibrosis. N Engl J Med 2014; 370:2083–92.
86. Richeldi L, du Bois RM, Raghu G, Azuma A, Brown KK, Costabel U, et al. Efficacy and safety of nintedanib in idiopathic pulmonary fibrosis [published erratum appears in N Engl J Med 2015;373:782]. N Engl J Med 2014;370:2071–82.
87. Lancaster L, Albera C, Bradford WZ, Costabel U, du Bois RM, Fagan EA, et al. Safety of pirfenidone in patients with idiopathic pulmonary fibrosis: integrated analysis of cumulative data from 5 clinical trials. BMJ Open Respir Res 2016;3:e000105.

ARTHRITIS & RHEUMATOLOGY
Vol. 70, No. 10, October 2018, pp 1555–1556
DOI 10.1002/art.40669

IN MEMORIAM

Herbert Kaplan, MD, 1929–2018

Herbert Kaplan died peacefully with his family by his side in his home at Loomis Village, South Hadley, MA on June 23, 2018 at the age of 88. He was the son of a high school math teacher and a mother who remained at home to care for 3 children. He graduated with honors from the University of Oklahoma and received his MD degree from Albany Medical College and his postgraduate training at Duke University Hospital and Yale–New Haven Hospital. He was a member of Phi Beta Kappa and Alpha Omega Alpha. After his training he served as Assistant Chief of Medical Services at the US Army Hospital in Munich, Germany. Following this he moved to Denver, where he began his 4-decade private practice of rheumatology.

Herb's professional career was marked by an indelible footprint of excellence at every milestone. He was a founding member (with Walter Briney, MD) of the Denver Arthritis Clinic, which became the prototype for the development of many similar groups (private practice and traditional academic settings) that were focused on personal and comprehensive care. He was the quintessential compassionate and caring physician clinician/rheumatologist who was an attentive and careful listener. He intuitively knew the importance of eye contact and the significance of a reassuring "healing touch."

Herb's personal mentoring philosophy included the importance of traditional medical diagnostic and therapeutic core values and stressed the language of humanity and kindness. His keen intellect, endless energy, and devotion to understanding emerging scientific advances served to enhance his diagnostic and therapeutic skills and fortify patient confidence and trust. These attributes played important roles, in his view, along with his humor and attention to detail, in improving patients' lives. His numerous students have included a number of individuals who have made important contributions to rheumatology and other fields, including Jim O'Dell, President of the ACR in 2011–2012.

Commitments to teaching, authoring scientific communications, and community service focused on rheumatology were all part of Herb's overall devotion to rheumatology and medicine. He had a long affiliation with the Colorado Medical Center, where he was a Clinical Professor of Medicine. He was the recipient of the Outstanding Clinical Faculty Award and the Outstanding Service Award, and was the first Distinguished Clinical Professor of Medicine at the University of Colorado Department of Medicine. He was a member of the Department of Medicine at Rose Medical Center in Denver. In 1992, he was named Colorado Internist of the Year. In addition, he was active in the Arthritis Foundation (AF), Rocky Mountain Chapter and was Chair of its Board of Directors in 1988–1990. He was the recipient of the ACR Paulding Phelps Award (1996). He was an author or co-author of more than 50 scientific publications.

Herb championed rheumatology in multiple national and international venues. His involvement with the AF/ACR spanned nearly 40 years and he held multiple leadership positions, which culminated in his election as President of the ACR in 1993–1994. His leadership, vision, energy, attention to detail, and wit were legendary and much admired by his colleagues. The breathtaking successes that have characterized the ACR are largely due to the vision of Mark Andrejeski and the ACR staff, as well as the tireless efforts and expertise of many dedicated volunteers, including Herb. His special interests included, but were not limited to, "defining what rheumatologists do," increased funding for rheumatology research and education (in both the private practice and academic settings), future rheumatology workforce needs, increasing ACR leadership, gender equality (as partially evidenced in the title and content of his 1994 ACR Presidential Address: "My Granddaughter, The Rheumatologist"), mainstream marketing initiatives, fortifying interactions with the AF, expanding collaboration with other medical and legislative organizations, and stressing the importance of "hanging together" as an organization. His initiatives were innovative, his leadership inspirational, and, as a result of

his many ACR contributions, he became a Master of the ACR in 1995 and was the recipient of the ACR Presidential Gold Medal in 2012.

His advocacy for medicine throughout his career exemplified the core values of the ACR mission statement "Advancing Rheumatology," namely, professionalism, service to members, vitality of the profession, excellence in patient care, transparency, and innovation. During a recent interview with Dr. Aileen Pangan (*The Rheumatologist*, April 2018), the essence of his ongoing commitment to and respect for his specialty was reinforced when he once again stated that "Rheumatology should get more widespread recognition. It is a travesty to not be at the same level of importance as cardiology or pulmonology." His advice to young rheumatologists: 1) Take time off for vacation. 2) Treat your employees well. 3) Be a mentor; you learn by teaching. 4) Get involved with the ACR.

In private life Herb was a devoted family man, an experienced traveler, an enthusiastic photographer, and an avid sailor, mountain biker, and cross country skier. He is survived by his wife of 67 years Beatrice (Bea) Swire Kaplan, 3 daughters Laura Kaplan Bensen, Janet Kaplan-Bucciarelli, and Susan Kaplan Jacobs, their spouses, 8 grandchildren, 1 step-grandson, and 4 great-grandchildren.

Joseph D. Croft, Jr., MD
Georgetown University Medical Center
Washington, DC

ARTHRITIS & RHEUMATOLOGY
Vol. 70, No. 10, October 2018, pp 1557–1564
DOI 10.1002/art.40546

An Economic Evaluation of Stopping Versus Continuing Tumor Necrosis Factor Inhibitor Treatment in Rheumatoid Arthritis Patients With Disease Remission or Low Disease Activity

Results From a Pragmatic Open-Label Trial

An Tran-Duy,[1] Marjan Ghiti Moghadam,[1] Martijn A. H. Oude Voshaar,[1] Harald E. Vonkeman,[1] Annelies Boonen,[2] Philip Clarke,[3] Geoff McColl,[3] Peter M. ten Klooster,[1] T. R. Zijlstra,[4] Willem F. Lems,[5] N. Riyazi,[6] E. N. Griep,[7] J. M. W. Hazes,[8] Robert Landewé,[9] Hein J. Bernelot Moens,[10] Piet L. C. M. van Riel,[11] Mart A. F. J. van de Laar,[1] and T. L. Jansen,[12] for the Dutch National POET Collaboration

Objective. **To evaluate, from a societal perspective, the incremental cost-effectiveness of withdrawing tumor necrosis factor inhibitor (TNFi) treatment compared to continuation of these drugs within a 1-year, randomized trial among rheumatoid arthritis patients with longstanding, stable disease activity or remission.**

Methods. **Data were collected from a pragmatic, open-label trial. Cost-utility analysis was performed using the nonparametric bootstrapping method, and a cost-effectiveness acceptability curve was constructed using the net-monetary benefit framework, where a willingness-to-accept threshold (WTA) was defined as the minimal cost saved that a patient accepted for each quality-adjusted life year (QALY) lost.**

Results. **A total of 531 patients were randomized to the stop group and 286 patients to the continuation group. Withdrawal of TNFi treatment resulted in a >60% reduction of the total drug cost, but led to an increase of ~30% in other health care expenditures. Compared to continuation, stopping TNFi resulted in a mean yearly cost saving of €7,133 (95% confidence interval [95% CI] €6,071, €8,234]) and was associated with a mean loss of QALYs of 0.02 (95% CI 0.002, 0.040). Mean saved cost per QALY lost and per extra flare incurred in the stop group compared to the continuation group was €368,269 (95% CI €155,132, €1,675,909) and €17,670 (95% CI €13,650, €22,721), respectively. At a WTA of €98,438 per QALY lost, the probability that stopping TNFi treatment is cost-effective was 100%.**

Conclusion. **Although an official WTA is not defined, the mean saved cost of €368,269 per QALY**

The Netherlands Trial Register identifier: NTR3112.

Supported by The Netherlands Organization for Health Research and Development and the Government of The Netherlands, Ministry of Health, Welfare and Sport (grant 40-00506-98-12001).

[1]An Tran-Duy, PhD (current address: University of Melbourne, Melbourne, Victoria, Australia), Marjan Ghiti Moghadam, MD, Martijn A. H. Oude Voshaar, PhD, Harald E. Vonkeman, MD, PhD, Peter M. ten Klooster, PhD, Mart A. F. J. van de Laar, MD, PhD: Arthritis Center Twente, Medisch Spectrum Twente, and University of Twente, Enschede, The Netherlands; [2]Annelies Boonen, MD, PhD: Maastricht University Medical Center and Maastricht University, Maastricht, The Netherlands; [3]Philip Clarke, PhD, Geoff McColl, MD, PhD: University of Melbourne, Melbourne, Victoria, Australia; [4]T. R. Zijlstra, MD, PhD: Isala Medical Center, Zwolle, The Netherlands; [5]Willem F. Lems, MD, PhD: VU University Medical Center and Reade Medical Center, Amsterdam, The Netherlands; [6]N. Riyazi, MD, PhD: Haga Medical Center, The Hague, The Netherlands; [7]E. N. Griep, MD, PhD: Antonius Medical Center, Sneek, The Netherlands; [8]J. M. W. Hazes, MD, PhD: Erasmus University Medical Center, Rotterdam, The Netherlands; [9]Robert Landewé, MD, PhD: AMC Amsterdam, Amsterdam, The Netherlands; [10]Hein J. Bernelot Moens, MD, PhD: Ziekenhuisgroep Twente, Almelo and Hengelo, The Netherlands; [11]Piet L. C. M. van Riel, MD, PhD: Radboud University Medical Center, Nijmegen, The Netherlands; [12]T. L. Jansen, MD, PhD: Viecurie Medical Center, Venlo, The Netherlands.

Address correspondence to Marjan Ghiti Moghadam, MD, Medical Spectrum Twente, Department of Rheumatology, Koningsplein 1, 7512KZ Enschede, The Netherlands. E-mail: m.ghiti@hotmail.com.

Submitted for publication August 30, 2017; accepted in revised form April 24, 2018.

lost seems acceptable in The Netherlands, given existing data on willingness to pay.

Rheumatoid arthritis (RA) is a progressive, immune-mediated inflammatory disease that has a prevalence of ~1% in developed countries (1). The disease is characterized by synovial inflammation and with time may involve articular damage, disability, and extra-articular manifestations. Besides its negative impact on the health of individual patients, RA imposes a significant and increasing economic burden on health care systems and societies in the form of health care resource utilization and (paid) productivity loss (2).

The main goal in the treatment of RA is to suppress inflammatory activity to control pain and prevent unfavorable outcomes such as structural damage and functional disability. Accumulating evidence suggests that optimal clinical outcomes may be achieved if treatment is started early and adjusted to reach predefined disease activity targets (3,4). The subpopulation of patients receiving biologic disease-modifying antirheumatic drugs (bDMARDs), including tumor necrosis factor inhibitors (TNFi), in this treat-to-target strategy has increased over time and accounted for up to 20% of the population of RA patients in various Western health care systems (5,6). Although it is widely believed that the introduction of bDMARDs has contributed to the overall improved clinical picture of severe RA, particularly in patients with methotrexate-refractory disease (7), their high cost has raised the question of whether bDMARDs could be discontinued in patients who achieve long-term, stable controlled disease, without negatively affecting their health (8).

As health care budgets are limited and money can be spent only once, savings from stopping treatment with bDMARDs could be used to reinvest in other treatments or increase access to bDMARDs for a larger proportion of the RA patient population. The recently completed Potential Optimalisation of Expediency and Effectiveness of TNFi (POET) trial aimed to evaluate the clinical course of patients in whom TNFi treatment was withdrawn, compared to that of patients who continued to receive TNFi (9). The results showed that patients who in whom TNFi treatment was withdrawn were >3 times as likely to experience a disease flare compared to patients who continued their TNFi treatment. However, disease control could typically be quickly regained upon TNFi restart. Although the withdrawal of TNFi is evidently associated with lower medication costs, this may be offset by higher non–drug-related health care costs or by lasting impact on patients' overall quality of life. From the health economic point of view, it is currently unclear whether the benefits of discontinuation of TNFi outweigh the harms. The present study aimed to evaluate, from a societal perspective, the 1-year trial–based cost utility and cost-effectiveness of withdrawing TNFi compared to continuation of these drugs in RA patients with longstanding stable disease, to inform rheumatologists and patients about balance between savings and health forgone.

PATIENTS AND METHODS

Study design and patients. The study outcomes and design of the POET study (NTR3112) are described in detail elsewhere (9). Briefly, this pragmatic, open-label trial was performed at 47 rheumatology centers in The Netherlands and included 817 adult patients fulfilling the American College of Rheumatology 1987 classification criteria for RA (10) who were treated with TNFi for at least 1 year. In addition, patients met 1 of the following criteria: 1) Disease Activity Score in 28 joints (DAS28) <3.2 for at least 6 months preceding inclusion (n = 672) or 2) perceived by a rheumatologist as having remission or low disease activity for at least 6 months prior to inclusion, with DAS28 <3.2 at baseline and C-reactive protein level <10 mg/liter at least once in the 6-month period prior to inclusion (n = 145). Patients were randomized to either the stop group (n = 531) or the continuation group (n = 286). After inclusion, TNFi were withdrawn in the stop group but maintained in the continuation group. Any other treatment decisions were made by rheumatologists with their patient and continued unchanged as much as possible in both groups. The primary outcome measure of the study was occurrence of disease flares, defined as a DAS28 increase of ≥0.6 compared to baseline and a current DAS28 level of ≥3.2.

Follow-up procedures. Patients were assessed at baseline and at least once every 3 months thereafter, for a period of 1 year. At each visit, components of the DAS28, the Health Assessment Questionnaire (HAQ) disability index (DI) (11,12), and the EuroQol 5-domain 3-level (EQ-5D-3L) questionnaire (13) were evaluated, laboratory tests conducted, and patient-reported outcomes recorded. Patient-reported outcomes included adverse events, days of sick leave, and frequencies of health care resource utilization. Restart of a TNFi was allowed when a flare occurred; for ethical reasons this included cases where the patient's perception of a flare could not be objectively verified.

Health economic outcomes. At each visit, patients answered the EQ-5D-3L questionnaire and reported the frequencies of health care resource utilization and number of days of sick leave (in those with a paid job) during the past 3 months. The health care resource utilization included visits to rheumatologists and general practitioners, visits to nurse specialists, physiotherapists, and psychologists, numbers of diagnostic and laboratory tests, days in hospital, and hours of formal and informal care.

For each patient, the health utility at 3-month visits was computed using the Dutch tariffs for EQ-5D-3L (14), and quality-adjusted life years (QALYs) were computed as the area under the EQ-5D-3L curve. Nondrug direct costs were calculated based on patient-reported frequencies of

health care resource utilization. The unit costs were retrieved from the Dutch Guideline for Economic Evaluations in Healthcare. Drug costs were calculated based on the doses of drug used and the medication prices. Indirect costs for those patients with a paid job were calculated using the friction-cost method with a 3-month friction period and were based on the number of hours absent from work and the average wage per hour for each age group and sex (15). The unit costs and prices published before the current year (2016) were adjusted to the current year using the consumer price index for The Netherlands (16). Costs were not discounted because of the short time horizon of 12 months.

Statistical and cost-effectiveness analyses. Between 10% and 15% of observations contained missing values for costs or utilities (for details, see Supplementary Figure 1, available on the *Arthritis & Rheumatology* web site at http://onlinelibrary.wiley.com/doi/10.1002/art.40546/abstract). For the cost-effectiveness analysis, these were replaced with estimates using multiple imputation, as recommended by the International Society for Pharmacoeconomics and Outcomes Research for cost-effectiveness analysis alongside clinical trials (17). For each of the 10 imputed data sets, cost-effectiveness analysis was performed using the nonparametric bootstrapping method (18). Five thousand bootstrap samples were generated, from which the expected costs and QALYs over the 1-year follow-up in each treatment group and the ratios of incremental cost to incremental QALYs or flares (ICERs) were computed (19). Manca et al recommended an adjustment of QALYs before calculation of ICERs when there was an imbalance in the mean baseline health utility between 2 trial arms (20). Because mean baseline health utility and other patient characteristics in our study were almost equal between the stop and continuation groups, in the main analyses and presentation of the results we used QALYs and costs unadjusted for these negligible differences.

To examine the effect of QALYs and cost adjustment on ICERs, we used the regression-based method proposed by Manca et al (20), in which linear regression models for patient-specific QALYs and costs were fitted to the observed data, with predictors for QALYs being treatment and baseline health utility, and predictors for costs being treatment, age, sex, disease duration, DAS28 score, and HAQ DI score. Then we used the coefficients for the treatment as the differential QALYs and costs for the adjustment. We applied a Box-Cox transformation for QALYs and a log transformation for costs to meet the assumptions of normal distribution and equal variance of the error term in the linear models (21). The results were pooled across imputed data sets using Rubin's rules (22) to take into account the uncertainty introduced by the missing data. Because the distribution of costs was skewed, the "approximate bootstrap confidence" (ABC) algorithm (23) was used to estimate the confidence intervals (CIs), instead of the usual symmetric CI proposed by Rubin (22). For each imputed data set, a confidence density curve was constructed for each of the outcome variables. The 10 confidence density curves were then combined by averaging the y-values to obtain the average density function, on which the 95% CIs were established by determining the areas under the curve that corresponded to 5% and 95% percentiles. For each imputed data set, a cost-effectiveness acceptability curve was constructed using the net-monetary benefit (NMB) framework (24), where an expected NMB was calculated as the difference between the willingness-to-accept threshold (WTA) for each QALY lost multiplied by the mean QALYs ($\bar{E}_i$), and the mean cost obtained from each bootstrap replication ($\bar{C}_i$) : $NMB = WTA \times \bar{E}_i - \bar{C}_i$. The Consolidated Health Economic Evaluation Reporting Standards (CHEERS) were followed to report the present study (for the CHEERS checklist, see Supplementary Table 1, available on the *Arthritis & Rheumatology* web site at http://onlinelibrary.wiley.com/doi/10.1002/art.40546/abstract).

RESULTS

Baseline characteristics were similar in both groups (Table 1). The majority of the patients had long-standing, erosive disease and utility scores reasonably close to general population norms (25). The sample was further characterized by low disease activity at baseline according to the DAS28, as per the inclusion criteria, and low disability according to HAQ DI scores.

Health outcomes. Mean DAS28 and HAQ DI scores in the continuation group were almost stable over time (Figure 1), while in the stop group the mean DAS28 score increased from baseline to month 3 and then gradually decreased during the rest of the year, and the mean HAQ DI score slightly increased over time. Post hoc analyses revealed significant differences in DAS28 scores at all follow-up visits ($P < 0.01$), except baseline ($P = 0.27$). No significant difference in HAQ DI scores between the 2 groups at any time point was observed.

The percentages of patients with 1 or 2 flares within 12 months were 41.1% and 8.1% in the stop group and 15.4% and 1.4% in the continuation group, respectively. No patients and only 0.6% of patients had

Table 1. Baseline characteristics of the patients*

Characteristic	Stop group (n = 531)	Continuation group (n = 286)
Age, mean ± SD years	60.1 ± 11.8	59.7 ± 10.6
Female, no. (%)	362 (68)	188 (66)
Disease duration, mean ± SD years	12.0 ± 8.8	11.1 ± 8.4
RF positive, no. (%)	238 (67.5)	178 (67.4)
Anti-CCP positive, no. (%)	332 (68.3)	179 (67.8)
Erosive disease, no. (%)	305 (62.8)	152 (57.6)
DAS28, mean ± SD	1.98 ± 0.76	2.05 ± 0.73
HAQ score, mean ± SD	0.63 ± 0.59	0.62 ± 0.55
EQ-5D-3L score, mean ± SD	0.83 ± 0.16	0.84 ± 0.13
Patients taking TNFi, no (%)		
Adalimumab	271 (51.1)	129 (45.1)
Etanercept	213 (40.2)	133 (46.5)
Infliximab	25 (4.7)	14 (4.9)
Golimumab	15 (2.8)	8 (2.8)
Certolizumab	7 (1.2)	2 (0.7)

* RF = rheumatoid factor; anti-CCP = anti–cyclic citrullinated peptide antibody; DAS28 = Disease Activity Score in 28 joints; HAQ = Health Assessment Questionnaire; EQ-5D-3L = EuroQol 5-domain 3-level measure; TNFi = tumor necrosis factor inhibitors.

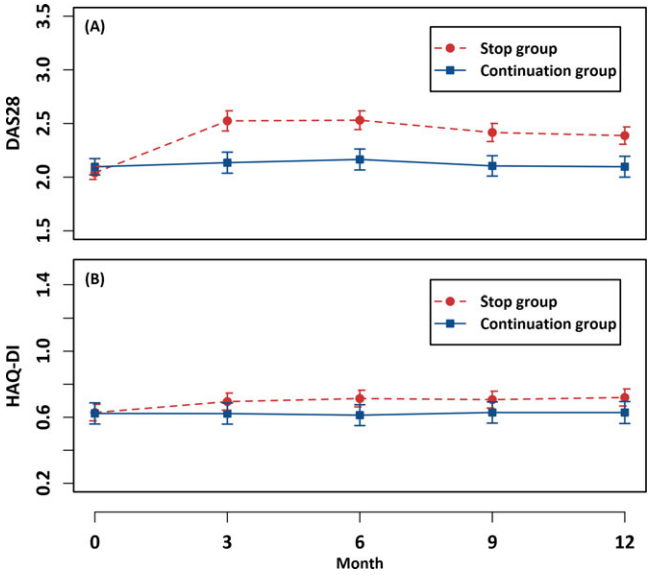

Figure 1. Mean Disease Activity Score in 28 joints (DAS28) and Health Assessment Questionnaire (HAQ) disability index (DI) at different points in time during the 1-year follow-up in the 2 treatment groups. Vertical bars represent 95% confidence intervals.

3 flares in the continuation and stop groups, respectively. On average, within 12 months each patient experienced 0.59 flares (95% CI 0.53, 0.64) in the stop group and 0.18 flares (95% CI 0.13, 0.24) in the continuation group.

Mean health utility in the continuation group slightly deteriorated during the first 6 months and then remained relatively stable during the rest of the year, while that in the stop group decreased within the first 3 months and then slightly increased until the end of the year (Figure 2). Except for month 3 ($P = 0.0005$), mean health utility was not significantly different at any time points between the 2 groups ($P > 0.05$).

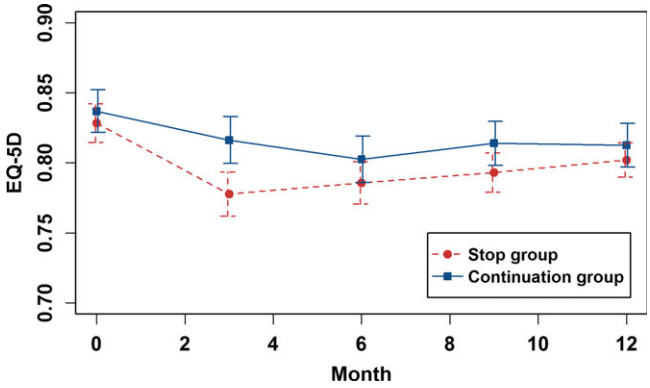

Figure 2. Mean EuroQol 5-domain (EQ-5D) 3-level measure scores at different points in time during the 1-year follow-up in the 2 treatment groups. Vertical bars represent 95% confidence intervals.

Health care, medication, and sick leave costs and QALYs. Table 2 shows means and 95% CIs of nondrug health care costs, drug costs, and sick leave costs (in euros) and of QALYs per patient per year with the 2 treatment strategies. A detailed overview of health care resource utilization in each category at baseline and cumulative over 1 year, as well as the corresponding unit prices, is provided in Supplementary Tables 2–6, available on the *Arthritis & Rheumatology* web site at http://onlinelibrary.wiley.com/doi/10.1002/art.40546/abstract. Withdrawal of TNFi resulted in a >60% reduction of the total drug cost, but led to an increase of ~30% for the other health care expenditures. Sick leave cost in the stop group was slightly lower than that in the continuation group, although the difference between the 2 groups was not significant. Since the cost of TNFi treatment was much larger than the increased expenditure in other cost components, the mean total cost incurred by each patient per year in the continuation group (€14,740 [95% CI €13,913, €15,676]) was almost double that in the stop group (€7,607 [95% CI €7,001, €8,261]). Mean QALY per patient in the stop and continuation groups was 0.79 (95% CI 0.781, 0.805) and 0.81 (95% CI 0.799, 0.829), respectively.

Incremental cost-effectiveness and uncertainty. An average patient in the stop group may save €7,133 (95% CI €6,071, €8,234) for society, but would lose 0.022 QALY (95% CI 0.002, 0.040) per year and experience 0.41 (95% CI 0.33, 0.48) more flares compared to an average patent in the continuation group. Mean saved cost per QALY lost and per extra flare incurred in the stop group compared to the continuation group was €368,269 (95% CI €155,132, €1,675,909) and €17,670 (95% CI €13,650, €22,721), respectively. When QALYs and costs were adjusted for differences in baseline health utility and patient characteristics, mean saved cost per QALY lost in the stop group compared to the continuation group (€371,457 [95% CI €156,291, €1,736,887]) was slightly higher than that when no adjustment was made. Because the difference in mean sick leave costs between the 2 groups was very small, mean costs saved from the health care perspective, per QALY lost (€366,642 [95% CI €152,396, €1,662,057]) and per flare increase (€17,587 [95% CI €13,575, €22,642]) were similar to those from the societal perspective. Hereafter, we focused on the outcomes and interpretation from the societal perspective.

A scatter plot of the incremental mean costs and QALYs resulting from 50,000 bootstrapped replications for 10 imputed data sets is provided in Figure 3. All differences in mean costs were negative. Approximately 1.5% of all data points fell in the southeast quadrant (i.e., saved cost with increased QALYs), indicating that the probability of TNFi withdrawal being

Table 2. Mean costs (€) and QALYs (95% confidence intervals) per patient per year in the 2 treatment groups*

	Stop group	Continuation group	Incremental
Nondrug health care cost	2,122 (1,684, 2,563)	1,663 (1,384, 1,958)	459 (70, 890)
Drug cost	4,894 (4,396, 5,402)	12,450 (11,427, 13,472)	−7,556 (−8,547, −6,629)
csDMARD	325 (220, 461)	324 (230, 471)	1 (−98, 121)
TNFi	4,568 (4,070, 5,067)	12,126 (11,106, 13,145)	−7,558 (−8,534, −6,643)
Sick leave cost	591 (450, 735)	626 (452, 804)	−35 (−226, 155)
Total cost	7,607 (7,001, 8,261)	14,740 (13,913, 15,676)	−7,133 (−8,234, −6,071)
QALYs	0.79 (0.781, 0.805)	0.81 (0.799, 0.829)	−0.022 (−0.040, −0.002)
ICER (€ per QALY)			368,269 (155,132, 1,675,909)

* QALYs = quality-adjusted life years; csDMARD = conventional synthetic disease-modifying antirheumatic drug; TNFi = tumor necrosis factor inhibitor; ICER = incremental cost-effectiveness ratio.

cost-effective at any level of WTA is negligible. At WTAs of €330,450 and €98,438, the probabilities of TNFi withdrawal being cost-effective were 0.5 and 1.0, respectively (Figure 4). If stopping TNFi is considered as the baseline comparator, it was almost certain that the continuation of TNFi was not cost-effective at a willingness-to-pay (WTP) of €100,000 per QALY gained.

DISCUSSION

Our analysis shows that stopping TNFi treatment in RA patients with stable controlled disease (remission or low disease activity) can save considerable cost, but results in a small QALY loss. At the beginning of this century, TNFi were developed, studied, and introduced to control inflammatory disease activity in patients with RA. Despite increasing budget impact over the first 15 years since the introduction of these drugs, evidence regarding the possibility of discontinuing TNFi in the maintenance phase is still sparse. Therefore, patients are frequently kept on TNFi treatment indefinitely. Up to now, TNFi have been recommended in most of the developed countries for management of RA and reimbursed for patients with persistently high disease activity despite adequate treatment with at least 2 conventional synthetic DMARDs (csDMARDs) (26–29). These recommendations were predominantly based on evidence of the favorable cost-effectiveness ratio of TNFi therapy compared to csDMARDs in patients with severe disease. For instance, a recent systematic literature review on economic aspects of treatment with TNFi to inform clinical recommendations by the European League Against Rheumatism showed that the incremental cost of the use of a TNFi after failure of 2 csDMARDs per QALY gain was <€60,000 (conversion applied) in 14 of 18 studies (30). Regardless of the majority of studies with outcomes in favor of the use of TNFi in this population, concerns continue to be raised about

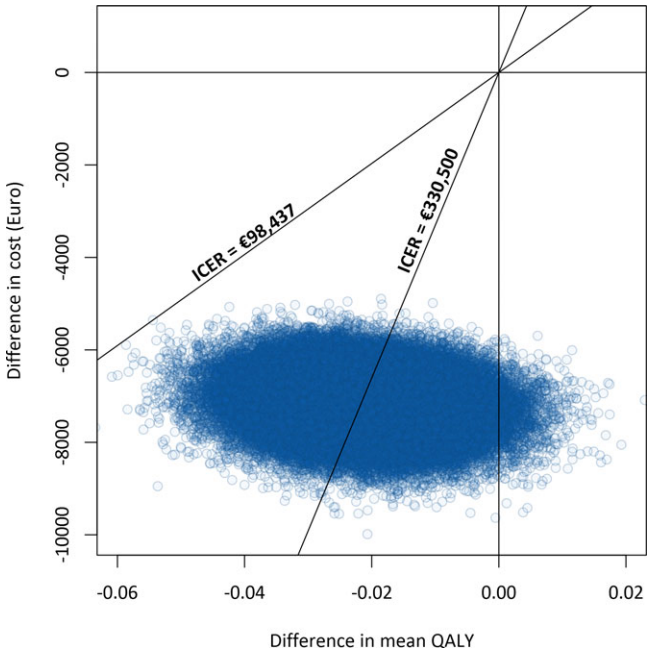

Figure 3. Scatter plot of incremental mean cost against incremental mean quality-adjusted life years (QALYs) with the stop strategy compared to the continuation strategy. Each data point was obtained from 1 bootstrap replication. ICER = incremental cost-effectiveness ratio. Color figure can be viewed in the online issue, which is available at http://onlinelibrary.wiley.com/doi/10.1002/art.40546/abstract.

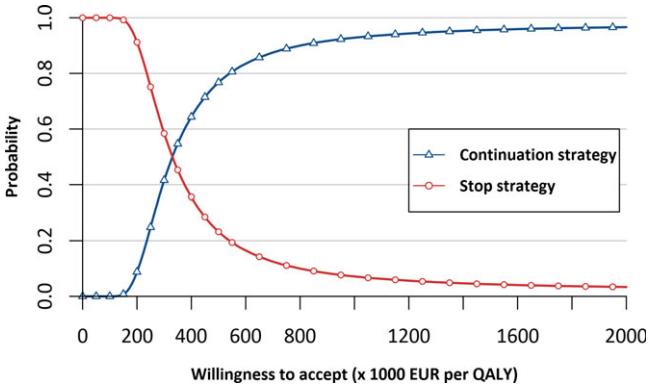

Figure 4. Cost-effectiveness acceptability curve for continuation and stop strategies. EUR = euros; QALY = quality-adjusted life year. Color figure can be viewed in the online issue, which is available at http://onlinelibrary.wiley.com/doi/10.1002/art.40546/abstract.

the substantial impact of TNFi therapy on the health care budgets, owing to the high prices of these drugs. For economic reasons, withdrawal of TNFi treatment has therefore been considered in patients with sustained low disease activity.

To date, approximately a dozen studies examining the effects of discontinuing TNFi treatment on clinical outcomes have been published (9,31–35). Due to the heterogeneity in study designs, characteristics of patients, definitions of low disease activity, and criteria for restarting TNFi therapy when failure was observed, the results between studies differed remarkably; the proportions of patients whose disease remained in remission or with low disease activity after discontinuation of TNFi ranged from 0% to 33% at 7 months, and from 13% to 80% at 12 months (32). Despite the fact that high treatment costs are a frequently cited motivation to conduct such studies, unfortunately no reports of previous discontinuation studies addressed preference-based health valuation such as the EQ-5D or health care costs, which are important to inform health policy decisions.

In the present study, we showed that the mean health utility did not significantly differ over time between patients in the stop and continuation groups, except for the first follow-up point after baseline. These results suggest that discontinuing TNFi treatment in patients with long-term stable disease is a strategy that over the course of 1 year is associated with considerable saved cost and negligible loss of quality of life. Very similar conclusions were reached in the Dose Reduction Strategy of Subcutaneous TNF inhibitors down-titration study, in which it was found that when using a TNFi down-titration approach guided by disease activity, an amount of €390,493 could be saved for each QALY lost, compared to continued tight control treatment. Together, these findings suggest significant potential for disinvestment decisions (i.e., to stop subsidizing therapies that are not cost-effective) (36). This could potentially free up resources that could be reallocated to other more cost-effective interventions. One way to do this would be to look for scope for implementing other more cost-effective interventions for the patients formerly receiving TNFi, as any improvement in their health status could offset the loss in QALYs due to discontinuation. Such an approach would avoid having to make trade-offs involving reducing the health of patients with RA.

While there is no explicit WTA threshold that could be used to judge whether or not TNFi should be discontinued, it is useful to consider the threshold for WTP, which is suggested to be between €20,000 and €73,000 per QALY in The Netherlands (37). The estimated saving per QALY lost of €368,269 is much higher than the maximal bound of this threshold range, suggesting that it would be cost-effective to discontinue TNFi in the maintenance phase while the patients are in a state of low disease activity or remission. Adjustment of QALYs and costs for differences in baseline health utility and patient characteristics resulted in a slightly higher saving than the above-mentioned value, which increases the likelihood that stopping TNFi is cost-effective.

Our study has strengths and weaknesses. It is based on the largest randomized controlled trial on discontinuing TNFi in RA patients with stable low disease activity, with high-quality data owing to a strictly electronic data collection protocol. Generalizability of the results to the overall population of patients withdrawing from TNFi is probably high, since our study was based on a pragmatic trial with relatively few inclusion and exclusion criteria being maintained during the recruitment. We used advanced methods, i.e., a combination of multiple imputation, bootstrap, and ABC algorithm to capture the uncertainty surrounding the study results. However, our findings on the cost-effectiveness of stopping TNFi are valid only for an intervention duration of 12 months. Studies on the WTA thresholds in patients with RA are important to support decision making. Since patients with different disease durations and numbers of failed TNFi may respond differently to the discontinuation of the current TNFi, more research on response to discontinuation is needed.

In conclusion, stopping TNFi treatment in RA patients with stable low disease activity, on average, was associated with a cost saving of €7,133, a loss of 0.022 QALYs, and an increase of 0.41 flares per patient per year. Although an official WTA threshold is not available, we found that the mean saved cost of €368,269 per QALY lost would be cost-effective in The Netherlands, given existing data on the WTP and the WTA:WTP ratio. If the WTA threshold is €100,000, the probability that stopping TNFi is cost-effective is approximately 1.

ACKNOWLEDGMENTS

The authors thank all patients, rheumatology nurses, and rheumatologists at the participating centers, as well as the members of the Steering Committee: Renée Allaart (University Medical Center Leiden), Annelies Boonen (Maastricht University Medical Center), Reinhard Bos (Medical Center Leeuwarden), Liesbeth Brouwer (University Medical Center Groningen), Alfons den Broeder (Sint Maartens Clinic), Danielle Gerlag (Amsterdam Medical Center), Mieke

Hazes (Erasmus University Medical Center), Willem Lems (VU Medical Center), Dirkjan van Schaardenburg (Reade), Janneke Tekstra (University Medical Center Utrecht), and Harald Vonkeman (Arthritis Center Twente MST & University of Twente), and Gerardine Willemsen (patients association), Huib Kooiman (Dutch Ministry of Health, Welfare and Sport), and Benien Vingerhoeds (Netherlands Organization for Health Research and Development).

AUTHOR CONTRIBUTIONS

All authors were involved in drafting the article or revising it critically for important intellectual content, and all authors approved the final version to be submitted for publication. Dr. Moghadam had full access to all of the data in the study and takes responsibility for the integrity of the data and the accuracy of the data analysis.

Study conception and design. Tran-Duy, Vonkeman, Boonen, Clarke, Landewé, van Riel, van de Laar, Jansen.

Acquisition of data. Moghadam, Voshaar, Vonkeman, ten Klooster, Zijlstra, Lems, Riyazi, Griep, Hazes, Landewé, Moens, van de Laar, Jansen.

Analysis and interpretation of data. Tran-Duy, Boonen, Clarke, McColl, ten Klooster.

REFERENCES

1. Gabriel SE, Michaud K. Epidemiological studies in incidence, prevalence, mortality, and comorbidity of the rheumatic diseases. Arthritis Res Ther 2009;11:229.
2. Boonen A, Severens JL. The burden of illness of rheumatoid arthritis. Clin Rheumatol 2011;30 Suppl 1:S3–8.
3. Smolen JS, Breedveld FC, Burmester GR, Bykerk V, Dougados M, Emery P, et al. Treating rheumatoid arthritis to target: 2014 update of the recommendations of an international task force. Ann Rheum Dis 2016;75:3–15.
4. Singh JA, Saag KG, Bridges SL Jr, Akl EA, Bannuru RR, Sullivan MC, et al. 2015 American College of Rheumatology guideline for the treatment of rheumatoid arthritis. Arthritis Rheumatol 2016; 68:1–26.
5. Yazici Y, Shi N, John A. Utilization of biologic agents in rheumatoid arthritis in the United States: analysis of prescribing patterns in 16,752 newly diagnosed patients and patients new to biologic therapy. Bull NYU Hosp Jt Dis 2008;66:77–85.
6. Huscher D, Mittendorf T, von Hinuber U, Kotter I, Hoese G, Pfafflin A, et al. Evolution of cost structures in rheumatoid arthritis over the past decade. Ann Rheum Dis 2015;74:738–45.
7. Bongartz T, Sutton AJ, Sweeting MJ, Buchan I, Matteson EL, Montori V. Anti-TNF antibody therapy in rheumatoid arthritis and the risk of serious infections and malignancies: systematic review and meta-analysis of rare harmful effects in randomized controlled trials. JAMA 2006;295:2275–85.
8. Scott DL. Biologics-based therapy for the treatment of rheumatoid arthritis. Clin Pharmacol Ther 2012;91:30–43.
9. Moghadam GM, Vonkeman HE, ten Klooster PM, Tekstra J, van Schaardenburg D, Starmans-Kool M, et al. Stopping tumor necrosis factor inhibitor treatment in patients with established rheumatoid arthritis in remission or with stable low disease activity: a pragmatic multicenter, open-label randomized controlled trial. Arthritis Rheumatol 2016;68:1810–7.
10. Arnett FC, Edworthy SM, Bloch DA, McShane DJ, Fries JF, Cooper NS, et al. The American Rheumatism Association 1987 revised criteria for the classification of rheumatoid arthritis. Arthritis Rheum 1988;31:315–24.
11. Ramey DR, Raynauld JP, Fries JF. The Health Assessment Questionnaire 1992: status and review. Arthritis Care Res 1992;5:119–29.
12. Bruce B, Fries JF. The health assessment questionnaire (HAQ). Clin Exp Rheumatol 2005;23:14.
13. The EuroQol Group. EuroQol: a new facility for the measurement of health-related quality of life. Health Policy 1990;16:199–208.
14. Lamers LM, McDonnell J, Stalmeier PF, Krabbe PF, Busschbach JJ. The Dutch tariff: results and arguments for an effective design for national EQ-5D valuation studies. Health Econ 2006;15:1121–32.
15. StatLine. Gemiddeld inkomen van personen naar kenmerken en naar regio. Centraal Bureau voor de Statistiek (CBS). 2017. URL: http://statline.cbs.nl.
16. StatLine. Consumentenprijzen. Centraal Bureau voor de Statistiek (CBS). 2017. URL: http://statline.cbs.nl.
17. Ramsey S, Willke R, Briggs A, Brown R, Buxton M, Chawla A, et al. Good research practices for cost-effectiveness analysis alongside clinical trials: the ISPOR RCT-CEA Task Force report. Value Health 2005;8:521–33.
18. Barber JA, Thompson SG. Analysis of cost data in randomized trials: an application of the non-parametric bootstrap. Stat Med 2000;19:3219–36.
19. Briggs AH, Wonderling DE, Mooney CZ. Pulling cost-effectiveness analysis up by its bootstraps: a non-parametric approach to confidence interval estimation. Health Econ 1997;6:327–40.
20. Manca A, Hawkins N, Sculpher MJ. Estimating mean QALYs in trial-based cost-effectiveness analysis: the importance of controlling for baseline utility. Health Econ 2005;14:487–96.
21. Box GE, Cox DR. An analysis of transformations. J R Stat Soc Series B (Methodological) 1964:211–52.
22. Rubin DB. Multiple imputation for nonresponse in surveys. New York: John Wiley & Sons; 2004.
23. Efron B. Missing data, imputation, and the bootstrap. J Am Stat Assoc 1994;89:463–75.
24. Hoch JS, Briggs AH, Willan AR. Something old, something new, something borrowed, something blue: a framework for the marriage of health econometrics and cost-effectiveness analysis. Health Econ 2002;11:415–30.
25. Szende A, Janssen B, Cabases J. Self-reported population health: an international perspective based on EQ-5D. Dordrecht: Springer; 2014.
26. Emery P, van Vollenhoven R, Ostergaard M, Choy E, Combe B, Graninger W, et al. Guidelines for initiation of anti-tumour necrosis factor therapy in rheumatoid arthritis: similarities and differences across Europe. Ann Rheum Dis 2009;68:456–9.
27. Singh JA, Furst DE, Bharat A, Curtis JR, Kavanaugh AF, Kremer JM, et al. 2012 update of the 2008 American College of Rheumatology recommendations for the use of disease-modifying antirheumatic drugs and biologic agents in the treatment of rheumatoid arthritis. Arthritis Care Res (Hoboken) 2012;64:625–39.
28. Smolen JS, Landewe R, Breedveld FC, Dougados M, Emery P, Gaujoux-Viala C, et al. EULAR recommendations for the management of rheumatoid arthritis with synthetic and biological disease-modifying antirheumatic drugs. Ann Rheum Dis 2010;69: 964–75.
29. Smolen JS, Landewe R, Breedveld FC, Buch M, Burmester G, Dougados M, et al. EULAR recommendations for the management of rheumatoid arthritis with synthetic and biological disease-modifying antirheumatic drugs: 2013 update. Ann Rheum Dis 2014;73:492–509.
30. Schoels M, Wong J, Scott DL, Zink A, Richards P, Landewe R, et al. Economic aspects of treatment options in rheumatoid arthritis: a systematic literature review informing the EULAR recommendations for the management of rheumatoid arthritis. Ann Rheum Dis 2010;69:995–1003.
31. Navarro-Millan I, Sattui SE, Curtis JR. Systematic review of tumor necrosis factor inhibitor discontinuation studies in rheumatoid arthritis. Clin Ther 2013;35:1850–61.
32. Yoshida K, Sung YK, Kavanaugh A, Bae SC, Weinblatt ME, Kishimoto M, et al. Biologic discontinuation studies: a systematic review of methods. Ann Rheum Dis 2014;73:595–9.

33. Kavanaugh A, Lee SJ, Curtis JR, Greenberg JD, Kremer JM, Soto L, et al. Discontinuation of tumour necrosis factor inhibitors in patients with rheumatoid arthritis in low-disease activity: persistent benefits: data from the Corrona registry. Ann Rheum Dis 2015;74:1150–5.
34. Tanaka Y, Hirata S, Kubo S, Fukuyo S, Hanami K, Sawamukai N, et al. Discontinuation of adalimumab after achieving remission in patients with established rheumatoid arthritis: 1-year outcome of the HONOR study. Ann Rheum Dis 2015;74:389–95.
35. Van Vollenhoven RF, Ostergaard M, Leirisalo-Repo M, Uhlig T, Jansson M, Larsson E, et al. Full dose, reduced dose or discontinuation of etanercept in rheumatoid arthritis. Ann Rheum Dis 2016;75:52–8.
36. Karnon J, Carlton J, Czoski-Murray C, Smith K. Informing disinvestment through cost-effectiveness modelling. Appl Health Econ Health Policy 2009;7:1–9.
37. Raad voor de Volksgezondheig en Zorg. Zicht op zinnige en duurzame zorg. Quantes, Rijswijk. URL: http://rvz.net.

ARTHRITIS & RHEUMATOLOGY
Vol. 70, No. 10, October 2018, pp 1565–1571
DOI 10.1002/art.40536

Serious Infections in Rheumatoid Arthritis Offspring Exposed to Tumor Necrosis Factor Inhibitors

A Cohort Study

Évelyne Vinet,[1] Cristiano De Moura,[2] Christian A. Pineau,[3] Michal Abrahamowicz,[3] Jeffrey R. Curtis,[4] and Sasha Bernatsky[1]

Objective. **To evaluate the risk of serious infections in rheumatoid arthritis (RA) offspring exposed to tumor necrosis factor inhibitors (TNFi) in the gestational period compared to unexposed RA offspring, as well as to children from the general population.**

Methods. **We used US claim data (2011–2015) to identify 2,989 offspring born to women who have RA and a randomly selected group of 14,596 control children, matched ≥4:1 for maternal age, year of delivery, and state of residence. We defined TNFi exposure based on ≥1 filled prescription during pregnancy. We ascertained serious infections based on ≥1 hospitalization, with infection as a primary diagnosis, at ≤12 months of life. We performed multivariable analyses, adjusting for maternal demographics, comorbidities, pregnancy complications, and drugs.**

Results. **Among RA offspring, 380 (12.7%) were exposed to TNFi during pregnancy. The percentage of serious infections in RA offspring with no TNFi exposure (2.0%; 95% confidence interval [95% CI] 1.5, 2.6) was similar to that in non-RA offspring (1.9%; 95% CI 1.9, 2.2), while the percentage of serious infections in RA offspring with TNFi exposure was 3.2% (95% CI 1.5, 5.6). In multivariable analyses, we were unable to establish an increased risk of serious infections in RA offspring exposed to TNFi versus both non-RA offspring (odds ratio [OR] 1.7, 95% CI 0.8, 3.7) and RA offspring unexposed to TNFi (OR 1.4, 95% CI 0.7, 2.8).**

Conclusion. **We did not demonstrate a marked excess risk for serious infections in RA offspring exposed to TNFi during pregnancy versus unexposed RA offspring or general population controls.**

In North America, infections are the leading cause of mortality in children age <5 years, accounting for >30% of deaths (1). Tumor necrosis factor inhibitors (TNFi) are important drugs in the treatment of rheumatoid arthritis (RA), being used in one-third of patients (2). Since animal studies did not show fetal risk, TNFi have been commonly and increasingly used during pregnancy, now prescribed in 20% of RA pregnancies, representing a 3-fold increase over the past 10 years (2). Despite existing concerns that these potent drugs may cause immunosuppression, there are limited data on the risk of serious infection in exposed offspring.

During pregnancy, there is active transplacental transport of maternal circulating immunoglobulins (IgG) through their Fc portion (3). TNFi are all monoclonal IgG with an Fc part, except for etanercept and certolizumab, which are, respectively, a fusion protein with an Fc portion and a PEGylated Fab fragment without an Fc component (4,5). Thus, most TNFi are actively transported across the placenta, with some reaching higher fetal than maternal blood levels. For instance, infliximab

Supported by the Department of Medicine of the McGill University Health Centre. Dr. Vinet's work was supported by Fonds de Recherche en Santé du Québec (Clinical Research Scholar Junior 1 Award). Dr. Curtis' work was supported by the Patient Centered Outcomes Research Institute.

[1]Évelyne Vinet, MD, PhD, Sasha Bernatsky, MD, PhD: McGill University Health Center and McGill University, Montreal, Quebec, Canada; [2]Cristiano De Moura, PhD: McGill University, Montreal, Quebec, Canada; [3]Christian A. Pineau, MD, Michal Abrahamowicz, PhD: McGill University Health Center, Montreal, Quebec, Canada; [4]Jeffrey R. Curtis, MD, MS, MPH: University of Alabama at Birmingham.

Dr. Curtis has received consulting fees from AbbVie, Bristol-Myers Squibb, Eli Lilly and Company, Myriad, Roche/Genentech, and UCB (less than $10,000 each) and from Amgen, CORRONA, Janssen, and Pfizer (more than $10,000 each).

Address correspondence to Évelyne Vinet, MD, PhD, Research Institute of the McGill University Health Centre, 5252 Boulevard de Maisonneuve Ouest, Office 3D.57, Montréal, Quebec H4A 3S5, Canada. E-mail: evelyne.vinet@mcgill.ca.

Submitted for publication January 19, 2018; accepted in revised form April 17, 2018.

and adalimumab have the highest transplacental transfer (reaching cord blood median levels at, respectively, 160% and 150% of maternal blood levels), while etanercept and certolizumab display the lowest passage (cord blood median levels at, respectively, 4–7% and <0.25% of maternal blood levels) (4–8).

As fetuses could be exposed to therapeutic (and potentially supratherapeutic) TNFi doses, there are concerns that they could cause immunosuppression in the offspring. These concerns were initially raised following the case report in 2010 of a mother with Crohn's disease receiving infliximab throughout pregnancy (9). After an uncomplicated delivery, her healthy infant received a BCG vaccine at 3 months of age and died of disseminated tuberculosis (TB). Due to the potential for immunosuppression in exposed offspring and because of the TNFi differential half-life and transplacental transfer, the European League Against Rheumatism recommends discontinuing infliximab and adalimumab before 20 weeks of gestation and etanercept before 31–32 weeks to minimize the risk of infections in offspring, while they state that certolizumab can be continued throughout pregnancy (10). The British Society of Rheumatology guidelines for use of drugs during pregnancy also state that certolizumab is compatible with all 3 trimesters of pregnancy, but differ slightly in recommending that infliximab be discontinued before 16 weeks, and that etanercept and adalimumab be stopped before the end of the second trimester (8).

Until now, there has been no reported study on the risk of infection in RA offspring exposed in utero to TNFi versus unexposed offspring. Therefore, we aimed to evaluate serious infections in RA offspring exposed to TNFi in the preconception and/or gestational period compared to unexposed RA offspring, as well as to children from the general population.

PATIENTS AND METHODS

Data source and study population. We assembled the Pregnancies in RA Mothers and Outcomes in Offspring in the United States (PAROUS) cohort, a population-based cohort of children born to women who have RA and a matched control group of children born to unaffected mothers, using MarketScan commercial databases (January 1, 2011 to December 30, 2015). The MarketScan commercial database is a large prospective US database of >230 million subjects with employer-provided health insurance (11). It contains data on hospitalizations, outpatient visits, and drug prescription claims.

To create the PAROUS cohort, we identified women ages 15–45 years as RA subjects (using the International Classification of Diseases, Ninth and/or Tenth Revisions [ICD-9/10] code 714/M05) if they had any of the following: 1) ≥1 hospitalization with a diagnosis of RA at or prior to delivery, or 2) ≥2 physician visits with a diagnosis of RA, the first occurring at any time prior to the delivery and the second at any point during the study period. This RA case definition demonstrated a high sensitivity (83%) and excellent specificity (99%) when using physician diagnosis as a reference (12). A group of women without RA was randomly selected and matched ≥4:1 for age, year of delivery, and geographic location (i.e., state, division, and region) of the primary beneficiary's residence. Only women continuously enrolled within MarketScan with medical and pharmacy coverage for ≥12 months prior to delivery were included in PAROUS. We then identified the children born live to RA and unexposed women, linking mothers with their infants deterministically using family identifiers and delivery dates corresponding to birth year. Children were followed up from birth until 12 months of age, first event of interest (i.e., serious infection), end of commercial insurance eligibility, death, or end of study period (December 30, 2015), whichever came first.

Delivery was defined using any inpatient hospital admission record including a pregnancy-related diagnosis or procedure code for vaginal or caesarean delivery identified by the relevant ICD-9/10 codes and/or procedure codes (see Supplementary Table 1, available on the *Arthritis & Rheumatology* web site at http://onlinelibrary.wiley.com/doi/10.1002/art.40536/abstract). We excluded deliveries with diagnostic and/or procedure codes related to a molar pregnancy, spontaneous abortion or termination, and ectopic pregnancy.

Exposure. We defined TNFi exposure based on ≥1 filled prescription for adalimumab, certolizumab, etanercept, golimumab, infliximab, and/or ≥1 infusion procedure claim for golimumab and/or infliximab during the preconception and/or gestational periods. We identified the date of the last menstrual period (i.e., onset of gestational period) based on the delivery date after applying a validated algorithm to term and preterm deliveries separately (13). We further categorized TNFi exposure according to the timing of the filled prescription or the infusion procedure date in relation to the gestational period.

The main exposure categories were as follows: 1) RA offspring with TNFi exposure at any time during pregnancy (i.e., any prescription filled or infusion procedure claim during the gestational period), 2) RA offspring with TNFi exposure in the last 12 weeks of pregnancy (i.e., any prescription filled or infusion procedure claim within 12 weeks of delivery), 3) RA offspring with TNFi in the preconception period only (i.e., at least 1 prescription filled or infusion procedure claim in the 12 weeks preceding the gestational period, but none within the gestational period), 4) RA offspring without TNFi exposure (i.e., no prescription filled or infusion procedure claim within the gestational period and the 12 weeks preceding it), and 5) children born to non-RA mothers without TNFi exposure (i.e., no prescription filled or infusion procedure claim within the preconception and gestational periods).

Outcome measure. The outcome of interest was serious infection occurring in the offspring. We ascertained serious infections in the offspring based on ≥1 hospitalization with infection within the first 12 months of life, with a relevant diagnostic code, as primary reason for admission (i.e., hospitalization where the primary diagnosis was an infection, including ICD-9/10 coding by organism and/or organ involvement). This approach of identifying serious infections has been shown to have a high sensitivity (80%) and specificity (84%) when using chart review as a reference (14). We only considered the first event if >1 event was identified.

Assessment of covariates. We assessed the following maternal comorbidity and pregnancy complications based on at least 1 physician billing and/or hospitalization with relevant diagnostic codes: pregestational diabetes mellitus, gestational diabetes mellitus, and preterm birth. We also identified in utero drug exposures to systemic corticosteroids, nonbiologic disease-modifying antirheumatic drugs (DMARDs) (i.e., hydroxychloroquine, sulfasalazine, methotrexate, and leflunomide), and biologic DMARDs other than TNFi (i.e., rituximab, abatacept, and tocilizumab), based on at least 1 prescription filled and/or perfusion procedure claim by the mother during the gestational period.

Statistical analysis. We used descriptive statistics to characterize the different exposure groups and calculated crude measures of risk (i.e., proportions and incidence rates) with 95% confidence intervals (95% CIs). As mean follow-up time for offspring was very similar across exposure groups (ranging from 285 to 296 days), we performed univariable and multivariable analyses using a generalized estimating equation (GEE) method to estimate the odds ratio (OR) for the outcome of interest (i.e., serious infections), for children born to women with RA with different TNFi exposures, relative to RA offspring unexposed to TNFi, as well as to unexposed children from unaffected mothers. The GEE method accounts for correlation between observations, which might arise from including >1 offspring from the same mother. In addition, we assessed the robustness of our effect estimates by conducting exploratory univariable and multivariable Cox proportional hazards analyses, which provided very similar results. In our multivariable analyses, we adjusted for maternal age, pregestational diabetes mellitus, gestational diabetes mellitus, preterm birth, and medications (i.e., corticosteroids and nonbiologic and biologic DMARDs). All analyses were performed using SAS, version 9.4.

Patient involvement. Patient advocates from the Canadian Arthritis Patient Alliance (CAPA) were involved in setting the research question, developing the study protocol, and interpreting the study findings. We plan to disseminate the results of the research to relevant patient communities (e.g., CAPA, the Arthritis Society, the Arthritis Foundation, CreakyJoints, and the ArthritisPower patient registry).

RESULTS

We identified 2,989 RA offspring and 14,596 matched offspring unexposed to maternal RA (see the patient selection flow chart, Supplementary Figure 1, available on the *Arthritis & Rheumatology* web site at http://onlinelibrary.wiley.com/doi/10.1002/art.40536/abstract). Among RA offspring, 380 (12.7%) were exposed to TNFi during pregnancy, 133 (4.4%) were unexposed during pregnancy but exposed in the preconception period, and 2,476 (82.8%) were unexposed during both the pregnancy and preconception periods. Mean maternal age was similar across all RA groups and non-RA mothers (Table 1).

Among mothers with RA a higher proportion had pregestational diabetes mellitus and a higher proportion experienced pregnancy complications, such as preterm births and gestational diabetes mellitus (Table 1), compared to unaffected mothers. In addition, in utero drug exposures to corticosteroids and nonbiologic DMARDs were more frequent in RA offspring compared to offspring of non-RA mothers.

Over the first year of life, the percentage of serious infections in RA offspring with no TNFi exposure (2.0%; 95% CI 1.5, 2.6) was almost identical to that in non-RA offspring (1.9%; 95% CI 1.7, 2.2), while the percentage of serious infections in RA offspring with TNFi exposure was 3.2% (95% CI 1.5, 5.6). With regard to TNFi exposure in the third trimester, the percentage of serious infections was 3.2% (95% CI 1.2, 7.7), while for TNFi exposure in the preconception period only, it was 1.5% (95% CI 0.3, 5.9) (Table 2).

In multivariable analyses, we did not find an increased risk of serious infections in RA offspring

Table 1. Maternal characteristics of children included in the PAROUS cohort (n = 17,585)*

Characteristic	RA and TNFi pregnancy (n = 380)	RA and TNFi preconception (n = 133)	RA and no TNFi (n = 2,476)	Non-RA (n = 14,596)
Maternal age, mean ± SD years	32.6 ± 4.1	32.0 ± 4.4	32.5 ± 4.4	32.4 ± 4.9
Maternal comorbidities, no. (%)				
Preexisting hypertension	58 (15.3)	17 (12.8)	387 (15.6)	1,409 (9.7)
Preexisting diabetes mellitus	26 (6.8)	8 (6.0)	208 (8.4)	754 (5.2)
Asthma	21 (5.5)	11 (8.3)	201 (8.1)	665 (4.6)
In utero drug exposures, no. (%)				
Corticosteroids	213 (56.1)	62 (46.6)	667 (26.9)	285 (2.0)
Nonbiologic DMARDs	74 (19.5)	23 (17.3)	379 (15.3)	9 (0.1)
Other biologic DMARDs	2 (0.5)	0 (0.0)	31 (1.3)	0 (0.0)
Obstetric outcomes, no. (%)				
Gestational diabetes mellitus	82 (21.6)	26 (19.6)	483 (19.5)	2,384 (16.3)
Multiple birth	17 (4.5)	2 (1.5)	81 (3.3)	479 (3.3)
Preterm birth	45 (11.8)	20 (15.0)	273 (11.0)	1,313 (9.0)

* PAROUS = Pregnancies in RA Mothers and Outcomes in Offspring in the United States; RA = rheumatoid arthritis; TNFi = tumor necrosis factor inhibitors; DMARDs = disease-modifying antirheumatic drugs.

Table 2. Crude absolute risk estimates of serious infections in offspring included in the PAROUS cohort by exposure categories*

Exposure categories	Serious infection events, no.	Person-years	Serious infections, % (95% CI)	Incidence rate per 100 person-years (95% CI)
Non-RA (n = 14,596)	279	11,592	1.9 (1.7, 2.2)	2.4 (2.1, 2.7)
RA and no TNFi (n = 2,476)	49	1,977	2.0 (1.5, 2.6)	2.5 (1.9, 3.3)
RA and TNFi preconception (n = 133)	2	106	1.5 (0.3, 5.9)	1.9 (0.5, 7.6)
RA and TNFi pregnancy (n = 380)	12	287	3.2 (1.5, 5.6)	4.2 (2.4, 7.4)
RA and TNFi third trimester (n = 156)	5	118	3.2 (1.2, 7.7)	4.2 (1.8, 10.2)

* PAROUS = Pregnancies in RA Mothers and Outcomes in Offspring in the United States; 95% CI = 95% confidence interval; RA = rheumatoid arthritis; TNFi = tumor necrosis factor inhibitors.

exposed to TNFi versus non-RA offspring (OR for TNFi pregnancy 1.7 [95% CI 0.8, 3.7], OR for TNFi preconception 0.9 [95% CI 0.2, 3.9]) (Table 3 and Figure 1). The OR estimates for serious infections in RA offspring exposed to TNFi during pregnancy versus unexposed RA offspring were fairly wide and precluded a definitive conclusion (OR 1.4, 95% CI 0.7, 2.8), as were the results when we restricted TNFi exposure to the third trimester versus unexposed RA offspring (OR 1.4, 95% CI 0.5, 3.6).

When we looked at the percentage of serious infections in RA offspring exposed to specific TNFi (Table 4), we observed a trend toward more serious infections in RA offspring exposed to infliximab as opposed to those exposed to other TNFi (absolute risk difference 5.4%; 95% CI −1.1, 20.4). However, the 95% CIs for all the estimates were overlapping and, particularly in the case of golimumab and certolizumab, very imprecise.

We evaluated the risk of serious infections in RA offspring exposed to infliximab as opposed to other TNFi in an exploratory multivariable analysis, adjusting for maternal age and in utero corticosteroid exposure (but unable to control for preterm birth and gestational diabetes mellitus since no case occurred for these covariates). Again, there was a trend for an increased risk of serious infections in RA offspring exposed to infliximab during pregnancy versus RA offspring exposed to other TNFi, although the 95% CI included the possibility of no difference (OR 3.0, 95% CI 0.7, 11.8).

Table 3. Unadjusted and adjusted ORs for the risk of serious infections comparing different exposure categories in the PAROUS cohort*

Comparison	Unadjusted OR (95% CI)	Adjusted OR (95% CI)
TNFi pregnancy vs. non-RA offspring	1.7 (0.9, 3.0)	1.7 (0.8, 3.7)
TNFi preconception vs. non-RA offspring	0.8 (0.2, 3.2)	0.9 (0.2, 3.9)
TNFi pregnancy vs. unexposed RA offspring	1.6 (0.9, 3.1)	1.4 (0.7, 2.8)
TNFi third trimester vs. unexposed RA offspring	1.6 (0.6, 4.2)	1.4 (0.5, 3.6)

* ORs = odds ratios; PAROUS = Pregnancies in RA Mothers and Outcomes in Offspring in the United States; 95% CI = 95% confidence interval; TNFi = tumor necrosis factor inhibitors; RA = rheumatoid arthritis.

The most frequent type of serious infections in RA offspring exposed to TNFi, unexposed RA offspring, and non-RA offspring was acute bronchiolitis due to respiratory syncytial virus, accounting for 36% (95% CI 14, 64), 31% (95% CI 19, 46), and 33% (95% CI 27, 38) of cases, respectively, in these 3 groups (Table 5). Among all cases of serious infection occurring in RA offspring (exposed and unexposed to TNFi), we did not identify any case of TB.

DISCUSSION

Within the largest cohort of RA offspring exposed to TNFi ever assembled, we did not detect a marked excess risk associated with overall TNFi exposure during the preconception and gestational period. In addition, we did not identify any cases of TB.

We observed a trend in the risk of serious infections in RA offspring exposed to infliximab, as opposed to other TNFi, during pregnancy. In a recent study of 80 pregnant women with inflammatory bowel disease (IBD) exposed to adalimumab or infliximab, investigators assessed maternal and cord blood levels of TNFi (15). The median ratio of infant-to-mother drug concentration at birth was 1.21 for adalimumab (95% CI 0.94, 1.49) and 1.97 for infliximab (95% CI 1.50, 2.43). The investigators showed that the mean half-life of infliximab and adalimumab was, respectively, 3.7 and 2.0 times longer in infants than in adult nonpregnant patients. This translated to a longer mean time to drug clearance in infants exposed in utero to infliximab as opposed to those exposed to adalimumab (respectively, 7.3 months [95% CI 6.2, 8.3] and 4.0 months [95% CI 2.9, 5.0]) (15). Of note, drug concentrations were detectable up to 12 months of age in offspring exposed to infliximab. These data suggest that the pharmacokinetic properties of TNFi (i.e., their half-life) combined with their

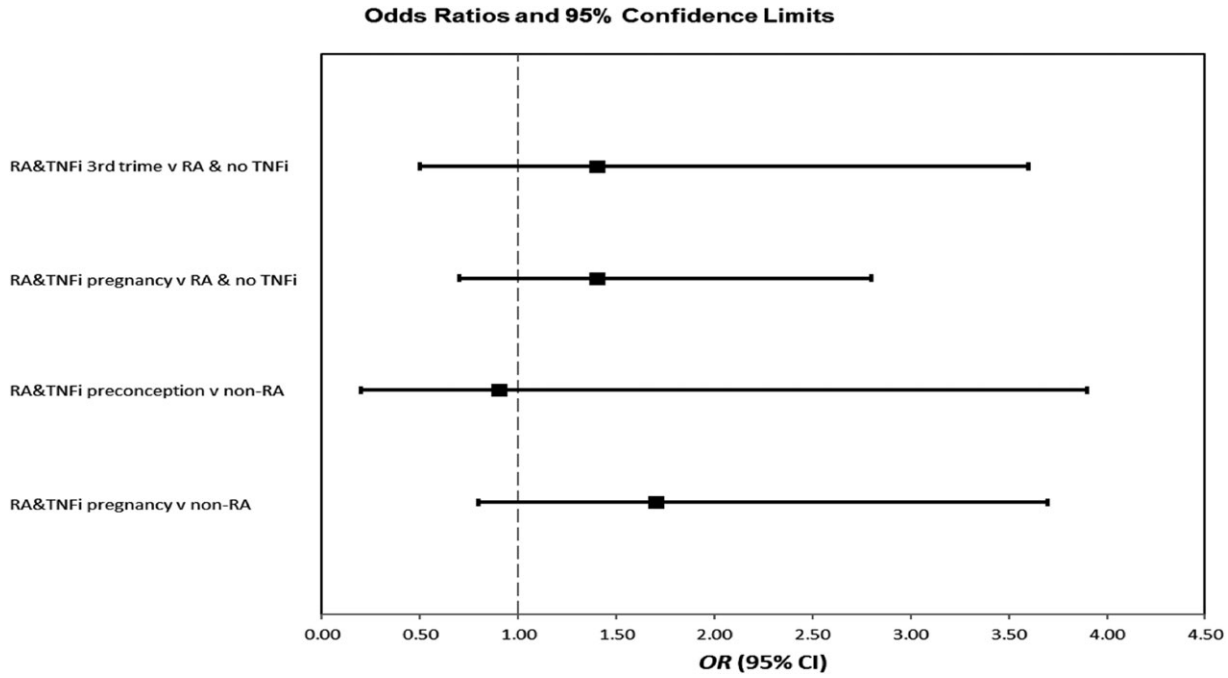

Figure 1. Forest plot of the effect estimates for the risk of serious infections comparing offspring in the Pregnancies in RA Mothers and Outcomes in Offspring in the United States cohort with different exposure categories. RA = rheumatoid arthritis; TNFi = tumor necrosis factor inhibitor; trime = trimester; OR = odds ratio; 95% CI = 95% confidence interval.

immunologic structure (i.e., harboring an Fc fragment or not) influence drug levels in exposed offspring and the potential risk of having a serious infection.

Our study has many strengths. It is the first study to evaluate the risk of serious infections in RA offspring exposed to TNFi, using an RA group and general population unexposed group as comparators. Owing to the availability of data on maternal medical diagnoses and prescription claims preceding delivery, we were able to account for important confounding factors, such as other medications, and present adjusted effect estimates for each comparison. Another strength of our study resides in the use of a large health plan database, which allowed us to assess a rare outcome in RA offspring exposed to TNFi. In addition, we used case definitions for RA and serious infections that have been shown to be valid in prior studies (12,14). Moreover, our data source (i.e., MarketScan) has been extensively used for the conduct of pharmacoepidemiologic studies in rheumatic diseases, particularly related to biologic DMARDs (such as TNFi) and RA outcomes (16–19).

Table 4. Percent of serious infections according to type of TNFi in RA offspring exposed during pregnancy*

TNFi	Serious infections, % (95% CI)
Adalimumab (n = 108)	1.9 (0.3, 7.2)
Certolizumab (n = 19)	0.0 (0.0, 20.9)
Etanercept (n = 195)	3.6 (1.6, 7.6)
Golimumab (n = 10)	0.0 (0.0, 34.5)
Infliximab (n = 37)	8.1 (2.1, 23.0)

* TNFi = tumor necrosis factor inhibitor; RA = rheumatoid arthritis; 95% CI = 95% confidence interval.

Table 5. Most frequent types of serious infections across exposure categories*

Types of serious infection	Cases of serious infection		
	RA offspring exposed to TNFi in pregnancy and/or preconception (n = 14)	RA offspring unexposed to TNFi (n = 49)	Non-RA offspring (n = 279)
Acute bronchiolitis due to RSV	36 (14, 64)	31 (19, 46)	33 (27, 38)
Acute bronchiolitis due to other organisms	36 (14, 64)	20 (11, 34)	18 (14, 23)
Viral meningitis	7 (1, 31)	8 (3, 19)	4 (2, 7)
Other	21 (6, 51)	41 (27, 56)	55 (49, 61)

* Values are the % (95% confidence interval). TNFi = tumor necrosis factor inhibitors; RA = rheumatoid arthritis; RSV = respiratory syncytial virus.

Furthermore, administrative database studies like ours are less prone to selection bias or recall bias compared to drug or pregnancy registries, which might differentially select drug-exposed subjects based on certain characteristics and/or outcomes or collect exposure information after the outcome has occurred (20).

We must acknowledge some potential limitations, particularly TNFi exposure misclassification. Exposure to TNFi was defined based on filled prescriptions, except for infliximab and golimumab exposures, which were also identified by infusion procedure codes. There might be some concerns that filled prescriptions may not have reflected actual use. However, it is likely that most women who filled a prescription for TNFi took at least 1 dose, because within the MarketScan commercial database the vast majority of subjects have out-of-pocket costs associated with prescriptions filled (21). Thus, we believe this would not have invalidated our findings.

As MarketScan (like most administrative databases) does not provide information on the gestational age at birth and/or the last menstrual period, we estimated the gestational period by applying a validated algorithm to term and preterm deliveries separately (13). Thus, misclassification of TNFi during the gestational period is possible. However, since our sensitivity analysis restricted to RA offspring exposed to TNFi in the 12 weeks prior to delivery showed a similar effect estimate to the one obtained in our primary analysis, we do not think that misclassification explains all of our study findings.

Since MarketScan does not explicitly record RA activity measures, our study might be subject to residual confounding by this factor. However, we adjusted for important drug exposures, such as the use of steroids and nonbiologic DMARDs, which might be associated with high disease activity. Thus, by accounting for medication exposures, this might have at least partially controlled for disease activity.

To date, there have been limited data on the risk of serious infections in children born to mothers with inflammatory conditions such as IBD and exposed in utero to TNFi. Mahadevan et al have reported findings from the Pregnancy in Inflammatory Bowel Diseases And Neonatal Outcomes (PIANO) registry, a US prospective cohort of pregnant women with IBD and their offspring followed up until 12 months after delivery (22). PIANO includes 102 offspring exposed to TNFi monotherapy, 59 offspring exposed to combination therapy with TNFi and thiopurines, as well as an unexposed group of 265 children. The authors reported an increased risk of infections at 12 months of age in offspring exposed to combination therapy with TNFi and thiopurines relative to the unexposed group (relative risk [RR] 1.50, 95% CI 1.08, 2.09). However, they did not report a specific effect estimate for the risk of infections in children exposed to TNFi monotherapy (compared to unexposed offspring). In addition, the study results have only been reported in abstract form so far.

In the study mentioned above that evaluated 80 IBD offspring exposed in utero to adalimumab or infliximab, Julsgaard et al assessed the risk of infections in the first year of life, as reported by the mothers (15). The investigators did not observe an increased risk of infections in children exposed to TNFi monotherapy after the thirtieth gestational week compared to those who were only exposed before the thirtieth gestational week (RR 0.54, 95% CI 0.26, 1.16). However, offspring exposed to both TNFi and thiopurines had a ≥2-fold increase in the risk of infections compared to those only exposed to TNFi (RR 2.7, 95% CI 1.09, 6.78). These study findings and the preliminary results from the PIANO registry suggest that TNFi are associated with a potential increase in the risk of infections in IBD offspring when used in combination with thiopurines during pregnancy.

In summary, we did not observe a marked excess risk for serious infections in RA offspring exposed to TNFi during pregnancy, including the third trimester, versus unexposed RA offspring and children from the general population. However, we cannot exclude a differential risk according to specific TNFi, with infliximab potentially resulting in a 3-fold increase in the risk of serious infections compared to other TNFi. More studies are needed to further evaluate whether the risk of serious infections in exposed offspring is influenced by individual TNFi characteristics.

AUTHOR CONTRIBUTIONS

All authors were involved in drafting the article or revising it critically for important intellectual content, and all authors approved the final version to be submitted for publication. Dr. Vinet had full access to all of the data in the study and takes responsibility for the integrity of the data and the accuracy of the data analysis.

Study conception and design. Vinet, De Moura, Curtis, Bernatsky.
Acquisition of data. Vinet, Abrahamowicz, Curtis, Bernatsky.
Analysis and interpretation of data. Vinet, De Moura, Pineau, Abrahamowicz, Curtis, Bernatsky.

REFERENCES

1. Black RE, Cousens S, Johnson HL, Lawn JE, Rudan I, Bassani DG, et al. Global, regional, and national causes of child mortality in 2008: a systematic analysis. Lancet 2010;375:1969–87.
2. Desai RJ, Huybrechts KF, Bateman BT, Hernandez-Diaz S, Mogun H, Gopalakrishnan C, et al. Patterns and secular trends in use of immunomodulatory agents during pregnancy in women with rheumatic conditions. Arthritis Rheumatol 2016;68:1183–9.

3. Suzuki T, Ishii-Watabe A, Tada M, Kobayashi T, Kanayasu-Toyoda T, Kawanishi T, et al. Importance of neonatal FcR in regulating the serum half-life of therapeutic proteins containing the Fc domain of human IgG1: a comparative study of the affinity of monoclonal antibodies and Fc-fusion proteins to human neonatal FcR. J Immunol 2010;184:1968–76.
4. Mahadevan U, Wolf DC, Dubinsky M, Cortot A, Lee SD, Siegel CA, et al. Placental transfer of anti–tumor necrosis factor agents in pregnant patients with inflammatory bowel disease. Clin Gastroenterol Heptol 2013;11:286–92.
5. Mariette X, Förger F, Abraham B, Flynn AD, Moltó A, Flipo RM, et al. Lack of placental transfer of certolizumab pegol during pregnancy: results from CRIB, a prospective, postmarketing, pharmacokinetic study. Ann Rheum Dis 2018;77:228–33.
6. Murashima A, Watanabe N, Ozawa N, Saito H, Yamaguchi K. Etanercept during pregnancy and lactation in a patient with rheumatoid arthritis: drug levels in maternal serum, cord blood, breast milk and the infant's serum. Ann Rheum Dis 2009;68:1793–4.
7. Berthelsen BG, Fjeldsøe-Nielsen H, Nielsen CT, Hellmuth E. Etanercept concentrations in maternal serum, umbilical cord serum, breast milk and child serum during breastfeeding. Rheumatology (Oxford) 2010;49:2225–7.
8. Flint J, Panchal S, Hurrell A, van de Venne M, Gayed M, Schreiber K, et al. BSR and BHPR guideline on prescribing drugs in pregnancy and breastfeeding. Part I. Standard and biologic disease modifying anti-rheumatic drugs and corticosteroids. Rheumatology (Oxford) 2016;55:1693–7.
9. Cheent K, Nolan J, Shariq S, van de Venne M, Gayed M, Schreiber K, et al. Case report: fatal case of disseminated BCG infection in an infant born to a mother taking infliximab for Crohn's disease. J Crohns Colitis 2010;4:603–5.
10. Skorpen CG, Hoeltzenbein M, Tincani A, Fischer-Betz R, Elefant E, Chambers C, et al. The EULAR points to consider for use of antirheumatic drugs before pregnancy, and during pregnancy and lactation. Ann Rheum Dis 2016;75:795–810.
11. Marketscan Research Database. URL: https://truvenhealth.com/your-healthcare-focus/analytic-research/marketscan-research-databases.
12. Widdifield J, Bombardier C, Bernatsky S, Paterson JM, Green D, Young J, et al. An administrative data validation study of the accuracy of algorithms for identifying rheumatoid arthritis: the influence of the reference standard on algorithm performance. BMC Musculoskelet Disord 2014;15:216.
13. Margulis AV, Setoguchi S, Mittleman MA, Glynn RJ, Dormuth CR, Hernandez-Diaz S. Algorithms to estimate the beginning of pregnancy in administrative databases. Pharmacoepidemiol Drug Saf 2013;22:16–24.
14. Henriksen DP, Nielsen SL, Laursen CB, Hallas J, Lassen AT. How well do discharge diagnoses identify hospitalised patients with community-acquired infections? A validation study. PLoS One 2014;9:e92891.
15. Julsgaard M, Christensen LA, Gibson PR, Gearry RB, Fallingborg J, Hvas CL, et al. Concentrations of adalimumab and infliximab in mothers and newborns, and effects on infection. Gastroenterology 2016;151:110–9.
16. Bonafede MM, Curtis JR, McMorrow D, Mahajan P, Chen CI. Treatment effectiveness and treatment patterns among rheumatoid arthritis patients after switching from a tumor necrosis factor inhibitor to another medication. Clinicoecon Outcomes Res 2016;8:707–15.
17. Xie F, Yun H, Bernatsky S, Curtis JR. Risk of gastrointestinal perforation among rheumatoid arthritis patients receiving tofacitinib, tocilizumab, or other biologic treatments. Arthritis Rheumatol 2016;68:2612–7.
18. Curtis JR, Xie F, Smith C, Saag KG, Chen L, Beukelman T, et al. Changing trends in opioid use among patients with rheumatoid arthritis in the United States. Arthritis Rheumatol 2017;69:1733–40.
19. Curtis JR, Xie F, Yun H, Bernatsky S, Winthrop KL. Real-world comparative risks of herpes virus infections in tofacitinib and biologic-treated patients with rheumatoid arthritis. Ann Rheum Dis 2016;75:1843–7.
20. Andrade SE, Scott PE, Davis RL, Li DK, Getahun D, Cheetham TC. Validity of health plan and birth certificate data for pregnancy research. Pharmacoepidemiol Drug Saf 2013;22:7–15.
21. Curkendall S, Patel V, Gleeson M, Campbell RS, Zagari M, Dubois R. Compliance with biologic therapies for rheumatoid arthritis: do patient out-of-pocket payments matter? Arthritis Rheum 2008;59:1519–26.
22. Mahadevan U, Martin CF, Sandler RS, Kane SV, Dubinsky M, Lewis JD. 865 PIANO: a 1000 patient prospective registry of pregnancy outcomes in women with IBD exposed to immunomodulators and biologic therapy. Gastroenterol Hepatol (N Y) 2012;8 Suppl 5:1–24.

ARTHRITIS & RHEUMATOLOGY
Vol. 70, No. 10, October 2018, pp 1572–1576
DOI 10.1002/art.40537

BRIEF REPORT

Leg Length Inequality and Hip Osteoarthritis in the Multicenter Osteoarthritis Study and the Osteoarthritis Initiative

Chan Kim,[1] Michael Nevitt,[2] Ali Guermazi,[1] Jingbo Niu,[1] Margaret Clancy,[1] Irina Tolstykh,[2] Pia M. Jungmann,[3] Nancy E. Lane,[4] Neil A. Segal,[5] William F. Harvey,[6] Cora E. Lewis,[7] and David T. Felson[8]

Objective. **Studies suggest that persons with a leg length inequality (LLI) of ≥2 cm have an increased risk of developing knee osteoarthritis (OA) in that limb. The present study was undertaken to examine whether LLI also confers an increased risk of hip OA.**

Methods. **Using long limb radiographs from subjects in the Multicenter Arthritis Study (MOST) and the Osteoarthritis Initiative (OAI), we measured LLI and scored hip radiographs that were obtained at baseline and 3–5-year follow-up. The associations of LLI of ≥1 cm and LLI of ≥2 cm with radiographic hip OA were examined cross-sectionally and longitudinally, assessing risk in shorter limbs and longer limbs compared to limbs from subjects with no LLI. We carried out logistic regression analyses with generalized estimating equations and adjusted for age, sex, body mass index, height, and cohort of origin.**

Results. **There were 1,966 subjects from the MOST and 2,627 subjects from the OAI. Twelve percent had LLI of ≥1 cm and 1% had LLI of ≥2 cm. For LLI ≥1 cm, the adjusted odds ratio for prevalent hip OA in the shorter leg was 1.47 (95% confidence interval [95% CI] 1.07–2.02) and for LLI ≥2 cm, it was 2.15 (95% CI 0.87–5.34). For LLI ≥1 cm, the odds of incident hip OA in the shorter leg were 1.39 (95% CI 0.81–2.39) while for LLI ≥2 cm, they were 4.20 (95% CI 1.26–14.03). We found no increased risk of hip OA in longer limbs.**

Conclusion. **Our findings suggest that, as with knee OA, legs that are at least 2 cm shorter than the contralateral leg are at increased risk of hip OA.**

Hip osteoarthritis (OA) is a significant source of morbidity and a major cause of disability in the US. In the urban/suburban community of Framingham, MA, the age-standardized prevalence of symptomatic hip OA was found to be 4.2% (1). Not much is known about modifiable risk factors for hip OA that could help identify treatment strategies.

One potential risk factor for hip OA is leg length inequality (LLI). In the Multicenter Osteoarthritis Study (MOST), we found that among persons with LLI of least 1 cm, the incidence, prevalence, and progression of knee OA in the shorter leg were increased compared to the longer limb (2). The shorter leg is likely to sustain increased impact force of the foot during gait, thus transmitting a greater impulse up the ipsilateral leg. LLI is easily treatable and could be modifiable. However, the longitudinal association of LLI and hip OA has not been well characterized. LLI of ≥1 cm is uncommon (~10–15% of subjects in the

This article was prepared using an Osteoarthritis Initiative (OAI) public-use data set, and its contents do not necessarily reflect the opinions or views of the OAI Study Investigators, the NIH, or the private funding partners of the OAI. The OAI is a public–private partnership between the NIH (contracts N01-AR-2-2258, N01-AR-2-2259, N01-AR-2-2260, N01-AR-2-2261, and N01-AR-2-2262) and private funding partners (Merck Research Laboratories, Novartis Pharmaceuticals, GlaxoSmithKline, and Pfizer, Inc.) and is conducted by the OAI Study Investigators. Private sector funding for the OAI is managed by the Foundation for the NIH. The authors of this article are not part of the OAI investigative team. The OAI was also funded by the National Institute of Arthritis and Musculoskeletal and Skin Diseases (grant HHSN-268201000019C).

Supported by the NIH (grants AG-018393, AR-047785, AG-018820, AG-018832, AG-018947, and AG-019069).

[1]Chan Kim, MD, Ali Guermazi, MD, PhD, Jingbo Niu, DSc, Margaret Clancy, MPH, MS: Boston University School of Medicine, Boston, Massachusetts; [2]Michael Nevitt, PhD, MPH, Irina Tolstykh, PhD: University of California, San Francisco; [3]Pia M. Jungmann, MD: University Hospital Zurich, University of Zurich, Zurich, Switzerland; [4]Nancy E. Lane, MD: University of California, Davis; [5]Neil A. Segal, MD, MS: University of Kansas Medical Center, Kansas City; [6]William F. Harvey, MD: Tufts Medical Center, Boston, Massachusetts; [7]Cora E. Lewis, MD, MSPH: University of Alabama at Birmingham; [8]David T. Felson, MD, MPH: Boston University School of Medicine, Boston, Massachusetts, and NIHR Manchester Musculoskeletal Biomedical Research Centre, University of Manchester, Manchester, UK.

Dr. Guermazi has received consulting fees and/or speaking fees from TissueGene, GE, AstraZeneca, Sanofi, and OrthoTrophix (less than $10,000 each) and from MerckSerono and Pfizer (more than $10,000 each) and owns stock in Boston Imaging Core LB, LLC.

Address correspondence to David T. Felson, MD, MPH, Clinical Epidemiology Research & Training Unit, Boston University School of Medicine, 650 Albany Street, Boston, MA 02118. E-mail: dfelson@bu.edu.

Submitted for publication January 2, 2018; accepted in revised form April 19, 2018.

MOST), and LLI of ≥2 cm is rare (~1% in the MOST). Furthermore, hip OA has a lower prevalence and incidence than knee OA. Therefore, in the present study examining the association of LLI with hip OA, we combined data from the MOST and the Osteoarthritis Initiative (OAI), 2 large longitudinal cohort studies of OA, in order to increase the size of the study population.

PATIENTS AND METHODS

Multicenter Osteoarthritis Study. The MOST is a multicenter longitudinal community-based study of 3,026 participants ages 50–79 years with or at risk for knee OA. MOST participants were recruited from 2 US communities: Birmingham, AL and Iowa City, IA. Details of the study population have been published elsewhere (3–5). Subjects were excluded if they had bilateral total knee replacement, rheumatoid arthritis, ankylosing spondylitis, psoriatic arthritis, reactive arthritis, or a history of cancer (except for nonmelanoma skin cancer), needed dialysis, were unable to walk without the help of another person or use of a walker, or planned to move out of the area in the subsequent 3 years. Long limb radiographs obtained at baseline and 60 months were used to assess LLI and radiographic hip OA.

Long limb length evaluation. Leg lengths were measured as the distance from the center of the femoral head to the tibial midplafond point (the most distal portion of the tibia directly over the talar dome), and LLI was recorded as the difference between legs in these lengths. A detailed description of the leg length measurement in the MOST has been published (2).

Hip OA evaluation. Long limb radiographs were read independently by 2 trained investigators, 1 an experienced musculoskeletal radiologist (AG) and the other a rheumatologist trained in reading hip radiographs (CK), for individual features of radiographic OA of the hip (RHOA) in accordance with the Osteoarthritis Research Society International (OARSI) atlas (6,7). Definite femoral and acetabular osteophytes and superolateral and superomedial joint space narrowing (JSN) were defined as OARSI atlas grades of ≥2. Hips were classified as having definite RHOA based on the individual radiographic features present, using the following criteria (8): 1) a Croft grade of ≥2 (presence of 2 or more of the following: definite osteophytes, definite JSN, sclerosis, cysts, or deformity); 2) definite JSN plus OARSI grade ≥1 femoral osteophytes; 3) definite femoral osteophytes regardless of the presence of other radiographic features; or 4) definite superolateral JSN or OARSI grade ≥3 superomedial JSN regardless of other features. The rheumatologist read all of the radiographs, and the radiologist read a selected number of radiographs including all of those the rheumatologist had classified as showing RHOA. Intraobserver agreement (κ) was 0.80 for the presence/absence of RHOA in a sample of 168 radiographs that were reread with the readers being unaware of previous scores. Among 90 radiographs that were read as negative for OA by the rheumatologist, the radiologist classified 5 as showing OA. If there was a disagreement between readers, the classification made by the radiologist was used.

Osteoarthritis Initiative. The OAI is a multicenter longitudinal cohort study of OA in 4,796 persons ages 45–79 years recruited during 2003–2005 at 4 centers: Columbus, OH, Providence, RI, Baltimore, MD, and Pittsburgh, PA. The researchers recruited participants if they had or were at increased risk for knee OA. A description of the OAI is available at www.oai.ucsf.edu. Inclusion criteria required that participants had to be ambulatory (use of assistive devices such as canes and walkers was allowed) with no plans to move away from the area for at least 3 years. Subjects were excluded if they had a history of bilateral total knee replacement, bilateral bone-on-bone radiographic knee OA, rheumatoid arthritis, contraindications to magnetic resonance imaging, or comorbidities that might interfere with the ability to participate in a study for 4 years. The long limb radiographs used to measure leg length were obtained at 12-month, 24-month, 36-month, or 48-month follow-up visits (26%, 40%, 30%, and 4% of subjects, respectively). Pelvic radiographs were obtained at baseline and 48-month follow-up and were used to assess radiographic hip OA.

Long limb length evaluation. The long limb measurements were performed by the same readers who read the MOST radiographs, using the same protocol.

Hip OA evaluation. In contrast to the MOST, in which long limb radiographs were used to assess RHOA, the OAI participants underwent standard weight-bearing anteroposterior pelvic radiography, which was used to assess RHOA. The pelvic radiographs were read by 2 musculoskeletal radiologists (including 1 of the authors [PMJ]) and a rheumatologist (NEL) for individual radiographic features of hip OA, using the OARSI atlas (6). A detailed radiograph reading protocol has been published (7). RHOA was defined by the same criteria applied in the MOST cohort (8). Test–retest agreement (κ) for the presence/absence of RHOA was 0.77 in a sample of 189 radiographs reassessed under blinded conditions.

Analyses. Analyses were restricted to subjects with available leg length data from both limbs. Subjects with a total knee or total hip replacement in either limb at baseline were excluded. If outcome data were missing in 1 hip (usually unreadable hip joint due to poor radiograph quality), the contralateral limb was still included in the analysis. We performed analyses using 2 different definitions of LLI (≥1 cm and ≥2 cm). For analyses evaluating LLI of ≥1 cm, LLI was categorized as either <1 cm (referent) or ≥1 cm. For analyses of LLI of ≥2 cm, LLI was categorized as <1 cm (referent), 1 to <2 cm, or ≥2 cm. For each LLI category we examined the risk of hip OA in the shorter limb separately from the risk in the longer limb. First, we examined the cross-sectional association of LLI with the prevalence of RHOA using logistic regression models with generalized estimating equations. We then examined the longitudinal

Table 1. Characteristics of the study subjects from the MOST and the OAI*

	MOST (n = 1,966)	OAI (n = 2,627)
Age, mean ± SD years	61.9 ± 7.9	61.0 ± 9.1
Sex, no. (%) male	777 (39.5)	1,114 (42.4)
Race, no. (%) white	1,671 (85.0)	2,144 (81.6)
BMI, mean ± SD kg/m^2	29.9 ± 5.1	28.2 ± 4.6
Height, mean ± SD cm	169.4 ± 9.4	168.2 ± 9.5
Leg length difference category, no. (%)		
Difference <1 cm	1,709 (86.9)	2,285 (87.0)
Difference between 1 cm and 2 cm	240 (12.2)	304 (11.6)
Difference ≥2 cm	17 (0.9)	28 (1.1)

* MOST = Multicenter Osteoarthritis Study; OAI = Osteoarthritis Initiative; BMI = body mass index.

Table 2. Relationship between leg length inequality of ≥1 cm and hip OA*

	Degree of leg length inequality		
	From –1 cm to 1 cm	Shorter limb when LLI is ≥1 cm	Longer limb when LLI is ≥1 cm
Prevalent hip OA			
Hips, n/N (%)	450/7,969 (5.6)	51/587 (8.7)	39/588 (6.6)
Crude OR (95% CI)	Referent	1.58 (1.16–2.16)	1.18 (0.84–1.67)
Adjusted OR (95% CI)†	Referent	1.47 (1.07–2.02)	1.09 (0.77–1.55)
Incident hip OA			
Hips, n/N (%)	141/6,971 (2.0)	15/505 (3.0)	17/516 (3.3)
Crude OR (95% CI)	Referent	1.50 (0.89–2.53)	1.65 (1.00–2.72)
Adjusted OR (95% CI)†	Referent	1.39 (0.81–2.39)	1.56 (0.93–2.60)

* OA = osteoarthritis; LLI = leg length inequality; n/N = number of hips with the outcome (prevalent hip OA or incident hip OA)/number of hips in the LLI category; OR = odds ratio; 95% CI = 95% confidence interval.
† Adjusted for age, sex, race (white/nonwhite), body mass index, and height (sex-specific quartiles).

relationship of baseline LLI with incident hip OA. Incident hip OA was defined as a hip without RHOA at baseline that had developed RHOA at follow-up. Although total hip replacements at baseline were excluded, total hip replacements were not excluded from the follow-up period, and a patient with a total hip replacement was considered to have incident hip OA. Analyses were adjusted for age, sex, race (white/nonwhite), body mass index, height (sex-specific quartiles), and cohort of origin.

RESULTS

Characteristics of the subjects from both cohorts are shown in Table 1. There were 1,966 subjects from the MOST and 2,627 subjects from the OAI who had complete data and were included in the analysis.

In the combined analysis of the MOST and OAI cohorts with LLI ≥1 cm, the adjusted odds ratio (OR) for prevalent RHOA in the shorter leg was 1.47 (95% confidence interval [95% CI] 1.07–2.02) and the OR for prevalent RHOA in the longer leg was 1.09 (95% CI 0.77–1.55) (Table 2). With LLI ≥2 cm, the adjusted OR for prevalent RHOA in the shorter leg and in the longer leg was 2.15 (95% CI 0.87–5.34) and 1.31 (95% CI 0.46–3.74), respectively (Table 3). For incident RHOA with LLI ≥1 cm, the OR in the shorter leg was 1.39 (95% CI 0.81–2.39) and the OR in the longer leg was 1.56 (95% CI 0.93–2.60). With LLI ≥2 cm, the OR for incident RHOA was 4.20 (95% CI 1.26–14.03) in the shorter leg and 1.32 (95% CI 0.20–8.66) in the longer leg (Tables 2 and 3).

DISCUSSION

Our study provides mixed evidence that, in individuals with LLI, the shorter limb is at increased risk of radiographic hip OA. With LLI ≥1 cm, the shorter limb had a significant 1.47-fold odds of prevalent RHOA in both cohorts combined. With LLI ≥2 cm, the OR for prevalent RHOA in the shorter leg was increased (2.15 [95% CI 0.87–5.34]) but the increase did not reach statistical significance. The lack of significance may be due to limited numbers of subjects with this degree of LLI.

For incident RHOA, there was not a significant association with LLI ≥1 cm. Among subjects with LLI ≥2 cm, there was a significant 4.2-fold increased odds of incident RHOA in the shorter limb. However, this positive association was based on small numbers.

Minor degrees of LLI are common and have been reported to occur in up to 70–90% of the population (9–11). LLI may be congenital or acquired, with causes including trauma, infection, and scoliosis causing pelvic tilt

Table 3. Relationship between leg length inequality of ≥2 cm and hip OA*

	Degree of leg length inequality				
	From –1 cm to 1 cm	Shorter limb when LLI is ≥1 cm but ≤2 cm	Longer limb when LLI is ≥1 cm but ≤2 cm	Shorter limb when LLI is ≥2 cm	Longer limb when LLI is ≥2 cm
Prevalent hip OA					
Hips, n/N (%)	450/7,969 (5.6)	45/543 (8.3)	35/543 (6.4)	6/44 (13.6)	4/45 (8.9)
Crude OR (95% CI)	Referent	1.50 (1.09–2.08)	1.15 (0.80–1.65)	2.60 (1.09–6.22)	1.62 (0.58–4.57)
Adjusted (95% CI)†	Referent	1.41 (1.01–1.97)	1.07 (0.74–1.55)	2.15 (0.87–5.34)	1.31 (0.46–3.74)
Incident hip OA					
Hips, n/N (%)	141/6,971 (2.0)	12/469 (2.6)	16/478 (3.3)	3/36 (8.3)	1/38 (2.6)
Crude OR (95% CI)	Referent	1.30 (0.73–2.30)	1.67 (1.00–2.79)	4.17 (1.26–13.76)	1.41 (0.23–8.47)
Adjusted OR (95% CI)†	Referent	1.20 (0.66–2.16)	1.57 (0.93–2.66)	4.20 (1.26–14.03)	1.32 (0.20–8.66)

* OA = osteoarthritis; LLI = leg length inequality; n/N = number of hips with the outcome (prevalent hip OA or incident hip OA)/number of hips in the LLI category; OR = odds ratio; 95% CI = 95% confidence interval.
† Adjusted for age, sex, race (white/nonwhite), body mass index, and height (sex-specific quartiles).

(12–14). However, the degree of LLI at which it becomes clinically significant is controversial (9,10,15–18). In this study, we chose to assess LLI of ≥1 cm and ≥2 cm.

Although it is known that LLI causes abnormal loading of the lower extremities, the pathophysiology of its contribution to lower extremity OA is not completely understood. The shorter leg sustains increased impact force with foot strike during gait, thus transmitting a greater impulse up the ipsilateral leg. A prior cross-sectional study of hip OA and LLI by Gofton and Trueman showed an increased prevalence of RHOA in the longer limb in hip arthroplasty patients (19). In that study, RHOA in the longer limb was postulated to occur because the longer limb sustained excessive load while weight bearing. In cross-sectional data from the Johnston County Osteoarthritis Study in which LLI was assessed using a physical examination measure, there was an association between shorter leg length and ipsilateral right hip OA but not left hip OA (20). In a longitudinal analysis, there was a nonsignificant trend toward development of hip OA in the shorter limb (21). In the present study, there was a modest increase in prevalent RHOA in the shorter limb in the crude analyses, whereas we found a significant association of LLI ≥2 cm with incident hip OA. In a study of LLI and knee OA in subjects from the MOST, higher rates of prevalent and incident knee OA occurred in the shorter limb (2).

A limitation of the present study is the fact that severe hip OA with femoral head flattening may shorten the affected limb; thus, the direction of causality in the cross-sectional analyses is uncertain. In most cases of hip OA, however, leg length should not be affected. Our finding of a positive association of incident hip OA in the shorter leg with LLI ≥2 cm was based on small numbers (3 of 36 subjects with LLI ≥2 cm developed hip OA in the combined cohort). Similarly, the Johnston County incident hip OA results were based on single-digit numbers of outcomes for LLI ≥2 cm (9 hips with RHOA of 62 hips in the shorter leg versus 3 hips with RHOA of 57 hips in the longer leg). In general, marked LLI is uncommon and its consequences are difficult to study even in large cohorts. Furthermore, the follow-up period in the present study (60 months in subjects from the MOST and 48 months in subjects from the OAI) may not be long enough to detect robust numbers of new hip OA cases. Because our cohorts included participants at risk for or with knee OA, the findings may not be generalizable to the general population. In the MOST specifically, RHOA was assessed on long limb radiographs, and the limitations of this method have been discussed previously (1,22).

LLI is likely treatable with shoe modifications such as heel lifts, which are simple and inexpensive. Hip OA is a disease with few significant modifiable risk factors, and current nonsurgical treatment modalities are of only moderate efficacy. The present study provides evidence to suggest that equalizing leg lengths may reduce the risk of hip OA.

In summary, leg length inequality increased the risk of prevalent and incident radiographic hip osteoarthritis, with a greater effect on risk in the shorter limb. Leg length inequality is easily correctable, so this association might identify a correctable cause of hip OA.

AUTHOR CONTRIBUTIONS

All authors were involved in drafting the article or revising it critically for important intellectual content, and all authors approved the final version to be published. Dr. Felson had full access to all of the data in the study and takes responsibility for the integrity of the data and the accuracy of the data analysis.

Study conception and design. Kim, Nevitt, Guermazi, Tolstykh, Harvey, Lewis, Felson.

Acquisition of data. Kim, Nevitt, Guermazi, Clancy, Tolstykh, Jungmann, Lane, Segal, Lewis.

Analysis and interpretation of data. Kim, Nevitt, Guermazi, Niu, Tolstykh, Lane, Segal, Harvey.

REFERENCES

1. Kim C, Linsenmeyer KD, Vlad SC, Guermazi A, Clancy MM, Niu J, et al. Prevalence of radiographic and symptomatic hip osteoarthritis in an urban United States community: the Framingham Osteoarthritis Study. Arthritis Rheumatol 2014;66:3013–7.
2. Harvey WF, Yang M, Cooke TD, Segal NA, Lane N, Lewis CE, et al. Association of leg-length inequality with knee osteoarthritis: a cohort study. Ann Intern Med 2010;152:287–95.
3. Guermazi A, Roemer FW, Hayashi D, Crema MD, Niu J, Zhang Y, et al. Assessment of synovitis with contrast-enhanced MRI using a whole-joint semiquantitative scoring system in people with, or at high risk of, knee osteoarthritis: the MOST study. Ann Rheum Dis 2011;70:805–11.
4. Guermazi A, Hayashi D, Roemer FW, Zhu Y, Niu J, Crema MD, et al. Synovitis in knee osteoarthritis assessed by contrast-enhanced magnetic resonance imaging (MRI) is associated with radiographic tibiofemoral osteoarthritis and MRI-detected widespread cartilage damage: the MOST study. J Rheumatol 2014;41:501–8.
5. Stefanik JJ, Neogi T, Niu J, Roemer FW, Segal NA, Lewis CE, et al. The diagnostic performance of anterior knee pain and activity-related pain in identifying knees with structural damage in the patellofemoral joint: the Multicenter Osteoarthritis Study. J Rheumatol 2014;41:1695–702.
6. Altman RD, Gold GE. Atlas of individual radiographic features in osteoarthritis, revised. Osteoarthritis Cartilage 2007;15 Suppl A:A1–56.
7. Joseph GB, Hilton JF, Jungmann PM, Lynch JA, Lane NE, Liu F, et al. Do persons with asymmetric hip pain or radiographic hip OA have worse pain and structure outcomes in the knee opposite the more affected hip? Data from the Osteoarthritis Initiative. Osteoarthritis Cartilage 2016;24:427–35.
8. Arden NK, Lane NE, Parimi N, Javaid KM, Lui LY, Hochberg MC, et al. Defining incident radiographic hip osteoarthritis for epidemiologic studies in women. Arthritis Rheum 2009;60:1052–9.
9. Woerman AL, Binder-Macleod SA. Leg length discrepancy assessment: accuracy and precision in five clinical methods of evaluation. J Orthop Sports Phys Ther 1984;5:230–9.
10. Knutson GA. Anatomic and functional leg-length inequality: a review and recommendation for clinical decision-making. Part I. Anatomic leg-length inequality: prevalence, magnitude, effects and clinical significance. Chiropr Osteopat 2005;13:11.

11. Knutson GA. Anatomic and functional leg-length inequality: a review and recommendation for clinical decision-making. Part II. The functional or unloaded leg-length asymmetry. Chiropr Osteopat 2005;13:12.
12. Murray KJ, Azari MF. Leg length discrepancy and osteoarthritis in the knee, hip and lumbar spine. J Can Chiropr Assoc 2015; 59:226–37.
13. Gurney B. Leg length discrepancy. Gait Posture 2002;15:195–206.
14. Papaioannou T, Stokes I, Kenwright J. Scoliosis associated with limb-length inequality. J Bone Joint Surg Am 1982;64:59–62.
15. Beal MC. The short leg problem. J Am Osteopath Assoc 1977; 76:745–51.
16. Subotnick SI. Limb length discrepancies of the lower extremity (the short leg syndrome). J Orthop Sports Phys Ther 1981;3:11–6.
17. Cathie AG. The influence of the lower extremities upon the structural integrity of the body. J Am Osteopath Assoc 1950; 49:443–6.
18. Friberg O. Clinical symptoms and biomechanics of lumbar spine and hip joint in leg length inequality. Spine 1983;8:643–51.
19. Gofton JP, Trueman GE. Studies in osteoarthritis of the hip. Part II. Osteoarthritis of the hip and leg-length disparity. Can Med Assoc J 1971;104:791–9.
20. Golightly YM, Allen KD, Renner JB, Helmick CG, Salazar A, Jordan JM. Relationship of limb length inequality with radiographic knee and hip osteoarthritis. Osteoarthritis Cartilage 2007;15:824–9.
21. Golightly YM, Allen KD, Helmick CG, Schwartz TA, Renner JB, Jordan JM. Hazard of incident and progressive knee and hip radiographic osteoarthritis and chronic joint symptoms in individuals with and without limb length inequality. J Rheumatol 2010; 37:2133–40.
22. Kim C, Nevitt MC, Niu J, Clancy MM, Lane NE, Link TM, et al. Association of hip pain with radiographic evidence of hip osteoarthritis: diagnostic test study. BMJ 2015;351:h5983.

ARTHRITIS & RHEUMATOLOGY
Vol. 70, No. 10, October 2018, pp 1577–1587
DOI 10.1002/art.40545

Functional Characterization of the Osteoarthritis Genetic Risk Residing at *ALDH1A2* Identifies rs12915901 as a Key Target Variant

Colin Shepherd,[1] Dongxing Zhu,[2] Andrew J. Skelton,[1] Jennifer Combe,[1] Harrison Threadgold,[1] Linyi Zhu,[3] Tonia L. Vincent,[3] Paul Stuart,[4] Louise N. Reynard,[1] and John Loughlin[1]

Objective. **To identify the functional single-nucleotide polymorphisms (SNPs) and mechanisms conferring increased risk of hand osteoarthritis (OA) at the *ALDH1A2* locus, which is a retinoic acid regulatory gene.**

Methods. **Tissue samples from 247 patients with knee, hip, or hand OA who had undergone joint surgery were included. RNA-sequencing analysis was used to investigate differential expression of *ALDH1A2* and other retinoic acid signaling pathway genes in cartilage. Expression of *ALDH1A2* in joint tissues obtained from multiple sites was quantified using quantitative reverse transcription–polymerase chain reaction. Allelic expression imbalance (AEI) was measured by pyrosequencing. The consequences of *ALDH1A2* depletion by RNA interference were assessed in primary human chondrocytes. In silico and in vitro analyses were used to pinpoint which, among 62 highly correlated SNPs, could account for the association at the locus.**

Results. ***ALDH1A2*** **expression was observed across multiple joint tissue samples, including osteochondral tissue from the hand. The expression of *ALDH1A2* and of several retinoic acid signaling genes was different in diseased cartilage compared to non-diseased cartilage, with *ALDH1A2* showing lower levels in OA cartilage. Experimental depletion of *ALDH1A2* resulted in changes in the expression levels of a number of chondrogenic markers, including *SOX9*. In addition, reduced expression of the OA risk–conferring allele was witnessed in a number of joint tissues, with the strongest effect in cartilage. The intronic SNP rs12915901 recapitulated the AEI observed in patient tissues, while the Ets transcription factors were identified as potential mediators of this effect.**

Conclusion. **The *ALDH1A2* locus seems to increase the risk of hand OA through decreased expression of *ALDH1A2* in joint tissues, with the effect dependent on rs12915901. These findings indicate a mechanism that may now be targeted to modulate OA risk.**

Osteoarthritis (OA) is a common age-related disease that is characterized by the focal loss of cartilage, and that is accompanied by pathologic alterations to additional joint tissues (1). There are no disease-modifying drugs for OA, with arthroplasty of the hips and knees being a common procedure.

Epidemiologic studies have reported an OA heritability of >40% at individual skeletal sites (2), while data sets from candidate-gene and genome-wide association studies have revealed that OA is polygenic, with the evidence indicating that there is no risk-conferring loci of large singular impact. As such, the disease is genetically complex and multifactorial.

Supported by Arthritis Research UK (grant 20771 and Centre for OA Pathogenesis grant 20205), the Medical Research Council, the MRC–Arthritis Research UK Centre for Integrated Research into Musculoskeletal Ageing, and the European Union under the Seventh Framework Program (grant 305815; project D-BOARD). Funds to assist recruitment of patients and processing of tissue were provided by the NIHR Newcastle Biomedical Research Centre and awarded to the Newcastle upon Tyne NHS Foundation Trust and Newcastle University.

[1]Colin Shepherd, PhD, Andrew J. Skelton, MSc, Jennifer Combe, BSc, Harrison Threadgold, MSc, Louise N. Reynard, PhD, John Loughlin, PhD: Newcastle University, Newcastle upon Tyne, UK; [2]Dongxing Zhu, PhD: Newcastle University, Newcastle upon Tyne, UK, and Guangzhou Institute of Cardiovascular Disease, The Second Affiliated Hospital, and Guangzhou Medical University, Guangzhou, China; [3]Linyi Zhu, PhD, Tonia L. Vincent, MD, PhD: Arthritis Research UK Centre for OA Pathogenesis, University of Oxford, Oxford, UK; [4]Paul Stuart, FRCS: Newcastle University Teaching Hospitals NHS Trust, Freeman Hospital, Newcastle upon Tyne, UK.

Drs. Shepherd and Zhu contributed equally to this work.

Address correspondence to Colin Shepherd, PhD, or John Loughlin, PhD, Institute of Genetic Medicine, Newcastle University, International Centre for Life, Newcastle upon Tyne NE2 4HH, UK. E-mail: colin.shepherd@ncl.ac.uk or john.loughlin@ncl.ac.uk.

Submitted for publication December 5, 2017; accepted in revised form April 26, 2018.

To date, the OA loci identified are typically located within regions of the genome harboring genes encoding proteins involved in joint development, maturation, or homeostasis and that tend to contribute to disease susceptibility only at particular skeletal sites (2–5). An example of this is the hand OA–associated single-nucleotide polymorphisms (SNPs) in *ALDH1A2* (6). *ALDH1A2* codes for the enzyme RALDH2, which synthesizes the morphogen retinoic acid. Studies have shown that retinoic acid has pivotal roles in the development and maintenance of the skeleton, with its effect mediated at the gene transcriptional level (7,8).

The association of *ALDH1A2* with OA risk was discovered in Icelanders and replicated in cohorts from the UK and Netherlands in studies using proxy SNPs rs3204689 and rs4238326. The greatest odds ratio in the combined analysis was 1.46 for rs3204689 ($P = 1.1 \times 10^{-11}$). None of the SNPs that correlate ($r^2 > 0.8$) with rs3204689 or rs4238326 are nonsynonymous, implying that the association acts by modulating gene expression as a quantitative trait locus (eQTL). The presence of an eQTL operating on *ALDH1A2* was confirmed using the 3′-untranslated region (3′-UTR) SNP rs3204689. An average 17.4% excess expression of *ALDH1A2* messenger RNA (mRNA) from the non-risk G allele, relative to the risk-conferring C allele, was reported in knee and hip cartilage samples (6). This is equivalent to a 15% reduction in *ALDH1A2* expression in the presence of the risk allele.

In this study, we aimed to expand the allelic expression imbalance (AEI) analysis into other synovial joint tissues and to the trapezium of patients who had undergone a trapeziectomy due to hand OA. We carried out a broad analysis of the expression of *ALDH1A2* and genes involved in the retinoic acid pathway. Finally, we performed experiments to identify a SNP or SNPs in the association signal that recapitulate the AEI effect observed in patient tissues and which could, therefore, be functional candidate SNPs.

PATIENTS AND METHODS

Patients. Joint tissue samples were obtained through 2 centers in the UK, Newcastle and Oxford. The Newcastle collection was undertaken essentially as previously described (9). The Newcastle and North Tyneside Research Ethics Committee granted ethics approval for the collection. Each donor provided verbal and written informed consent (REC reference no. 14/NE/1212). Samples were collected from 1) patients with primary hip or knee OA who had undergone joint replacement surgery, 2) patients with primary hand OA who had undergone trapeziectomy, and 3) patients who had undergone hip replacement due to a neck-of-femur (NOF) fracture. For patients with hand OA, cartilage could not be readily separated from fractured subchondral bone; therefore these samples comprised subchondral bone with attached cartilage (i.e., osteochondral samples). Tissue preparation and grinding was performed as described previously (10).

DNA and RNA were extracted from the cartilage, bone, and trapezieum samples using TRIzol reagent (Life Technologies). For the synovium and fat pad, DNA and RNA were extracted using an E.Z.N.A. DNA/RNA isolation kit (Omega Biotek, VWR) (11). Primary human chondrocytes were prepared and cultured as previously reported (12).

The Oxford Musculoskeletal Biobank collection provided samples of OA trapezium. Patients gave their informed consent for sample collection (REC reference no. 09/H0606/11). Trapezium cartilage was dissected from the bone within 2 hours of surgical removal from the joint, and the tissue was then snap frozen in liquid nitrogen and stored at −80°C. Cartilage and bone tissue were ground using a Cryo-Cup Grinder (Biospec). RNA was extracted from cartilage using an RNeasy Micro kit (Qiagen). DNA was extracted from the bone using DNAzol (Thermo Fisher Scientific).

Further details regarding both the Newcastle and Oxford patients can be found in Supplementary Table 1 (available on the *Arthritis & Rheumatology* web site at http://onlinelibrary.wiley.com/doi/10.1002/art.40545/abstract).

Quantitation of gene expression. Synthesis of complementary DNA (cDNA) and analysis by quantitative reverse transcription–polymerase chain reaction (qRT-PCR) were performed as described previously (9). Predesigned TaqMan assays (Integrated DNA Technologies) were used to quantify expression of the housekeeping genes *HPRT1*, *18S*, and *GAPDH* and the target genes *COL2A1*, *COL10A1*, *SOX9*, *ACAN*, *ADAMTS5*, *VEGFA*, *RUNX2*, and *MMP13*. For target genes *ALDH1A2*, *RARA*, *RARB*, *RARG*, *RXRA*, *RXRB*, *CRABP2*, and *CYP26B1*, primers were designed using the Roche probe library system (see Supplementary Table 2, available on the *Arthritis & Rheumatology* web site at http://onlinelibrary.wiley.com/doi/10.1002/art.40545/abstract). *P* values were calculated using a Mann-Whitney 2-tailed exact test.

RNA-sequencing (RNA-seq) analysis. RNA-seq analysis was performed on the cartilage of 10 patients with hip OA and 6 patients with NOF fracture (non-OA controls) (the RNA-seq data have been deposited in the NCBI Gene Expression Omnibus [accession no. GSE111358]). Quality of the raw sequencing data was assessed using Fastqc (version 0.11.5) and compiled for experiment-wide context using MultiQC (version 1.0dev) (13,14). Salmon software (version 0.8.2) was used to quantify raw Fastq files, based on an index derived from Gencode V24 transcript sequences (15,16). Salmon was run in sequence and G/C bias correction models, with 100 bootstraps. Abundance estimations were analyzed in R (version 3.4.1), and estimates were imported using Tximport (version 1.4.0) (17–19). Statistical modeling was performed using DESeq2 (version 1.16.1) (20) to library-scale normalize the raw counts and fit a negative binomial generalized linear model. Hypothesis testing was performed using the DESeq2 implementation of the Wald test. Statistical significance of the analyzed genes was determined on the basis of a false discovery rate–corrected *P* value of <0.01 and a fold change filter of 2.

Genotyping. The rs3204689 SNP was genotyped by a restriction fragment length polymorphism assay. The SNP was

amplified by PCR using the primers listed in Supplementary Table 3 (available on the *Arthritis & Rheumatology* web site at http://onlinelibrary.wiley.com/doi/10.1002/art.40545/abstract). The discriminatory enzyme was *SfcI* (New England Biolabs), which cuts at the non-risk G allele.

The rs4238326 SNP was genotyped by pyrosequencing (see Supplementary Table 3 for the primers used). PCR products were analyzed using the PyroMark Q24 MDx platform (Qiagen), with use of the sequencing primer listed in Supplementary Table 3 and PyroMark Gold Q96 reagents, in accordance with the manufacturer's instructions.

Determination of allelic expression imbalance (AEI). AEI at rs3204689 was quantified by pyrosequencing, using the pyrosequencing methods described above and the PCR and sequencing primers listed in Supplementary Table 3. Analysis of the results was performed as described previously (9). *P* values were calculated using a Mann-Whitney 2-tailed exact test.

Determination of mRNA stability. Chondrocytes were isolated from the cartilage of 4 patients with knee OA who were heterozygous at rs3204689. The cells were seeded in 6-well plates at 400,000 cells per well, and then treated with 5 μg/ml actinomycin D (Sigma-Aldrich) for 0, 4, 8, 12, and 24 hours. Nucleic acid was extracted using TRIzol reagent (Life Technologies), and expression of *ALDH1A2* was measured by qRT-PCR.

AEI at rs3204689 was assessed by pyrosequencing. Expression of *ALDH1A2* mRNA in the combined group of patients was compared at each time point relative to time 0. *P* values were calculated using a Mann-Whitney 2-tailed exact test.

RNA interference (RNAi). RNAi was performed in chondrocytes isolated from the cartilage of 3 patients with knee OA, essentially as described previously (9). For each patient, the cells were seeded in each well of a 6-well plate at a density of 350,000 cells per well. Cells were transfected with 50 n*M* Dharmacon ON-TARGET*plus* SMARTpool small interfering RNA (siRNA) targeted against *ALDH1A2* (L-008118-00) or a nontargeting siRNA as the control (D-001810-10-20). RNA and protein were extracted concurrently using the Nucleospin RNA/protein kit (Macherey-Nagel). Gene expression was assessed by qRT-PCR using cDNA synthesized from RNA extracted from each well, with 5 technical repeats per analyzed gene. *P* values were calculated using a Student's 2-tailed *t*-test.

Immunoblotting. For immunoblot analysis of RALDH2 depletion following RNAi, 10 μg of protein was resolved on 10% (weight/volume) sodium dodecyl sulfate–polyacrylamide gel electrophoresis (SDS-PAGE) gels. Blots were probed with an anti-ALDH1A2 antibody (HPA010022; Atlas Antibodies) or anti-GAPDH antibody (Cell Signaling Technology). RALDH2 depletion was quantified using ImageJ software (21), with RALDH2 values normalized to the levels of anti-GAPDH. *P* values were calculated using Student's 2-tailed *t*-test.

For immunoblot analysis of RALDH2 in ground trapezium bone samples, cellular protein was extracted with radioimmunoprecipitation assay buffer. Twenty micrograms of clarified lysate was resolved by SDS-PAGE and immunoblotted as described above.

Luciferase reporter assays. DNA regions surrounding the 39 SNPs selected for analysis were cloned and used for luciferase reporter analysis, essentially as described previously (9). Primer sequences are listed in Supplementary Table 4 (available on the *Arthritis & Rheumatology* web site at http://onlinelibrary.wiley.com/doi/10.1002/art.40545/abstract). The cell lines SW1353 and HEK 293 (both from ATCC) were seeded at 10,000 cells per well in 96-well plates, and after 24 hours, they were transfected with the firefly and *Renilla* luciferase constructs. *P* values were calculated using a Mann-Whitney 2-tailed exact test.

Electrophoretic mobility shift assays (EMSAs). Nuclear protein was extracted from SW1353 and HEK 293 cells as previously described (22). For each allele of each of the 8 SNPs studied, forward and reverse single-stranded DY682-labeled oligonucleotides (Eurofins MWG Operon), spanning 15 bp each side of the SNP (see Supplementary Table 5, available on the *Arthritis & Rheumatology* web site at http://onlinelibrary.wiley.com/doi/10.1002/art.40545/abstract), were annealed to generate double-stranded probes. EMSAs were then undertaken as previously described (22). For rs12915901, an Ets random competitor probe was used as a negative control (see Supplementary Table 6, available on the *Arthritis & Rheumatology* web site at http://onlinelibrary.wiley.com/doi/10.1002/art.40545/abstract).

RESULTS

Quantitative expression of *ALDH1A2* in joint tissues. We measured *ALDH1A2* expression by qRT-PCR in the cartilage, fat pad, synovium, and trabecular bone from OA patients who had undergone knee or hip joint replacement surgery. Expression was also measured in osteochondral tissue from patients who had undergone a trapeziectomy. Expression was highest in the cartilage and lowest in the bone and trapezium. In fact, the expression of *ALDH1A2* was below the limit of detection (established as a threshold cycle value of ≥40) in 17 of the 25 bone samples and 2 of the 8 trapezium samples (Figure 1A).

Having confirmed expression of *ALDH1A2* mRNA in the joint tissues, including samples from the trapezium of patients who underwent a trapeziectomy, we next confirmed expression of the RALDH2 protein by immunoblotting of the protein extracted from the trapezium tissue of patients with hand OA (see Supplementary Figure 1, available on the *Arthritis & Rheumatology* web site at http://onlinelibrary.wiley.com/doi/10.1002/art.40545/abstract).

Using RNA-seq data from the cartilage of OA patients and that from non-OA controls (i.e., age-matched patients with NOF fracture) who had undergone hip replacement surgery, we characterized the expression pattern of the *ALDH1A2* transcript isoforms. The Ensembl database (available at http://www.ensembl.org/index.html) lists 25 isoforms for this gene, of which 8 are predicted to be protein coding. Nine of the 25 isoforms were expressed in the analyzed

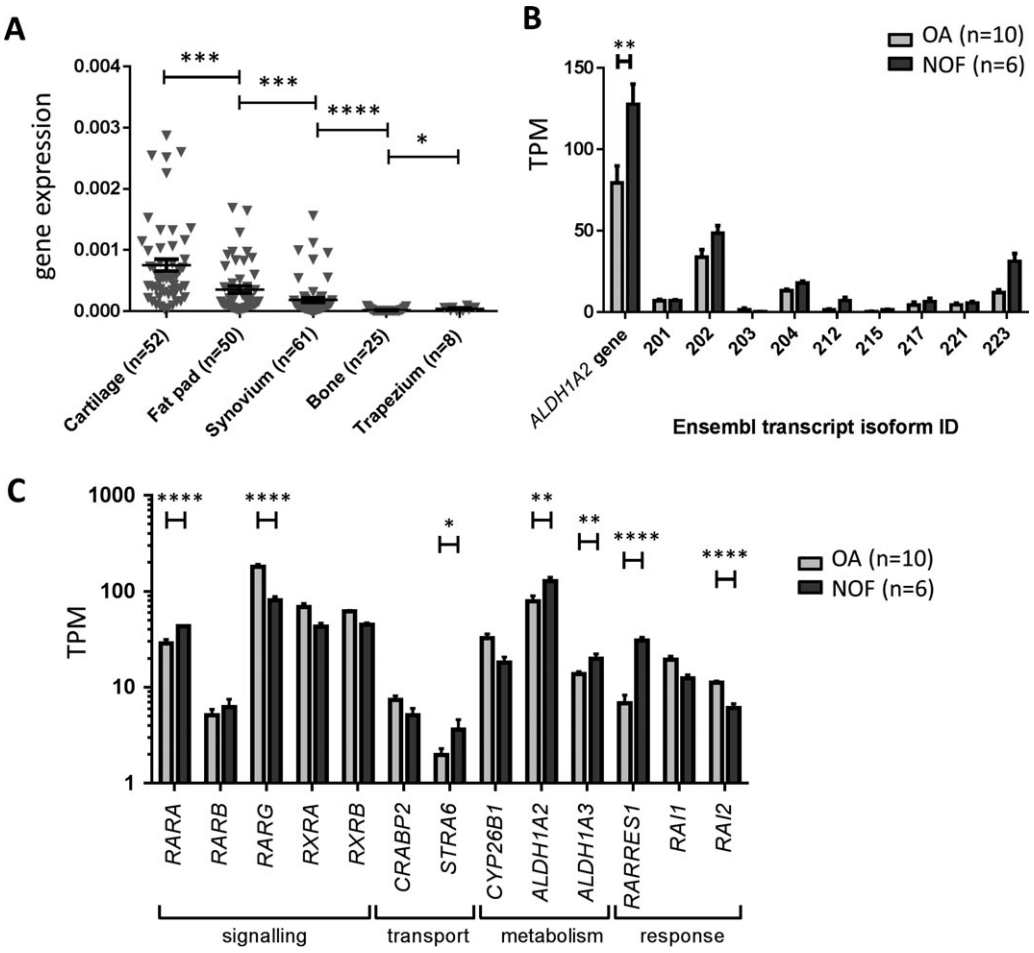

Figure 1. Expression analysis of *ALDH1A2* and retinoic acid pathway genes in multiple tissue samples from patients with osteoarthritis (OA). **A,** Expression of *ALDH1A2* mRNA was measured by quantitative reverse transcription–polymerase chain reaction in OA cartilage, fat pad, synovium, bone, and trapezium. **B,** Expression of *ALDH1A2* gene and transcript isoforms (designated by their Ensembl database identification [ID] numbers) was measured in hip cartilage from OA patients and patients with neck-of-femur (NOF) fracture as controls, using RNA-sequencing data. The category "*ALDH1A2* gene" represents all isoforms combined. **C**, Expression of a panel of retinoic acid pathway genes was measured in hip cartilage from OA patients and non-OA NOF controls, using RNA-sequencing data. The data for *ALDH1A2* are replotted for comparison. In **C**, transcripts per million (TPM) kilobase values are plotted as the $\log^{10}$. *P* values were calculated using Mann-Whitney 2-tailed exact test in **A** and Wald test within the DESeq2 package in **B** and **C**. In **A,** symbols represent individual samples; horizontal lines with bars show the mean ± SEM. In **B** and **C,** results are the mean ± SEM. * = $P < 0.05$; ** = $P < 0.01$; *** = $P < 0.001$; **** = $P < 0.0001$.

cartilage above a mean transcripts-per-million threshold of 1, including 4 of the 8 protein-coding isoforms (Figure 1B) (see also Supplementary Table 7, available on the *Arthritis & Rheumatology* web site at http://onlinelibrary.wiley.com/doi/10.1002/art.40545/abstract). When assessing expression of all *ALDH1A2* isoforms combined (designated the *ALDH1A2* gene in Figure 1B), there was a 0.3-fold decrease in *ALDH1A2* expression in the OA cartilage compared to the non-OA control cartilage ($P < 0.01$).

Differential expression of RA pathway genes in OA cartilage. The reduced expression of *ALDH1A2* in OA compared to non-OA cartilage prompted us to investigate our RNA-seq data for the relative expression of other genes active in the retinoic acid pathway (see Supplementary Table 8, available on the *Arthritis & Rheumatology* web site at http://onlinelibrary.wiley.com/doi/10.1002/art.40545/abstract). Of a panel of 13 genes selected as a representative cross-section of the retinoic acid pathway, and due to their relatively abundant levels of expression, several of these genes were differentially expressed between OA cartilage and non-OA control cartilage (Figure 1C). *RARRES1*, which codes for retinoic acid receptor responder 1, was one of the most significantly differentially expressed genes, with a 2.4-fold decreased expression in OA cartilage (P =

6×10^{-12}). The results of this analysis imply that there is a widespread differential regulation of the retinoic acid pathway between OA and non-OA cartilage.

AEI analysis of *ALDH1A2*. The investigators who reported the association of OA risk with *ALDH1A2* observed a reduction in expression of the OA risk–conferring allele of the gene in AEI analysis. We replicated this observation, detecting an average reduction of 28% in the expression of the risk C allele in the cartilage of patients who were heterozygous at rs3204689 ($P < 0.0001$), with the majority of patients demonstrating AEI (Figure 2A).

In our expanded analysis, we observed an average reduction of 14% in the expression of the risk C allele in the fat pad ($P < 0.0001$) (Figure 2B) and a reduction of 15% in the bone samples ($P = 0.001$)

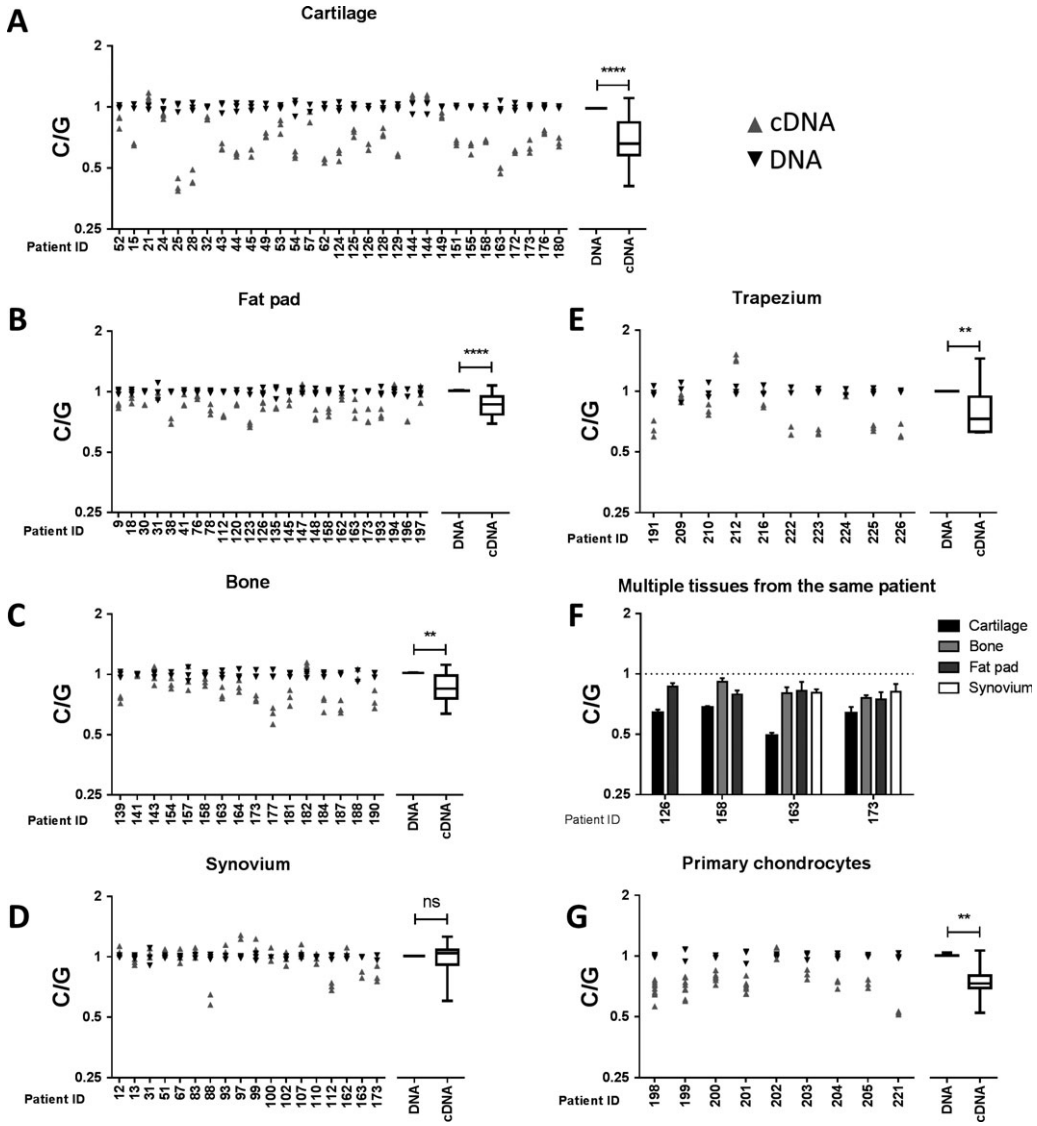

Figure 2. Allelic expression imbalance (AEI) analysis of *ALDH1A2*. **A–E** and **G**, AEI analysis of rs3204689 was carried out in osteoarthritis (OA) patient cartilage (n = 31) (**A**), fat pad (n = 24) (**B**), bone (n = 16) (**C**), synovium (n = 18) (**D**), trapezium (n = 10) (**E**), and primary chondrocytes (n = 9) (**G**). Plots in the left panels show the risk/non-risk (C/G) allelic ratios, with a ratio of <1 indicating decreased expression of the C allele. The right panels show the mean values for DNA and cDNA from all patients combined, with results represented as box-and-whisker plots, in which the lines within the box represent the median, the box represents the 25th to 75th percentiles, and the whiskers represent the minimum and maximum values. A minimum of 3 technical repeats were performed for each patient's DNA and cDNA. *P* values were calculated using Mann-Whitney 2-tailed exact test. **F,** AEI analysis was carried out in 4 OA patients for whom cartilage samples and tissue from at least one other site were available. The broken horizontal line indicates a C/G ratio of 1, which is indicative of no allelic imbalance. Values are the mean ± SD AEI plotted for each individual in each tissue tested. Individual patients are designated by their anonymized identification (ID) numbers. ** = $P < 0.01$; **** = $P < 0.0001$. NS = not significant.

(Figure 2C), whereas in the synovium, the reduction was nonsignificant (average reduction 2%; $P > 0.05$) (Figure 2D). We observed an average reduction of 18% in the expression of the risk allele in the trapezium ($P < 0.01$) (Figure 2E). Despite the nonsignificant AEI observed in synovium samples, there were individuals who did demonstrate clear AEI in the synovium (patients 88 and 112 in Figure 2D).

The reduction in expression of the OA risk allele was less profound in these noncartilaginous joint tissues, as was most clearly demonstrated when we compared AEI ratios in 4 patients for whom cartilage tissue and tissue from at least 1 other site from the same joint could be concurrently analyzed. In each patient, cartilage showed a larger AEI than that observed in any of the noncartilaginous tissue samples (Figure 2F).

It is noteworthy that in a small number of patients, the OA risk–conferring C allele was expressed at a higher level, rather than a lower level, than was the non-risk allele (Figures 2A–E). This was most obvious in the synovium of patient 97 (Figure 2D) and the osteochondral trapezium of patient 212 (Figure 2E).

Finally, we assessed AEI stability during tissue culture by extracting chondrocytes from the knee cartilage of 9 OA patients who were heterozygous at rs3204689, culturing the cells in monolayer for a minimum of 10 days and then undertaking AEI analysis (Figure 2G). We observed an average reduction of 25% in the expression of the risk allele ($P = 0.004$), which is comparable to the reduction seen in OA cartilage tissue samples (Figure 2A), thus suggesting that the AEI is stable during cell division in vitro.

Effect of knockdown of *ALDH1A2* on chondrocyte gene expression. Having demonstrated that the OA risk–conferring C allele of rs3204689 is correlated with decreased expression of *ALDH1A2*, we next modeled this effect. Chondrocytes were isolated from the knee cartilage of 3 OA patients, and then cultured in monolayer and subjected to *ALDH1A2* knockdown by RNAi. Compared to the effects of the scrambled siRNA control, siRNA targeting *ALDH1A2* achieved a mean knockdown at the *ALDH1A2* mRNA level of 89% ($P < 0.0001$) (Figure 3A), with a 22% reduction at the protein level ($P < 0.05$) (Figure 3B).

We next assessed the effect of this knockdown of *ALDH1A2* on the expression of 7 retinoic acid pathway genes (*RARA*, *RARB*, *RARG*, *RXRA*, *RXRB*, *CRABP2*, and *CYP26B1*) and 8 chondrogenic genes (*SOX9*, *ADAMTS5*, *MMP13,* *ACAN*, *COL2A1*, *COL10A1*, *RUNX2*, and *VEGFA*). Depletion of *ALDH1A2* correlated with a significant reduction in the expression of *RARB* ($P = 0.001$), *SOX9* ($P = 0.002$), *ADAMTS5* ($P = 0.007$), *ACAN* ($P = 0.04$), and *VEGFA* ($P = 0.004$) (Figures 3C–G). Therefore, in this model system, depletion of *ALDH1A2* transcript and of its protein in OA knee cartilage had a significant impact on genes that encode regulators of cartilage homeostasis.

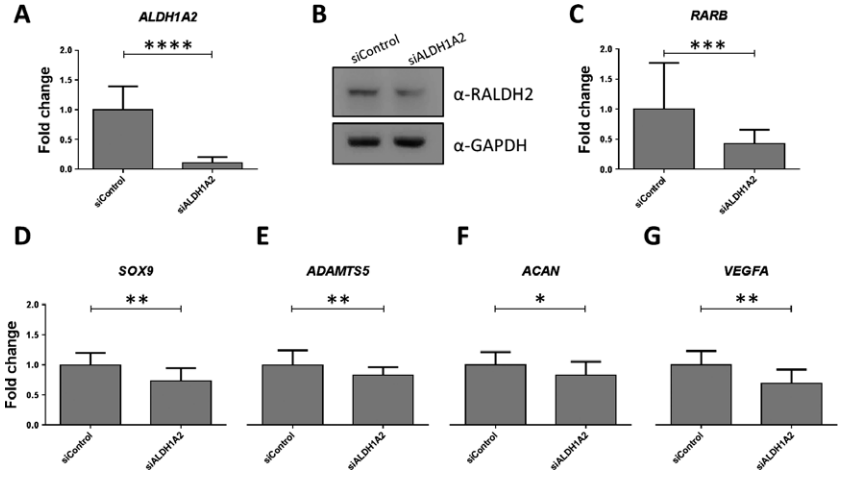

Figure 3. Effects of knockdown of *ALDH1A2* in primary chondrocytes from patients with osteoarthritis (OA). **A,** *ALDH1A2* knockdown with small interfering RNA (siRNA) targeting *ALDH1A2* (siALDH1A2) was carried out in cultured knee chondrocytes from 3 OA patients, in comparison to the effects of a nontargeting siRNA control (siControl). *ALDH1A2* expression was measured by quantitative reverse transcription–polymerase chain reaction. Values represent the mean ± SD fold change in expression compared to siControl, with the data combined for the 3 patients. **B,** Representative results from immunoblotting demonstrate depletion of RALDH2 protein following *ALDH1A2* knockdown. GAPDH was used as a loading control. **C–G**, The fold change in expression of *RARB* **(C)**, *SOX9* **(D)**, *ADAMTS5* **(E)**, *ACAN* **(F)**, and *VEGFA* **(G)** following *ALDH1A2* knockdown, relative to that with the siControl, was assessed in chondrocytes from the 3 OA patients combined. Values are the mean ± SD. *P* values were calculated using Student's 2-tailed *t*-test. * = $P < 0.05$; ** = $P < 0.01$; *** = $P < 0.001$; **** = $P < 0.0001$.

Lack of involvement of UTR SNPs in regulating transcript stability. The 3′-UTRs offer binding sites for microRNAs (miRNAs) that can regulate transcript stability. The 3′-UTR of *ALDH1A2* contains 2 SNPs that correlate with the rs3204689 association signal: rs3204689 itself and rs9325 (r^2 = 0.96 with rs3204689). A search of TargetScan (http://www.targetscan.org/vert_71/) revealed that both of these SNPs reside within predicted miRNA binding sites. In order to assess whether the eQTL operating on *ALDH1A2* was the result of miRNA-mediated transcript degradation, we measured AEI in cultured chondrocytes following treatment with the transcriptional inhibitor actinomycin D. If the ratio of AEI endures following treatment, this would imply that the AEI results from differential transcription between alleles, rather than differential transcript stability.

We investigated chondrocytes from 4 patients with knee OA who were heterozygous at rs3204689. Levels of *ALDH1A2* mRNA expression were significantly decreased in the chondrocytes after 12 hours (P < 0.01) and 24 hours (P < 0.0001) of actinomycin D treatment, compared to time 0 (Figure 4A), but the allelic ratio remained stable for the duration of the time course in each patient's cells (Figure 4B). These data therefore support the notion that an effect on transcription, rather than transcript stability, is the mechanism through which the association signal impacts on *ALDH1A2* expression.

Triage to identify functional candidate SNPs. We aimed to identify SNPs that correlated with the OA association signal, and in which the 2 SNP alleles demonstrated differential transcriptional activity. Such SNPs would be strong functional candidates responsible for the AEI. To achieve this, we applied a triage system that had 3 sequential stages: 1) identification of SNPs showing a correlation ($r^2 \geq 0.8$) with either rs3204689 or rs4238326 and that could be predicted in silico to be potentially functional; 2) luciferase reporter analysis of both alleles of these SNPs in transformed cell lines; and 3) further functional characterization by EMSA of the SNPs that demonstrated AEI in the luciferase analysis.

SNPs correlated with the OA association signal. Using HaploReg version 4.1 (http://archive.broadinstitute.org/mammals/haploreg/haploreg.php), we identified 54 SNPs that strongly correlated with rs3204689 and 8 SNPs that strongly correlated with rs4238326 (each $r^2 \geq 0.8$) (see Supplementary Tables 9 and 10, available on the *Arthritis & Rheumatology* web site at http://onlinelibrary.wiley.com/doi/10.1002/art.40545/abstract). All resided within the gene body or immediately downstream of *ALDH1A2*, and encompassed a 145-kb region.

We screened all 62 of these SNPs, as well as rs3204689 and rs4238326, for predicted transcriptional functionality using RegulomeDB (http://www.regulomedb.org) (for more details on the RegulomeDB scores, see Supplementary Figure 2, available on the *Arthritis & Rheumatology* web site at http://onlinelibrary.wiley.com/doi/10.1002/art.40545/abstract). This analysis identified 38 positive SNPs (as indicated by the RegulomeDB scores listed in Supplementary Tables 9 and 10), and these were taken forward for luciferase analysis. We also included rs4646563, despite there being no supporting RegulomeDB data for this SNP, as it resides close to the CpG dinucleotide cg12031962, which marks an *ALDH1A2* methylation QTL (mQTL) that we described in a previous report (23). In total, we took forward 39 SNPs for luciferase analysis.

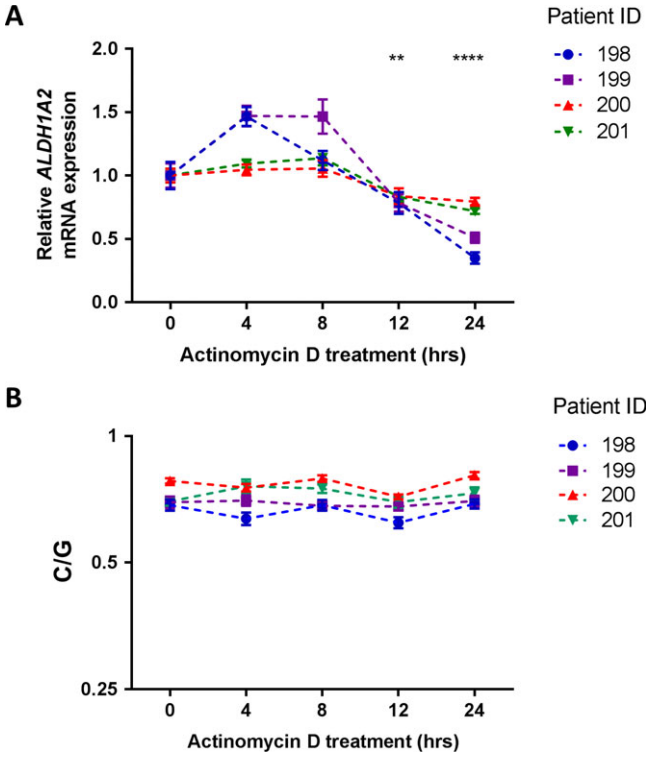

Figure 4. *ALDH1A2* transcript stability in osteoarthritis (OA) chondrocytes. **A,** Chondrocytes from 4 OA patients were cultured in the presence of actinomycin D for 0, 4, 8, 12, or 24 hours and the effects on *ALDH1A2* mRNA expression were assessed by quantitative reverse transcription–polymerase chain reaction. At each time point, the mean ± SEM *ALDH1A2* mRNA expression level in the 4 patients combined was compared to time 0. P values were calculated using a Mann-Whitney 2-tailed exact test. **B,** The allelic ratio (C/G) at rs3204689 was determined by pyrosequencing in the chondrocytes from the 4 OA patients at each time point. Values are the mean ratio determined from 6 technical repeats. Individual patients are designated by their anonymized identification (ID) numbers. ** = P < 0.01; **** = P < 0.0001.

Allelic expression differences identified at 8 SNPs by luciferase analysis. For these 39 SNPs, each allele was cloned into a pGL3-promoter plasmid (with multiple SNPs cloned together if they were <200 bp apart) and relative luciferase activity was compared in 2 human cell lines, SW1353 chondrosarcoma cells and HEK 293 cells. The former was chosen because of its chondrocyte origin, and the latter because it abundantly expresses *ALDH1A2*.

Six constructs encompassing a total of 8 SNPs displayed significant allelic differences in transcriptional activity ($P < 0.05$) (Figures 5A and B). These SNPs were rs4646636, rs12915901, rs4646563, and rs4646586, which correlated with rs3204689, and rs11071365, rs11071366, rs4646571, and rs4646572, which correlated with rs4238326.

Of the 8 SNPs, rs12915901 was particularly noteworthy in that both the A and G alleles of this SNP acted as an enhancer in both cell types (normalized luciferase activity >1.0), with the A allele (equivalent to the risk-conferring C allele of rs3204689) showing lower expression relative to the non-risk G allele in both cell types. The relative reduction in expression of the risk allele observed for rs12915901 was 15% in SW1353 cells and 14% in HEK 293 cells. These reductions are comparable to those observed in OA patient cartilage (28%), fat pad (14%), and bone (15%) for the C allele of rs3204689 (Figure 2). As such, rs12915901 recapitulated the AEI seen in OA patients. The additional 7 SNPs that displayed allelic differences in transcriptional activity did not meet the same criteria as met by rs12915901.

EMSA characterization of differential allelic binding at rs12915901. We used EMSAs to characterize protein complex binding to each of the 8 positive SNPs that emerged from our luciferase analysis. This analysis revealed differential allelic binding of 2 protein complexes to rs12915901 (results in SW1353 cells in Figure 6A; results in HEK 293 cells in Supplementary Figure 3A, available on the *Arthritis & Rheumatology* web site at http://onlinelibrary.wiley.com/doi/10.1002/art.40545/abstract). We found no consistent allelic differences in protein complex binding for the other 7 SNPs analyzed. The 2 rs12915901 complexes bound almost exclusively to the non-risk G allele of the SNP, with the higher molecular weight complex competing much less efficiently with the A allele than with the G allele competitor (Figure 6B).

A search of the online databases JASPAR (http://jaspar.genereg.net) and UniProbe (http://the_brain.bwh.harvard.edu/uniprobe/) identified the Ets family of transcription factors as potentially binding to rs12915901 and its flanking sequence, but only for the non-risk G allele: the highly conserved Ets DNA binding domain is 5′-GGAA-3′, which is intact for the G allele of rs12915901 but is abolished in the A allele, with the sequence changing to 5′-GAAA-3′ (underline indicates the rs12915901 base).

This hypothetical loss of Ets binding was consistent with our EMSA data, in that the 2 protein complexes bind to the G allele but not the A allele of the SNP. We therefore used an Ets competitor sequence in our EMSA. This competed very efficiently for binding to the 2 protein complexes, implying that they do

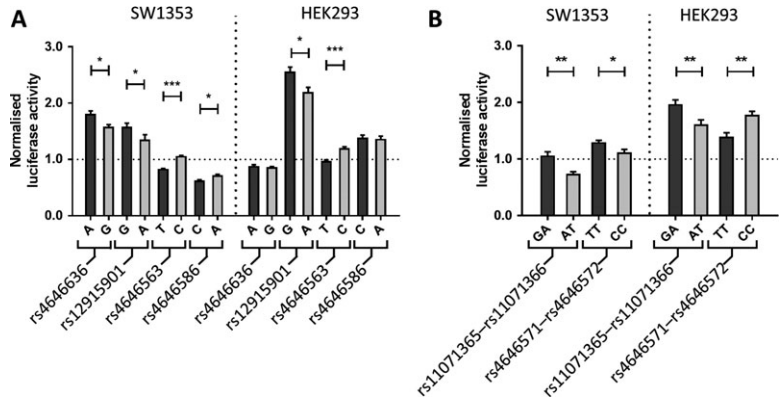

Figure 5. Luciferase reporter analysis of single-nucleotide polymorphism (SNP) alleles. Four SNPs correlating with rs3204689 (**A**) and 2 SNP pairs correlating with rs4238326 (**B**) demonstrated allelic expression differences in SW1353 and HEK 293 cells. Values are plotted as the mean ± SEM normalized luciferase activity from 6 biologic repeats, each with 6 technical repeats. For each SNP, the osteoarthritis risk–associated allele is shown as light gray–shaded bars. The horizontal dashed line indicates no difference in expression relative to the *Renilla* transfection control (normalized luciferase activity value of 1.0). *P* values were calculated using a Mann-Whitney 2-tailed exact test. * = $P < 0.05$; ** = $P < 0.01$; *** = $P < 0.001$.

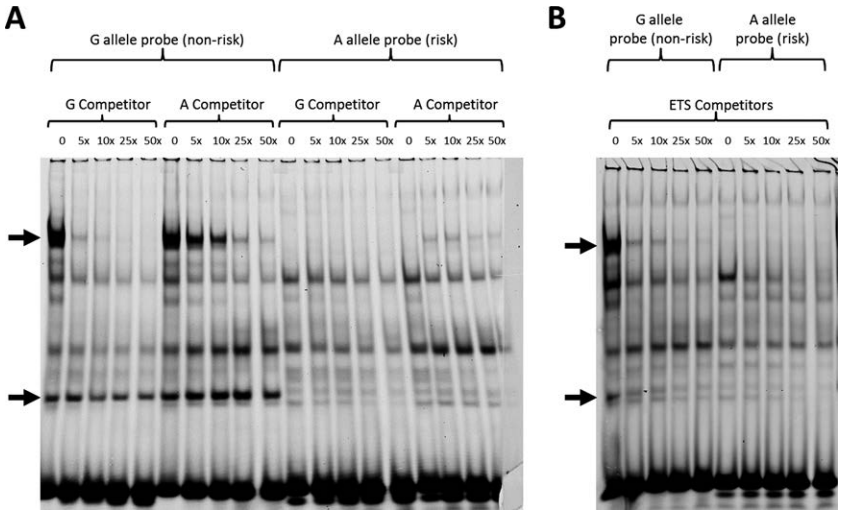

Figure 6. Electrophoretic mobility shift assay (EMSA) analyses of expression of the rs12915901 G and A alleles in SW1353 cells. **A,** Increasing concentrations of unlabeled G allele and the A allele competitor were added to the EMSA reactions containing cell nuclear extract and a G or A allele probe. **B,** Increasing concentrations of an unlabeled Ets competitor were added to the EMSA reaction containing a G allele or an A allele probe. **Arrows** indicate 2 complexes binding with much greater affinity to the G allele than to the A allele.

contain at least 1 Ets transcription factor (Figure 6B and Supplementary Figure 3B, http://onlinelibrary.wiley.com/doi/10.1002/art.40545/abstract). A random competitor sequence had no effect (data not shown). Ets is one of the largest family of transcription factors, with 29 Ets genes in humans. Using our RNA-seq data, we determined that the majority of these Ets transcription factors were expressed in cartilage.

DISCUSSION

Retinoic acid plays a crucial role in organism development (24), via its regulatory effects on chondrogenesis and osteogenesis (25). Its synthesis involves the oxidation of retinaldehyde to retinoic acid. This step is catalyzed by the RALDH enzymes, of which there are 3 in humans (RALDH1, RALDH2, and RALDH3), each coded for by a separate gene (*ALDH1A1*, *ALDH1A2*, and *ALDH1A3*). RALDH2/*ALDH1A2* is pivotal, with knockout of the mouse ortholog being lethal (24).

A 2014 report discussing an association with OA of SNPs at the *ALDH1A2* locus (6) was the first occasion in which the retinoic acid pathway had been associated with OA at a genome-wide significance level, and those findings highlighted the fact that a molecule key to early postnatal development can have an impact on a disease that tends to develop in older individuals. That prior report contained a number of features common in OA genetic studies: 1) the signal is to a gene involved in a regulatory pathway; 2) the functional effect of the genetic susceptibility is on gene expression; and 3) the signal is not a risk factor for disease at all skeletal sites examined (2,4,5).

We set out to replicate and expand upon the findings included in the 2014 study. We confirmed that the risk-conferring C allele of rs3204689 correlated with reduced expression of *ALDH1A2* in cartilage, and demonstrated that this effect was common in the fat pad and bone of OA patients, albeit to a lower degree. AEI was less common in the synovium examined. Our data suggest that the functional consequence of the genetic risk is not uniform across joint tissues, with cartilage being the major target tissue. The fact that cartilage showed a more pronounced AEI when we studied several joint tissue sites from the same individual suggests that nongenetic modulators have a role. We have previously demonstrated that *ALDH1A2* is subject to an mQTL that correlates with the association signal (23). A detailed analysis of DNA CpG methylation and *ALDH1A2* AEI in multiple joint tissues from the same donor is clearly merited.

We examined osteochondral tissue from patients with hand OA who had undergone a trapeziectomy. Severe thumb OA was one of the clinical phenotypes for which an association with *ALDH1A2* was demonstrated in the 2014 report. In the present study, we observed statistically significant AEI in the osteochondral tissue, confirming, for the first time, that the risk allele at this locus correlates with decreased expression of *ALDH1A2* in the trapezium of patients with hand OA.

Our RNA-seq data revealed reduced expression of *ALDH1A2* in OA hip cartilage compared to non-OA

hip cartilage. Reduction in expression in OA cartilage, combined with carriage of 1 or 2 copies of the low-expressing C allele of rs3204689, may be the risk-conferring scenario. In the same RNA-seq data set, we observed differential expression of several retinoic acid–related genes. This implies that a systemic alteration in the activity of the retinoic acid pathway occurs in OA. We are not aware of any reports that have discussed a significant association of any of the other investigated retinoic acid genes with OA, but an analysis of these genes as candidate genes may be worthwhile.

A functional role of retinoic acid and retinoic acid receptors in the pathogenesis of OA has been described. Increased concentrations of retinoic acid receptor ligands were previously reported in synovial fluid samples extracted from patients with OA as compared to non-OA controls (26). These increased concentrations of retinoic acid metabolites and derivatives are suggested to be detrimental to cartilage through the stimulation of catabolic processes in chondrocyte explant cultures. Paradoxically, our data suggest that decreased *ALDH1A2* expression, and, by extrapolation, decreased retinoic acid availability, may also compromise cartilage integrity through modulation of *SOX9* expression. The catabolic effects of altered retinoic acid levels in cartilage perhaps suggest that the tight regulation of retinoic acid production during development is also critical for the long-term maintenance of healthy cartilage.

The results of our studies utilizing treatment of chondrocytes with actinomycin D suggest that the alterations in allelic expression occur as a result of the effects on the rate of transcription rather than on transcript stability, while our knockdown of *ALDH1A2* resulted in the reduced expression of several genes, including the gene coding for the key chondrogenic transcription factor *SOX9*. A recent report highlighted the finding that *ALDH1A2* expression is a positive determinant of *SOX9* expression in chondrocytes (27), thereby supporting our own observations.

Our in silico and in vitro analyses of SNPs correlating with the OA association signal identified the *ALDH1A2* intronic SNP rs12915901 as a SNP exhibiting differences in allelic activity that matched the allelic effects seen in our patient-based studies. Our EMSA analyses implicated the Ets family of transcription factors as positive regulators of expression. Members of this family have previously been reported to have a role in OA via regulation of the expression of chondrogenic genes (28,29). Detailed analysis of these Ets transcription factors in the context of the *ALDH1A2* association signal and *ALDH1A2* expression is now warranted.

We analyzed several samples of OA trapezieum tissue, but the vast majority of our tissue came from hip or knee arthroplasties, reflecting the small volume of hand OA surgical procedures undertaken relative to hip and knee procedures. In our quantification of *ALDH1A2* expression, the trapezium samples displayed relatively low levels compared to the hip and knee cartilage samples. We posit therefore that where the expression of the gene is already low, as in the hand, that joint may not be able to tolerate further reduction in expression brought about by carriage of the risk allele.

In conclusion, we have characterized the eQTL operating on *ALDH1A2* in multiple joint tissue sites, including trapezium samples obtained from patients with hand OA. We highlight the functional effect of decreased *ALDH1A2* expression in human chondrocytes and show that retinoic acid–related genes are differentially expressed between OA diseased cartilage and non-OA control cartilage. Our findings prioritize a SNP as a functional variant potentially responsible for the modulation of *ALDH1A2* expression. Experiments building on our findings can now be planned to develop strategies to mitigate the effect of the risk of OA conferred by *ALDH1A2*.

ACKNOWLEDGMENTS

We thank surgeons at the Newcastle upon Tyne Hospitals NHS Foundation Trust for providing us with access to patient samples, and the research nurses for facilitating this access. We thank the hand surgical team at the Nuffield Orthopedic Hospital, Oxford. We thank the patients for donating their tissue. We thank the Newcastle Bone and Joint Biobank for assistance in patient sample collection. We thank Dr. Amanda Villalvilla for technical advice.

AUTHOR CONTRIBUTIONS

All authors were involved in drafting the article or revising it critically for important intellectual content, and all authors approved the final version to be published. Drs. Shepherd and Loughlin had full access to all of the data in the study and take responsibility for the integrity of the data and the accuracy of the data analysis.

Study conception and design. Shepherd, D. Zhu, Reynard, Loughlin.

Acquisition of data. Shepherd, D. Zhu, Skelton, Combe, Threadgold, L. Zhu, Vincent, Stuart.

Analysis and interpretation of data. Shepherd, D. Zhu, Skelton, Reynard, Loughlin.

REFERENCES

1. Loeser RF, Goldring SR, Scanzello CR, Goldring MB. Osteoarthritis: a disease of the joint as an organ [review]. Arthritis Rheum 2012;64:1697–707.
2. Loughlin J. Genetic indicators and susceptibility to osteoarthritis. Br J Sports Med 2011;45:278–82.

3. MacGregor AJ, Li Q, Spector TD, Williams FM. The genetic influence on radiographic osteoarthritis is site specific at the hand, hip and knee. Rheumatology (Oxford) 2009;48:277–80.
4. Reynard LN. Analysis of genetics and DNA methylation in osteoarthritis: what have we learnt about the disease? Semin Cell Dev Biol 2017;62:57–66.
5. Reynard LN, Loughlin J. Insights from human genetic studies into the pathways involved in osteoarthritis. Nat Rev Rheumatol 2013;9:573–83.
6. Styrkarsdottir U, Thorleifsson G, Helgadottir HT, Bomer N, Metrustry S, Bierma-Zeinstra S, et al. Severe osteoarthritis of the hand associates with common variants within the ALDH1A2 gene and with rare variants at 1p31. Nat Genet 2014;46:498–502.
7. Weston AD, Hoffman LM, Underhill TM. Revisiting the role of retinoid signaling in skeletal development. Birth Defects Res C Embryo Today 2003;69:156–73.
8. Zeller R. The temporal dynamics of vertebrate limb development, teratogenesis and evolution. Curr Opin Genet Dev 2010;20:384–90.
9. Gee F, Rushton MD, Loughlin J, Reynard LN. Correlation of the osteoarthritis susceptibility variants that map to chromosome 20q13 with an expression quantitative trait locus operating on NCOA3 and with functional variation at the polymorphism rs116855380. Arthritis Rheumatol 2015;67:2923–32.
10. Wilkins JM, Southam L, Price AJ, Mustafa Z, Carr A, Loughlin J. Extreme context specificity in differential allelic expression. Hum Mol Genet 2007;16:537–46.
11. Shepherd C, Skelton AJ, Rushton MD, Reynard LN, Loughlin J. Expression analysis of the osteoarthritis genetic susceptibility locus mapping to an intron of the MCF2L gene and marked by the polymorphism rs11842874. BMC Med Genet 2015;16:108.
12. Bui C, Barter MJ, Scott JL, Xu Y, Galler M, Reynard LN, et al. cAMP response element-binding (CREB) recruitment following a specific CpG demethylation leads to the elevated expression of the matrix metalloproteinase 13 in human articular chondrocytes and osteoarthritis. FASEB J 2012;26:3000–11.
13. Andrews S. FastQC. 2010. URL: http://www.bioinformatics.babraham.ac.uk/projects/fastqc/.
14. Ewels P, Magnusson M, Lundin S, Kaller M. MultiQC: summarize analysis results for multiple tools and samples in a single report. Bioinformatics 2016;32:3047–8.
15. Harrow J, Frankish A, Gonzalez JM, Tapanari E, Diekhans M, Kokocinski F, et al. GENCODE: the reference human genome annotation for The ENCODE Project. Genome Res 2012;22:1760–74.
16. Patro R, Duggal G, Love MI, Irizarry RA, Kingsford C. Salmon provides fast and bias-aware quantification of transcript expression. Nat Methods 2017;14:417–9.
17. Soneson C, Love MI, Robinson MD. Differential analyses for RNA-seq: transcript-level estimates improve gene-level inferences. F1000Res 2015;4:1521.
18. Team RC. R: a language and environment for statistical computing. R Foundation for Statistical Computing, Vienna, Austria. URL: https://www.r-project.org/.
19. Wickham H, François R, Henry L, Müller K. RStudio. dplyr: a grammar of data manipulation. R package version 042. 2016. URL: https://dplyr.tidyverse.org/.
20. Love MI, Huber W, Anders S. Moderated estimation of fold change and dispersion for RNA-seq data with DESeq2. Genome Biol 2014;15:550.
21. Schneider CA, Rasband WS, Eliceiri KW. NIH Image to ImageJ: 25 years of image analysis. Nat Methods 2012;9:671–5.
22. Syddall CM, Reynard LN, Young DA, Loughlin J. The identification of trans-acting factors that regulate the expression of GDF5 via the osteoarthritis susceptibility SNP rs143383. PLoS Genet 2013;9:e1003557.
23. Rushton MD, Reynard LN, Young DA, Shepherd C, Aubourg G, Gee F, et al. Methylation quantitative trait locus analysis of osteoarthritis links epigenetics with genetic risk. Hum Mol Genet 2015;24:7432–44.
24. Niederreither K, Subbarayan V, Dolle P, Chambon P. Embryonic retinoic acid synthesis is essential for early mouse post-implantation development. Nat Genet 1999;21:444–8.
25. Williams JA, Kane M, Okabe T, Enomoto-Iwamoto M, Napoli JL, Pacifici M, et al. Endogenous retinoids in mammalian growth plate cartilage: analysis and roles in matrix homeostasis and turnover. J Biol Chem 2010;285:36674–81.
26. Davies MR, Ribeiro LR, Downey-Jones M, Needham MR, Oakley C, Wardale J. Ligands for retinoic acid receptors are elevated in osteoarthritis and may contribute to pathologic processes in the osteoarthritic joint. Arthritis Rheum 2009;60:1722–32.
27. Unguryte A, Bernotiene E, Bagdonas E, Garberyte S, Porvaneckas N, Jorgensen C. Human articular chondrocytes with higher aldehyde dehydrogenase activity have stronger expression of COL2A1 and SOX9. Osteoarthritis Cartilage 2016;24:873–82.
28. Ohta Y, Okabe T, Larmour C, Di Rocco A, Maijenburg MW, Phillips A, et al. Articular cartilage endurance and resistance to osteoarthritic changes require transcription factor Erg. Arthritis Rheumatol 2015;67:2679–90.
29. Otero M, Peng H, Hachem KE, Culley KL, Wondimu EB, Quinn J, et al. ELF3 modulates type II collagen gene (COL2A1) transcription in chondrocytes by inhibiting SOX9-CBP/p300-driven histone acetyltransferase activity. Connect Tissue Res 2017;58:15–26.

ARTHRITIS & RHEUMATOLOGY
Vol. 70, No. 10, October 2018, pp 1588–1596
DOI 10.1002/art.40551

Association of Inflammatory Bowel Disease and Acute Anterior Uveitis, but Not Psoriasis, With Disease Duration in Patients With Axial Spondyloarthritis

Results From Two Belgian Nationwide Axial Spondyloarthritis Cohorts

Gaëlle Varkas,[1] Nathan Vastesaeger,[2] Heleen Cypers,[1] Roos Colman,[3] Thomas Renson,[1] Liesbet Van Praet,[4] Philippe Carron,[1] Frank Raeman,[5] Mieke Devinck,[5] Lieve Gyselbrecht,[5] Luc Corluy,[5] Yves Piette,[5] Jan Lenaerts,[5] Kristof Thevissen,[5] Benedicte Vanneuville,[5] Filip Van den Bosch,[1] and Dirk Elewaut [1]

Objective. **To determine the link between extraarticular manifestations (EAMs) and baseline characteristics in patients with axial spondyloarthritis (SpA), and to define their potentially differential prognostic value in 2 large, independent Belgian axial SpA cohorts with distinct recruitment periods.**

Methods. **Information on demographic and clinical characteristics and extraarticular manifestations (EAMs) was obtained from patients with axial SpA originating from the (Be)Giant (Belgian Inflammatory Arthritis and Spondylitis) cohort, which includes consecutive axial SpA patients whose data have been collected since 2010, and from the ASPECT (Ankylosing Spondylitis Patients Epidemiological Cross-sectional Trial) cohort, a Belgian registry of cross-sectional data collected between February 2004 and February 2005 from consecutive patients with ankylosing spondylitis (AS) or probable AS.**

Results. **Among the 1,250 Belgian patients studied, disease duration was associated with risk of developing inflammatory bowel disease (IBD), with an increase in risk by 20% per 10 years of disease duration (relative risk [RR] 1.2, $P = 0.026$), and associated with risk of developing acute anterior uveitis, with an increase in risk by 30% per 10 years of disease duration (RR 1.3, $P < 0.001$). In the subgroup of 171 newly diagnosed patients with prospective follow-up data, higher mean C-reactive protein levels over time were demonstrated in those with acute anterior uveitis or IBD compared to those without EAMs or those with psoriasis alone (each $P = 0.01$).**

Conclusion. **The risk of developing acute anterior uveitis or IBD, but not psoriasis, in patients with axial SpA seems to increase with disease duration and appears to be linked to a higher cumulative exposure to inflammation, thus providing a possible explanation for the differential structural progression observed in those with axial SpA.**

The prevalence of extraarticular manifestations (EAMs) in patients with ankylosing spondylitis (AS) is well-known, with hazard ratios (HRs) compared to the general population of 15.5 for acute anterior uveitis, 1.5

The ASPECT cohort was collected and supported by Merck Sharp & Dohme. The (Be)Giant cohort was supported by an unrestricted grant from AbbVie. Dr. Elewaut's work was supported by Scientific Research–Flanders, the Research Council of Ghent University, and the Belspo Agency (Interuniversity Attraction Pole grant Devrepair; project P7/07).

[1]Gaëlle Varkas, MD, PhD, Heleen Cypers, MD, PhD, Thomas Renson, MD, Philippe Carron, MD, PhD, Filip Van den Bosch, MD, PhD, Dirk Elewaut, MD, PhD: Ghent University Hospital and VIB Center for Inflammation Research, Ghent University, Ghent, Belgium; [2]Nathan Vastesaeger, MD, PhD: Merck Sharp & Dohme, Antwerp, Belgium; [3]Roos Colman, MSc: Biostatistics Unit of the Faculty of Medicine and Health Sciences, Ghent University, Ghent, Belgium; [4]Liesbet Van Praet, MD, PhD: Ghent University Hospital, Ghent, Belgium; [5]Frank Raeman, MD, Mieke Devinck, MD, Lieve Gyselbrecht, MD, Luc Corluy, MD, Yves Piette, MD, Jan Lenaerts, MD, Kristof Thevissen, MD, Benedicte Vanneuville, MD: (Be)Giant Consortium, Ghent, Belgium.

Drs. Van den Bosch and Elewaut contributed equally to this work.

Dr. Van den Bosch has received consulting fees and/or speaking fees from AbbVie, Celgene, Janssen, Merck, Novartis, Pfizer, and UCB (less than $10,000 each). Dr. Elewaut has received speaking fees from Boehringer Ingelheim, Pfizer, UCB, Merck, Novartis, Janssen, and AbbVie (less than $10,000 each) and research support from those companies.

Address correspondence to Dirk Elewaut, MD, PhD, Department of Rheumatology, Ghent University Hospital, De Pintelaan 185, Ghent 9000, Belgium. E-mail: Dirk.elewaut@ugent.be.

Submitted for publication September 23, 2017; accepted in revised form May 1, 2018.

for skin psoriasis, and 3.3 for inflammatory bowel disease (IBD) (1). Similarly, increasing frequencies of EAMs in different stages of disease have been reported across observational cohorts such as the GESPIC (German Spondyloarthritis Inception Cohort) and the DESIR (Devenir des Spondyloarthropathies Indifférenciées Récentes) cohort of patients with inflammatory back pain (IBP) (2,3). Nevertheless, research on the potential value of these EAMs as tools for the stratification of patients and for disease prognosis is scarce.

In patients with axial SpA, radiographic progression has been shown to be associated with baseline clinical characteristics, such as an elevated C-reactive protein (CRP) level, hip involvement, HLA–B27 positivity, smoking, structural damage, and evidence of inflammation on magnetic resonance imaging (MRI) (4–6). Meanwhile, acute anterior uveitis in patients with axial SpA has been found to be strongly associated with the presence of HLA–B27 (7,8), while gut inflammation has been shown to be associated with the severity of sacroiliitis (9), both of which were previously recognized as a predisposing factor for structural progression in axial SpA. However, the presence of psoriasis in patients with axial SpA has been associated with less evidence of inflammation on MRI and less frequent radiographic damage (10).

Therefore, in the present study our goal was to examine any potential link of psoriasis with baseline clinical characteristics in patients with axial SpA in comparison to that in axial SpA patients who develop acute anterior uveitis or IBD, and to explore the role of exposure to systemic inflammation over time—with CRP as a surrogate marker—as a potential explanation for the discrepancy in structural progression between patients displaying these different types of EAMs. We anticipated that the axial SpA patients with IBD and/or acute anterior uveitis would display more inflammation, rendering them more prone to structural progression.

PATIENTS AND METHODS

Patients and study design. The analyzed data originated from the (Be)Giant (Belgian Inflammatory Arthritis and Spondylitis) cohort, which includes consecutive patients diagnosed as having SpA since 2010, and from the ASPECT (Ankylosing Spondylitis Patients Epidemiological Cross-sectional Trial) cohort, which is a large cohort of consecutive patients diagnosed as having AS or probable AS, from whom data were obtained between February 2004 and February 2005.

The (Be)Giant is an observational cohort comprising both patients with peripheral SpA and patients with axial SpA, of which the subset of 227 patients with axial SpA was analyzed in the present study, and part of this cohort has been previously described in a study by Van Praet et al (11). The ASPECT registry is a Belgian cross-sectional database containing information on 847 axial SpA patients who fulfilled the modified New York criteria for AS (12). The aim of ASPECT was to describe the phenotype of an average axial SpA patient in a Belgian rheumatology practice (6,12) prior to the initiation of anti–tumor necrosis factor (anti-TNF) therapy for axial SpA. Another 176 patients in the ASPECT cohort who did not fulfill the criterion of radiographic damage in the modified New York criteria were classified as having probable AS. Similar to the (Be)Giant cohort, all patients in the ASPECT cohort received their clinical diagnosis of axial SpA from a rheumatologist prior to inclusion.

Considering that some of the patients in the ASPECT cohort had received a diagnosis of probable AS, the baseline characteristics did not differ from those in a contemporary population of patients with nonradiographic axial SpA. Moreover, 76.6% of patients (108 of 141 [n = 35 with missing data]) were HLA–B27 positive, of whom 63.9% (69 of 108) fulfilled the Assessment of SpondyloArthritis international Society (ASAS) clinical criteria for SpA (13), based on the combined presence of HLA–B27 positivity and ≥2 typical characteristics of SpA (i.e., IBP, arthritis, enthesitis, acute anterior uveitis, skin psoriasis, IBD, family history, and elevated CRP level). Unfortunately, no data on dactylitis and/or the patients' response to nonsteroidal antiinflammatory drug (NSAID) therapy were available, nor were there any MRI data available at that time. Therefore, this cohort of patients with probable AS mirrors the phenotype of patients who we currently classify as having nonradiographic axial SpA (6). By introducing a large cohort of axial SpA patients who received their diagnosis in an unbiased manner (due to the introduction of EAMs as a criterion in the 2009 ASAS criteria for SpA), an extra dimension was added to the analysis.

Both observational cohorts and the study protocol were authorized by the local ethics committee of the University Hospital of Ghent. Written informed consent was obtained from all patients prior to inclusion.

Variables. Sex, age, disease duration, HLA–B27 status, enthesitis, arthritis, CRP level, fulfillment of disease classification criteria, family history, and scores on the Bath Ankylosing Spondylitis Disease Activity Index (BASDAI) (scale 0–10) (14) and Bath Ankylosing Spondylitis Functional Index (BASFI) (scale 0–10) (15) were collected from patients in the ASPECT and (Be)Giant cohorts. The outcome measures (EAMs, psoriasis, IBD, acute anterior uveitis, arthritis, and enthesitis) were recoded into dichotomous variables as present versus absent. Paradoxical psoriasis was not included in the analysis. In the (Be)Giant cohort, only EAMs documented by a physician in the electronic patient file were included. In the ASPECT cohort, past or present EAMs were collected by the treating rheumatologist at the time of inclusion in the cohort. For the prospective analysis, data on the CRP level were collected through a thorough file search within the electronic files of the patients who had not yet been treated with anti-TNF agents, both prospectively and retrospectively up to 1 year prior to diagnosis and up to 4.5 years after inclusion. Patients were included when at least 2 CRP values were available, obtained over at least a 6-month interval. CRP values collected by the general practitioner were not included, as these were more likely to represent an infectious episode.

Statistical analysis. The statistical analysis was performed using SPSS version 24. Significance was set at an alpha level of 0.05.

The nonparametric Mann-Whitney U test was applied to asses any differences in the continuous variables between the (Be)Giant and ASPECT cohorts, and between the patients with acute anterior uveitis and/or IBD and the patients without EAMs or those with skin psoriasis only. For variables with a parametric distribution, the Student's *t*-test was applied. The chi-square test for a 2×2 table was employed to identify differences in sex, HLA–B27 status, presence of acute anterior uveitis, presence of psoriasis, and presence of IBD between the cohorts and subgroups, as well as to identify differences in family history, presence of arthritis, and presence of enthesitis.

The association of the presence of EAMs with different patient characteristics was analyzed by multiple logistic regression. Variables were selected on the basis of clinical relevance. The number of variables entered in the model was based on ~10 events per variable. The Hosmer and Lemeshow goodness-of-fit test was evaluated for model fit, with no signs of overfitting observed. The relative risk (RR) associated with the odds ratio (OR) was calculated using the following formula, as recommended by Grant (16): $RR = OR/(1 - p + [p \times OR])$, where p represents the baseline risk. Since the CRP level was collected from patients at the time of diagnosis in the (Be)Giant cohort, but was collected at a cross-sectional inclusion time point in the ASPECT cohort, an interaction between CRP and the cohort variable was included in the model to correct for differential effect across the cohorts. However, this interaction was not significant. There were no signs of collinearity between the variables. Interactions of the variables with the cohort variable were explored, but none were significant. Sensitivity analyses in which we excluded patients treated with anti-TNF therapy were conducted.

In the prospective analysis, the cumulative exposure to log-transformed CRP (log[CRP]) over time was calculated by linear mixed models analysis, with the group and time point (and their interaction) as fixed factors and subjects as a random factor. Since the outcome variable CRP was log-transformed, the results of this model are presented on the original scale (mg/dl) as the geometric mean, with corresponding 95% confidence interval. Similarly, the proportion of patients with measurements of CRP above the cutoff level of 0.5 mg/dl per group was analyzed by mixed logistic regression, with the group and time point as fixed factors and subjects as a random factor.

RESULTS

Baseline characteristics of the patients. The baseline characteristics of the 928 patients who fulfilled the modified New York criteria for AS, including 847 in the ASPECT cohort and 81 in the (Be)Giant cohort, and 322 patients with nonradiographic axial SpA, including 176 in the ASPECT cohort and 146 in the (Be)Giant cohort, were compared across the cohorts. All of the baseline demographic and clinical characteristics of these patients (Table 1) were consistent with the data reported previously in cohorts of patients with early or established disease. The higher proportion of patients in the (Be)Giant cohort with elevated CRP levels can be explained by the fact that the serum collection took place at the time of diagnosis as opposed to the time of inclusion, regardless of time of diagnosis, in the ASPECT cohort.

Cross-sectional analysis of EAMs in patients with axial SpA. *Prevalence of EAMs at inclusion.* The prevalence of EAMs at the time of inclusion was not significantly different across the cohorts despite the inclusion of patients at different stages of disease. Overall, 34.4% of patients in the (Be)Giant cohort had already experienced EAMs prior to inclusion, as compared to 39.7% of patients in the ASPECT cohort experiencing EAMs by the time of inclusion (*P* not significant). Overlap between the different EAMs (psoriasis, IBD, and acute anterior uveitis) appeared to be limited, even in patients with

Table 1. Baseline characteristics of the patients in the (Be)Giant and ASPECT cohorts by diagnosis*

	AS			Nonradiographic axial SpA		
	(Be)Giant cohort (n = 81)	ASPECT cohort (n = 847)	*P*	(Be)Giant cohort (n = 146)	ASPECT cohort (probable AS) (n = 176)	*P*
Male, no. (%)	44 (54.3)	575 (68)	0.012	68 (46.6)	87 (49.4)	NS
Age, mean ± SD years	35.3 ± 10.8	44.6 ± 12.1	<0.001	32.6 ± 9.0	39.7 ± 11.2	<0.001
Symptom duration, median (range) years	10.3 (0.1–44.8)	16.3 (0.1–66.2)	<0.001	3.3 (0.0–32.6)	6.0 (0.0–39.4)	<0.001
HLA–B27+, no. (%)	66 (83.5)	560 (83)	NS	99 (68.8)	108 (76.6)	NS
Elevated CRP, no. (%)†	45 (57.0)	351 (42.6)	0.014	51 (36.2)	42 (23.9)	0.017
BASDAI, median (range)	4.1 (0.4–9.2)	5.5 (0.0–10.0)	<0.001	4.3 (0.0–9.6)	4.8 (0.2–9.1)	0.037
BASFI, median (range)	2.7 (0.0–8.5)	5.2 (0.0–10.0)	<0.001	2.3 (0.0–8.2)	3.4 (0.0–9.8)	<0.001
Anti-TNF therapy, no. (%)	3 (3.7)	98 (11.6)	0.030	3 (2.0)	6 (3.4)	NS
Positive family history, no. (%)	33 (41.8)	395 (46.6)	NS	62 (44.6)	69 (39.2)	NS
Arthritis (ever), no. (%)‡	13 (16)	490 (57.9)	<0.001	33 (22.9)	98 (55.7)	<0.001

* AS = ankylosing spondylitis; SpA = spondyloarthritis; NS = not significant; BASDAI = Bath Ankylosing Spondylitis Disease Activity Index (scale 0–10); BASFI = Bath Ankylosing Spondylitis Functional Index (scale 0–10); anti-TNF = anti–tumor necrosis factor.

† Levels of C-reactive protein (CRP) in the (Be)Giant (Belgian Inflammatory Arthritis and Spondylitis) cohort were collected at diagnosis, whereas CRP values in the ASPECT (Ankylosing Spondylitis Patients Epidemiological Cross-sectional Trial) cohort were collected at a cross-sectional time point.

‡ Arthritis in patients in the ASPECT cohort was recorded as present at the clinical discretion of the treating rheumatologist, whereas it was defined as clinical suspicion combined with objective confirmation by ultrasound in the (Be)Giant cohort.

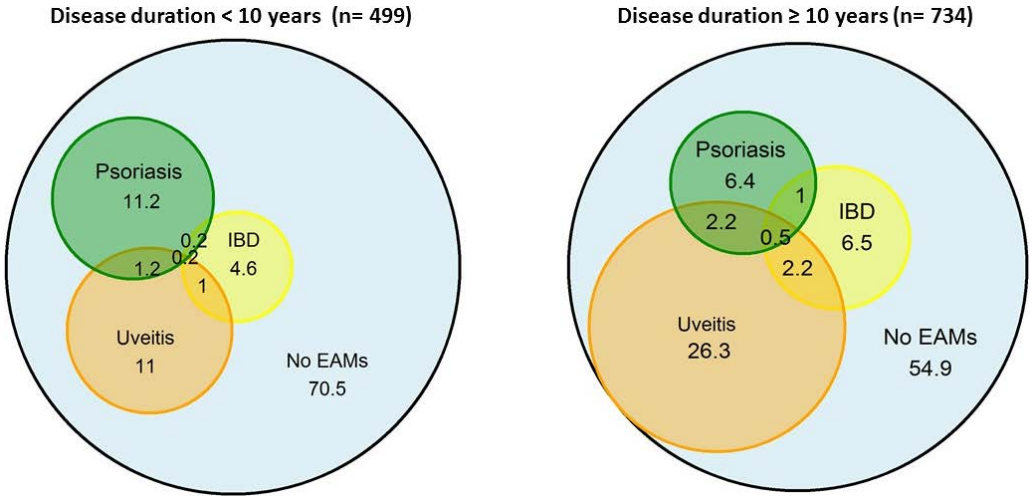

Figure 1. Distribution of extraarticular manifestations (EAMs) according to disease duration groups of <10 years versus ≥10 years in patients with axial spondyloarthritis (SpA) from the ASPECT (Ankylosing Spondylitis Patients Epidemiological Cross-sectional Trial) cohort and (Be)Giant (Belgian Inflammatory Arthritis and Spondylitis) cohort. The Venn diagrams of data from the cross-sectional analysis show the overlap in EAMs in axial SpA patients. Values are the percentage of patients in each EAM cluster. IBD = inflammatory bowel disease.

longstanding disease (Figure 1). After stratification of patients based on who did or did not fulfill the ASAS classification criteria, the prevalence of EAMs remained comparable between the 2 groups (Figure 2).

Features associated with EAMs. The presence or history of any EAM at the time of inclusion was significantly associated with disease duration in analyses corrected for age, sex, classification criteria present, BASFI score, BASDAI score, CRP level, and HLA–B27 status. The overall increase in the risk of developing EAMs was 20% per 10 years of disease duration (RR 1.2, $P < 0.001$). Interestingly, we also found a significant association between the risk of EAMs and the time point of inclusion (pre–ASAS criteria versus post–ASAS criteria), with a 30% increase in risk in patients considered to have met the ASAS criteria (RR 1.3, $P = 0.047$). This finding might be explained by the implementation of the ASAS criteria, which incorporates the presence of EAMs. Conceivably, this made physicians more aware of these features of SpA, which would lead to referral. Disease duration nevertheless remained an independent predictor of the risk of developing EAMs in multivariate analyses, after correction for multiple variables, including the specific cohort as a factor.

We noticed that patients in the ASPECT cohort who were already taking anti-TNF medication at baseline were more likely to have already encountered an EAM (RR 1.5, $P = 0.004$). This was clearly manifested in patients who developed IBD, in whom a significant association with taking an anti-TNF agent at the time of inclusion was noted, with an increase in the RR of 140%. Indeed, uncontrolled IBD is more likely to be recognized as an indication for biologic therapy than is psoriasis or acute anterior uveitis.

Moreover, a 20% increased risk of developing IBD was noted per 10 years of disease duration in the patient cohorts, in addition to an increase in the risk by

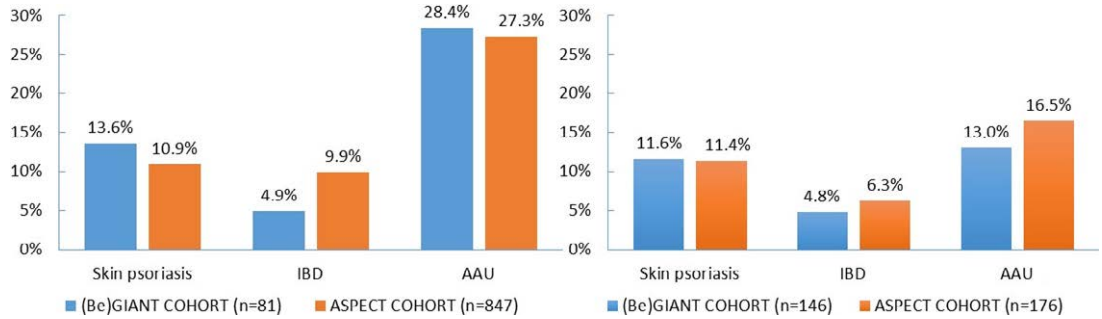

Figure 2. Comparison of the frequency of EAMs at the time of inclusion between patients with ankylosing spondylitis (left) and patients with nonradiographic axial spondyloarthritis (right) in the (Be)Giant and ASPECT cohorts. EAMs include skin psoriasis, IBD, and acute anterior uveitis (AAU). Values above the bars are the percentage of patients. See Figure 1 for other definitions.

Table 2. Variables associated with the presence or history of extraarticular manifestations at presentation*

	OR (95% CI)	RR	*P*
IBD†			
Disease duration, per 10 years	1.3 (1.0–1.6)	1.2	0.026
HLA–B27 negativity	1.8 (1.0–3.2)	1.7	0.049
Baseline anti-TNF therapy	2.8 (1.4–5.3)	2.4	0.002
Acute anterior uveitis‡			
Disease duration, per 10 years	1.5 (1.3–1.8)	1.3	<0.001
HLA–B27 positivity	2.7 (1.6–4.4)	1.9	<0.001
Psoriasis§			
HLA–B27 negativity	2.1 (1.3–3.4)	1.9	0.002
Sex, male	1.6 (1.0–2.5)	1.5	0.041

* OR = odds ratio; 95% CI = 95% confidence interval; RR = relative risk; IBD = inflammatory bowel disease; anti-TNF = anti–tumor necrosis factor.
† Corrected for sex, cohort, C-reactive protein (CRP) level, classification criteria present, Bath Ankylosing Spondylitis Disease Activity Index (BASDAI) score, and Bath Ankylosing Spondylitis Functional Index (BASFI) score.
‡ Corrected for cohort, age, classification criteria present ($P = 0.064$), BASDAI score, BASFI score, CRP level, sex, and anti-TNF therapy at baseline.
§ Corrected for cohort, age, classification criteria present, BASDAI score, BASFI score, CRP level, disease duration, and anti-TNF therapy at baseline.

70% in those with HLA–B27 negativity. Similarly, acute anterior uveitis was linked to disease duration, with an increase in risk by 30%, and, as expected, those with HLA–B27 positivity also had an increased risk, by 90%. In contrast, the risk of developing skin psoriasis as an EAM was solely associated with HLA–B27 negativity, with an increase in risk of 90%, and with male sex, with an increase in risk of 50% (Table 2).

Another surrogate of the inflammatory burden, peripheral arthritis, showed a marked increase in risk, by 20%, per 10 years of disease duration (RR 1.2, $P < 0.001$), whereas in those receiving anti-TNF therapy at baseline, the increase in risk was 50% (RR 1.5, $P = 0.005$). However, with regard to enthesitis, the association with disease duration did not reach statistical significance ($P = 0.096$) (data not shown).

Linkage of IBD and acute anterior uveitis to cumulative exposure to inflammation in patients with axial SpA in a prospective analysis. A striking observation was that only IBD and acute anterior uveitis appeared to be associated with disease duration in the patient cohorts, which may be reflective of a higher cumulative load of inflammation over time in these patients. To test this hypothesis, a subanalysis of 171 patients from the (Be)Giant cohort with newly diagnosed axial SpA for whom prospective follow-up data were available was conducted. A comparison of the geometric mean CRP value over time was made between patients who developed IBD or acute anterior uveitis and those who did not.

Overall, 5.3% of patients (9 of 171) presented with IBD and 16.4% (28 of 171) presented with acute anterior uveitis. Psoriasis was present in 8.8% of patients in this subset (15 of 171) at the end of follow-up. Overlap of the EAMs was present in only 5.8% of patients (10 of 171), with 0.6% of the patients (1 of 171) developing IBD and acute anterior uveitis, 2.9% (5 of 171) developing both acute anterior uveitis and psoriasis, and 2.3% (4 of 171) developing IBD and psoriasis. Patient characteristics at

Table 3. Baseline characteristics of the patients exhibiting IBD and/or acute anterior uveitis compared to patients without EAMs or with psoriasis only*

	IBD and/or acute anterior uveitis (n = 47)	Without EAMs or with psoriasis only (n = 124)
Male, no. (%)	22 (46.8)	63 (50.8)
Fulfilled modified New York criteria, no. (%)	23 (48.9)	40 (32.3)†
Age, mean ± SD years	35.3 ± 8.2	33.1 ± 8.7
Symptom duration, median (range) years	5.1 (0.3–22.7)	3.9 (0.0–28.4)
HLA–B27+, no. (%)	39 (83.0)	88 (71.5)
SPARCC score of the SI joints, median (range)‡	9.4 (0.0–60.75)	10.1 (0.0–54.8)
BASDAI score, mean ± SD	3.7 ± 1.9	4.0 ± 2.0
CRP level at baseline, median (range) mg/dl	0.40 (0.0–2.4)	0.35 (0.0–6.7)
BASFI score, median (range)	2.3 (0.0–6.6)	2.3 (0.0–8.5)
ASDAS, mean ± SD	2.4 ± 0.8	2.5 ± 0.9
SJC, median (range)	0.0 (0.0–1.0)	0.0 (0.0–6.0)
Enthesitis, no. (%)	8 (17.4)	13 (10.3)
Chronic gut inflammation, no. (%)§	19 (47.5)	17 (21.5)¶

* EAMs = extraarticular manifestations; NS = not significant; BASDAI = Bath Ankylosing Spondylitis Disease Activity Index (scale 0–10); CRP = C-reactive protein; BASFI = Bath Ankylosing Spondylitis Functional Index (scale 0–10); ASDAS = Ankylosing Spondylitis Disease Activity Score (score >2.1 but <3.5 indicates high disease activity); SJC = swollen joint count.
† $P = 0.044$ versus other group.
‡ The Spondyloarthritis Research Consortium of Canada (SPARCC) score is an index for scoring inflammation of the sacroiliac (SI) joints by magnetic resonance imaging (scale 0–72).
§ Combination of both overt inflammatory bowel disease (IBD) and microscopic chronic gut inflammation.
¶ $P = 0.004$ versus other group.

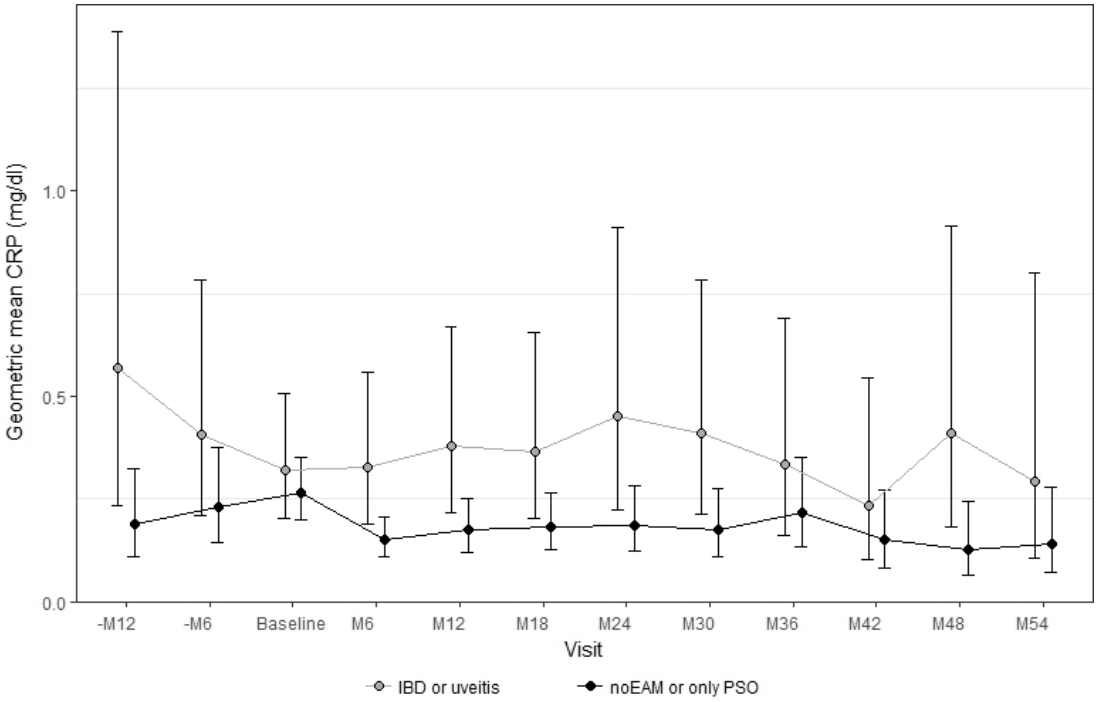

Figure 3. Evolution of the C-reactive protein (CRP) level over time in patients with IBD or acute anterior uveitis compared to patients without EAMs or patients with only skin psoriasis (PSO) in the prospective (Be)GIANT cohort. Values are the cumulative exposure to change in log-transformed CRP levels over time, calculated by linear mixed models. The results of this model are presented on the original scale (mg/dl) as the geometric mean with corresponding 95% confidence interval. M = month (see Figure 1 for other definitions).

the time of inclusion did not differ between the groups, except for a higher percentage of AS in the IBD and/or acute anterior uveitis group ($P = 0.044$).

Because microscopic gut inflammation occurs in ~50% of patients with SpA and is linked to more severe sacroiliac inflammation, we also determined the presence of gut inflammation in relation to the presence of clinically overt EAMs. Gut inflammation (including both acute and chronic microscopic gut inflammation and clinically overt IBD) was present in 60% of patients in the IBD and/or acute anterior uveitis group compared to 41.8% of patients in the group without EAMs or with psoriasis only ($P = 0.06$). Chronic gut inflammation (which resembles Crohn's disease) and/or overt IBD was present in 47.5% of patients in the IBD and/or acute anterior uveitis group compared to only 21.5% of patients in the subset without EAMs or with psoriasis alone ($P = 0.004$) (Table 3).

Both groups presented with high disease activity at baseline, as defined by an Ankylosing Spondylitis Disease Activity Score of >2.1 (Table 3). The mean follow-up time in patients with acute anterior uveitis or IBD and patients without EAMs or with psoriasis alone was 28.9 months and 26.9 months, respectively (*P* not significant).

Consistent with our hypothesis, we observed significantly higher geometric mean CRP values over time in patients with IBD or acute anterior uveitis compared to those without EAMs or those with psoriasis alone ($P = 0.01$) (Figure 3). In addition, in more than 37% of the patients with IBD and/or acute anterior uveitis, the CRP measurements reached ≥0.5 mg/dl, compared to 24.5% of patients without EAMs or those with psoriasis alone displaying a CRP level of ≥0.5 mg/dl ($P = 0.057$).

Thus, patients with axial SpA who develop IBD or acute anterior uveitis experience higher levels of CRP over time, as well as a higher frequency of gut inflammation and AS, as compared to axial SpA patients without EAMs or with skin psoriasis only.

DISCUSSION

In this study, a striking association between acute anterior uveitis, IBD, and disease duration in axial SpA was found. Surprisingly, this was not the case for psoriasis. We show that this duality could reflect an overall differential cumulative exposure to inflammation over time, with higher exposure in patients with IBD and/or acute anterior uveitis. To our knowledge, this is the first study to link a discriminative association of IBD and/or acute anterior uveitis, as opposed to psoriasis, to structural progression in axial SpA.

It is well-known that the genetic predisposition and cytokine-driven pathways of AS and psoriasis, acute anterior uveitis, and IBD are closely linked (1,17–21). The common physiopathology in the spectrum of SpA is illustrated by the shared success of anti-TNF therapy. Nevertheless, the variable success of other modes of action, such as the interleukin-17 (IL-17) and anti–IL-12/IL-23 pathways (22), illustrates the differences in tissue-specific responses.

The major histocompatibility complex region HLA–Cw6 has been shown to be increased in frequency in patients with psoriatic skin disease, whereas HLA–B27 was more closely related to joint disease in patients with psoriatic arthritis (23). Besides the lack of association with HLA–B27 in the present and previous studies (24,25), only a few shared loci were found between patients with AS and patients with psoriasis. In sharp contrast, much more overlap was reported between patients with AS and patients with IBD, with at least 23 shared loci (26). Likewise, the genetic overlap between AS and acute anterior uveitis is much greater than with psoriasis (27).

In addition to the genetic component, imaging features in patients with axial SpA with or without psoriasis (or psoriasis patients with spondylitis) seem to present differently, with sacroiliitis being preferentially located unilaterally, aberrant expression of syndesmophytes, and more frequent involvement of the cervical spine (28–32). Consistent with the results of the present study, psoriasis was associated with less inflammation, as evidenced on MRI of the spine and sacroiliac joints, and with less radiographic damage in a follow-up study of patients with early disease (10). Recently, Costantino et al reported on the possible existence of different phenotypes in the DESIR cohort of patients with IBP, with the analysis showing clustering of patients based on specific phenotypes, such as a cluster of patients with predominantly axial symptoms and a better response to NSAIDs in contrast to a cluster of patients with IBP and more prominent peripheral disease, consisting of arthritis, dactylitis, and enthesitis closely linked to psoriasis (33). Accordingly, our study findings revealed a similar trend toward a higher range of swollen joint counts in patients without EAMs or in patients displaying psoriasis.

A similar overall prevalence of the different EAMs was observed at the time of inclusion in both cohorts, which mirrors data from the DESIR cohort and the GESPIC cohort of patients with AS or nonradiographic axial SpA (2,3). In concordance with our results, the prevalence of acute anterior uveitis in AS has been reported to increase with disease duration or with duration of IBP (34–36). However, up until now, no investigators have been able to determine the association of IBD or psoriasis with disease duration, which is most likely attributable to the underrepresentation of patients with a shorter disease duration (34). Similarly, in the GESPIC cohort, no significant difference in EAM frequencies was observed between axial SpA patients with >5 years of symptom duration and axial SpA patients with ≤5 years of symptom duration, although the prevalence of both IBD and acute anterior uveitis was distinctly lower compared to that in other cohorts containing patients with a longer disease duration. Notably, this was not the case for psoriasis (3).

Remarkably, even in those with longstanding disease, overlap between EAMs appeared to be rather limited in axial SpA. Nevertheless, in a study by Wendling et al, an association between IBD with SpA and psoriasis in a well-established cohort of patients with IBP was found (36), while a lower prevalence of acute anterior uveitis in patients with IBD and SpA as compared to patients with classic AS has been reported (35,37–39). These seemingly contradictory results might be explained by overlap with peripheral disease, in which the link with EAMs is clearly different.

In the present study, a higher mean CRP level over time was observed in axial SpA patients with IBD or acute anterior uveitis compared to patients without EAMs or psoriasis only. Since CRP is a key predictor of radiographic progression over time, it may contribute to the divergent radiographic findings between these groups. Although our findings are indicative of an association between the presence of certain EAMs and CRP levels, these findings do not necessarily portray a causal relationship. The appearance of IBD or acute anterior uveitis may just as well be an expression of cumulative exposure to systemic inflammation. Alternatively, patients with IBD or acute anterior uveitis might simply develop more inflammation. Interestingly, patients with IBD and/or acute anterior uveitis not only displayed a higher CRP level over time, but also had a significantly higher frequency of AS at inclusion. In addition, a higher proportion of patients with IBD and/or acute anterior uveitis had gut inflammation, especially chronic gut inflammation, which in turn has been linked to more severe inflammation of the sacroiliac joints on MRI (9). The results of this analysis support the hypothesis that the overall exposure to systemic inflammation differs according to the spectrum of EAM in patients with axial SpA, potentially entailing a higher risk of structural progression in patients with IBD and/or acute anterior uveitis as compared to patients with psoriasis. As these EAMs frequently seem to occur early in the disease, and prior to diagnosis, they may be an early indication of risk of progressive disease.

Possible limitations of this study include the cross-sectional design of the ASPECT study compared to the

prospective nature of the (Be)Giant cohort. However, by including the cohort as a variable in our model, we corrected for this potential confounder, rendering our results independently associated with the presence of EAMs. Likewise, by including an interaction of CRP with the cohort in our model, we corrected for a possible differential effect of CRP in the different cohorts, as CRP values at diagnosis were not available in the ASPECT cohort, thus explaining the lower CRP values in the ASPECT patients compared to the (Be)Giant patients at baseline.

From a conceptual point of view, our data suggest that we should reconsider whether acute anterior uveitis, IBD, and psoriasis are 3 entities equally associated with axial SpA, even though a strong association between psoriasis and peripheral SpA has been established in the past. Overall, the risk of developing acute anterior uveitis or IBD, but not psoriasis, seems to increase with disease duration in axial SpA and appears to be linked to a higher cumulative exposure to inflammation.

AUTHOR CONTRIBUTIONS

All authors were involved in drafting the article or revising it critically for important intellectual content, and all authors approved the final version to be published. Dr. Elewaut had full access to all of the data in the study and takes responsibility for the integrity of the data and the accuracy of the data analysis.

Study conception and design. Varkas, Vastesaeger, Cypers, Van den Bosch, Elewaut.

Acquisition of data. Varkas, Vastesaeger, Cypers, Renson, Van Praet, Carron, Raeman, Devinck, Gyselbrecht, Corluy, Piette, Lenaerts, Thevissen, Vanneuville, Van den Bosch, Elewaut.

Analysis and interpretation of data. Varkas, Vastesaeger, Colman, Renson, Carron, Van den Bosch, Elewaut.

ROLE OF THE STUDY SPONSOR

Merck Sharp & Dohme provided support and collected patients for the ASPECT cohort. Merck Sharp & Dohme had no role in the study design or in the collection, analysis, or interpretation of the data, the writing of the manuscript, or the decision to submit the manuscript for publication. Publication of this article was not contingent upon approval by Merck Sharp & Dohme.

REFERENCES

1. Stolwijk C, Essers I, van Tubergen A, Boonen A, Bazelier MT, De Bruin ML, et al. The epidemiology of extra-articular manifestations in ankylosing spondylitis: a population-based matched cohort study. Ann Rheum Dis 2015;74:1373–8.
2. Dougados M, d'Agostino MA, Benessiano J, Berenbaum F, Breban M, Claudepierre P, et al. The DESIR cohort: a 10-year follow-up of early inflammatory back pain in France: study design and baseline characteristics of the 708 recruited patients. Joint Bone Spine 2011;78:598–603.
3. Rudwaleit M, Haibel H, Baraliakos X, Listing J, Märker-Hermann E, Zeidler H, et al. The early disease stage in axial spondylarthritis: results from the German Spondyloarthritis Inception Cohort. Arthritis Rheum 2009;60:717–27.
4. Poddubnyy D, Haibel H, Listing J, Märker-Hermann E, Zeidler H, Braun J, et al. Baseline radiographic damage, elevated acute-phase reactant levels, and cigarette smoking status predict spinal radiographic progression in early axial spondylarthritis. Arthritis Rheum 2012;64:1388–98.
5. Maksymowych WP, Chiowchanwisawakit P, Clare T, Pedersen SJ, Østergaard M, Lambert RG. Inflammatory lesions of the spine on magnetic resonance imaging predict the development of new syndesmophytes in ankylosing spondylitis: evidence of a relationship between inflammation and new bone formation. Arthritis Rheum 2009;60:93–102.
6. Vander Cruyssen B, Ribbens C, Boonen A, Mielants H, de Vlam K, Lenaerts J, et al. The epidemiology of ankylosing spondylitis and the commencement of anti-TNF therapy in daily rheumatology practice. Ann Rheum Dis 2007;66:1072–7.
7. Feltkamp TE, Ringrose JH. Acute anterior uveitis and spondyloarthropathies. Curr Opin Rheumatol 1998;10:314–8.
8. Juanola X, Loza Santamaria E, Cordero-Coma M, SENTINEL Working Group. Description and prevalence of spondyloarthritis in patients with anterior uveitis: the SENTINEL Interdisciplinary Collaborative Project. Ophthalmology 2016;123:1632–6.
9. Van Praet L, Jans L, Carron P, Jacques P, Glorieus E, Colman R, et al. Degree of bone marrow oedema in sacroiliac joints of patients with axial spondyloarthritis is linked to gut inflammation and male sex: results from the GIANT cohort. Ann Rheum Dis 2014;73:1186–9.
10. Chung HY, Machado P, van der Heijde D, D'Agostino MA, Dougados M. HLA-B27 positive patients differ from HLA-B27 negative patients in clinical presentation and imaging: results from the DESIR cohort of patients with recent onset axial spondyloarthritis. Ann Rheum Dis 2011;70:1930–6.
11. Van Praet L, Van den Bosch FE, Jacques P, Carron P, Jans L, Colman R, et al. Microscopic gut inflammation in axial spondyloarthritis: a multiparametric predictive model. Ann Rheum Dis 2013;72:414–7.
12. Van der Linden S, Valkenburg HA, Cats A. Evaluation of diagnostic criteria for ankylosing spondylitis: a proposal for modification of the New York criteria. Arthritis Rheum 1984;27:361–8.
13. Rudwaleit M, van der Heijde D, Landewé R, Akkoc N, Brandt J, Chou CT, et al. The Assessment of SpondyloArthritis international Society classification criteria for peripheral spondyloarthritis and for spondyloarthritis in general. Ann Rheum Dis 2010;70:25–31.
14. Garrett S, Jenkinson T, Kennedy LG, Whitelock H, Gaisford P, Calin A. A new approach to defining disease status in ankylosing spondylitis: the Bath Ankylosing Spondylitis Disease Activity Index. J Rheumatol 1994;21:2286–91.
15. Calin A, Garrett S, Whitelock H, Kennedy LG, O'Hea J, Mallorie P, et al. A new approach to defining functional ability in ankylosing spondylitis: the development of the Bath Ankylosing Spondylitis Functional Index. J Rheumatol 1994;21:2281–5.
16. Grant RL. Converting an odds ratio to a range of plausible relative risks for better communication of research findings. BMJ 2014;348:f7450.
17. Ellinghaus D, Jostins L, Spain SL, Cortes A, Bethune J, Han B, et al. Analysis of five chronic inflammatory diseases identifies 27 new associations and highlights disease-specific patterns at shared loci. Nat Genet 2016;48:510–8.
18. Lee FI, Bellary SV, Francis C. Increased occurrence of psoriasis in patients with Crohn's disease and their relatives. Am J Gastroenterol 1990;85:962–3.
19. Catsarou-Catsari A, Katsambas A, Theodoropoulos P, Stratigos J. Ophthalmological manifestations in patients with psoriasis. Acta Derm Venereol 1984;64:557–9.
20. Lolli E, Saraceno R, Calabrese E, Ascolani M, Scarozza P, Chiricozzi A, et al. Psoriasis phenotype in inflammatory bowel disease: a case-control prospective study. J Crohns Colitis 2015;9:699–707.
21. Eppinga H, Poortinga S, Thio HB, Nijsten TE, Nuij V, van der Woude CJ, et al. Prevalence and phenotype of concurrent psoriasis and inflammatory bowel disease. Inflamm Bowel Dis 2017;23:1783–92.

22. Hueber W, Sands BE, Lewitzky S, Vandemeulebroecke M, Reinisch W, Higgins PD, et al. Secukinumab, a human anti-IL-17A monoclonal antibody, for moderate to severe Crohn's disease: unexpected results of a randomised, double-blind placebo-controlled trial. Gut 2012;61:1693–700.
23. Rahman P, Elder JT. Genetic epidemiology of psoriasis and psoriatic arthritis. Ann Rheum Dis 2005;64 Suppl 2:ii37–9.
24. Essers I, Ramiro S, Stolwijk C, Blaauw M, Landewe R, van der Heijde D, et al. Characteristics associated with the presence and development of extra-articular manifestations in ankylosing spondylitis: 12-year results from OASIS. Rheumatology (Oxford) 2015;54:633–40.
25. Linssen A, Feltkamp TE. B27 positive diseases versus B27 negative diseases. Ann Rheum Dis 1988;47:431–9.
26. International Genetics of Ankylosing Spondylitis Consortium, Cortes A, Hadler J, Pointon JP, Robinson PC, Karaderi T, et al. Identification of multiple risk variants for ankylosing spondylitis through high-density genotyping of immune-related loci. Nat Genet 2013;45:730–8.
27. Robinson PC, Claushuis TA, Cortes A, Martin TM, Evans DM, Leo P, et al. Genetic dissection of acute anterior uveitis reveals similarities and differences in associations observed with ankylosing spondylitis. Arthritis Rheumatol 2015;67:140–51.
28. McEwen C, DiTata D, Lingg C, Porini A, Good A, Rankin T. Ankylosing spondylitis and spondylitis accompanying ulcerative colitis, regional enteritis, psoriasis and Reiter's disease: a comparative study. Arthritis Rheum 1971;14:291–318.
29. Gladman DD. Psoriatic arthritis. Rheum Dis Clin North Am 1998;24:829–44.
30. Salvarani C, Macchioni P, Cremonesi T, Mantovani W, Battistel B, Rossi F, et al. The cervical spine in patients with psoriatic arthritis: a clinical, radiological and immunogenetic study. Ann Rheum Dis 1992;51:73–7.
31. Helliwell PS, Hickling P, Wright V. Do the radiological changes of classic ankylosing spondylitis differ from the changes found in the spondylitis associated with inflammatory bowel disease, psoriasis, and reactive arthritis? Ann Rheum Dis 1998;57:135–40.
32. Jadon DR, Sengupta R, Nightingale A, Lindsay M, Korendowych E, Robinson G, et al. Axial disease in psoriatic arthritis study: defining the clinical and radiographic phenotype of psoriatic spondyloarthritis. Ann Rheum Dis 2016;76:701–7.
33. Costantino F, Aegerter P, Dougados M, Breban M, D'Agostino MA. Two phenotypes are identified by cluster analysis in early inflammatory back pain suggestive of spondyloarthritis: results from the DESIR cohort. Arthritis Rheumatol 2016;68:1660–8.
34. Stolwijk C, van Tubergen A, Castillo-Ortiz JD, Boonen A. Prevalence of extra-articular manifestations in patients with ankylosing spondylitis: a systematic review and meta-analysis. Ann Rheum Dis 2015;74:65–73.
35. Zeboulon N, Dougados M, Gossec L. Prevalence and characteristics of uveitis in the spondyloarthropathies: a systematic literature review. Ann Rheum Dis 2008;67:955–9.
36. Wendling D, Prati C, Demattei C, Miceli-Richard C, Daures JP, Dougados M. Impact of uveitis on the phenotype of patients with recent inflammatory back pain: data from a prospective multicenter French cohort. Arthritis Care Res (Hoboken) 2012;64:1089–93.
37. Palm O, Moum B, Ongre A, Gran JT. Prevalence of ankylosing spondylitis and other spondyloarthropathies among patients with inflammatory bowel disease: a population study (the IBSEN study). J Rheumatol 2002;29:511–5.
38. Zippi M, Corrado C, Pica R, Avallone EV, Cassieri C, De Nitto D, et al. Extraintestinal manifestations in a large series of Italian inflammatory bowel disease patients. World J Gastroenterol 2014;20:17463–72.
39. Isene R, Bernklev T, Hoie O, Munkholm P, Tsianos E, Stockbrugger R, et al. Extraintestinal manifestations in Crohn's disease and ulcerative colitis: results from a prospective, population-based European inception cohort. Scand J Gastroenterol 2015;50:300–5.

DOI 10.1002/art.40716

Errata

In the article by Wilkinson et al in the August 2017 issue of *Arthritis & Rheumatology* (Matriptase Induction of Metalloproteinase-Dependent Aggrecanolysis In Vitro and In Vivo: Promotion of Osteoarthritic Cartilage Damage by Multiple Mechanism [pages 1601–1611]), the name of one of the authors was omitted. Hui Wang, MD (Newcastle University, Newcastle upon Tyne, UK [current address: University of Aberdeen, Aberdeen, UK]) should have been listed as the second author.

DOI 10.1002/art.40719

In the review by Zaid et al in the April 2018 issue of *Arthritis & Rheumatology* (Chikungunya Arthritis: Implications of Acute and Chronic Inflammation Mechanisms on Disease Management [pages 484–495]), the terminology used throughout the text to describe clinical manifestations associated with chikungunya virus infection should have been "chikungunya virus disease" or "CHIKVD," rather than "chikungunya virus." The authors would like to highlight the stark distinction between the two terms: specifically, "chikungunya virus" refers to the pathogen, and "chikungunya virus disease" refers to the range of clinical manifestations (as discussed in detail in the article) of the disease caused by the pathogen.

In addition, the authors would like to clarify that the findings described in reference 36 (Hoarau et al, J Immunol 2010) suggesting that chikungunya virus antigen persists in the tissues of patients with chronic chikungunya disease have not yet been confirmed in other studies (e.g., Chang et al, in the same issue of *Arthritis & Rheumatology* [pages 578–584]). Clearly more studies are needed to determine the extent of RNA/antigen persistence in chronic CHIKVD.

We regret the errors.

22. Hueber W, Sands BE, Lewitzky S, Vandemeulebroecke M, Reinisch W, Higgins PD, et al. Secukinumab, a human anti-IL-17A monoclonal antibody, for moderate to severe Crohn's disease: unexpected results of a randomised, double-blind placebo-controlled trial. Gut 2012;61:1693–700.
23. Rahman P, Elder JT. Genetic epidemiology of psoriasis and psoriatic arthritis. Ann Rheum Dis 2005;64 Suppl 2:ii37–9.
24. Essers I, Ramiro S, Stolwijk C, Blaauw M, Landewe R, van der Heijde D, et al. Characteristics associated with the presence and development of extra-articular manifestations in ankylosing spondylitis: 12-year results from OASIS. Rheumatology (Oxford) 2015;54:633–40.
25. Linssen A, Feltkamp TE. B27 positive diseases versus B27 negative diseases. Ann Rheum Dis 1988;47:431–9.
26. International Genetics of Ankylosing Spondylitis Consortium, Cortes A, Hadler J, Pointon JP, Robinson PC, Karaderi T, et al. Identification of multiple risk variants for ankylosing spondylitis through high-density genotyping of immune-related loci. Nat Genet 2013;45:730–8.
27. Robinson PC, Claushuis TA, Cortes A, Martin TM, Evans DM, Leo P, et al. Genetic dissection of acute anterior uveitis reveals similarities and differences in associations observed with ankylosing spondylitis. Arthritis Rheumatol 2015;67:140–51.
28. McEwen C, DiTata D, Lingg C, Porini A, Good A, Rankin T. Ankylosing spondylitis and spondylitis accompanying ulcerative colitis, regional enteritis, psoriasis and Reiter's disease: a comparative study. Arthritis Rheum 1971;14:291–318.
29. Gladman DD. Psoriatic arthritis. Rheum Dis Clin North Am 1998;24:829–44.
30. Salvarani C, Macchioni P, Cremonesi T, Mantovani W, Battistel B, Rossi F, et al. The cervical spine in patients with psoriatic arthritis: a clinical, radiological and immunogenetic study. Ann Rheum Dis 1992;51:73–7.
31. Helliwell PS, Hickling P, Wright V. Do the radiological changes of classic ankylosing spondylitis differ from the changes found in the spondylitis associated with inflammatory bowel disease, psoriasis, and reactive arthritis? Ann Rheum Dis 1998;57:135–40.
32. Jadon DR, Sengupta R, Nightingale A, Lindsay M, Korendowych E, Robinson G, et al. Axial disease in psoriatic arthritis study: defining the clinical and radiographic phenotype of psoriatic spondyloarthritis. Ann Rheum Dis 2016;76:701–7.
33. Costantino F, Aegerter P, Dougados M, Breban M, D'Agostino MA. Two phenotypes are identified by cluster analysis in early inflammatory back pain suggestive of spondyloarthritis: results from the DESIR cohort. Arthritis Rheumatol 2016;68:1660–8.
34. Stolwijk C, van Tubergen A, Castillo-Ortiz JD, Boonen A. Prevalence of extra-articular manifestations in patients with ankylosing spondylitis: a systematic review and meta-analysis. Ann Rheum Dis 2015;74:65–73.
35. Zeboulon N, Dougados M, Gossec L. Prevalence and characteristics of uveitis in the spondyloarthropathies: a systematic literature review. Ann Rheum Dis 2008;67:955–9.
36. Wendling D, Prati C, Demattei C, Miceli-Richard C, Daures JP, Dougados M. Impact of uveitis on the phenotype of patients with recent inflammatory back pain: data from a prospective multicenter French cohort. Arthritis Care Res (Hoboken) 2012;64:1089–93.
37. Palm O, Moum B, Ongre A, Gran JT. Prevalence of ankylosing spondylitis and other spondyloarthropathies among patients with inflammatory bowel disease: a population study (the IBSEN study). J Rheumatol 2002;29:511–5.
38. Zippi M, Corrado C, Pica R, Avallone EV, Cassieri C, De Nitto D, et al. Extraintestinal manifestations in a large series of Italian inflammatory bowel disease patients. World J Gastroenterol 2014;20:17463–72.
39. Isene R, Bernklev T, Hoie O, Munkholm P, Tsianos E, Stockbrugger R, et al. Extraintestinal manifestations in Crohn's disease and ulcerative colitis: results from a prospective, population-based European inception cohort. Scand J Gastroenterol 2015;50:300–5.

DOI 10.1002/art.40716

Errata

In the article by Wilkinson et al in the August 2017 issue of *Arthritis & Rheumatology* (Matriptase Induction of Metalloproteinase-Dependent Aggrecanolysis In Vitro and In Vivo: Promotion of Osteoarthritic Cartilage Damage by Multiple Mechanism [pages 1601–1611]), the name of one of the authors was omitted. Hui Wang, MD (Newcastle University, Newcastle upon Tyne, UK [current address: University of Aberdeen, Aberdeen, UK]) should have been listed as the second author.

DOI 10.1002/art.40719

In the review by Zaid et al in the April 2018 issue of *Arthritis & Rheumatology* (Chikungunya Arthritis: Implications of Acute and Chronic Inflammation Mechanisms on Disease Management [pages 484–495]), the terminology used throughout the text to describe clinical manifestations associated with chikungunya virus infection should have been "chikungunya virus disease" or "CHIKVD," rather than "chikungunya virus." The authors would like to highlight the stark distinction between the two terms: specifically, "chikungunya virus" refers to the pathogen, and "chikungunya virus disease" refers to the range of clinical manifestations (as discussed in detail in the article) of the disease caused by the pathogen.

In addition, the authors would like to clarify that the findings described in reference 36 (Hoarau et al, J Immunol 2010) suggesting that chikungunya virus antigen persists in the tissues of patients with chronic chikungunya disease have not yet been confirmed in other studies (e.g., Chang et al, in the same issue of *Arthritis & Rheumatology* [pages 578–584]). Clearly more studies are needed to determine the extent of RNA/antigen persistence in chronic CHIKVD.

We regret the errors.

ARTHRITIS & RHEUMATOLOGY
Vol. 70, No. 10, October 2018, pp 1597–1609
DOI 10.1002/art.40535

Toll-Like Receptor 9 Deficiency Breaks Tolerance to RNA-Associated Antigens and Up-Regulates Toll-Like Receptor 7 Protein in *Sle1* Mice

Teja Celhar,[1] Hiroko Yasuga,[1] Hui Yin Lee,[1] Olga Zharkova,[1] Shubhita Tripathi,[1] Susannah I. Thornhill,[1] Hao K. Lu,[1] Bijin Au,[2] Lina H. K. Lim,[3] Thomas P. Thamboo,[3] Shizuo Akira,[4] Edward K. Wakeland,[5] John E. Connolly,[2] and Anna-Marie Fairhurst[1]

Objective. **Toll-like receptors (TLRs) 7 and 9 are important innate signaling molecules with opposing roles in the development and progression of systemic lupus erythematosus (SLE). While multiple studies support the notion of a dependency on TLR-7 for disease development, genetic ablation of TLR-9 results in severe disease with glomerulonephritis (GN) by a largely unknown mechanism. This study was undertaken to examine the suppressive role of TLR-9 in the development of severe lupus in a mouse model.**

Methods. **We crossed *Sle1* lupus-prone mice with TLR-9–deficient mice to generate *Sle1*TLR-9$^{-/-}$ mice. Mice ages 4.5–6.5 months were evaluated for severe autoimmunity by assessing splenomegaly, GN, immune cell populations, autoantibody and total Ig profiles, kidney dendritic cell (DC) function, and TLR-7 protein expression. Mice ages 8–10 weeks were used for functional B cell studies, Ig profiling, and determination of TLR-7 expression.**

Results. ***Sle1*TLR-9$^{-/-}$ mice developed severe disease similar to TLR-9–deficient *MRL* and *Nba2* models. *Sle1*TLR-9$^{-/-}$ mouse B cells produced more class-switched antibodies, and the autoantibody repertoire was skewed toward RNA-containing antigens. GN in these mice was associated with DC infiltration, and purified *Sle1*TLR-9$^{-/-}$ mouse renal DCs were more efficient at TLR-7–dependent antigen presentation and expressed higher levels of TLR-7 protein. Importantly, this increase in TLR-7 expression occurred prior to disease development, indicating a role in the initiation stages of tissue destruction.**

Conclusion. **The increase in TLR-7–reactive immune complexes, and the concomitant enhanced expression of their receptor, promotes inflammation and disease in *Sle1*TLR9$^{-/-}$ mice.**

The pattern-recognition receptors Toll-like receptor 7 (TLR-7) and TLR-9 are intracellular sensors of single-stranded RNA and double-stranded DNA (dsDNA), respectively (1). Upon binding microbial nucleic acids, signaling cascades are activated to rapidly induce an inflammatory immune response designed to clear the pathogen (1). Several mechanisms prevent the activation of TLR-7 and TLR-9 by self nucleic acids, including endosomal localization, tight regulation of their trafficking, and proteolytic processing prior to receptor activation (2,3). In systemic lupus erythematosus (SLE), however, a unique combination of self nucleic acid overload and the presence of antinuclear autoantibodies (ANAs) leads to aberrant TLR-7/9 activation (4,5). The immune complexes (ICs) formed between ANAs and their respective antigens (RNA/DNA and RNA/DNA-associated proteins) deposit in tissues where they cause chronic inflammation and ultimately lead to irreversible

Supported by core funding from Singapore Immunology Network, Agency for Science, Technology, and Research (grant to Dr. Fairhurst) and Institute of Molecular and Cell Biology, Agency for Science, Technology, and Research (grant to Dr. Connolly).

[1]Teja Celhar, PhD, Hiroko Yasuga, BSc, Hui Yin Lee, BSc, Olga Zharkova, PhD, Shubhita Tripathi, MSc, Susannah I. Thornhill, PhD, Hao K. Lu, PhD, Anna-Marie Fairhurst, PhD: Singapore Immunology Network, Agency for Science, Technology, and Research, Singapore; [2]Bijin Au, BSc, John E. Connolly, PhD: Institute of Molecular and Cell Biology, Agency for Science, Technology, and Research, Singapore; [3]Lina H. K. Lim, PhD, Thomas P. Thamboo, MD: National University Hospital, Singapore; [4]Shizuo Akira, PhD: Osaka University, Osaka, Japan; [5]Edward K. Wakeland, PhD: University of Texas Southwestern Medical Center, Dallas.

Address correspondence to Anna-Marie Fairhurst, PhD, Singapore Immunology Network, Agency for Science, Technology, and Research, 8A Biomedical Grove, #03-06 Immunos, 138648 Singapore. E-mail: annamarie_fairhurst@immunol.a-star.edu.sg.

Submitted for publication January 30, 2018; accepted in revised form April 17, 2018.

organ damage (6). Due to the similarities between TLR-7 and TLR-9 expression and shared signaling pathways, it has been predicted that the deletion of either of these receptors would be beneficial in terms of disease progression. Unexpectedly, TLR-9 deletion caused disease exacerbation in multiple models of spontaneous and induced lupus, while TLR-7 proved to be essential for disease development (7–14). These data suggest that the system is more complex than originally thought; however, the means by which TLR-9 prevents progression to severe disease are largely unknown.

Supporting the notion of their divergent in vivo roles, analysis of TLR-7/9 messenger RNA (mRNA) expression reveals a separation in regulatory mechanisms. TLR-7 is rapidly induced in human immune cells following stimulation with bacteria, viruses, lipopolysaccharide (LPS), CpG, interferon-α (IFNα), and SLE patient serum (15–19). However, TLR-9 can be induced in B cells, but is either down-regulated or unchanged in other cell types (16–20). We have previously shown this in human dendritic cell (DC) subsets, where plasmacytoid DCs (pDCs), BDCA-1+, and BDCA-3+ DCs all up-regulated TLR-7 mRNA in response to IFNα or influenza, but TLR-9 mRNA was down-regulated in pDCs (15). These differences suggest a separation of TLR-7/9 receptor roles, which might have important implications in SLE. Abundant immune complex–bound TLR-7/9 ligands and inflammatory mediators such as IFNα in SLE serum can chronically interfere with the expression of TLR-7 and TLR-9, disrupting homeostatic mechanisms to retain tolerance. Studies involving TLR-9– and/or TLR-7–deficient autoimmune mice can significantly contribute to the understating of these mechanisms, since TLRs are highly conserved in vertebrates (21) and humans and mice with lupus share the same autoantibody repertoire (22).

In this study we set out to examine the cellular mechanisms by which TLR-9 deficiency results in severe lupus nephritis. We bred B6.NZM2410-derived *Sle1* congenic mice, which develop mild autoimmune traits, with TLR-9–deficient mice to generate *Sle1*TLR-9$^{-/-}$ mice (23,24). By ages 4–6.5 months, female *Sle1*TLR9$^{-/-}$ mice developed severe autoimmunity, characterized by splenomegaly and kidney disease, similar to findings in TLR-9–deficient *MRL* and *Nba2* mice (8,10). Glomerulonephritis (GN) was associated with DC infiltration, and upon extraction, *Sle1*TLR-9$^{-/-}$ mouse renal DCs were more efficient at TLR-7–dependent antigen presentation than *Sle1* mouse controls. A comprehensive analysis of intracellular TLR-7 protein expression revealed an increase in TLR-7 expression in renal DCs and macrophages, which positively correlated with their recruitment into the kidney. Importantly, this increase in TLR-7 occurred prior to disease development, indicating a role in the initiation stages of tissue destruction. Additionally, our data show that, in the absence of TLR-9, *Sle1* mouse B cells are primed to produce more class-switched antibodies, and the autoantibody repertoire is skewed toward RNA-containing antigens. In summary, this study provides a unique understanding of the protective role TLR-9 plays in the development of autoimmunity and identifies the TLR-7 pathway as a critical instigator of disease development.

MATERIALS AND METHODS

Mice. Mice were bred at the Biomedical Resource Center (Singapore) or the University of Texas Southwestern Medical Center. The derivations of the B6.*Sle1* (*Sle1*), TLR-9$^{-/-}$, and TLR-7$^{-/-}$ mouse strains have been described previously (23–25). TLR-9$^{-/-}$ and TLR-7$^{-/-}$ mice (backcrossed to B6 more than 10 generations) and OT-II–transgenic mice were bred with *Sle1* mice (defined by the microsatellite markers D1Mit17, D1Mit113, and D1Mit202). SLE disease traits were evaluated in 4.5–6.5-month-old female mice, and functional cellular assessments were conducted using 8–10-week-old female mice. The care and use of laboratory animals conformed to the National Institutes of Health guidelines, and all experimental procedures were conducted according to an Institutional Animal Care and Use Committee–approved animal protocol.

Pathologic assessment of mouse kidneys. Proteinuria was assessed using Albustix (Bayer). Blood urea nitrogen (BUN) was assessed using a QuantiChrom Urea Assay Kit (BioAssay Systems). For evaluation of GN, mouse kidneys were fixed in formalin and embedded in paraffin, and 3-μm sections were stained with hematoxylin and eosin and with periodic acid–Schiff. Microscopic morphologic analysis was performed by an independent pathologist (TPT) according to the International Society of Nephrology/Renal Pathology Society 2003 criteria for the classification of lupus nephritis (26).

Autoantibody enzyme-linked immunosorbent assays (ELISAs). Serum autoantibodies were measured using ELISAs to detect antinucleosomes (histones and dsDNA), anti-dsDNA, anti–U1 small nuclear RNP (anti–U1 snRNP), or anti-RNA as previously described (27,28). Bound IgG was detected with alkaline phosphatase–conjugated anti-mouse IgG (Jackson ImmunoResearch) using paranitrophenyl phosphate as a substrate (Sigma). Absorbance was measured at 405/410 nm. Results are shown as arbitrary units (AU) that were calculated as absorbance at 405 nm (sample minus blank). For anti-RNA, serial dilutions of pooled serum from diseased mice were used to construct a standard curve.

ANA Luminex assay. An AtheNA Multi-Lyte ANA III Test System (Zeus Scientific) was used to measure 10 analytes (autoantibodies to SSA 52, SSA 60, SSB, Sm, RNP, Scl-70, Jo-1, centromere B, ribosomal P, and dsDNA) according to the recommendations of the manufacturer, with a goat polyclonal secondary antibody to mouse IgG heavy and light chains (Dylight 550; Abcam). Samples were run on a

Luminex 200 system using Luminex 100 IS software and analyzed using AtheNA Multi-Lyte Test System data analysis software (Zeus Scientific). Unit values reported are IU/ml for dsDNA and AU/ml for the remaining analytes.

Ig isotyping assays. Ig subtypes (IgA, IgG1, IgG2a/c, IgG2b, IgG3, and IgM) were measured using a mouse Ig isotyping bead panel (EMD Millipore), according to the recommendations of the manufacturer. This panel is designed to detect IgG2a (from BALB/c mice), which cross-reacts with IgG2c from mice on the B6 background, which we have labeled as IgG2a/c (29). Luminex plates were read on a Flexmap 3D System (Luminex) with Bio-Plex Manager version 6.0 software (Bio-Rad). IgM concentrations from cell culture supernatants were analyzed with an IgM ELISA (eBioscience) according to the recommendations of the manufacturer.

Microscopy. ANA screening was performed with NOVA Lite HEp-2 slides and the *Crithidia luciliae* indirect immunofluorescence test (CLIFT) using NOVA Lite dsDNA *Crithidia luciliae* substrate slides (both from Inova Diagnostics) according to the recommendations of the manufacturer. Sera were diluted 200-fold for HEp-2 and 40-fold for CLIFT, and a goat anti-mouse IgG DyLight 488 secondary antibody (Abcam) was used for detection. CLIFT slides were counterstained with DAPI. All images were obtained using a Zeiss LSM 800 upright confocal microscope with Zeiss Zen (Blue edition) software at 100× and 200× magnification for HEp-2 and CLIFT, respectively. HEp-2 staining patterns were evaluated by 2 independent investigators according to the International Consensus on Antinuclear Antibody Patterns. Confocal images of splenic germinal centers were obtained with an Olympus FV1000 confocal laser scanning microscope and were processed with FluoView (Olympus).

Flow cytometric analysis and cell sorting. Single-cell suspensions of the mouse spleen and kidneys were obtained as previously described with additional collagenase digestion for splenic DC analysis (30). Cells were blocked for 15 minutes in staining buffer (phosphate buffered saline with 1% fetal calf serum and 15 m*M* HEPES) containing 20% 2.4G2 hybridoma supernatant and incubated on ice for 30 minutes with the antibodies listed in Supplementary Table 1 (available on the *Arthritis & Rheumatology* web site at http://onlinelibrary.wiley.com/doi/10.1002/art.40535/abstract). When a biotin-conjugated antibody was used, cells were washed and incubated for an additional 30 minutes with a streptavidin-conjugated fluorophore. Red blood cell lysis was achieved using BD FACS lysing solution, followed by washing and resuspension in 1% paraformaldehyde. For sorting of live kidney cells, ACK lysis buffer (Lonza) was used, and cells were resuspended in staining buffer. For intracellular staining with anti–TLR-7, the BD Cytofix/Cytoperm fixation/permeabilization solution kit was used according to the recommendations of the manufacturer. Acquisition and analysis were completed using a BD Canto II, BD Fortessa, BD LSR II, or BD Symphony system, with FlowJo 10 for Windows (Tree Star). Mouse kidney cells were sorted using BD Aria II, Aria IV, and Aria V.

In vitro B cell stimulation. Mouse splenocytes stained with 5,6-carboxyfluorescein succinimidyl ester (CFSE) were resuspended in complete RPMI media, consisting of RPMI 1640 (Gibco Life Technologies) supplemented with 10% fetal bovine serum (HyClone; ThermoFisher Scientific), 15 m*M* HEPES, 100 μg/ml streptomycin, 100 units/ml penicillin, 200 μ*M* L-glutamine,10 μ*M* nonessential amino acids, 100 μ*M* sodium pyruvate (all from Gibco), and 45 μ*M* 2-mercaptoethanol (Sigma-Aldrich). They were plated at 1.5×10^6 cells/ml in round-bottomed 96-well plates in the presence of either CpG-B (ODN 1826), R848, or LPS-EB Ultrapure (all from InvivoGen) at the indicated concentrations. Activation was measured by CD69 and CD86 up-regulation at 24 hours, and proliferation at 72 hours was measured by CFSE dilution using flow cytometry. Ig subtype analysis in supernatants was measured 96 hours after stimulation.

Renal DC antigen presentation assay. Mouse kidneys cells were sorted, and cells were seeded in a 96-well plate at 1×10^4 cells per well. Where indicated, cells sorted from multiple mice were pooled to achieve sufficient cell numbers. Cells were stimulated overnight with or without 1 μg/ml R848 (InvivoGen), and then incubated with 10 μg/ml ovalbumin (Sigma-Aldrich). After 4 hours, medium was replaced with CFSE-stained *Sle1*OT-II mouse splenocytes at 2×10^5 cells per well. After 5 days of incubation, T cell proliferation was assessed by CFSE dilution.

Statistical analysis. Data were analyzed using GraphPad Prism 7.01 for Windows. Normal distribution was assessed using the Kolmogorov-Smirnov test. Gaussian data were analyzed using Student's *t*-test for 2 comparisons and ordinary one-way analysis of variance with post hoc Bonferroni adjustment for multiple comparisons for 3 or more comparisons. Nonparametric data were assessed using the Mann-Whitney test for 2 comparisons and the Kruskal-Wallis test with post hoc Dunn's multiple comparisons test for 3 or more comparisons. Where indicated, a multiple *t*-test corrected with the Holm-Sidak method was used.

RESULTS

Severe autoimmune disease in *Sle1* mice with genetic ablation of TLR-9. Cohorts of 4.5–6.5-month-old female *Sle1*TLR-$9^{-/-}$ mice and controls were analyzed for pathologic traits associated with common models of SLE. Genetic ablation of TLR-9 in *Sle1* mice resulted in splenomegaly and the expansion of all major leukocyte subsets (Figures 1A and B). There was a significant increase in CD11b+ cell numbers in *Sle1* mice versus wild-type C57BL/6J (B6) mice and in TLR-$9^{-/-}$ mice versus wild-type mice, indicating that both genetic components contribute to splenic myeloid cell expansion (Figure 1B). We detected an expansion of germinal center B cells in *Sle1*TLR-$9^{-/-}$ mice compared to *Sle1* controls, similar to observations in *Sle1b*TLR-$9^{-/-}$ and MRL/+TLR-$9^{-/-}$ mice (Figures 1C and D and Supplementary Table 2, available on the *Arthritis & Rheumatology* web site at http://onlinelibrary.wiley.com/doi/10.1002/art.40535/abstract) (9,31). We also observed increases in CD138+B220− plasma cell numbers (Supplementary Table 2) and a decreased frequency of marginal zone B cells (Supplementary Figure 1A, available on the *Arthritis & Rheumatology* web site at http://onlinelibrary.wiley.com/doi/10.1002/art.40535/abstract), which are characteristics of lupus

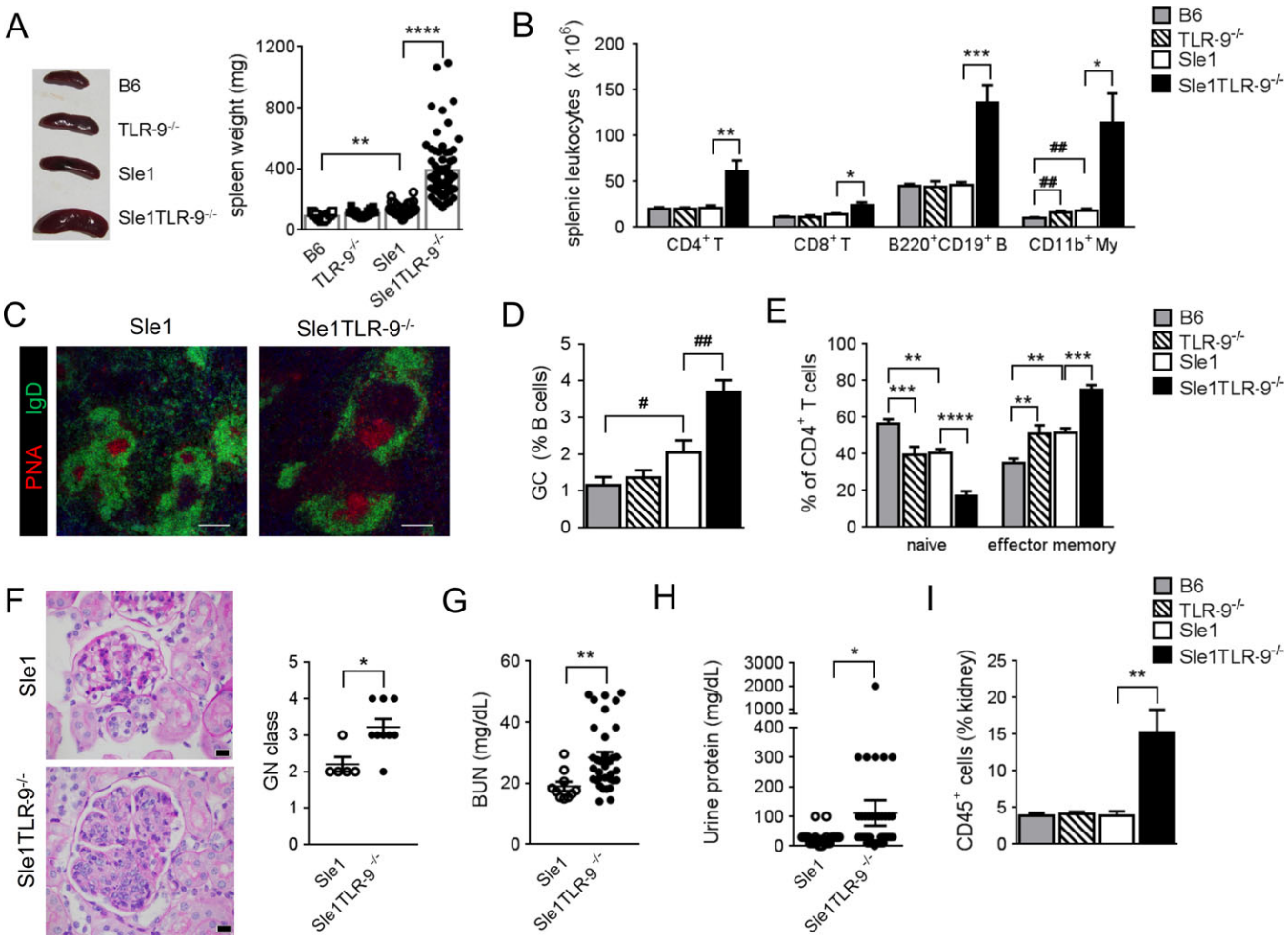

Figure 1. Severe disease in Toll-like receptor 9 (TLR-9)–deficient mice. Female B6, TLR-9$^{-/-}$, *Sle1*, and *Sle1*TLR-9$^{-/-}$ mice ages 4.5–6.5 months were analyzed for lupus disease features. **A**, Left, Representative spleens from the indicated mouse strains. Right, Cumulative splenic weights for the indicated mouse strains. Symbols represent individual mice; bars show the mean (n = 30–65 mice/group). **B**, Numbers of leukocytes of each subset in the spleens of mice of the indicated strains. My = myeloid cells. **C**, Representative images of germinal center (GC) staining in the spleens of *Sle1* and *Sle1*TLR-9$^{-/-}$ mice. PNA = peanut agglutinin. Bars = 200 μm; original magnification × 100. **D**, GC frequency measured by flow cytometric analysis of GL-7+Fas+ cells and presented as the percentage of B cells (CD19+B220+). **E**, Flow cytometric analysis of naive (CD62L^{high} CD44^{low}) and effector memory (CD62L^{low}CD44^{high}) CD4+ T cells in the spleens of mice of the indicated strains. **F**, Left, Representative photomicrographs of an *Sle1* mouse glomerulus with mild segmental mesangial proliferation and an *Sle1*TLR-9$^{-/-}$ mouse glomerulus with global endocapillary proliferation. Periodic acid–Schiff stained. Bars = 20 μm; original magnification × 600. Right, Kidney glomerulonephritis (GN) class (I–IV represented as 1–4) in *Sle1* and *Sle1*TLR-9$^{-/-}$ mice. **G** and **H**, Functional assessment of mouse kidneys. Blood urea nitrogen (BUN) (**G**) and urinary protein levels (measured by Albustix) (**H**) were determined. **I**, Infiltration of CD45+ leukocytes into the mouse kidney, assessed by flow cytometry. All flow cytometry data (in **B**, **D**, **E**, and **I**) are from 2–5 separate cohorts with a total of 6–17 mice per group. In **B**, **D**, **E**, and **I**, bars show the mean ± SEM. In **F**–**H**, circles represent individual mice; horizontal lines and error bars show the mean ± SEM. * = $P < 0.05$; ** = $P < 0.01$; *** = $P < 0.001$; **** = $P < 0.0001$, by one-way analysis of variance (with Bonferroni adjustment for multiple comparisons) for parametric data or Kruskal-Wallis test (with Dunn's multiple comparison test) for nonparametric data, taking into consideration all 4 groups; # = $P < 0.05$; ## = $P < 0.01$, by Student's *t*-test for parametric data or Mann-Whitney test for nonparametric data, taking into consideration only 2 groups.

models overexpressing TLR-7 (32,33). CD4+ and CD8+ T cells from *Sle1*TLR-9$^{-/-}$ mice had a more activated phenotype, with higher percentages of CD62L^{low} CD44^{high} effector memory cells and CD4+ follicular helper T cells, and increased programmed death 1 and inducible costimulator expression, consistent with observations in S*le1b*TLR-9$^{-/-}$ mice and in *Sle1* mouse models overexpressing TLR-7, such as *Sle1*Tg7 (15,31,32) (Figure 1E, Supplementary Figures 1B–D, and Supplementary Table 2).

Analysis of the splenic CD11b+ myeloid lineage revealed increases in the numbers of $Gr1^{high}$ polymorphonuclear leukocytes (PMNs) and SSC-A^{high} eosinophils in *Sle1*TLR-$9^{-/-}$ mice compared to controls (Supplementary Table 2 and Supplementary Figure 1E). $Gr1^{-/low}$ cells represented the majority of the expanding myeloid population (Supplementary Figure 1E) and were further analyzed for CD11c and major histocompatibility complex (MHC) class II expression (Supplementary Figure 1F). Conventional CD11b+ DCs (cDCs) expressing MHC class II, and a possible precursor, which lacks MHC class II, were increased; both were previously characterized in the *Sle1*Tg7 model (Supplementary Figure 1F and Supplementary Table 2) (15). Splenic F4/80+CD64+$CD11b^{intermediate}$ macrophage, CD8+ DC, and pDC numbers, but not frequencies, were increased due to increased cellularity in TLR-9–deficient *Sle1* mice (Supplementary Table 2).

Pathologic analysis confirmed that the majority of *Sle1*TLR-$9^{-/-}$ mice developed severe GN (class III–IV), characterized by segmental to global endocapillary proliferation of the glomeruli (Figure 1F). Increased serum BUN levels and urinary protein levels confirmed these findings (Figures 1G and H). GN was associated with an infiltration of CD45+ leukocytes into the mouse kidney, consisting mainly of T cells and CD11b+ myeloid cells (Figure 1I and Supplementary Table 2). CD11b+ cells were mostly $Gr1^{-/low}$, as determined previously in *Sle1*Tg7 mice (Supplementary Figure 1G) (15). B cells and pDCs comprised minor populations in the kidney infiltrates and were not significantly increased in the absence of TLR-9 (Supplementary Table 2).

TLR-9 deficiency in *Sle1* mice skews the autoantibody profile toward RNA-associated autoantigens. Previous studies have shown that TLR-9 deletion on the MRL mouse background results in a shift from homogenous nuclear to cytoplasmic ANA HEp-2 staining patterns and the loss of binding to mitotic chromatin (7–9). This coincides with lower levels of antinucleosome antibodies, but not with lower anti-dsDNA antibody titers as measured by ELISA (8). Similarly, elimination of TLR-9 decreased antinucleosome/chromatin antibodies in B6.Fas/*lpr*, Plcg2*Ali5*, and B6*Nba2* mice, while anti-dsDNA levels measured by ELISA were increased or unchanged (10,13,34).

Next, we examined the autoantibody profile in *Sle1*TLR-$9^{-/-}$ mice, using a variety of methods for clarity. Microscopy of HEp-2 cells revealed that serum autoantibodies from *Sle1*TLR-$9^{-/-}$ mice bound primarily to the cytoplasm, with some nucleolar specificity, in contrast to *Sle1* mouse sera, which bound primarily to the nucleus (Figures 2A–C). All *Sle1*TLR-$9^{-/-}$ mouse sera tested lost the ability to bind mitotic chromatin (Figures 2A and D). Consistent with this finding, the levels of antinucleosome autoantibodies were significantly decreased in *Sle1*TLR-$9^{-/-}$ mice compared to *Sle1* controls (Figure 2E). However, we detected increased levels of anti-dsDNA antibodies using an in-house ELISA and a commercial Luminex-based assay (Figure 2E and Supplementary Figure 2F, available on the *Arthritis & Rheumatology* web site at http://onlinelibrary.wiley.com/doi/10.1002/art.40535/abstract). In clinical practice, dsDNA ELISAs have shown low specificity and poor correlation with superior detection assays, such as CLIFT (35,36). We therefore tested *Sle1*TLR-$9^{-/-}$ samples from Figures 2A–D with the CLIFT assay, and 6 of 8 serum samples showed positive kinetoplast staining, confirming the presence of anti-dsDNA antibodies despite negative chromatin staining (Supplementary Figures 2A and B). High levels of anti-dsDNA as determined by anti-dsDNA ELISA did not correlate with positive CLIFT findings (Supplementary Figure 2C), confirming low specificity of the ELISA. Discrepancies between ELISA and CLIFT for anti-dsDNA measurement in TLR-$9^{-/-}$ lupus models have also been observed by other groups and are due to a number of factors, including the origin and purity of the DNA antigen used for ELISA (8,13).

The cytoplasmic HEp-2 staining pattern of *Sle1*TLR-$9^{-/-}$ mouse serum is characteristic of RNA-reactive antibodies (33,37) (Figures 2A and C), which we confirmed by anti-RNA ELISA (Figure 2E). Moreover, cytoplasmic staining intensity positively correlated with anti-RNA titers (Supplementary Figures 2D and E). Additionally, anti-snRNP autoantibody levels were higher in *Sle1*TLR-$9^{-/-}$ mice than *Sle1* mice (Figure 2E). A Luminex autoantigen assay confirmed this change and detected significant increases in several other RNA-associated autoantibodies, including anti-SSA 52 and 60, anti-SSB, anti-Sm, and anti–ribosomal P (Supplementary Figure 2F). Analyses of serum Ig levels by Luminex showed that TLR-9 deficiency resulted in significantly higher concentrations of total IgG2a/c, IgG2b, and IgM antibodies compared to *Sle1* controls, while IgA concentrations were decreased (Figure 2F).

Systemic up-regulation of TLR-7 in diseased *Sle1*TLR-$9^{-/-}$ mice. Increased TLR-7 expression leads to an augmentation in autoimmunity (15,27,33). However, it is unknown if TLR-$9^{-/-}$ mice express higher levels of TLR-7 protein. Bossaller et al recently showed an infiltration of $Ly6G^{high}Ly6C^{high}$ cells with higher levels of TLR-7 in the peritoneal cavity of TLR-$9^{-/-}$BALB/c mice with pristane-induced lupus (14). Therefore, we assessed

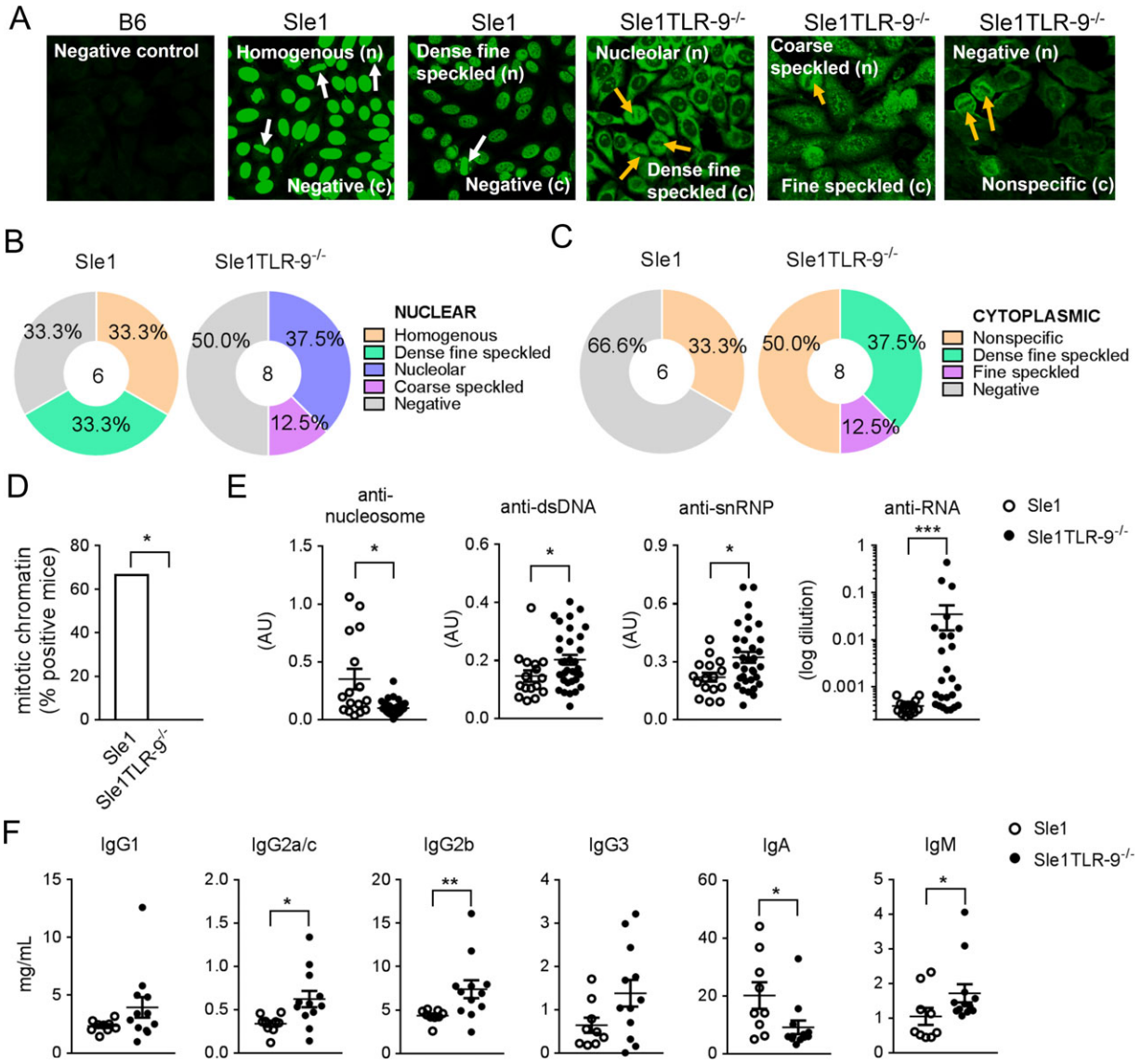

Figure 2. Toll-like receptor 9 (TLR-9) deletion in mice breaks tolerance to RNA-associated antibodies. **A**, Representative microscopy images of nuclear (**n**) and cytosolic (**c**) HEp-2 staining patterns of serum autoantibodies from B6, *Sle1*, and *Sle1*TLR-9$^{-/-}$ mice ages 4.5–6.9 months. **White arrows** show mitotic chromosome staining; **orange arrows** indicate the absence of mitotic chromosome staining. **B** and **C**, Analysis of nuclear (**B**) and cytoplasmic (**C**) staining patterns determined by HEp-2 staining and microscopy. **D**, Percentage of *Sle1* and *Sle1*TLR-9$^{-/-}$ mice with mitotic chromatin positivity. Serum for HEp-2 staining was obtained from 3 independent cohorts with a total of 6 *Sle1* mice and 8 *Sle1*TLR-9$^{-/-}$ mice. **E**, Levels of antinucleosome (double-stranded DNA [dsDNA]/histone), anti-dsDNA, anti–small nuclear RNP (anti-snRNP), and anti-RNA autoantibodies in *Sle1* and *Sle1*TLR-9$^{-/-}$ mice. Serum dilutions were 1:100 for anti-RNA and 1:200 for all other autoantibodies. AU represents absorbance at 405 nm (sample minus blank). Values for anti-RNA antibodies are represented as logarithmic values of dilutions calculated from a standard curve. **F**, Levels of IgG subtypes in sera from *Sle1* and *Sle1*TLR-9$^{-/-}$ mice analyzed by Luminex. In **E** and **F**, mouse sera were from 6 independent cohorts. Circles represent individual mice; horizontal lines and error bars show the mean ± SEM. All data presented are from 4.5–6.9-month-old mice. Parametric data were assessed by one-way analysis of variance (with Bonferroni adjustment for multiple comparisons) or Student's *t*-test, and nonparametric data were assessed by Kruskal-Wallis test (with Dunn's multiple comparison test) or Mann-Whitney test. Significance in **D** was determined by Fisher's exact test. * = $P < 0.05$; ** = $P < 0.01$; *** = $P < 0.001$.

TLR-7 expression by flow cytometry using the same antibody clone (A9410). We verified binding specificity using TLR-7–deficient B6 mice (TLR-7$^{-/-}$) and a fluorescence minus one control. Our analyses showed that TLR-7 levels were significantly higher in B cells, pDCs, CD11b+ DCs, F4/80+ macrophages, and in the CD11c+MHCII–

precursor population in *Sle1*TLR-9$^{-/-}$ mice than in *Sle1* controls (Figure 3A). TLR-7 expression positively correlated with the expansion of CD11b+ DCs and CD11c+ MHCII− subsets, but not with pDC frequencies (Figures 3B–D). TLR-7 was expressed in splenic PMNs and at significantly higher levels in TLR-9–deficient *Sle1* mice (Supplementary Figure 3A, available on the *Arthritis & Rheumatology* web site at http://onlinelibrary.wiley.com/doi/10.1002/art.40535/abstract). No differences were observed in splenic CD11b+Gr-1^{intermediate} cells, which had highly variable TLR-7 expression (Supplementary Figure 3B). As expected, TLR-7 expression was not detected in CD3+ T cells or CD8+ DCs (Supplementary Figures 3C and D).

Regulation of IgG production by TLR-9 in *Sle1* lupus-prone mice. Given the essential role of humoral immunity in the development of SLE, we assessed B cell functional responses to TLR-7 in young prediseased mice. We stimulated mouse splenocytes with the TLR-7 ligand R848 and TLR-4 ligand LPS as a TLR-7–independent

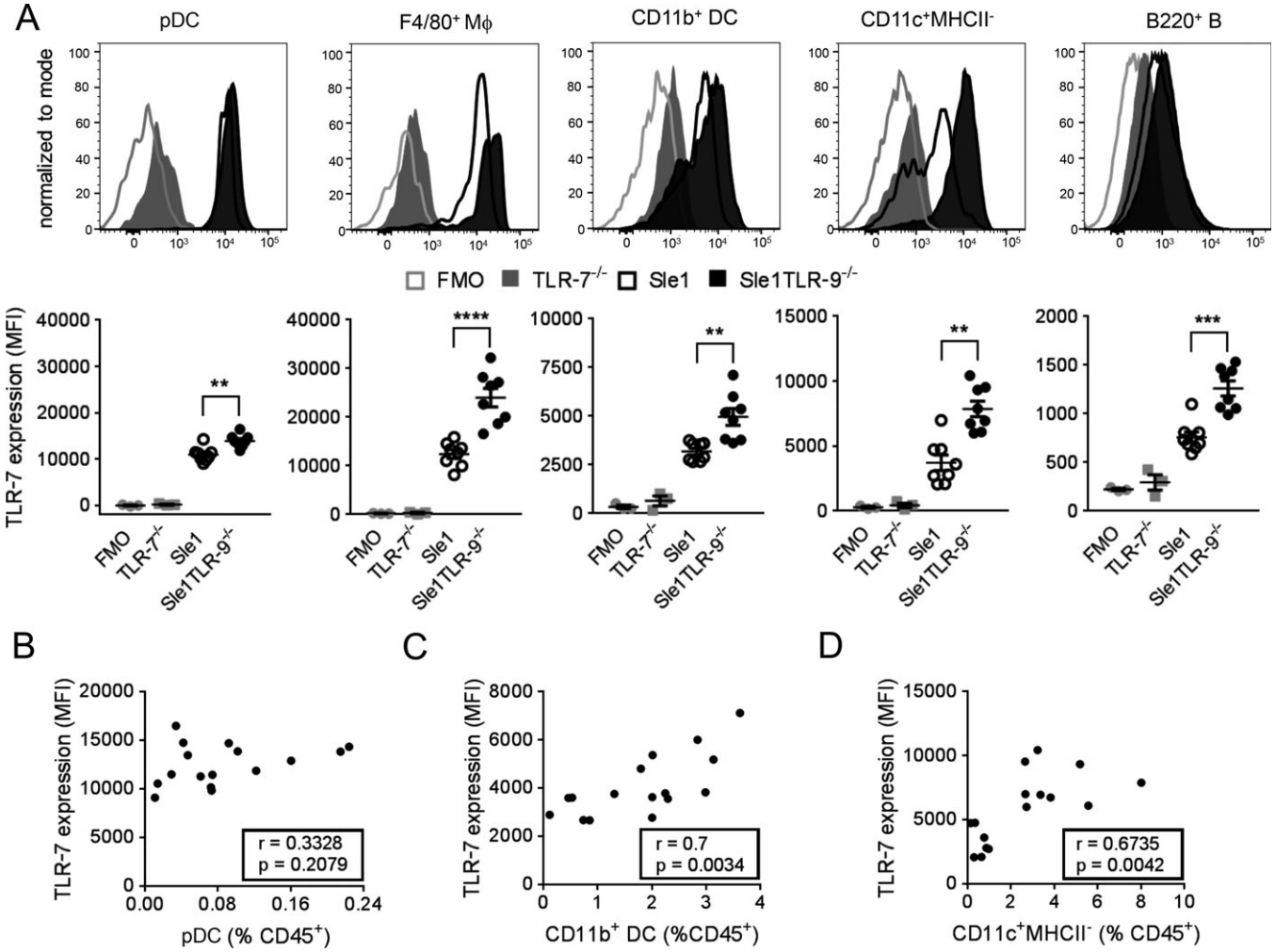

Figure 3. Regulation of Toll-like receptor 7 (TLR-7) protein expression in the mouse spleen by TLR-9 deficiency. **A**, Representative histograms (top) and median fluorescence intensity (MFI) data (bottom) for TLR-7 expression, measured by intracellular flow cytometry, in the indicated spleen cell subsets in *Sle1* and *Sle1*TLR-9$^{-/-}$ mice ages 5.7–6.4 months. Results are from 3 independent experiments each conducted with a TLR-7$^{-/-}$ and fluorescence minus one (FMO) control (n = 8 *Sle1* mice, 8 *Sle1*TLR-9$^{-/-}$ mice, 3 TLR-7$^{-/-}$ controls, and 3 FMO controls). Symbols represent individual samples; horizontal lines and error bars show the mean ± SEM. Mϕ = macrophage. **B–D**, Correlation of leukocyte expansion in *Sle1* and *Sle1*TLR-9$^{-/-}$ mouse spleens with TLR-7 expression in plasmacytoid dendritic cells (pDCs) (**B**), CD11b+ DCs (**C**), and CD11c+ major histocompatibility complex class II (MHCII)− cells (**D**). Parametric data were assessed by Student's *t*-test, and nonparametric data were assessed by Mann-Whitney test. Correlations were determined using Spearman's rank correlation for nonparametric data and Pearson's correlation for parametric data. ** = $P < 0.01$; *** = $P < 0.001$; **** = $P < 0.0001$.

signal. We used flow cytometry assays to measure B cell survival, activation, and proliferation and did not detect any significant differences between *Sle1* and *Sle1*TLR-9$^{-/-}$ mice within a wide range of R848 concentrations, in contrast to the findings of an earlier study in B6.TLR-9$^{-/-}$ CD19+B220+ mouse splenocytes (38) (Figures 4A and B and Supplementary Figures 4A–C, available on the *Arthritis & Rheumatology* web site at http://onlinelibrary.wiley.com/doi/10.1002/art.40535/abstract). Consistent with the lack of increased activation upon TLR-7 ligation, we

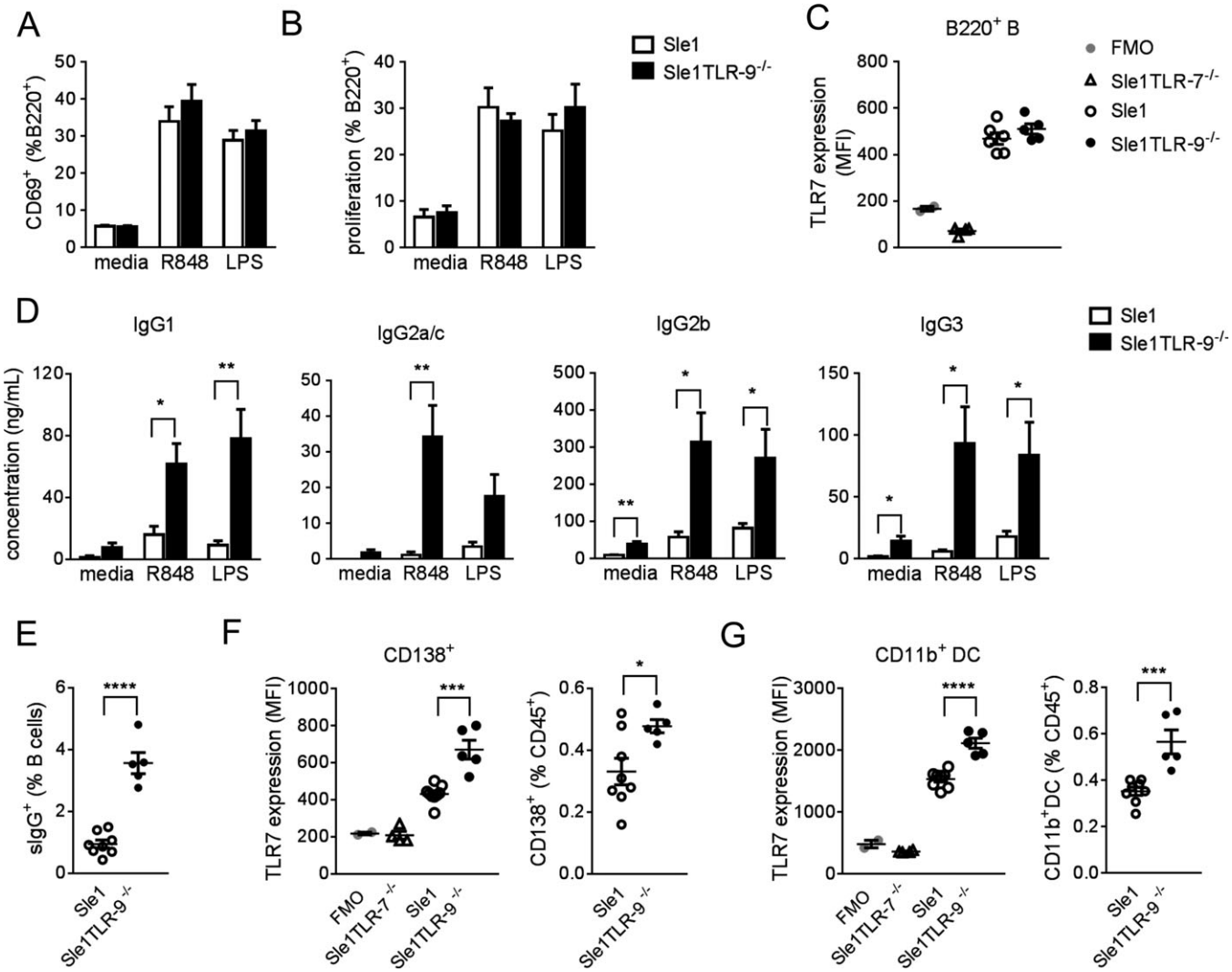

Figure 4. Regulation of antibody production by Toll-like receptor 9 (TLR-9) in *Sle1* mice. **A** and **B**, B cell (B220+) activation (**A**) and proliferation (**B**) in splenocytes from young (8–10-week-old) *Sle1* and *Sle1*TLR-9$^{-/-}$ mice that were left untreated (media), stimulated with R848 (0.01 μg/ml), or stimulated with lipopolysaccharide (LPS; 1 μg/ml). B cell activation was measured by flow cytometry after 24 hours of stimulation and is shown as the percentage of CD69+ cells. B cell proliferation was measured according to the 5,6-carboxyfluorescein succinimidyl ester dilution after 72 hours of stimulation. **C**, TLR-7 expression, measured by intracellular flow cytometry, in mouse splenic B220+ B cells. TLR-7–deficient *Sle1* mice (*Sle1*TLR-7$^{-/-}$) (n = 4) and fluorescence minus one (FMO) samples were used as negative controls. MFI = median fluorescence intensity. **D**, Levels of IgG subtypes, measured by Luminex, in *Sle1* and *Sle1*TLR-9$^{-/-}$ mouse culture supernatants collected after 96 hours of incubation. Cultures were left untreated, stimulated with R848, or stimulated with LPS. **E**, Expression of surface IgG (sIgG) (IgG1/IgG2a/IgG2b/IgG3) on freshly isolated B220+CD19+ splenocytes from *Sle1* and *Sle1*TLR-9$^{-/-}$ mice. **F** and **G**, TLR-7 expression and frequencies of splenic CD138+ plasma/plasmablasts (**F**) and CD11b+ dendritic cells (DCs) (**G**) in *Sle1* and *Sle1*TLR-9$^{-/-}$ mice. In **A**, **B**, and **D**, bars show the mean ± SEM from 2–3 independent experiments (n = 9–15 mice per group). Data were assessed by multiple *t*-tests, and statistical significance was corrected using the Holm-Sidak method. In **C**, **E**, **F**, and **G**, data are from 1 representative experiment with 8–10-week-old mice (n = 8 *Sle1* and 5 *Sle1*TLR-9$^{-/-}$ mice). Circles represent individual mice; horizontal lines and error bars show the mean ± SEM. Significance was determined by Student's *t*-test. * = $P < 0.05$; ** = $P < 0.01$; *** = $P < 0.001$; **** = $P < 0.0001$.

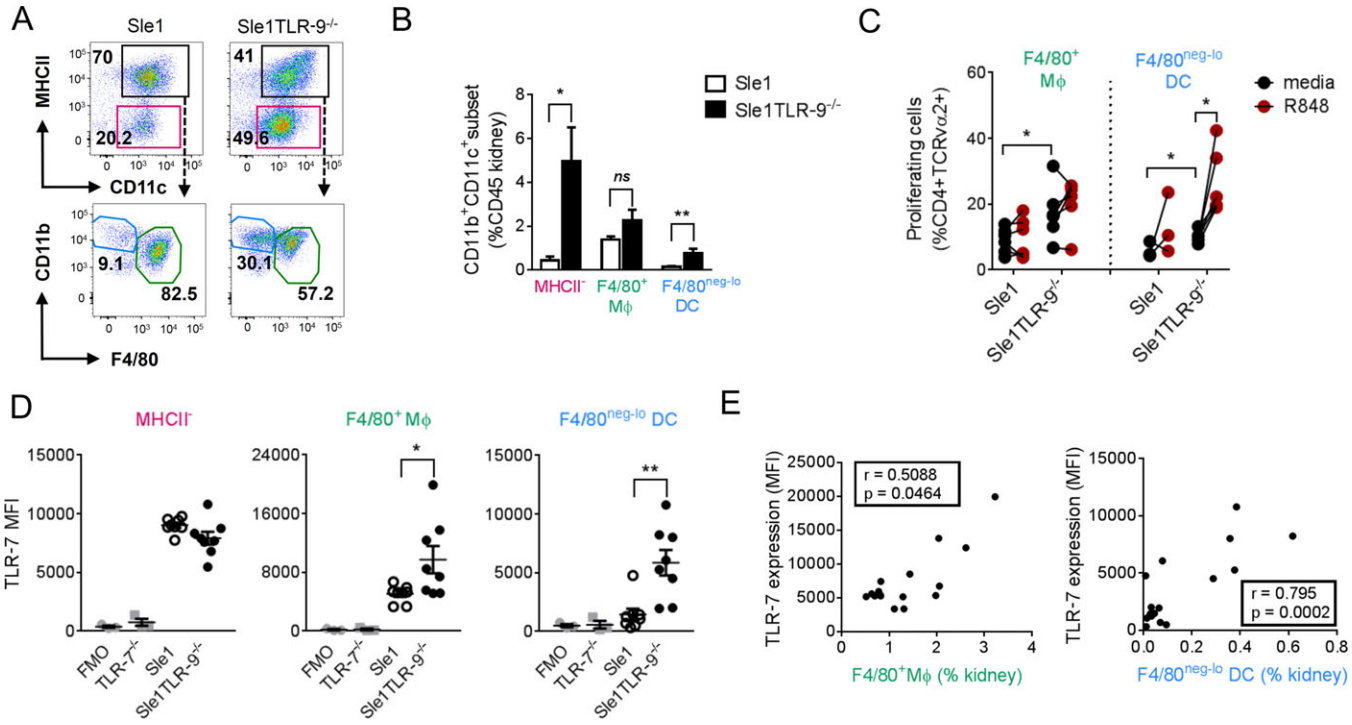

Figure 5. Infiltration of dendritic cells (DCs) with increased Toll-like receptor 7 (TLR-7) protein expression into *Sle1*TLR-9$^{-/-}$ mouse kidneys. **A**, Analysis of renal CD45+CD11b+Gr-1$^{-/low}$ subsets using antibodies to CD11c, major histocompatibility complex class II (MHCII), F4/80, and CD11b. The magenta boxed area includes the CD11c+MHCII− precursor population. The black boxed area includes the CD11c+MHCII+ cells. CD11c+MHCII+ cells were further subdivided into F4/80+ macrophages (Mϕ; green encircled area) and F4/80$^{-/low}$ DCs (blue encircled area). **B**, Cumulative frequencies of renal CD11b+Gr-1− subsets identified in **A** in *Sle1* and *Sle1*TLR-9$^{-/-}$ mice. Bars show the mean ± SEM. Data are from 3 independent cohorts of 4.5–6.5-month-old mice with a total of 9–16 mice per group. **C**, Proliferation of CD4+TCRvα2+ *Sle1*OT-II cells exposed to ovalbumin-pulsed F4/80+ macrophages or F4/80$^{-/low}$ DCs, with or without prior stimulation with R848. Circles represent cells sorted from an individual mouse (n = 6), except for *Sle1* F4/80$^{-/low}$ DCs that were pooled to a total of 3 samples due to low cell numbers. **D**, Analysis of TLR-7 protein expression, using flow cytometry, in the CD11b+Gr-1− subsets identified in **A** in *Sle1* and *Sle1*TLR-9$^{-/-}$ mice. Symbols represent individual samples; horizontal lines and error bars show the mean ± SEM. **E**, Correlation of TLR-7 expression in *Sle1* and *Sle1*TLR-9$^{-/-}$ mice with percentages of renal macrophage and DC infiltration. Data in **D** and **E** are from 3 independent experiments with a total of 8 mice (ages 5.7–6.4 months) per group. Each experiment was conducted with a TLR-7$^{-/-}$ and a fluorescence minus one (FMO) control (a total of 3 each). Parametric data were assessed by one-way analysis of variance (with Bonferroni adjustment for multiple comparisons) or Student's *t*-test, and nonparametric data were assessed by Kruskal-Wallis test (with Dunn's multiple comparison test) or Mann-Whitney test. Correlations were determined using Spearman's rank correlation for nonparametric data and Pearson's correlation for parametric data. * = $P < 0.05$; ** = $P < 0.01$. NS = not significant; MFI = median fluorescence intensity.

did not detect an increase in TLR-7 protein in B cells in young mice (Figure 4C). However, analyses of supernatants collected on day 4 revealed that *Sle1*TLR-9$^{-/-}$ mouse cultures produced significantly higher amounts of IgG upon stimulation with R848 or LPS (Figure 4D). Moreover, in the absence of any stimulation, *Sle1*TLR-9$^{-/-}$ B cells spontaneously released IgG2b and IgG3, in contrast to their *Sle1* counterparts (Figure 4D).

No differences were detected between *Sle1*TLR-9$^{-/-}$ mice and *Sle1* mice in IgM and IgGA production, suggesting an increase in IgG isotype switching (Supplementary Figure 4D). We thus stained freshly isolated mouse splenocytes with a cocktail of anti-IgG1/IgG2a/IgG2b/IgG3 antibodies and analyzed them by flow cytometry (gating strategy is shown in Supplementary Figure 4E). We confirmed that *Sle1*TLR-9$^{-/-}$ mouse B cells expressed significantly more surface IgG than their *Sle1* mouse counterparts (Figure 4E). Additionally, the frequencies of CD138+ plasma/plasmablast cells were increased and they expressed significantly higher TLR-7 protein levels in the absence of TLR-9 (Figure 4F and Supplementary Figure 4F). Extrafollicular plasmablast responses and antibody switching in lupus have been attributed to DCs (39). We detected increased frequencies of splenic CD11b+ DCs with higher TLR-7 expression in *Sle1*TLR-9$^{-/-}$ mice (Figure 4G). This early stage expansion of TLR-7–high DCs might play a role in the increase in CD138+ plasma/plasmablasts and IgG-switched B cells in *Sle1*TLR-9$^{-/-}$ mice.

Kidney disease in *Sle1*TLR-9$^{-/-}$ mice is characterized by infiltrating renal cDCs that overexpress TLR-7. To further understand kidney pathogenesis in *Sle1*TLR-9$^{-/-}$ mice, we characterized renal leukocyte infiltrates, using a similar flow cytometry strategy as previously described for *Sle1* mice overexpressing TLR-7 (*Sle1*Tg7) (15). The majority of infiltrating cells in *Sle1*TLR-9$^{-/-}$ mouse kidneys were CD11b+Gr-1$^{-/low}$ (Supplementary Figure 1G). These consisted of 3 CD11c+ populations: MHCII−, F4/80+ macrophages, and F4/80$^{-/low}$ DCs (Figures 5A and B). As in *Sle1*Tg7 mice, the proportions of MHCII− and F4/80$^{-/low}$ DCs were increased in the kidneys of *Sle1*TLR-9$^{-/-}$ mice compared to *Sle1* mice, while the proportions of macrophages did not change significantly (15) (Figure 5B).

We then assessed the ability of DCs to present antigen and induce T cell proliferation by purifying renal DCs, or macrophages as a control, and exposing them to ovalbumin before culturing with *Sle1*OT-II T cells (15). Unstimulated DCs from *Sle1*TLR-9$^{-/-}$ mouse kidneys induced more T cell proliferation than those from *Sle1* controls, which was enhanced with the TLR-7 ligand R848 (Figure 5C and Supplementary Figure 5A, available on the *Arthritis & Rheumatology* web site at http://onlinelibrary.wiley.com/doi/10.1002/art.40535/abstract). Renal macrophages did not show augmented T cell proliferation with R848, consistent with earlier data from bone-marrow derived and peritoneal macrophages (40). Both renal DCs and macrophages had increased TLR-7 protein expression in the absence of TLR-9, and the levels positively correlated with the percentage of infiltrating renal DCs and macrophages (Figures 5D and E). Additionally, TLR-7 expression was increased in TLR-9–deficient *Sle1* kidney Gr1^{intermediate} CD11b+ cells, but not in pDCs and B cells (Supplementary Figure 5B). We did not detect TLR-7 expression in kidney PMNs and T cells (data not shown). To assess whether the increases in TLR-7 occurred prior to the development of GN, we analyzed younger *Sle1*TLR-9$^{-/-}$ mice with less severe disease, as confirmed by splenic weight and a lack of significant CD45+ kidney infiltration (Supplementary Figure 5C). Expression of TLR-7 was increased in *Sle1*TLR-9$^{-/-}$ mouse kidney F4/80+ macrophages and F4/80$^{-/low}$ DCs, but not in MHCII− cells, similar to their older counterparts (Supplementary Figure 5D).

DISCUSSION

Over the last decade, multiple studies have supported the notion of a fundamental role of TLR-7 in SLE disease development; however, little progress has been made to elucidate the regulatory role of TLR-9 (7–10,12–14,27,31–34,41). Moreover, the lack of data from human studies has reduced enthusiasm for understanding the cellular and molecular roles in TLR-9–deficient mice. In the present study, we have shown for the first time that TLR-7 is increased at the protein level prior to disease onset in TLR-9–deficient *Sle1* mice. Our data also show that in B cells, TLR-9 maintains tolerance to RNA and RNA-associated antigens, prevents antibody switching and antibody production, and regulates B cell maturation. Thus, in the absence of TLR-9, there is an accumulation of TLR-7–reactive RNA/anti-RNA–associated ICs that can activate the increased TLR-7 in DCs and B cells (Figure 6). This essentially yields an identical kidney inflammation phenotype to that observed in *Sle1*Tg7 mice, which have a modest increase in TLR-7 expression (15).

We and others have proposed a multistep model of lupus pathogenesis whereby there is an initial loss of tolerance to self, which, together with an additional immune alteration, leads to the progression of severe disease (42–44). We propose that the loss of tolerance to RNA plays a key role in the transition to active disease. Surprisingly, anti-RNA antibodies have not been studied extensively, despite showing high specificity for SLE (28). However, autoantibodies to RNA-associated molecules, such as snRNP, Sm, SSA/Ro, and SSB/La, are well characterized, and the presence of anti-Sm antibodies is part of the immunologic criteria for SLE diagnosis (45).

BWR4, an anti-RNA antibody derived from (NZB × NZW)F_1 mice, forms ICs in vitro by binding RNA present in the tissue culture supernatant (37). These RNA-containing ICs then activate cells through a B cell receptor (BCR)– and TLR-7–dependent mechanism. We showed that *Sle1*TLR-9$^{-/-}$ mouse serum predominantly produces a cytoplasmic HEp-2 staining pattern, similar to the anti-RNA antibody BWR4 (37). The increase in the cytoplasmic HEp-2 staining pattern and/or increased anti-RNA antibody levels are common to the few TLR-9–deficient model systems that have been examined (8,9,14). Increased levels of RNA-associated autoantibodies, such as anti-Sm, U1 snRNP-1, PM/Scl-100, and/or anti–ribosomal P, were also observed in TLR-9$^{-/-}$ models that develop severe kidney disease (8–10). On the other hand, when TLR-9 was eliminated on a milder autoimmune background, such as *Sle1b*, there was no increase in anti-Sm/RNP IgG (31). This might have important implications for human SLE, since there is evidence that anti-Sm and anti-snRNP antibodies are present immediately preceding the manifestation of clinical symptoms (42).

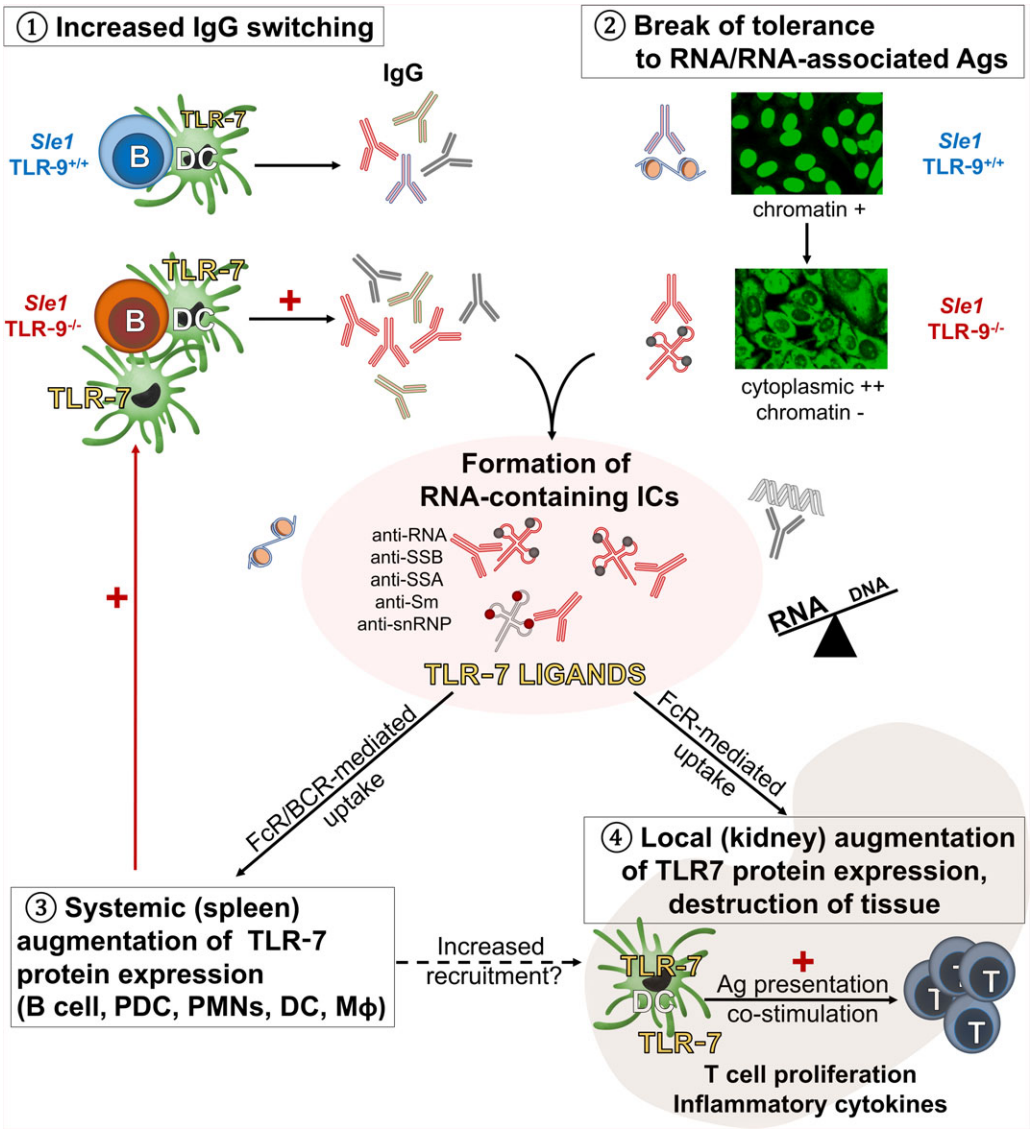

Figure 6. Schematic overview of the proposed mechanisms leading to severe disease in the absence of Toll-like receptor 9 (TLR-9). (1) B cells from prediseased *Sle1*TLR-9$^{-/-}$ mice are primed to produce more IgG-switched antibodies, most likely due to the presence of increased numbers of CD11b+ dendritic cells (DCs) with increased TLR-7 protein expression. (2) In the absence of TLR-9, the autoantibody repertoire shifts toward RNA/RNA-associated antigens (Ags), which leads to the generation of RNA-containing immune complexes (ICs). These complexes act as TLR-7 ligands through Fc receptor (FcR) and B cell receptor (BCR)–mediated uptake and induce TLR-7 protein expression through a positive feedback loop at the systemic (3) and organ (4) levels. A simultaneous increase in the levels of TLR-7 and its ligands leads to ongoing inflammation and tissue destruction through various mechanisms, including T cell proliferation and inflammatory cytokine generation. Anti-snRNP = anti–small nuclear RNP; pDCs = plasmacytoid DCs; PMNs = polymorphonuclear leukocytes; Mϕ = macrophages.

Aside from the autoantibody switch to RNA specificity, our data also suggest that the concomitant increase in TLR-7 plays a crucial role in the progression to end-organ damage. Since SLE serum and the TLR-7 agonist R848 have been shown to increase TLR-7 expression (19,46), the RNA-associated ICs in the circulation can increase TLR-7 through a positive feedback loop. This is supported by clinical data that shows a preferentially higher TLR-7 expression in SLE patients with an anti-RNA–associated antibody profile (47). Additionally, it has recently been shown that RNA-associated antibodies are more prone to form circulating ICs compared to antibodies to dsDNA (48). U1 RNA, which forms the U1 snRNP complex together with Sm and RNP proteins (49), is elevated in the circulation of SLE patients and correlates with disease activity (50).

Thus, while anti-RNA/RNA-associated antibodies might be less common than anti-dsDNA in SLE patients (28,49), they can form ICs more easily and enhance disease progression through TLR-7 binding and up-regulation (Figure 6).

In our earlier investigations we proposed that renal cDCs play a fundamental role in disease progression given their location, their increased inflammatory properties, and the correlation of their expansion with disease progression (15). Consistent with the findings of this study, *Sle1*TLR-9$^{-/-}$ renal cDCs have increased levels of TLR-7 protein and have an increased ability to stimulate T cells following TLR-7 ligation. Furthermore, TLR-7 in these populations correlated with leukocyte infiltration. Importantly, our analyses in younger mice indicated that the increase in renal cDCs occurred prior to significant leukocyte infiltration, suggesting that cDCs play a crucial role in disease progression.

In summary, we have identified multiple roles for the innate dsDNA receptor, TLR-9, in preventing the systemic inflammation and progression to severe disease in a lupus-prone mouse strain. In B cells, TLR-9 prevents excessive Ig production and the switch to RNA-reactive antibody production. In addition, TLR-9 controls TLR-7 at the protein level, most likely in an indirect manner by preventing TLR-7 ligands from being generated and by favoring DNA sensing over RNA sensing in the endosome (51). In the absence of TLR-9, the concomitant increase in the levels of TLR-7 and its ligands leads to ongoing inflammation and tissue destruction.

ACKNOWLEDGMENTS

We would like to thank Katja Lakota, PhD and Tinka Svec, MSc (The University Medical Centre Ljubljana, Ljubljana, Slovenia) for scoring of the HEp-2 slides and subsequent discussion. We thank the staff of the Flow Cytometry cores at Singapore Immunology Network and Institute of Molecular and Cell Biology, Agency for Science, Technology. and Research, for assistance with acquisition and sorting.

AUTHOR CONTRIBUTIONS

All authors were involved in drafting the article or revising it critically for important intellectual content, and all authors approved the final version to be published. Drs. Celhar and Fairhurst had full access to all of the data in the study and take responsibility for the integrity of the data and the accuracy of the data analysis.

Study conception and design. Celhar, Lim, Akira, Wakeland, Connolly, Fairhurst.

Acquisition of data. Celhar, Yasuga, Lee, Zharkova, Tripathi, Thornhill, Lu, Au, Lim, Thamboo.

Analysis and interpretation of data. Celhar, Au, Thamboo, Fairhurst.

REFERENCES

1. Akira S, Uematsu S, Takeuchi O. Pathogen recognition and innate immunity. Cell 2006;124:783–801.
2. Lee BL, Barton GM. Trafficking of endosomal Toll-like receptors. Trends Cell Biol 2014;24:360–9.
3. Mouchess ML, Arpaia N, Souza G, Barbalat R, Ewald SE, Lau L, et al. Transmembrane mutations in Toll-like receptor 9 bypass the requirement for ectodomain proteolysis and induce fatal inflammation. Immunity 2011;35:721–32.
4. Celhar T, Magalhaes R, Fairhurst AM. TLR7 and TLR9 in SLE: when sensing self goes wrong. Immunol Res 2012;53:58–77.
5. Marshak-Rothstein A. Toll-like receptors in systemic autoimmune disease. Nat Rev Immunol 2006;6:823–35.
6. Podolska MJ, Biermann MH, Maueroder C, Hahn J, Herrmann M. Inflammatory etiopathogenesis of systemic lupus erythematosus: an update. J Inflamm Res 2015;8:161–71.
7. Nickerson KM, Christensen SR, Shupe J, Kashgarian M, Kim D, Elkon K, et al. TLR9 regulates TLR7- and MyD88-dependent autoantibody production and disease in a murine model of lupus. J Immunol 2010;184:1840–8.
8. Christensen SR, Shupe J, Nickerson K, Kashgarian M, Flavell RA, Shlomchik MJ. Toll-like receptor 7 and TLR9 dictate autoantibody specificity and have opposing inflammatory and regulatory roles in a murine model of lupus. Immunity 2006;25:417–28.
9. Nickerson KM, Wang Y, Bastacky S, Shlomchik MJ. Toll-like receptor 9 suppresses lupus disease in Fas-sufficient MRL mice. PLoS One 2017;12:e0173471.
10. Santiago-Raber ML, Dunand-Sauthier I, Wu T, Li QZ, Uematsu S, Akira S, et al. Critical role of TLR7 in the acceleration of systemic lupus erythematosus in TLR9-deficient mice. J Autoimmun 2010;34:339–48.
11. Wu X, Peng SL. Toll-like receptor 9 signaling protects against murine lupus. Arthritis Rheum 2006;54:336–42.
12. Jackson SW, Scharping NE, Kolhatkar NS, Khim S, Schwartz MA, Li QZ, et al. Opposing impact of B cell-intrinsic TLR7 and TLR9 signals on autoantibody repertoire and systemic inflammation. J Immunol 2014;192:4525–32.
13. Yu P, Wellmann U, Kunder S, Quintanilla-Martinez L, Jennen L, Dear N, et al. Toll-like receptor 9-independent aggravation of glomerulonephritis in a novel model of SLE. Int Immunol 2006;18:1211–9.
14. Bossaller L, Christ A, Pelka K, Nundel K, Chiang PI, Pang C, et al. TLR9 deficiency leads to accelerated renal disease and myeloid lineage abnormalities in pristane-induced murine lupus. J Immunol 2016;197:1044–53.
15. Celhar T, Hopkins R, Thornhill SI, De Magalhaes R, Hwang SH, Lee HY, et al. RNA sensing by conventional dendritic cells is central to the development of lupus nephritis. Proc Natl Acad Sci U S A 2015;112:E6195–204.
16. Bourke E, Bosisio D, Golay J, Polentarutti N, Mantovani A. The toll-like receptor repertoire of human B lymphocytes: inducible and selective expression of TLR9 and TLR10 in normal and transformed cells. Blood 2003;102:956–63.
17. Miettinen M, Veckman V, Latvala S, Sareneva T, Matikainen S, Julkunen I. Live Lactobacillus rhamnosus and Streptococcus pyogenes differentially regulate Toll-like receptor (TLR) gene expression in human primary macrophages. J Leukoc Biol 2008; 84:1092–100.
18. Zarember KA, Godowski PJ. Tissue expression of human Toll-like receptors and differential regulation of Toll-like receptor mRNAs in leukocytes in response to microbes, their products, and cytokines. J Immunol 2002;168:554–61.
19. Garcia-Romo GS, Caielli S, Vega B, Connolly J, Allantaz F, Xu Z, et al. Netting neutrophils are major inducers of type I IFN production in pediatric systemic lupus erythematosus. Sci Transl Med 2011;3:73ra20.
20. Bernasconi NL, Onai N, Lanzavecchia A. A role for Toll-like receptors in acquired immunity: up-regulation of TLR9 by BCR

triggering in naive B cells and constitutive expression in memory B cells. Blood 2003;101:4500–4.
21. Roach JC, Glusman G, Rowen L, Kaur A, Purcell MK, Smith KD, et al. The evolution of vertebrate Toll-like receptors. Proc Natl Acad Sci U S A 2005;102:9577–82.
22. Plotz PH. The autoantibody repertoire: searching for order. Nat Rev Immunol 2003;3:73–8.
23. Morel L, Mohan C, Yu Y, Croker BP, Tian N, Deng A, et al. Functional dissection of systemic lupus erythematosus using congenic mouse strains. J Immunol 1997;158:6019–28.
24. Hemmi H, Takeuchi O, Kawai T, Kaisho T, Sato S, Sanjo H, et al. A Toll-like receptor recognizes bacterial DNA. Nature 2000;408:740–5.
25. Hemmi H, Kaisho T, Takeuchi O, Sato S, Sanjo H, Hoshino K, et al. Small anti-viral compounds activate immune cells via the TLR7 MyD88-dependent signaling pathway. Nat Immunol 2002; 3:196–200.
26. Weening JJ, D'Agati VD, Schwartz MM, Seshan SV, Alpers CE, Appel GB, et al, on behalf of the International Society of Nephrology and Renal Pathology Society Working Group on the Classification of Lupus Nephritis. The classification of glomerulonephritis in systemic lupus erythematosus revisited [published erratum appears in Kidney Int 2004;65:1132]. Kidney Int 2004; 65:521–30.
27. Fairhurst AM, Hwang SH, Wang A, Tian XH, Boudreaux C, Zhou XJ, et al. Yaa autoimmune phenotypes are conferred by overexpression of TLR7. Eur J Immunol 2008;38:1971–8.
28. Blanco F, Kalsi J, Isenberg DA. Analysis of antibodies to RNA in patients with systemic lupus erythematosus and other autoimmune rheumatic diseases. Clin Exp Immunol 1991;86:66–70.
29. Martin RM, Brady JL, Lew AM. The need for IgG2c specific antiserum when isotyping antibodies from C57BL/6 and NOD mice. J Immunol Methods 1998;212:187–92.
30. Wang A, Fairhurst AM, Tus K, Subramanian S, Liu Y, Lin F, et al. CXCR4/CXCL12 hyperexpression plays a pivotal role in the pathogenesis of lupus. J Immunol 2009;182:4448–58.
31. Soni C, Wong EB, Domeier PP, Khan TN, Satoh T, Akira S, et al. B cell-intrinsic TLR7 signaling is essential for the development of spontaneous germinal centers. J Immunol 2014;193: 4400–14.
32. Hwang SH, Lee H, Yamamoto M, Jones LA, Dayalan J, Hopkins R, et al. B cell TLR7 expression drives anti-RNA autoantibody production and exacerbates disease in systemic lupus erythematosus-prone mice. J Immunol 2012;189:5786–96.
33. Deane JA, Pisitkun P, Barrett RS, Feigenbaum L, Town T, Ward JM, et al. Control of toll-like receptor 7 expression is essential to restrict autoimmunity and dendritic cell proliferation. Immunity 2007;27:801–10.
34. Lartigue A, Courville P, Auquit I, Francois A, Arnoult C, Tron F, et al. Role of TLR9 in anti-nucleosome and anti-DNA antibody production in lpr mutation-induced murine lupus. J Immunol 2006;177:1349–54.
35. Zigon P, Lakota K, Cucnik S, Svec T, Ambrozic A, Sodin-Semrl S, et al. Comparison and evaluation of different methodologies and tests for detection of anti-dsDNA antibodies on 889 Slovenian patients' and blood donors' sera. Croat Med J 2011;52:694–702.
36. Ghirardello A, Villalta D, Morozzi G, Afeltra A, Galeazzi M, Gerli R, et al. Evaluation of current methods for the measurement of serum anti double-stranded DNA antibodies. Ann N Y Acad Sci 2007;1109:401–6.
37. Lau CM, Broughton C, Tabor AS, Akira S, Flavell RA, Mamula MJ, et al. RNA-associated autoantigens activate B cells by combined B cell antigen receptor/Toll-like receptor 7 engagement. J Exp Med 2005;202:1171–7.
38. Desnues B, Macedo AB, Roussel-Queval A, Bonnardel J, Henri S, Demaria O, et al. TLR8 on dendritic cells and TLR9 on B cells restrain TLR7-mediated spontaneous autoimmunity in C57BL/6 mice. Proc Natl Acad Sci U S A 2014;111:1497–502.
39. Teichmann LL, Ols ML, Kashgarian M, Reizis B, Kaplan DH, Shlomchik MJ. Dendritic cells in lupus are not required for activation of T and B cells but promote their expansion, resulting in tissue damage. Immunity 2010;33:967–78.
40. Celhar T, Pereira-Lopes S, Thornhill SI, Lee HY, Dhillon MK, Poidinger M, et al. TLR7 and TLR9 ligands regulate antigen presentation by macrophages. Int Immunol 2016;28:223–32.
41. Pisitkun P, Deane JA, Difilippantonio MJ, Tarasenko T, Satterthwaite AB, Bolland S. Autoreactive B cell responses to RNA-related antigens due to TLR7 gene duplication. Science 2006;312:1669–72.
42. Arbuckle MR, McClain MT, Rubertone MV, Scofield RH, Dennis GJ, James JA, et al. Development of autoantibodies before the clinical onset of systemic lupus erythematosus. N Engl J Med 2003;349:1526–33.
43. Fairhurst AM, Wandstrat AE, Wakeland EK. Systemic lupus erythematosus: multiple immunological phenotypes in a complex genetic disease. Adv Immunol 2006;92:1–69.
44. Kanta H, Mohan C. Three checkpoints in lupus development: central tolerance in adaptive immunity, peripheral amplification by innate immunity and end-organ inflammation. Genes Immun 2009;10:390–6.
45. Petri M, Orbai AM, Alarcón GS, Gordon C, Merrill JT, Fortin PR, et al. Derivation and validation of the Systemic Lupus International Collaborating Clinics classification criteria for systemic lupus erythematosus. Arthritis Rheum 2012;64:2677–86.
46. Marshall JD, Heeke DS, Gesner ML, Livingston B, Van Nest G. Negative regulation of TLR9-mediated IFN-α induction by a small-molecule, synthetic TLR7 ligand. J Leukoc Biol 2007;82: 497–508.
47. Chauhan SK, Singh VV, Rai R, Rai M, Rai G. Distinct autoantibody profiles in systemic lupus erythematosus patients are selectively associated with TLR7 and TLR9 upregulation. J Clin Immunol 2013;33:954–64.
48. Ahlin E, Mathsson L, Eloranta ML, Jonsdottir T, Gunnarsson I, Ronnblom L, et al. Autoantibodies associated with RNA are more enriched than anti-dsDNA antibodies in circulating immune complexes in SLE. Lupus 2012;21:586–95.
49. Migliorini P, Baldini C, Rocchi V, Bombardieri S. Anti-Sm and anti-RNP antibodies. Autoimmunity 2005;38:47–54.
50. Doedens JR, Jones WD, Hill K, Mason MJ, Gersuk VH, Mease PJ, et al. Blood-borne RNA correlates with disease activity and IFN-stimulated gene expression in systemic lupus erythematosus. J Immunol 2016;197:2854–63.
51. Fukui R, Saitoh S, Matsumoto F, Kozuka-Hata H, Oyama M, Tabeta K, et al. Unc93B1 biases Toll-like receptor responses to nucleic acid in dendritic cells toward DNA- but against RNA-sensing. J Exp Med 2009;206:1339–50.

ARTHRITIS & RHEUMATOLOGY
Vol. 70, No. 10, October 2018, pp 1610–1616
DOI 10.1002/art.40550

BRIEF REPORT

Anti–Calponin 3 Autoantibodies: A Newly Identified Specificity in Patients With Sjögren's Syndrome

Julius Birnbaum, Ahmet Hoke, Aliya Lalji, Peter Calabresi, Pavan Bhargava, and Livia Casciola-Rosen

Objective. **Autoantibodies are clinically useful for phenotyping patients across the spectrum of autoimmune rheumatic diseases. Using serum from a patient with Sjögren's syndrome (SS), we detected a new specificity by immunoblotting. This study was undertaken to identify this autoantibody and to evaluate its disease specificity.**

Methods. **A prominent 40-kd band was detected when immunoblotting was performed using SS patient serum and lysate from rat dorsal root ganglia (DRGs). Using 2-dimensional gel electrophoresis and liquid chromatography tandem mass spectrometry peptide sequencing, the autoantigen was identified as calponin 3. Anti–calponin 3 antibodies were evaluated in sera from patients with primary SS (n = 209), patients with systemic lupus erythematosus (SLE; n = 138), patients with myositis (n = 138), patients with multiple sclerosis (MS; n = 44), and healthy controls (n = 46) by enzyme-linked immunosorbent assay. Expression of calponin 3 was assessed by immunohistochemistry.**

Results. **Calponin 3 was identified as a new autoantigen. Anti–calponin 3 antibodies were detected in 23 (11.0%) of the 209 SS patients, 12 (8.7%) of the 138 SLE patients, 7 (5.1%) of the 138 myositis patients, 3 (6.8%) of the 44 MS patients, and 1 (2.2%) of the 46 healthy controls. Among SS patients, the frequency of anti–calponin 3 antibodies was highest in those with neuropathies (7 [17.9%] of 39). In this subset, the frequency of anti–calponin 3 antibodies differed significantly from that in the control group (P = 0.02). Calponin 3 was expressed primarily in rat DRG perineuronal satellite cells but not neurons.**

Conclusion. **Calponin 3 is a novel autoantigen. Antibodies against this protein are found in SS and associate with the subset of patients experiencing neuropathies. Intriguingly, we found that calponin 3 is expressed in DRG perineuronal satellite cells, suggesting that these may be a target in SS.**

Autoantibodies across the spectrum of autoimmune rheumatic diseases are of significant clinical utility because they may serve as diagnostic biomarkers, help to define prognosis, and provide insight into pathogenesis. In Sjögren's syndrome (SS), antibodies may be associated with specific types of extraglandular disease or help to define mechanisms of end-organ damage (1). In this study, we defined and validated a new autoantibody specificity, anti–calponin 3, in a cohort of patients with SS. We also examined the frequency of these antibodies in subgroups of SS patients classified according to neuropathic pain and peripheral nerve status. Interestingly, although the frequency of these antibodies in the overall SS group was not significantly different from that in the healthy control group (11.0% versus 2.2%; P = 0.09), the difference was significant when the subset of patients with SS with neuropathy was compared to controls (17.9% versus 2.2%; P = 0.02). Since patients with systemic lupus erythematosus (SLE) and myositis may share underlying mechanisms of robust humoral autoimmunity with SS (e.g., anti–Ro 52, anti–Ro 60, and anti-La) (2), we also examined the frequency of anti–calponin 3 antibodies in these disease groups. Anti–calponin 3 antibodies were found in both of these patient cohorts, albeit less frequently than in the SS cohort (8.7% and 5.1%, respectively).

Interestingly, our immunohistochemical studies showed that calponin 3 is expressed in perineuronal

Supported by the NIH (grants R01-DE-12354, K23-AR-064279 [to Dr. Birnbaum], and R37-NS-041435 [to Dr. Calabresi]), the Jerome L. Greene Foundation, the Dr. Miriam and Sheldon G. Adelson Medical Research Foundation (grant to Dr. Hoke), and a Career Transition Award from the Multiple Sclerosis Society. The Johns Hopkins Rheumatic Disease Research Core Center, where the assays were performed, is supported by NIH grants P30-AR-053503 and P30-AR-070254.

Julius Birnbaum, MD, MHS, Ahmet Hoke, MD, PhD, FRCPC, Aliya Lalji, MD, Peter Calabresi, MD, Pavan Bhargava, MD, Livia Casciola-Rosen, PhD: Johns Hopkins University, Baltimore, Maryland.

Address correspondence to Julius Birnbaum, MD, MHS, Division of Rheumatology, Department of Neurology, The Johns Hopkins University School of Medicine, 5200 Eastern Avenue, Mason F. Lord Building, Center Tower, Suite 4000, Baltimore, MD 21224. E-mail: jbirnba2@jhmi.edu.

Submitted for publication November 26, 2017; accepted in revised form May 1, 2018.

satellite cells but not neurons of rat dorsal root ganglia (DRGs). While anti-DRG antibodies that primarily target DRG neurons have been identified in several neurologic diseases (3), our findings provide the first example in which a novel antibody specificity is primarily directed against satellite cells. Such findings may provide insight into SS neurologic disease.

PATIENTS AND METHODS

Study type and cohorts. We studied a cross-sectional cohort of SS patients (n = 209) consecutively enrolled from 2008 to 2015. Patients were evaluated at the Jerome L. Greene Sjögren's Syndrome Center at Johns Hopkins University. The diagnosis of SS was made using the 2002 American–European Consensus Group criteria (4), since patients could be enrolled prior to publication of the 2012 American College of Rheumatology classification criteria (5). Since the Center encompasses a Neuro-Rheumatology Clinic, this cohort is enriched with patients referred for evaluation of potential neuropathies, performed by a board-certified neurologist and rheumatologist (JB). SS patients without neuropathies were evaluated by a rheumatologist.

For some analyses, we identified the following 3 patient subsets within the cohort of 209 SS patients: those with a neuropathy (n = 39), those who described neuropathic-type pain but did not have a neuropathy (n = 71) (see below), and those without neuropathies (n = 99). Peripheral nerve status was evaluated using a validated neuropathic pain symptoms questionnaire, neurologic examination, nerve conduction studies to assess large myelinated Aβ fibers, and punch skin biopsies to assess the intra-epidermal nerve-fiber density of nonmyelinated nerves. The Self-Administered Leeds Assessment of Neuropathic Symptoms and Signs pain scale was used to ascertain the presence of neuropathic-type pain (6). Findings of neurologic examination and nerve conduction studies were used to define patients with large-fiber neuropathies, including large-fiber sensory neuronopathies, axonal sensory or sensorimotor polyneuropathies, and vasculitic neuropathies (7). Findings of neurologic examination and skin biopsies were used to classify patients as having small-fiber neuropathies (8).

Table 1 shows that compared to SS patients without neuropathies, the subsets of SS patients with neuropathy and with neuropathic-type pain without neuropathy had lower frequencies of most known antibody specificities, including antinuclear antibodies (ANAs) ≥1:320, anti–Ro 52, anti–Ro 60, and anti-La/SSB antibodies, rheumatoid factor, and polyclonal gammopathy. This enrichment of seronegative disease by patients with SS with small-fiber and neuropathic pain accounts for the lower frequency of antibodies compared to previously described SS cohorts (5,9).

Sera obtained from 138 SLE patients seen consecutively at the Johns Hopkins Lupus Center, and from 138 myositis patients seen at the Johns Hopkins Myositis Center were also studied. Forty-four serum samples from patients with multiple sclerosis (MS) were obtained from the Johns Hopkins Multiple Sclerosis Center Biorepository; diagnosis of MS was based on the 2010 revised McDonald criteria (10). Sera from 46 healthy individuals were used as controls.

The study protocol was approved by the Johns Hopkins Institutional Review Board. All patients provided written informed consent to participate.

Cell culture and lysates. Human skeletal muscle cells from a single donor, human keratinocytes (both from Lonza), HeLa cells, fibroblasts, and Jurkat cells were cultured using standard techniques. An immortalized rat DRG neuronal cell line, 50B11, was cultured and differentiated as previously described (11). The cells were lysed in buffer A containing Nonidet P40, 20 m*M* Tris pH 7.4, 150 m*M* NaCl, 1 m*M* EDTA, and protease inhibitors. HeLa cells were transiently transfected with DNA encoding full-length human calponin 3 (OriGene) or vector alone using Lipofectamine 2000, per the manufacturer's protocol (Invitrogen), and lysed as described above.

Immunoblotting. Gel samples prepared from cell lysates or recombinant full-length human calponin 3 were electrophoresed on 10% sodium dodecyl sulfate (SDS)–polyacrylamide gels and transferred to nitrocellulose membranes. Primary antibody incubations were performed using a

Table 1. Demographic and immunologic features of the SS cohorts*

Characteristic	SS (n = 209)	SS without neuropathic pain (n = 99)	SS with neuropathy (n = 39)†	SS with neuropathic-type pain without neuropathy (n = 71)
Age, mean ± SD years	52.5 ± 13.5	52.5 ± 13.9	55.8 ± 12.3	50.8 ± 13.2
Sex, female	185/209 (88.5)	93/99 (93.9)	28/39 (71.8)	64/71 (90.1)
Race, white	178/209 (85.2)	81/99 (81.8)	32/39 (82.1)	65/71 (91.5)
ANA ≥1:320	132/199 (66.3)	70/96 (72.9)	26/38 (68.4)	36/65 (55.4)
RF positive	80/196 (40.8)	52/92 (56.5)	10/37 (27.0)	18/67 (26.9)
Anti–Ro 52 positive	155/208 (74.5)	86/98 (87.8)	27/39 (69.2)	42/71 (59.2)
Anti–Ro 60 positive	137/205 (66.8)	76/99 (76.8)	23/37 (62.2)	38/69 (55.0)
Anti-La/SSB positive	83/208 (39.9)	45/98 (45.9)	9/39 (23.1)	29/71 (40.8)
Polyclonal gammopathy	78/193 (40.4)	42/87 (48.3)	12/39 (30.8)	24/67 (35.8)
Anti–calponin 3	23/209 (11.0)	10/99 (10.1)	7/39 (17.9)	6/71 (8.5)

* Except where indicated otherwise, values are the no./no. assessed (%). SS = Sjögren's syndrome; ANA = antinuclear antibody; RF = rheumatoid factor.

† Subtypes of neuropathies included 19 patients with pure small-fiber neuropathies, 4 patients with mixed small-fiber neuropathies and large-fiber sensory neuronopathies, 4 patients with mixed small-fiber neuropathies and large-fiber axonal sensorimotor polyneuropathies, 5 patients with large-fiber sensory neuronopathies, and 7 patients with large-fiber axonal sensorimotor polyneuropathies.

polyclonal anti–calponin 3 antibody (Abcam), an anti-FLAG antibody (Sigma-Aldrich), the prototype patient serum (SJ193; 1:5,000 dilution), or serum from a healthy individual (1:5,000 dilution). Blots were subsequently incubated with horseradish peroxidase (HRP)–conjugated secondary antibodies (Jackson ImmunoResearch), visualized using chemiluminescence (Pierce), and imaged using a FluorChem imaging platform (Protein Simple).

Proteomic identification. Cultured rat DRGs were lysed in isoelectric focusing buffer (8*M* urea, 2*M* thiourea, 4% CHAPS, 1% dithiothreitol, and protease inhibitors) and run on 2-dimensional gels (first dimension, pI range 3–10; second dimension, 10% SDS–polyacrylamide gel electrophoresis) as previously described (12). The spot corresponding to the protein of interest was determined by immunoblotting using the prototype patient serum (SJ193) (12). Preparative 2-dimensional gels were subsequently run and stained with GelCode Blue (Thermo Scientific), and the protein spot of interest was plucked, as well as a "blank" gel plug. These were sent to the Johns Hopkins Mass Spectrometry and Proteomics Facility for liquid chromatography tandem mass spectrometry peptide sequencing as previously described (11).

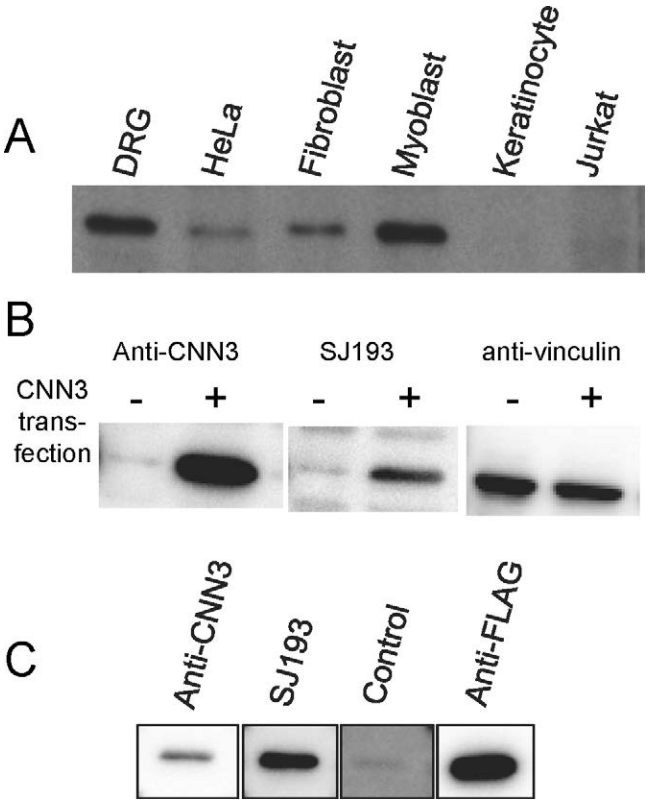

Figure 1. Identification of a new 40-kd autoantigen and confirmation that it is calponin 3 (CNN3). **A**, Immunoblotting of a panel of lysates made from different cell types with serum from a patient with Sjögren's syndrome (SJ193). Equal protein amounts were loaded in each gel lane. An unidentified 40-kd band was blotted and was expressed at varying levels in the different lysates. DRG = dorsal root ganglion. **B**, Immunoblotting of equal protein amounts of lysates made from cells transfected with calponin 3 DNA or with vector alone. Lysates were immunoblotted with anti–calponin 3 antibody, serum SJ193, or antivinculin antibody. **C**, Immunoblotting of recombinant calponin 3 (50 ng/lane) with anti–calponin 3 antibody, serum SJ193, a control serum, or anti–FLAG antibody. A 40-kd band, corresponding to calponin 3, was immunoblotted by all except the control serum.

Calponin 3 antibody enzyme-linked immunosorbent assay (ELISA). Recombinant full-length human calponin 3 was purchased from OriGene. Purity and specificity were confirmed by Coomassie staining and by immunoblotting with anti–FLAG and anti–calponin 3 antibodies (Figure 1C). ELISA plates were coated with 50 ng/well of calponin 3 (overnight at 4°C). ELISAs were performed using sera diluted 1:100 in 1% bovine serum albumin/phosphate buffered saline (PBS)–Tween, followed by incubation with HRP-labeled goat anti-human antibody (1:10,000; Jackson ImmunoResearch) and color development with SureBlue peroxidase reagent (KPL). The prototype serum was included as a reference in every ELISA (optical density in the linear range of the assay), and all absorbances at 450 nm were calibrated relative to it.

Anti–calponin 3 immunostaining. Lumbar DRGs were dissected from adult female Sprague-Dawley rats, fixed in 4% paraformaldehyde overnight, and then transferred to 15% and then 30% sucrose in PBS. DRGs were cryosectioned and stained with polyclonal anti–calponin 3 antibody (Acris) overnight (4°C; 1:200 dilution). After blocking in goat serum, calponin 3–positive cells were visualized using an ImmPRESS HRP goat anti-rabbit IgG (peroxidase) polymer detection kit (Vector). Sections were counterstained with eosin to better visualize the neuronal structures.

Statistical analysis. Bivariate associations between anti–calponin 3 antibodies, known antibody specificities, and subsets of comparator groups were evaluated by chi-square test or Fisher's exact test.

RESULTS

Identification and validation of calponin 3 as a new autoantibody specificity. Antibodies against DRGs have been identified primarily in paraneoplastic disorders (3) and are associated with a wide variety of peripheral nervous system disorders. Given the frequency and wide spectrum of neuropathies in SS, we screened sera from this autoimmune disease spectrum by immunoblotting to evaluate if any novel specificities were enriched in DRG lysates.

A panel of lysates (equal protein amounts of each) from rat DRGs and human HeLa, fibroblast, myoblast, keratinocyte, and Jurkat cells was immunoblotted with SS patient sera (1:5,000 dilution). Serum SJ193 immunoblotted a novel 40-kd band (Figure 1A). This serum was known to have high-titer anti–Ro 60 antibodies and was negative for Ro 52 and SSB antibodies. When lysates were run on 2-dimensional gels, the 40-kd protein was noted to have a pI of ~5.7. Since this 40-kd protein was also detected by other sera, we sought to identify this new specificity.

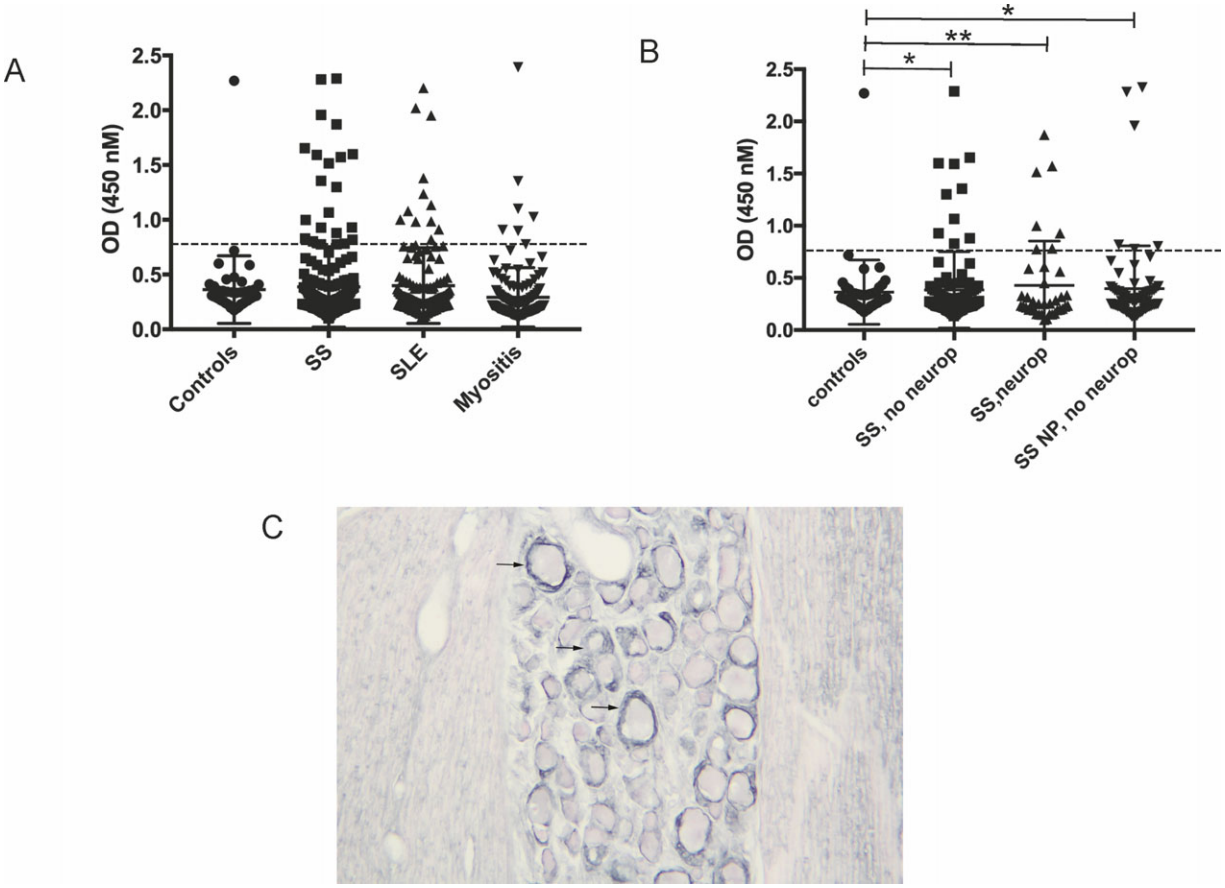

Figure 2. Detection of autoantibodies against calponin 3 in patients with Sjögren's syndrome (SS) and systemic lupus erythematosus (SLE), and expression of calponin 3 in perineuronal satellite cells in rat dorsal root ganglia (DRGs). **A**, Levels of anti–calponin 3 antibody in healthy controls (n = 46), patients with SS (n = 209), patients with SLE (n = 138), and patients with myositis (n = 138). Anti–calponin 3 antibodies were detected in 11.0% of the patients with SS ($P = 0.09$ versus controls), 8.7% of the patients with SLE ($P = 0.19$ versus controls), 5.1% of the patients with myositis ($P = 0.68$ versus controls), and 2.2% of the controls. **B**, Levels of anti–calponin 3 antibody in healthy controls and the 209 patients with SS subgrouped by neurologic status as patients without neuropathy (neurop), patients with neuropathy, and patients with neuropathic-type pain (NP) without neuropathy. Antibodies against calponin 3 were associated (denoted **) with the subgroup of SS patients with neuropathy versus normal controls ($P = 0.02$). In contrast, this association was not seen (denoted *) in patients with SS with neuropathic-type pain without neuropathy ($P = 0.24$ versus controls) or in SS patients without neuropathy ($P = 0.17$ versus controls). In **A** and **B**, antibodies against calponin 3 were assayed by enzyme-linked immunosorbent assay, as described in Patients and Methods. Each symbol represents an individual serum sample; horizontal and vertical lines show the mean ± SD. Broken lines show the cutoff for positivity. **C**, Staining of adult rat DRGs with a commercial anti–calponin 3 antibody. Staining was primarily seen in perineuronal cells (**arrows**) surrounding DRG neurons. Original magnification × 200.

For autoantigen identification, we selected rat DRGs as the source material because the 40-kd protein was prominently represented (Figure 1A). Proteomic analysis was performed by selecting the spot corresponding to the unidentified 40-kd protein on a 2-dimensional gel as described in Patients and Methods. Post-pluck blotting confirmed that the pluck had captured the protein of interest. Among the peptides identified by mass spectrometric sequencing, calponin 3 was the top hit; peptides gave 21% coverage. Since the molecular weight and pI of calponin 3 were consistent with those of the 40-kd protein, we prioritized calponin 3 for validation.

We confirmed that the 40-kd protein was indeed calponin 3 as follows. Lysates were made from HeLa cells transiently transfected with calponin 3 DNA or empty vector. Robust calponin 3 expression in the transfected cell lysates only was confirmed by immunoblotting with a commercial anti–calponin 3 antibody (Figure 1B). Identical data were obtained when the transfected lysates were blotted with serum SJ193 (Figure 1B). Vinculin immunoblots confirmed equal protein loading (Figure 1B). In a second validation approach, immunoblotting was performed using recombinant FLAG-tagged human calponin 3. This was detected robustly by

a rabbit anti–calponin 3 antibody, an anti-FLAG monoclonal antibody, and the prototype serum. As expected, a control human serum did not immunoblot the purified protein (Figure 1C).

Anti–calponin 3 antibodies in patients with SS, SLE, or MS. To determine the prevalence of antibodies against calponin 3 in patients with SS and in other autoimmune disease cohorts, we developed an ELISA. Sera were designated antibody positive if the relative absorbance value was >4 SD higher than the mean value obtained from assaying 46 healthy controls. Note that in the control set, there was a single outlier with a high absorbance. To calculate the mean in the control group, the outlier was excluded. This outlier was included in determining how many antibody-positive sera there were in the control set. The levels of calponin 3 antibodies in the 3 autoimmune rheumatic disease cohorts studied, as well as the healthy controls, are shown in Figure 2A. Anti–calponin 3 antibodies were detected in 23 (11.0%) of 209 SS patients, 12 (8.7%) of 138 SLE patients, 3 (6.8%) of 44 MS patients, and 7 (5.1%) of 138 myositis patients.

Compared to controls, these antibodies were detected at a frequency that approached significance in the SS cohort ($P = 0.09$). The frequency of this antibody in the SLE and myositis cohorts did not differ significantly from that in controls ($P = 0.19$ for SLE patients versus controls and $P = 0.68$ for myositis patients versus controls). This was also true when the myositis cohort was analyzed as 3 separate groups (patients with dermatomyositis, patients with inclusion body myositis, and patients who were anti–hydroxymethylglutaryl-coenzyme A reductase positive).

Since the antibody was discovered using lysates from rat DRGs (which have been implicated in SS neuropathies) and because the P value for the SS cohort tended toward significance, we subsequently subgrouped the 209 SS patients into 3 sets based on neurologic findings and evaluated the frequency of anti–calponin 3 antibodies in each subgroup versus healthy controls (Figure 2B). This analysis showed that calponin 3 antibodies were significantly associated with the SS neuropathy group (7 [17.9%] of 39; $P = 0.02$). In contrast, anti–calponin 3 antibodies were not associated with SS without neuropathy (10 [10.1%] of 99; $P = 0.17$) or with SS with neuropathic-type pain without neuropathy (6 [8.5%] of 71; $P = 0.24$). There was no statistically significant difference in the presence of anti–calponin 3 antibodies among these 3 subgroups ($P = 0.27$). Within the group of 39 patients with neuropathies, we did not find demographic, clinical, or other immunologic differences when comparing patients with versus those without anti–calponin 3 antibodies. Furthermore, there was no difference in the frequency of anti–calponin 3 antibodies between patients with non–length-dependent neuropathies (i.e. non–length-dependent small-fiber neuropathies and large-fiber sensory neuronopathies) and those with length-dependent neuropathies (12.5% [2 of 16] versus 21.7% [5 of 23]; $P = 0.68$). There was no difference in the frequency of ANA ≥1:320 in SS patients with versus those without anti–calponin 3 antibodies (69.6% [16 of 23] versus 65.9% [116 of 176]; $P = 0.90$), nor with anti–Ro 52, anti–Ro 60, and anti-La/SSB antibodies, rheumatoid factor, or polyclonal gammopathy (data not shown).

Expression of calponin 3 in rat DRG perineuronal satellite cells but not neurons. Calponin 3 is widely expressed, including by neurons and glial cells in the central nervous system (13). However, its expression in the peripheral nervous system is unknown. To address this, adult rat DRGs were immunostained using a commercial anti–calponin 3 antibody. Robust calponin 3 staining was noted in perineuronal satellite cells in rat DRGs. Satellite cells surrounding both large and small DRG neurons were stained with anti–calponin 3 antibody (Figure 2C), but none of the DRG neurons stained.

DISCUSSION

We have identified anti–calponin 3 antibodies as a novel specificity found in 11.0% of SS patients. The frequency of these antibodies trended toward significance when compared to healthy controls ($P = 0.09$). Anti–calponin 3 antibodies were also found, albeit at lower frequencies, in SLE (8.7%), myositis (5.1%), and MS (6.8%). Our study also demonstrated that calponin 3 is expressed mainly in nonneuronal satellite cells but not in DRG neurons.

When the SS patients were subgrouped according to neuropathic pain and peripheral nerve status, we found that those with neuropathies had a significantly increased frequency of anti–calponin 3 antibodies compared to healthy controls ($P = 0.02$). This was not noted in patients without neuropathies or in any of the other cohorts evaluated. The spectrum of neuropathies seen in the anti–calponin 3–positive SS patients was informative. It included SS patients with non–length-dependent small-fiber neuropathies and large-fiber sensory neuronopathies (Table 1), which are associated with cytotoxic CD8 T cell injury of small-sized and large-sized DRGs (7,14). It is noteworthy that when we immunodepleted calponin 3 antibodies from sera that also had antibodies against Ro 52 and Ro 60, these reactivities remained unchanged, indicating that these

associations are not due to antibody cross-reactivity (results are available upon request from the corresponding author). Further studies are warranted to evaluate the specificity of anti–calponin 3 antibodies in larger cohorts of well-defined SS patients with peripheral neuropathies.

We determined the expression of calponin 3 in rat DRGs versus other nonneuronal cells by immunostaining. Calponin 3 was expressed most robustly in nonneuronal satellite cells compared to DRG neurons. These findings are notable given that other antibodies associated with immune-mediated neurologic disorders exclusively target neuronal DRGs while sparing nonneuronal satellite cells. The significance of this observation is presently unclear, but given that anti–calponin 3 antibodies were associated with neuropathy and pain, the mechanism that leads to neuropathic behavior is likely to be indirect. Satellite cells play an important neurotrophic role for DRGs (15), and antibodies that target satellite cells may contribute either to sensitization or neurotoxic injury to DRGs. Interestingly, we did not detect calponin 3 by immunohistochemistry in skeletal muscle paraffin sections (data not shown). Calponin 3 is an actin-binding protein expressed in several other tissues (cartilage, brain, and trophoblasts) (13). By binding to the cytoskeleton, it may play a regulatory role in the development of osteoarthritis, neurite outgrowth, seizures, and trophoblast fusion. Future studies can similarly evaluate how the functional role of anti–calponin 3 antibodies may give new insights into the pathogenesis of neuropathies in SS patients with these autoantibodies.

Some limitations of our study should be noted. There were differences in the recruitment of patients with SS compared to the SLE and myositis cohorts. Patients in the latter 2 cohorts were consecutively enrolled. In contrast, there was recruitment bias in the SS cohort because patients were enrolled from the Neuro-Rheumatology Clinic, which is enriched with SS patients with peripheral neuropathies. However, this bias was crucial in enabling us to identify a significant association between anti–calponin 3 antibodies and the subgroup of SS patients with peripheral neuropathies.

In summary, we identified a novel anti–calponin 3 antibody in serum from a patient with SS. We have shown that these antibodies are found more frequently in SS patients than SLE, myositis, and MS patients. Among SS patients, these antibodies are significantly associated with the subset of patients who have peripheral neuropathies. These studies highlight the importance of applying subgroup filters to understand antibody associations.

ACKNOWLEDGMENTS

We acknowledge the Johns Hopkins University Proteomics Core Facility for performing the proteomic identification. We are grateful to the Johns Hopkins Myositis and Lupus Centers for use of their banked serum cohorts as disease controls. We thank Dr. Alan Baer for evaluation of SS patients without neuropathies, Dr. Michelle Petri for evaluation of patients in the Hopkins SLE cohort, and the faculty of the Johns Hopkins Myositis Center for evaluation of the myositis patient cohort.

AUTHOR CONTRIBUTIONS

All authors were involved in drafting the article or revising it critically for important intellectual content, and all authors approved the final version to be published. Dr. Birnbaum had full access to all of the data in the study and takes responsibility for the integrity of the data and the accuracy of the data analysis.

Study conception and design. Birnbaum, Hoke, Lalji, Calabresi, Bhargava, Casciola-Rosen.

Acquisition of data. Birnbaum, Hoke, Lalji, Calabresi, Bhargava, Casciola-Rosen.

Analysis and interpretation of data. Birnbaum, Hoke, Lalji, Calabresi, Bhargava, Casciola-Rosen.

REFERENCES

1. Both T, Dalm VA, van Hagen PM, van Daele PL. Reviewing primary Sjögren's syndrome: beyond the dryness - from pathophysiology to diagnosis and treatment. Int J Med Sci 2017;14:191–200.
2. Frank MB, McCubbin V, Trieu E, Wu Y, Isenberg DA, Targoff IN. The association of anti-Ro52 autoantibodies with myositis and scleroderma autoantibodies. J Autoimmun 1999;12:137–42.
3. Pignolet BS, Gebauer CM, Liblau RS. Immunopathogenesis of paraneoplastic neurological syndromes associated with anti-hu antibodies: a beneficial antitumor immune response going awry. Oncoimmunology 2013;2:e27384.
4. Vitali C, Bombardieri S, Jonsson R, Moutsopoulos HM, Alexander EL, Carsons SE, et al, and the European Study Group on Classification Criteria for Sjögren's Syndrome. Classification criteria for Sjögren's syndrome: a revised version of the European criteria proposed by the American-European Consensus Group. Ann Rheum Dis 2002;61:554–8.
5. Shiboski SC, Shiboski CH, Criswell LA, Baer AN, Challacombe S, Lanfranchi H, et al, for the Sjögren's International Collaborative Clinical Alliance (SICCA) Research Groups. American College of Rheumatology classification criteria for Sjögren's syndrome: a data-driven, expert consensus approach in the Sjögren's International Collaborative Clinical Alliance Cohort. Arthritis Care Res (Hoboken) 2012;64:475–87.
6. Bennett MI, Smith BH, Torrance N, Potter J. The S-LANSS score for identifying pain of predominantly neuropathic origin: validation for use in clinical and postal research. J Pain 2005; 6:149–58.
7. Birnbaum J. Peripheral nervous system manifestations of Sjögren syndrome: clinical patterns, diagnostic paradigms, etiopathogenesis, and therapeutic strategies. Neurologist 2010;16:287–97.
8. McArthur JC, Stocks EA, Hauer P, Cornblath DR, Griffin JW. Epidermal nerve fiber density: normative reference range and diagnostic efficiency. Arch Neurol 1998;55:1513–20.
9. Sene D, Cacoub P, Authier FJ, Haroche J, Creange A, Saadoun D, et al. Sjögren syndrome-associated small fiber neuropathy: characterization from a prospective series of 40 cases. Medicine (Baltimore) 2013;92:e10–8.

10. Polman CH, Reingold SC, Banwell B, Clanet M, Cohen JA, Filippi M, et al. Diagnostic criteria for multiple sclerosis: 2010 revisions to the McDonald criteria. Ann Neurol 2011;69:292–302.
11. Chen W, Mi R, Haughey N, Oz M, Hoke A. Immortalization and characterization of a nociceptive dorsal root ganglion sensory neuronal line. J Peripher Nerv Syst 2007;12:121–30.
12. Cottrell TR, Hall JC, Rosen A, Casciola-Rosen L. Identification of novel autoantigens by a triangulation approach. J Immunol Methods 2012;385:35–44.
13. Liu R, Jin P. Calponin isoforms CNN1, CNN2, and CNN3: regulators for actin cytoskeleton functions in smooth muscle and non-muscle cells. Gene 2016;585:143–53.
14. Griffin JW, Cornblath DR, Alexander E, Campbell J, Low PA, Bird S, et al. Ataxic sensory neuropathy and dorsal root ganglionitis associated with Sjögren's syndrome. Ann Neurol 1990;27:304–15.
15. Huang LY, Gu Y, Chen Y. Communication between neuronal somata and satellite glial cells in sensory ganglia. Glia 2013;61: 1571–81.

ARTHRITIS & RHEUMATOLOGY
Vol. 70, No. 10, October 2018, pp 1617–1625
DOI 10.1002/art.40539

Molecular Profiling and Clonal Tracking of Secreted Rheumatoid Factors in Primary Sjögren's Syndrome

Jing J. Wang,[1] Joanne H. Reed,[2] Alex D. Colella,[1] Amanda J. Russell,[2] William Murray-Brown,[1] Tim K. Chataway,[3] Katherine J. L. Jackson,[2] Christopher C. Goodnow,[2] and Tom P. Gordon[1]

Objective. **Rheumatoid factors (RFs) are associated with systemic disease in primary Sjögren's syndrome (SS) and may be pathogenic as mixed cryoglobulins. Current detection methods cannot resolve RFs at a molecular level. This study was undertaken to perform the first proteomic and transcriptomic analysis of secreted and membrane-bound IgM-RF in primary SS and identify unique heavy-chain peptide signatures for RF clonotype tracking.**

Methods. **Purified heavy chains of serum RFs from 15 patients with primary SS were subjected to de novo mass spectrometric sequencing. The circulating B cell Ig repertoire was determined by massively parallel sequencing of *IGH* RNA from matched peripheral blood mononuclear cells (n = 7). RF-specific heavy-chain third complementarity-determining region (CDR3) peptides were identified by searching RF heavy-chain peptide sequences against the corresponding *IGH* RNA sequence libraries. Heavy-chain CDR3 peptides were used as biomarkers to track serum RF clonotypes using quantitative multiple reaction monitoring.**

Results. **Serum RFs were clonally restricted and composed of shared sets of IgM heavy-chain variable region (Ig V_H) 1–69, 3–15, 3–7, and 3–74 subfamilies. Cryoprecipitable RFs from patients with mixed cryoglobulinemia (MC) were distinguishable from nonprecipitating RFs by a higher frequency of amino acid substitutions and identification of stereotypic heavy-chain CDR3 transcripts. Potentially pathogenic RF clonotypes were detected in serum by multiple reaction monitoring years before patients presented with MC. Levels of Ig V_H4–34 IgM-RF decreased following immunosuppression and remission of MC.**

Conclusion. **Cryoprecipitable RF clonotypes linked to vasculitis in primary SS have different molecular profiles than nonprecipitating RFs, suggesting different underlying mechanisms of production. The combined omics workflow presented herein provides molecular biomarkers for tracking and removal of pathogenic RF clones.**

Rheumatoid factors (RFs) are commonly found in the serum and saliva of patients with primary Sjögren's syndrome (SS) and are associated with high Ig levels, the presence of anti-Ro/SSA and anti-La/SSB, and extraglandular manifestations (1–5). Reflecting the prominent B cell hyperactivity in primary SS, RFs along with anti-Ro/La autoantibodies are produced years before the clinical onset and diagnosis of the disease, akin to their appearance before joint disease in rheumatoid arthritis (6–8). Serum RFs have recently been shown to be independent predictors of lymphoma in primary SS, where they are hypothesized to be linked to lymphomagenesis via chronic stimulation of RF-positive B cells by anti-Ro/La immune complexes (6,9–14). Providing further evidence of the pathologic importance of RFs in primary SS, overexpression of stereotypic RF clonotypes, notably of the Ig heavy-chain variable region (Ig V_H) 1–69, 4–34, and 3–7 subfamilies, can lead to precipitation of IgG/IgM-RF complexes and mixed cryoglobulinemia (MC), which is associated with higher mortality and is a strong predictor of lymphoma development (14–16).

Serum RFs have been detected for decades in the clinical setting by semiquantitative agglutination methods, such as nephelometry or enzyme-linked immunosorbent assay. While simple to perform, these methods lack the

Supported by the Australian National Health and Medical Research Council (grant 1041900 to Dr. Gordon and Early Career Fellowship grant 1090759 to Dr. Wang), NSW Health (Early-Mid Career fellowship to Dr. Reed), and Arthritis South Australia (LSS Support Group grant to Dr. Reed).

[1]Jing J. Wang, PhD, Alex D. Colella, PhD, William Murray-Brown, PhD, Tom P. Gordon, MD, PhD: Flinders University and SA Pathology, Bedford Park, South Australia, Australia; [2]Joanne H. Reed, PhD, Amanda J. Russell, BSc, Katherine J. L. Jackson, PhD, Christopher C. Goodnow, PhD: Garvan Institute of Medical Research, Darlinghurst, New South Wales, Australia; [3]Tim K. Chataway, PhD: Flinders University, Bedford Park, South Australia, Australia.

Address correspondence to Tom P. Gordon, MD, PhD, Department of Immunology, Flinders Medical Centre, Flinders University, Flinders Drive, Bedford Park, South Australia 5042, Australia. E-mail: t.gordon@flinders.edu.au.

Submitted for publication August 29, 2017; accepted in revised form April 19, 2018.

resolving power to profile clonality, Ig V_H subfamily composition, and/or V-region somatic mutations. Changes in the levels of individual RF clonotypes in complex serum mixtures, some of which may be pathogenic, are thus invisible to these assays. Antiidiotypic antibody detection methods partly address this issue, but these methods are unable to profile the global V-region repertoire and individualized heavy-chain third complementarity-determining regions (CDR3). Heavy-chain CDR3 generate most of the diversity in the human repertoire as well as being a major determinant of binding specificity, thus serving—along with details of the *IGHV* and *IGHJ* gene segments—as clonotypic markers of an antibody (17). While hybridoma and recombinant antibody technologies can provide full nucleotide sequences of antibodies, single-cell methods do not generally reflect the overall secreted (serum) RF repertoire (18). Direct sequencing of serum antibody repertoires by mass spectrometry (MS) is limited currently by technical difficulties in sequencing heavy-chain CDR3 peptides. Theoretically, this limitation could be addressed by reference to the nucleotide sequences of Ig RNAs from peripheral blood lymphocytes in the same patient, provided the serum autoantibody is also expressed as RNA by circulating cells and provided the B cell RNA repertoire could be sequenced at sufficient depth to detect rare circulating B cells or plasmablasts (19–21).

Given the clinical importance of RFs in primary SS and other systemic rheumatic diseases, there is a need for biomarkers in sera for identification and tracking of pathogenic RF clonotypes that can be tailored to individual patients. Molecular profiling of Ig V_H subfamily expression and somatic mutations may also provide insights into mechanisms of RF production in different subsets of patients and/or lead to novel molecular biomarkers of responsiveness to biologics (22). Based on recently developed proteomic workflows that can perform de novo sequencing on microgram amounts of autoantibodies in sera, we present a simple purification method for MS-based sequencing of heavy chains of serum RFs and analysis of their Ig V_H subfamily composition (23–25). We then identify heavy-chain CDR3 markers by a combined proteomic and RNA repertoire approach and monitor the expression of specific RF clonotypes by quantitative proteomics.

PATIENTS AND METHODS

Patients and controls. Sera were obtained from 15 patients with primary SS whose sera were RF positive by nephelometry (Table 1). Blood samples were obtained at different time points from patients SS1, SS2, and SS4 for the longitudinal study, while a single blood sample was obtained from each of the remaining 12 patients. At the same time serum was collected, non-coagulated blood was obtained from a subset of these patients (n = 7), and peripheral blood mononuclear cells (PBMCs) were prepared with Ficoll-Histopaque and cryopreserved in RPMI 1640, 50% fetal calf serum, and 10% DMSO. Patients with primary SS fulfilled at least 4 of the 6 American–European Consensus Group Criteria (26). The patients were not being treated with any immunomodulatory medications at the time of initial blood sampling, except for patients SS1 and SS5, who were taking azathioprine 100 mg daily and prednisolone 5 mg daily, respectively. Patient SS4 was started on prednisolone and methotrexate after a baseline blood sample was obtained. The study was approved by the Clinical Ethics Committee of Flinders Medical Centre. Control sera were obtained from 10 healthy donors, 5 RF-negative SS patients, and 3 asymptomatic subjects positive for IgM-RF and anti-Ro/La without sicca symptoms, MC, or other features of primary SS. Demographic and serologic characteristics are shown in Table 1. The European League Against Rheumatism Sjögren's Syndrome Disease Activity Index (ESSDAI) was scored as previously described (27).

Purification of heavy chains of serum RF. IgM-RFs were purified from serum by a heat-aggregated IgG (HAGG) precipitation method. Briefly, 20 μl of HAGG obtained by heating human intravenous Ig (Flebogamma; Grifols) at 20 mg/ml for 30 minutes at 63°C was mixed with 60 μl patient serum and incubated at 4°C for 1 hour to allow IgM-RF HAGG complex formation. Following centrifugation at 14,000 revolutions per minute (rpm) for 20 minutes, the IgM-RF HAGG pellet was washed twice with cold Milli-Q water and subjected to reduced sodium dodecyl sulfate–polyacrylamide gel electrophoresis (SDS-PAGE) to separate the 75-kd RF heavy-chain band from the residual HAGG migrating at 50 kd.

Serum samples from patients with MC were collected at 37°C, placed at 4°C for 72 hours, and centrifuged at 4°C at 14,000 rpm for 20 minutes. Cryoprecipitates were washed twice in cold Milli-Q water and identified as type II by IgM immunofixation (28). Cryoglobulins were solubilized at 37°C, and 75-kd RF heavy chains were isolated by reduced SDS-PAGE as described above.

Mass spectrometry. IgM heavy-chain gel bands at 75 kd were excised from reduced SDS-PAGE and digested with Pierce trypsin protease (ThermoFisher Scientific) and chymotrypsin (Promega), separately. Digested peptides were analyzed using a TripleTOF 5600+ mass spectrometer (AB Sciex) coupled to an Ekspert NanoLC 415 HPLC (Eksigent) as previously described (23,25). Purification of IgM-RF from individual patient sera was carried out on at least 2 independent occasions, and the RF heavy-chain tryptic and chymotryptic digests from each purification were subjected to MS as 2 technical replicates, respectively.

Protein sequence data analysis. MS data files were first analyzed using ProteinPilot 5.0.1 (AB Sciex), and post-calibrated Mascot generic files were exported for combined de novo amino acid sequencing and database matching by Peaks Studio version 8.0 software (Bioinformatics Solutions) using combined IMGT (F + ORF + in-frame P) version 3.1.2 (http://www.imgt.org), NCBI (NCBI Human Database), and Uniprot 2016-12 databases. The parameters for database searches, data refinement, and Ig V_H gene family assignments have been described previously (23,24,29). Briefly, the parameters include a maximum of 2 missed cleavages, precursor mass/charge tolerance of <10 parts per million, product ion error tolerance of 0.02 daltons, and

Table 1. Characteristics of the patients with primary SS*

Patient/ age/sex	Disease duration, years	Autoantibodies			Total IgG, mg/ml‡	RF <14 IU/ml‡	Low C3 (<0.85 gm/liter)	Low C4 (<0.12 gm/liter)	Lymphopenia (<1.5 × 10^9/liter)	Clinical features	ESSDAI
		Ro 52†	Ro 60†	La†							
SS1/49/F	30	+	+	+	12.8	69	–	+	+	Salivary gland enlargement, purpura, MC	14
SS2/61/F	7	+	+	+	15.7	300	+	+	+	Purpura, MC	18
SS3/76/F	30	+	+	+	11.1	329	–	+	+	Salivary gland enlargement, purpura, MC	20
SS4/68/F	20	+	+	+	17.4	320	+	+	+	Salivary gland enlargement, urticarial vasculitis, arthritis, MC	15
SS5/36/F	17	+	+	+	15.4	19	–	–	–	Interstitial nephritis, tubular acidosis, baby with CHB	10
SS6/45/F	16	+	+	+	27.2	210	+	+	+	Persistent cough, Raynaud's phenomenon	7
SS7/56/F	22	+	+	+	12.2	346	–	–	–	Salivary gland enlargement, arthritis	6
SS8/44/F	1	+	+	–	19.6	220	–	–	+	Arthralgia	4
SS9/61/F	8	+	+	+	32.6	220	–	–	+	Salivary gland enlargement, purpura	14
SS10/59/F	6	+	+	+	26.8	320	–	–	–	Neutropenia, Raynaud's phenomenon	4
SS11/26/F	9	+	+	+	59	190	–	+	+	Mild fever, salivary gland enlargement, purpura	17
SS12/59/F	9	+	+	+	28.7	430	+	–	+	Salivary gland enlargement	8
SS13/66/F	10	+	+	–	13.3	110	–	–	–	Salivary gland enlargement, erythema multiforme	5
SS14/46/F	19	+	+	+	26.5	36	–	+	–	Salivary gland enlargement	4
SS15/75/F	10	+	+	+	35.8	190	+	+	+	Salivary gland enlargement	9

* SS = Sjögren's syndrome; RF = rheumatoid factor; ESSDAI = European League Against Rheumatism Sjögren's Syndrome Disease Activity Index; MC = mixed cryoglobulinemia; CHB = congenital heart block.
† Measured by line blot immunoassay.
‡ Measured by nephelometry.

precursor charge state of +2 to +4. The Ig V_H region gene family is assigned based on the presence of a unique peptide corresponding to the gene family.

Massively parallel *IGH* repertoire sequencing of PBMCs. RNA was prepared from 0.5–8 million thawed PBMCs using an RNeasy kit (Qiagen). Complementary DNA was synthesized from 0.5 μg RNA using oligo(dT) and random hexamer primers. A 2-step polymerase chain reaction (PCR) approach was used to generate Ig heavy-chain amplicons for deep sequencing. The first step uses forward primers binding leader peptide sequences of V segments and reverse primers binding μ constant regions (30), incorporating a universal 5′ sequence for the Illumina Nextera protocol. Using the resulting IgM amplicons as templates, the second PCR step uses the Nextera Index kit and incorporates sample barcodes to allow pooling of multiple samples, before massively parallel sequencing on an Illumina MiSeq with 300-bp paired end reads to a depth of at least 1 million read pairs per sample.

***IGH* RNA nucleotide sequence analysis.** Ig heavy-chain amplicon libraries were processed using MiXCR software to identify B cell clonal lineages and to determine their frequencies within each patient's IgM repertoire (31). Clonal lineages are defined as having matching V and J gene segment usage, >90% nucleotide sequence identity, and same length CDR3. Individualized *IGH* reference databases for each patient were generated from productive Ig heavy-chain amino acid sequences. Translated sequences were generated by aligning merged paired-end amplicons (32) against the IMGT human reference *IGHV*, *IGHD*, and *IGHJ* gene segments (33) using a local installation of IgBLAST (34) before extracting in-frame Ig heavy-chain amino acid sequences from the IgBLAST output.

Multiple reaction monitoring. A quantitative proteomics approach was developed using multiple reaction monitoring, targeting specific RF clonotypes. This involved the mass spectrometer repeating a 3-second cycle that comprised an MS scan of all intact peptide ions, followed by the isolation and fragmentation of 29 different peptide masses corresponding to unique RF clonotype peptides. A TripleTOF 5600+ mass spectrometer (AB Sciex) coupled to an Ekspert nano415 HPLC (Eksigent) was used to perform this analysis. Multiple reaction monitoring data files were processed using Multiquant 1.2 software (AB Sciex) that performed peak detection and integration on 5 different fragment ions per RF peptide targeted. These fragment ions were selected since they were sufficient to represent a unique spectral signature of each peptide. The peak areas for all 5 fragment ions were then summed to provide a quantitative measure of heavy-chain CDR3 peptide levels expressed as spectral counts per second.

RESULTS

Purification of RF heavy chains from primary SS sera. We have developed a combined omics workflow to analyze secreted (serum) IgM-RF repertoires in patients

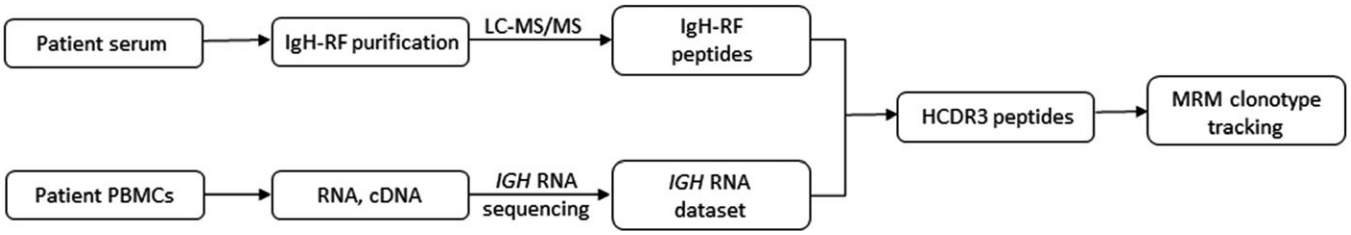

Figure 1. Combined omics workflow for serum rheumatoid factor heavy-chain (IgH-RF) repertoire analysis. RF heavy chains are purified from serum and digested with enzymes to generate peptides for liquid chromatography mass spectrometry/mass spectrometry (LC-MS/MS). IgM heavy-chain variable region peptide sequences are analyzed by combined de novo sequencing and database matching. In parallel, total RNA from peripheral blood mononuclear cells (PBMCs) is reverse transcribed, and more than 1 million IgM heavy-chain RNA nucleotide sequences are obtained by massively parallel DNA sequencing. RF heavy-chain peptide sequences are searched against the matched *IGH* RNA data set to identify clonotypic heavy-chain third complementarity-determining region (HCDR3) peptides, which are then used for multiple reaction monitoring (MRM)–based clonotype tracking.

with primary SS (Figure 1). The initial proteomics arm involves purification of RF heavy-chain protein from as little as 60 μl of patient serum using HAGG as a surrogate immune complex to precipitate RFs, followed by high-resolution mass spectrometric sequencing of in-gel digests. The serum RF heavy chains bound to HAGG migrate as 75-kd bands on reduced SDS-PAGE and can be sequenced directly without additional purification steps. The method specifically isolates RF heavy chains since no 75-kd bands are observed in HAGG pulldown/SDS-PAGE of sera from healthy controls or patients with primary SS who are seronegative for RF by nephelometry (see Supplementary Figure 1, available on the *Arthritis & Rheumatology* web site at http://onlinelibrary.wiley.com/doi/10.1002/art.40539/abstract). Furthermore, RF activity as assessed by nephelometry is undetectable in the supernatant after HAGG pulldown. While sequencing the 75-kd heavy chains, this method does not separate RF light chains from HAGG light chains, which both migrate at 25 kd. RF heavy chains can be gel purified and prepared for sequencing within hours, shortening earlier autoantibody sequencing methods by days (35).

Serum RF heavy chains from primary SS patients express shared sets of Ig V_H subfamilies. Mass spectrometric sequencing of heavy-chain peptides was performed on in-gel trypsin and chymotrypsin digests of purified RF heavy chains from 15 unrelated patients with anti-Ro/La antibody–positive primary SS and 3 asymptomatic subjects who were positive for IgM-RFs and anti-Ro/La. This represents the largest direct sequencing study of secreted systemic autoantibodies to date (35). We applied highly stringent methods for peptide selection to minimize

Table 2. Proteomic profiling of Ig V_H composition of serum RF heavy chains in patients with primary SS*

	Ig V_H1–3	Ig V_H1–69	Ig V_H3–15	Ig V_H3–23	Ig V_H3–7	Ig V_H3–74	Ig V_H4–34	Ig V_H4–61	Ig V_H5–51	Ig V_H7–4
SS1	+	+†	–	–	+†	–	–	–	–	+
SS2	–	+†	–	–	+†	–	–	–	–	–
SS3	–	+†	–	–	–	–	–	–	–	–
SS4	–	+†	+	–	+	+	+†	–	–	–
SS5	–	–	+	–	+	+	–	–	+	–
SS6	–	–	+	–	+	+	–	+	–	–
SS7	–	–	+	–	+	+	–	–	+	–
SS8	–	–	+	–	+	+	–	+	–	–
SS9	–	+	+	–	+	+	–	–	–	–
SS10	–	+	–	+	+	+	–	+	–	–
SS11	–	+	+	+	+	–	–	–	–	–
SS12	–	+	–	+	+	+	–	–	–	–
SS13	–	+	+	–	+	–	–	–	–	–
SS14	–	+	+	–	+	–	–	–	–	–
SS15	–	–	–	+	+	+	–	–	–	–
AS1	–	–	+	+	+	+	–	–	–	–
AS2	+	+	+	–	+	+	–	–	–	–
AS3	–	–	+	–	+	+	–	–	–	–

* IgM heavy-chain variable region (Ig V_H) subfamily peptide sequence maps are available from the corresponding author upon request. SS = Sjögren's syndrome; AS = asymptomatic subject positive for rheumatoid factor (RF).
† Cryoprecipitable RF.

false-positive antibody repertoire matches, by requiring b- and/or y-ions for each amino acid in the peptides. Representative high-confidence spectra are available from the corresponding author upon request. Combined de novo amino acid sequencing and database matching revealed shared oligoclonal patterns with common expression of Ig V_H 3–7 in 14 of 15 patients, Ig V_H 1–69 in 10 of 15 patients, and Ig V_H 3–15 and 3–74 subfamilies in 9 of 15 patients. RF heavy-chain proteomes from the 3 RF-positive asymptomatic subjects revealed similar profiles of heavy-chain subfamily expression as seen in the patients with primary SS (Table 2).

Sequencing of 75-kd heavy chains from washed cryoglobulins from patients SS1–SS4 revealed Ig V_H 1–69/3–7 cryoglobulins for patients SS1 and SS2 with dominant utilization of Ig V_H 3–7 for patient SS1 and of Ig V_H 1–69 for patient SS2; Ig V_H 1–69 cryoglobulins for patient SS3; and Ig V_H 1–69/4–34 (Ig V_H 4–34 dominant) cryoglobulins for patient SS4, which were homologous with their serum RF heavy-chain counterparts. Dominant Ig V_H region usage was determined by spectral counts of Ig V_H subfamily–specific peptides and read counts from *IGH* RNA-Seq libraries (data not shown). Our finding of multiple RF cryoglobulins in 3 patients is consistent with recent reports of oligoclonal RF in type II MC (36).

A comparison between the numbers of V-region amino acid substitutions in cryoprecipitable and nonprecipitating RF heavy chains from the Ig V_H 1–69 and 3–7 subfamilies showed a significant increase in the overall frequency of amino acid substitutions in the heavy chains of cryoprecipitable RFs versus the heavy chains of nonprecipitating RFs (P = 0.0006 by Mann-Whitney U test) (Supplementary Figure 2, available on the *Arthritis & Rheumatology* web site at http://onlinelibrary.wiley.com/doi/10.1002/art.40539/abstract).

Identification of RF heavy-chain CDR3 peptides by combined proteotranscriptomics. A limitation of the single proteomic workflow is that clonality cannot be established because accurate heavy-chain CDR3 peptide sequences are difficult to identify because of the small amounts of available heavy chains for de novo sequencing and lack of reference databases for rearranged V–D–J segments. We therefore searched our serum MS/MS V-region peptide libraries against corresponding massively parallel *IGH* RNA data from the same patient, identifying matched heavy-chain CDR3 peptide/RNA sequences for the 6 cryoprecipitable RF heavy chains in patients SS1, SS2, and SS4 with MC. These patients shared the stereotypic (rearrangements utilizing the same gene segments with similar heavy-chain CDR3 amino acid composition

Table 3. Matched heavy-chain CDR3 peptide and transcript signatures of RF heavy-chain clonotypes from patients with primary SS with MC*

Patient	Ig V_H	Ig D_H	Ig J_H	Translated heavy-chain CDR3 sequences (% of total IgM transcripts)	Matched heavy-chain CDR3 peptide sequences
SS1	3–7†	3–22	3‡	ARGDYYDSGGSDWVDAFDVW (2.6)	YCARGDYY (peptide 1)§ DSGGSDWVDAF (peptide 2)§
SS1	1–69	3–22	4¶	ARGPGDSSGYYYFFW (0.014)# ARGPGDSGGYYYFFW (0.02)# ARGPGDSSGYDYW (<0.0001) ARGPGDSSGYSAFDYW (<0.0001)	CARGPGDSSGY CARGPGDSGGY
SS2	1–69†	3–22	4¶	AREYERDSSGYYYLYW (12.0)** AREYERDSSGYYFLYW (9.2)** AREYERESSGYYYLYW (0.4)**	YCAREY (peptide 3)§ ERESSGYY (peptide 4)§ ERDSSGYY (peptide 5)§ LYWGQGTL FLYWGQGTL
SS2	3–7	3–22	3‡	ARGDYYDSGGSDWVDAFDVW (0.0002)	YCARGDYY DSGGSDWVDAF
SS4	4–34†	5–18/5–5 3–16/3–10	5 5	ARSYEEHLGFDPW (0.0008)†† ARSYDEHLGFDPW (0.0006)††	YCARSY (peptide 6)§ EEHLGFDPW (peptide 7)§ EHDLGFDPW (peptide 8)§
SS4	1–69	3–9 6–6	4 4	AGSFDSGDPPKPFNYW (<0.0001) AREFGAAPGRESYFAYW (<0.0001)	DSGDPPKPF FCAREF GAAPGRESY

* CDR3 = third complementarity-determining region; SS = Sjögren's syndrome; MC = mixed cryoglobulinemia; Ig V_H = IgM heavy-chain variable region; Ig D_H = IgM heavy-chain diversity region; Ig J_H = IgM heavy-chain joining region.
† Dominant rheumatoid factor (RF) heavy-chain clonotypes sequenced in cryoglobulins from each patient.
‡ V3–7 stereotypic RF heavy chain.
§ Peptide sequence used as a surrogate peptide in multiple reaction monitoring.
¶ RF-WOL (Wa) stereotypic heavy-chain idiotype.
# Mutational variants arising within a clonal lineage.
** Mutational variants arising within a clonal lineage.
†† Mutational variants arising within a clonal lineage.

in unrelated subjects) *IGVH1-69*/*D3-22*/*J4* rearrangement of the RF-WOL (Wa) idiotype expressed by patients with SS-related mucosa-associated lymphoid tissue (MALT)–type lymphoma, hepatitis C virus–infected patients with cryoglobulinemia, and patients with chronic lymphocytic leukemia (37–42). In addition, cryoprecipitable IgM-RFs from unrelated patients SS1 and SS2 shared an identical *IGHV3-7*/*D3-22*/*J3* rearrangement and heavy-chain CDR3 sequence (ARGDYYDSGGSDWVDAFDVW), providing a rare example of a secreted public clonotype (Table 3). Stereotypic Ig V_H 3–7/D_H3–22/J_H3, denoted as Ig V_H3–7 RF, has also been found in SS-related MALT lymphoma and chronic lymphocytic leukemia (10,38,41). Matched peptide and RNA heavy-chain CDR3 sequences were also detected in serum and PBMCs from patient SS4 with RF cryoglobulins encoded by the inherently autoreactive Ig V_H4–34 subfamily (43).

In contrast to the heavy-chain CDR3 protein–RNA matches identified for cryoprecipitable RFs, no matched heavy-chain CDR3 peptide sequences were found for any of the soluble RFs encoded by the Ig V_H 1, 3, 4, and 5 subfamilies in patients SS5, SS6, SS8, and SS10 when searched against their *IGH* RNA data sets, despite identical sample processing and bioinformatics analysis. We infer that the B cell and/or plasma cell precursors of soluble RFs in these patients do not circulate or are present in low levels that are undetectable by the *IGH* RNA sequencing protocol used in this study. This is corroborated by a recent report that proteomic-sequenced antibodies may not be detected in B cells sequenced in parallel from the same patient, since only a fraction of the B cell repertoire is sampled from humans (21). Given the heterogeneity of heavy-chain CDR3 sequences, it is also possible that some heavy-chain CDR3 do not digest well, giving rise to peptides that are either too small, large, hydrophilic, or hydrophobic to be adequately resolved by MS.

Tracking of serum RFs in SS patients with MC by quantitative multiple reaction monitoring/MS using heavy-chain CDR3 peptide markers. Having identified serum heavy-chain CDR3 peptide markers of clinically important cryoprecipitable RFs, we next developed a novel multiple reaction monitoring/MS platform to investigate whether specific RF antibodies sequenced from patients SS1 and SS2 with MC were detectable in stored serum samples obtained years before the patients presented with MC. In this context, multiple reaction monitoring involves targeting of heavy-chain CDR3 peptides unique to particular RF clonotypes, which when fragmented produce a quantifiable spectral fingerprint specific to the heavy-chain CDR3 sequence.

For patient SS1, RF heavy-chain CDR3 peptides associated with Ig V_H3–7 clonotypes were identified in a serum sample stored in 2012, at a time when the patient did not have clinical features of MC. However, when she presented 3 years later with cutaneous vasculitis and MC, multiple reaction monitoring/MS revealed an ~10-fold

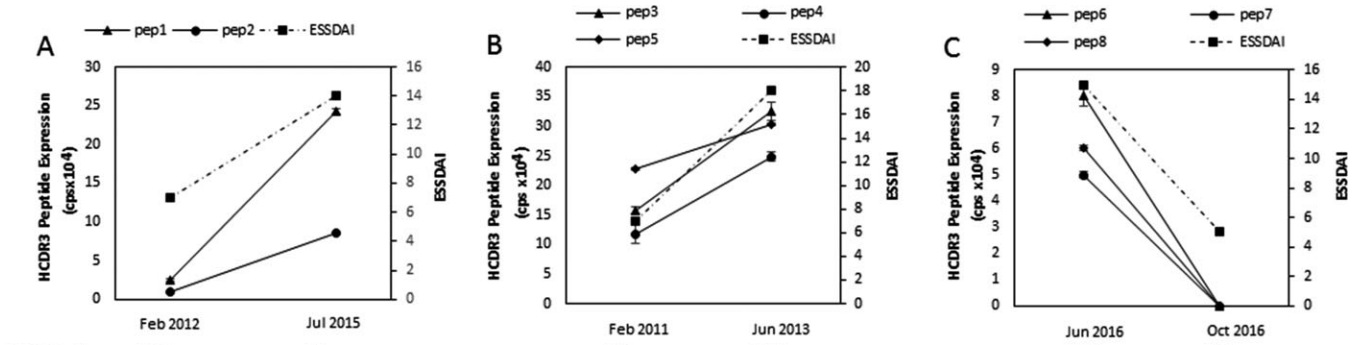

Figure 2. Tracking of serum rheumatoid factor (RF) clonotypes in patients with primary Sjögren's syndrome (SS) by multiple reaction monitoring/mass spectrometry using specific heavy-chain third complementarity-determining region (HCDR3) peptide (pep) markers. **A**, In patient SS1, Ig V_H3–7 clonotype expression showed a 10-fold increase from 2012 to 2015, when the patient presented with mixed cryoglobulinemia (MC) and cutaneous vasculitis (CV). **B**, Similarly, in patient SS2, Ig V_H1–69 clonotype expression increased 2-fold over 2 years concordant with the development of MC and CV. **C**, In patient SS4, levels of the Ig V_H4–34 clonotype became undetectable after 4 months of prednisolone and methotrexate treatment associated with the disappearance of MC and remission of urticarial vasculitis (UV). The amino acid sequences of surrogate peptides (peptides 1–8) are shown in Table 3. Heavy-chain CDR3 peptides are expressed as spectral counts per second (cps). Data are the mean ± SEM of 4 replicates. ESSDAI = European League Against Rheumatism Sjögren's Syndrome Disease Activity Index; cryo = cryoglobulin.

increase in the serum level of the RF-specific clonotypes (Figure 2A). Similarly for patient SS2, there was a 2-fold increase in Ig V_H1–69 heavy-chain CDR3 peptide expression in serum from 2011 to 2013, concordant with the development of MC and cutaneous vasculitis (Figure 2B). Taken together, these preliminary results suggest that cryoprecipitable RF clonotypes are stable moieties that persist in sera over years but can be detected by targeted multiple reaction monitoring/MS before precipitation as IgG-RF complexes and development of MC.

We then assessed changes in the levels of cryoprecipitable IgM-RFs utilizing Ig V_H4–34 for patient SS4 following treatment with prednisolone (25 mg daily) and methotrexate (15 mg weekly) for MC. After 4 months of therapy, serum heavy-chain CDR3 peptide levels became undetectable, concordant with a decrease in RF levels by nephelometry, disappearance of the cryoglobulin, and remission of the patient's urticarial vasculitis (Figure 2C). These observations suggest that levels of selected RF clonotypes assayed by quantitative multiple reaction monitoring/MS may have potential as molecular biomarkers of responsiveness to therapy.

DISCUSSION

In this study, we performed the first proteomic profiling of secreted (serum) RF responses in primary SS using a simple purification method for RF heavy chains followed by de novo Ig sequencing and database matching. As reported for other systemic autoantibodies in lupus and primary SS, such as anti-Ro/La, anti-Sm, and anti–ribosomal P, serum IgM-RF repertoires express shared sets of Ig V_H subfamilies and reveal moderate levels of somatic hypermutation (23–25,29,44,45). While an early study of RF hybridomas reported a diverse usage of germline-encoded Ig V_H genes in primary SS, single-cell studies provide a limited view of the actual secreted RF repertoire in comparison with direct high-resolution mass spectrometric sequencing (46). We used a combined Ig peptide RNA sequencing approach for RF clonal matching between serum and peripheral B cells, with the translational goal of identifying specific heavy-chain CDR3 peptide barcodes expressed by IgM-RF cryoglobulins. To verify and quantify expression of clonotypic peptides in patient sera, a quantitative proteomic platform was designed for targeted identification and monitoring of pathogenic RF clonotypes in patients presenting with MC, with preliminary findings revealing changes in levels of specific clonotypes over time and following treatment.

The molecular analysis of RFs described here differentiates pathogenic, cryoprecipitable RFs from apparently benign, nonprecipitating RFs, in terms of a higher frequency of amino acid substitutions and identification of matched heavy-chain CDR3 RNAs in the peripheral blood B cells. The cryoprecipitable RF clonotypes, linked to the development of systemic vasculitis and higher mortality in primary SS, expressed stereotypic RF idiotypes of the RF-WOL (Wa) and Ig V_H3–7 RF families that have been reported in MALT lymphomas from primary SS patients, consistent with the notion that chronic stimulation of these RF-positive B cells by circulating anti-Ro/La immune complexes can lead to their transition to malignant lymphoma (9–14).

The different molecular characteristics of these RF subsets may reflect separate mechanisms of production. We surmise that soluble RFs are sustained by Toll-like receptor–driven activation of naive RF-positive B cells in extracellular foci, with T cells having a facultative role with low rates of somatic hypermutation, as shown in experimental models of RF production (47). Intermittent waves of plasmablasts generated by this mechanism may not be sampled in peripheral blood, accounting for the absence of matched B cell receptor (BCR) transcripts. In contrast, we suggest that the precipitating RFs linked to immune complex formation are secreted by repetitive recall responses on RF-positive memory B cells derived from rounds of affinity maturation in germinal centers, leading to continuous release of B cell precursors into the circulation.

Combined omics profiling of RFs requires specialized technology yet represents a major advance over conventional RF detection methods such as agglutination and solid-phase immunoassay. Here we present the first multiple reaction monitoring technology for tracking expression of specific human autoantibodies in complex serum samples. Once a set of personalized heavy-chain CDR3 sequences has been identified by BCR repertoire sequencing and matched to secreted proteomes, selected RF clonotypes can plausibly be tracked in serial samples over years with MS precision and accuracy. Furthermore, multiple reaction monitoring/MS technology can readily be multiplexed to quantitate multiple RF marker peptides (and other autoantibodies of interest) in small volumes of individual sera. The workflow described herein can be used for molecular profiling of RFs in patients with rheumatoid arthritis and other systemic autoimmune diseases, and readily adapted for targeted detection of other systemic autoantibodies. Furthermore, RF heavy-chain molecular biomarkers hold promise for the monitoring of individual RF responses to conventional and biologic therapies for primary SS (22,48). Given that RF is an independent predictor of lymphoma in patients with primary SS (12), it will be interesting to sequence serum RFs to search for associations with particular Ig V_H expression profiles

and mutational patterns in patients progressing from initial presentation to MC and to lymphoma.

In summary, this first combined omics analysis of the serum RF repertoire in a prototypical systemic autoimmune disease reveals a restricted yet convergent repertoire, consistent with the idea that these specific germline V(D)J combinations have an affinity for identical epitopes on IgG Fc with further shaping by somatic selection. The discovery of public and individualized RF heavy-chain peptides requires further investigation with respect to their utility as diagnostic and prognostic biomarkers in longitudinal studies of larger patient cohorts. Determination of heavy-chain CDR3 markers of pathogenic RF subsets linked to systemic vasculitis, the main autoimmune cause of death in patients with primary SS (49), may have a therapeutic application in terms of the selective removal of precursor B cell clonotypes by an antiidiotypic approach. Finally, it is likely that molecular profiling studies of RFs and other systemic autoantibodies using the workflow described herein will set the scene for further integrative studies of human autoimmunity, by providing specific BCR repertoire biomarkers for phenotypic and single-cell analyses of autoreactive B cell clones.

ACKNOWLEDGMENTS

The authors would like to thank all patients and volunteers for their participation in this study.

AUTHOR CONTRIBUTIONS

All authors were involved in drafting the article or revising it critically for important intellectual content, and all authors approved the final version to be published. Prof. Gordon had full access to all of the data in the study and takes responsibility for the integrity of the data and the accuracy of the data analysis.

Study conception and design. Wang, Reed, Colella, Chataway, Goodnow, Gordon.

Acquisition of data. Wang, Reed, Colella, Russell, Murray-Brown, Chataway, Jackson, Goodnow, Gordon.

Analysis and interpretation of data. Wang, Reed, Collela, Chataway, Jackson, Goodnow, Gordon.

REFERENCES

1. Cummings NA, Schall GL, Asofsky R, Anderson LG, Talal N. Sjögren's syndrome: newer aspects of research, diagnosis, and therapy. Ann Intern Med 1971;75:937–50.
2. Bournia VK, Vlachoyiannopoulos PG. Subgroups of Sjögren syndrome patients according to serological profiles. J Autoimmun 2012;39:15–26.
3. Kyriakidis NC, Kapsogeorgou EK, Tzioufas AG. A comprehensive review of autoantibodies in primary Sjögren's syndrome: clinical phenotypes and regulatory mechanisms. J Autoimmun 2014; 51:67–74.
4. Markusse HM, Otten HG, Vroom TM, Smeets TJ, Fokkens N, Breedveld FC. Rheumatoid factor isotypes in serum and salivary fluid of patients with primary Sjögren's syndrome. Clin Immunol Immunopathol 1993;66:26–32.
5. Talal N. Recent developments in the immunology of Sjögren's syndrome (autoimmune exocrinopathy). Scand J Rheumatol Suppl 1986;61:76–82.
6. Theander E, Jonsson R, Sjöström B, Brokstad K, Olsson P, Henriksson G. Prediction of Sjögren's syndrome years before diagnosis and identification of patients with early onset and severe disease course by autoantibody profiling. Arthritis Rheumatol 2015;67:2427–36.
7. Tan EM, Smolen JS. Historical observations contributing insights on etiopathogenesis of rheumatoid arthritis and role of rheumatoid factor. J Exp Med 2016;213:1937–50.
8. Kroese FG, Abdulahad WH, Haacke E, Bos NA, Vissink A, Bootsma H. B-cell hyperactivity in primary Sjögren's syndrome. Expert Rev Clin Immunol 2014;10:483–99.
9. Bende RJ, Slot LM, Hoogeboom R, Wormhoudt TA, Adeoye AO, Guikema JE, et al. Stereotypic rheumatoid factors that are frequently expressed in mucosa-associated lymphoid tissue–type lymphomas are rare in the labial salivary glands of patients with Sjögren's syndrome. Arthritis Rheumatol 2015;67:1074–83.
10. Martin T, Weber JC, Levallois H, Labouret N, Soley A, Koenig S, et al. Salivary gland lymphomas in patients with Sjögren's syndrome may frequently develop from rheumatoid factor B cells. Arthritis Rheum 2000;43:908–16.
11. Nocturne G, Mariette X. Sjögren Syndrome-associated lymphomas: an update on pathogenesis and management. Br J Haematol 2015;168:317–27.
12. Nocturne G, Virone A, Ng WF, Le Guern V, Hachulla E, Cornec D, et al. Rheumatoid factor and disease activity are independent predictors of lymphoma in primary Sjögren's syndrome. Arthritis Rheumatol 2016;68:977–85.
13. Routsias JG, Goules JD, Charalampakis G, Tzima S, Papageorgiou A, Voulgarelis M. Malignant lymphoma in primary Sjögren's syndrome: an update on the pathogenesis and treatment. Semin Arthritis Rheum 2013;43:178–86.
14. Tzioufas AG, Boumba DS, Skopouli FN, Moutsopoulos HM. Mixed monoclonal cryoglobulinemia and monoclonal rheumatoid factor cross-reactive idiotypes as predictive factors for the development of lymphoma in primary Sjögren's syndrome. Arthritis Rheum 1996;39:767–72.
15. Retamozo S, Gheitasi H, Quartuccio L, Kostov B, Corazza L, Bove A, et al. Cryoglobulinaemic vasculitis at diagnosis predicts mortality in primary Sjögren syndrome: analysis of 515 patients. Rheumatology (Oxford) 2016;55:1443–51.
16. Papageorgiou A, Voulgarelis M, Tzioufas AG. Clinical picture, outcome and predictive factors of lymphoma in Sjögren syndrome. Autoimmun Rev 2015;14:641–9.
17. Xu JL, Davis MM. Diversity in the CDR3 region of V(H) is sufficient for most antibody specificities. Immunity 2000;13:37–45.
18. Lindop R, Arentz G, Thurgood LA, Reed JH, Jackson MW, Gordon TP. Pathogenicity and proteomic signatures of autoantibodies to Ro and La. Immunol Cell Biol 2012;90:304–9.
19. Cheung WC, Beausoleil SA, Zhang X, Sato S, Schieferl SM, Wieler JS, et al. A proteomics approach for the identification and cloning of monoclonal antibodies from serum. Nat Biotechnol 2012;30:447–52.
20. Wine Y, Boutz DR, Lavinder JJ, Miklos AE, Hughes RA, Hoi KH, et al. Molecular deconvolution of the monoclonal antibodies that comprise the polyclonal serum response. Proc Natl Acad Sci U S A 2013;110:2993–8.
21. Guthals A, Gan Y, Murray L, Chen Y, Stinson J, Nakamura G, et al. De novo MS/MS sequencing of native human antibodies. J Proteome Res 2017;16:45–54.
22. Verstappen GM, van Nimwegen JF, Vissink A, Kroese FG, Bootsma H. The value of rituximab treatment in primary Sjögren's syndrome. Clin Immunol 2017;182:62–71.
23. Al Kindi MA, Chataway TK, Gilada GA, Jackson MW, Goldblatt FM, Walker JG, et al. Serum SmD autoantibody proteomes are clonally restricted and share variable-region peptides. J Autoimmun 2015;57:77–81.

24. Al Kindi MA, Colella AD, Beroukas D, Chataway TK, Gordon TP. Lupus anti-ribosomal P autoantibody proteomes express convergent biclonal signatures. Clin Exp Immunol 2016;184:29–35.
25. Wang JJ, Al Kindi MA, Colella AD, Dykes L, Jackson MW, Chataway TK, et al. IgV peptide mapping of native Ro60 autoantibody proteomes in primary Sjögren's syndrome reveals molecular markers of Ro/La diversification. Clin Immunol 2016; 173:57–63.
26. Vitali C, Bombardieri S, Jonsson R, Moutsopoulos HM, Alexander EL, Carsons SE, et al, and the European Study Group on Classification Criteria for Sjögren's Syndrome. Classification criteria for Sjögren's syndrome: a revised version of the European criteria proposed by the American-European Consensus Group. Ann Rheum Dis 2002;61:554–8.
27. Seror R, Bowman SJ, Brito-Zeron P, Theander E, Bootsma H, Tzioufas A, et al. EULAR Sjögren's syndrome disease activity index (ESSDAI): a user guide. RMD Open 2015;1:e000022.
28. Kallemuchikkal U, Gorevic PD. Evaluation of cryoglobulins. Arch Pathol Lab Med 1999;123:119–25.
29. Arentz G, Thurgood LA, Lindop R, Chataway TK, Gordon TP. Secreted human Ro52 autoantibody proteomes express a restricted set of public clonotypes. J Autoimmun 2012;39:466–70.
30. Tiller T, Meffre E, Yurasov S, Tsuiji M, Nussenzweig MC, Wardemann H. Efficient generation of monoclonal antibodies from single human B cells by single cell RT-PCR and expression vector cloning. J Immunol Methods 2008;329:112–24.
31. Bolotin DA, Poslavsky S, Mitrophanov I, Shugay M, Mamedov IZ, Putintseva EV, et al. MiXCR: software for comprehensive adaptive immunity profiling. Nat Methods 2015;12:380–1.
32. Magoc T, Salzberg SL. FLASH: fast length adjustment of short reads to improve genome assemblies. Bioinformatics 2011;27: 2957–63.
33. Lefranc MP, Giudicelli V, Duroux P, Jabado-Michaloud J, Folch G, Aouinti S, et al. IMGT(R), the international ImMunoGeneTics information system(R) 25 years on. Nucleic Acids Res 2015; 43:D413–22.
34. Ye J, Ma N, Madden TL, Ostell JM. IgBLAST: an immunoglobulin variable domain sequence analysis tool. Nucleic Acids Res 2013;41:W34–40.
35. Al Kindi MA, Colella AD, Chataway TK, Jackson MW, Wang JJ, Gordon TP. Secreted autoantibody repertoires in Sjögren's syndrome and systemic lupus erythematosus: a proteomic approach. Autoimmun Rev 2016;15:405–10.
36. De Re V, De Vita S, Sansonno D, Gasparotto D, Simula MP, Tucci FA, et al. Type II mixed cryoglobulinaemia as an oligo rather than a mono B-cell disorder: evidence from GeneScan and MALDI-TOF analyses. Rheumatology (Oxford) 2006;45:685–93.
37. Knight GB, Agnello V, Bonagura V, Barnes JL, Panka DJ, Zhang QX. Human rheumatoid factor cross-idiotypes. Part IV. Studies on WA XId-positive IgM without rheumatoid factor activity provide evidence that the WA XId is not unique to rheumatoid factors and is distinct from the 17.109 and G6 XIds. J Exp Med 1993;178:1903–11.
38. Bende RJ, Aarts WM, Riedl RG, de Jong D, Pals ST, van Noesel CJ. Among B cell non-Hodgkin's lymphomas, MALT lymphomas express a unique antibody repertoire with frequent rheumatoid factor reactivity. J Exp Med 2005;201:1229–41.
39. Charles ED, Green RM, Marukian S, Talal AH, Lake-Bakaar GV, Jacobson IM, et al. Clonal expansion of immunoglobulin M+CD27+ B cells in HCV-associated mixed cryoglobulinemia. Blood 2008;111:1344–56.
40. Charles ED, Orloff MI, Nishiuchi E, Marukian S, Rice CM, Dustin LB. Somatic hypermutations confer rheumatoid factor activity in hepatitis C virus–associated mixed cryoglobulinemia. Arthritis Rheum 2013;65:2430–40.
41. Hoogeboom R, Wormhoudt TA, Schipperus MR, Langerak AW, Dunn-Walters DK, Guikema JE, et al. A novel chronic lymphocytic leukemia subset expressing mutated IGHV3-7-encoded rheumatoid factor B-cell receptors that are functionally proficient. Leukemia 2013;27:738–40.
42. Newkirk MM, Mageed RA, Jefferis R, Chen PP, Capra JD. Complete amino acid sequences of variable regions of two human IgM rheumatoid factors, BOR and KAS of the Wa idiotypic family, reveal restricted use of heavy and light chain variable and joining region gene segments. J Exp Med 1987;166:550–64.
43. Richardson C, Chida AS, Adlowitz D, Silver L, Fox E, Jenks SA, et al. Molecular basis of 9G4 B cell autoreactivity in human systemic lupus erythematosus. J Immunol 2013;191:4926–39.
44. Lindop R, Arentz G, Chataway TK, Thurgood LA, Jackson MW, Reed JH, et al. Molecular signature of a public clonotypic autoantibody in primary Sjögren's syndrome: a "forbidden" clone in systemic autoimmunity. Arthritis Rheum 2011;63:3477–86.
45. Thurgood LA, Arentz G, Lindop R, Jackson MW, Whyte AF, Colella AD, et al. An immunodominant La/SSB autoantibody proteome derives from public clonotypes. Clin Exp Immunol 2013;174:237–44.
46. Elagib KE, Borretzen M, Jonsson R, Haga HJ, Thoen J, Thompson KM, et al. Rheumatoid factors in primary Sjögren's syndrome (pSS) use diverse VH region genes, the majority of which show no evidence of somatic hypermutation. Clin Exp Immunol 1999;117: 388–94.
47. Sweet RA, Ols ML, Cullen JL, Milam AV, Yagita H, Shlomchik MJ. Facultative role for T cells in extrafollicular Toll-like receptor-dependent autoreactive B-cell responses in vivo. Proc Natl Acad Sci U S A 2011;108:7932–7.
48. Verstappen GM, Meiners PM, Corneth OB, Visser A, Arends S, Abdulahad WH, et al. Attenuation of follicular helper T cell–dependent B cell hyperactivity by abatacept treatment in primary Sjögren's syndrome. Arthritis Rheumatol 2017;69:1850–61.
49. Ramos-Casals M, Anaya JM, García-Carrasco M, Rosas J, Bové A, Claver G, et al. Cutaneous vasculitis in primary Sjögren syndrome: classification and clinical significance of 52 patients. Medicine (Baltimore) 2004;83:96–106.

ARTHRITIS & RHEUMATOLOGY
Vol. 70, No. 10, October 2018, pp 1626–1633
DOI 10.1002/art.40538

Association Between Reappearance of Myeloperoxidase–Antineutrophil Cytoplasmic Antibody and Relapse in Antineutrophil Cytoplasmic Antibody–Associated Vasculitis

Subgroup Analysis of Nationwide Prospective Cohort Studies

Haruki Watanabe,[1] Ken-Ei Sada,[1] Yoshinori Matsumoto,[1] Masayoshi Harigai,[2] Koichi Amano,[3] Hiroaki Dobashi,[4] Shouichi Fujimoto,[5] Joichi Usui,[6] Kunihiro Yamagata,[6] Tatsuya Atsumi,[7] Shogo Banno,[8] Takahiko Sugihara,[9] Yoshihiro Arimura,[10] Seiichi Matsuo,[11] Hirofumi Makino,[12] the Japan Research Committee of the Ministry of Health, Labour, and Welfare for Intractable Vasculitis, and the Research Committee of Intractable Renal Disease of the Ministry of Health, Labour, and Welfare of Japan

Objective. **To evaluate clinical links between levels of myeloperoxidase (MPO)–antineutrophil cytoplasmic antibody (ANCA) and relapse in patients with ANCA-associated vasculitis (AAV) using a data set from 2 nationwide prospective cohort studies.**

Methods. **From the cohort studies, MPO-ANCA–positive patients who achieved remission during the 6 months after remission induction therapy were enrolled. We measured MPO-ANCA levels at months 0, 3, 6, 12, 18, 24, and at the time of relapse. The primary outcome measure was relapse. A nested case–control analysis and multivariable analysis were performed to investigate the relationship between ANCA reappearance and relapse.**

Results. **Of 271 patients, 183 were classified as having microscopic polyangiitis, 34 as having granulomatosis with polyangiitis, 15 as having eosinophilic granulomatosis with polyangiitis, and 39 were unclassifiable. The median age was 73 years, and 165 (61%) were female. In 195 patients (72%), MPO-ANCA levels decreased to normal levels within 6 months after commencement of treatment, and MPO-ANCA reappeared in 73 of 181 patients (40%) with complete follow-up data. Reappearance of MPO-ANCA was more frequent in patients with relapse than in 75 age- and sex-matched control patients without relapse (odds ratio 26.2 [95% confidence interval 8.2–101], $P < 0.0001$) after adjustment for confounding factors.**

Supported by the Ministry of Health, Labour and Welfare, Japan (grant nannti-ippann-004) and the Japan Agency for Medical Research and Development (grants 17ek0109104 and 17ek0109121).

[1]Haruki Watanabe, MD, Ken-Ei Sada, MD, PhD, Yoshinori Matsumoto, MD, PhD: Okayama University Graduate School of Medicine, Dentistry and Pharmaceutical Sciences, Okayama, Japan; [2]Masayoshi Harigai, MD, PhD: Tokyo Women's Medical University, Tokyo, Japan; [3]Koichi Amano, MD, PhD: Saitama Medical Center, Saitama Medical University, Kawagoe, Japan; [4]Hiroaki Dobashi, MD, PhD: Kagawa University, Kita-gun, Miki-cho, Japan; [5]Shouichi Fujimoto, MD, PhD: University of Miyazaki, Miyazaki, Japan; [6]Joichi Usui, MD, PhD, Kunihiro Yamagata, MD, PhD: University of Tsukuba, Tsukuba, Japan; [7]Tatsuya Atsumi, MD, PhD: Hokkaido University, Sapporo, Japan; [8]Shogo Banno, MD, PhD: Aichi Medical University School of Medicine, Nagakute, Japan; [9]Takahiko Sugihara, MD, PhD: Tokyo Metropolitan Geriatric Hospital, Tokyo, Japan; [10]Yoshihiro Arimura, MD, PhD (current address: Kichijoji Asahi Hospital, Tokyo, Japan): Kyorin University School of Medicine, Tokyo, Japan; [11]Seiichi Matsuo, MD, PhD: Nagoya University Graduate School of Medicine, Aichi, Japan; [12]Hirofumi Makino, MD, PhD: Okayama University, Okayama, Japan.

Dr. Sada has received speaking fees and/or honoraria from Chugai Pharmaceutical (less than $10,000). Dr. Harigai has received honoraria from Takeda Pharmaceutical (less than $10,000) and from Ayumi, Abbott Japan, Astellas Pharma, Bristol-Myers Squibb, Chugai Pharmaceutical, Eisai, Janssen Pharmaceutical, Mitsubishi Tanabe Pharma, Santen Pharmaceutical, Teijin Pharma, Taisho Toyama Pharmaceutical, Nippon Kayakuand, and Pfizer Japan (more than $10,000 each). Dr. Makino has received consulting fees from AbbVie and Teijin Pharma (less than $10,000 each).

Address correspondence to Ken-Ei Sada, MD, PhD, Department of Nephrology, Rheumatology, Endocrinology and Metabolism, Okayama University Graduate School of Medicine, Dentistry and Pharmaceutical Sciences, 2-5-1 Shikata-cho, Kita-ku, Okayama City 700-8558, Japan. E-mail: sadakenn@md.okayama-u.ac.jp.

Submitted for publication November 29, 2017; accepted in revised form April 19, 2018.

Conclusion. **Reappearance of MPO-ANCA could be a clinically useful biomarker for predicting relapse in patients with MPO-ANCA–positive AAV in remission. This suggests that routine MPO-ANCA monitoring should be implemented in this patient population.**

Antineutrophil cytoplasmic antibody (ANCA) was first discovered in 1982 in sera from patients with segmental necrotizing glomerulonephritis (1). Two major antigens of ANCA were detected in the late 1980s: myeloperoxidase (MPO) and proteinase 3 (PR3) (2). The diagnostic utility of ANCA testing has been widely accepted, and ANCA has been used for the classification or the diagnosis of ANCA-associated vasculitis (AAV) (3,4). While PR3-ANCA is generally regarded as a marker for granulomatosis with polyangiitis (GPA) (2), MPO-ANCA is regarded as a marker for microscopic polyangiitis (MPA)/renal limited vasculitis (5).

Although it has been well documented that patients with PR3-ANCA have a higher risk of relapse than those with MPO-ANCA (6), the usefulness of monitoring ANCA levels to predict disease activity, especially relapse, is controversial. In 2012, a meta-analysis showed that persistence of, or a rise in, ANCA during remission is modestly predictive of future disease relapse (7). Two recent studies have shown that an increase in MPO-ANCA levels seems to be a reliable marker for future relapse (8,9), but there was variation in the period of observation of the patients and the timing of ANCA evaluation (8). Inconsistent intervals of ANCA evaluation may underestimate the reappearance of ANCA, and long intervals between ANCA reappearance and relapse may make the relevance obscure. Therefore, it is difficult to draw a firm conclusion about the association between MPO-ANCA transition and relapse from previous studies.

MPO-ANCA is predominant in patients with AAV in Japan. Thus, cohorts of Japanese patients with AAV are suitable for investigating the clinical relevance of monitoring MPO-ANCA. The aim of this study was to investigate the association between the transition of MPO-ANCA at predetermined time points over a 24-month period in patients with incident AAV. We also aimed to evaluate their clinical features, then determine the association between reappearance of MPO-ANCA and relapse using data sets from 2 nationwide prospective cohort studies in Japan.

PATIENTS AND METHODS

Database. We previously conducted 2 nationwide prospective cohort studies. In the former study (Remission Induction Therapy in Japanese Patients With ANCA-Associated Vasculitides [UMIN000001648]), consecutive patients with newly diagnosed AAV were enrolled between April 2009 and December 2010 from 22 tertiary care institutions, while 53 tertiary care institutions participated in the latter study (Remission Induction Therapy in Japanese Patients with ANCA-associated Vasculitides and Rapidly Progressive Glomerulonephritis [UMIN000005136]) from April 2011 to March 2014 (for a list of participating tertiary care institutions, see Appendix A). For both studies, the criteria for enrollment were 1) diagnosis of AAV by the site investigators, 2) fulfilling the criteria for primary systemic vasculitis as proposed by the European Medicines Agency algorithm (3), and 3) starting immunosuppressive treatment based on the discretion of the site investigators. The exclusion criteria were 1) age younger than 20 years, 2) prevalent AAV, 3) serologic evidence of hepatitis B or C virus infection, and 4) a history of malignancy. The Baseline data recorded for each patient consisted of demographic information, laboratory data, disease activity according to the Birmingham Vasculitis Activity Score (BVAS) 2003, disease severity, and imaging data. The disease severity of the enrolled patients was classified as localized, early systemic, generalized, or severe, according to the European Vasculitis Study Group–defined disease severity types (10). Patients with threatened vital organ function were classified as having generalized disease, and patients with organ failure were classified as having severe disease. Detailed definitions of disease severity were described in our previous report (11). Follow-up data consisted of laboratory findings, treatments, and outcomes at months 3, 6, 12, 18, and 24, and at the time of relapse.

Patient selection and outcome measures. In this analysis, patients with MPO-ANCA–associated vasculitis (MPO-AAV) who achieved remission by month 6 after initiation of remission induction therapy were enrolled. Disease activity was determined systematically using the BVAS 2003 (12). Remission was defined as a BVAS score of 0 on 2 consecutive occasions at least 1 month apart, according to the European League Against Rheumatism recommendations (10), plus a daily glucocorticoid dosage of ≤15 mg prednisolone by month 6. Renal remission was also defined as stable or decreasing creatinine levels and the absence of red cell casts (13,14). Stable or decreasing creatinine was evaluated using the BVAS component ("Rise in creatinine >30% or creatinine clearance fall >25%"). Patients without follow-up data within 6 months were excluded.

The primary outcome measure of this study was relapse. Relapse was defined as the recurrence or new onset of clinical signs and symptoms attributable to active vasculitis. Secondary outcome measures included cumulative and overall end-stage renal disease (ESRD)–free survival rates. ESRD was defined as dependence on dialysis or an irreversible increase in serum creatinine levels of >5.6 mg/dl (500 moles/liter).

ANCA measurements and definition of status. In each institution, MPO-ANCA was evaluated using commercial assays according to the manufacturers' instructions. During the study period, the fluorescent enzyme immunoassay (FEIA) EliA (cutoff 3.5 IU/ml; ThermoFisher Diagnostics), chemiluminescent enzyme immunoassay MPO-STACIA MEBLux test (cutoff 3.5 units/ml), and enzyme-linked immunosorbent assays (ELISAs) Mesacup-2 test, MPO-ANCA test (BS) (cutoff 9 units/ml; MBL), Nephroscholar MPO-ANC II kit (cutoff 20 units/ml; Nipro), and Euroimmun (cutoff 20 relative units/ml) had been

available in clinical practice in Japan. Negative conversion was defined when a patient presented with disappearance of MPO-ANCA without relapse by month 6, or had a relapse by month 6 with disappearance of MPO-ANCA before the relapse. Reappearance of MPO-ANCA was defined as conversion from negative to positive after fulfilling the above definition of negative conversion.

Statistical analysis. The enrolled patients were initially divided into 2 groups: a negative conversion group and a non–negative conversion group. Baseline data, treatments, and outcomes were compared between the 2 groups. Subsequently, the negative conversion group was divided into 2 subgroups: those with reappearance of MPO-ANCA and those without. Laboratory data at baseline and at the time of negative conversion of MPO-ANCA, treatments, and outcomes were compared between the 2 groups. Continuous variables were compared using the Mann-Whitney U test or Welch's *t*-test depending on data distribution, and categorical variables were compared using the chi-square test or Fisher's direct probability test, as appropriate.

In the present study, a nested case–control analysis was performed to analyze the relationship between relapse and ANCA reappearance. In the negative conversion group, we identified cases who experienced relapse and controls who did not experience relapse, who were matched for age, sex, observational period, and timing of ANCA evaluation. Then, multivariable analysis was performed using a logistic regression model to adjust for confounding factors. Age, sex, AAV type, and BVAS score were included as potential confounders based on previous reports (15,16). *P* values less than 0.05 were considered significant. All statistical analyses were performed using the JMP 9.0 software package (SAS Institute).

Ethical considerations. This study was approved by the Ethics Committee of the Okayama University Graduate School of Medicine, Dentistry and Pharmaceutical Sciences (authorization no. 1610-007) and was conducted according to the principles of the Declaration of Helsinki. Informed consent was obtained from all patients to participate in the study, as well as permission to have their data published.

RESULTS

Patient characteristics. A flow chart describing patient selection is shown in Figure 1. Of 477 patients enrolled in the 2 cohort studies, 271 patients were included in this analysis. Of those, 183 were classified as having MPA, 34 as having GPA, 15 as having eosinophilic granulomatosis with polyangiitis (EGPA), and 39 were unclassifiable. Among the unclassifiable patients, organ involvements were as follows: general 28 (72%), cutaneous mucous membranes/eyes 6 (15%), ear/nose/throat 2 (5.1%), chest 11 (28%), cardiovascular 1 (2.5%), abdominal 1 (2.5%), renal 22 (56%), and nervous system 16 (41%). The median age of the patients was 73 years (interquartile range [IQR] 65–78 years), and 165 (61%) were female.

Comparison of patients with and those without negative conversion of MPO-ANCA. Of the 271 enrolled patients, 195 patients (72%) were classified into the negative conversion group. To investigate relationships between clinical manifestations and negative conversion of MPO-ANCA, characteristics of the negative conversion group and non–negative conversion group were compared (Table 1). All EGPA patients exhibited negative conversion of MPO-ANCA. The disease severity was similar in the 2 groups. Although renal involvement was less frequent in the negative conversion group

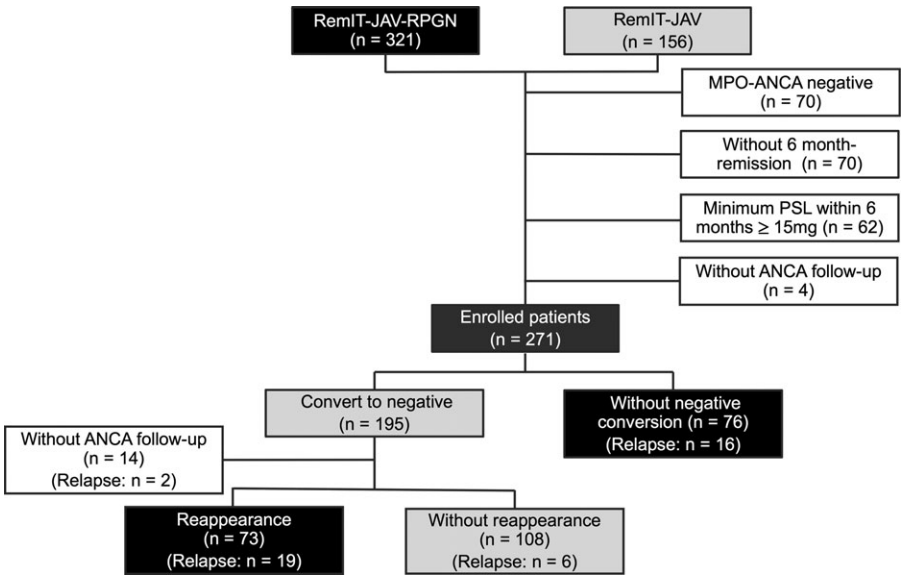

Figure 1. Flow chart showing allocation of patients to the study groups. RemIT-JAV-RPGN = Remission Induction Therapy in Japanese Patients With ANCA-Associated Vasculitides and Rapidly Progressive Glomerulonephritis; MPO-ANCA = myeloperoxidase–antineutrophil cytoplasmic antibody; PSL = prednisolone.

Table 1. Comparison of patients with and those without negative conversion of MPO-ANCA*

Variables at baseline	Negative conversion group (n = 195)	Non–negative conversion group (n = 76)
Male/female, no.	75/120	31/45
Age, median (IQR) years	72 (65–78)	74 (67–80)
EGPA/GPA/MPA/unclassifiable, no.	15/23/129/28	0/11/54/11
Localized/early systemic/generalized/severe, no.	7/31/123/34	3/15/42/16
Serum creatinine, median (IQR) mg/dl	1.1 (0.7–3.1)	1.5 (0.8–3.4)
C-reactive protein, median (IQR) mg/dl	7.1 (1.8–11.8)	6.4 (1.6–11.6)
BVAS score, median (IQR)	15 (12–20)	16 (12–21)
Renal involvement, no. (%)	152 (78)†	69 (91)
Interstitial lung disease, no. (%)	87 (45)	37 (49)
Glucocorticoid, median (IQR) mg/day‡	40 (30–50)	40 (30–46)
Glucocorticoid pulse therapy, no. (%)	84 (43)	28 (37)
CYC, no. (%)§	66 (34)	28 (37)
Concomitant immunosuppressants (AZA/MTX/others), no.	15/2/9	9/0/9

* MPO-ANCA = myeloperoxidase–antineutrophil cytoplasmic antibody; IQR = interquartile range; EGPA = eosinophilic granulomatosis with polyangiitis; GPA = granulomatosis with polyangiitis; MPA = microscopic polyangiitis; BVAS = Birmingham Vasculitis Activity Score; CYC = cyclophosphamide; AZA = azathioprine; MTX = methotrexate.
† $P < 0.015$ versus non–negative conversion group.
‡ Prednisolone equivalent.
§ During the initial 3 weeks of treatment.

compared to the other group (78% versus 91%; $P = 0.015$), the frequency of renal involvement was similar in the 2 groups if patients with EGPA were not included (147 of 180 [82%] versus 69 of 76 [91%]; $P = 0.09$). Of the 271 patients, 43 (16%) experienced relapse; at the time of relapse, MPO-ANCA was positive in 27 patients and negative in 11 patients. In the other 5 patients, data on ANCA were not available. Relapse rates, overall survival rates, and renal survival rates were similar in the 2 groups (relapse rate 14% in the negative conversion

Table 2. Comparison of patients with and those without reappearance of MPO-ANCA*

	With MPO-ANCA reappearance (n = 73)	Without MPO-ANCA reappearance (n = 108)
Variables at baseline		
Male/female, no.	30/43	39/69
Age, median (IQR) years	71 (62–76)	74 (65–78)
EGPA/GPA/MPA/unclassifiable, no.	8/9/51/5	7/12/67/22
BVAS score, median (IQR)	14 (12–21)	16 (12–20)
Renal involvement, no. (%)	59 (81)	82 (76)
Interstitial lung disease, no. (%)	37 (51)	47 (44)
Serum creatinine, median (IQR) mg/dl	1.1 (0.7–2.2)	1.1 (0.7–3.6)
C-reactive protein, median (IQR) mg/dl	4.7 (1.0–10.9)	7.6 (2.2–12.4)
Initial glucocorticoid, median (IQR) mg/day†	40 (30–50)	40 (30–50)
Glucocorticoid pulse therapy, no. (%)	32 (44)	48 (44)
CYC, no. (%)‡	27 (37)	36 (33)
Variables at the time of negative conversion of MPO-ANCA		
Serum creatinine, median (IQR) mg/dl	1.0 (0.7–1.5)	1.0 (0.7–1.9)
C-reactive protein, median (IQR) mg/dl	0.09 (0.03–0.32)	0.08 (0.02–0.28)
Glucocorticoid, median (IQR) mg/day†	12.5 (10–15)§	15 (11–18)
Concomitant immunosuppressants, no. (%)	37 (51)	53 (49)
Concomitant immunosuppressants (CYC/RTX/AZA/MTX/others), no.	27/1/5/0/4	35/0/13/1/4

* MPO-ANCA = myeloperoxidase–antineutrophil cytoplasmic antibody; IQR = interquartile range; EGPA = eosinophilic granulomatosis with polyangiitis; GPA = granulomatosis with polyangiitis; MPA = microscopic polyangiitis; BVAS = Birmingham Vasculitis Activity Score; CYC = cyclophosphamide; RTX = rituximab; AZA = azathioprine; MTX = methotrexate.
† Prednisolone equivalent.
‡ During the initial 3 weeks of treatment.
§ $P < 0.015$ versus without MPO-ANCA reappearance group.

group versus 21% in the non–negative conversion group [P = 0.19]; overall survival rate 7% versus 4% [P = 0.57]; and renal survival rate 11% versus 8% [P = 0.65], respectively). The median number of days to the conversion (positive to negative) of MPO-ANCA was similar between patients with and those without relapse (114 days [IQR 102–129 days] versus 114 days [IQR 98–141 days]; P = 0.75).

Comparison of patients with and those without reappearance of MPO-ANCA. Next, we investigated the association between reappearance of MPO-ANCA and clinical features (Table 2). Of 195 patients in the negative conversion group, 14 patients were excluded due to insufficient follow-up data (Figure 1). After negative conversion of MPO-ANCA, 73 of 181 patients (40%) experienced reappearance of MPO-ANCA by month 24. Patient demographics, disease severity, and organ involvement at baseline and types of induction treatment did not differ in the reappearance and nonreappearance groups. Median levels of serum creatinine and C-reactive protein at the time of negative conversion were similar. However, the median daily prednisolone dosage at the time of negative conversion was lower in the reappearance group (12.5 mg/day [IQR 10–15] versus 15 mg/day [IQR 11–18]; P = 0.015). Of all 43 patients with relapse, 19 patients experienced reappearance of MPO-ANCA at a mean of 34 days before the relapse: the glucocorticoid doses from 3 to 12 months were smaller in patients with reappearance compared to those without reappearance (Figure 1 and Supplementary Table 1, available on the *Arthritis & Rheumatology* web site at http://onlinelibrary.wiley.com/doi/10.1002/art.40538/abstract). Of 181 patients in the negative conversion group with sufficient follow-up data, 25 patients (14%) experienced relapse.

In patients with renal involvement (n = 141), 17 of 21 patients with relapse and 42 of 120 patients without relapse experienced the reappearance of MPO-ANCA (81% versus 35%; P = 0.0002). In patients without renal involvement (n = 40), patients with relapse experienced the reappearance of MPO-ANCA more frequently than those without relapse, but the difference was not significant (2 of 4 [50%] versus 12 of 36 [33%]; P = 0.6). We implemented a nested case–control analysis as described in Patients and Methods. As controls, 75 age-, sex-, observational period-, and timing of ANCA evaluation–matched patients were selected from those who had not experienced relapse in the negative conversion group. Characteristics of the patients with and those without relapse are shown in Table 3. Although AAV types, disease activity, laboratory data, organ involvement, and treatment were similar in the 2 groups, reappearance of MPO-ANCA was observed more frequently in patients with relapse than those without (76% versus 12%; P < 0.0001), and the odds ratio (OR) was 23.2

Table 3. Characteristics of the patients who experienced relapse and the controls who did not experience relapse from the negative conversion group*

	Cases (n = 25)	Controls (n = 75)
Variables at baseline		
Male/female, no.	12/13	36/39
Age, median (IQR) years	72 (67–79)	73 (66–77)
EGPA/GPA/MPA/unclassifiable, no.	2/4/17/2	5/7/52/11
BVAS score, median (IQR)	14 (13–23)	15 (12–21)
Renal involvement, no. (%)	21 (84)	58 (77)
Interstitial lung disease, no. (%)	14 (56)	36 (48)
Serum creatinine, median (IQR) mg/dl	1.0 (0.7–1.7)	1.3 (0.7–3.1)
C-reactive protein, median (IQR) mg/dl	7.5 (3.7–11.9)	7.6 (2.1–12.3)
Initial glucocorticoid, median (IQR) mg/day†	40 (30–50)	35 (30–50)
Glucocorticoid pulse therapy, no. (%)	7 (28)	31 (41)
CYC, no. (%)‡	10 (40)	21 (28)
Variables at the time of negative conversion of MPO-ANCA		
Serum creatinine, median (IQR) mg/dl	1.0 (0.7–1.5)	1.1 (0.8–1.6)
C-reactive protein, median (IQR) mg/dl	0.1 (0.03–0.35)	0.1 (0.03–0.26)
Glucocorticoid, median (IQR) mg/day†	12.5 (10–16)	15 (11–17.5)
Concomitant immunosuppressants (CYC/AZA/others), no.	12/2/2	23/8/5
Reappearance of MPO-ANCA, no. (%)	19 (76)§	9 (12)
Observational period, median (IQR) days	374 (260–539)	395 (365–558)

* IQR = interquartile range; EGPA = eosinophilic granulomatosis with polyangiitis; GPA = granulomatosis with polyangiitis; MPA = microscopic polyangiitis; BVAS = Birmingham Vasculitis Activity Score; CYC = cyclophosphamide; MPO-ANCA = myeloperoxidase–antineutrophil cytoplasmic antibody; AZA = azathioprine; MTX = methotrexate.
† Prednisolone equivalent.
‡ During the initial 3 weeks of treatment.
§ P < 0.0001 versus controls.

(95% confidence interval [95% CI] 7.3–73.5). The median duration from negative to positive conversion was shorter in patients with relapse compared to those without relapse (238 days [IQR 105–378 days] versus 363 days [IQR 270–479 days]; $P = 0.036$). After adjustment for potential confounders (age, sex, AAV type, and BVAS score) using multivariable analysis, the reappearance of MPO-ANCA was still the superior statistically significant predictor for relapse (OR 26.2 [95% CI 8.2–101], $P < 0.0001$).

Relapse among the patients with reappearance of MPO-ANCA. Although patients with reappearance of MPO-ANCA were more likely to experience relapse, some patients with reappearance of MPO-ANCA did not experience relapse. To elucidate the factor associated with relapse in patients with reappearance of MPO-ANCA, characteristics of patients with relapse (n = 19) and without relapse (n = 54) among the patients with reappearance of MPO-ANCA (see Supplementary Table 2, available on the *Arthritis & Rheumatology* web site at http://onlinelibrary.wiley.com/doi/10.1002/art.40538/abstract) were compared. Demographics and clinical characteristics, including organ involvement, laboratory data, and types of treatments, were comparable. Laboratory data and treatment at negative conversion of MPO-ANCA also did not differ significantly between the 2 groups. The survival rate tended to be lower in patients with relapse compared to those without, but the difference was not statistically significant (11% in patients with relapse versus 2% in those without; $P = 0.16$).

DISCUSSION

In the present study, MPO-ANCA negative conversion occurred in 72% of patients with MPO-AAV after remission induction therapy within 6 months. After negative conversion of MPO-ANCA, reappearance occurred in 40% of patients and was associated with a subsequent or concomitant relapse. The reappearance of MPO-ANCA may be a promising marker for relapse.

The proportion of ANCA-negative conversion has been investigated in several studies, which were included in the previous meta-analysis (7). In the studies using immunofluorescence for the evaluation of ANCA, the proportion of conversion from positive to negative after induction treatment varied from 38% to 100% (17–20). In the studies using ELISA for ANCA detection, 64–79% of PR3-ANCA–positive patients and 74–80% of MPO-ANCA–positive patients achieved ANCA negativity (8,9,21,22). Therefore, methods for ANCA detection may affect the dispersion of the proportions of negative conversion. An ELISA was used for detection of ANCA in our study, so our negative conversion rate was consistent with these previous results.

Negative conversion of MPO-ANCA may be related to disease classification. This is the first study to explore the factors related to ANCA seroconversion. In the present study, all EGPA patients experienced negative conversion of MPO-ANCA. Renal involvement was also significantly related to negative conversion, but was insignificant when EGPA patients were excluded. This is also the first study to evaluate ANCA seroconversion in patients with EGPA (21,23).

Elevation of ANCA levels has been reported to predict relapse, but the definition of elevation ranges widely from a 130% to a 400% increase, and the interval between ANCA measurements also varies (7) anywhere from 1 to 6 months. To address the variability, Kemna et al determined the optimal cutoff value of the slope of ANCA transition (24), but it requires several calculations. On the other hand, several studies have evaluated the association of ANCA conversion from negative to positive with relapse, and cytoplasmic or PR3-ANCA is generally reported to accompany or closely precede relapse (19,21,22,25). Two previous studies showed that MPO-ANCA conversion from negative to positive was significantly associated with relapse (8,9). The results were consistent with those of the present study, but our study also had key strengths, i.e., the homogeneous patient population (MPO-AAV just after induction treatment), the unified interval of time between ANCA measurements, and the matched observational period. Kemna et al also suggested that ANCA rise was more useful for prediction of relapse in patients with nonpersistently positive ANCA compared to those with persistently positive ANCA (24). The ANCA reappearance seemed to be more useful for prediction of the subsequent relapse in clinical settings than the ANCA rise. One of the limitations of their study was the heterogeneity, in that they included patients during remission after a relapse, with both MPO- and PR3-ANCA.

We confirmed that the ANCA reappearance was a useful biomarker for relapse in patients with renal involvement. Previous studies showed that monitoring ANCA was useful for predicting relapse in patients with renal vasculitis (9,24,26). Regarding other related factors, Yamaguchi et al reported that lung involvement was significantly associated with relapse in renal AAV (adjusted hazard ratio 2.29 [95% CI 1.13–4.65], $P = 0.022$) in addition to a rise in ANCA, in a study using multivariate analysis (9). Therefore, a rise in ANCA could predict relapse in patients with renal involvement. In this study, only 4 patients without renal involvement experienced relapse,

and a larger study is necessary to address the association of ANCA reappearance with relapse in nonrenal AAV patients.

The present study has several limitations. First, this was a subanalysis of observational studies, although data were collected prospectively. Second, different assay kits for ANCA were used in the participating institutions, and the rise in titer could not be evaluated. Because the concordances of MPO-ANCA positivity among commercial kits using ELISA, chemiluminescent immunoassay, and FEIA were high according to a previous study (27), we deemed it possible to assess the ANCA reappearance in our patients with different assay kits. To the best of our knowledge, this is the largest study evaluating the association between ANCA transition and relapse and the first study in which the association between ANCA status and relapse was validated by case–control analysis. Moreover, the homogeneity of enrolled patients (remitted MPO-AAV) was a strength of our study.

In conclusion, negative conversion of MPO-ANCA after remission induction therapy was not associated with subsequent relapse and survival, but reappearance of MPO-ANCA after the negative conversion can be a useful biomarker for predicting relapse in patients with MPO-AAV in remission. This suggests that routine MPO-ANCA monitoring should be implemented in this patient population.

ACKNOWLEDGMENTS

The authors thank Keiko Hongo, Tomomi Maruyama, Eri Katsuyama, Takayuki Katsuyama, Mariko Narazaki, Noriko Toyota-Tatebe, and Kouichi Sugiyama for their significant assistance in data management.

AUTHOR CONTRIBUTIONS

All authors were involved in drafting the article or revising it critically for important intellectual content, and all authors approved the final version to be submitted for publication. Dr. Sada had full access to all of the data in the study and takes responsibility for the integrity of the data and the accuracy of the data analysis.

Study conception and design. Watanabe, Sada, Matsumoto, Harigai.

Acquisition of data. Watanabe, Sada, Matsumoto, Harigai, Amano, Dobashi, Fujimoto, Usui, Yamagata, Atsumi, Banno, Sugihara, Arimura, Matsuo, Makino.

Analysis and interpretation of data. Watanabe, Sada, Harigai.

REFERENCES

1. Davies DJ, Moran JE, Niall JF, Ryan GB. Segmental necrotising glomerulonephritis with antineutrophil antibody: possible arbovirus aetiology? Br Med J (Clin Res Ed) 1982;285:606.
2. Damoiseaux J, Cohen Tervaert JW. Autoantibodies in vasculitis. In: Ball GV, Fessler BJ, Bridges SL, editors. Oxford textbook of vasculitis. Oxford: Oxford University Press; 2014. p. 61–9.
3. Watts R, Lane S, Hanslik T, Hauser T, Hellmich B, Koldingsnes W, et al. Development and validation of a consensus methodology for the classification of the ANCA-associated vasculitides and polyarteritis nodosa for epidemiological studies. Ann Rheum Dis 2007;66:222–7.
4. Sada KE, Yamamura M, Harigai M, Fujii T, Arimura Y, Makino H. Issues associated with the Ministry of Health, Labour and Welfare diagnostic criteria for antineutrophil cytoplasmic antibody-associated vasculitides: reclassification of patients in the prospective cohort study of remission induction therapy in Japanese patients with ANCA-associated vasculitides according to the MHLW criteria. Mod Rheumatol 2015;25:657–9.
5. Sada KE, Yamamura M, Harigai M, Fujii T, Dobashi H, Takasaki Y, et al. Classification and characteristics of Japanese patients with antineutrophil cytoplasmic antibody-associated vasculitis in a nationwide, prospective, inception cohort study. Arthritis Res Ther 2014;16:R101.
6. Specks U, Merkel PA, Seo P, Spiera R, Langford CA, Hoffman GS, et al. Efficacy of remission-induction regimens for ANCA-associated vasculitis. N Engl J Med 2013;369:417–27.
7. Tomasson G, Grayson PC, Mahr AD, Lavalley M, Merkel PA. Value of ANCA measurements during remission to predict a relapse of ANCA-associated vasculitis: a meta-analysis. Rheumatology (Oxford) 2012;51:100–9.
8. Terrier B, Saadoun D, Sène D, Ghillani P, Amoura Z, Deray G, et al. Antimyeloperoxidase antibodies are a useful marker of disease activity in antineutrophil cytoplasmic antibody-associated vasculitides. Ann Rheum Dis 2009;68:1564–71.
9. Yamaguchi M, Ando M, Kato S, Katsuno T, Kato N, Kosugi T, et al. Increase of antimyeloperoxidase antineutrophil cytoplasmic antibody (ANCA) in patients with renal ANCA-associated vasculitis: association with risk to relapse. J Rheumatol 2015;42:1853–60.
10. Hellmich B, Flossmann O, Gross WL, Bacon P, Cohen-Tervaert JW, Guillevin L, et al. EULAR recommendations for conducting clinical studies and/or clinical trials in systemic vasculitis: focus on anti-neutrophil cytoplasm antibody-associated vasculitis. Ann Rheum Dis 2007;66:605–17.
11. Sada KE, Harigai M, Amano K, Atsumi T, Fujimoto S, Yuzawa Y, et al. Comparison of severity classification in Japanese patients with antineutrophil cytoplasmic antibody-associated vasculitis in a nationwide, prospective, inception cohort study. Mod Rheumatol 2016;26:730–7.
12. Flossmann O, Bacon P, de Groot K, Jayne D, Rasmussen N, Seo P, et al. Development of comprehensive disease assessment in systemic vasculitis. Ann Rheum Dis 2007;66:283–92.
13. Jayne D, Rasmussen N, Andrassy K, Bacon P, Tervaert JW, Dadoniene J, et al. A randomized trial of maintenance therapy for vasculitis associated with antineutrophil cytoplasmic autoantibodies. N Engl J Med 2003;349:36–44.
14. De Groot K, Harper L, Jayne DR, Flores Suarez LF, Gregorini G, Gross WL, et al. Pulse versus daily oral cyclophosphamide for induction of remission in antineutrophil cytoplasmic antibody-associated vasculitis: a randomized trial. Ann Intern Med 2009;150:670–80.
15. Oh YJ, Ahn SS, Park ES, Jung SM, Song JJ, Park YB, et al. Chest and renal involvements, Birmingham Vascular Activity Score more than 13.5 and five factor score (1996) more than 1 at diagnosis are significant predictors of relapse of microscopic polyangiitis. Clin Exp Rheumatol 2017;Suppl 103:47–54.
16. Kitagawa K, Furuichi K, Sagara A, Shinozaki Y, Kitajima S, Toyama T, et al. Risk factors associated with relapse or infectious complications in Japanese patients with microscopic polyangiitis. Clin Exp Nephrol 2016;20:703–11.
17. Tervaert JW, van der Woude FJ, Fauci AS, Ambrus JL, Velosa J, Keane WF, et al. Association between active Wegener's granulomatosis and anticytoplasmic antibodies. Arch Intern Med 1989;149:2461–5.

18. Nowack R, Grab I, Flores-Suarez LF, Schnulle P, Yard B, van der Woude FJ. ANCA titres, even of IgG subclasses, and soluble CD14 fail to predict relapses in patients with ANCA-associated vasculitis. Nephrol Dial Transplant 2001;16:1631–7.
19. Gaskin G, Savage CO, Ryan JJ, Jones S, Rees AJ, Lockwood CM, et al. Anti-neutrophil cytoplasmic antibodies and disease activity during long-term follow-up of 70 patients with systemic vasculitis. Nephrol Dial Transplant 1991;6:689–94.
20. Kerr GS, Fleisher TA, Hallahan CW, Leavitt RY, Fauci AS, Hoffman GS. Limited prognostic value of changes in antineutrophil cytoplasmic antibody titer in patients with Wegener's granulomatosis. Arthritis Rheum 1993;36:365–71.
21. Girard T, Mahr A, Noël LH, Cordier JF, Lesavre P, André MH, et al. Are antineutrophil cytoplasmic antibodies a marker predictive of relapse in Wegener's granulomatosis? A prospective study. Rheumatology (Oxford) 2001;40:147–51.
22. Sanders JS, Huitma MG, Kallenberg CG, Stegeman CA. Prediction of relapses in PR3-ANCA-associated vasculitis by assessing responses of ANCA titres to treatment. Rheumatology (Oxford) 2006;45:724–9.
23. Jayne DR, Gaskin G, Pusey CD, Lockwood CM. ANCA and predicting relapse in systemic vasculitis. QJM 1995;88:127–33.
24. Kemna MJ, Damoiseaux J, Austen J, Winkens B, Peters J, van Paassen P, et al. ANCA as a predictor of relapse: useful in patients with renal involvement but not in patients with nonrenal disease. J Am Soc Nephrol 2015;26:537–42.
25. Pettersson E, Heigl Z. Antineutrophil cytoplasmic antibody (cANCA and pANCA) titers in relation to disease activity in patients with necrotizing vasculitis: a longitudinal study. Clin Nephrol 1992;37:219–28.
26. Koh JH, Kemna MJ, Cohen Tervaert JW, Kim WU. Can an increase in antineutrophil cytoplasmic autoantibody titer predict relapses in antineutrophil cytoplasmic antibody–associated vasculitis? [editorial]. Arthritis Rheumatol 2016;68:1571–3.
27. Damoiseaux J, Csernok E, Rasmussen N, Moosig F, van Paassen P, Baslund B, et al. Detection of antineutrophil cytoplasmic antibodies (ANCAs): a multicentre European Vasculitis Study Group (EUVAS) evaluation of the value of indirect immunofluorescence (IIF) versus antigen-specific immunoassays. Ann Rheum Dis 2017; 76:647–53.

APPENDIX A: JAPAN RESEARCH COMMITTEE OF THE MINISTRY OF HEALTH, LABOUR, AND WELFARE FOR INTRACTABLE VASCULITIS, AND RESEARCH COMMITTEE OF INTRACTABLE RENAL DISEASE OF THE MINISTRY OF HEALTH, LABOUR, AND WELFARE OF JAPAN

In addition to the authors, the following investigators and institutions participated in this study: Department of Human Resource Development of Dialysis Therapy for Kidney Disease, Okayama University Graduate School of Medicine, Dentistry and Pharmaceutical Sciences (Hitoshi Sugiyama); Department of Internal Medicine and Rheumatology, Juntendo University School of Medicine (Yoshinari Takasaki); Faculty of Health Sciences, Hokkaido University (Akihiro Ishizu); Department of the Control for Rheumatic Diseases, Graduate School of Medicine, Kyoto University (Takao Fujii); Department of Pathology, Keio University School of Medicine (Yasunori Okada); Department of Respiratory Medicine, Toho University Omori Medical Center (Sakae Homma); Department of Nephrology, Internal Medicine, Nagoya University Graduate School of Medicine (Naotake Tsuboi); Department of Clinical Pathology and Immunology, Kobe University Graduate School of Medicine (Shunichi Kumagai); Department of Nephrology and Dialysis, Kitano Hospital, Tazuke Kofukai Medical Research Institute (Eri Muso); Department of Rheumatology, Shimane University Faculty of Medicine (Yohko Murakawa); Division of Rheumatology, Department of Medical Oncology and Immunology, Nagoya City University Graduate School of Medical Science (Shogo Banno); Department of Hematology, Clinical Immunology and Infectious Diseases, Ehime University Graduate School of Medicine (Hitoshi Hasegawa); Division of Nephrology, Department of Internal Medicine, Jichi Medical University (Wako Yumura); Department of Cardiovascular Medicine, Kyoto Prefectural University School of Medicine (Hiroaki Matsubara); Division of Nephrology, Tokyo Medical University Hachioji Medical Center (Masaharu Yoshida); Department of Dermatology, Kitasato University School of Medicine (Kensei Katsuoka); Division of Immunology and Rheumatology, Department of Internal Medicine 3, Hamamatsu University School of Medicine (Noriyoshi Ogawa); Department of Hematology, Nephrology, and Rheumatology, Akita University Graduate School of Medicine (Atsushi Komatsuda); Department of Rheumatology, Niigata Rheumatic Center (Satoshi Ito); Department of Immunology and Rheumatology, Division of Advanced Preventive Medical Sciences, Nagasaki University Graduate School of Biomedical Sciences (Atsushi Kawakami); Department of Nephrology, Iwate Prefectural Central Hospital (Izaya Nakaya); Division of Nephrology and Rheumatology, Department of Internal Medicine, Fukuoka University School of Medicine (Takao Saito); Shimane University, Faculty of Medicine, Division of Nephrology (Takafumi Ito); Department of Hemodialysis and Apheresis, Yokohama City University Medical Center (Nobuhito Hirawa); Center for Rheumatology, Okayama Saiseikai General Hospital (Masahiro Yamamura); Department of Medical Technology, School of Health Sciences, Faculty of Medicine, Niigata University (Masaaki Nakano); Department of Medicine, Kidney Center, Tokyo Women's Medical University (Kosaku Nitta); Division of Nephrology and Hypertension, Kashiwa Hospital, Jikei University (Makoto Ogura); Department of Respiratory Medicine, Allergy and Clinical Immunology, Nagoya City University Graduate School of Medical Sciences (Taio Naniwa); Division of Rheumatology and Allergology, Department of Internal Medicine, St. Marianna University School of Medicine (Shoichi Ozaki); Department of Nephrology and Endocrinology, Graduate School of Medicine, The University of Tokyo (Junichi Hirahashi); Division of Kidney and Hypertension, Department of Internal Medicine, Jikei University School of Medicine (Tatsuo Hosoya); Department of Nephrology and Laboratory Medicine, Faculty of Medicine, Institute of Medical, Pharmaceutical and Health Sciences, Kanazawa University (Takashi Wada); Division of Nephrology, Department of Internal Medicine, Juntendo University Faculty of Medicine (Satoshi Horikoshi); Institute of Rheumatology, Tokyo Women's Medical University (Yasushi Kawaguchi); Division of Clinical Immunology, Graduate School of Comprehensive Human Sciences, University of Tsukuba (Taichi Hayashi); Department of Nephrology, Hypertension, Diabetology, Endocrinology and Metabolic, Fukushima Medical University (Tsuyoshi Watanabe); Department of Nephrology, Japanese Red Cross Nagoya Daini Hospital (Daijo Inaguma); Department of Integrated Therapy for Chronic Kidney Disease, Kyushu University (Kazuhiko Tsuruya); Niigata Prefectural Shibata Hospital (Noriyuki Homma); Division of Rheumatology, Department of Internal Medicine, Keio University School of Medicine (Tsutomu Takeuchi); Division of Cardiology, Nephrology, Pulmonology and Neurology, Department of Internal Medicine, Asahikawa Medical University (Naoki Nakagawa); Kurobe City Hospital (Shinichi Takeda); National Fukuoka Higashi Medical Center (Ritsuko Katabuchi); Division of Nephrology, Department of Medicine, Faculty of Medical Sciences, University of Fukui (Masayuki Iwano); Tokyo Medical University Ibaraki Medical Center (Masaki Kobayashi).

ARTHRITIS & RHEUMATOLOGY
Vol. 70, No. 10, October 2018, pp 1634–1643
DOI 10.1002/art.40547

Lysophosphatidic Acid Receptor 1 Antagonist SAR100842 for Patients With Diffuse Cutaneous Systemic Sclerosis

A Double-Blind, Randomized, Eight-Week Placebo-Controlled Study Followed by a Sixteen-Week Open-Label Extension Study

Yannick Allanore,[1] Oliver Distler,[2] Alexandre Jagerschmidt,[3] Stephane Illiano,[3] Laetitia Ledein,[3] Eric Boitier,[4] Inoncent Agueusop,[5] Christopher P. Denton,[6] and Dinesh Khanna[7]

Objective. **Preclinical studies suggest a role for lysophosphatidic acid (LPA) in the pathogenesis of systemic sclerosis (SSc). We undertook this study to assess SAR100842, a potent selective oral antagonist of the LPA_1 receptor, for safety, biomarkers, and clinical efficacy in patients with diffuse cutaneous SSc (dcSSc).**

Methods. **An 8-week double-blind, randomized, placebo-controlled study followed by a 16-week open-label extension with SAR100842 was performed in patients with early dcSSc who had a baseline modified Rodnan skin thickness score (MRSS) of at least 15. The primary end point was safety during the double-blind phase of the trial. Exploratory end points included the identification of an LPA-induced gene signature in patients' skin.**

Results. **Seventeen of 32 patients were randomly assigned to receive placebo and 15 to receive SAR100842; 30 patients participated in the open-label extension study. The most frequent adverse events reported for SAR 100842 during the blinded phase were headache, diarrhea, nausea, and falling, and the safety profile was acceptable during the open-label extension. At week 8, the reduction in MRSS was numerically greater in the SAR100842 group than in the placebo group (mean ± SD change −3.57 ± 4.18 versus −2.76 ± 4.85; treatment effect −1.2 [95% confidence interval −4.37, 2.02]; P = 0.46). A greater reduction of LPA-related genes was observed in skin samples from the SAR100842 group at week 8, indicating LPA_1 target engagement.**

Conclusion. **SAR100842, a selective orally available LPA_1 receptor antagonist, was well tolerated in patients with dcSSc. The MRSS improved during the study although the difference was not significant, and**

ClinicalTrials.gov identifier: NCT01651143.
Supported by Sanofi.

[1]Yannick Allanore, MD, PhD: Rheumatology A Department, Cochin Hospital, Paris Descartes University, Paris, France; [2]Oliver Distler, MD, PhD: University Hospital Zurich, Zurich, Switzerland; [3]Alexandre Jagerschmidt, PhD, Stephane Illiano, PhD, Laetitia Ledein, PhD: Sanofi R&D, Chilly-Mazarin, France; [4]Eric Boitier, PhD: Sanofi R&D, Alfortville, France; [5]Inoncent Agueusop, PhD: Sanofi R&D, Frankfurt am Main, Germany; [6]Christopher P. Denton, MD, PhD: Royal Free Hospital, London, UK; [7]Dinesh Khanna, MD, MSc: University of Michigan, Ann Arbor.

Drs. Allanore and Distler contributed equally to this work. Drs. Denton and Khanna contributed equally to this work.

Dr. Allanore has received consulting fees from Actelion, Bayer, Biogen, Genentech-Roche, Galapagos, Medac, Pfizer, Sanofi, Servier, and UCB (less than $10,000 each) and research support from Bristol-Myers Squibb, Genentech-Roche, Inventiva, Pfizer, and Sanofi. Dr. Distler has received consulting fees and/or speaking fees from AbbVie, iQone Healthcare, 4D Science, Actelion, Active Biotec, Bayer, Biogen Idec, Bristol-Myers Squibb, Boehringer Ingelheim, ChemomAb, EpiPharm, EspeRare Foundation, Genentech-Roche, GlaxoSmithKline, Inventiva, Eli Lilly and Company, Medac, Mepha, MedImmune, Mitsubishi Tanabe Pharma, Pharmacyclics, Pfizer, Sanofi, Serodapharm, and Sinoxa (less than $10,000 each), research support from Actelion, Bayer, Boehringer Ingelheim, Pfizer, and Sanofi, and holds a patent licensed for mir-29 for the treatment of systemic sclerosis. Drs. Jagerschmidt, Illiano, Ledein, Boitier, and Agueusop own stock or stock options in Sanofi. Dr. Denton has received consulting fees and/or speaking fees from Actelion, Bayer, GlaxoSmithKline, CSL Behring, Merck-Serono, Genentech-Roche, Inventiva, and Sanofi-Aventis (less than $10,000 each). Dr. Khanna has received consulting fees from Actelion, Bristol-Myers Squibb, CSL Behring, Inventiva, EMD Merck-Serono, Sanofi-Aventis, GlaxoSmithKline, Corbus, Cytori, and UCB (less than $10,000 each), Bayer, Boehringer Ingelheim, Corbus, and Genentech-Roche (more than $10,000 each), and research support from Bayer, Bristol-Myers Squibb, and Pfizer, and owns stock or stock options in Eicos Sciences, Inc. (now CiViBioPharma, Inc.).

Address correspondence to Yannick Allanore, MD, PhD, Service de Rhumatologie A, Hôpital Cochin, Université Paris Descartes, 27 Rue du Faubourg St. Jacques, 75014 Paris, France (e-mail: yannick.allanore@aphp.fr); or to Dinesh Khanna, MD, MSc, University of Michigan Scleroderma Program, Division of Rheumatology/Department of Internal Medicine, Suite 7C27, 300 North Ingalls Street, SPC 5422, Ann Arbor, MI 48109 (e-mail: khannad@med.umich.edu).

Submitted for publication July 6, 2017; accepted in revised form April 24, 2018.

additional gene signature analysis suggested target engagement. These results need to be confirmed in a larger controlled trial.

Systemic sclerosis (SSc) is characterized by fibrosis of the skin and internal organs, prominent alterations of the microvasculature, and frequent abnormalities of cellular and humoral immunity (1). SSc is an orphan disease with high morbidity, which strongly impairs the quality of life, and it has a high case-specific mortality (2). The high burden of severe skin and internal organ involvement in the early stages of diffuse cutaneous SSc (dcSSc) has been highlighted by many cohort studies. Safe and effective treatments for skin and other manifestations of dcSSc are lacking (3).

The pathogenesis of SSc is complex, and at present there is no unifying theory that may explain all its aspects. There is consensus that early vascular events associated with autoimmunity and inflammation lead to fibroblast activation and differentiation, promoting subsequent fibrosis. A broad range of biologic processes interact in SSc, and these include involvement of key profibrotic cytokines and growth factors, an imbalance in Th1/Th2/Th17/Treg cell systems promoting inflammation and fibrosis, and activation of B cells promoting production of autoantibodies (1).

Lysophosphatidic acid (LPA) is a lipid mediator that signals through specific G protein–coupled receptors, designated LPA_1 through LPA_6. It is generated at sites of inflammation or cell injury by the action of lysophospholipase D, also known as autotaxin, on lysophosphatidylcholine and other lysophospholipids (4). LPA exerts various physiologic effects on the receptors of parenchymal cells with some tissue specificities with regard to the various receptors (5–7). LPA mediates a variety of cell activities, including mitogenesis, cell differentiation, cell survival, cytoskeletal reorganization, cell migration, and extracellular matrix production. Recent studies of circulating markers, in vitro cell activation, or animal models have suggested that LPA is involved, and plays an important role, in the pathogenesis of SSc. The role of LPA has also been demonstrated in several animal models of organ fibrosis independently of SSc (8–11).

SAR100842 is a potent selective LPA_1 receptor antagonist (Sanofi R&D). In vivo, SAR100842 reversed dermal thickening and significantly inhibited myofibroblast differentiation and reduced collagen content in a mouse model of skin fibrosis. Similar antifibrotic properties were observed using the *Tsk1* mouse model (Illiano S, et al: unpublished observations). Mechanistic investigations showed that the antifibrotic effects of LPA_1 blockade could be mediated partly via inhibition of the Wnt signaling pathway. Taking into account the promise of LPA_1 receptor blockade in preclinical models of fibrosis and the unmet need of patients with early dcSSc, we performed a randomized proof of biologic activity study assessing the effects of SAR100842 in patients with early dcSSc.

PATIENTS AND METHODS

Study design. This was a double-blind, randomized, placebo-controlled, 8-week phase IIa study followed by an open-label extension study for 16 weeks (see Supplementary Figure 1, available on the *Arthritis & Rheumatology* web site at http://onlinelibrary.wiley.com/doi/10.1002/art.40547/abstract). The objective was to investigate the effects of orally administered SAR100842 in patients with dcSSc, characterizing safety as well as plasma pharmacokinetics and pharmacodynamics, with a focus on clinical efficacy and on SSc-related biomarkers. In the double-blind phase of the study, SAR100842 at 300 mg or matching placebo was administered orally twice a day (in the treatment arm, patients received 100 mg plus 200 mg tablets of SAR100842 twice daily for a total daily dose of 600 mg). Following a screening period of up to 14 days, eligible patients were randomized. Clinical and biologic parameters were assessed, and skin biopsy samples were obtained from a predefined area of the forearm at baseline and end of treatment (week 8).

Patients who had completed the 8-week treatment and who did not meet any discontinuation criteria (see Amended Clinical Trial Protocol 5, http://onlinelibrary.wiley.com/doi/10.1002/art.40547/abstract) were invited to participate in the open-label noncontrolled 16-week extension phase of the study with the same dosage of SAR100842 as in the initial part of the trial. Patients were evaluated at the end of the extension phase (week 24) for clinical and biologic assessments including 2 additional skin biopsies in those who consented.

The dose of 300 mg twice a day was selected for the study based on activity/efficacy data from in vitro pharmacology models and in vivo animal disease models as well as on the safety profile observed in healthy volunteers (Illiano S, et al: unpublished observations). The duration of 8 weeks was chosen based on expert opinion, which suggested that an 8-week treatment duration would be sufficient to demonstrate significant changes in SSc-related biomarkers. This design reduced the exposure of dcSSc patients to an experimental drug in this phase IIa study, while it provided the necessary data on safety and activity to support full development of the drug. A total of 12 active clinical sites located in Switzerland, France, the UK, Italy, and the US participated in this study.

Patients. Patients met the 1980 American College of Rheumatology (ACR) preliminary classification criteria for SSc (12), with diffuse cutaneous involvement according to the criteria of LeRoy et al (13), and had disease duration of less than 36 months since the onset of the first SSc manifestation other than Raynaud's phenomenon. Other key inclusion criteria were a baseline modified Rodnan skin thickness score (MRSS) $\geq$15 of 51 (14) together with an area of definite involvement of the mid-volar forearm allowing 4-mm skin biopsy samples.

Immunosuppressive therapies stable for 4 weeks prior to enrollment were permitted including prednisolone up to 10 mg/day, methotrexate up to 25 mg/week, azathioprine up to 100 mg/day, and mycophenolate mofetil up to 2 gm/day (for

exclusion criteria for medication dosages, see Amended Clinical Trial Protocol 5, http://onlinelibrary.wiley.com/doi/10.1002/art.40547/abstract). We excluded patients experiencing orthostatic hypotension (postural reduction of systolic blood pressure by >20 mm Hg or reduction of diastolic blood pressure by >10 mm Hg), moderate-to-severe postural dizziness, or presyncope or syncope within the last 6 months of screening. These exclusion criteria were related to the current knowledge of the study drug obtained in phase I studies.

Study end points. The primary end point was safety and tolerability during the 8-week treatment period. Secondary end points were change from baseline to week 8 in skin and blood biomarkers, changes from baseline to week 8 in the MRSS and Scleroderma Health Assessment Questionnaire (SHAQ) (15), safety and tolerability during the extension treatment period, and pharmacokinetics. Skin biopsy samples were used for RNA extraction, and some messenger RNA (mRNA) biomarkers were assessed using quantitative reverse transcription–polymerase chain reaction (qRT-PCR), including cartilage oligomeric matrix protein (COMP), thrombospondin 1 (TSP-1), plasminogen activator inhibitor 1, Wnt-2, and secreted Frizzled-related protein 4 (sFRP-4). Other skin biopsy samples were dedicated to immunohistochemistry. Labeling for α-smooth muscle actin (α-SMA) was performed on serial slides, and skin thickness (histology) was evaluated. LPA markers were selected based on literature data and internal confirmation using dermal fibroblasts from SSc patients treated with LPA. The choice of other markers (COMP, TSP-1, type I collagen, and α-SMA) was based on literature data selecting genes or proteins that may play a key role in the evolution of fibrosis in SSc patients (16,17).

To explore the effect of SAR100842 on the LPA pathway, we used the results of a parallel study performed using cultured dermal fibroblasts from patients with SSc. LPA gene expression response was defined in the cultured dermal fibroblasts study. This LPA response was used in combination with the expression profile in patient skin biopsy samples for identifying an LPA signature, according to a guided clustering algorithm. The goal of using this data integration approach was to ensure that the identified gene cluster with high LPA treatment response was also consistently expressed and correlated in skin biopsy samples. The identified fibroblast LPA signature was subsequently reduced to a single composite biomarker called the pathway activation index (PAI), computed as the coefficient of a robust regression on the expression matrix of the LPA signature at each treatment visit (median polish algorithm) (18). The PAI was then used as a surrogate biomarker for investigating SAR100842 treatment response. Exploratory end points were change from baseline to week 24 on the MRSS and SHAQ, and also the change in pain or pruritus from baseline to week 8 and week 24.

Statistical analysis. *Sample size determination.* No formal sample size calculation was performed for this proof of biologic activity study, and the sample size for the study was based on empirical considerations.

Safety analyses. The safety analyses were based on the safety population of all randomized patients who actually received at least 1 dose of the investigational medicinal product, and they were performed according to the treatment actually received in the core or extension phases of the study. The safety analyses were descriptive.

Efficacy analyses. The efficacy analyses were based on the modified intent-to-treat (ITT) population, which included all randomized patients who had actually received at least 1 dose of the investigational medicinal product and who had undergone at least 1 measurement after administration of the investigational medicinal product during the blinded period of the study (the double-blind phase). The modified ITT population for the open-label extension phase included all randomized patients who did actually receive at least 1 dose of the investigational medicinal product during the open-label extension phase and who had undergone at least 1 measurement after administration of the investigational medicinal product during the open-label extension phase.

An analysis of covariance (ANCOVA) was performed for the total MRSS and the Health Assessment Questionnaire disability index (HAQ DI) score (19) on the change from baseline to week 8 in the modified ITT population, with treatment group as the main factor and the baseline MRSS and HAQ DI scores centered on their means in the modified ITT population as a continuous covariate. Student's *t*-test was used to determine the superiority of 300 mg SAR100842 twice a day over placebo at week 8, with a nominal 2-sided Type I error rate of 5%. The analysis of other SHAQ variables was purely descriptive. All other secondary end points were described by treatment and analyzed within an ANCOVA.

Biomarker analyses. The biomarker analyses were based on the population of all randomized and treated patients who received at least 4 weeks of study drug with at least a baseline and a postbaseline assessment. Prior to all statistical analyses, mRNA data were normalized. Each biomarker was analyzed using descriptive statistics. For each of the skin biomarkers related to the disease (i.e., COMP, TSP-1, and type I collagen mRNAs and α-SMA [16]), the change from baseline to week 8 measurement was analyzed using a rank ANCOVA, with treatment group as fixed effect and baseline value as covariate.

Target engagement. SSc fibroblasts were prepared from forearm biopsy samples following established outgrowth conditions and were cultured in Ham's F-12 medium with 10% heat-inactivated fetal calf serum, 100 units/ml penicillin, 100 μg/ml streptomycin, and 0.3 mg/ml L-glutamine. Dermal fibroblasts from 4 healthy volunteers and 10 SSc patients were seeded and treated with vehicle or LPA at 10 μ*M* for 24 hours. Supernatants were removed and cells were rinsed and stored, and total RNA was purified using an RNeasy Mini kit (Qiagen). The same methodology was used to extract RNA from skin biopsy samples from patients in Sanofi study no. ACT12339. Gene expression was measured by whole transcriptome profiling analysis using Affymetrix GeneChip Human Genome U133 Plus 2.0 arrays. From each array result, a probe cell intensity data file was computed, which represented an individual gene expression profile. Samples were clustered based on Euclidean distance and correlation for evaluating the similarity of the quality of each array to the quality of the other arrays. We performed principal components analysis on expression data as well as on quality control metrics of the raw data provided by the Affymetrix platform (R-package simpleaffy; https://rdrr.io/bioc/simpleaffy/).

The guided clustering algorithm (18) was used for the identification of a set of genes that had high LPA perturbation in the cell culture study and that were consistently expressed in the skin biopsy samples from patients with SSc. A logistic regression model was computed for each probe set separately, with the LPA treatment label as the outcome variable (LPA = 1, placebo = 0) and the probe set as the independent variable. Each model was adjusted by fibroblast type (normal/SSc). The coefficient of the probe set in the model was used as the LPA activation strength for weighting the probe sets. The obtained weights were

used in conjunction with the expression profile in skin biopsy samples at baseline to extract the LPA signature. The LPA signature was condensed into 1 surrogate marker called the PAI. Descriptive statistics of change in the LPA PAI from baseline to the end of the 8-week treatment period were computed by treatment arm. The difference between SAR100842 and placebo was investigated using the following equation:

$$\Delta PAI_{\text{main part}} = \beta_0 + \beta_1 \times \text{treatment} + \beta_2 \times PAI_{\text{scaled baseline}} + \xi$$

where β_0 is the mean effect, β_1 is the treatment effect, β_2 is the PAI value effect at baseline, and ξ represents residuals from the model. Targeted gene expression analysis of selected LPA-related and fibrosis genes was carried out in the same skin biopsy samples using qRT-PCR.

Ethics approval. The protocol and its amendments were submitted to independent ethics committees and/or institutional review boards for review and written approval. All patients provided written informed consent prior to the conduct of any study-related procedures, and the optional skin biopsy informed consent form was obtained from patients who agreed to the collection of skin biopsy samples. In addition, dermal fibroblasts were grown from skin biopsy samples obtained from another cohort of SSc patients fulfilling the ACR/European League Against Rheumatism 2013 classification criteria (20). The procedure was approved by the local ethics committee (University of Naples), and patients signed informed consent forms.

RESULTS

Baseline characteristics of the patients, flow of enrollment into the study, discontinuations, and compliance. Of 48 patients screened, 16 (33.3%) were determined to be ineligible. Thirty-two patients were randomized into the study; for a period of 8 weeks, 15 received 300 mg SAR100842 twice a day and 17 received placebo twice a day. Patients in each group had comparable demographic characteristics at baseline, consistent with the overall population of dcSSc patients (Table 1).

One patient receiving SAR100842 discontinued treatment on personal request but was included in the modified ITT analysis. Of the 32 patients initially randomized to the double-blind phase, 30 were enrolled into the open-label extension phase (16 initially treated with placebo and 14 initially treated with SAR100842). One patient in the placebo/SAR100842 group and 1 patient in the SAR100842/SAR100842 group requested to discontinue treatment due to adverse events (AEs). The mean overall compliance was comparably high between treatment groups (99.6% in the placebo group versus 98.5% in the SAR100842 group).

Table 1. Baseline characteristics of the patients*

	Placebo (n = 17)	SAR100842 (n = 15)	All (n = 32)
Age, mean ± SD years	50.6 ± 11.3	48.8 ± 10.3	49.8 ± 10.7
Female	12 (71)	9 (60)	21 (66)
Caucasian/white	13 (76)	13 (87)	26 (81)
Weight, mean ± SD kg	70.6 ± 16.8	75.1 ± 19.3	72.7 ± 17.9
Current smoker	3 (18)	2 (13)	5 (16)
Disease duration, mean ± SD months	19.6 ± 7.4	20.4 ± 8.9	20.0 ± 8.0
Raynaud's phenomenon	17 (100)	14 (93)	31 (97)
Digital ulcers (past or current)	6 (35)	4 (27)	10 (31)
Joint synovitis	5 (29)	4 (27)	9 (28)
Tendon friction rubs	6 (35)	7 (47)	13 (41)
Renal crisis	1 (6)	0	1 (3)
Dyspnea (significant)	7 (41)	2 (13)	9 (28)
Fibrosis on plain radiograph	3 (18)	1 (7)	4 (13)
ACA positive	1 (6)	0	1 (3)
Anti–Scl-70 positive	5 (29)	4 (27)	9 (28)
Anti–RNA polymerase III positive	4 (24)	8 (53)	12 (38)
MRSS			
Mean ± SD	24.8 ± 7.8	22.7 ± 8.2	23.8 ± 7.9
Median (range)	23 (15–38)	21 (15–44)	22 (15–44)
HAQ DI score			
Mean ± SD	1.27 ± 0.75	1.23 ± 0.77	1.25 ± 0.75
Median (range)	1.25 (0.0–2.5)	1.38 (0.0–2.4)	1.37 (0.0–2.5)
Previous immunosuppressive or steroid medications	14 (82)	10 (67)	24 (75)
Mycophenolate mofetil	5 (29)	7 (47)	12 (38)
Methotrexate	9 (53)	1 (7)	10 (31)
Systemic steroids	8 (47)	6 (40)	14 (44)
Topical steroids	1 (6)	1 (7)	2 (6)

* Except where indicated otherwise, values are the number (%). ACA = anticentromere antibody; MRSS = modified Rodnan skin thickness score; HAQ DI = Health Assessment Questionnaire disability index.

Good safety and tolerability of SAR100842. Overall, SAR100842 was well tolerated. AEs are described in Supplementary Table 1, http://onlinelibrary.wiley.com/doi/10.1002/art.40547/abstract. Eighty percent of patients in the SAR100842 group versus 71% of patients in the placebo group reported at least 1 treatment-emergent AE. However, most treatment-emergent AEs were mild to moderate in intensity. There was 1 treatment-emergent serious AE (SAE) in the SAR100842 group (syncope) in a patient with a medical history of syncope in childhood. In the open-label extension phase, 2 patients reported a treatment-emergent SAE, 1 in each group. Dyspnea was reported in 1 patient 6 days after switching from placebo to SAR100842, and this was considered to be related to the investigational medicinal product, while an infected digital ulcer in another patient was not considered to be drug-related. Two patients discontinued prematurely due to treatment-emergent AEs, 1 for moderate arthritis in the SAR100842/SAR100842 group and 1 for pruritus, skin discoloration, and facial swelling in the placebo/SAR100842 group. With regard to the laboratory safety assessments, no safety concern emerged from the various laboratory parameters (see Supplementary Table 2, http://onlinelibrary.wiley.com/doi/10.1002/art.40547/abstract).

Efficacy as determined by change in MRSS during the controlled and extension phases. A primary analysis was conducted in the modified ITT population on patients who were treated until week 8. There was a numerically greater decrease from baseline in the total MRSS in the SAR100842 group compared to the placebo group, although the difference did not reach statistical significance (mean ± SD change −3.57 ± 4.18 versus −2.76 ± 4.85; treatment effect −1.2 [95% confidence interval {95% CI} −4.37, 2.02]; $P = 0.46$) (median change −4.00 [interquartile range {IQR} −5, −1] versus −1.00 [IQR −5, 0], respectively) (Figure 1).

After 24 weeks of treatment, patients in the SAR 100842/SAR100842 group experienced a clinically meaningful decrease in total MRSS versus baseline (mean ± SD change −7.36 ± 4.24; median change −7.50), and a high percentage (78.6%) of patients improved by at least 5 points (the definition of responders). Patients initially receiving 8 weeks of placebo also demonstrated an improvement in MRSS after 24 weeks (mean ± SD change −7.31 ± 4.59; median change from baseline −7.00), with a responder rate of 69.2%.

Changes in quality of life during controlled and extension phases. There was no statistically significant difference between the SAR100842 and placebo groups in change in HAQ DI total score from baseline to week 8 (mean ± SD change 0.00 ± 0.33 in the placebo group versus −0.14 ± 0.30 in the SAR100842 group; treatment effect −0.1 [95% CI −0.38, 0.09]). However, it should be pointed out that the mean absolute difference from baseline observed in the SAR100842 group (−0.14) was clinically meaningful; indeed, a HAQ DI score improvement of ≥0.14 is considered to be the minimum clinically important difference in patients with SSc. In contrast to the improvement between baseline and week 8, the improvement seen in the mean HAQ DI total score was clinically meaningful from baseline to week 24 in both the placebo/SAR100842 group and the SAR100842/SAR100842 group (mean ± SD change −0.23 ± 0.30 versus −0.15 ± 0.33, respectively), and the percentages of patients whose HAQ DI total scores decreased by ≥ −0.14 were comparable in the 2 groups.

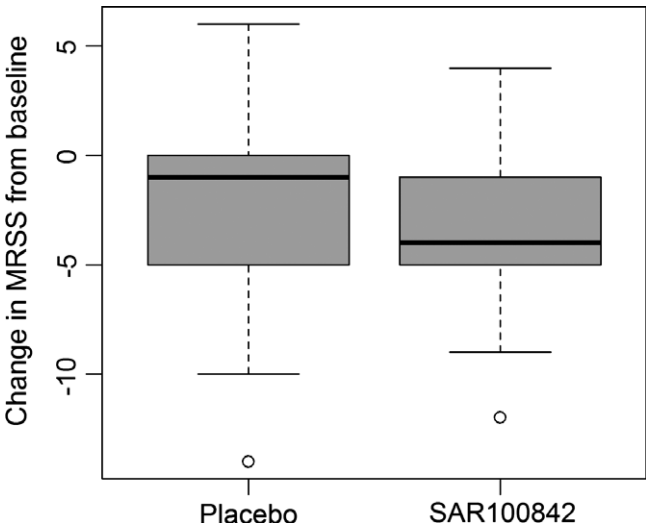

Figure 1. Change in modified Rodnan skin thickness score (MRSS) from baseline to week 8 in the modified intent-to-treat population. Data are presented as box plots, where the boxes represent the 25th to 75th percentiles, the lines within the boxes represent the median, and the lines outside the boxes represent the 10th and 90th percentiles. Circles indicate outliers.

Effects on pruritus and pain during controlled and extension phases. Based on the preclinical rationale, LPA receptor antagonists may be effective against pruritus. Interestingly, despite a low baseline value, there was numerical improvement in the SAR100842 group and worsening in the placebo group (mean ± SD change −0.37 ± 3.92 versus 0.25 ± 1.79) in the severity of pruritus assessed by patients from baseline to week 8 using a 0–10-cm visual analog scale. Similarly, reduced pruritus severity was observed in SAR100842/SAR100842-treated patients compared to placebo/SAR100842-treated patients (mean ± SD change −1.38 ± 2.85 versus −0.84 ± 1.67). Compared to week 8, the severity of pruritus was further decreased at week 24 in patients initially treated with SAR100842 or placebo. The severity of pain assessed by

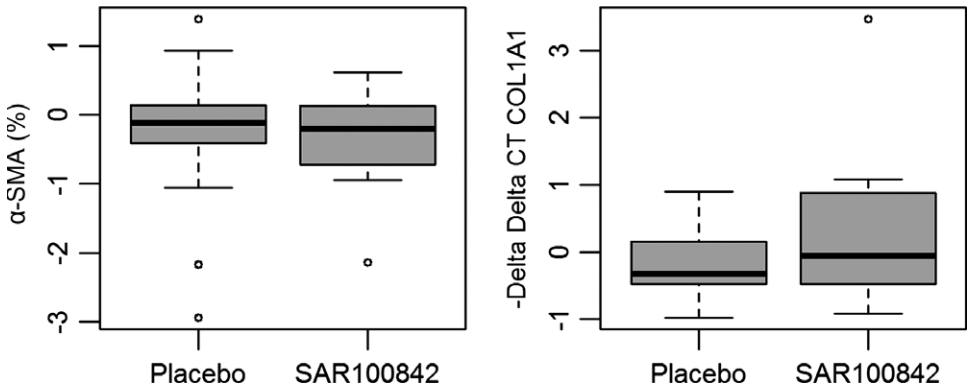

Figure 2. Changes in the skin fibrosis markers α-smooth muscle actin (α-SMA) and type I collagen from baseline to week 8. Data are presented as box plots, where the boxes represent the 25th to 75th percentiles, the lines within the boxes represent the median, and the lines outside the boxes represent the 10th and 90th percentiles. Circles indicate outliers.

patients using a numerical pain scale was low at baseline in the study population, and no conclusion could be drawn.

No significant differences between groups in skin and blood biomarker end points. There was no statistically significant differential expression of any skin mRNA and protein biomarkers or blood protein biomarkers between placebo- and SAR100842-treated patients. Type I collagen and α-SMA were used as fibrosis markers and were not modulated by SAR100842 treatment (Figure 2). Disease signature was evaluated using either the 4-gene biomarker as described by Farina et al (16) or a combination of TSP-1 and COMP. No changes in these genes were correlated with change in MRSS (Table 2). However, after 8 weeks there was a trend toward a reduction in TSP-1 with SAR100842 compared to placebo, although this did not reach statistical significance (Figure 3). We also evaluated the gene for membrane-spanning 4 domains, subfamily A, member 4A (a marker of M2-type macrophages). The expression of this marker, such as in the 2-gene signature (17), was not modulated by SAR 100842 and was not correlated with the change in MRSS (not shown).

Global change in gene expression in skin samples at 8 weeks between vehicle- and SAR100842-treated patients was evaluated using a stringent cutoff for false discovery rate ($P = 0.05$) or less stringent criteria ($P = 0.1$). No significant difference was observed under any conditions. Data obtained using a cutoff for a false discovery rate of <0.1 are presented in Supplementary Table 3, http://onlinelibrary.wiley.com/doi/10.1002/art.40547/abstract.

Table 2. Absence of correlation of change in 4 gene biomarkers with change in MRSS*

Gene	Correlation of change in gene with change in MRSS	*P*
COMP	0.01	0.96
TSP1	0.0074	0.97
SIGLEC1	0.043	0.82
IFF44	−0.031	0.87

* MRSS = modified Rodnan skin thickness score.

SAR100842 induces target engagement in the LPA pathway. There was a nonsignificant numerical reduction from baseline in some LPA pathway biomarkers (plasminogen activator inhibitor 1, Wnt-2, and sFRP-4) in SAR 100842-treated patients compared to placebo-treated patients (Figure 4). Although the decrease in these biomarkers was not significant, it is of interest since they have been shown to be regulated by LPA and SAR100842 in dermal fibroblasts from SSc patients. Thus, a post hoc analysis was performed to identify a more global LPA signature in SSc dermal fibroblasts and skin biopsy samples and to evaluate the impact of SAR100842 on this signature in patient skin to assess target engagement.

The signature was identified using both microarray data obtained in SSc dermal fibroblasts treated for 24 hours with LPA and microarray data from skin biopsy samples from SSc patients at baseline. A guided clustering method was performed to give weight to genes that were expressed at a significant level following LPA treatment but that were also expressed at a significant level in skin biopsy samples. This led to a list of 47 genes identified as an LPA signature (see Supplementary Table 4, http://onlinelibrary.wiley.com/doi/10.1002/art.40547/abstract). This signature reflects pathways such as those for proliferation and epidermal growth factor signaling, which are known to be mechanistically part of LPA responses in other cell types. These genes were reduced to a unique surrogate biomarker in 1 dimension called the PAI, using the median polish algorithm (21). The PAI was extracted as a row effect as it represents the summary expression in each patient. A significant decrease in the

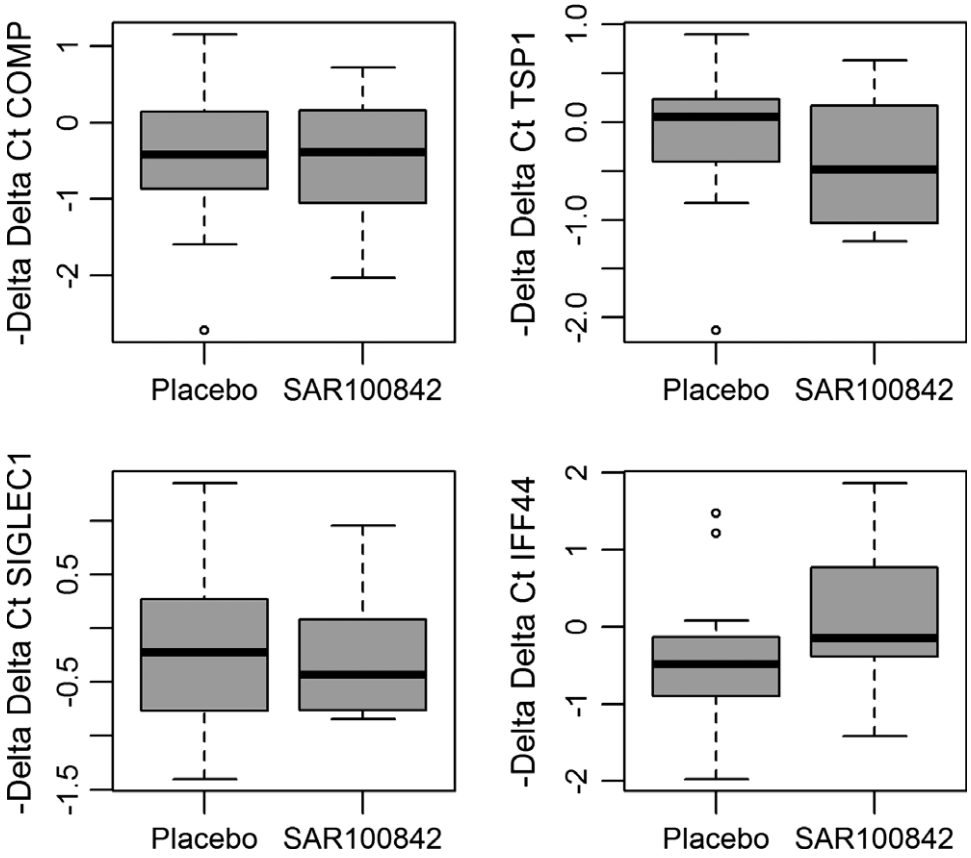

Figure 3. Changes from baseline to week 8 in 4 gene biomarkers of skin fibrosis. Data are presented as box plots, where the boxes represent the 25th to 75th percentiles, the lines within the boxes represent the median, and the lines outside the boxes represent the 10th and 90th percentiles. Circles indicate outliers.

PAI was observed in the SAR100842 group ($P = 0.0089$) (Figure 5).

DISCUSSION

LPA is a phospholipid growth factor that targets cells through a number of cell surface receptors, and it has been implicated in the pathogenesis of SSc. Of greatest interest, it appears that it may contribute to excessive tissue fibrosis, mainly through LPA_1 receptor activation (5), as observed in SSc. Recent findings further emphasize the key roles of autotaxin and the LPA axis in SSc (22). SAR100842 is a low molecular weight, selective inhibitor of the LPA_1 receptor that is being developed as a potential novel therapy for SSc with the aim of reducing or even reversing the progression of fibrosis. This phase IIa study is the first to assess oral administration of SAR100842 in patients with early dcSSc. The safety and tolerability of SAR100842 was the primary outcome measure, and SAR100842 was shown to be well tolerated in patients with dcSSc.

In preclinical studies, the administration of SAR 100842 to rats at doses up to 2,000 mg/kg/day caused no toxicologically relevant effects. Findings related to the compound were limited to a slightly higher incidence of regurgitation in females at a high dose, and the present study did not show any specific gastrointestinal AEs in SSc patients. In previous phase I studies, the safety profile was very good, and overall the most frequently reported SAR100842-related AEs were headache, symptomatic orthostatic hypotension or postural dizziness, and flatulence. Those AEs were not severe or serious. In the present study, both in the short-term double-blind phase and in the longer term open-label extension phase, no safety signals emerged regarding vital signs, orthostatic hypotension, electrocardiography, or laboratory parameters. A common toxicologic concern with antifibrotic agents is whether patients may exhibit a delay in normal wound healing. Studies with LPA receptor antagonists using incisional and excisional wounding in rats have been reassuring (22), but it is noteworthy that in the present study, although one-third of patients had digital ulcerations at

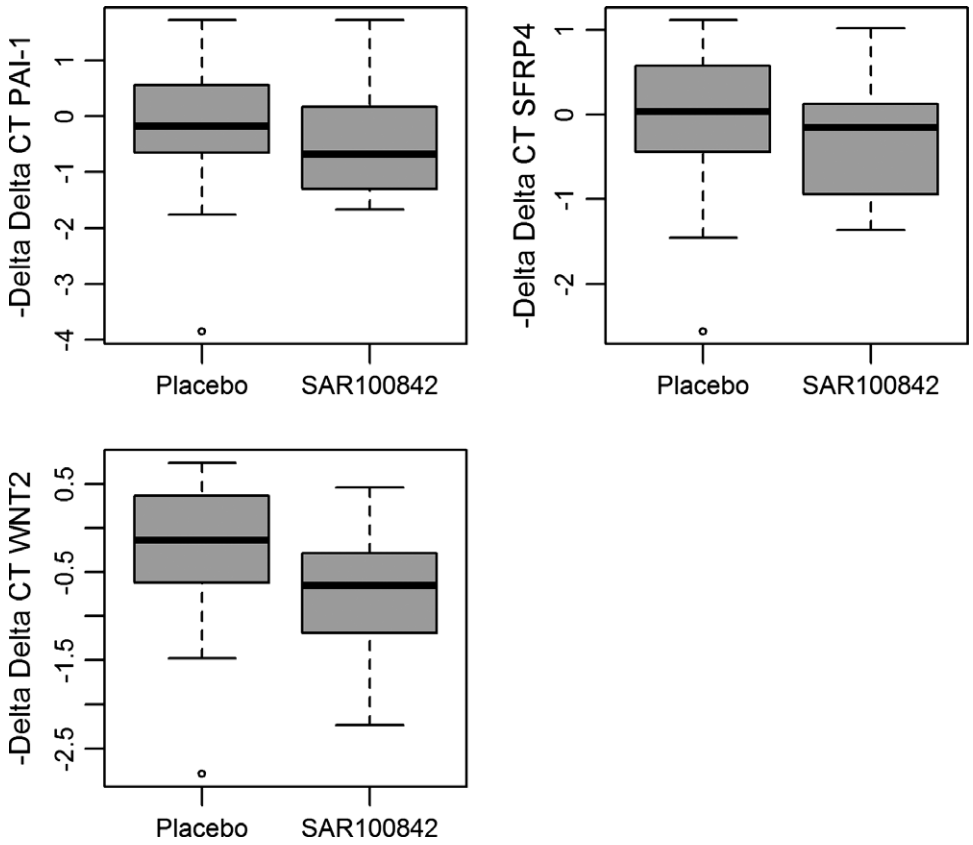

Figure 4. Changes from baseline to week 8 in lysophosphatidic acid pathway markers. Data are presented as box plots, where the boxes represent the 25th to 75th percentiles, the lines within the boxes represent the median, and the lines outside the boxes represent the 10th and 90th percentiles. Circles indicate outliers.

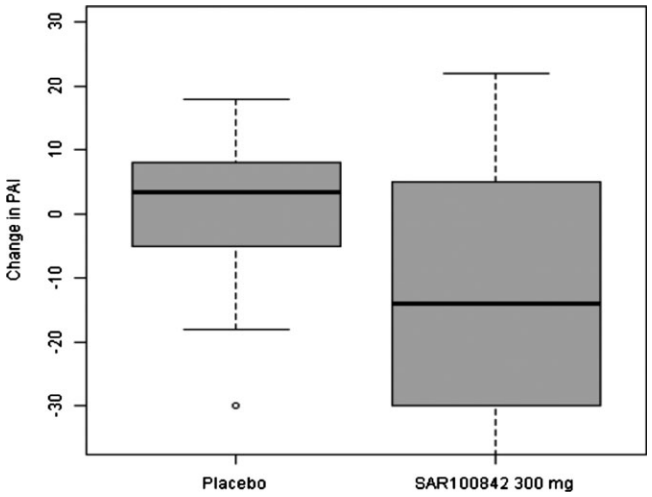

Figure 5. Change in the pathway activation index (PAI) from baseline to week 8. Data are presented as box plots, where the boxes represent the 25th to 75th percentiles, the lines within the boxes represent the median, and the lines outside the boxes represent the 10th and 90th percentiles. Circles indicate outliers.

baseline, no overt safety concerns emerged for them, confirming the good safety profile in SSc patients.

The clinical efficacy of SAR100842 was part of the secondary end points, but no effect was expected on the MRSS after 8 weeks of treatment because the MRSS is slow in changing. Nevertheless, at the end of the double-blind period, a numerically greater decrease in total MRSS score from baseline in the SAR100842 group compared to the placebo group was detected without reaching statistical significance (treatment effect −1.2 [95% CI −4.37, 2.02]; median change −4.00 versus −1.00, respectively). Also, there was a numerically greater reduction without reaching statistical significance in the HAQ DI score in the SAR100842 group (treatment effect −0.1 [95% CI −0.38, 0.09]). These findings are promising; they might be due to the mechanism of action of SAR100842 and/or they might also be explained by a large proportion of subjects receiving background immunosuppressive medications. These findings were supportive of the effect observed after 24 weeks of treatment, when patients experienced a clinically meaningful decrease in total MRSS

(median change −7.50) and a high percentage of them (78.6%) improved by at least 5 points from baseline (responders) (23); similar benefit was observed in the HAQ DI score. Although these were secondary end points and had weak statistical power, the size of the decreases must be noted and is larger than that observed in other trials targeting the same SSc population. Furthermore, the similar trend observed for skin changes and quality of life is encouraging and promising for future trials. Nevertheless, and despite being encouraging, the open-label data should be interpreted with caution.

This study must be interpreted while taking its limitations into account. The sample size was not large but was consistent with the design of a proof of biologic activity study looking primarily at safety. The duration may be considered short, and most trials are expected to last more than 6 months, but the observed changes in MRSS in this population are promising. SSc is a systemic disease and organ involvement defines the prognosis. No data could be provided on organ involvement from the present study, and this will have to be addressed in the future.

Pharmacodynamic and biomarker assessments were part of the secondary end points. There was no statistically significant differential expression of any biomarker between the 2 groups of patients.

Using a new unbiased statistical analysis, a guided clustering algorithm allowed the identification of a set of genes that had high LPA perturbation in the cell culture study and that were consistently expressed and correlated with similar expression in skin samples from patients. This LPA signature was then reduced to 1 dimension, and change in the resulting PAI was computed in skin biopsy samples from patients treated with placebo versus patients treated with SAR100842. A significant effect of SAR100842 on change from baseline in the PAI was indicative of an effect of SAR100842 on the LPA signature (15 patients per treatment arm), demonstrating target engagement upon SAR100842 treatment for 8 weeks.

The optimal clinical trial duration for patients with SSc is still unknown. Some observations regarding collagen metabolism suggest that a clinical trial duration of 24 weeks or longer might be recommended. Indeed, in the phase II tocilizumab data (24), the 2-gene biomarker was able to differentiate tocilizumab from placebo at 24 weeks. The biomarkers in clinical trials of SSc have been shown to correlate with skin fibrosis (as seen here) rather than to predict skin progression. In addition, the collagen turnover (which is a product of collagen production and collagen degradation) may require several weeks to be modulated, and this also depends on whether the pharmacologic agent directly (e.g., knockout) or indirectly (the current inhibitor) targets collagen products. A longer version of this trial with clinical and biologic outcome measures at 4–6 months might have shown statistically significant differences.

This study demonstrates that LPA_1 blockade by SAR100842 is well tolerated in patients with early dcSSc. The results show target engagement with SAR100842 as well as some promising clinical and biologic changes. Nevertheless, treatment effect cannot be inferred from skin fibrosis biomarkers, but these biomarkers may be informative as shown in other recent trials (24–26). Taken together, these results suggest the potential clinical benefit of SAR100842 in dcSSc patients with unmet needs (27), and SAR100842 deserves evaluation in confirmatory trials.

AUTHOR CONTRIBUTIONS

All authors were involved in drafting the article or revising it critically for important intellectual content, and all authors approved the final version to be published. Drs. Allanore and Khanna had full access to all of the data in the study and take responsibility for the integrity of the data and the accuracy of the data analysis.

Study conception and design. Allanore, Distler, Jagerschmidt, Illiano, Ledein, Boitier, Agueusop, Denton, Khanna.

Acquisition of data. Allanore, Distler, Denton, Khanna.

Analysis and interpretation of data. Allanore, Distler, Jagerschmidt, Illiano, Denton, Khanna.

ROLE OF THE STUDY SPONSOR

Sanofi was involved in the design and conduct of the study, oversaw the collection, management, and statistical analysis of the data, and contributed to the interpretation of the data and the preparation, review, and approval of the manuscript. The final decision on manuscript submission was made by the authors. Publication of this article was not contingent upon approval by Sanofi.

REFERENCES

1. Denton CP. Systemic sclerosis: from pathogenesis to targeted therapy. Clin Exp Rheumatol 2015;33:S3–7.
2. Elhai M, Meune C, Avouac J, Kahan A, Allanore Y. Trends in mortality in patients with systemic sclerosis over 40 years: a systematic review and meta-analysis of cohort studies. Rheumatology (Oxford) 2012;51:1017–26.
3. Nagaraja V, Denton CP, Khanna D. Old medications and new targeted therapies in systemic sclerosis. Rheumatology (Oxford) 2015;54:1944–53.
4. Zhao Y, Natarajan V. Lysophosphatidic acid (LPA) and its receptors: role in airway inflammation and remodeling. Biochim Biophys Acta 2013;1831:86–92.
5. Swaney JS, Chapman C, Correa LD, Stebbins KJ, Broadhead AR, Bain G, et al. Pharmacokinetic and pharmacodynamic characterization of an oral lysophosphatidic acid type 1 receptor-selective antagonist. J Pharmacol Exp Ther 2011;336:693–700.
6. Tigyi G. Aiming drug discovery at lysophosphatidic acid targets. Br J Pharmacol 2010;161:241–70.
7. Rancoule C, Pradère JP, Gonzalez J, Klein J, Valet P, Bascands JL, et al. Lysophosphatidic acid-1-receptor targeting agents for fibrosis. Expert Opin Investig Drugs 2011;20:657–67.
8. Tokumura A, Carbone LD, Yoshioka Y, Morishige J, Kikuchi M, Postlethwaite A, et al. Elevated serum levels of arachidonoyl-

lysophosphatidic acid and sphingosine 1-phosphate in systemic sclerosis. Int J Med Sci 2009;6:168–76.
9. Ohashi T, Yamamoto T. Antifibrotic effect of lysophosphatidic acid receptors LPA1 and LPA3 antagonist on experimental murine scleroderma induced by bleomycin. Exp Dermatol 2015;24:698–702.
10. Castelino FV, Seiders J, Bain G, Brooks SF, King CD, Swaney JS, et al. Amelioration of dermal fibrosis by genetic deletion or pharmacologic antagonism of lysophosphatidic acid receptor 1 in a mouse model of scleroderma. Arthritis Rheum 2011;63:1405–15.
11. Yin Z, Carbone LD, Gotoh M, Postlethwaite A, Bolen AL, Tigyi GJ, et al. Lysophosphatidic acid-activated Cl^- current activity in human systemic sclerosis skin fibroblasts. Rheumatology (Oxford) 2010;49:2290–7.
12. Subcommittee for Scleroderma Criteria of the American Rheumatism Association Diagnostic and Therapeutic Criteria Committee. Preliminary criteria for the classification of systemic sclerosis (scleroderma). Arthritis Rheum 1980;23:581–90.
13. LeRoy EC, Black C, Fleischmajer R, Jablonska S, Krieg T, Medsger TA Jr, et al. Scleroderma (systemic sclerosis): classification, subsets and pathogenesis. J Rheumatol 1988;15:202–5.
14. Clements P, Lachenbruch P, Seibold J, White B, Weiner S, Martin R, et al. Inter and intraobserver variability of total skin thickness score (modified Rodnan TSS) in systemic sclerosis. J Rheumatol 1995;22:1281–5.
15. Steen VD, Medsger TA Jr. The value of the Health Assessment Questionnaire and special patient-generated scales to demonstrate change in systemic sclerosis patients over time. Arthritis Rheum 1997;40:1984–91.
16. Farina G, Lafyatis D, Lemaire R, Lafyatis R. A four-gene biomarker predicts skin disease in patients with diffuse cutaneous systemic sclerosis. Arthritis Rheum 2010;62:580–8.
17. Rice LM, Ziemek J, Stratton EA, McLaughlin SR, Padilla CM, Mathes AL, et al. A longitudinal biomarker for the extent of skin disease in patients with diffuse cutaneous systemic sclerosis. Arthritis Rheumatol 2015;67:3004–15.
18. Maneck M, Schrader A, Dieter K, Spang R. Genomic data integration using guided clustering. Bioinformatics 2011;27:2231–8.
19. Fries JF, Spitz P, Kraines RG, Holman HR. Measurement of patient outcome in arthritis. Arthritis Rheum 1980;23:137–45.
20. Van den Hoogen F, Khanna D, Fransen J, Johnson SR, Baron M, Tyndall A, et al. 2013 classification criteria for systemic sclerosis: an American College of Rheumatology/European League Against Rheumatism collaborative initiative. Arthritis Rheum 2013;65:2737–47.
21. Mosteller F, Tukey JW. Data analysis and regression: a second course in statistics. Reading (MA): Addison-Wesley; 1977.
22. Castelino FV, Bain G, Pace VA, Black KE, George L, Probst CK, et al. An autotaxin/lysophosphatidic acid/interleukin-6 amplification loop drives scleroderma fibrosis. Arthritis Rheumatol 2016;68:2964–74.
23. Khanna D, Furst DE, Hays RD, Park GS, Wong WK, Seibold JR, et al. Minimally important difference in diffuse systemic sclerosis: results from the D-penicillamine study. Ann Rheum Dis 2006;65:1325–9.
24. Khanna D, Denton CP, Jahreis A, van Laar JM, Frech TM, Anderson ME, et al. Safety and efficacy of subcutaneous tocilizumab in adults with systemic sclerosis (faSScinate): a phase 2, randomised, controlled trial. Lancet 2016;387:2630–40.
25. Quillinan NP, McIntosh D, Vernes J, Haq S, Denton CP. Treatment of diffuse systemic sclerosis with hyperimmune caprine serum (AIMSPRO): a phase II double-blind placebo-controlled trial. Ann Rheum Dis 2014;73:56–61.
26. Rice LM, Padilla CM, McLaughlin SR, Mathes A, Ziemek J, Goummih S, et al. Fresolimumab treatment decreases biomarkers and improves clinical symptoms in systemic sclerosis patients. J Clin Invest 2015;125:2795–807.
27. Khanna D, Distler J, Sandner P, Distler O. Emerging strategies for treatment of systemic sclerosis. J Scleroderma Relat Disord 2016;1:186–93.

ARTHRITIS & RHEUMATOLOGY
Vol. 70, No. 10, October 2018, pp 1644–1653
DOI 10.1002/art.40534

CCL21 as a Potential Serum Biomarker for Pulmonary Arterial Hypertension in Systemic Sclerosis

Anna-Maria Hoffmann-Vold,[1] Roger Hesselstrand,[2] Håvard Fretheim,[1] Thor Ueland,[1] Arne K. Andreassen,[3] Cathrine Brunborg,[3] Vyacheslav Palchevskiy,[4] Øyvind Midtvedt,[3] Torhild Garen,[3] Pål Aukrust,[1] John A. Belperio,[4] and Øyvind Molberg[1]

Objective. **Systemic sclerosis (SSc) is a major cause of pulmonary arterial hypertension (PAH). Murine models indicate key roles for chemokines CCL19 and CCL21 and their receptor CCR7 in lung inflammation leading to PAH. The objective of this study was to assess the chemokine CCL19–CCL21 axis in patients with SSc-related PAH.**

Methods. **Serum samples obtained from 2 independent prospective SSc cohorts (n = 326), patients with idiopathic PAH (n = 12), and healthy control subjects (n = 100) were analyzed for CCL19/CCL21 levels, by enzyme-linked immunosorbent assay. The levels were defined as either high or low, using the mean + 2 SD value in controls as the cutoff value. Risk stratification at the time of PAH diagnosis and PAH-related events were performed. Descriptive and Cox regression analyses were conducted.**

Results. **CCL21 levels were higher in patients with SSc compared with controls and were elevated prior to the diagnosis of PAH. PAH was more frequent in patients with high CCL21 levels (≥0.4 ng/ml) than in those with low CCL21 levels (33.3% versus 5.3% [$P < 0.001$]). In multivariate analyses, CCL21 was associated with PAH (hazard ratio [HR] 5.1, 95% CI 2.39–10.76 [$P < 0.001$]) and occurrence of PAH-related events (HR 4.7, 95% CI 2.12–10.46, $P < 0.001$). Risk stratification at the time of PAH diagnosis alone did not predict PAH-related events. However, when risk at diagnosis was combined with high or low CCL21 level, there was a significant predictive effect (HR 1.3, 95% CI 1.03–1.60 [$P = 0.027$]). A high CCL21 level was associated with decreased survival ($P < 0.001$).**

Conclusion. **CCL21 appears to be a promising marker for predicting the risk of SSc-related PAH and PAH progression. CCL21 may be part of a dysregulated immune pathway linked to the development of lung vascular damage in SSc.**

Systemic sclerosis (SSc) is a complex autoimmune disorder characterized by progressive fibrosis of the skin and internal organs, vascular pathology, and distinct autoantibodies in serum (1). Mortality is high, and precapillary pulmonary hypertension (PH) and interstitial lung disease (ILD) are major causes (2–4). The 2 main forms of PH in SSc are pulmonary arterial hypertension (PAH) (World Health Organization [WHO] group 1) and PH secondary to ILD (WHO group 3 PH). It is important to differentiate these forms, because SSc-related PAH may respond to targeted PH therapies, particularly if treatment is introduced at an early stage when vascular damage is not too advanced, while SSc-related PH complicating ILD (PH-ILD) is resistant to current therapies (5–8).

Unfortunately, the onset of PH in patients with SSc is typically insidious, resulting in delayed diagnosis (9). Multimodal screening by echocardiography, N-terminal pro–brain natriuretic peptide (NT-proBNP) tests, and pulmonary function tests (PFTs) may reduce diagnostic delay (10–12), but this is an expensive strategy that primarily detects established PH and does not differentiate PAH from PH-ILD. Hence, there is an unmet need for early and specific PAH (WHO group 1) markers in SSc for early diagnosis.

Immune processes originating in the lungs appear to drive the development of PAH (13), and various

Supported by the Norwegian Women's Public Health Association and the Norwegian Rheumatology Foundation, Oslo, Norway.

[1]Anna-Maria Hoffmann-Vold, PhD, Håvard Fretheim, MD, Thor Ueland, PhD, Pål Aukrust, PhD, Øyvind Molberg, PhD: Oslo University Hospital, Rikshospitalet, and University of Oslo, Oslo, Norway; [2]Roger Hesselstrand, PhD: Lund University, Lund, Sweden; [3]Arne K. Andreassen, PhD, Cathrine Brunborg, MS, Øyvind Midtvedt, MD, Torhild Garen, MS: Oslo University Hospital, Rikshospitalet, Oslo, Norway; [4]Vyacheslav Palchevskiy, PhD, John A. Belperio, MD: David Geffen School of Medicine at UCLA, Los Angeles, California.

Address correspondence to Anna-Maria Hoffmann-Vold, PhD, Oslo University Hospital, Rikshospitalet, Pb 4950 Nydalen, 0424 Oslo, Norway. E-mail: a.m.hoffmann-vold@medisin.uio.no.

Submitted for publication November 15, 2017; accepted in revised form April 17, 2018.

studies indicate that these immune processes may leave distinct fingerprints in the systemic circulation (14–17). A prime example is the high systemic level of chemokine CXCL4 that was recently identified in SSc-related PAH (16). Surprisingly, the CXCL4 level was also elevated in patients in whom ILD was developing, indicating low specificity for PAH (16). The effects of age were not assessed in the CXCL4 study. This was unfortunate, because age is a risk factor for SSc-related PAH (18,19) and appears to influence systemic chemokine levels (20,21).

Data derived from murine models support the notion of PAH as an immune-driven process and have identified chemokine receptor CCR7 and its ligands CCL19 and CCL21 as potential factors in PAH development (22). This chemokine axis is essential for directing naive T cells to dendritic cells in lymph nodes but is also highly inducible in the periphery, with selective induction of CCL21 in lung tissue (23). Mice deficient in CCR7 have perivascular lung inflammation and develop PAH (24), and there are indications of dysregulated CCR7 and/or CCL21 in human PAH (25,26). These observations are consistent with the notion that CCL21 is a potent regulator of angiogenesis (27) and a marker of vascular inflammation and damage in human cardiovascular diseases (28,29).

We hypothesized that the CCR7–CCL19/CCL21 axis could be dysregulated in SSc-related PAH. To approach this issue, we analyzed serum samples from a large, prospective, well-characterized SSc cohort covering the whole spectrum of disease severities, including complete longitudinal data sets on PAH and ILD (30–32). Follow-up analyses were performed in patients with idiopathic PAH, and the data were validated in an independent cohort of patients with SSc-related PAH (33).

PATIENTS AND METHODS

Study cohorts. All included SSc patients from the unselected, prospective Oslo University Hospital SSc cohort met the American College of Rheumatology/European League Against Rheumatism 2013 classification criteria for SSc (31) and had serum samples and complete longitudinal data on cardiopulmonary disease development available (as detailed below) (30). As internal controls, we included serum samples from 12 patients with idiopathic PAH at the Department of Cardiology, Oslo University Hospital and from 100 healthy blood donors. All serum samples were collected in Nunc tubes (Thermo Fisher), processed within 30 minutes, and stored according to the Oslo University Hospital protocol. For validation, we selected SSc patients with and those without PAH from the prospective Lund University Hospital SSc cohort. All patients selected from the Lund cohort met the inclusion criteria described above. The study was conducted in compliance with the Declaration of Helsinki and was approved by the Data Protection Authority in Norway (No.2006/119). Informed consent was obtained from all included subjects.

Clinical parameters. Clinical data including SSc subset (1), autoantibody status, smoking history, and vital status were retrieved from the Oslo University Hospital and Lund University Hospital SSc registries (34). Disease onset was defined as the first non–Raynaud's phenomenon manifestation of SSc, and disease duration was defined as the period from disease onset until study end (June 2017) or time of death.

Serial assessments of ILD. Paired PFTs and high-resolution computed tomography (HRCT) lung images from baseline and the last available follow-up visit were analyzed as previously described (30,32,35). Briefly, the extent of lung fibrosis was expressed as the percentage of total lung volume, and PFTs were carried out according to the American Thoracic Society/European Respiratory Society guidelines, using an automated Vmax V6200 system (SensorMedics) (30,36).

PH surveillance, diagnostic procedures, and PAH risk stratification at diagnosis. Annual PH surveillance procedures in the Oslo and Lund SSc cohorts include complete clinical examination, echocardiography with estimated systolic pulmonary artery pressure (PAP), PFTs, 6-minute walk test, and NT-proBNP test. These data were retrieved for the baseline visit and the last available assessment (follow-up). The threshold for referral for right-sided heart catheterization (RHC) is low, and the indication is based on clinical suspicion of PH, typically due to increasing or unexplained dyspnea, a significant decline in the diffusing capacity for carbon monoxide (DLCO), increasing NT-proBNP levels, and a systolic blood pressure of >40 mm Hg as determined by echocardiography. In January 2014, the DETECT algorithm was added to the Oslo University Hospital SSc protocol, and all patients with a DETECT score of >35 were referred for RHC (37).

PH was diagnosed by RHC according to the European Society of Cardiology (ESC) guidelines, using a Swan-Ganz pulmonary artery thermodilution catheter (Baxter Healthcare) (38,39). A follow-up RHC was conducted if it was clinically indicated. Differentiation between SSc-related PAH (WHO group 1) and PH-ILD (WHO group 3) was performed as previously described (11), with SSc-related PAH defined as the presence of precapillary PH and the absence of significant lung fibrosis (<10% on HRCT) and forced vital capacity (FVC) of >70% of the predicted value at both baseline and follow-up, with other causes of precapillary PH ruled out (6). Risk stratification at the time of PAH diagnosis was performed using the low-risk, intermediate-risk, and high-risk grouping system suggested in the 2015 ESC guidelines (38). Patients with ≥1 measure of poor prognosis were considered to be at high risk, and those with ≥1 measure of intermediate prognosis were considered to be at intermediate risk. The composite outcome measure "PAH-related events" was defined as previously described (40) and included PAH progression, end-stage PAH, hospitalization for PAH worsening, and all-cause mortality.

Chemokine enzyme-linked immunosorbent assay. Blood samples from all patient populations (SSc, idiopathic PAH, and controls) at Oslo University Hospital and Lund University Hospital were obtained according to the same standardized procedures, and processing and storing of blood samples were similar in these cohorts. The European League Against Rheumatism (EULAR)/EULAR Scleroderma Trial and Research

recommendations for biobanking (41) were followed. Samples were centrifuged at room temperature within 30 minutes, and serum aliquots were stored at −70°C until assayed. Circulating CCL19 and CCL21 were analyzed in all samples by enzyme immunoassay (R&D Systems) using undiluted serum in all included samples at Oslo University Hospital, and all samples were measured in duplicate. The 100 healthy control samples were drawn from blood bank donors. The Norwegian law for blood donors is strict, allowing inclusion of only healthy individuals without cardiovascular disease, immune deficiencies, any chronic disease, or infection.

Statistical analysis. Analyses were performed using IBM SPSS software version 22 and Stata version 14. Pearson's chi-square test, Fisher's exact test, or *t*-test for independent samples was used as appropriate. For correlation analyses, Pearson's or Kendall's tau-b coefficients were applied as appropriate, and Cohen's criteria for correlation were applied (<0.3 = medium correlation, and <0.5 = strong correlation). Cox regression analyses with hazard ratios (HRs) and 95% confidence intervals (95% CIs) were applied to analyze cardiopulmonary outcome measures. The association, predictive value, and the prognostication of CCL21 in relation to PAH were evaluated by Cox regression analyses. Independent risk factors from univariable analyses with a significance level of 20%, along with all variables of known clinical importance were included in the multivariable Cox regression analysis. A manual backward stepwise elimination procedure was performed to identify independent risk factors for PAH (42). Multivariable analyses were preceded by an estimation of the correlation between risk factors. To avoid multicollinearity between age at onset and CCL21 levels, separate models including either CCL21 (model 1) or age at onset (model 2) were constructed and discriminated by the C index (values >0.7 were considered acceptable). Cumulative survival rates were computed using the Kaplan-Meier method, and significance was determined by log rank test. Items with significant effects on survival were entered into the Cox proportional hazards model.

RESULTS

Serum levels of CCL21 in the SSc cohort and controls. In total, 298 SSc patients from the prospective Oslo University Hospital SSc cohort were included (Figure 1). Demographics and clinical characteristics of the subjects are shown in Table 1. The serum levels of CCL19 did not differ between the groups (Figure 2A). The mean ± SD CCL21 levels in serum were higher in SSc patients (0.36

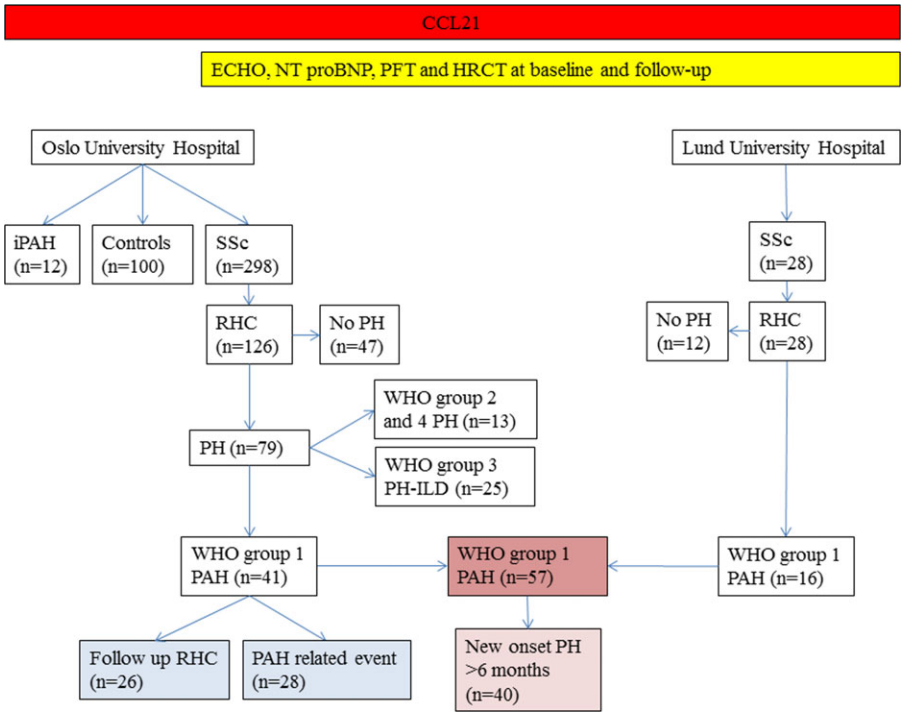

Figure 1. Flow chart of the included patients from the Oslo University Hospital and Lund University Hospital cohorts. Inclusion of all subjects from the Oslo and Lund cohorts, the number of right-sided heart catheterizations (RHCs) conducted, and the frequency of pulmonary hypertension (PH), categorized according to World Health Organization (WHO) groups for PH, are shown. All included subjects had sera analyzed for CCL21 (red bar) and all patients had available clinical data (yellow bar). Systemic sclerosis (SSc) patients with pulmonary arterial hypertension (PAH) (dark pink–shaded box) were included in the association studies. Light pink–shaded box indicates predictive studies, and blue-shaded boxes indicate prognotication studies. Echo = echocardiography; NT-proBNP = N-terminal pro–brain natriuretic peptide; PFT = pulmonary function test; HRCT = high-resolution computed tomography; iPAH = idiopathic PAH. Color figure can be viewed in the online issue, which is available at http://onlinelibrary.wiley.com/doi/10.1002/art.40534/abstract.

Table 1. Demographics, clinical characteristics, and CCL21 levels in patients from the Oslo University Hospital and Lund University Hospital cohorts*

	SSc-PH				
	Total, Oslo (n = 298)	PAH, Oslo (n = 41)	PAH, Lund (n = 16)	PH-ILD, Oslo (n = 25)	iPAH, Oslo (n = 12)
Age at onset, years†	56 ± 13.9	66.8 ± 8.2	68.6 ± 10.3	59.5 ± 10.2	40.3 ± 14.5
Time from onset to PH, years	NA	12.1 ± 10.8	15.2 ± 6.5	8.7 ± 5.6	0 (0)
Time from serum sampling to PH, years	NA	−2.1 ± 3.8	−2.6 ± 0.7	−1.4 ± 2.7	0.07 ± 1.2
Male, no. (%)	55 (18.5)	9 (22)	2 (12.5)	9 (36)	2 (16.7)
Deceased, no. (%)	99 (31.6)	21 (51.2)	11 (68.8)	15 (60)	4 (33.3)
Diffuse cutaneous SSc, no. (%)	78 (26.2)	4 (9.8)	0 (0)	6 (24)	NA
ACAs, no. (%)	127 (46.9)	25 (69.4)	8 (50)	5 (20)	NA
mPAP at diagnosis, mm Hg	NA	39.1 ± 11.9	38.5 ± 10.1	36.3 ± 11.6	55.1 ± 17.1
CCL21 at baseline, pg/ml	0.36 ± 0.24	0.51 ± 0.2	0.60 ± 0.3	0.33 ± 0.1	0.26 ± 0.1

* None of the parameters were significantly different between patients with pulmonary arterial hypertension (PAH) in the Oslo University Hospital and the Lund University Hospital cohorts. Except where indicated otherwise, values are the mean ± SD. SSc-PH = systemic sclerosis–related pulmonary hypertension; PH-ILD = PH-related interstitial lung disease; iPAH = idiopathic PAH; NA = not applicable; ACAs = anticentromere antibodies; mPAP = mean pulmonary artery pressure.
† Defined as disease onset in the total cohort and PAH onset in all other cohorts.

± 0.24 ng/ml) compared with those in 100 healthy controls (0.18 ± 0.06 ng/ml [$P < 0.001$]) (Figure 2B). CCL21 levels did not differ between patients with limited cutaneous SSc and patients with diffuse cutaneous SSc (Figure 2C), across major SSc-related autoantibodies (Figure 2D), or in patient with and those without SSc-related ILD. In the Oslo cohort, the highest CCL21 levels were in SSc patients with PAH (n = 41) followed by patients with PH secondary to ILD (n = 25) (Figure 2E and Table 1). The CCL19 level was not elevated in patients with PAH. The finding of elevated CCL21 levels in patients with SSc-related PAH was confirmed in an independent cohort from Lund University Hospital (n = 28). CCL21 levels were similar in PAH patients from the Oslo (n = 41) and Lund cohorts (n = 16) (Table 1). Additionally, elevated CCL21 levels were not observed in the limited number of patients with idiopathic PAH (n = 12) (Figure 2E).

A CCL21 level of ≥0.40 ng/ml (i.e., more than +2 SD of the mean level in healthy controls) was identified in 90 of 298 SSc patients in the Oslo cohort. These 90 patients were defined as the "CCL21 high" subset, while the remaining 208 patients with a CCL21 level of <0.40 ng/ml were defined as the "CCL21 low" subset. Patients in these 2 subsets were similar with regard to disease duration but differed in age at disease onset and sex distribution. We did not observe that use of immunosuppressive drugs had any impact on the CCL21 analyses.

Absolute risk of cardiopulmonary disease in the CCL21 high and CCL21 low subsets of SSc patients. Among the 298 SSc patients from the Oslo cohort, 126 (43.3%) underwent at least 1 RHC during the observation period and was diagnostic for PAH in 41 SSc patients with WHO group 1 (PAH) and 25 with WHO group 3 (PH-ILD) (Figure 1). Patients with WHO groups 2, 4, and 5 (n = 13) were excluded from further analyses. In the CCL21 high subset, we estimated the absolute risk of developing PAH during the observation period to be 33.3% (30 of 90 patients), while it was 5.3% (11 of 208 patients) in the CCL21 low subset. Hence, as a stand-alone PAH test item in this unselected SSc cohort, serum CCL21 showed 80% specificity and 73% sensitivity.

Analyses of RHC parameters indicated more severe PAH in the CCL21 high subset (Table 2), and further analyses showed that the CCL21 level correlated with the cardiac index (r = −0.28, $P = 0.019$), pulmonary vascular resistance (r = 0.5, $P = 0.004$), and Svo_2 (r = −0.34, $P = 0.045$). Consistent with the RHC data, we observed higher baseline estimated systolic PAP and plasma NT-proBNP levels in the CCL21 high subset (Table 2). Moreover, the CCL21 high subset had lower DLco values at baseline compared with the low CCL21 subset (mean ± SD 62.6 ± 22.9 versus 70.6 ± 20.8; $P = 0.004$) and an increased frequency of a decrease in the DLco of >15% per year (50 ± 25.5% versus 35 ± 39.8%; $P = 0.015$). CCL21 was also correlated with the C-reactive protein (CRP) level (r = 0.4, $P < 0.001$) and the erythrocyte sedimentation rate (ESR) (r = 0.4, $P < 0.001$). Parameters associated with SSc-related ILD (baseline FVC, annual FVC deterioration, baseline extent of lung fibrosis, and annual progression of lung fibrosis) did not differ between the CCL21 high and CCL21 low subsets. The mean ± SD time from disease onset to PAH diagnosis was shorter in the CCL21

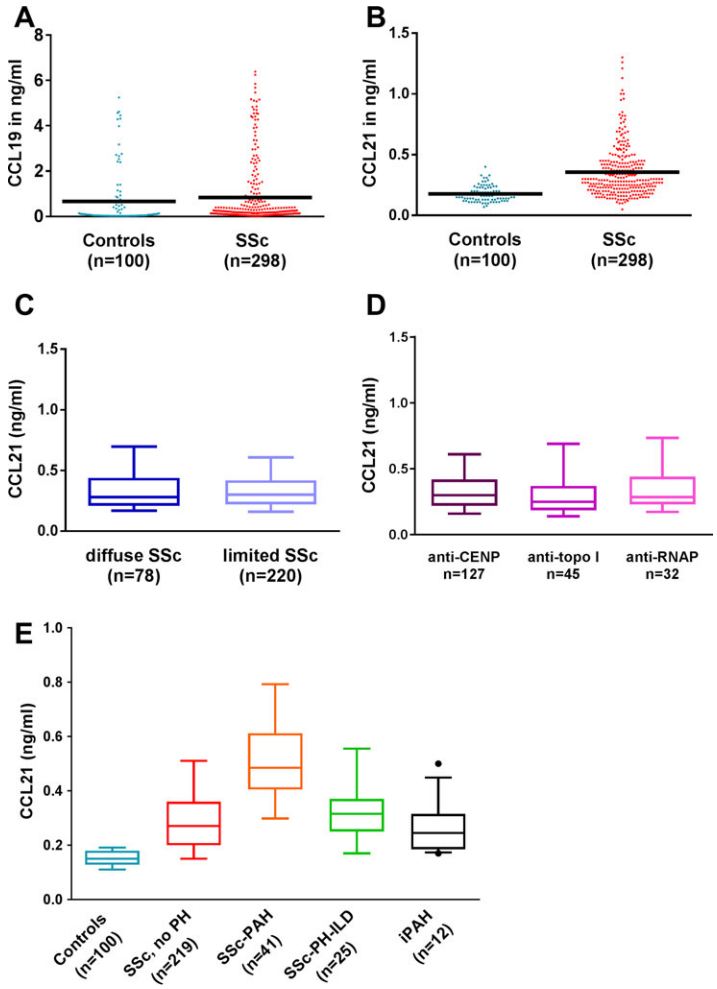

Figure 2. **A** and **B**, CCL19 levels (**A**) and CCL21 levels (**B**) in healthy control subjects and patients with SSc from the Oslo University Hospital cohort. Horizontal lines show the mean. **C,** CCL21 levels in SSc patients categorized as having diffuse cutaneous SSc or limited cutaneous SSc. **D,** CCL21 levels stratified by positivity for anticentromere (anti-CENP), anti–topoisomerase I (anti–topo I), and anti–RNAP III (anti-RNAP) antibodies. **E,** CCL21 levels in healthy control subjects, patients with SSc, patients with SSc-related PAH (SSc-PAH), patients with PH-related interstitial lung disease (PH-ILD), and patients with iPAH. In **C–E,** data are presented as box plots, where the boxes represent the 25th to 75th percentiles, the lines within the boxes represent the median, and the lines outside the boxes represent the 10th and 90th percentiles. The circle represents an outlier. See Figure 1 for other definitions.

high subset than in the CCL21 low subset (6.8 ± 7.1 years versus 15.4 ± 16.3 years; $P = 0.04$).

Associations between CCL21 and PAH in SSc. For these analyses, we included all patients in the Oslo and Lund cohorts who had undergone an RHC procedure. In 57 patients (41 from the Oslo cohort and 16 from the Lund cohort), PAH was diagnosed during the observation period (Figure 1). Univariable Cox regression analyses showed that CCL21 was associated with PAH (HR 3.3, 95% CI 1.81–5.97 [$P < 0.001$]) and age at onset (HR 1.12, 95% CI 1.08–1.15 [$P < 0.001$]). There was a significant correlation between CCL21 and age at onset (r = 0.4, $P < 0.001$), and 2 separate multivariable models were chosen to avoid multicollinearity (1 including CCL21 and 1 including age). C-index analyses of the 2 models showed superiority of the model that included CCL21 (model 1) compared with the model including age at onset (model 2) (C index 0.89 and 0.84, respectively). In the superior multivariable model, we observed that CCL21, anticentromere antibodies (ACAs), systolic PAP by echocardiography, and DLCO were independently associated with PAH (Table 3).

CCL21 and prediction of PAH development in the SSc cohort. To estimate the predictive value of CCL21 for development of PAH, we analyzed data for patients in whom the serum samples used for CCL21 analyses had

Table 2. Risk of cardiopulmonary disease in the low CCL21 and high CCL21 subsets of patients in the Oslo University Hospital SSc cohort*

	Total cohort (n = 298)	Low CCL21 (n = 208)	High CCL21 (n = 90)	P†
Right-sided heart catheterization				
Diagnostic for PAH, no. (%)	41 (13.8)	11 (5.3)	30 (33.3)	<0.001
Baseline mPAP, mm Hg	37.8 ± 11.4	35.9 ± 12.2	38.2 ± 10.2	0.499
Follow-up mPAP, mm Hg‡	36.2 ± 11.9	29.0 ± 10.4	40.3 ± 11.0	0.020
Baseline cardiac index, liters/minute/m^2	2.7 ± 0.83	3.2 ± 1.0	2.5 ± 0.66	0.029
Follow-up cardiac index, liters/minute/m^2‡	3.0 ± 0.87	3.5 ± 0.99	2.7 ± 0.71	0.049
Baseline PVR, Wood units	2.2 ± 1.9	5.3 ± 3.2	7.5 ± 4.5	0.147
Follow-up PVR, Wood units‡	4.8 ± 3.4	3.2 ± 2.0	6.5 ± 3.9	0.005
Estimated systolic PAP by echocardiography, mm Hg				
Baseline	27.7 ± 19.2	33.6 ± 19.1	56.6 ± 34.3	0.043
Follow-up	34.9 ± 35.0	55.2 ± 25.5	69.3 ± 29.1	0.162
Serum NT-proBNP, pmoles/liter				
Baseline	73.5 ± 304.4	26.7 ± 36.6	128.3 ± 172.7	0.004
Follow-up	201.5 ± 576.9	58.0 ± 101.7	348.7 ± 398.1	0.001
Cardiovascular events				
Myocardial infarction, no. (%)	3 (7.3)	2 (1.0)	1 (1.1)	0.681
Angina pectoris, no. (%)	4 (9.8)	1 (0.5)	3 (3.3)	0.190

* Except where indicated otherwise, values are the mean ± SD. SSc = systemic sclerosis; PAH = pulmonary arterial hypertension; mPAP = mean pulmonary artery pressure; PVR = pulmonary vascular resistance; NT-proBNP = N-terminal pro–brain natriuretic peptide.
† Low CCL21 versus high CCL21.
‡ Measured in 25 patients in the low CCL21 subset and 16 patients in the high CCL21 subset.

been obtained >6 months prior to RHC, before PAH was diagnosed in the patients. Such pre-PAH samples were available for 40 patients (Figure 1). The clinical characteristics of the 40 patients with pre-PAH samples did not differ from those of the 17 other Oslo/Lund cohort patients with SSc-related PAH. Again, due to strong collinearity between CCL21 and age at onset, we used 2 models to avoid multicollinearity and found that the model that included CCL21 (model 1) was superior to model 2 (C index 0.89 and 0.82, respectively). Using this model, we showed that factors independently predicting PAH were CCL21, ACAs, systolic PAP, and DLCO (Table 3).

Table 3. CCL21 and other variables associated with PAH and predictive of PAH*

	Associated with PAH		Predictive of PAH	
Variable	HR (95% CI)	P	HR (95% CI)	P
CCL21	5.1 (2.39–10.76)	<0.001	3.3 (1.52–7.10)	0.003
ACAs	2.6 (1.40–4.67)	0.002	2.9 (1.38–6.14)	0.005
Systolic PAP	1.02 (1.01–1.03)	<0.001	1.02 (1.01–1.03)	0.002
DLCO, % predicted	0.98 (0.96–0.99)	0.010	0.97 (0.95–0.99)	0.001

* Adjusted multivariable Cox regression analyses included all patients with systemic sclerosis in the Oslo University Hospital and Lund University Hospital cohorts who had pulmonary arterial hypertension (PAH) diagnosed by right-sided heart catheterization and for whom data on CCL21 were available (n = 57). The model used for the prediction of PAH development included 40 patients in whom the serum samples used for the CCL21 analysis had been obtained >6 months before the diagnosis of PAH (i.e., pre-PAH serum samples). HR = hazard ratio; 95% CI = 95% confidence interval; ACAs = anticentromere antibodies; PAP = pulmonary artery pressure (by echocardiography); DLCO = diffusing capacity for carbon monoxide.

Utility of CCL21 for predicting PAH in patients with SSc. The value of CCL21 for predicting PAH-related events was assessed in the 41 patients with SSc-related PAH from the Oslo University Hospital cohort. At the time of PAH diagnosis, 12 of these 41 patients (29%) belonged to the low-risk subgroup, as defined by the 2015 ESC guidelines, while 32% had an intermediate risk and 39% had a high risk. CCL21 levels were significantly higher in the high-risk group compared with the intermediate- and low-risk subgroups ($P < 0.001$). During the observation period, 28 (68%) of 41 patients developed a PAH-related composite event. In univariable analyses, baseline variables associated with the development of a PAH event were CCL21 (HR 4.7, 95% CI 2.12–10.46 [$P < 0.001$]), syncope (HR 5.9, 95% CI 1.59–21.53 [$P = 0.008$]), New York Heart Association functional class (43) (HR 2.3, 95% CI 1.17–4.46 [$P = 0.016$]), age at onset (HR 1.12, 95% CI 1.08–1.16 [$P < 0.001$]), and SvO_2 (HR 0.95, 95% CI 0.91–0.99 [$P = 0.025$]). Due to high intervariable correlations, no further multivariable analyses were performed. None of the 3 risk groups (low, intermediate, and high) predicted the development of PAH-related events (HR 1.6, 95% CI 0.99–2.50 [$P = 0.055$]). However, when risk at diagnosis was combined with high or low CCL21 levels,

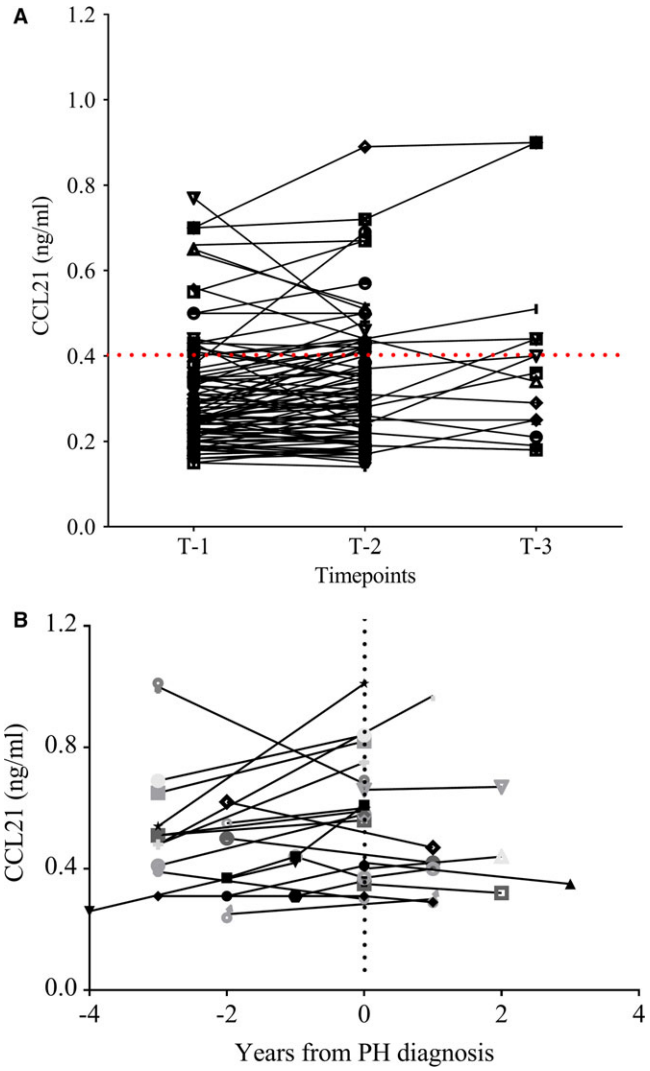

Figure 3. Serial measurements of CCL21. **A,** Serial measurements of CCL21 in serum samples obtained at different time points (>12 months apart) from 126 patients with SSc. Broken red line indicates the cutoff value. **B,** Serial measurements of CCL21 in serum samples obtained at different time points (>2 months apart) from 20 SSc patients in whom PAH was diagnosed. Lines connect the data points for each patient. Each symbol represents a different patient. See Figure 1 for definitions. Color figure can be viewed in the online issue, which is available at http://onlinelibrary.wiley.com/doi/10.1002/art.40534/abstract.

resulting in 6 risk groups, the predictive value was significant (HR 1.3, 95% CI 1.03–1.60 [$P = 0.027$]).

Follow-up RHC was performed in 26 (63.4%) of 41 patients. Analyses of serial RHC demonstrated that an increase in the mean pulmonary artery pressure from diagnosis to follow-up differed between the CCL21 high and CCL21 low subsets (9.1 mm Hg versus 1.6 mm Hg; $P = 0.031$). PAH treatment did not differ between the CCL21 high and CCL21 low subsets (data not shown).

Longitudinal assessment of CCL21 in the Oslo and Lund cohorts. At least 2 serum samples obtained at different time points (>12 months apart) were available for 126 (38.7%) of 326 SSc patients from the combined (Oslo and Lund) cohort. Analyses of these paired samples showed that the serum levels of CCL21 were stable across time in the vast majority of patients (Figure 3A). The cohort of 126 SSc patients with available serial serum samples included 20 patients in whom the first serum sample had been drawn at a time point before PAH was diagnosed by RHC (pre-PAH sample), while the last sample was drawn after PAH was diagnosed (post-PAH sample) (Figure 3B). Combined analyses of these pre-PAH and post-PAH samples showed that the level of CCL21 was elevated prior to PAH diagnosis and remained stably elevated over time, even after initiation of PAH treatment (Figure 3B).

High CCL21 level and survival in SSc. Eighty-seven (29%) of 298 patients in the Oslo University Hospital SSc cohort and 16 (57%) of 28 patients in the Lund University Hospital SSc cohort died during the observation period; no causes of deaths were available. Patients with high CCL21 levels had reduced 5-year and 10-year cumulative survival compared with patients with low CCL21 levels (87% and 71% versus 96% and 91%, respectively [$P < 0.001$ by log rank test]). CCL21 (HR 2.1, 95% CI 1.21–3.70 [$P = 0.008$]) and age at onset (HR 1.1 95% CI 1.07–1.11 [$P < 0.001$]) were associated with mortality in univariate Cox proportional hazard analyses of the combined cohorts. We found that the model that included age (model 2) was superior to the model that included CCL21 (model 1) (C index 0.84 and 0.88, respectively).

DISCUSSION

There is an unmet need for biomarkers that allow for earlier detection of precapillary PH in patients with SSc. Here, we present data indicating the potential of CCL21 as a serum marker associated with early precapillary PH, with the strongest association with PAH, the predictive value for development of PAH, and progression of PAH. This observation may have implications for clinical practice, and it should contribute to new hypotheses about the immune mechanisms operative in SSc-associated cardiopulmonary involvement that certainly could include CCL21–CCR7 interactions.

From a clinical point of view, we believe that the observed ability of CCL21 to predict PAH development is of key importance. The results of the current study suggest that a high CCL21 level in patients with SSc is specific for PAH and could be integrated with other

known risk factors such as age, sex, the FVC:DLco ratio, and ACA status in an improved algorithm for earlier detection and diagnosis of PAH (9,18). The serial sample analyses showed that serum levels of CCL21 were elevated prior to the diagnosis of PAH, indicating that the CCL21 level may be useful as a marker used to predict the development of PAH, but validation studies in independent cohorts, and prospective studies in unselected patient cohorts, with repeat serum samplings from disease onset and onward, are required to fully elucidate its predictive value in SSc. Additionally, our findings indicate that the CCL21 level may be helpful in risk stratification at the time of PAH diagnosis, thereby aiding decisions regarding treatment.

Earlier studies of SSc-related PH, including DETECT, focused on PH markers, such as echocardiographic right-sided heart strain measures and NT-proBNP (10,11). Those studies provided valuable information but were designed to detect established PH and did not differentiate between the 2 major subtypes of SSc-related PH. Because of these limitations, there is an ongoing search for new markers linked to the pathogenesis of SSc-related PH. With the critical role of immune genes in SSc (44), and the body of evidence linking aberrant immune activation to PH development (14), the focus has been on markers with established or presumed immunologic functions. In 2014, van Bon et al reported that the CXCL4 level in plasma was highly elevated in patients with early diffuse cutaneous SSc and predicted the development of SSc-associated ILD and PAH (16). This report of an association with both ILD and PAH contrasts with the findings in the current study, in which we concluded, based on complete longitudinal data sets (i.e., paired PFTs and lung HRCTs) that CCL21 was not associated with ILD. Thus, it is likely that CXCL4 and CCL21 mark different immune pathways related to SSc-related PAH. Because most studies of potential SSc-related PAH markers have not included ILD analyses, we do not know whether the CCL21 level is unique as a selective PAH marker (15,17,45,46).

Interestingly, we observed that CCL21 levels were lower in patients with idiopathic PAH compared with those in patients with SSc-related PAH, indirectly supporting the notion that the mechanisms behind these PAH forms may differ (47). These data should, however, be cautiously interpreted, because the number of cases of idiopathic PAH was low. Moreover, the patients with idiopathic PAH were younger than the patients with SSc-related PAH.

Due to the links between CCR7–CCL21 and vascular inflammation, it is tempting to speculate that CCL21 could mark pathways linked to angiogenesis, inflammation, and vascular damage. This notion is supported by the staining pattern of SSc-related PAH we observed (data not shown), which indicated that CCL21, expressed on endothelial cells, could recruit CCR7-positive mononuclear cells to the vascular wall and induce inflammation. This concept was also supported by the fact that CCL21 was correlated with the CRP level and the ESR, both of which are mononuclear cell markers.

In contrast to other immune-mediated systemic diseases, SSc is more severe in patients with an older age at disease onset (1). This is also true for SSc-related PAH, in which older age at onset is a negative prognostic factor (9). In the current study, we observed an age-dependent increase in CCL21 levels in both patients with SSc and controls. Studies of age-associated immune dysregulation indicated that this age effect was physiologic (20,21,48), but because it occurred in a setting in which there was a clear impact of age, we needed expert statistical advice to handle it correctly. The favored solution was to apply separate models for CCL21 and age at onset (see Patients and Methods).

We observed that high CCL21 levels were associated with reduced survival but appeared to have less influence on mortality compared with age at onset. This minor impact of CCL21 on mortality probably reflects that PAH, even though it is an important mortality risk factor, accounts for only 12% of all SSc deaths in Norway (3).

The current study has major strengths. First, it was performed in a large SSc cohort with complete longitudinal data sets for ILD and PH/PAH, and serial serum samples were available for one-third of the patients. Second, the study included control populations and a replication cohort with comparable SSc characteristics. Third, due to the unique personal identification numbers in Norway and the official mortality statistics, we had no "loss to follow-up." The most important limitations were interindividual variations in disease duration and observational length, which were attributable to the cohort study design in which patients are included consecutively and then followed up annually. Also, the controls and SSc patients were not completely matched for age and sex. This may have had a minor effect on the cutoff value used to define the high CCL21 and low CCL21 subsets but had no impact on the data regarding PAH. Finally, the blood samples from the Oslo and Lund cohorts were obtained at 2 different sites, which could possibly influence the chemokine levels.

In conclusion, our results indicate that CCL21 has promise for predicting the risk of pulmonary vascular disease associated with SSc. The data also indicate that CCL21 may be part of a dysregulated immune pathway

that is operative in SSc and may be linked to the development of lung vascular damage. Further clinical and mechanistic studies are warranted to elucidate the roles of the CCR7–CCL21 axis in SSc.

AUTHOR CONTRIBUTIONS

All authors were involved in drafting the article or revising it critically for important intellectual content, and all authors approved the final version to be published. Dr. Hoffman-Vold had full access to all of the data in the study and takes responsibility for the integrity of the data and the accuracy of the data analysis.

Study conception and design. Hoffmann-Vold, Ueland, Aukrust, Molberg.
Acquisition of data. Hoffmann-Vold, Hesselstrand, Andreassen, Palchevskiy, Midtvedt, Garen, Belperio, Molberg.
Analysis and interpretation of data. Hoffmann-Vold, Fretheim, Brunborg, Molberg.

REFERENCES

1. Allanore Y, Simms R, Distler O, Trojanowska M, Pope J, Denton CP, et al. Systemic sclerosis. Nat Rev Dis Primers 2015;1:150–2.
2. Tyndall AJ, Bannert B, Vonk M, Airo P, Cozzi F, Carreira PE, et al. Causes and risk factors for death in systemic sclerosis: a study from the EULAR Scleroderma Trials and Research (EUSTAR) database. Ann Rheum Dis 2010;69:1809–15.
3. Hoffmann-Vold AM, Molberg O, Midtvedt O, Garen T, Gran JT. Survival and causes of death in an unselected and complete cohort of Norwegian patients with systemic sclerosis. J Rheumatol 2013;40:1127–33.
4. Rubio-Rivas M, Royo C, Simeón C, Corbella X, Fonollosa V. Mortality and survival in systemic sclerosis: systematic review and meta-analysis. Semin Arthritis Rheum 2014;44:208–19.
5. Le Pavec J, Girgis RE, Lechtzin N, Mathai SC, Launay D, Hummers LK, et al. Systemic sclerosis–related pulmonary hypertension associated with interstitial lung disease: impact of pulmonary arterial hypertension therapies. Arthritis Rheum 2011;63:2456–64.
6. Hoeper MM, Bogaard HJ, Condliffe R, Frantz R, Khanna D, Kurzyna M, et al. Definitions and diagnosis of pulmonary hypertension. J Am Coll Cardiol 2013;62 Suppl:D42–50.
7. Hassoun PM, Zamanian RT, Damico R, Lechtzin N, Khair R, Kolb TM, et al. Ambrisentan and tadalafil up-front combination therapy in scleroderma-associated pulmonary arterial hypertension. Am J Respir Crit Care Med 2015;192:1102–10.
8. Pulido T, Adzerikho I, Channick RN, Delcroix M, Galie N, Ghofrani HA, et al. Macitentan and morbidity and mortality in pulmonary arterial hypertension. N Engl J Med 2013;369:809–18.
9. Chaisson NF, Hassoun PM. Systemic sclerosis-associated pulmonary arterial hypertension. Chest 2013;144:1346–56.
10. Hao Y, Thakkar V, Stevens W, Morrisroe K, Prior D, Rabusa C, et al. A comparison of the predictive accuracy of three screening models for pulmonary arterial hypertension in systemic sclerosis. Arthritis Res Ther 2015;17:7.
11. Coghlan JG, Denton CP, Grunig E, Bonderman D, Distler O, Khanna D, et al. Evidence-based detection of pulmonary arterial hypertension in systemic sclerosis: the DETECT study. Ann Rheum Dis 2014;73:1340–9.
12. Khanna D, Gladue H, Channick R, Chung L, Distler O, Furst DE, et al. Recommendations for screening and detection of connective tissue disease–associated pulmonary arterial hypertension. Arthritis Rheum 2013;65:3194–201.
13. Pattanaik D, Brown M, Postlethwaite B, Postlethwaite A. Pathogenesis of systemic sclerosis. Front Immunol 2015;6:272.
14. Rabinovitch M, Guignabert C, Humbert M, Nicolls MR. Inflammation and immunity in the pathogenesis of pulmonary arterial hypertension. Circ Res 2014;115:165–75.
15. Affandi AJ, Radstake TR, Marut W. Update on biomarkers in systemic sclerosis: tools for diagnosis and treatment. Semin Immunopathol 2015;37:475–87.
16. Van Bon L, Affandi AJ, Broen J, Christmann RB, Marijnissen RJ, Stawski L, et al. Proteome-wide analysis and CXCL4 as a biomarker in systemic sclerosis. N Engl J Med 2014;370:433–43.
17. Becker MO, Kill A, Kutsche M, Guenther J, Rose A, Tabeling C, et al. Vascular receptor autoantibodies in pulmonary arterial hypertension associated with systemic sclerosis. Am J Respir Crit Care Med 2014;190:808–17.
18. Lefèvre G, Dauchet L, Hachulla E, Montani D, Sobanski V, Lambert M, et al. Survival and prognostic factors in systemic sclerosis–associated pulmonary hypertension: a systematic review and meta-analysis. Arthritis Rheum 2013;65:2412–23.
19. Chung L, Farber HW, Benza R, Miller DP, Parsons L, Hassoun PM, et al. Unique predictors of mortality in patients with pulmonary arterial hypertension associated with systemic sclerosis in the REVEAL registry. Chest 2014;146:1494–504.
20. Seidler S, Zimmermann HW, Bartneck M, Trautwein C, Tacke F. Age-dependent alterations of monocyte subsets and monocyte-related chemokine pathways in healthy adults. BMC Immunol 2010;11:30.
21. Shaw AC, Goldstein DR, Montgomery RR. Age-dependent dysregulation of innate immunity. Nat Rev Immunol 2013;13:875–87.
22. Comerford I, Harata-Lee Y, Bunting MD, Gregor C, Kara EE, McColl SR. A myriad of functions and complex regulation of the CCR7/CCL19/CCL21 chemokine axis in the adaptive immune system. Cytokine Growth Factor Rev 2013;24:269–83.
23. Lo JC, Chin RK, Lee Y, Kang HS, Wang Y, Weinstock JV, et al. Differential regulation of CCL21 in lymphoid/nonlymphoid tissues for effectively attracting T cells to peripheral tissues. J Clin Invest 2003;112:1495–505.
24. Larsen KO, Yndestad A, Sjaastad I, Loberg EM, Goverud IL, Halvorsen B, et al. Lack of CCR7 induces pulmonary hypertension involving perivascular leukocyte infiltration and inflammation. Am J Physiol Lung Cell Mol Physiol 2011;301:L50–9.
25. Bull TM, Coldren CD, Moore M, Sotto-Santiago SM, Pham DV, Nana-Sinkam SP, et al. Gene microarray analysis of peripheral blood cells in pulmonary arterial hypertension. Am J Respir Crit Care Med 2004;170:911–9.
26. Perros F, Dorfmuller P, Montani D, Hammad H, Waelput W, Girerd B, et al. Pulmonary lymphoid neogenesis in idiopathic pulmonary arterial hypertension. Am J Respir Crit Care Med 2012; 185:311–21.
27. Pickens SR, Chamberlain ND, Volin MV, Pope RM, Talarico NE, Mandelin AM II, et al. Role of the CCL21 and CCR7 pathways in rheumatoid arthritis angiogenesis. Arthritis Rheum 2012;64: 2471–81.
28. Halvorsen B, Dahl TB, Smedbakken LM, Singh A, Michelsen AE, Skjelland M, et al. Increased levels of CCR7 ligands in carotid atherosclerosis: different effects in macrophages and smooth muscle cells. Cardiovasc Res 2014;102:148–56.
29. Finsen AV, Ueland T, Sjaastad I, Ranheim T, Ahmed MS, Dahl CP, et al. The homeostatic chemokine CCL21 predicts mortality in aortic stenosis patients and modulates left ventricular remodeling. PLoS One 2014;9:e112172.
30. Hoffmann-Vold AM, Aaløkken TM, Lund MB, Garen T, Midtvedt Ø, Brunborg C, et al. Predictive value of serial high-resolution computed tomography analyses and concurrent lung function tests in systemic sclerosis. Arthritis Rheumatol 2015;67:2205–12.
31. Van den Hoogen F, Khanna D, Fransen J, Johnson SR, Baron M, Tyndall A, et al. 2013 classification criteria for systemic sclerosis: an American College of Rheumatology/European League Against Rheumatism collaborative initiative. Arthritis Rheum 2013;65:2737–47.
32. Hoffmann-Vold AM, Tennoe AH, Garen T, Midtvedt O, Abraityte A, Aalokken TM, et al. High level of chemokine CCL18 is associated with pulmonary function deterioration, lung fibrosis progression, and reduced survival in systemic sclerosis. Chest 2016;150:299–306.

33. Hesselstrand R, Wildt M, Ekmehag B, Wuttge DM, Scheja A. Survival in patients with pulmonary arterial hypertension associated with systemic sclerosis from a Swedish single centre: prognosis still poor and prediction difficult. Scand J Rheumatol 2011;40: 127–32.
34. Hoffmann-Vold AM, Midtvedt O, Molberg O, Garen T, Gran JT. Prevalence of systemic sclerosis in south-east Norway. Rheumatology (Oxford) 2012;51:1600–5.
35. Hansell D, Bankier A, MacMahon H, McLoud T, Muller N, Remy J. Fleischner Society: glossary of terms for thoracic imaging. Radiology 2008;246:697–722.
36. Quanjer PH, Tammeling GJ, Cotes JE, Pedersen OF, Peslin R, Yernault JC. Lung volumes and forced ventilatory flows. Report working party standardization of lung function tests, European Community for Steel and Coal. Official statement of the European Respiratory Society. Eur Respir J Suppl 1993; 16:5–40.
37. Hoffmann-Vold AM, Fretheim H, Midtvedt O, Kilian K, Angelshaug M, Chaudhary A, et al. Frequencies of borderline pulmonary hypertension before and after the DETECT algorithm: results from a prospective systemic sclerosis cohort. Rheumatology (Oxford) 2018;57:480–7.
38. Galie N, Humbert M, Vachiery JL, Gibbs S, Lang I, Torbicki A, et al. 2015 ESC/ERS guidelines for the diagnosis and treatment of pulmonary hypertension: the Joint Task Force for the Diagnosis and Treatment of Pulmonary Hypertension of the European Society of Cardiology (ESC) and the European Respiratory Society (ERS). Endorsed by: Association for European Paediatric and Congenital Cardiology (AEPC), International Society for Heart and Lung Transplantation (ISHLT). Eur Heart J 2016;37:67–119.
39. Gude E, Simonsen S, Geiran OR, Fiane AE, Gullestad L, Arora S, et al. Pulmonary hypertension in heart transplantation: discrepant prognostic impact of pre-operative compared with 1-year post-operative right heart hemodynamics. J Heart Lung Transplant 2010;29:216–23.
40. Sitbon O, Channick R, Chin KM, Frey A, Gaine S, Galie N, et al. Selexipag for the treatment of pulmonary arterial hypertension. N Engl J Med 2015;373:2522–33.
41. Beyer C, Distler JH, Allanore Y, Aringer M, Avouac J, Czirjak L, et al. EUSTAR biobanking: recommendations for the collection, storage and distribution of biospecimens in scleroderma research. Ann Rheum Dis 2011;70:1178–82.
42. Moons KG, Kengne AP, Woodward M, Royston P, Vergouwe Y, Altman DG, et al. Risk prediction models: I. Development, internal validation, and assessing the incremental value of a new (bio)-marker. Heart 2012;98:683–90.
43. The Criteria Committee of the New York Heart Association. Nomenclature and Criteria for Diagnosis of Diseases of the Heart and Great Vessels. 9th ed. Boston: Little Brown; 1994. p. 253–6.
44. Broen JC, Radstake TR, Rossato M. The role of genetics and epigenetics in the pathogenesis of systemic sclerosis. Nat Rev Rheumatol 2014;10:671–81.
45. Reiseter S, Molberg O, Gunnarsson R, Lund MB, Aalokken TM, Aukrust P, et al. Associations between circulating endostatin levels and vascular organ damage in systemic sclerosis and mixed connective tissue disease: an observational study. Arthritis Res Ther 2015;17:231.
46. Damico R, Kolb TM, Valera L, Wang L, Housten T, Tedford RJ, et al. Serum endostatin is a genetically determined predictor of survival in pulmonary arterial hypertension. Am J Respir Crit Care Med 2015;191:208–18.
47. Overbeek MJ, Vonk MC, Boonstra A, Voskuyl AE, Vonk-Noordegraaf A, Smit EF, et al. Pulmonary arterial hypertension in limited cutaneous systemic sclerosis: a distinctive vasculopathy. Eur Respir J 2009;34: 371–9.
48. Pawelec G, Goldeck D, Derhovanessian E. Inflammation, ageing and chronic disease. Curr Opin Immunol 2014;29:23–8.

ARTHRITIS & RHEUMATOLOGY
Vol. 70, No. 10, October 2018, pp 1654–1660
DOI 10.1002/art.40541

BRIEF REPORT

Whole-Exome Sequencing to Identify Rare Variants and Gene Networks That Increase Susceptibility to Scleroderma in African Americans

Pravitt Gourh,[1] Elaine F. Remmers,[2] Steven E. Boyden,[2] Theresa Alexander,[3] Nadia D. Morgan,[4] Ami A. Shah,[4] Maureen D. Mayes,[5] Ayo Doumatey,[2] Amy R. Bentley,[2] Daniel Shriner,[2] Robyn T. Domsic,[6] Thomas A. Medsger Jr.,[6] Virginia D. Steen,[7] Paula S. Ramos,[8] Richard M. Silver,[8] Benjamin Korman,[9] John Varga,[9] Elena Schiopu,[10] Dinesh Khanna,[10] Vivien Hsu,[11] Jessica K. Gordon,[12] Lesley Ann Saketkoo,[13] Heather Gladue,[14] Brynn Kron,[15] Lindsey A. Criswell,[15] Chris T. Derk,[16] S. Louis Bridges Jr.,[17] Victoria K. Shanmugam,[18] Kathleen D. Kolstad,[19] Lorinda Chung,[20] Reem Jan,[21] Elana J. Bernstein,[22] Avram Goldberg,[23] Marcin Trojanowski,[24] Suzanne Kafaja,[25] Kathleen M. Maksimowicz-McKinnon,[26] James C. Mullikin,[27] Adebowale Adeyemo,[2] Charles Rotimi,[2] Francesco Boin,[15] Daniel L. Kastner,[2] and Fredrick M. Wigley[4]

Objective. **Whole-exome sequencing (WES) studies in systemic sclerosis (SSc) patients of European American (EA) ancestry have identified variants in the *ATP8B4* gene and enrichment of variants in genes in the extracellular matrix (ECM)–related pathway that increase SSc susceptibility. This study was undertaken to evaluate the association of the *ATP8B4* gene and the ECM-related pathway with SSc in a cohort of African American (AA) patients.**

Methods. **SSc patients of AA ancestry were enrolled from 23 academic centers across the US under the Genome Research in African American Scleroderma Patients consortium. Unrelated AA individuals without serologic evidence of autoimmunity who were enrolled in the Howard University Family Study were used as unaffected controls. Functional variants in genes reported in the 2 WES studies in EA patients with SSc were selected for gene association**

Dr. Gourh is recipient of a Scientist Development award from the Rheumatology Research Foundation. Ms Morgan's work was supported by the NIH (National Institute of Arthritis and Musculoskeletal and Skin Diseases [NIAMS] grant T32-AR-048522) and the Rheumatology Research Foundation (Scientist Development award). Dr. Shah's work was supported by the NIH (NIAMS grant K23-AR-061439). Dr. Mayes' work was supported by NIAMS grant P50-AR-054144 from the Centers of Research Translation, NIH grants N01-AR-02251 and R01-AR-055258, and the Department of Defense Congressionally Directed Medical Research Program (grants W81XWH-07–1–011 and WX81XWH-13–1-0452). Dr. Ramos' work was supported by the NIH (grants K01-AR-067280, R03-AR-065801, and P60-AR-062755) and the South Carolina Clinical and Translational Research Institute (Medical University of South Carolina) through the NIH (grants UL1-RR-029882 and UL1-TR-000062). Dr. Silver's work was supported by the NIH (grant P60-AR-062755) and the South Carolina Clinical and Translational Research Institute (Medical University of South Carolina) through the NIH (grants UL1-RR-029882 and UL1-TR-000062). Dr. Khanna's work was supported by NIAMS grant K24-AR-063120. Dr. Shanmugam's work was supported by the NIH (grant R01-NR-013888 from the National Institute of Nursing Research), the Defense Advanced Research Projects Agency, and the Scleroderma Research Foundation. Dr. Boin's work was supported by the Nina Ireland Program for Lung Health.

[1]Pravitt Gourh, MD: NIAMS and National Human Genome Research Institute, NIH, Bethesda, Maryland; [2]Elaine F. Remmers, PhD, Steven E. Boyden, PhD, Ayo Doumatey, PhD, Amy R. Bentley, PhD, Daniel Shriner, PhD, Adebowale Adeyemo, MD, Charles Rotimi, PhD, Daniel L. Kastner, MD, PhD: National Human Genome Research Institute, NIH, Bethesda, Maryland; [3]Theresa Alexander, MS: NIAMS, NIH, Bethesda, Maryland; [4]Nadia D. Morgan, MBBS, MHS, Ami A. Shah, MD, MHS, Fredrick M. Wigley, MD: Johns Hopkins University School of Medicine, Baltimore, Maryland; [5]Maureen D. Mayes, MD, PhD: University of Texas McGovern Medical School, Houston; [6]Robyn T. Domsic, MD, MPH, Thomas A. Medsger Jr., MD: University of Pittsburgh, Pittsburgh, Pennsylvania; [7]Virginia D. Steen, MD: Georgetown University School of Medicine, Washington, DC; [8]Paula S. Ramos, PhD, Richard M. Silver, MD: Medical University of South Carolina, Charleston; [9]Benjamin Korman, MD, John Varga, MD: Northwestern University Feinberg School of Medicine, Chicago, Illinois; [10]Elena Schiopu, MD, Dinesh Khanna, MD, MSc: University of Michigan, Ann Arbor; [11]Vivien Hsu, MD: Robert Wood Johnson University, New Brunswick, New Jersey; [12]Jessica K. Gordon, MD, MSc: Hospital for Special Surgery, New York, New York; [13]Lesley Ann Saketkoo, MD, MPH: Tulane University School of Medicine, New Orleans, Louisiana; [14]Heather Gladue, DO: Arthritis and Osteoporosis Consultants of the Carolinas, Charlotte, North Carolina; [15]Brynn Kron, BS, Lindsey A. Criswell, MD, MPH, Francesco Boin, MD: University of California, San Francisco; [16]Chris T. Derk, MD, MS: University of Pennsylvania, Philadelphia; [17]S. Louis Bridges Jr., MD, PhD: University of Alabama at Birmingham; [18]Victoria K. Shanmugam, MD, MRCP: The George Washington University, Washington, DC; [19]Kathleen D. Kolstad, MD, PhD: Stanford University School of Medicine, Stanford, California; [20]Lorinda Chung, MD, MS: Stanford University School of Medicine, Stanford, California, and Palo Alto VA Health Care System, Palo Alto, California; [21]Reem Jan, MBBS: University of Chicago Pritzker School of Medicine, Chicago, Illinois; [22]Elana J. Bernstein, MD, MS: New York Presbyterian Hospital, Columbia University, New York, New York; [23]Avram Goldberg, MD: New York University Langone Medical Center, New York, New York; [24]Marcin Trojanowski, MD: Boston University School of Medicine,

testing using the optimized sequence kernel association test (SKAT-O) and pathway analysis by Ingenuity Pathway Analysis in 379 patients and 411 controls.

***Results*. Principal components analysis demonstrated that the patients and controls had similar ancestral backgrounds, with roughly equal proportions of mean European admixture. Using SKAT-O, we examined the association of individual genes that were previously reported in EA patients and none remained significant, including *ATP8B4* ($P = 0.98$). However, we confirmed the previously reported association of the ECM-related pathway with enrichment of variants within the *COL13A1*, *COL18A1*, *COL22A1*, *COL4A3*, *COL4A4*, *COL5A2*, *PROK1*, and *SERPINE1* genes (corrected $P = 1.95 \times 10^{-4}$).**

***Conclusion*. In the largest genetic study in AA patients with SSc to date, our findings corroborate the role of functional variants that aggregate in a fibrotic pathway and increase SSc susceptibility.**

Systemic sclerosis (SSc; scleroderma) is a chronic multisystem disease, characterized by fibrosis of the skin and internal organs, systemic vasculopathy, and autoimmunity. Compared with individuals of European American (EA) ancestry, African Americans (AA) in the US have a higher incidence and prevalence of SSc (1). SSc occurs at an earlier age in persons of AA descent compared to EA and is more likely to be manifested as diffuse skin involvement and the presence of anti–topoisomerase I or antifibrillarin antibodies—features that are associated with severe disease and a worse outcome (2). AA individuals are more likely to develop severe interstitial lung disease (ILD) or pulmonary arterial hypertension. This lung disease accounts for the major overall SSc-related deaths in all racial groups (3).

The etiology of SSc is unknown, but several environmental agents and genetic variants have been implicated. A strong role of genetic etiologic factors has been suggested by family studies in SSc, which have demonstrated an absolute risk of 1.6% in families as compared to 0.026% in the general population (4). Candidate gene, family-based, and genome-wide association studies (GWAS) investigating common variants, that have been conducted mostly in EA patients with SSc, have revealed autoimmune disease susceptibility loci that are not unique to SSc (5). These studies focused on common variants that have been able to only partially account for SSc heritability. Rare variants (minor allele frequency [MAF] <0.5%) and low-frequency variants (MAF 0.5–5%) have recently been implicated in several diseases and could account for a portion of the missing data on SSc heritability.

Recent reports suggest an increased burden of rare coding variants in genes and pathways of complex diseases beyond the common variants identified by GWAS (6,7). Various techniques used to identify genes with aggregation of deleterious variants include candidate gene Sanger sequencing for a hypothesis-driven approach. Next generation sequencing platforms, including whole-exome sequencing (WES) and whole-genome sequencing, provide hypothesis-neutral approaches. Gao et al (6) recently performed WES in 78 EA patients with SSc and found an enrichment in functional *ATP8B4* variants as compared to controls ($P = 2.77 \times 10^{-7}$). Furthermore, a single missense variant (rs55687265) was associated with SSc ($P = 9.35 \times 10^{-10}$), and when this variant was removed, the *ATP8B4* gene–based association was eliminated. Mak et al (7) performed WES in 32 EA patients with SSc, identifying 70 genes enriched for deleterious variants in the diffuse SSc subset; they reported significant enrichment of variants in the *COL4A3*, *COL4A4*, *COL5A2*, *COL13A1,* and *COL22A1* genes in the extracellular matrix (ECM)–related pathway ($P = 0.002$). Given the potential importance of the findings of these prior smaller WES studies in EA patients with SSc, we investigated their significance in a larger cohort of AA patients with SSc by performing WES gene and pathway-based association testing.

Our understanding of genetic susceptibility in AA patients with SSc is limited and restricted to HLA antigens, due to the lack of extensive studies in the AA population (8). The Genome Research in African American Scleroderma Patients (GRASP) consortium was created

Boston, Massachusetts; [25]Suzanne Kafaja, MD: David Geffen School of Medicine, University of California, Los Angeles; [26]Kathleen M. Maksimowicz-McKinnon, DO: Henry Ford Health System, Detroit, Michigan; [27]James C. Mullikin, PhD: National Human Genome Research Institute, NIH Intramural Sequencing Center, Rockville, Maryland.

Drs. Boin, Kastner, and Wigley contributed equally to this work.

Dr. Mayes has received consulting fees from Mitsubishi Tanabe, Astellas, Boehringer Ingelheim, Gerson Lehrman Group, Smart Analyst, and Guidepoint Global (less than $10,000 each). Dr. Domsic has received consulting fees from Eicos Sciences (less than $10,000). Dr. Khanna has received consulting fees from Actelion, Bristol-Myers Squibb, CSL Behring, Inventiva, EMD Merck-Serono, Sanofi-Aventis, GlaxoSmithKline, Corbus, Cytori, and UCB (less than $10,000 each), Bayer, Boehringer Ingelheim, Corbus, and Genentech-Roche (more than $10,000 each), and research support from Bayer, Bristol-Myers Squibb, and Pfizer, and owns stock or stock options in Eicos Sciences, Inc. (now CiViBioPharma, Inc.). Dr. Saketkoo has received consulting fees from Axon Pharma (less than $10,000). Dr. Gladue has received consulting fees from Pfizer, AbbVie, and Actelion (less than $10,000 each) and from Horizon Pharmaceuticals (more than $10,000). Dr. Derk has received research support from Gilead, Actelion, and Cytori. Dr. Shanmugam has received research support from AbbVie. Dr. Bernstein has received consulting fees from Genentech (less than $10,000).

Address correspondence to Pravitt Gourh, MD, National Institute of Arthritis and Musculoskeletal and Skin Diseases, National Human Genome Research Institute, NIH, Building 10, Room 5-SEN-3481, 10 Center Drive, Bethesda, MD 20892. E-mail: pravitt.gourh@nih.gov.

Submitted for publication March 6, 2018; accepted in revised form April 26, 2018.

to assemble a large cohort of AA patients with SSc in order to conduct systematic and comprehensive genetic studies. Within the cohort, 400 AA patients with SSc and 482 controls have undergone WES, and studies of select genes from the WES analysis are being replicated in an independent series for confirmation. Herein we present the results of our analyses for gene-level associations and pathway associations in genes that were previously reported in WES studies of 76 EA patients with SSc by Gao et al and 32 EA patients with SSc by Mak et al (6,7). We replicated a collective enrichment of coding and deleterious variants in genes of the fibrotic pathway in AA patients with SSc.

PATIENTS AND METHODS

Study population. AA patients with SSc were enrolled in the GRASP consortium from 23 academic centers in the US (see Supplementary Table 1, available on the *Arthritis & Rheumatology* web site at http://onlinelibrary.wiley.com/doi/10.1002/art.40541/abstract). Enrolled patients self-identified as African American. All patients met the 1980 American College of Rheumatology (ACR) or the 2013 ACR/European League Against Rheumatism classification criteria for SSc (9,10) or had at least 3 of the 5 features of CREST syndrome (calcinosis, Raynaud's phenomenon, esophageal dysmotility, sclerodactyly, telangiectasias) (11). Control samples were obtained from the Howard University Family Study, a population-based study of AA families and unrelated individuals enrolled in the Washington, DC metropolitan area (12). Only unrelated individuals were included as controls. Sera obtained from controls were tested for antinuclear antibodies (ANAs) by indirect immunofluorescence, and only those with a titer of <1:80 were included in this study. DNA was extracted from samples of whole blood or saliva.

Sequence analysis. WES was performed on 400 SSc and 482 control samples using SeqCap EZ Human Exome + UTR Probes (Roche), and libraries were sequenced on the HiSeq 2000 platform (Illumina) using 2 × 100-bp paired-end reads. WES data were analyzed using the computational resources of the NIH high-performance computing Biowulf cluster (http://hpc.nih.gov). Multiple variant and sample quality control filters were used prior to analyses (see Supplementary Methods, available on the *Arthritis & Rheumatology* web site at http://onlinelibrary.wiley.com/doi/10.1002/art.40541). The sequence data shown in this study are accessible from the Sequence Read Archive under the accession number SRP140756.

Identity by descent, admixture, and principal components analyses. Identity by descent analysis was performed using common variants (MAF >5%) from the sequence data after linkage disequilibrium (LD) pruning (r^2 <0.5) for estimating kinship coefficients. In order to remove familial relatedness, only 1 sample with the highest call rate was included from individuals with pi-hat >0.085. We used the ADMIXTURE software tool (13) and the 1000 Genomes populations as references for estimation of population admixture in our patients and controls. Principal components analysis (PCA) was used to estimate population stratification. A set of 35,280 markers (LD pruned [r^2 <0.5] and MAF >5%) was used to compute principal components and the top ten principal component eigenvalues were used to correct for population stratification using SNP & Variation Suite v8.7.1 (Golden Helix). Samples that clustered within the European cluster were removed from the analysis.

Statistical analysis. Gene-level testing was performed using an optimized sequence kernel association test (SKAT-O) with Madsen and Browning marker weighting and was corrected for ancestry using the top 10 principal components. Functional variants (missense, nonsense, and splice site) with a MAF of <0.05 present on 20 candidate genes as reported by Gao et al (6), and functional variants of all frequencies present on 87 genes from the diffuse disease and ILD subsets of SSc patients analyzed by Mak et al (7) were examined for association in the GRASP cohort (see Supplementary Figure 1, available on the *Arthritis & Rheumatology* web site at http://onlinelibrary.wiley.com/doi/10.1002/art.40541/abstract). In order to account for multiple gene testing, Bonferroni correction was applied for the total number of tests performed. This included 20 tests for the Gao et al study and 87 for the Mak et al study, which yielded *P* value significance thresholds of 0.0025 and 0.00057, respectively (6,7). Ingenuity Pathway Analysis (IPA) software was used to identify canonical pathways with all of the reported genes in the studies by Gao and colleagues and Mak and colleagues. *P* values for pathways were generated using Fisher's right-tailed exact test and were corrected for multiple testing using the Benjamini-Hochberg false discovery rate criterion.

RESULTS

Patient characteristics. A few controls (2.17%) were ANA+ (titer ≥1:80) and were excluded from the study. As we had hypothesized, there were more female subjects in the SSc cohort as compared to the control cohort (Table 1). Detailed sociodemographic, clinical, and serologic characteristics of the GRASP cohort have been reported by Morgan et al (11). In order to address population stratification, we performed PCA and plots showed that the patients and controls in the GRASP cohort were well-matched and that there was no major stratification at a global genomic level (Figure 1 and Supplementary

Table 1. Clinical and serologic characteristics of the African American patients with SSc and healthy controls*

	SSc patients (n = 379)	Healthy controls (n = 411)
Sex, male/female	64 (16.9)/315 (83.1)	217 (52.8)/194 (47.2)
SSc skin involvement		
Limited	166 (43.8)	–
Diffuse	188 (49.6)	–
Autoantibodies		
Anticentromere	44 (11.6)	–
Anti–topoisomerase I	107 (28.2)	–
Pulmonary arterial hypertension	73 (19.3)†	–
Interstitial lung disease	114 (30.1)‡	–

* Values are the number (%) of patients with systemic sclerosis (SSc) and unaffected controls.
† Data are based on right-sided heart catheterization.
‡ Data are based on computed tomography of the chest.

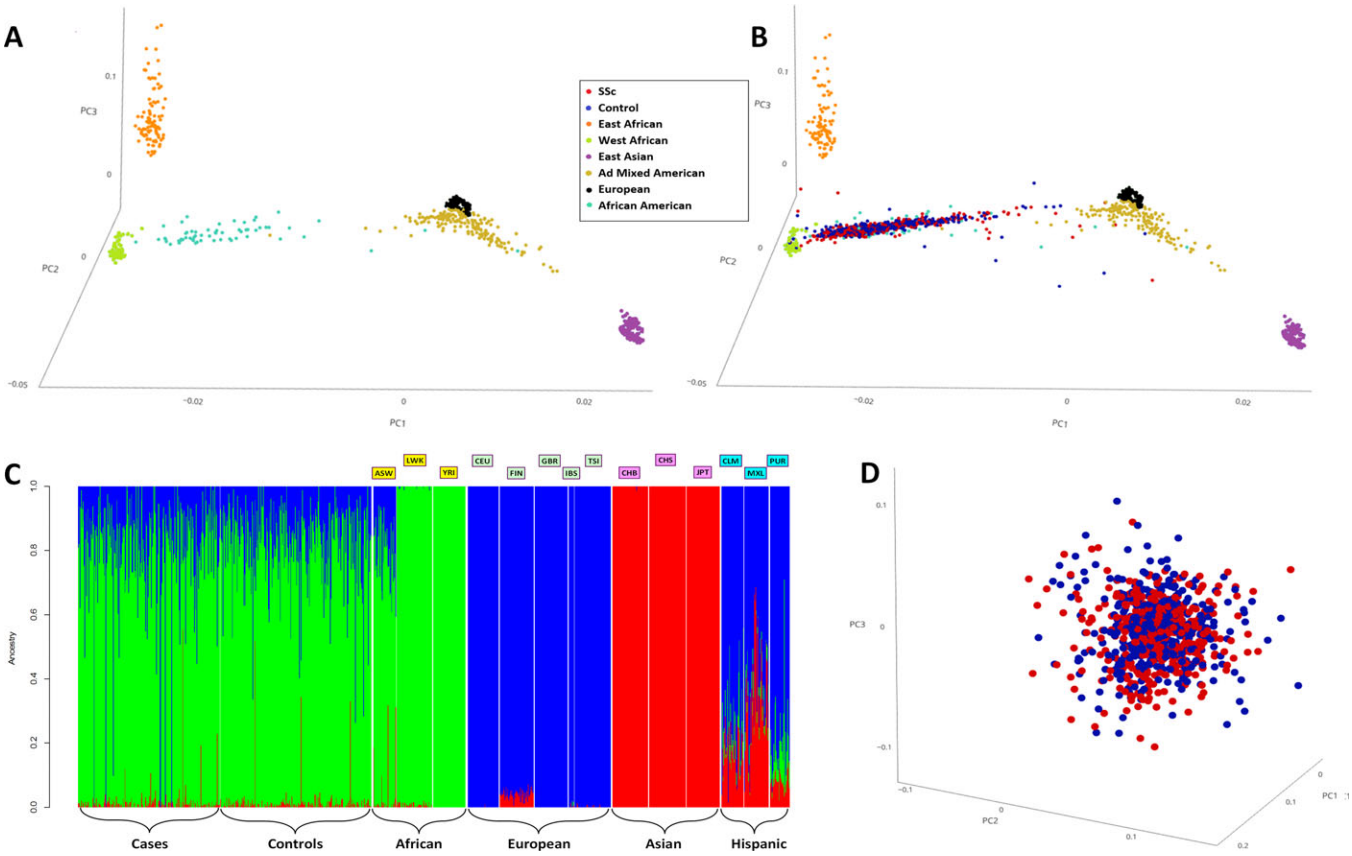

Figure 1. **A** and **B,** Three-dimensional principal components analysis (PCA) plots of the 1000 Genomes populations (**A**) and the 1000 Genomes populations along with the systemic sclerosis (SSc) patients and controls from the present study (**B**). Each dot represents an individual subject. Patients with SSc (red), controls (blue), Americans of admixture (Colombians from Medellin, Colombia [CLM], subjects of Mexican Ancestry from Los Angeles, California [MXL], and Puerto Ricans from Puerto Rico [PUR]) (gold), African Americans (light blue), East Africans (Luhya in Webuye, Kenya [LWK]) (orange), East Asians (Han Chinese in Beijing [CHB], Southern Han Chinese [CHS], and Japanese in Tokyo, Japan [JPT]) (purple), Europeans (Utah Residents of North and Western Europe ancestry [CEU], Finnish in Finland [FIN], British in England and Scotland [GBR], Iberian population in Spain [IBS], and Toscani in Italy [TSI]) (black), and West Africans (Yoruba in Ibadan, Nigeria [YRI]) (light green) are shown. **C**, Admixture plot of the 1000 Genomes populations along with the SSc patients and controls from the present study. Each individual subject is represented as a vertical bar. The y-axis depicts contributions from African (green), European (blue), Asian (red), and Hispanic ancestries. The results in cases and controls are similar to each other and similar to those in the Americans of African Ancestry in southwestern US (ASW) group from the 1000 Genomes project. **D**, Three-dimensional PCA with the top 3 principal components. Each dot represents an individual subject. Patients with SSc (red) and controls (blue) are shown.

Figures 2 and 3, available at http://online.library.wiley.com/doi/10.1002/art.40541/abstract).

Results of sequence analysis. A total of 400 SSc and 482 control exomes were sequenced using the same platform and were analyzed simultaneously. After filtration for quality control, 379 SSc cases and 411 controls remained and were used for further analysis (see Supplementary Methods, available at http://online.library.wiley.com/doi/10.1002/art.40541/abstract). An average of 90% of targeted bases produced high-confidence calls, and mean depth of coverage was 47× in the targeted region. The transition-to-transversion ratio for the coding region was 3.29, and the ratio for heterozygous-to-nonreference homozygous variants was 2.6.

PCA was performed for fine characterization of genetic ancestry. A 3-dimensional PCA plot depicted the AA patients to be spread between the West African and European clusters based on their degree of European admixture (Figures 1A and B, and Supplementary Figures 2 and 3, http://online.library.wiley.com/doi/10.1002/art.40541/abstract). The GRASP samples were closer to the West African cluster and distinct from the East African cluster, confirming West Africa as the main ancestral home of the AA patients. The admixture proportions in GRASP samples were similar to those in AA persons in the 1000 Genomes Project (Americans of African Ancestry in southwestern US), with major contributions from West African and European ancestries and a minor

contribution from Asian ancestry, likely representing Native American admixture (Figure 1C). The mean ± SD individual European admixture was 16.98 ± 12.4% in the SSc samples and 16.52 ± 11.7% in controls, and the difference was not statistically significant ($P = 0.59$, by *t*-test) (see Supplementary Figure 4, available at http://online.library.wiley.com/doi/10.1002/art.40541/abstract). The PCA plot also confirmed that the patients and controls were very ancestrally similar to each other (Figure 1D).

Gene-level analysis. All variants in the 20 genes, as described in the report by Gao and colleagues (6), were included for gene-level testing by SKAT-O with the top 10 principal components as covariates. The *ATP8B4* gene-level association reported in EA patients did not reach statistical significance in the GRASP cohort ($P = 0.98$) (see Supplementary Tables 2 and 3, available at http://online.library.wiley.com/doi/10.1002/art.40541/abstract). A missense variant (rs55687265), which was found to be the primary signal for association in the *ATP8B4* gene in the study by Gao et al (6), had similar frequency in the SSc patients and controls and was not statistically significant in the GRASP cohort ($P = 0.84$) (Supplementary Table 4, http://online.library.wiley.com/doi/10.1002/art.40541/abstract).

The 87 unique genes that were identified in the study by Mak and colleagues (7) were evaluated in the GRASP cohort by SKAT-O. For the *COL4A4* gene, the *P* value was 0.038, but this did not remain significant after correction for multiple testing (see Supplementary Table 5, available at http://online.library.wiley.com/doi/10.1002/art.40541/abstract). Upon examining the subset of SSc patients with diffuse disease, we discovered the *MSR1* gene ($P = 0.01$), and when evaluating the subset of SSc patients with ILD we identified the *ZNF492* gene ($P = 0.01$), the *FOLR3* gene ($P = 0.03$), and the *STAB1* gene ($P = 0.04$). After correction for multiple testing, however, these associations were not statistically significant (see Supplementary Tables 6 and 7, available at http://online.library.wiley.com/doi/10.1002/art.40541/abstract). The growth differentiation factor 2 gene (*GDF-2*) was reported by Mak et al to have a potential enrichment of variants by burden ratio (7) and was significant with an uncorrected *P* value of 0.00029 in the study by Gao et al (6). In the GRASP cohort this gene initially showed significance (uncorrected $P = 0.04$), but it did not remain significant after correction for multiple testing (see Supplementary Table 2, available at http://online.library.wiley.com/doi/10.1002/art.40541/abstract).

Pathway-based analysis. IPA was used to predict pathways enriched with gene variants. Gene-level association results from the SKAT-O analysis of the 20 genes from the study by Gao et al and the 87 genes from the study by Mak et al (6,7), in all SSc patients, were used for pathway prediction. None of the pathways that were predicted based on the gene list from the study by Gao and colleagues were statistically significant after correction for multiple testing. The hepatic fibrosis/hepatic stellate cell activation pathway, identified with IPA based on the gene list in the study by Mak and colleagues, comprised not only the *COL13A1, COL22A1, COL4A3, COL4A4,* and *COL5A2* genes, but additionally included the *COL18A1, PROK1,* and *SERPINE1* genes belonging to the same pathway (see Supplementary Table 8, available at http://online.library.wiley.com/doi/10.1002/art.40541/abstract). In the GRASP cohort, this was the only pathway that was statistically significant after correction for multiple testing (corrected $P = 1.95 \times 10^{-4}$) (Table 2). After correction for multiple testing, the hepatic fibrosis/hepatic stellate cell activation pathway was the only significant pathway in the subset of SSc patients with diffuse disease (Table 2).

Table 2. Pathway analysis of the candidate genes in the GRASP cohort*

Ingenuity pathway	*P*†	Corrected *P*‡
All SSc patients versus controls		
Hepatic fibrosis/hepatic stellate cell activation	2.09×10^{-6}	1.95×10^{-4}
Melatonin degradation III	0.005	0.22
Coagulation system	0.01	0.29
Complement system	0.01	0.29
Atherosclerosis signaling	0.02	0.34
Diffuse SSc subset of patients versus controls		
Hepatic fibrosis/hepatic stellate cell activation	2.27×10^{-6}	2.14×10^{-4}
Melatonin degradation III	0.005	0.22
Coagulation system	0.01	0.29
Complement system	0.01	0.29
Atherosclerosis signaling	0.02	0.36

* Data depict the top 5 pathways and results from the optimized sequence kernel association test of the 87 genes (from the study by Mak et al [7]) in all patients with systemic sclerosis (SSc) and in the diffuse SSc patient subset. The Ingenuity Pathway Analysis program was used for predicting pathways. GRASP = Genome Research in African American Scleroderma Patients.
† By Fisher's right-tailed exact test.
‡ Corrected for multiple testing using the Benjamini-Hochberg correction.

DISCUSSION

In this large cohort of AA patients with SSc, we examined the 20 candidate genes as identified by Gao et al and the 87 candidate genes as identified by Mak et al in their recent WES studies of EA patients with SSc (6,7). Despite having a much larger sample size than these original studies, we were unable to replicate the *ATP8B4* gene association or the rs55687265 variant in the *ATP8B4* gene in the present study. We were, however, able to replicate the association with the ECM-related pathway, but found no additional associations.

One of the greatest accomplishments achieved as a result of this investigation is the establishment of the GRASP cohort, which comprised a large sample of AA patients with SSc and controls with similar ancestral backgrounds. The GRASP cohort will serve as a valuable resource for future transethnic genomic studies in SSc.

Based on the genes reported as candidates for association in the study by Mak et al (7), pathway analysis in the GRASP cohort highlighted a fibrotic pathway that had enrichment of genes with functional variants involved in ECM biology. The gene list included several genes in the collagen family and genes involved in fibrinolysis and angiogenesis. The clustering of these genes into a fibrosis network corresponds to the excessive synthesis and deposition of ECM proteins observed in SSc and, thus, could be a potential candidate for targeted therapy. The *GDF2* gene (also known as bone morphogenetic protein 9) that was evaluated in the present study and identified in the studies by Gao et al and Mak et al (6,7) did not reach statistical significance after correction for multiple testing, but remains an interesting candidate gene involved in modulation of the ECM.

In the GRASP cohort, the ancestries of AA patients as well as the controls were primarily derived from West Africa, and on average the AA patients and controls had similar proportions of African, European, and Asian (likely Native American) descent. The patients and controls were recruited from different geographic locations in the US and, using PCA and the ADMIXTURE software tool, we were able to demonstrate that there was no major population stratification between the patients and controls.

Ancestry-specific associations have previously been identified in complex diseases. Similar to the *PADI4* gene association in Asians and the *PTPN22* gene association in Europeans with rheumatoid arthritis, it may be the case that there are differences in SSc susceptibility loci in different ancestral populations (14). The admixture of the AA population is a recent event in human admixture history and, as we have demonstrated, contains varying amounts of European and Asian ancestries. This difference in genetic architecture could explain the lack of association of the *ATP8B4* gene and the rs55687265 variant in AA patients with SSc.

In the original report of the association of the rs55687265 variant with scleroderma in EA patients by Gao and colleagues (6), the discovery set contained 78 patients in whom the likelihood of association was significant (odds ratio [OR] 6.11, $P = 9.35 \times 10^{-10}$) and the replication set had 415 patients in whom a significant association was found (OR 1.86, $P = 0.01$). Nevertheless, a recent study of 7,426 SSc patients and 13,087 controls of European ancestry was also unable to replicate the association with the rs55687265 variant (15). This underscores the importance of replication in genetics studies in large well-established cohorts to demonstrate reproducibility, provide a better estimate of effect size, and confirm that the original association is not due to unidentified biases present in a single study. We expect that, upon completion of the GRASP targeted resequencing and final analysis of ~400 genes, at least a few of these genes will show a statistically significant association with scleroderma and increase our understanding of molecular pathways involved in SSc pathogenesis.

ACKNOWLEDGMENT

We thank Dr. Kalpana Manthiram for critical reading of the manuscript.

AUTHOR CONTRIBUTIONS

All authors were involved in drafting the article or revising it critically for important intellectual content, and all authors approved the final version to be published. Dr. Gourh had full access to all of the data in the study and takes responsibility for the integrity of the data and the accuracy of the data analysis.

Study conception and design. Gourh, Remmers, Boin, Kastner, Wigley.

Acquisition of data. Gourh, Remmers, Morgan, Shah, Mayes, Doumatey, Bentley, Shriner, Domsic, Medsger, Steen, Ramos, Silver, Korman, Varga, Schiopu, Khanna, Hsu, Gordon, Saketkoo, Gladue, Kron, Criswell, Derk, Bridges, Shanmugam, Kolstad, Chung, Jan, Bernstein, Goldberg, Trojanowski, Kafaja, Maksimowicz-McKinnon, Mullikin, Adeyemo, Rotimi, Boin, Kastner, Wigley.

Analysis and interpretation of data. Gourh, Remmers, Boyden, Alexander.

REFERENCES

1. Mayes MD, Lacey JV Jr, Beebe-Dimmer J, Gillespie BW, Cooper B, Laing TJ, et al. Prevalence, incidence, survival, and disease characteristics of systemic sclerosis in a large US population. Arthritis Rheum 2003;48:2246–55.
2. Ioannidis JP, Vlachoyiannopoulos PG, Haidich AB, Medsger TA Jr, Lucas M, Michet CJ, et al. Mortality in systemic sclerosis: an international meta-analysis of individual patient data. Am J Med 2005;118:2–10.
3. Poudel DR, Jayakumar D, Danve A, Sehra ST, Derk CT. Determinants of mortality in systemic sclerosis: a focused review. Rheumatol Int 2017. E-pub ahead of print.
4. Arnett FC, Cho M, Chatterjee S, Aguilar MB, Reveille JD, Mayes MD. Familial occurrence frequencies and relative risks for systemic sclerosis (scleroderma) in three United States cohorts. Arthritis Rheum 2001;44:1359–62.
5. Radstake TR, Gorlova O, Rueda B, Martin JE, Alizadeh BZ, Palomino-Morales R, et al. Genome-wide association study of systemic sclerosis identifies CD247 as a new susceptibility locus. Nat Genet 2010;42:426–9.
6. Gao L, Emond MJ, Louie T, Cheadle C, Berger AE, Rafaels N, et al. Identification of rare variants in ATP8B4 as a risk factor for systemic sclerosis by whole-exome sequencing. Arthritis Rheumatol 2016;68:191–200.
7. Mak AC, Tang PL, Cleveland C, Smith MH, Connolly MK, Katsumoto TR, et al. Whole-exome sequencing for identification of potential causal variants for diffuse cutaneous systemic sclerosis. Arthritis Rheumatol 2016;68:2257–62.

8. Arnett FC, Gourh P, Shete S, Ahn CW, Honey RE, Agarwal SK, et al. Major histocompatibility complex (MHC) class II alleles, haplotypes and epitopes which confer susceptibility or protection in systemic sclerosis: analyses in 1300 Caucasian, African-American and Hispanic cases and 1000 controls. Ann Rheum Dis 2010;69:822–7.
9. Subcommittee for Scleroderma Criteria of the American Rheumatism Association Diagnostic and Therapeutic Criteria Committee. Preliminary criteria for the classification of systemic sclerosis (scleroderma). Arthritis Rheum 1980;23:581–90.
10. Van den Hoogen F, Khanna D, Fransen J, Johnson SR, Baron M, Tyndall A, et al. 2013 classification criteria for systemic sclerosis: an American College of Rheumatology/European League Against Rheumatism collaborative initiative. Arthritis Rheum 2013;65:2737–47.
11. Morgan ND, Shah AA, Mayes MD, Domsic RT, Medsger TA Jr, Steen VD, et al. Clinical and serological features of systemic sclerosis in a multicenter African American cohort: analysis of the genome research in African American scleroderma patients clinical database. Medicine (Baltimore) 2017;96:e8980.
12. Adeyemo A, Gerry N, Chen G, Herbert A, Doumatey A, Huang H, et al. A genome-wide association study of hypertension and blood pressure in African Americans. PLoS Genet 2009;5:e1000564.
13. Alexander DH, Novembre J, Lange K. Fast model-based estimation of ancestry in unrelated individuals. Genome Res 2009;19:1655–64.
14. Kochi Y, Suzuki A, Yamada R, Yamamoto K. Ethnogenetic heterogeneity of rheumatoid arthritis-implications for pathogenesis. Nat Rev Rheumatol 2010;6:290–5.
15. López-Isac E, Bossini-Castillo L, Palma AB, Assassi S, Mayes MD, Simeón CP, et al. Analysis of ATP8B4 F436L missense variant in a large systemic sclerosis cohort. Arthritis Rheumatol 2017;69:1337–8.

ARTHRITIS & RHEUMATOLOGY
Vol. 70, No. 10, October 2018, pp 1661–1672
DOI 10.1002/art.40533

Inhibitory Regulation of Skin Fibrosis in Systemic Sclerosis by Apelin/APJ Signaling

Yoko Yokoyama, Akiko Sekiguchi, Chisako Fujiwara, Akihiko Uchiyama, Akihito Uehara, Sachiko Ogino, Ryoko Torii, Osamu Ishikawa, and Sei-ichiro Motegi

Objective. **Apelin/APJ signaling has been determined to regulate cardiac and arterial fibrosis and to be involved in the pathogenesis of pulmonary arterial hypertension. Our objective was to elucidate the role of apelin in skin fibrosis in systemic sclerosis (SSc).**

Methods. **Expression of apelin/APJ in normal and SSc fibroblasts was compared. Effects of small interfering RNA depletion and the addition of apelin in fibroblasts were analyzed. The effect of apelin injections on bleomycin-induced dermal fibrosis in mice was investigated. We analyzed the effects of the biased agonist of APJ, MM07, on skin fibrosis in vitro and in vivo.**

Results. **The expression of apelin in SSc fibroblasts was significantly lower than that in normal fibroblasts. Serum apelin levels were negatively correlated with the modified Rodnan skin thickness score in SSc patients. Stimulation with transforming growth factor β1 (TGFβ1) inhibited apelin expression in fibroblasts, suggesting that activation of TGFβ1 signaling in SSc might be responsible for reduced apelin expression in SSc fibroblasts. Small interfering RNA depletion of apelin from fibroblasts significantly enhanced fibrosis-related gene expression, and treatment with apelin protein significantly inhibited TGFβ1 signaling in fibroblasts. Administration of apelin significantly inhibited bleomycin-induced dermal fibrosis in mice. We demonstrated that MM07 had greater potential than apelin to inhibit fibrosis in vivo and in vitro.**

Conclusion. **Collectively, TGFβ1 signaling and apelin signaling may counteract each other in the fibrotic process of SSc. Inhibitory regulation of TGFβ1-induced skin fibrosis by apelin/APJ signaling may be involved in the pathogenesis of SSc and could be a therapeutic target for fibrosis in SSc patients.**

Systemic sclerosis (SSc) is an autoimmune connective tissue disorder characterized by the development of fibrosis in the skin and internal organs as well as by vascular dysfunction, including Raynaud's phenomenon (RP), digital ulcers, and pulmonary arterial hypertension (PAH) (1–5). These complications account for the high morbidity and mortality of SSc patients. Although several treatments for vascular dysfunction are approved, there are no approved targeted therapies for fibrosis. Therefore, there is a great need for novel therapies for fibrosis.

The secreted protein apelin is a selective endogenous ligand of the G protein–coupled receptor APJ, and apelin/APJ signaling mainly regulates cardiovascular functions, fluid homeostasis, angiogenesis, and adipose tissue functions (6–13). Apelin expression is widely distributed in various peripheral tissues and is mainly produced by vascular endothelial cells (ECs), adipocytes, and epithelial cells (6–13). APJ is expressed ubiquitously, especially in ECs and vascular smooth muscle cells (VSMCs) (6–13).

Regarding the regulation of cardiovascular functions, it has been reported that apelin is secreted by ECs and pericytes and binds to APJ, resulting in the dilation of blood vessels and increased blood flow (9,10). Apelin/APJ signaling also regulates the parallel alignment of arteries and veins in the skin (11). Many studies have indicated the important roles of apelin/APJ signaling in the pathogenesis of cardiovascular diseases, including atherosclerosis, coronary heart disease, heart failure, hypertension, myocardial ischemia-reperfusion injury, and PAH (12–18). Recently, it has been reported that the expression of apelin in pulmonary arterial ECs in PAH patients was significantly reduced. In addition, the down-regulation of apelin/APJ signaling induced the inhibition of microRNA-424/503 (miR-424/503) and enhanced the expression of fibroblast

Supported by the Japan Society for the Promotion of Science (KAKENHI grant 26461459 to Ms Yokoyama).

Yoko Yokoyama, Akiko Sekiguchi, MD, Chisako Fujiwara, MD, Akihiko Uchiyama, MD, PhD, Akihito Uehara, MD, PhD, Sachiko Ogino, Ryoko Torii, Osamu Ishikawa, MD, PhD, Sei-ichiro Motegi, MD, PhD: Gunma University Graduate School of Medicine, Maebashi, Japan.

Address correspondence to Sei-ichiro Motegi, MD, PhD, Department of Dermatology, Gunma University Graduate School of Medicine, 3-39-22 Showa, Maebashi, Gunma 371-8511, Japan. E-mail: smotegi@gunma-u.ac.jp.

Submitted for publication March 6, 2017; accepted in revised form April 12, 2018.

growth factor 2 (FGF-2) and its receptor FGF receptor 1 (FGFR-1), resulting in EC and VSMC proliferation (12). It has also been reported that hypoxia-induced PAH was exacerbated in apelin-knockout mice (13). These findings suggest that decreased apelin expression in ECs is associated with the pathogenesis of PAH.

There is growing evidence that apelin is associated with tissue fibrosis. Interstitial fibrosis of the heart was enhanced in apelin-knockout mice with chronic pressure overload by surgical constriction of the aorta (14,15). Apelin/APJ signaling inhibited cardiac fibrosis by inhibiting transforming growth factor β (TGFβ) signaling (16,17). Also, it has been reported that administration of apelin significantly inhibited TGFβ-induced epithelial–mesenchymal transition and attenuated unilateral ureteral obstruction–induced renal tubulointerstitial fibrosis (19,20). In contrast, several studies showed that activated apelin/APJ signaling was associated with the initiation and maintenance of liver fibrosis (21,22).

With respect to the role of apelin in SSc, a recent study has shown that the prevalence of severe vascular involvement, including intractable skin ulcers, renal crisis, and PAH, was significantly higher in patients with elevated serum apelin levels in late stage SSc (>10 years), suggesting that apelin might be involved in the pathogenesis of vasculopathy in SSc (23). However, the roles of apelin in the development of skin fibrosis in SSc have not been fully investigated. In this study, we examined the association of serum apelin levels with clinical and laboratory features in SSc patients, the effect of small interfering RNA (siRNA) depletion of apelin and the effect of the addition of apelin on fibrosis in fibroblasts in vitro, and the effect of apelin injections on bleomycin-induced dermal fibrosis in mice. Furthermore, we examined the effect of the synthetic biased agonist of APJ, MM07 (24,25), on fibrosis in vitro and in vivo.

PATIENTS AND METHODS

Patients and clinical assessments. All SSc patients fulfilled the preliminary classification criteria of the American College of Rheumatology (ACR) (26) and the ACR/European League Against Rheumatism 2013 classification criteria (27). Sera were obtained from 67 Japanese patients with SSc (61 women, mean ± SD age 60 ± 2.3 years). Of these 67 patients, 41 had limited cutaneous SSc (lcSSc) and 26 had diffuse cutaneous SSc (dcSSc) according to the classification by LeRoy et al (28). Skin sclerosis was assessed using the modified Rodnan skin thickness score (MRSS) (29). We obtained human dermal fibroblasts from skin biopsy samples from the affected dorsal forearm areas of 5 dcSSc patients and 7 age-, race-, and sex-matched healthy volunteers. For immunohistochemical staining of apelin, we obtained human skin tissues from skin biopsy samples from the affected dorsal forearm areas of 11 dcSSc patients and 8 age-, race-, and sex-matched healthy volunteers. The study was approved by the institutional review board and the local research ethics committee of Gunma University. All of the patients and volunteers provided informed consent before participating in the study. This study was conducted according to the principles of the Declaration of Helsinki.

Interstitial lung disease (ILD) was defined as the presence of bibasilar interstitial fibrosis or a ground-glass shadow on high-resolution computed tomography scans. PAH was defined as an elevated right ventricular systolic pressure (>35 mm Hg) as assessed by echocardiography and subsequently as an elevated mean pulmonary artery pressure (>25 mm Hg) as assessed by cardiac catheterization.

Cell culture. Human dermal fibroblasts were cultured in Dulbecco's modified Eagle's medium (DMEM) and 10% fetal bovine serum and were used before passage 8.

Reverse transcription–polymerase chain reaction (RT-PCR) analysis. Human dermal fibroblasts were incubated in DMEM with or without [Pyr^1]-Apelin-13 (Tocris), MM07 (cyclo [1-6]CRPRLCHKGPMPF; synthesized by Sigma-Aldrich) (25), or recombinant human TGFβ1 (R&D Systems) for the indicated periods of time. To examine the effect of apelin on production of TGFβ1-induced α-smooth muscle actin (α-SMA), collagen α1(I), tissue inhibitor of metalloproteinases 1 (TIMP-1), and sphingosine kinase 1 (SPK-1), the cells were pretreated with apelin or MM07 for 60 minutes and then stimulated with TGFβ1 (1 ng/ml) for 24 hours. Total RNA was isolated by RNeasy Mini Kits (Qiagen) and analyzed by quantitative RT-PCR (qRT-PCR) (for further details, see Supplementary Patients and Methods, available on the *Arthritis & Rheumatology* web site at http://onlinelibrary.wiley.com/doi/10.1002/art.40533/abstract).

To inhibit the expression of apelin, siRNA specific for human apelin messenger RNA (mRNA) was designed by and purchased from Thermo Fisher Scientific. Human dermal fibroblasts (5×10^5 cells per 60-mm plate) were transfected with 10 n*M* apelin siRNA or AllStars negative control siRNA (Qiagen) using HiPerFect Transfection Reagent (Qiagen). After 48 hours, apelin, α-SMA, collagen α1(I), TIMP-1, SPK-1, TGFβ1, connective tissue growth factor (CTGF), and 18S mRNA levels were assessed by qRT-PCR.

Histochemical and immunofluorescence staining. Dermal fibroblasts from SSc patients or normal individuals were seeded in 8-well culture slides (BD Biosciences). Cells were then either left untreated or treated with TGFβ1 (1 ng/ml) and [Pyr^1]-Apelin-13 (100 n*M*) or MM07 (10 n*M*) for 24 hours and fixed in 4% paraformaldehyde (PFA) in phosphate buffered saline (PBS) at room temperature for 1 hour. Frozen sections (4-μm thick) of human skin were also fixed in 4% PFA. After being blocked with 3% skim milk–PBS supplemented with 5% normal goat serum for 30 minutes at room temperature, cells were stained with rabbit anti-apelin antibody (Santa Cruz Biotechnology), rabbit anti-human APJ antibody (Abcam), anti–α-SMA antibody (Sigma), and anti–fibroblast surface protein antibody (Abcam) followed by Alexa Fluor 488– or Alexa Fluor 568–conjugated secondary antibodies (Invitrogen). Cells were mounted in ProLong Gold antifade reagent (Invitrogen). Quantification of the amount of staining was performed using ImageJ software version 1.46r (National Institutes of Health).

Next, 4-μm–thick sections of mouse skin tissue embedded in paraffin were stained with hematoxylin and eosin or Masson's trichrome. Skin fibrosis was quantified by measuring the thickness of the dermis, which was defined as the distance

from the epidermal–dermal junction to the dermal–subcutaneous junction, at 6 randomly selected microscopic fields. For immunohistochemical staining, tissue sections of human or mouse skin were treated for antigen retrieval with a pressure cooker for 10 minutes at 121°C. After blocking using Peroxidase Blocking (Dako) for 5 minutes and Protein Block (Dako) for 10 minutes, the sections were incubated with rabbit anti-apelin antibody, anti–α-SMA antibody, anti-CD3 antibody (Abcam), anti-CD68 antibody (AbD Serotec), and anti-CD31 antibody (Abcam). After washing, the sections were incubated with a horseradish peroxidase–labeled polymer-conjugated secondary antibody (ENVISION+; Dako). Finally, color was developed with 3,3′-diaminobenzidine tetrahydrochloride.

Western blotting. Western blot analyses were performed according to previously described protocols (30). To examine the effect of apelin or MM07 on TGFβ1-induced α-SMA or collagen α1(I) production, cells were pretreated with [Pyr^1]-Apelin-13 (100 n*M*) or MM07 (10 n*M*) for 60 minutes and then stimulated with TGFβ1 (1 ng/ml) for 48 hours. To examine the effect of apelin or MM07 on TGFβ1-induced phosphorylated Smad2/3, cells were pretreated with [Pyr^1]-Apelin-13 (100 n*M*) or MM07 (10 n*M*) for 60 minutes and then stimulated with TGFβ1 (1 ng/ml) for 3 hours (for further details, see Supplementary Patients and Methods, http://onlinelibrary.wiley.com/doi/10.1002/art.40533/abstract).

Bleomycin-induced skin fibrosis model. Dermal fibrosis was induced in 8-week-old C57BL/6 mice with injections of bleomycin. Injections of 300 μl of bleomycin (Nippon Kayaku) at a concentration of 1 mg/ml were given 5 times per week for 2 weeks as previously described (31,32). Injections of 300 μl of PBS were used as controls for treatment with bleomycin. To examine the effect of apelin, mice received intraperitoneally [Pyr^1]-Apelin-13 (0.1 μmoles/kg/day) dissolved in 100 μl of PBS or PBS alone 5 times per week for 2 weeks. To examine the effect of MM07, mice received intraperitoneally MM07 (0.01 μmoles/kg/day) dissolved in 100 μl of PBS or PBS alone 5 times per week for 2 weeks. In the therapeutic model, apelin or MM07 intraperitoneal injection was initiated 7 days after starting bleomycin treatment. C57BL/6 mice were purchased from Japan SLC. Mice were maintained in the Institute of Experimental Animal Research of Gunma University under specific pathogen–free conditions. All experiments were approved by the Gunma University Animal Care and Experimentation Committee and carried out in accordance with approved guidelines.

Measurement of serum apelin concentration. A specific enzyme-linked immunosorbent assay (ELISA) kit for human apelin-36 (Phoenix Pharmaceuticals) was used for measuring serum apelin levels. This ELISA kit has cross-reactivity with human apelin-12 and apelin-13; therefore, the summation of serum human apelin-12, apelin-13, and apelin-36 was measured.

Statistical analysis. *P* values were calculated by Student's *t*-test or one-way analysis of variance followed by Bonferroni post hoc test for multiple comparisons. A chi-square analysis was used to compare frequencies. Spearman's rank correlation coefficients were used to examine the relationship with clinical data between 2 continuous variables. Values are reported as the mean ± SEM, and numbers of experiments are indicated.

RESULTS

Significantly lower expression of apelin in SSc fibroblasts than in normal fibroblasts. We first examined the expression of apelin and APJ in the skin tissue and dermal fibroblasts from SSc patients and normal individuals. The mRNA levels of apelin in the whole-skin tissue, including epidermis and dermis from affected skin lesions in SSc patients, were significantly reduced compared with those in normal individuals (Figure 1A). Next, we examined the expression and distribution of apelin in the skin in normal individuals and SSc patients. The summary of the quantification of apelin staining in 11 SSc patients and 8 normal individuals is provided in Supplementary Table 1 (http://onlinelibrary.wiley.com/doi/10.1002/art.40533/abstract), and representative results are shown in Figure 1B. Immunohistochemical staining of apelin in dermal fibroblasts from SSc patients was reduced compared with that in those from normal individuals (Figure 1B; also see Supplementary Table 1). Staining of apelin in dermal small vessels from SSc patients was also reduced (Figure 1B; also see Supplementary Table 1). We also determined that apelin was expressed in CD31+ ECs and fibroblast surface protein–positive cells (which may be fibroblasts in the dermis) by immunofluorescence staining (see Supplementary Figure 1, http://onlinelibrary.wiley.com/doi/10.1002/art.40533/abstract).

Consistent with these findings, mRNA levels of apelin in SSc fibroblasts were significantly reduced compared with those in normal fibroblasts (Figure 1C). Furthermore, protein levels of apelin in SSc fibroblasts were significantly reduced (Figures 1D and E). Messenger RNA levels for the receptor of apelin, APJ, in normal and SSc fibroblasts were not changed (Figure 1F). We confirmed that the production of α-SMA, collagen α1(I), and TIMP-1 in SSc fibroblasts was significantly higher than that in normal fibroblasts (see Supplementary Figure 2, http://onlinelibrary.wiley.com/doi/10.1002/art.40533/abstract). These results suggest that suppression of apelin production in dermal fibroblasts might be associated with the pathogenesis of fibrosis in SSc.

Association of decreased serum apelin levels with skin sclerosis and peripheral vasculopathy in SSc patients. To examine the association of serum apelin levels with skin sclerosis and other clinical features, such as peripheral vascular disorder, we examined serum apelin levels in 67 SSc patients. We determined that serum apelin levels were negatively correlated with the MRSS in SSc patients (Figure 1G). In addition, we determined that serum apelin levels were negatively correlated with the MRSS in both early (<3 years, 10 patients) and late (≥10 years, 36 patients) stages of SSc ($P < 0.05$ for the early stage; $P < 0.01$ for the late stage) (see Supplementary Figure 3A, http://onlinelibrary.wiley.com/doi/10.1002/art.40533/abstract). Serum apelin levels did not differ between the early, middle, and late stages of the disease (see Supplementary Figure 3B) or between lcSSc and dcSSc (see Supplementary Figure 3C).

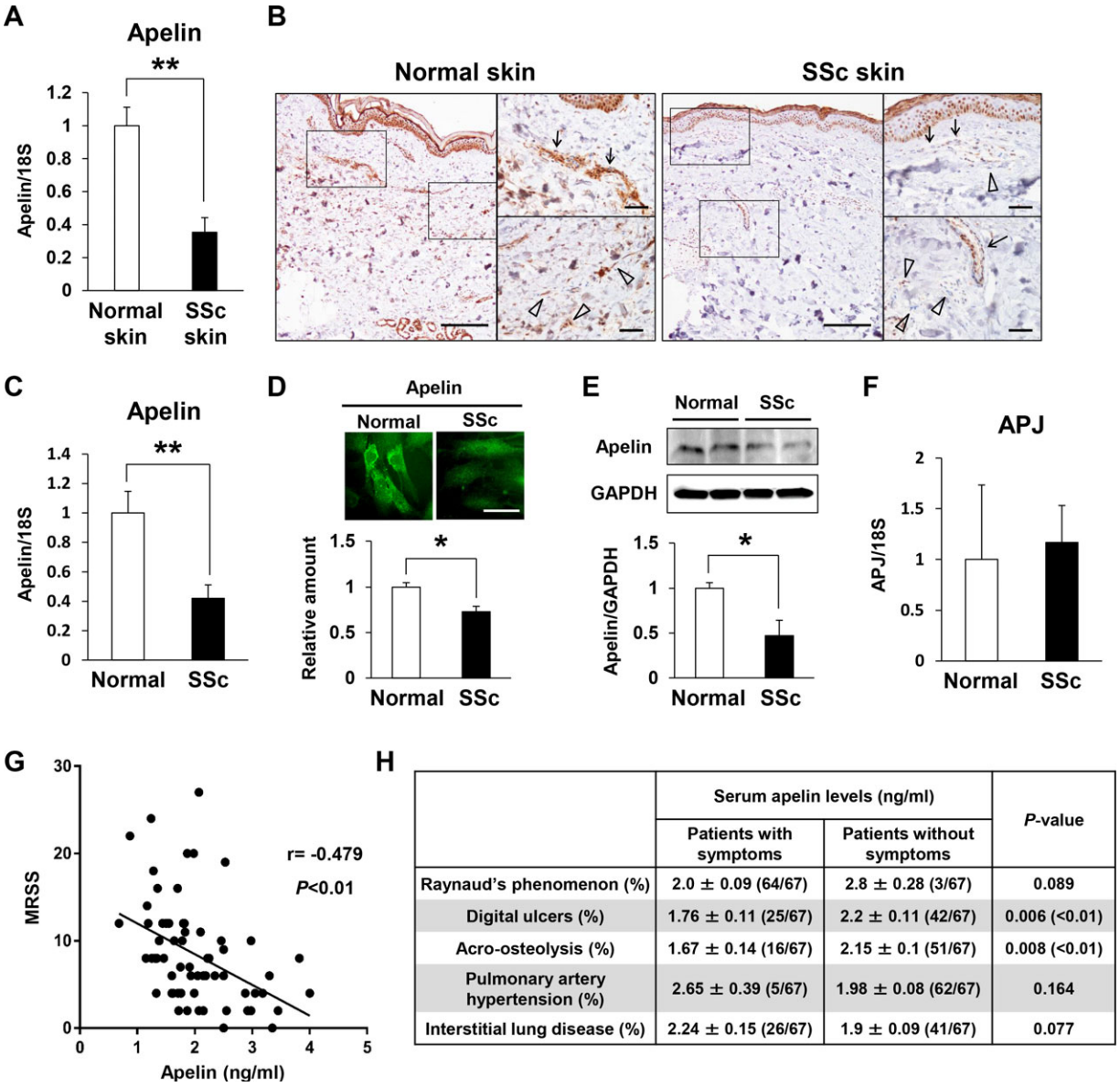

H

	Serum apelin levels (ng/ml)		*P*-value
	Patients with symptoms	Patients without symptoms	
Raynaud's phenomenon (%)	2.0 ± 0.09 (64/67)	2.8 ± 0.28 (3/67)	0.089
Digital ulcers (%)	1.76 ± 0.11 (25/67)	2.2 ± 0.11 (42/67)	0.006 (<0.01)
Acro-osteolysis (%)	1.67 ± 0.14 (16/67)	2.15 ± 0.1 (51/67)	0.008 (<0.01)
Pulmonary artery hypertension (%)	2.65 ± 0.39 (5/67)	1.98 ± 0.08 (62/67)	0.164
Interstitial lung disease (%)	2.24 ± 0.15 (26/67)	1.9 ± 0.09 (41/67)	0.077

Figure 1. Expression of apelin in systemic sclerosis (SSc) and normal fibroblasts, and serum apelin levels in SSc patients. **A,** Apelin mRNA in skin tissue from 4 healthy individuals and 6 SSc patients, determined using quantitative reverse transcription–polymerase chain reaction. ** = $P < 0.01$. **B,** Representative immunohistochemical staining of apelin in skin from SSc patients and normal individuals. Boxed areas in left panels are shown at higher magnification in right panels, which exhibit representative dermal small vessels (**arrows**) and dermal fibroblasts (**arrowheads**). Bars = 200 μm in left panels; 50 μm in right panels. **C** and **F,** Apelin mRNA levels (**C**) and APJ mRNA levels (**F**) in fibroblasts from 5 healthy individuals and 6 SSc patients. ** = $P < 0.01$. **D,** Expression of apelin in normal and SSc fibroblasts by immunofluorescence staining. Bar = 50 μm. Values are from 10 randomly chosen fibroblasts from 3 normal individuals and 3 SSc patients. * = $P < 0.05$. **E,** Apelin expression in 2 normal and 2 SSc fibroblasts by immunoblotting. Quantification of relative levels of apelin (normalized to GAPDH) was accomplished via densitometry using ImageJ software (National Institutes of Health) (n = 5 donors in each group). * = $P < 0.05$. **G,** Correlation of serum apelin levels with modified Rodnan skin thickness score (MRSS) in SSc patients. **H,** Association of serum apelin levels with clinical symptoms and organ involvement in 67 SSc patients. Values in **A**, **C–F**, and **H** are the mean ± SEM.

We also found that serum apelin levels in SSc patients with digital ulcers were significantly lower than those in patients without digital ulcers (mean ± SEM 1.76 ± 0.11 ng/ml versus 2.2 ± 0.11 ng/ml; $P < 0.01$) (Figure 1H). Serum apelin levels in SSc patients with acro-osteolysis (resorption of the terminal tuft of the digit) were also significantly lower than those in patients without acro-osteolysis (mean ± SEM 1.67 ± 0.14 ng/ml

versus 2.15 ± 0.1 ng/ml; $P < 0.01$) (Figure 1H). In contrast, serum apelin levels did not differ significantly between patients with and those without RP, PAH, and ILD. These results suggest that decreased serum apelin levels might be associated with skin sclerosis and peripheral vasculopathy, such as digital ulcers and acro-osteolysis, in SSc patients.

TGFβ1 stimulation–induced decreased apelin synthesis in fibroblasts. Next, we assessed the effects of TGFβ1 on apelin expression in normal and SSc fibroblasts. Apelin mRNA expression was significantly inhibited by TGFβ1 stimulation in a dose-dependent manner in normal and SSc fibroblasts (Figures 2A and B). In addition, levels of apelin protein were significantly decreased by TGFβ1 treatment in normal and SSc fibroblasts (Figures 2A and B). In contrast, APJ expression on the surface of normal and SSc fibroblasts was not changed by TGFβ1 stimulation (Figure 2C). These results suggest that activation of TGFβ1 signaling in SSc might be responsible for reduced apelin mRNA and protein expression in SSc fibroblasts.

Enhanced expression of α-SMA, collagen α1(I), and SPK-1 in fibroblasts resulting from siRNA depletion of apelin. Next, we analyzed the effects of siRNA depletion of apelin in normal fibroblasts (Figure 3). The expression of apelin mRNA in normal fibroblasts treated with siRNA specific for apelin was reduced by ~80% compared with that in fibroblasts treated with control siRNA. Small interfering RNA depletion of apelin significantly enhanced α-SMA and collagen α1(I) expression in normal fibroblasts. It has been reported that TGFβ1 induced the expression of α-SMA and TIMP-1 via SPK-1 in dermal fibroblasts

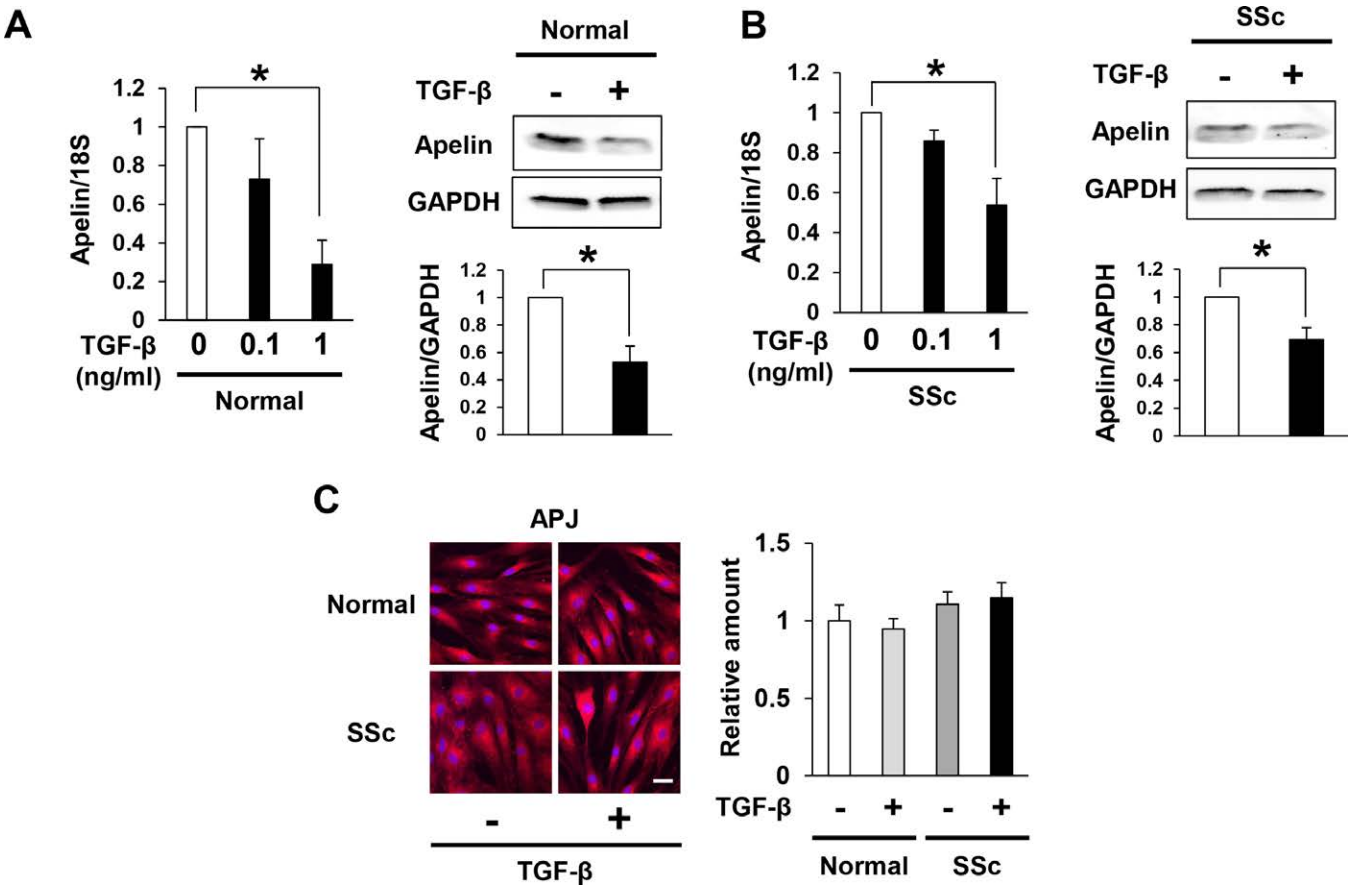

Figure 2. Decreased apelin synthesis in fibroblasts induced by stimulation with transforming growth factor β1 (TGFβ1). **A,** Apelin mRNA levels (left) and protein levels (right) in normal fibroblasts that were either left untreated or treated with TGFβ1. **B,** Apelin mRNA levels (left) and protein levels (right) in systemic sclerosis (SSc) fibroblasts that were either left either untreated or treated with TGFβ1. Values are the mean ± SEM from 3 experiments, relative to mRNA levels in fibroblasts not treated with TGFβ1. Quantification of relative levels of apelin (normalized to GAPDH protein levels) was accomplished via densitometry using ImageJ software (National Institutes of Health) (n = 3 donors in each group). The level of apelin in untreated normal or SSc fibroblasts was assigned a value of 1. * = $P < 0.05$. **C,** APJ staining in normal and SSc fibroblasts that were either left untreated or treated with TGFβ1. Bar = 50 μm. Values are the mean ± SEM from 10 randomly chosen fibroblasts from 3 normal individuals and 3 SSc patients.

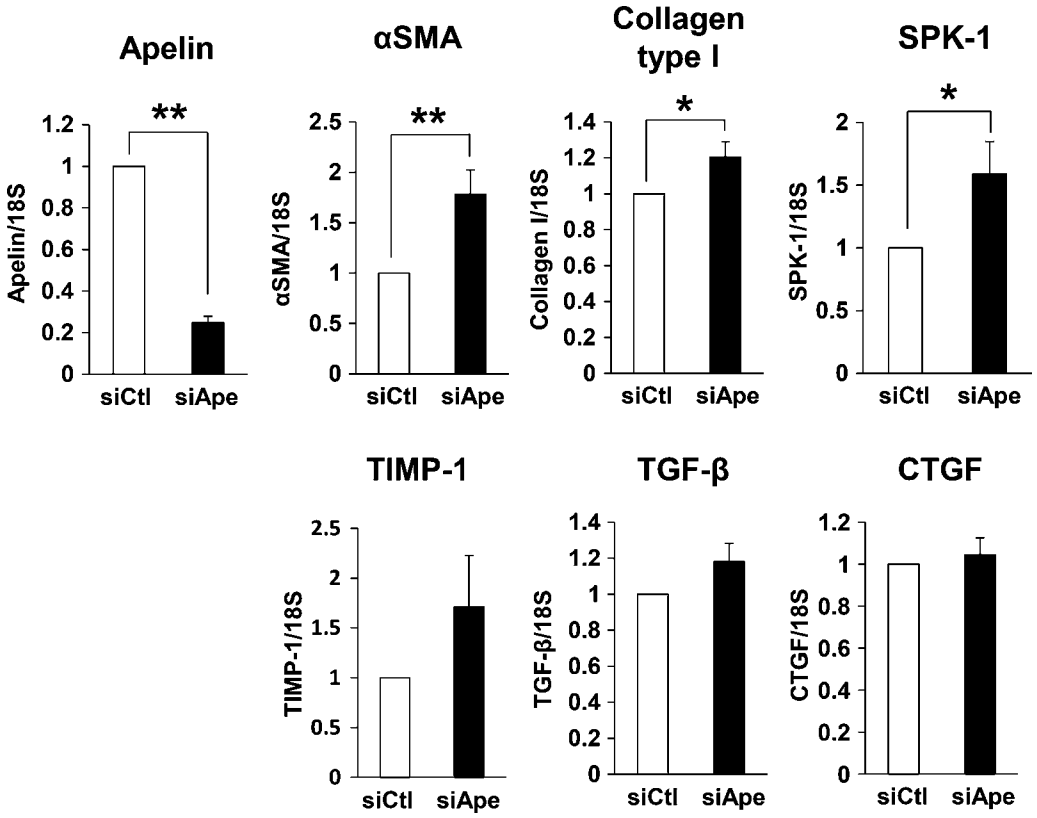

Figure 3. Small interfering RNA (siRNA) depletion of apelin enhances expression of α-smooth muscle actin (α-SMA), collagen α1(I), and sphingosine kinase 1 (SPK-1) in fibroblasts. Shown are levels of mRNA for apelin, α-SMA, collagen α1(I), SPK-1, tissue inhibitor of metalloproteinases 1 (TIMP-1), transforming growth factor β1 (TGFβ1), and connective tissue growth factor (CTGF) in control siRNA (siCtl)–treated and apelin siRNA (siApe)–treated normal fibroblasts, determined using quantitative reverse transcription–polymerase chain reaction. Quantification was normalized to 18S ribosomal RNA levels. Values are the mean ± SEM from 7 experiments using fibroblasts from 7 different donors, relative to levels of mRNA in control siRNA–treated fibroblasts. * = $P < 0.05$; ** = $P < 0.01$.

(33,34). We found that siRNA depletion of apelin significantly enhanced SPK-1 expression in normal fibroblasts. TIMP-1 mRNA expression in fibroblasts tended to be enhanced by siRNA depletion of apelin. These results suggest that apelin might have an inhibitory effect on mRNA expression of fibrosis-related genes in dermal fibroblasts.

Apelin inhibition of TGFβ1/Smad signaling and of TGFβ1-induced overexpression of α-SMA, collagen α1(I), TIMP-1, and SPK-1 in fibroblasts. To assess the inhibitory effect of apelin on fibrosis, we analyzed the effects of adding apelin ([Pyr^1]-Apelin-13) to fibroblasts. TGFβ1-induced α-SMA, collagen α1(I), TIMP-1, and SPK-1 mRNA overexpression in normal fibroblasts was inhibited by the addition of apelin in a dose-dependent manner (Figures 4A–D). TGFβ1-induced α-SMA and collagen α1(I) protein expression was also inhibited by the addition of apelin, as shown by Western blot (Figure 4E) and immunofluorescence staining (Figure 4G). In addition, the expression of collagen α1(I), α-SMA, CTGF, and TIMP-1 in SSc fibroblasts was also inhibited by the addition of apelin (see Supplementary Figure 4, http://onlinelibrary.wiley.com/doi/10.1002/art.40533/abstract).

It has been known that TGFβ1 induces α-SMA, collagen α1(I), SPK-1, and TIMP-1 production via phosphorylated Smad2/3 (33–36). We found that TGFβ1-induced phosphorylated Smad2/3 was inhibited by the addition of apelin (Figure 4F). The expression of TGFβ receptor types I and II was not changed by addition of apelin (see Supplementary Figure 5, http://onlinelibrary.wiley.com/doi/10.1002/art.40533/abstract). Administration of apelin did not affect the proliferation of fibroblasts (see Supplementary Figure 6A, http://onlinelibrary.wiley.com/doi/10.1002/art.40533/abstract), which suggests that there might be no toxicity of apelin in vitro. These results suggest that apelin might have an inhibitory action against TGFβ1-induced skin fibrosis.

Significant inhibition of bleomycin-induced dermal fibrosis in mice by apelin administration. Next, we examined the effect of apelin injections on bleomycin-induced dermal fibrosis in mice. Mice with

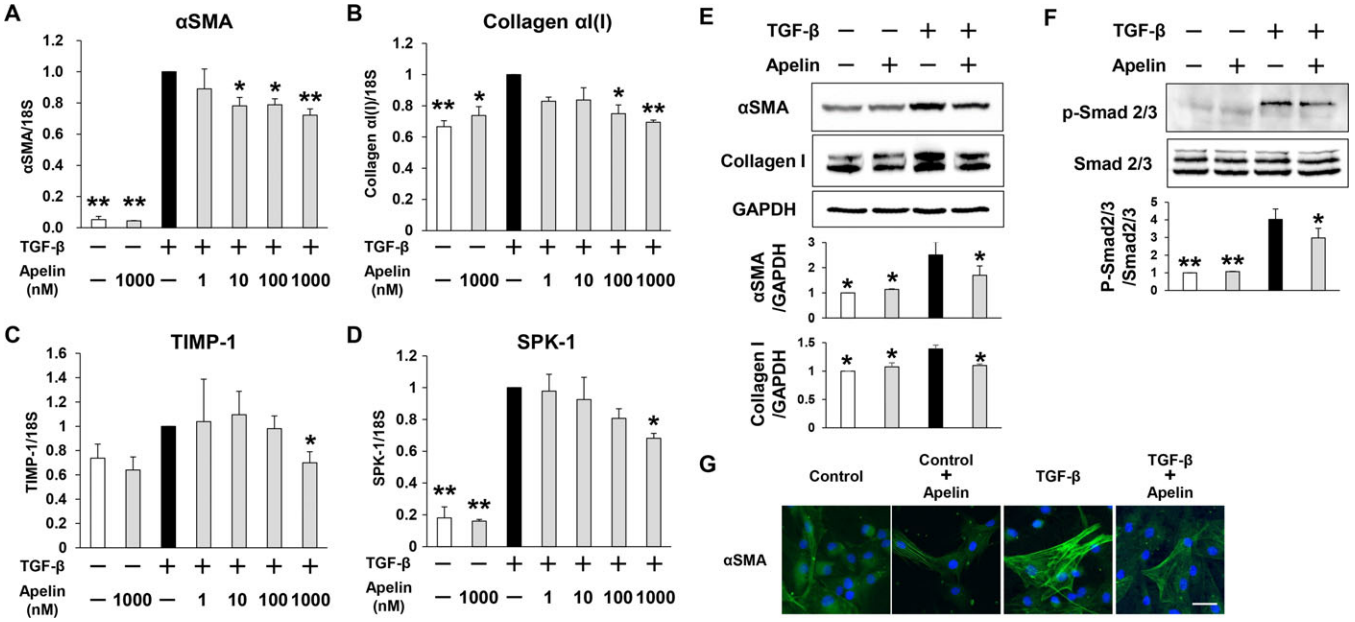

Figure 4. Apelin inhibits transforming growth factor β1 (TGFβ1)/Smad signaling and TGFβ1-induced overexpression of α-smooth muscle actin (α-SMA), collagen α1(I), tissue inhibitor of metalloproteinases 1 (TIMP-1), and sphingosine kinase 1 (SPK-1) in fibroblasts. **A–D,** Levels of mRNA for α-SMA (**A**), collagen α1(I) (**B**), TIMP-1 (**C**), and SPK-1 (**D**) in normal fibroblasts treated with apelin and/or TGFβ1 (1 ng/ml for 24 hours), determined using quantitative reverse transcription–polymerase chain reaction. **E,** Levels of α-SMA and collagen α1(I) protein in normal fibroblasts treated with apelin (100 n*M*) and/or TGFβ1 (1 ng/ml), determined by immunoblotting (n = 3 donors). **F,** Levels of pSmad2/3 and Smad2/3 protein in normal fibroblasts treated with apelin (100 n*M*) and/or TGFβ1 (1 ng/ml), determined by immunoblotting (n = 3 donors). Quantification of relative levels of α-SMA, collagen α1(I), and pSmad2/3 was accomplished via densitometry using ImageJ software (National Institutes of Health). The expression level in untreated fibroblasts was assigned a value of 1. Values are the mean ± SEM from 3 experiments, relative to levels of mRNA in fibroblasts treated with TGFβ1 without apelin. * = $P < 0.05$; ** = $P < 0.01$ versus cells treated with TGFβ1 without apelin. **G,** Immunofluorescence staining of α-SMA in dermal fibroblasts that were either left untreated or treated with TGFβ1 (1 ng/ml) and/or apelin (100 n*M*) for 24 hours. Bar = 50 μm.

bleomycin-induced dermal fibrosis received intraperitoneal injections of apelin or PBS. Bleomycin-enhanced dermal thickness was significantly suppressed by apelin injections (Figures 5A and B). We confirmed that bleomycin-induced dermal fibrosis, as revealed by Masson's trichrome staining, was significantly reduced by apelin injections (Figure 5C). The thickness of the subcutaneous adipose layer was significantly reduced by bleomycin, and apelin injections reversed bleomycin-induced suppression (see Supplementary Figure 7, http://onlinelibrary.wiley.com/doi/10.1002/art.40533/abstract). In addition, bleomycin-induced mRNA levels of IL-6, TGFβ1, and CTGF in lesional skin were significantly decreased by apelin injections (Figure 5D). The numbers of α-SMA+ myofibroblasts and CD3+ T cells were enhanced in lesional skin in bleomycin-treated mice, and apelin injections inhibited the numbers of these myofibroblasts and T cells in lesional skin (Figure 5E), while the number of CD68+ macrophages in lesional skin was not changed (Figure 5E). We noted the presence of dilated blood vessels in the dermis in lesional skin in apelin-injected mice (Figure 5F). The number of CD31+ blood vessels was not changed by apelin injections (Figure 5F). These results suggest that apelin might inhibit skin fibrosis in vivo.

Biased agonist of APJ, MM07, inhibits TGFβ1/Smad signaling and TGFβ1-induced overexpression of α-SMA and collagen α1(I) in fibroblasts in vitro and bleomycin-induced dermal fibrosis in mice. Finally, we investigated the effect of the synthetic biased agonist of APJ, MM07 (24,25), on fibrosis in vitro and in vivo. First, we assessed the inhibitory effect of MM07 on mRNA expression of fibrosis-related genes in fibroblasts. TGFβ1-induced α-SMA and collagen α1(I) mRNA overexpression was significantly inhibited by the addition of MM07 in a dose-dependent manner (Figures 6A and B). Interestingly, the inhibitory effect of MM07 on TGFβ1-induced gene expression in fibroblasts was higher than that of apelin ([Pyr^1]-Apelin-13) (compare Figures 6A and B with Figures 4A and B). Additionally, TGFβ1-induced α-SMA and collagen α1(I) protein expression was also inhibited by the addition of MM07, as shown by Western blot (Figure 6C) and immunofluorescence staining (Figure 6E). TGFβ1-induced phosphorylated Smad2/3 was also inhibited by the addition of MM07 (Figure 6D). Administration of MM07 did not affect the proliferation of fibroblasts

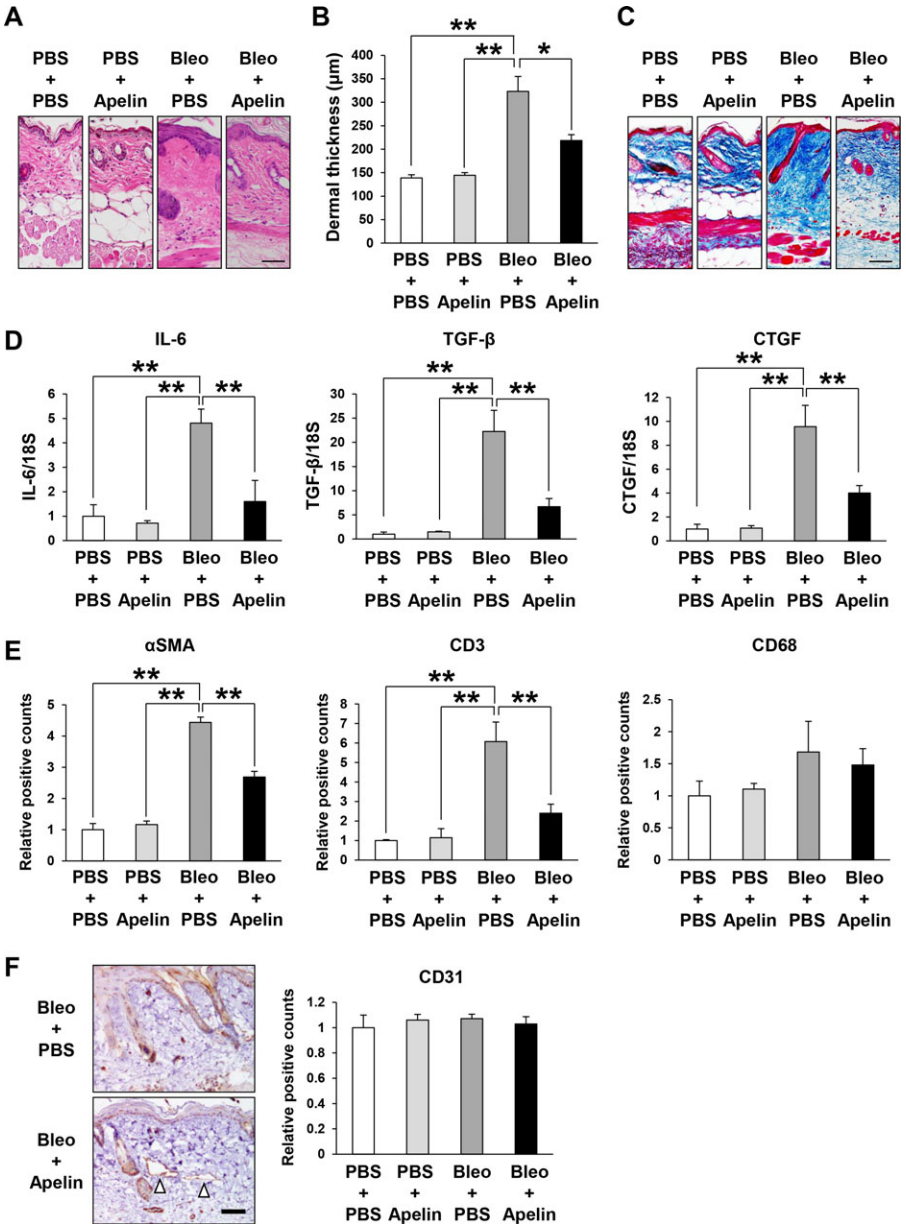

Figure 5. Administration of apelin significantly inhibits bleomycin (Bleo)–induced dermal fibrosis in mice. **A** and **C,** Representative images of hematoxylin and eosin staining (**A**) or Masson's trichrome staining (**C**) of the skin in mice treated with subcutaneous injections of phosphate buffered saline (PBS) or bleomycin and subsequently treated with intraperitoneal injections of PBS or apelin ([Pyr^1]-Apelin-13). Bars = 50 μm. **B,** Quantification of dermal thickness of lesional skin in mice, determined in 3 random microscopic fields in 6 mice per group. **D,** Levels of mRNA for interleukin-6 (IL-6), transforming growth factor β1 (TGFβ1), and connective tissue growth factor (CTGF) in skin of PBS- or bleomycin-treated mice subsequently injected with PBS or apelin, determined using quantitative reverse transcription–polymerase chain reaction (n = 3 mice per group), relative to levels of mRNA in skin of control mice. **E,** Numbers of α-smooth muscle actin (α-SMA)–positive myofibroblasts, infiltrating CD3+ T cells, and CD68+ macrophages in the dermis, determined by counting cells in 5 random microscopic fields in 3–6 mice per group. **F,** Representative imaging of CD31 staining of the skin in bleomycin-treated mice subsequently treated with PBS or apelin. **Arrowheads** indicate dilated small vessels. Bar = 50 μm. The number of CD31+ vessels in the dermis was determined by counting in 5 random microscopic fields in 3–6 mice per group. Values are the mean ± SEM. * = $P < 0.05$; ** = $P < 0.01$.

(see Supplementary Figure 6B, http://onlinelibrary.wiley.com/doi/10.1002/art.40533/abstract), which suggests that there might be no toxicity of MM07.

Next, we examined the effect of MM07 on bleomycin-induced dermal fibrosis in mice. Bleomycin-enhanced dermal thickness was significantly inhibited

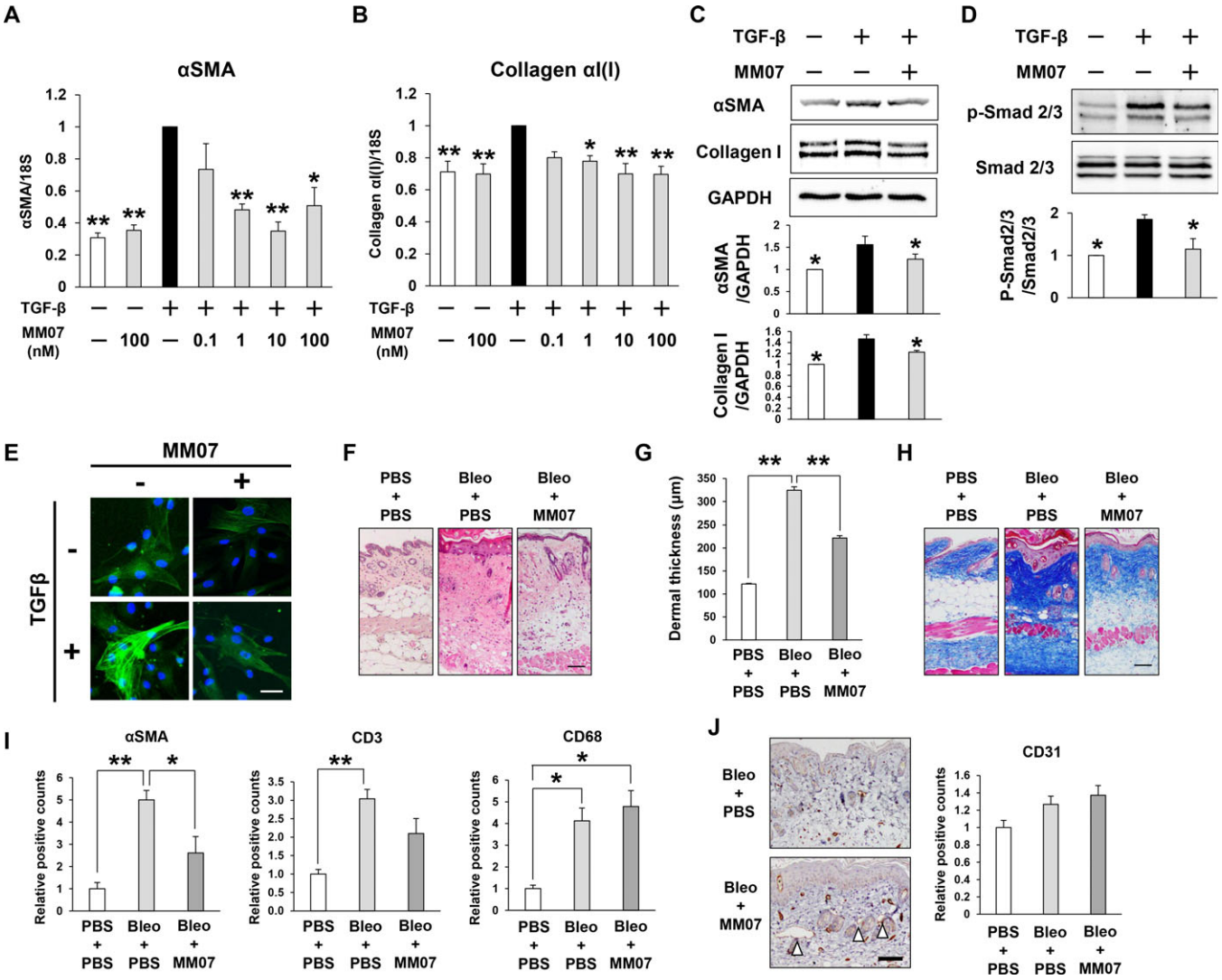

Figure 6. MM07 inhibits transforming growth factor β1 (TGFβ1)–induced fibrosis in fibroblasts in vitro and bleomycin (Bleo)–induced dermal fibrosis in mice. **A** and **B,** Levels of mRNA for α-smooth muscle actin (α-SMA) (**A**) and collagen α1(I) (**B**) in normal fibroblasts treated with MM07 and/or TGFβ1 (n = 4 donors). **C** and **D,** Levels of α-SMA and collagen α1(I) (**C**) and levels of pSmad2/3 and Smad2/3 (**D**) in normal fibroblasts treated with MM07 and/or TGFβ1, determined by immunoblotting (n = 3 donors). Quantification of relative expression levels was accomplished via densitometry using ImageJ software (National Institutes of Health). Values are the mean ± SEM. * = $P < 0.05$; ** = $P < 0.01$ versus cells treated with TGFβ1 without MM07. **E,** Immunofluorescence staining of α-SMA in fibroblasts that were either left untreated or treated with TGFβ1 and/or MM07. Bar = 50 μm. **F** and **H,** Representative images of hematoxylin and eosin staining (**F**) or Masson's trichrome staining (**H**) of the skin in mice treated with subcutaneous injections of phosphate buffered saline (PBS) or bleomycin and subsequently treated with intraperitoneal injections of PBS or MM07. Bars = 50 μm. **G,** Quantification of dermal thickness in mice, determined in 3 random microscopic fields in 6 mice per group. **I** and **J,** Numbers of α-SMA+ myofibroblasts, CD3+ T cells, CD68+ macrophages (**I**), and CD31+ vessels (**J**; right) in the dermis, determined by counting in 5 random microscopic fields in 6 mice per group. **J,** Left, Representative imaging of CD31 staining in bleomycin-treated mice treated with PBS or MM07. **Arrowheads** indicate dilated dermal small vessels. Bar = 50 μm. Values are the mean ± SEM. * = $P < 0.05$; ** = $P < 0.01$.

by intraperitoneal injections of MM07 (Figures 6F and G). We confirmed that the amount of collagen in the skin revealed by Masson's trichrome staining was enhanced by bleomycin, and this enhancement was inhibited by MM07 treatment (Figure 6H). The numbers of α-SMA+ myofibroblasts, CD3+ T cells, and CD68+ macrophages were increased in lesional skin in bleomycin-treated mice, and MM07 injections significantly decreased the number of bleomycin-induced myofibroblasts in lesional skin (Figure 6I), while the number of CD68+ macrophages in lesional skin was not changed by MM07 treatment (Figure 6I). Similar to the results with apelin-injected mice, dilated dermal small

vessels in lesional skin were noted in MM07-injected mice (Figure 6J). The number of CD31+ blood vessels was not changed by MM07 injections (Figure 6J).

Finally, we examined the effect of apelin/MM07 on fibrosis in the therapeutic model. Apelin/MM07 injections were initiated 7 days after starting bleomycin treatment. We found that bleomycin-enhanced dermal thickness tended to be inhibited by injections of apelin/MM07, but these differences did not reach statistical significance (see Supplementary Figure 8, http://onlinelibrary.wiley.com/doi/10.1002/art.40533/abstract). The numbers of bleomycin-induced α-SMA+ myofibroblasts and CD68+ macrophages were significantly decreased by apelin/MM07 injections. These results suggest that the biased agonist of APJ, MM07, might inhibit TGFβ1/Smad signaling and TGFβ1-induced fibrosis in fibroblasts in vitro and might inhibit skin fibrosis in vivo.

DISCUSSION

It has been reported that reduced apelin expression was associated with cardiac, renal, and pulmonary artery fibrosis (12,19,37). Consistent with these findings, we determined that apelin expression was significantly reduced in SSc fibroblasts in lesional skin compared with that in normal fibroblasts. Furthermore, we found that the expression of apelin was significantly inhibited by TGFβ1 stimulation in normal and SSc fibroblasts, suggesting that activation of TGFβ1 signaling in SSc fibroblasts might be partly responsible for reduced apelin expression in SSc fibroblasts.

Several studies have examined serum apelin levels in patients with fibrotic diseases or SSc-related diseases. Serum apelin levels were decreased in patients with cardiac, renal, and pulmonary fibrosis and PAH (13,38,39). In contrast, serum apelin levels were elevated in patients with liver fibrosis (40). In this study, we determined that serum apelin levels were negatively correlated with skin sclerosis in SSc patients, which suggests that decreased serum apelin levels might be associated with skin fibrosis in SSc. It has been reported that apelin/APJ signaling plays an important role in the pathogenesis of cardiovascular diseases, including PAH (18). In addition, apelin/APJ signaling regulates cardiovascular tone, blood pressure, blood flow, and parallel alignment of arteries and veins in the skin (9–11). We found that apelin staining of dermal small vessels in SSc patients was decreased and that serum apelin levels in SSc patients with peripheral vasculopathy, such as digital ulcers and acro-osteolysis, were significantly reduced. Therefore, reduced apelin production may also be involved in the pathogenesis of peripheral vasculopathy as well as PAH in SSc.

Recent studies indicate that microRNA can regulate fibrosis in human dermal fibroblasts and may be involved in the pathogenesis of skin fibrosis in SSc (41). Nagpal et al reported that TGFβ1 induced expression of miR-125b and that overexpression of miR-125b inhibited the expression of apelin in cardiac fibroblasts, suggesting that TGFβ1 might suppress the expression of apelin via miR-125b in cardiac fibroblasts (37). Apelin deficiency in pulmonary artery ECs led to increased expression of FGF-2 and FGFR-1 via decreased expression of miR-424 and miR-503 (42). Furthermore, miR-130/301 regulated the apelin–miR-424/503–FGF-2 regulatory axis (12). These findings suggest that microRNA may be involved in the inhibition of apelin expression in fibroblasts by TGFβ1. Additional studies are warranted to elucidate the role of microRNA in the regulation of apelin expression in fibroblasts.

In SSc fibroblasts, TGFβ1/Smad signaling is generally activated, resulting in myofibroblast transition and collagen overproduction (43). TGFβ1 binds to TGFβ receptor types I and II, induces the phosphorylation of Smad2/3, and subsequently binds to Smad4. A Smad complex translocates to the nucleus and enhances the expression of target genes, such as those for α-SMA, collagen α1(I), and CTGF (44). SPK-1 is an important component of TGFβ1/Smad signaling and the key mediator of collagen and α-SMA production (33,34,45). With respect to the regulation of TGFβ1/Smad signaling by apelin, Pchejetski et al reported that apelin suppressed the expression of SPK-1 and collagen production in cardiac fibroblasts in vitro (16). In addition, previous studies have revealed that apelin inhibited the TGFβ1-induced increase of phosphorylated Smad2/3 in vitro and attenuated the up-regulation of TGFβ receptor I and its downstream Smad signaling in vivo (19).

In the present study, we assessed the role of apelin in TGFβ1/Smad signaling in dermal fibroblasts. We determined that siRNA depletion of apelin enhanced α-SMA, collagen α1(I), and SPK-1 expression in fibroblasts and that addition of apelin inhibited TGFβ1-induced overexpression of α-SMA, collagen α1(I), TIMP-1, SPK-1, and phosphorylated Smad2/3 in fibroblasts. However, expression of TGFβ receptor types I and II was not inhibited by apelin. These results are consistent with previous findings and suggest that apelin might inhibit TGFβ1/Smad signaling, myofibroblast differentiation, and TGFβ1-induced skin fibrosis. These results also indicate that inhibitory regulation by apelin may be mediated by inhibition of phosphorylation of Smad2/3. However, the precise mechanisms by which apelin inhibits TGFβ1/Smad signaling are unknown, and further studies are needed.

Several studies demonstrated that the administration of apelin significantly inhibited fibrosis in animal

models, such as models of myocardial infarction, renal interstitial fibrosis, and pulmonary fibrosis (16,19,46,47). In our study, we demonstrated that the administration of apelin inhibited skin fibrosis in bleomycin-induced fibrosis. These in vivo results were consistent with our in vitro results, which suggested that apelin might have therapeutic potential by blocking TGFβ1/Smad signaling under pathogenic conditions. We also noticed that several dermal small vessels in lesional skin were dilated in apelin-injected mice, suggesting that injected apelin might act both on ECs and on fibroblasts in the skin.

Apelin produced by adipocytes acts as an adipokine (7). Several studies suggested the possible contribution of adipokines, such as leptin and adiponectin, to the pathologic process of SSc (48,49). Marangoni et al reported that adipose tissue loss and adipocyte–myofibroblast transition might be primary events in the pathogenesis of cutaneous fibrosis in SSc (50). Since SSc patients had significantly lower body mass indexes and fat tissue compared with normal individuals (51), reduced fat tissue in SSc patients may subsequently result in the reduced apelin/APJ signaling in SSc fibroblasts and, in turn, in enhanced fibrosis in SSc.

Collectively, we propose a model for the role of apelin in the regulation of skin fibrosis in SSc (see Supplementary Figure 9, http://onlinelibrary.wiley.com/doi/10.1002/art.40533/abstract). In SSc fibroblasts, activated TGFβ1 signaling inhibits apelin production, and reduced adipose tissue may lead to a decreased amount of apelin. These changes may attenuate the inhibitory effect of apelin on TGFβ1/Smad signaling and collagen production, resulting in the acceleration of skin fibrosis. TGFβ1 signaling and apelin signaling may counteract each other in the fibrotic process of SSc. The current findings provide new insight into the regulation of fibrosis by apelin/APJ signaling in SSc fibroblasts.

It has been reported that infusion of apelin leads to vasodilation in humans in vivo (25). However, since chronic administration of apelin causes receptor desensitization by β-arrestin–mediated internalization of APJ, there is a limitation for the clinical use of apelin. MM07 is the cyclic apelin peptide that preferentially activates G protein responses with low potency in β-arrestin–mediated receptor internalization (24). It is of interest that an intrabrachial infusion of MM07 increased the forearm blood flow in human volunteers without any severe adverse effects (25). We demonstrated that MM07 inhibited TGFβ1/Smad signaling and TGFβ1-induced fibrosis in fibroblasts in vitro, and that administration of MM07 significantly inhibited bleomycin-induced dermal fibrosis in mice. Furthermore, we demonstrated that MM07 had greater potential than apelin to inhibit fibrosis in vivo and in vitro. These results suggest that administration of MM07 may have therapeutic efficacy for fibrosis in SSc patients. Further clinical investigation is needed to determine the efficacy and safety of the clinical use of MM07. In conclusion, the inhibitory regulation of fibrosis by apelin/APJ signaling may be involved in the pathogenesis of SSc and could be a therapeutic target for fibrosis in SSc.

AUTHOR CONTRIBUTIONS

All authors were involved in drafting the article or revising it critically for important intellectual content, and all authors approved the final version to be published. Dr. Motegi had full access to all of the data in the study and takes responsibility for the integrity of the data and the accuracy of the data analysis.

Study conception and design. Yokoyama, Ishikawa, Motegi.

Acquisition of data. Yokoyama, Sekiguchi, Fujiwara, Uchiyama, Uehara, Ogino, Torii, Motegi.

Analysis and interpretation of data. Yokoyama, Sekiguchi, Fujiwara, Uchiyama, Uehara, Ogino, Torii, Motegi.

REFERENCES

1. Trojanowska M. Cellular and molecular aspects of vascular dysfunction in systemic sclerosis. Nat Rev Rheumatol 2010;6:453–60.
2. Asano Y. Future treatments in systemic sclerosis. J Dermatol 2010;37:54–70.
3. Jinnin M. Mechanisms of skin fibrosis in systemic sclerosis. J Dermatol 2010;37:11–25.
4. Motegi S, Yamada K, Toki S, Uchiyama A, Kubota Y, Nakamura T, et al. Beneficial effect of botulinum toxin A on Raynaud's phenomenon in Japanese patients with systemic sclerosis: a prospective, case series study. J Dermatol 2016;43:56–62.
5. Motegi S, Toki S, Hattori T, Yamada K, Uchiyama A, Ishikawa O. No association of atherosclerosis with digital ulcers in Japanese patients with systemic sclerosis: evaluation of carotid intima-media thickness and plaque characteristics. J Dermatol 2014; 41:604–8.
6. Tatemoto K, Hosoya M, Habata Y, Fujii R, Kakegawa T, Zou MX, et al. Isolation and characterization of a novel endogenous peptide ligand for the human APJ receptor. Biochem Biophys Res Commun 1998;251:471–6.
7. Boucher J, Masri B, Daviaud D, Gesta S, Guigné C, Mazzucotelli A, et al. Apelin, a newly identified adipokine up-regulated by insulin and obesity. Endocrinology 2005;146:1764–71.
8. Lee DK, Cheng R, Nguyen T, Fan T, Kariyawasam AP, Liu Y, et al. Characterization of apelin, the ligand for the APJ receptor. J Neurochem 2000;74:34–41.
9. Kidoya H, Ueno M, Yamada Y, Mochizuki N, Nakata M, Yano T, et al. Spatial and temporal role of the apelin/APJ system in the caliber size regulation of blood vessels during angiogenesis. EMBO J 2008;27:522–34.
10. Kidoya H, Takakura N. Biology of the apelin-APJ axis in vascular formation. J Biochem 2012;152:125–31.
11. Kidoya H, Naito H, Muramatsu F, Yamakawa D, Jia W, Ikawa M, et al. APJ regulates parallel alignment of arteries and veins in the skin. Dev Cell 2015;33:247–59.
12. Kim J, Kang Y, Kojima Y, Lighthouse JK, Hu X, Aldred MA, et al. An endothelial apelin-FGF link mediated by miR-424 and miR-503 is disrupted in pulmonary arterial hypertension. Nat Med 2013;19:74–82.
13. Chandra SM, Razavi H, Kim J, Agrawal R, Kundu RK, de Jesus Perez V, et al. Disruption of the apelin-APJ system worsens hypoxia-induced pulmonary hypertension. Arterioscler Thromb Vasc Biol 2011;31:814–20.
14. Kuba K, Zhang L, Imai Y, Arab S, Chen M, Maekawa Y, et al. Impaired heart contractility in Apelin gene-deficient mice

associated with aging and pressure overload. Circ Res 2007;101: e32–42.
15. Sato T, Suzuki T, Watanabe H, Kadowaki A, Fukamizu A, Liu PP, et al. Apelin is a positive regulator of ACE2 in failing hearts. J Clin Invest 2013;123:5203–11.
16. Pchejetski D, Foussal C, Alfarano C, Lairez O, Calise D, Guilbeau-Frugier C, et al. Apelin prevents cardiac fibroblast activation and collagen production through inhibition of sphingosine kinase 1. Eur Heart J 2012;33:2360–9.
17. Siddiquee K, Hampton J, Khan S, Zadory D, Gleaves L, Vaughan DE, et al. Apelin protects against angiotensin II-induced cardiovascular fibrosis and decreases plasminogen activator inhibitor type-1 production. J Hypertens 2011;29:724–31.
18. Yu XH, Tang ZB, Liu LJ, Qian H, Tang SL, Zhang DW, et al. Apelin and its receptor APJ in cardiovascular diseases. Clin Chim Acta 2014;428:1–8.
19. Wang LY, Diao ZL, Zhang DL, Zheng JF, Zhang QD, Ding JX, et al. The regulatory peptide apelin: a novel inhibitor of renal interstitial fibrosis. Amino Acids 2014;46:2693–704.
20. Nishida M, Okumura Y, Oka T, Toiyama K, Ozawa S, Itoi T, et al. The role of apelin on the alleviative effect of angiotensin receptor blocker in unilateral ureteral obstruction-induced renal fibrosis. Nephron Extra 2012;2:39–47.
21. Melgar-Lesmes P, Casals G, Pauta M, Ros J, Reichenbach V, Bataller R, et al. Apelin mediates the induction of profibrogenic genes in human hepatic stellate cells. Endocrinology 2010;151: 5306–14.
22. Chen W, Oue T, Ueno T, Uehara S, Usui N, Fukuzawa M. Apelin is a marker of the progression of liver fibrosis and portal hypertension in patients with biliary atresia. Pediatr Surg Int 2013; 29:79–85.
23. Aozasa N, Asano Y, Akamata K, Noda S, Masui Y, Yamada D, et al. Serum apelin levels: clinical association with vascular involvements in patients with systemic sclerosis. J Eur Acad Dermatol Venereol 2013;27:37–42.
24. Yang P, Maguire JJ, Davenport AP. Apelin, Elabela/Toddler, and biased agonists as novel therapeutic agents in the cardiovascular system. Trends Pharmacol Sci 2015;36:560–7.
25. Brame AL, Maguire JJ, Yang P, Dyson A, Torella R, Cheriyan J, et al. Design, characterization, and first-in-human study of the vascular actions of a novel biased apelin receptor agonist. Hypertension 2015;65:834–40.
26. Subcommittee for Scleroderma Criteria of the American Rheumatism Association Diagnostic and Therapeutic Criteria Committee. Preliminary criteria for the classification of systemic sclerosis (scleroderma). Arthritis Rheum 1980;23:581–90.
27. Van den Hoogen F, Khanna D, Fransen J, Johnson SR, Baron M, Tyndall A, et al. 2013 classification criteria for systemic sclerosis: an American College of Rheumatology/European League Against Rheumatism collaborative initiative. Arthritis Rheum 2013;65: 2737–47.
28. LeRoy EC, Black C, Fleischmajer R, Jablonska S, Krieg T, Medsger TA Jr, et al. Scleroderma (systemic sclerosis): classification, subsets and pathogenesis. J Rheumatol 1988;15:202–5.
29. Clements P, Lachenbruch P, Seibold J, White B, Weiner S, Martin R, et al. Inter and intraobserver variability of total skin thickness score (modified Rodnan TSS) in systemic sclerosis. J Rheumatol 1995;22:1281–5.
30. Motegi S, Garfield S, Feng X, Sárdy M, Udey MC. Potentiation of platelet-derived growth factor receptor-β signaling mediated by integrin-associated MFG-E8. Arterioscler Thromb Vasc Biol 2011;31:2653–64.
31. Yamamoto T, Takagawa S, Katayama I, Yamazaki K, Hamazaki Y, Shinkai H, et al. Animal model of sclerotic skin. I: local injections of bleomycin induce sclerotic skin mimicking scleroderma. J Invest Dermatol 1999;112:456–62.
32. Kudo H, Jinnin M, Asano Y, Trojanowska M, Nakayama W, Inoue K, et al. Decreased interleukin-20 expression in scleroderma skin contributes to cutaneous fibrosis. Arthritis Rheumatol 2014;66:1636–47.
33. Yamanaka M, Shegogue D, Pei H, Bu S, Bielawska A, Bielawski J, et al. Sphingosine kinase 1 (SPHK1) is induced by transforming growth factor-β and mediates TIMP-1 up-regulation. J Biol Chem 2004;279:53994–4001.
34. Kono Y, Nishiuma T, Nishimura Y, Kotani Y, Okada T, Nakamura S, et al. Sphingosine kinase 1 regulates differentiation of human and mouse lung fibroblasts mediated by TGF-β1. Am J Respir Cell Mol Biol 2007;37:395–404.
35. Massagué J, Seoane J, Wotton D. Smad transcription factors. Genes Dev 2005;19:2783–810.
36. Kamato D, Burch ML, Piva TJ, Rezaei HB, Rostam MA, Xu S, et al. Transforming growth factor-β signalling: role and consequences of Smad linker region phosphorylation. Cell Signal 2013;25:2017–24.
37. Nagpal V, Rai R, Place AT, Murphy SB, Verma SK, Ghosh AK, et al. MiR-125b is critical for fibroblast-to-myofibroblast transition and cardiac fibrosis. Circulation 2016;133:291–301.
38. Goetze JP, Rehfeld JF, Carlsen J, Videbaek R, Andersen CB, Boesgaard S, et al. Apelin: a new plasma marker of cardiopulmonary disease. Regul Pept 2006;133:134–8.
39. Kocer D, Karakukcu C, Ozturk F, Eroglu E, Kocyigit I. Evaluation of fibrosis markers: apelin and transforming growth factor-β1 in autosomal dominant polycystic kidney disease patients. Ther Apher Dial 2016;20:517–22.
40. Kalafateli M, Triantos C, Tsochatzis E, Michalaki M, Koutroumpakis E, Thomopoulos K, et al. Adipokines levels are associated with the severity of liver disease in patients with alcoholic cirrhosis. World J Gastroenterol 2015;21:3020–9.
41. Makino T, Jinnin M. Genetic and epigenetic abnormalities in systemic sclerosis. J Dermatol 2016;43:10–8.
42. Bertero T, Lu Y, Annis S, Hale A, Bhat B, Saggar R, et al. Systems-level regulation of microRNA networks by miR-130/301 promotes pulmonary hypertension. J Clin Invest 2014;124:3514–28.
43. Varga JA, Trojanowska M. Fibrosis in systemic sclerosis. Rheum Dis Clin North Am 2008;34:115–43.
44. Blobe GC, Schiemann WP, Lodish HF. Role of transforming growth factor β in human disease. N Engl J Med 2000;342:1350–8.
45. Gellings Lowe N, Swaney JS, Moreno KM, Sabbadini RA. Sphingosine-1-phosphate and sphingosine kinase are critical for transforming growth factor-β-stimulated collagen production by cardiac fibroblasts. Cardiovasc Res 2009;82:303–12.
46. Visser YP, Walther FJ, el Laghmani H, van der Laarse A, Wagenaar GT. Apelin attenuates hyperoxic lung and heart injury in neonatal rats. Am J Respir Crit Care Med 2010;182:1239–50.
47. Azizi Y, Faghihi M, Imani A, Roghani M, Nazari A. Post-infarct treatment with [Pyr1]-apelin-13 reduces myocardial damage through reduction of oxidative injury and nitric oxide enhancement in the rat model of myocardial infarction. Peptides 2013;46:76–82.
48. Budulgan M, Dilek B, Dağ ŞB, Batmaz I, Yıldız İ, Sarıyıldız MA, et al. Relationship between serum leptin level and disease activity in patients with systemic sclerosis. Clin Rheumatol 2014;33:335–9.
49. Masui Y, Asano Y, Shibata S, Noda S, Aozasa N, Akamata K, et al. Serum adiponectin levels inversely correlate with the activity of progressive skin sclerosis in patients with diffuse cutaneous systemic sclerosis. J Eur Acad Dermatol Venereol 2012;26:354–60.
50. Marangoni RG, Korman BD, Wei J, Wood TA, Graham LV, Whitfield ML, et al. Myofibroblasts in murine cutaneous fibrosis originate from adiponectin-positive intradermal progenitors. Arthritis Rheumatol 2015;67:1062–73.
51. Marighela TF, Genaro Pde S, Pinheiro MM, Szejnfeld VL, Kayser C. Risk factors for body composition abnormalities in systemic sclerosis. Clin Rheumatol 2013;32:1037–44.

ARTHRITIS & RHEUMATOLOGY
Vol. 70, No. 10, October 2018, pp 1673–1684
DOI 10.1002/art.40554

The Antifibrotic Effect of A_{2B} Adenosine Receptor Antagonism in a Mouse Model of Dermal Fibrosis

Harry Karmouty-Quintana,[1] Jose G. Molina,[1] Kemly Philip,[1] Chiara Bellocchi,[2] Brent Gudenkauf,[3] Minghua Wu,[1] Ning-Yuan Chen,[1] Scott D. Collum,[1] Junsuk Ko,[1] Sandeep K. Agarwal,[4] Shervin Assassi,[1] Hongyan Zhong,[5] Michael R. Blackburn,[1] and Tingting Weng[1]

Objective. **Systemic sclerosis (SSc; scleroderma) is a chronic disease that affects the skin and various internal organs. Dermal fibrosis is a major component of this disease. The mechanisms that promote dermal fibrosis remain elusive. Elevations in tissue adenosine levels and the subsequent engagement of the profibrotic A_{2B} adenosine receptor (ADORA2B) have been shown to regulate fibrosis in multiple organs including the lung, kidney, and penis; however, the role of ADORA2B in dermal fibrosis has not been investigated. We undertook this study to test our hypothesis that elevated expression of ADORA2B in the skin drives the development of dermal fibrosis.**

Methods. **We assessed the involvement of ADORA2B in the regulation of dermal fibrosis using a well-established mouse model of dermal fibrosis. Using an orally active ADORA2B antagonist, we demonstrated how inhibition of ADORA2B results in reduced dermal fibrosis in 2 distinct experimental models. Finally, using human dermal fibroblasts, we characterized the expression of adenosine receptors.**

Results. **We demonstrated that levels of ADORA2B were significantly elevated in dermal fibrosis and that the therapeutic blockade of this receptor in vivo using an ADORA2B antagonist could reduce the production of profibrotic mediators in the skin and attenuate dermal fibrosis. Antagonism of ADORA2B resulted in reduced numbers of arginase-expressing macrophages and myofibroblasts and in reduced levels of the extracellular matrix proteins fibronectin, collagen, and hyaluronan.**

Conclusion. **These findings identify ADORA2B as a potential profibrotic regulator in dermal fibrosis and suggest that ADORA2B antagonism may be a useful approach for the treatment of SSc.**

Dermal fibrosis is a prominent feature of scleroderma (systemic sclerosis [SSc]), which is a chronic and complex autoimmune disease that affects the skin and various internal organs (1). It has been proposed that the dermal fibrosis seen in SSc is driven in part by pathways that are similar to those found in normal wound healing, including the regulation of inflammation (2), the recruitment and proliferation of fibroblasts (3), and extracellular matrix production (3). Despite efforts to understand the immunologic and pathologic pathways involved in this disease, the mechanisms that promote dermal fibrosis in SSc remain elusive, and there are no effective therapies to halt the progression of dermal fibrosis in SSc patients.

Adenosine is a signaling molecule that is produced in response to tissue injury and inflammation (4). Extracellular adenosine can regulate numerous cellular responses through engagement of 4 cell surface adenosine receptors (A_1 adenosine receptor [ADORA1], ADORA2A, ADORA2B, and ADORA3) (5). Consistent with the notion that dermal fibrosis is associated with the activation of wound healing pathways, chronic elevations in adenosine have been implicated in the regulation of dermal fibrosis through the engagement of ADORA2A on dermal

Supported by Gilead Sciences, Inc.
[1]Harry Karmouty-Quintana, PhD, Jose G. Molina, MD, Kemly Philip, MD, PhD, Minghua Wu, MD, PhD, Ning-Yuan Chen, BA, Scott D. Collum, BSc, Junsuk Ko, ScB, Shervin Assassi, MD, Michael R. Blackburn, PhD, Tingting Weng, PhD: McGovern Medical School, Houston, Texas; [2]Chiara Bellocchi, MD: McGovern Medical School, Houston, Texas, and Referral Center for Systemic Autoimmune Diseases, Fondazione IRCCS Ca' Granda Ospedale Maggiore Policlinico di Milano, Milan, Italy; [3]Brent Gudenkauf, BA: McGovern Medical School, Houston, Texas, and Texas Tech University Health Sciences Center, Lubbock; [4]Sandeep K. Agarwal, MD, PhD: Baylor College of Medicine, Houston, Texas; [5]Hongyan Zhong, PhD: Gilead Sciences, Inc., Foster City, California.

Dr. Zhong owns stock or stock options in Gilead Sciences, Inc.

Address correspondence to Tingting Weng, PhD, Department of Biochemistry and Molecular Biology, McGovern Medical School, 6431 Fannin Street, Houston, TX 77030. E-mail: Tingting.Weng@uth.tmc.edu.

Submitted for publication December 19, 2016; accepted in revised form May 8, 2018.

fibroblasts (6). Indeed, ADORA2A has been implicated in several processes pertinent to the regulation of wound healing and fibrosis (6). Similarly, ADORA2B has also been implicated in processes associated with wound healing and fibrosis (7,8). These include the ability of this receptor to regulate profibrotic activities on fibroblasts (9) and macrophages (10). Moreover, work using genetically modified mice and selective ADORA2B antagonists has demonstrated that this receptor is effective in regulating the progression of pulmonary fibrosis (11,12), kidney fibrosis (13), and fibrosis in the penis (14). However, the role of ADORA2B in dermal fibrosis has not been systematically investigated.

The goal of this study was to assess the involvement of ADORA2B in the regulation of dermal fibrosis using a well-established mouse model of dermal fibrosis that is elicited by the subcutaneous (SC) injection of bleomycin (15) as well as by using the TSK1 mouse model (16). Using the bleomycin model, we characterized the expression of the adenosine receptors and demonstrated that levels of ADORA2B were significantly elevated in dermal fibrosis. Moreover, the therapeutic blockade of this receptor in vivo using an ADORA2B antagonist was shown to reduce the production of profibrotic mediators in the skin and to attenuate dermal fibrosis both in the bleomycin model and in TSK1 mice. Experiments using human fibroblasts from normal or SSc patients revealed high expression of ADORA2B. We also found increased hyaluronan synthase 2 (HAS-2) expression and increased HA levels in SSc skin. Collectively, this study identifies ADORA2B as a potential profibrotic regulator in dermal fibrosis and suggests that ADORA2B antagonism may be a useful approach for the treatment of SSc.

MATERIALS AND METHODS

Mouse model of bleomycin-induced skin fibrosis and TSK1 mice. Male wild-type C57BL/6J mice were acquired from Envigo. Bleomycin (0.02 units/day/mouse; Teva Parenteral Medicines) dissolved in saline or saline alone was administered to 8-week-old mice by daily SC injections in 2 distinct sites on shaved backs of mice. On day 28, mice were killed, and lesional skin was obtained for protein lysates, total RNA, and histology (15). Each group consisted of 10 mice. In experiments using the ADORA2B antagonist GS-6201, the drug was provided mixed in chow starting on day 15 until the end of the study. Control mice received chow with vehicle. TSK1 mice were obtained from The Jackson Laboratory. Eight-week-old TSK1 mice were fed chow containing vehicle or GS-6201 for 30 days until the end of the study. Animal experiments were approved by the Animal Welfare Committee (AWC) of UTHealth (protocol no. AWC-13-043).

Histochemical studies and immunohistochemistry. Five-micrometer thick sections of paraffin-embedded skin tissues were stained with hematoxylin and eosin, Masson's trichrome (both from Sigma-Aldrich), or picrosirius red (Abcam). Skin fibrosis was quantified by measuring the thickness of the dermis, defined as the distance from the epidermal–dermal junction to the dermal–adipose layer junction, at 6 randomly selected sites/microscopic fields in each skin sample (15). To analyze the accumulated collagen content in the lesional skin, deparaffinized sections were stained with Masson's trichrome. Fibrosis in picrosirius red–stained skin was quantified using ImageJ and Macro Language software (National Institutes of Health; https://imagej.nih.gov/ij/docs/examples/stained-sections/index.html). Data were calculated as percentage of total area.

Immunohistochemistry was performed using antibodies against fibronectin (FN; Abcam), α-smooth muscle actin (α-SMA; Sigma-Aldrich), and arginase 1 (Bioss) or a biotinylated HA-binding protein (EMD Millipore). Bound antibodies were detected with secondary antibodies from a Vectastain kit (Vector). Fibroblasts were identified by their spindle morphology, and inflammatory cells were identified by round morphology. For immunofluorescence-stained slides, Vector Red (Vector) or Alexa Fluor 488 (Life Technologies) was used to visualize the primary antibody. Sections were mounted with medium containing DAPI or propidium iodide (Abcam) as counterstain.

For immunofluorescence experiments with human tissues, fluorescein isothiocyanate–conjugated anti–α-SMA (Sigma-Aldrich) was used. Antibodies against ADORA2B (Thermo Scientific) and HAS-2 (Santa Cruz Biotechnology) were conjugated to Texas Red (Santa Cruz Biotechnology). Slides were counterstained with DAPI. All imaging was performed with a Leica DM4000 (Leica Microsystems) equipped with a monochrome camera (DFC 3000G; Leica). For immunohistochemistry experiments with human tissues, antibodies against α-SMA (clone 1A4 mouse monoclonal; Sigma-Aldrich), ADORA2B, and HAS-2 were used. α-SMA was visualized with Vector Blue (Vector) using an ImmPRESS-AP Anti-Mouse IgG (alkaline phosphatase) Polymer Detection Kit (Vector). ADORA2B and HAS-2 were visualized with ImmPACT Diaminobenzidine Peroxidase Substrate (Vector) after incubation using an ImmPRESS HRP Anti-Rabbit IgG (peroxidase) Polymer Detection Kit (Vector). Morphometric evaluation of cells positive for α-SMA and ADORA2B or of cells positive for α-SMA and HAS-2 was performed by a scientist (KP) who was blinded with regard to group status. Evaluations were performed using a total of 10 control or 10 SSc double-stained skin samples. Demographic characteristics of the SSc patients and controls who donated tissue used for immunohistochemistry are presented in Supplementary Table 1, available on the *Arthritis & Rheumatology* web site at http://onlinelibrary.wiley.com/doi/10.1002/art.40554/abstract.

Determination of messenger RNA (mRNA) levels by quantitative reverse transcription–polymerase chain reaction (RT-PCR). Total RNA was isolated from lesional skin tissue using TRIzol reagent (Life Technologies) and purified with an RNeasy Mini kit (Qiagen). Quantitative RT-PCR was performed using validated gene expression assays for ADORA1, ADORA2A, ADORA2B, ADORA3, COL1A1, interleukin-6 (IL-6), monocyte chemoattractant protein 1 (MCP-1), HAS-2, and FN (Sigma-Aldrich). Cyclophilin A (PPIA) and β-actin were used as endogenous controls to normalize transcript levels of total RNA of each sample.

The following primers were used for this study: ADORA1 forward 5′-TGTGCCCGGAAATGTACTGG-3′, reverse 5′-TCTGTGGCCCAATGTTGATAAG-3′; ADORA2A forward 5′-TTCCACTCCGGTACAATGGC-3′, reverse 5′-CGATGGCGAATGACAGCAC-3′; ADORA2B forward 5′-GCGTCCCGCTCAG-

GTATAAAG-3′, reverse 5′-CGGAGTCAATCCAATGCCAAAG-3′; ADORA3 forward 5′-ACGGACTGGCTGAACATCAC-3′, reverse 5′-AGACAATGAAATAGACGGTGGTG-3′; COL1A1 forward 5′-GCTCCTCTTAGGGGCCACT-3′, reverse 5′-CCACG TCTCACCATTGGGG-3′; IL-6 forward 5′-ACCGCTATGAAG-TTCCTCTC-3′, reverse 5′-CTCCGACTTGTGAAGTGGTA-3′; MCP-1 forward 5′-AGCATCCACGTGTTGGCTC-3′, reverse 5′-TGGGATCATCTTGCTGGTG-3′; HAS-2 forward 5′-TGTGA-GAGGTTTCTATGTGTCCT-3′, reverse 5′-ACCGTACAGTCCA-AATGAGAAGT-3′; PPIA forward 5′-GAGCTGTTTGCAGAC-AAAGTTC-3′, reverse 5′-CCCTGGCACATGAATCCTGG-3′; β-actin forward 5′-GGCTGTATTCCCCTCCATCG-3′, reverse 5′-CCAGTTGGTAACAATGCCATGT-3′. Data were analyzed with GraphPad Prism software using the $2^{-\Delta\Delta Ct}$ method.

Quantification of tissue collagen. The collagen content of skin was determined using a Sircol Collagen Assay (Biocolor). Collagen content was normalized to total protein content (Bradford assay; Bio-Rad).

Plasma MCP-1 assay. MCP-1 enzyme-linked immunosorbent assays (ELISAs) were performed on plasma using a Quantikine ELISA kit (R&D Systems). Results are given as the mean ± SEM pg/ml.

Primary normal human dermal fibroblasts (HDFs). Primary normal HDFs were obtained from Lonza (batch no. 0000214247) and cultured according to instructions provided by Lonza. These cells originated from a 41-year-old woman undergoing either reduction mammaplasty or abdominoplasty. RNA isolation and RT-PCR for human adenosine receptors were performed as previously described (17). Cells were washed twice in Hanks' balanced salt solution and incubated in serum-free basal medium (Lonza) with or without the agonist 5′-*N*-ethylcarboxamidoadenosine (NECA) or the selective ADORA2B antagonist CVT-6694 (18) for 18 hours. The concentration of IL-6 in cell medium was then determined using ELISA kits (Thermo Fisher). In experiments using fibroblasts isolated from patients with SSc or healthy controls, 5 SSc and 5 control fibroblast cell lines from age- and sex-matched individuals were used. All experiments were performed in passage 6. Demographic characteristics of the SSc patients and controls who donated primary cells are summarized in Supplementary Table 2, http://onlinelibrary.wiley.com/doi/10.1002/art.40554/abstract.

Availability of data and material. The data sets used and/or analyzed during the current study are available on reasonable request from the corresponding author.

RESULTS

Elevated fibroproliferative lesions in the skin following bleomycin exposure. To demonstrate our ability to consistently induce fibrosis in the skin of mice, we injected bleomycin SC into a cohort of animals and assessed various fibrosis end points. Masson's trichrome staining of sections of skin from mice exposed to phosphate buffered saline or bleomycin demonstrated a consistent increase in dermal fibrosis in mice exposed to bleomycin (representative findings are shown in Supplementary Figure 1A, http://onlinelibrary.wiley.com/doi/10.1002/art.40554/abstract). These observations were consistent with increased quantifiable metrics of fibrosis including increased transcripts for collagen and FN in the skin of mice exposed to bleomycin (see Supplementary Figures 1B and C). These findings demonstrate our ability to consistently induce dermal fibrosis in mice using bleomycin.

Elevated ADORA2B expression in dermal fibrosis. Adenosine has been shown to play a detrimental role in several organs where aberrant tissue remodeling and the development of fibrosis are consequences of chronic injury (7,8). Our laboratory and those of others have attributed the profibrotic effects of adenosine to the engagement of ADORA2B (11); however, the involvement of this receptor in bleomycin-induced skin fibrosis has not been examined. To gain insight into the potential role of ADORA2B in dermal fibrosis, we examined transcript levels of ADORA2B and other adenosine receptors in RNA lysates generated from mice exposed to bleomycin. Results demonstrated that there was a significant increase in ADORA2B transcript levels in the fibrotic skin of mice exposed to bleomycin (see Supplementary Figure 1F, http://onlinelibrary.wiley.com/doi/10.1002/art.40554/abstract). Interestingly, transcript levels for ADORA1, ADORA2A, or ADORA3 (see Supplementary Figures 1D, E, and G) were not increased in this model. These findings suggest that ADORA2B is increased in association with dermal fibrosis.

Inhibition of dermal fibrosis by an ADORA2B antagonist. Previous studies have shown that treatment with ADORA2B antagonists during stages of active fibrosis can attenuate fibrosis in the lung (11,12), kidney (13), and penis (14). These findings led us to hypothesize that ADORA2B antagonism would attenuate dermal fibrosis following bleomycin exposure. To test this hypothesis, we examined the therapeutic efficacy of an ADORA2B antagonist in attenuating bleomycin-induced skin fibrosis. Mice were exposed to SC bleomycin, and a cohort was provided with chow containing the ADORA2B antagonist GS-6201 beginning on day 15 following bleomycin administration, a stage when skin fibrosis is already evident (15). On day 28, the skin of mice with exposure to bleomycin and GS-6201 treatment was examined for metrics of skin fibrosis. Mice exposed to bleomycin and treated with the ADORA2B antagonist GS-6201 exhibited reduced dermal fibrosis compared to bleomycin-exposed control chow–treated mice, as observed histologically in Masson's trichrome–stained skin sections (Figure 1A). These qualitative observations were validated with quantifiable analysis of skin fibrosis, including reduced dermal thickness assessed morphometrically (Figure 1B) and reduced collagen transcript levels (Figure 1C). We next stained skin sections with α-SMA to identify myofibroblasts. There were increased numbers of myofibroblasts within fibrotic lesions in mice exposed to bleomycin, and these increased

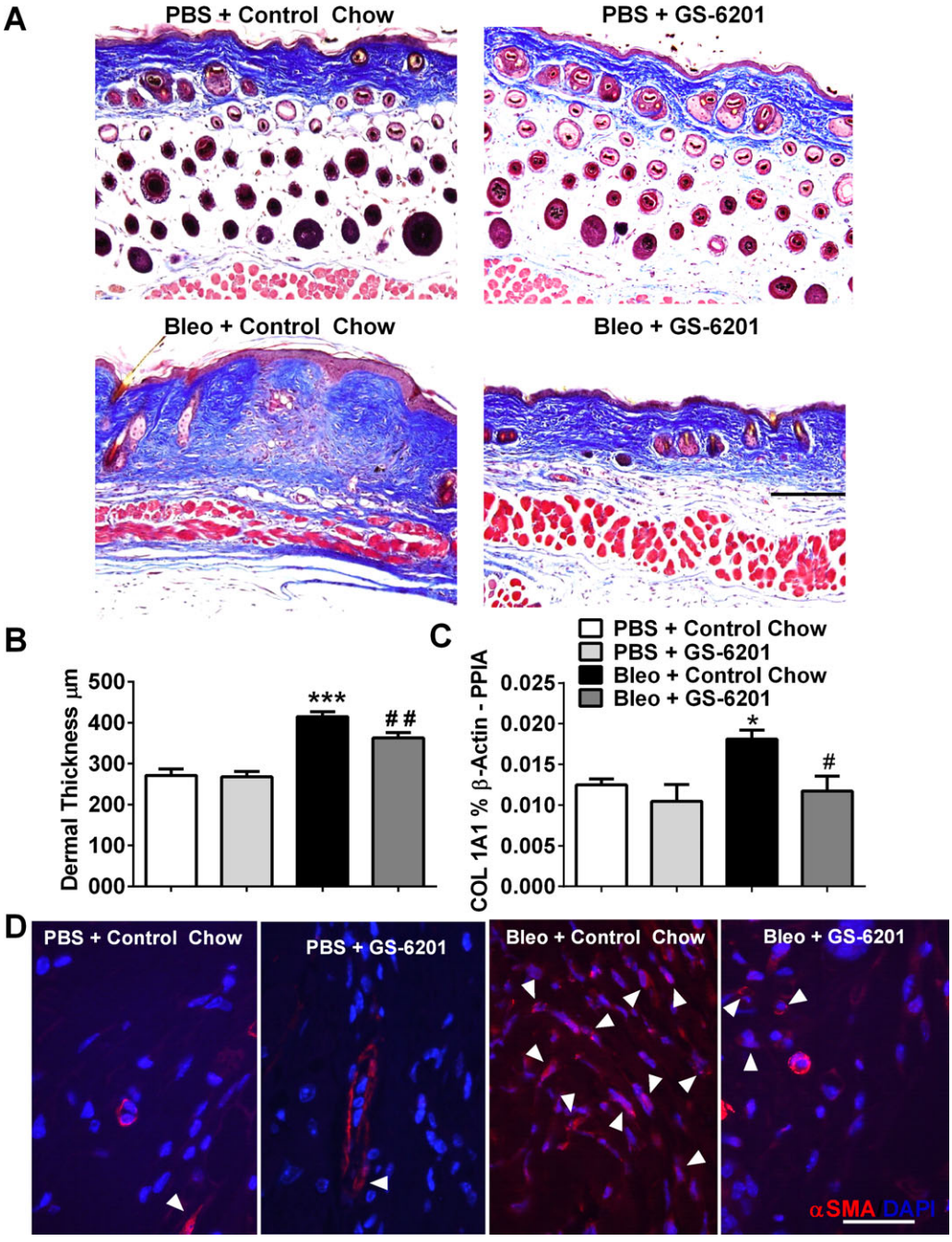

Figure 1. Attenuation of skin fibrosis by GS-6201. **A,** Masson's trichrome–stained skin sections from representative mice treated with phosphate buffered saline (PBS) plus control chow, PBS plus GS-6201, bleomycin (bleo) plus control chow, or bleomycin plus GS-6201. Bar = 500 µm. **B,** Dermal thickness assessed morphometrically from Masson's trichrome–stained skin sections from mice treated as shown in **A**. **C,** COL1A1 transcript levels in skin sections from mice treated as shown in **A**. PPIA = cyclophilin A. **D,** Immunofluorescence for α-smooth muscle actin (α-SMA; red) counterstained with DAPI (blue) in skin sections from mice treated as shown in **A**. **Arrowheads** indicate myofibroblasts. Bar = 25 µm. In **B** and **C**, values are the mean ± SEM. * = $P < 0.05$; *** = $P < 0.001$ versus PBS plus control chow. # = $P < 0.05$; ## = $P < 0.01$ versus bleomycin plus control chow, by analysis of variance.

numbers were attenuated in bleomycin-exposed mice treated with GS-6201 (Figure 1D).

Taken together, these observations demonstrate that treatment with GS-6201 starting on day 15 after the initiation of bleomycin exposure is able to halt the progression of dermal fibrosis. These experiments suggest a potential therapeutic role for GS-6201 in the treatment of skin fibrosis.

ADORA2B antagonism attenuates FN expression and reduces the number of alternatively activated macrophages found in dermal fibrosis. Further analysis of fibrotic lesions showed increased expression of the extracellular matrix molecule FN in mice exposed to SC bleomycin. Levels of FN were attenuated in bleomycin-exposed mice treated with GS-6201 (Figures 2A and C), further indicating the ability of this ADORA2B antagonist to regulate dermal fibrosis in this model.

Alternatively activated macrophages have been implicated in the regulation of fibrosis in various organs in part by the ability of ADORA2B on these cells to elicit the

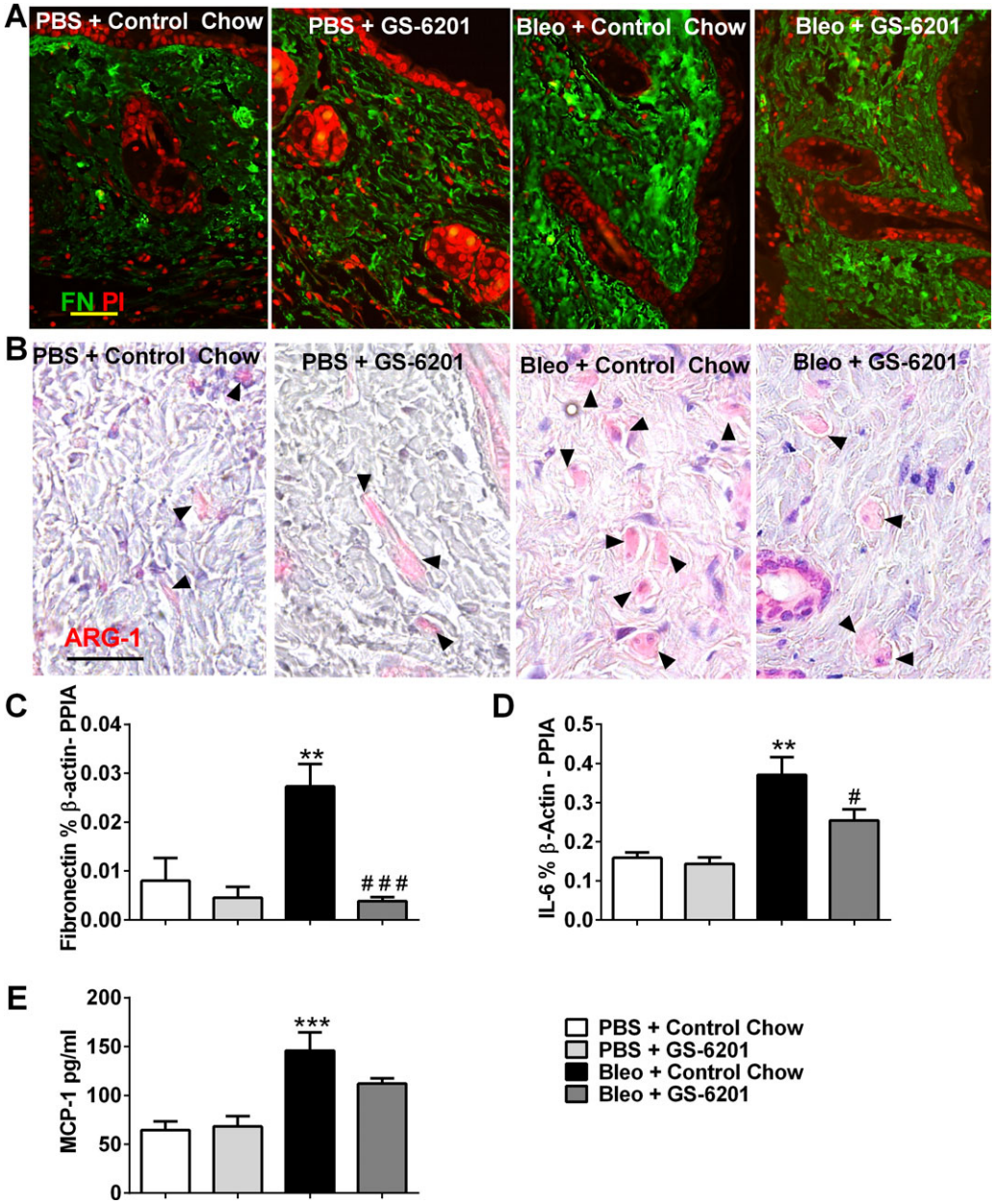

Figure 2. GS-6201 reduces fibronectin (FN) levels and numbers of alternatively activated macrophages. **A** and **B,** Immunofluorescence for FN (green) and counterstaining with propidium iodide (PI; red) (**A**) and immunohistochemical staining for arginase 1 (ARG-1) and counterstaining with hematoxylin (**B**) in skin sections from mice treated with phosphate buffered saline (PBS) plus control chow, PBS plus GS-6201, bleomycin (bleo) plus control chow, or bleomycin plus GS-6201. **Arrowheads** in **B** indicate ARG-1–positive cells. Bars = 50 μm. **C**–**E,** Transcript levels of FN (**C**) and interleukin-6 (IL-6) (**D**) and protein levels of monocyte chemoattractant protein 1 (MCP-1) (**E**) in skin sections from mice in the 4 treatment groups. Values are the mean ± SEM. ** = $P < 0.01$; *** = $P < 0.001$ versus PBS plus control chow. # = $P < 0.05$; ### = $P < 0.001$ versus bleomycin plus control chow, by analysis of variance. PPIA = cyclophilin A.

production of profibrotic molecules (19). To begin to assess whether a similar pathway may be active in dermal fibrosis, we stained tissue sections with arginase 1, a marker for alternatively activated macrophages (Figure 2B). Staining for arginase 1 demonstrated increased numbers of alternatively activated macrophages in bleomycin-exposed skin (Figure 2B). Interestingly, arginase 1–positive alternatively activated macrophages appeared to be less prevalent in the dermis of bleomycin-exposed mice treated with GS-6201 (Figure 2B). We have previously demonstrated that engagement of ADORA2B on alternatively activated macrophages regulates the production of the profibrotic molecule IL-6 (10,20) and of the immunoregulatory molecule MCP-1 (21). To determine if these molecules were regulated by ADORA2B signaling during dermal fibrosis, we measured IL-6 and MCP-1 transcripts in the skin of mice exposed to bleomycin with and without GS-6201 treatment. Results demonstrated significant elevations in

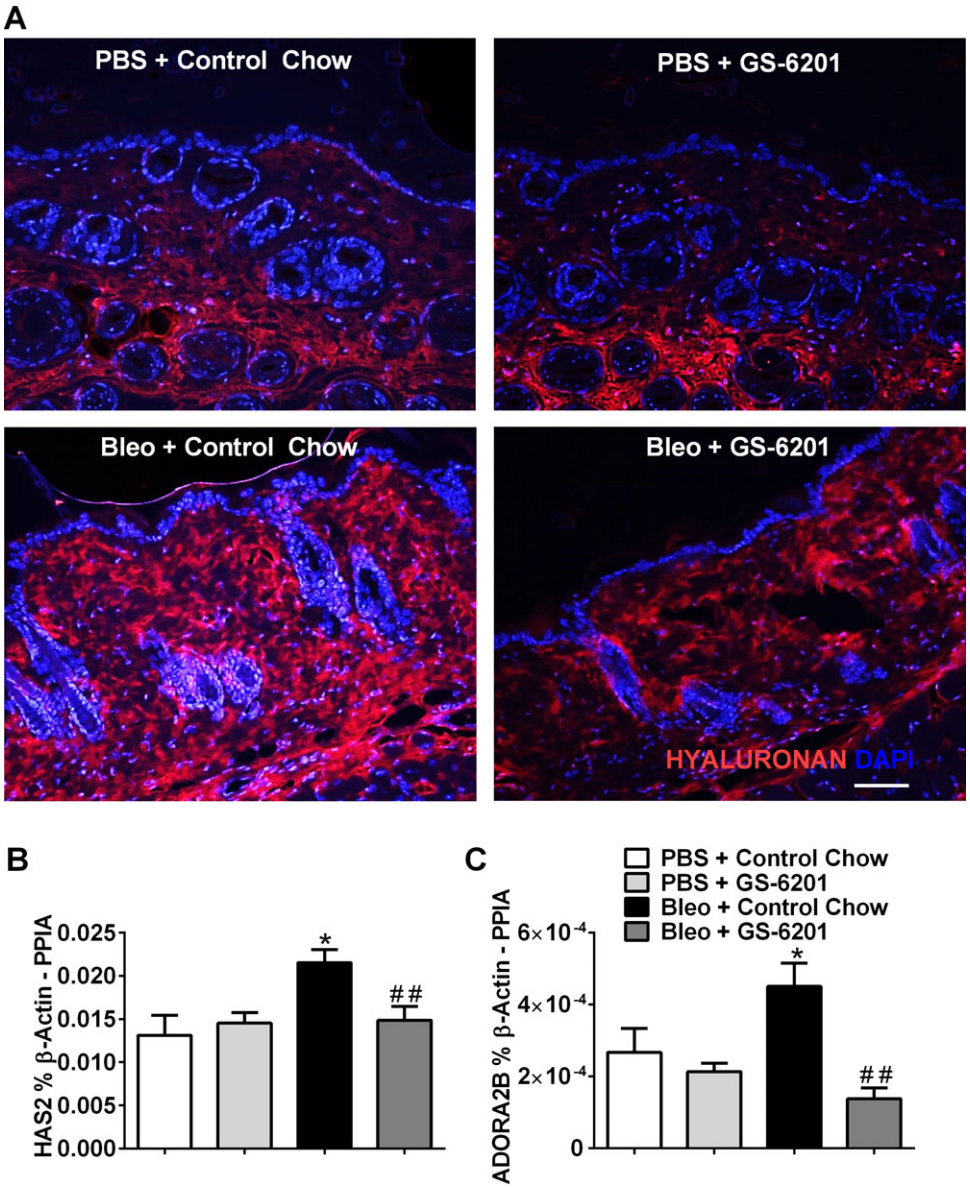

Figure 3. Increased levels of dermal hyaluronan (HA) in bleomycin (bleo)–exposed mice. **A,** Immunofluorescence for HA (red) and counterstaining with DAPI (blue) in skin sections from mice treated with phosphate buffered saline (PBS) plus control chow, PBS plus GS-6201, bleomycin plus control chow, or bleomycin plus GS-6201. Bar = 75 μm. **B** and **C,** Transcript levels of HA synthase 2 (HAS-2) (**B**) and A_{2B} adenosine receptor (ADORA2B) (**C**) in skin sections from mice in the 4 treatment groups. Values are the mean ± SEM. * = $P < 0.05$ versus PBS plus control chow. ## = $P < 0.01$ versus bleomycin plus control chow, by analysis of variance. PPIA = cyclophilin A.

IL-6 (Figure 2D) and MCP-1 (Figure 2E) in the skin of mice exposed to bleomycin. Furthermore, there was a significant reduction in IL-6 transcript levels in bleomycin-exposed mice treated with GS-6201 (Figure 2D) and a trend toward reduction in MCP-1 transcripts (Figure 2E). These findings demonstrate that GS-6201 treatment is able to reduce numbers of alternatively activated macrophages and attenuate fibrosis mediators in the skin of mice exposed to bleomycin.

Attenuation of HA pathways following treatment with an ADORA2B antagonist. Recent studies have shown that engagement of ADORA2B leads to enhanced HA production through increased expression of HAS-2 (22). HA has been implicated in mediating fibrosis through its interaction with fibroblasts (22); however, this profibrotic molecule has not been examined in dermal fibrosis. To address this gap in knowledge, we examined levels of HA and HAS-2 in the skin of mice exposed to bleomycin and determined the impact of GS-6201 treatment on these levels (Figure 3). Staining for HA revealed increased signals in bleomycin-exposed mice that were attenuated in bleomycin-exposed mice treated with GS-6201 (Figure 3A). These observations were consistent with increased HAS-2 expression in bleomycin-exposed mice that was attenuated in bleomycin-exposed mice treated with GS-6201 (Figure 3B). These findings suggest that ADORA2B-dependent up-regulation of HAS-2, and subsequently of HA, may impact dermal fibrosis (Figures 3B and C).

Attenuation of skin fibrosis in the TSK1 mouse following treatment with an ADORA2B antagonist. To investigate whether a similar antifibrotic effect could be achieved in a secondary model of dermal fibrosis, GS-6201 was administered to TSK1 mice, mice with genetically induced dermal fibrosis caused by fibrillin 1 mutation in which fibrotic changes are observed in the hyperdermal layer (16). Female TSK1 mice age 6–8 weeks were fed chow containing vehicle or GS-6201 for 30 days. Skin was collected on day 30 for fibrosis examination. As observed in the Masson's trichrome–stained sections, TSK1 mice

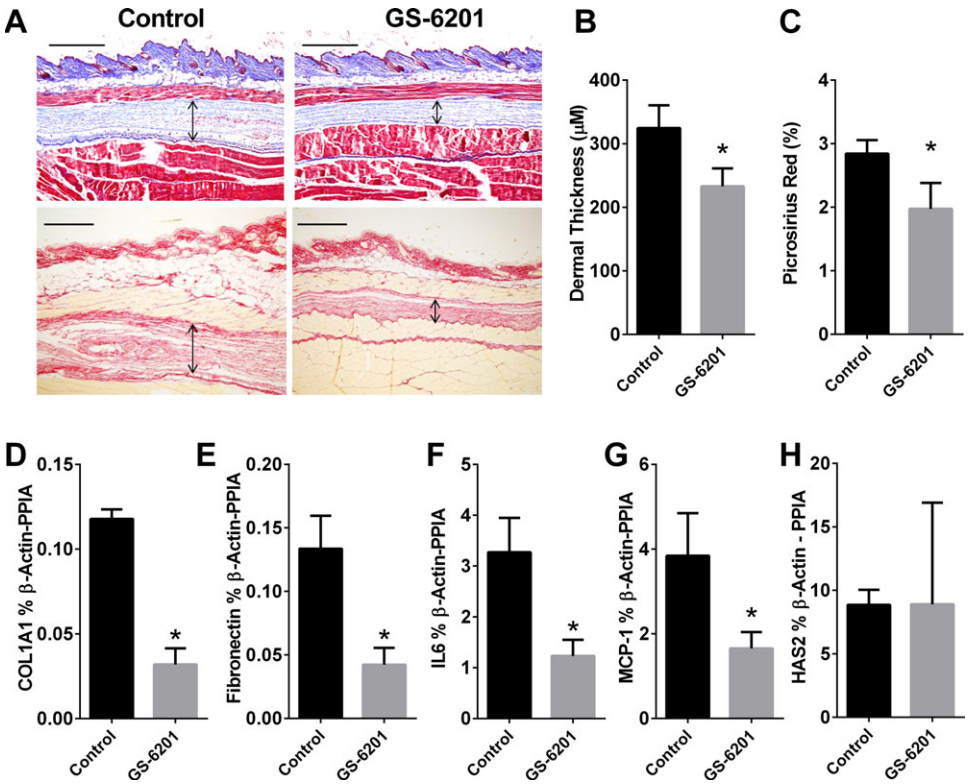

Figure 4. Reduction of dermal fibrosis by GS-6201 in TSK1 mice. Eight-week-old female TSK1 mice were fed control chow or chow containing GS-6201 for 30 days. **A,** After 30 days, skin was collected for Masson's trichrome staining or picrosirius red staining to evaluate skin thickness and collagen deposition. **Arrows** indicate extent of dermal fibrosis at the hyperdermal layer. Bar = 500 μm. **B,** Skin thickness at the hyperdermal layer was measured and quantified. **C,** Picrosirius red–stained skin was quantified, and data were expressed as percentage of the total area. **D**–**H,** Quantitative reverse transcription–polymerase chain reaction was performed to determine transcript levels of COL1A1 (**D**), fibronectin (**E**), interleukin-6 (IL-6) (**F**), monocyte chemoattractant protein 1 (MCP-1) (**G**), and hyaluronan synthase 2 (HAS-2) (**H**) in skin collected from TSK1 mice fed control chow or chow containing GS-6201. In **B**–**H**, values are the mean ± SEM. * = $P < 0.05$ versus control. PPIA = cyclophilin A.

treated with GS-6201 presented with reduced dermal fibrosis at the hyperdermal layer (Figure 4A). Analysis blinded with regard to dermal thickness confirmed a significant reduction in hyperdermal layer thickness (Figure 4B). These changes were consistent with reduced COL1A1 and FN expression levels (Figures 4D and E). In addition, we observed that both IL-6 and MCP-1 transcript expression levels were reduced in the skin of mice treated with GS-6201 (Figures 4F and G), which suggests that the ADORA2B antagonist is able to attenuate fibrosis mediators and inflammation markers associated with alternatively activated macrophages in TSK1 mice. However, HAS-2 transcript levels were not significantly altered in mice treated with GS-6201 compared to control mice (Figure 4H). Taken together, our findings demonstrate that treatment with GS-6201 can halt progression of dermal fibrosis in TSK1 mice.

High expression of ADORA1 and ADORA2B in normal HDFs. Our experiments to determine the expression levels of adenosine receptors in normal HDFs demonstrated that ADORA1 and ADORA2B, but not ADORA2A or ADORA3, were highly expressed in normal HDFs (Figure 5A). We found that normal HDFs treated with NECA, an adenosine receptor analog (18), led to increased levels of IL-6 in media, and that this was blocked by CVT-6694, a selective ADORA2B antagonist (Figure 5B). Interestingly, primary dermal fibroblasts cultured from normal donors or patients diagnosed as having SSc revealed that ADORA2B was the primary adenosine receptor expressed in dermal fibroblasts (Figure 5C). However, no significant differences in adenosine receptor expression were observed between normal and SSc dermal fibroblasts. Furthermore, assessment of mRNA expression levels for adenosine deaminase (ADA) and adenosine kinase, 2 enzymes involved in the degradation of adenosine, revealed a significant increase in adenosine kinase expression but not in ADA expression in SSc samples compared to normal samples (Figure 5D). ADA is normally responsible for extracellular adenosine degradation, while adenosine kinase usually degrades intracellular adenosine. In addition, there were no significant differences in CD73 expression levels, but HAS-2 expression levels were elevated in SSc fibroblasts compared to normal fibroblasts (Figure 5D).

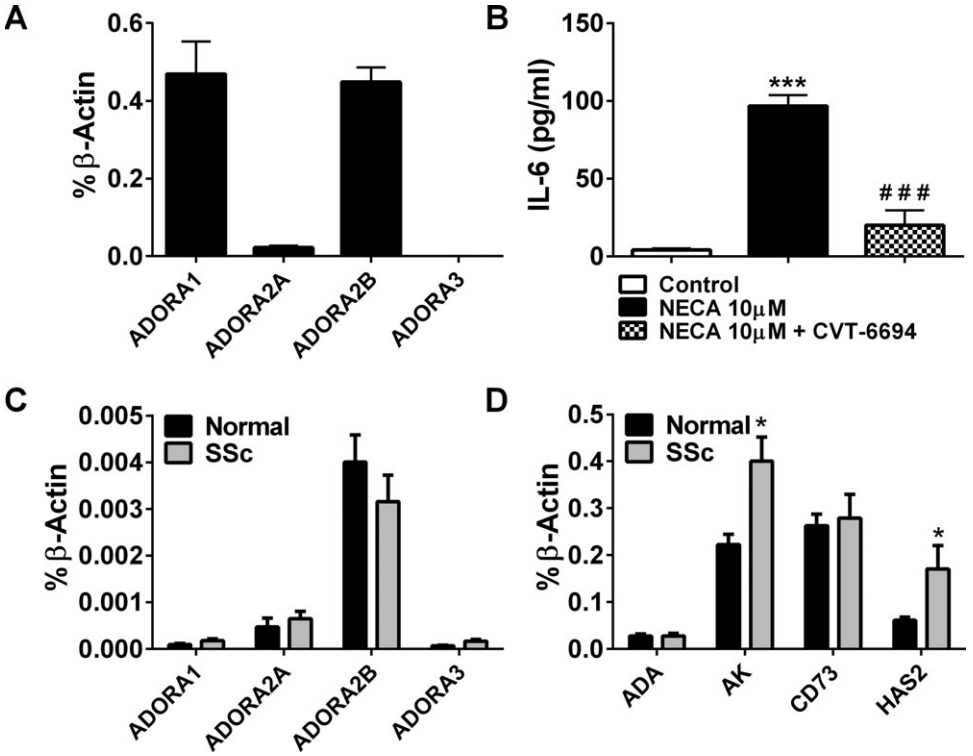

Figure 5. Adenosine receptors and A_{2B} adenosine receptor (ADORA2B) response in normal human dermal fibroblasts (HDFs). **A,** Adenosine receptor expression levels in normal HDFs (n = 3 experiments). **B,** Interleukin-6 (IL-6) release from normal HDFs (n = 4 experiments). Cells were incubated with 5′-*N*-ethylcarboxamidoadenosine (NECA) (10 μ*M*) with or without CVT-6694 (100 n*M*) for 18 hours. **C** and **D,** Adenosine receptor expression (**C**) and transcript levels for adenosine deaminase (ADA), adenosine kinase (AK), CD73, and hyaluronan synthase 2 (HAS-2) (**D**) in primary HDFs from 5 normal donors and 5 patients diagnosed as having systemic sclerosis (SSc). Values are the mean ± SEM. In **B**, *** = $P <$ 0.001 versus control; ### = $P < 0.001$ versus NECA alone, by analysis of variance. In **D**, * = $P < 0.05$ versus HDFs from normal donors, by *t*-test.

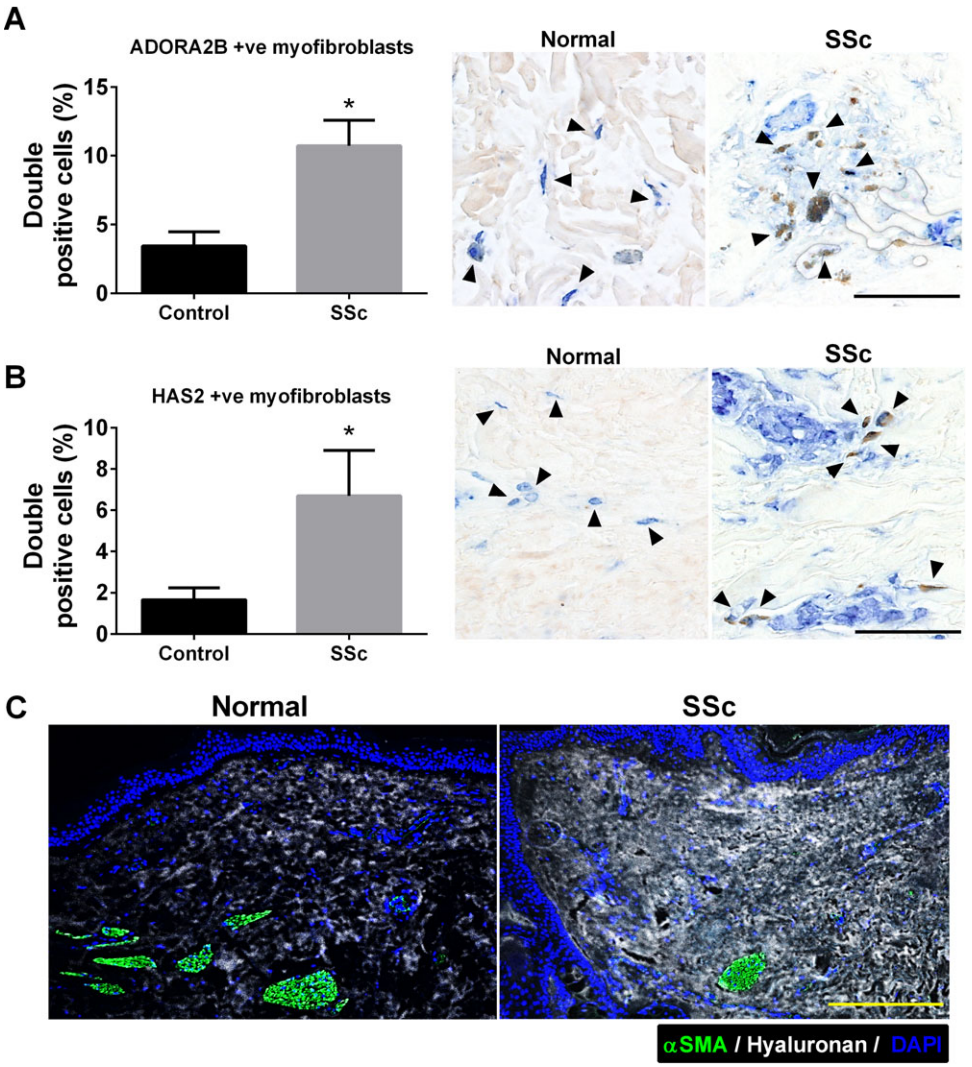

Figure 6. Expression of A_{2B} adenosine receptor (ADORA2B), hyaluronan, and hyaluronan synthase 2 (HAS-2) in human normal and systemic sclerosis (SSc) skin tissue. **A** and **B,** Immunofluorescence and morphometric evaluation of cells double positive for α-smooth muscle actin (α-SMA; blue) and ADORA2B (brown) (**A**) and of cells double positive for α-SMA and HAS-2 (brown) (**B**). **Arrowheads** in **A** indicate α-SMA and ADORA2B double-positive cells; **arrowheads** in **B** indicate α-SMA and HAS-2 double-positive cells. Bars = 100 μm. Values are the mean ± SEM. * = $P < 0.05$ versus control, by Student's 2-tailed *t*-test. **C,** Staining for α-SMA (green) and hyaluronan (white) with DAPI counterstaining (blue). Bar = 50 μm.

Similarly, immunofluorescence staining and subsequent morphometric evaluation revealed coexpression of ADORA2B and α-SMA in fibroblasts in normal and SSc skin (Figure 6A), with an increased number of ADORA2B-positive myofibroblasts in SSc skin compared to control skin (Figure 6A). In sections immunohistochemically stained for HAS-2 and α-SMA, we observed increased HAS-2–positive myofibroblasts in SSc skin compared to control skin (Figure 6B), which was consistent with increased HA deposition in SSc skin sections (Figure 6C).

DISCUSSION

Extracellular adenosine has been associated with the progression of several chronic diseases, including diseases in which fibrosis is a major component (7,8). Mice deficient in ADA exhibit progressive and chronic elevations in adenosine levels due to the absence of the enzyme that breaks down adenosine (23). These mice spontaneously develop fibrosis in many organs including the lung (24,25), liver (24), kidney (13), penis (14), and skin (26). These findings led to the hypothesis that chronic elevations

in adenosine serve as a profibrotic signal (7) and initiated a series of studies to investigate the mechanisms involved. With regard to skin fibrosis, substantial amounts of experimental work have demonstrated that adenosine generation (27) and its signaling through ADORA2A constitute a major profibrotic regulator in dermal fibrosis (6). Fernandez and colleagues have demonstrated that antagonism of ADORA2A in the ADA-deficient mouse model can attenuate adenosine-driven skin fibrosis (26). In addition, this group has shown that direct engagement of ADORA2A on dermal fibroblasts can access numerous profibrotic pathways (28–30). Thus, adenosine clearly plays a role in regulating dermal fibrosis through ADORA2A expressed on dermal fibroblasts.

Work from our laboratories has shown that ADORA2B plays an important role in the regulation of fibrosis in several organs (8). Moreover, the highly selective ADORA2B antagonist GS-6201 has been used in these studies to show that ADORA2B plays an important role in the regulation of pulmonary fibrosis (11). Treatment with GS-6201 was able to attenuate pulmonary fibrosis in ADA-deficient mice (11) and mice in which pulmonary fibrosis was induced by bleomycin (11,12). Importantly, in these studies, GS-6201 was given to mice after pulmonary fibrosis was well-established (12), demonstrating that blockade of this pathway was therapeutic. A major finding of the current study was that treatment with this same antagonist was also effective in attenuating dermal fibrosis in the SC bleomycin model and in TSK1 mice. Similar to studies on pulmonary fibrosis, GS-6201 was effective in attenuating several metrics of dermal fibrosis even though treatment was not initiated until late in the model. These findings provide the first evidence that ADORA2B plays a role in regulating dermal fibrosis, and they suggest that targeting this receptor may be an attractive approach for the treatment of fibrotic dermal disorders such as SSc.

Additional evidence to support a role for ADORA2B in dermal fibrosis was our finding that levels of this receptor were elevated in skin samples from mice exposed to SC bleomycin. Elevations in ADORA2B levels are commonly seen in fibrotic tissues in both mice and humans (12,20), where various profibrotic activities have been identified on different cell types. For example, ADORA2B levels are found to be elevated on myofibroblasts (9), where ADORA2B signaling can promote both the differentiation of myofibroblasts and the production of fibrosis mediators. In addition to its importance for myofibroblasts, ADORA2B has recently been shown to be important in regulating the function of a subtype of macrophages known as alternatively activated macrophages (10). Alternatively activated macrophages have been suggested to play an important role in the regulation of fibrosis in many organs (19), and a recent study has demonstrated that the expression of ADORA2B on this cell type contributes to the progression of pulmonary fibrosis in mice (10). ADORA2B is known to induce the production of the profibrotic molecule IL-6 from alternatively activated macrophages both in mice (10) and in humans (20) with pulmonary fibrosis, and genetically removing ADORA2B from macrophages is associated with reduced IL-6 production and reduced pulmonary fibrosis (10).

Similarly, in the current study, we demonstrate that IL-6 levels are elevated in the SC bleomycin model in conjunction with increased numbers of alternatively activated macrophages. Moreover, we show that treatment with an ADORA2B antagonist is associated with fewer alternatively activated macrophages and reduced production of IL-6 both in the SC bleomycin model and in TSK1 mice. Taken together, these results suggest that ADORA2B signaling on alternatively activated macrophages in fibrotic skin may regulate IL-6 production, which could regulate dermal fibrosis. In support of these studies, blockade of IL-6 was shown to lead to significant reduction in skin thickening in a randomized controlled trial in SSc patients (31).

We recently found that ADORA2B-driven fibrotic responses in the lungs of mice are also associated with increased HA signaling (22). Similarly, we demonstrated in the current study that there are substantial increases both in the enzyme that produces hyaluronan, HAS-2, and in HA itself in fibrotic lesions of mice exposed to bleomycin and in skin samples from patients with SSc. Moreover, treatment with GS-6201 was associated with decreased HAS-2 expression and with a reduction in HA in fibrotic skin. HA signaling contributes to the progression of fibrosis by stimulating profibrotic activities on fibroblasts (22), and our findings suggest that the ADORA2B-dependent regulation of this pathway may contribute to dermal fibrosis. These findings echo our observations in experimental models of lung injury in which treatment with GS-6201 or depletion of ADORA2B in myeloid cells reduced the extent of fibrotic deposition in the lungs and attenuated vascular remodeling and pulmonary hypertension (10,12). Further studies by our group identified increased HA as a modulator of enhanced fibrotic deposition and vascular remodeling (10,22) that can be targeted therapeutically (32). These observations have important implications for SSc, in which the development of interstitial lung disease or pulmonary hypertension is a serious complication (33,34).

Consistent with these results, in experiments using normal HDFs we demonstrate that both ADORA1 and ADORA2B are highly expressed in these cells and that activation of ADORA2B leads to increased levels of the

profibrotic cytokine IL-6. Interestingly, our data from primary cells isolated from SSc patients or controls did not show increased ADORA1 signals. This may be explained by the origin of the normal HDFs obtained from Lonza. These cells originated from 1 donor, a 41-year-old female who underwent reduction mammaplasty or abdominoplasty, while our results from primary cells represent average signals from cells obtained from the forearms of 5 controls and 5 SSc patients. Thus, we believe that our data from isolated primary fibroblasts may be more representative than the data from normal HDFs.

Our experiments using immunofluorescence showed expression of ADORA2B in fibroblasts in both normal and SSc tissue. These findings are significant as this response is likely augmented in fibrotic normal HDFs in which increased ADORA2B expression is expected (8). This is consistent with previously published data showing increased IL-6 levels from SSc skin lesions following exposure to ATP (35).

It is also important to point out that although our experiments in mice did not show increased ADORA2A levels, increased expression of ADORA2A has been shown in fibroblasts from SSc patients (36). Furthermore, activation of ADORA2A by CGS-21680 has been shown to stimulate fibroblast-to-myofibroblast differentiation in human SSc fibroblasts (36). In contrast, ADORA2A-deficient mice or mice treated with the ADORA2A antagonist ZM241385 have exaggerated dermal fibrosis due to abrogated production of transforming growth factor β and connective tissue growth factor (26,29). These studies clearly show an important role of adenosine signaling through ADORA2A in dermal fibrosis.

ADORA2A and ADORA2B are both coupled to adenylyl cyclase by the stimulatory G protein subunit (Gαs) and can induce intracellular cAMP levels. ADORA2B has the lowest affinity to extracellular adenosine; therefore, it is normally activated in pathologic conditions due to elevated extracellular adenosine (37). Previous studies in lymphocytes indicate that surface expression of ADORA2A is partially responsible for surface expression of ADORA2B in lymphocytes (38), indicating that activation of ADORA2A promotes ADORA2B signaling. The different turnover rate may contribute to the low ADORA2A expression in dermal fibroblasts. However, because ADORA2A has much higher affinity than ADORA2B, we believe that ADORA2A and ADORA2B both play potential roles during the pathogenesis of dermal fibrosis. Despite this, our results reveal that ADORA2B is the adenosine receptor most abundantly expressed both in normal and in SSc fibroblasts, yet no differences were identified in adenosine receptor expression between normal and SSc samples.

Taken together, these results point to the potential benefit of ADORA2A antagonists to treat human dermal fibrosis, in addition to ADORA2B antagonism. Interestingly, our data also show increased expression of adenosine kinase but not ADA in SSc skin samples. These results are significant since adenosine kinase metabolizes adenosine back to AMP intracellularly, while ADA degrades adenosine to inosine extracellularly. These results may suggest that in SSc, increased intracellular adenosine levels are present that lead to increased expression of adenosine kinase.

In conclusion, we have shown that the ADORA2B antagonist GS-6201 is effective in reducing dermal fibrosis in a mouse model of SC bleomycin exposure. These findings suggest that this receptor could play a role in regulating dermal fibrosis and that targeting this receptor may prove beneficial in the treatment of disorders such as SSc, in which dermal fibrosis is prominent. These studies were not able to resolve the relative difference between the ADORA2A and ADORA2B signaling pathways in dermal fibrosis; therefore, additional studies are needed to address this issue and to identify when and how best to promote the use of adenosine-based therapeutics for the treatment of dermal fibrosis.

ACKNOWLEDGMENT

We thank Kelly A. Volcik (UTHealth) for her help in revising the manuscript.

AUTHOR CONTRIBUTIONS

All authors were involved in drafting the article or revising it critically for important intellectual content, and all authors approved the final version to be published. Dr. Weng had full access to all of the data in the study and takes responsibility for the integrity of the data and the accuracy of the data analysis.

Study conception and design. Karmouty-Quintana, Agarwal, Zhong, Blackburn, Weng.

Acquisition of data. Karmouty-Quintana, Molina, Philip, Bellocchi, Gudenkauf, Chen, Collum, Ko, Zhong, Weng.

Analysis and interpretation of data. Karmouty-Quintana, Philip, Bellocchi, Gudenkauf, Wu, Chen, Collum, Ko, Assassi, Zhong, Weng.

ROLE OF THE STUDY SPONSOR

Gilead Sciences, Inc. had no role in the study design or in the collection, analysis, or interpretation of the data, the writing of the manuscript, or the decision to submit the manuscript for publication. Publication of this article was not contingent upon approval by Gilead Sciences, Inc.

REFERENCES

1. Charles C, Clements P, Furst DE. Systemic sclerosis: hypothesis-driven treatment strategies. Lancet 2006;367:1683–91.

2. Varga J, Abraham D. Systemic sclerosis: a prototypic multisystem fibrotic disorder. J Clin Invest 2007;117:557–67.
3. Varga J, Whitfield ML. Transforming growth factor-β in systemic sclerosis (scleroderma). Front Biosci (Schol Ed) 2009;1:226–35.
4. Fredholm BB. Adenosine, an endogenous distress signal, modulates tissue damage and repair. Cell Death Differ 2007;14: 1315–23.
5. Blackburn MR, Vance CO, Morschl E, Wilson CN. Adenosine receptors and inflammation. Handb Exp Pharmacol 2009:215–69.
6. Chan ES, Cronstein BN. Adenosine in fibrosis. Mod Rheumatol 2010;20:114–22.
7. Zhou Y, Schneider DJ, Blackburn MR. Adenosine signaling and the regulation of chronic lung disease. Pharmacol Ther 2009;123:105–16.
8. Karmouty-Quintana H, Xia Y, Blackburn MR. Adenosine signaling during acute and chronic disease states. J Mol Med (Berl) 2013;91:173–81.
9. Zhong H, Belardinelli L, Maa T, Zeng D. Synergy between A2B adenosine receptors and hypoxia in activating human lung fibroblasts. Am J Respir Cell Mol Biol 2005;32:2–8.
10. Karmouty-Quintana H, Philip K, Acero LF, Chen NY, Weng T, Molina JG, et al. Deletion of ADORA2B from myeloid cells dampens lung fibrosis and pulmonary hypertension. FASEB J 2015;29:50–60.
11. Sun CX, Zhong H, Mohsenin A, Morschl E, Chunn JL, Molina JG, et al. Role of A2B adenosine receptor signaling in adenosine-dependent pulmonary inflammation and injury. J Clin Invest 2006;116:2173–82.
12. Karmouty-Quintana H, Zhong H, Acero L, Weng T, Melicoff E, West JD, et al. The A2B adenosine receptor modulates pulmonary hypertension associated with interstitial lung disease. FASEB J 2012;26:2546–57.
13. Zhang W, Zhang Y, Wang W, Dai Y, Ning C, Luo R, et al. Elevated ecto-5'-nucleotidase-mediated increased renal adenosine signaling via A2B adenosine receptor contributes to chronic hypertension. Circ Res 2013;112:1466–78.
14. Wen J, Jiang X, Dai Y, Zhang Y, Tang Y, Sun H, et al. Increased adenosine contributes to penile fibrosis, a dangerous feature of priapism, via A2B adenosine receptor signaling. FASEB J 2010; 24:740–9.
15. Wu M, Schneider DJ, Mayes MD, Assassi S, Arnett FC, Tan FK, et al. Osteopontin in systemic sclerosis and its role in dermal fibrosis. J Invest Dermatol 2012;132:1605–14.
16. Walker MA, Harley RA, LeRoy EC. Inhibition of fibrosis in TSK mice by blocking mast cell degranulation. J Rheumatol 1987;14: 299–301.
17. Zhong H, Belardinelli L, Maa T, Feoktistov I, Biaggioni I, Zeng D. A(2B) adenosine receptors increase cytokine release by bronchial smooth muscle cells. Am J Respir Cell Mol Biol 2004; 30:118–25.
18. Kalla RV, Elzein E, Perry T, Li X, Gimbel A, Yang M, et al. Selective, high affinity A(2B) adenosine receptor antagonists: N-1 monosubstituted 8-(pyrazol-4-yl)xanthines. Bioorg Med Chem Lett 2008;18:1397–401.
19. Murray PJ, Wynn TA. Protective and pathogenic functions of macrophage subsets. Nat Rev Immunol 2011;11:723–37.
20. Zhou Y, Murthy JN, Zeng D, Belardinelli L, Blackburn MR. Alterations in adenosine metabolism and signaling in patients with chronic obstructive pulmonary disease and idiopathic pulmonary fibrosis. PLoS One 2010;5:e9224.
21. Pedroza M, Schneider DJ, Karmouty-Quintana H, Coote J, Shaw S, Corrigan R, et al. Interleukin-6 contributes to inflammation and remodeling in a model of adenosine mediated lung injury. PLoS One 2011;6:e22667.
22. Karmouty-Quintana H, Weng T, Garcia-Morales LJ, Chen NY, Pedroza M, Zhong H, et al. Adenosine A2B receptor and hyaluronan modulate pulmonary hypertension associated with chronic obstructive pulmonary disease. Am J Respir Cell Mol Biol 2013;49:1038–47.
23. Blackburn MR. Too much of a good thing: adenosine overload in adenosine-deaminase-deficient mice. Trends Pharmacol Sci 2003; 24:66–70.
24. Chunn JL, Mohsenin A, Young HW, Lee CG, Elias JA, Kellems RE, et al. Partially adenosine deaminase-deficient mice develop pulmonary fibrosis in association with adenosine elevations. Am J Physiol Lung Cell Mol Physiol 2006;290:L579–87.
25. Chunn JL, Molina JG, Mi T, Xia Y, Kellems RE, Blackburn MR. Adenosine-dependent pulmonary fibrosis in adenosine deaminase-deficient mice. J Immunol 2005;175:1937–46.
26. Fernandez P, Trzaska S, Wilder T, Chiriboga L, Blackburn MR, Cronstein BN, et al. Pharmacological blockade of A2A receptors prevents dermal fibrosis in a model of elevated tissue adenosine. Am J Pathol 2008;172:1675–82.
27. Fernandez P, Perez-Aso M, Smith G, Wilder T, Trzaska S, Chiriboga L, et al. Extracellular generation of adenosine by the ectonucleotidases CD39 and CD73 promotes dermal fibrosis. Am J Pathol 2013;183:1740–6.
28. Perez-Aso M, Fernandez P, Mediero A, Chan ES, Cronstein BN. Adenosine 2A receptor promotes collagen production by human fibroblasts via pathways involving cyclic AMP and AKT but independent of Smad2/3. FASEB J 2014;28:802–12.
29. Chan ES, Fernandez P, Merchant AA, Montesinos MC, Trzaska S, Desai A, et al. Adenosine A_{2A} receptors in diffuse dermal fibrosis: pathogenic role in human dermal fibroblasts and in a murine model of scleroderma. Arthritis Rheum 2006;54:2632–42.
30. Chan ES, Liu H, Fernandez P, Luna A, Perez-Aso M, Bujor AM, et al. Adenosine A(2A) receptors promote collagen production by a Fli1- and CTGF-mediated mechanism. Arthritis Res Ther 2013;15:R58.
31. Khanna D, Denton CP, Jahreis A, van Laar JM, Frech TM, Anderson ME, et al. Safety and efficacy of subcutaneous tocilizumab in adults with systemic sclerosis (faSScinate): a phase 2, randomised, controlled trial. Lancet 2016;387:2630–40.
32. Collum SD, Chen NY, Hernandez AM, Hanmandlu A, Sweeney H, Mertens TC, et al. Inhibition of hyaluronan synthesis attenuates pulmonary hypertension associated with lung fibrosis. Br J Pharmacol 2017;174:3284–301.
33. Wells AU, Steen V, Valentini G. Pulmonary complications: one of the most challenging complications of systemic sclerosis. Rheumatology (Oxford) 2009;48 Suppl 3:iii40–4.
34. Proudman SM, Stevens WM, Sahhar J, Celermajer D. Pulmonary arterial hypertension in systemic sclerosis: the need for early detection and treatment. Int Med J 2007;37:485–94.
35. Lo Monaco A, Gulinelli S, Castellino G, Solini A, Ferrari D, La Corte R, et al. Increased sensitivity to extracellular ATP of fibroblasts from patients affected by systemic sclerosis. Ann Rheum Dis 2007;66:1124–5.
36. Lazzerini PE, Natale M, Gianchecchi E, Capecchi PL, Montilli C, Zimbone S, et al. Adenosine A2A receptor activation stimulates collagen production in sclerodermic dermal fibroblasts either directly and through a cross-talk with the cannabinoid system. J Mol Med 2012;90:331–42.
37. Liu H, Xia Y. Beneficial and detrimental role of adenosine signaling in diseases and therapy. J Appl Physiol (1985) 2015;119: 1173–82.
38. Moriyama K, Sitkovsky MV. Adenosine A2A receptor is involved in cell surface expression of A2B receptor. J Biol Chem 2010; 285:39271–88.

ARTHRITIS & RHEUMATOLOGY
Vol. 70, No. 10, October 2018, pp 1685–1694
DOI 10.1002/art.40544

Risk Factors and Biomarkers for the Occurrence of Uveitis in Juvenile Idiopathic Arthritis

Data From the Inception Cohort of Newly Diagnosed Patients With Juvenile Idiopathic Arthritis Study

Christoph Tappeiner,[1] Jens Klotsche,[2] Claudia Sengler,[3] Martina Niewerth,[3] Ina Liedmann,[3] Karoline Walscheid,[4] Miha Lavric,[5] Dirk Foell,[5] Kirsten Minden,[2] and Arnd Heiligenhaus[4]

Objective. **To analyze the prognostic value of demographic, clinical, and therapeutic factors and laboratory biomarkers and to assess their role in predicting uveitis occurrence in patients with juvenile idiopathic arthritis (JIA).**

Methods. **Patients with JIA were enrolled within the first year after JIA diagnosis. Demographic and clinical parameters were documented. Serum samples were collected at study enrollment, at 3-month follow-up visits within the first year, and then every 6 months. A multivariable Cox regression analysis was performed to evaluate the impact of demographic, clinical, laboratory, and therapeutic parameters on uveitis onset.**

Results. **We included 954 JIA patients (67.2% female, 54.2% antinuclear antibody [ANA] positive, mean ± SD age at onset 7.1 ± 4.6 years). Uveitis occurred in 133 patients (observation period 44.5 months). Young age at JIA onset and ANA positivity were significantly associated with the onset of uveitis (both $P < 0.001$). Treatment of arthritis with methotrexate alone (hazard ratio [HR] 0.18 [95% confidence interval (95% CI) 0.12–0.29], $P < 0.001$) or combined with etanercept (HR 0.10 [95% CI 0.04–0.23], $P < 0.001$) or adalimumab (HR 0.09 [95% CI 0.01–0.61], $P = 0.014$) reduced the risk of uveitis onset and the occurrence of uveitis-related complications. Predictors of uveitis onset included elevated erythrocyte sedimentation rate at baseline (HR 2.36 [95% CI 1.38–4.02], $P = 0.002$) and continuing moderate or high disease activity during follow-up as measured by the 10-joint clinical Juvenile Arthritis Disease Activity Score (HR 4.30 [95% CI 2.51–7.37], $P < 0.001$). Additionally, S100A12 levels ≥250 ng/ml at baseline were significantly associated with the risk of uveitis (HR 2.10 [95% CI 1.15–3.85], $P = 0.016$).**

Conclusion. **Apart from demographic risk factors and treatment modalities, JIA disease activity scores and laboratory biomarkers could be used to better define the group of JIA patients at high risk of uveitis onset.**

Juvenile idiopathic arthritis (JIA) is a heterogeneous group of diseases with arthritis onset before age 16 years. In ~9–13% of patients with JIA, uveitis becomes manifest (1,2) and may lead to vision-threatening complications (3–5). Previous studies have identified different risk factors for uveitis onset in JIA, namely, oligoarthritis subtype, young age at arthritis onset, short duration of JIA disease, and antinuclear antibody (ANA) positivity (6–8). Uveitis occurrence is subject to geographic variations, with

The Inception Cohort of Newly diagnosed patients with Juvenile Idiopathic Arthritis study is funded by the German Federal Ministry of Education and Research (grants FKZ 01ER0812, 01ER0813, and 01ER0828).

[1]Christoph Tappeiner, MD: Inselspital, University of Bern, Bern, Switzerland, German Rheumatism Research Center, Berlin, Germany, and St. Franziskus Hospital, Muenster, Germany; [2]Jens Klotsche, PhD, Kirsten Minden, MD: German Rheumatism Research Center and Charité Universitätsmedizin Berlin, Berlin, Germany; [3]Claudia Sengler, MD, Martina Niewerth, MPH, Ina Liedmann: German Rheumatism Research Center, Berlin, Germany; [4]Karoline Walscheid, MD, Arnd Heiligenhaus, MD, PhD: St. Franziskus Hospital, Muenster, Germany; [5]Miha Lavric, PhD, Dirk Foell, MD: University of Muenster, Muenster, Germany.

Dr. Foell has received honoraria from Pfizer and Novartis (less than $10,000 each) and research grants from those companies. Dr. Minden has received honoraria from AbbVie, Roche/Chugai, Sanofi, Medac, and Pharm-Allergan (less than $10,000 each) and research grants from Pfizer, AbbVie, and Roche. Dr. Heiligenhaus has received honoraria from AbbVie, Alimera Sciences, Allergan, Merck Sharp & Dohme, Pfizer, Santen, and Xoma (less than $10,000 each) and research grants from Pfizer and Novartis.

Address correspondence to Christoph Tappeiner, MD, FEBO, Department of Ophthalmology, Inselspital, Bern University Hospital, 3010 Bern, Switzerland. E-mail: christoph.tappeiner@insel.ch.

Submitted for publication December 23, 2017; accepted in revised form April 26, 2018.

a higher rate in northern countries (e.g., Scandinavian countries and Germany) and a lower frequency in eastern and southern Asia (1,2,7). Furthermore, disease-modifying antirheumatic drug (DMARD) treatment in JIA patients may reduce the risk of uveitis onset, especially if instituted early in the course of disease (9).

Different molecular biomarkers have recently been investigated in arthritis patients in order to detect residual inflammation and the risk of arthritis flares after remission or after discontinuing treatment. A laboratory biomarker that offers the potential of a reliable outcome measure would be desirable for clinicians. An elevated erythrocyte sedimentation rate (ESR) may indicate activity of an autoimmune disease. Indeed, previous studies indicated an elevated risk of uveitis in JIA patients with an elevated ESR (10–13), while no such correlation was found in others (2,14). For other factors (e.g., C-reactive protein [CRP]), no correlation with uveitis risk in JIA has been found previously (10,12,13).

A new and promising approach is the determination of serum levels of S100 proteins, a group of damage-associated molecular pattern molecules expressed in cells of myeloid origin. S100 molecules mediate inflammatory responses of the innate immune system and recruit inflammatory cells to the site of tissue damage (15). S100A8/A9 complexes (myeloid-related protein 8 [MRP-8]/MRP-14; calprotectin) and S100A12 are calcium-binding proteins that mediate inflammatory responses through the receptor for advanced glycation end products and Toll-like receptors, after release from activated or necrotic cells (16). It has been shown that the MRPs S100A8 and S100A9 play a distinct role in neutrophil and monocyte activation (17). Analysis of these factors represents a promising tool for monitoring inflammation in JIA patients and in other (auto)inflammatory or autoimmune diseases (15,17–20). Indeed, serum levels of S100A8 and S100A9 have been shown to be useful for assessing the risk of further arthritis flares after methotrexate (MTX) withdrawal in JIA (21). Increased levels of S100A12 reflect neutrophil activation (15,20) and—similar to S100A8/A9—are useful for detecting low-level inflammation and predicting risk of relapses in JIA (19,22). Although it has been shown that elevated S100 serum levels reflect intraocular inflammation in JIA (23), no data are available about the impact of S100 serum protein levels on uveitis occurrence, outcome, and response to treatment. This would be a desirable monitoring instrument and prospective marker for assessing JIA patients at risk of uveitis manifestations or of a severe course of this ocular disease.

The aim of this study was to analyze the role of demographic factors, DMARD treatment, and laboratory biomarkers—particularly S100A12—to predict occurrence of uveitis in the prospective, controlled Inception Cohort of Newly diagnosed patients with Juvenile Idiopathic Arthritis (ICON-JIA).

PATIENTS AND METHODS

Patients and controls. The ICON-JIA study is a prospective, controlled, observational, multicenter study. We included patients with JIA defined according to the International League of Associations for Rheumatology classification (24) and with recent disease onset (diagnosis <12 months before enrollment). Eleven pediatric rheumatology centers in Germany are participating in this study (during the recruitment period, the units reached >33% of patients with incident JIA expected in the population in Germany). For more details on the ICON-JIA cohort study, see Sengler et al (25). For this analysis, the observation period ended at the last follow-up visit in patients without uveitis and on the date of occurrence of uveitis in patients who developed uveitis during the follow-up period. The loss to follow-up was low, with an annual dropout rate of 3.4% over the study period.

Data and blood sample collection. Patients were examined by a pediatric rheumatologist and an ophthalmologist quarterly during the first year and every 6 months thereafter. Various demographic and clinical data (e.g., count of joints with active disease [range 0–70] and global assessment of disease activity on a Numerical Rating Scale [21-point; 0–10]) and medical and family history were collected with standardized case report forms and questionnaires. JIA disease activity was evaluated using the 10-joint clinical Juvenile Arthritis Disease Activity Score (cJADAS-10). The cJADAS-10 (range 0–30) includes the physician's global assessment of disease activity, the parents' global assessment of overall well-being, and the number of joints with active disease (maximum of 10). The cJADAS-10 thresholds proposed by Consolaro and Ravelli (26) were applied to define disease activity states for oligoarticular and polyarticular JIA (≤1 = inactive; >1–≤1.5 and >1–≤2.5 = minimal; >1.5–≤4 and >2.5–≤8.5 = moderate; >4 and >8.5 = high, respectively).

At enrollment and at the follow-up visits every 3 months within the first year and every 6 months thereafter, standard inflammation markers (e.g., ESR, CRP level, and platelet count) and S100 proteins, cytokines, and chemokines were measured from serum samples. A double-sandwich enzyme-linked immunosorbent assay system was used to determine S100A12 levels. The ESR cutoff of ≥20 mm/hour was applied to define elevated ESR levels in accordance with the definition of the JADAS-10 (27). The readers of the laboratory assays were blinded with regard to the diagnosis. Additionally, immunoglobulins, autoantibodies (rheumatoid factor [RF] and ANAs), and HLA–B27 status were determined at inclusion. Ophthalmologic screening was performed according to current screening recommendations (2); findings were directly recorded with standardized questionnaires by the ophthalmologist who cared for the patient, and uveitis was classified according to the Standardization of Uveitis Nomenclature Working Group criteria (28).

Statistical analysis. Descriptive data were reported as the mean ± SD or the median and interquartile range for continuously distributed variables, as appropriate. Distributions of categorical variables were described by absolute and relative frequencies. A multivariable Cox regression analysis was performed to evaluate the associations of demographic, clinical (JADAS-10 score, etc.), laboratory (S100A12 and ESR), and

therapeutic parameters with uveitis onset. These analyses also included time-dependent covariates (change in disease severity across time and change in therapy) to model the change in the underlying risk of incidence of uveitis. A clinically meaningful threshold of 250 ng/ml for S100A12 levels was determined at the maximum of the Youden index based on receiver operating characteristic curve analysis (29). Missing values in categorical predictor variables were modeled by an additional category. Hazard ratios (HRs) are reported with 95% confidence intervals (95% CIs). *P* values less than 0.05 were considered significant. All statistical analyses were conducted using SAS software, version 9.3 (SAS Institute).

Ethics committee approval. The study was approved by the ethics committee of the Charité Universitätsmedizin Berlin. Subjects' consent was obtained according to the Declaration of Helsinki, and the design of the work conforms to the standards currently applied in Germany.

RESULTS

Demographic data. A total of 954 JIA patients were included in the study (67.2% female, 54.2% ANA positive, mean ± SD age at onset 7.1 ± 4.6 years) (Table 1). The mean ± SD follow-up time was 44.5 ± 22.8 months. Uveitis occurred in 133 patients (13.9%) during the observation period. Uveitis developed in 4 of these patients (0.4% of all JIA patients; 3.0% of all with uveitis) before the first JIA symptoms became manifest, with a mean ± SD duration of 11.0 ± 5.6 months between uveitis onset and first JIA symptoms. New uveitis onset was recorded for 65 (6.8% of all JIA patients; 48.9% of all with uveitis), 24 (2.5% of all JIA patients; 18.0% of all with uveitis), and 19 (2.0% of all JIA patients; 14.3% of all with uveitis) patients in the first, second, and third year, respectively, after first JIA symptoms. In 52 patients (5.5% of all JIA patients; 39.1% of all with uveitis), uveitis occurred after first JIA symptoms became manifest and before ICON-JIA study enrollment. A total of 21 patients (2.2% of all JIA patients; 15.8% of all with uveitis) developed uveitis after 3 years or later after JIA onset (see Supplementary Figure 1, available on the *Arthritis & Rheumatology* web site at http://onlinelibrary.wiley.com/doi/10.1002/art.40544/abstract).

Established risk factors for uveitis. The established risk factors for uveitis onset were analyzed in the total sample of 954 patients. Female sex, young age at JIA onset, the JIA category of oligoarthritis, and ANA positivity were significantly associated with the onset of uveitis in univariate analyses (Table 2). Moreover, ANA positivity (HR 2.79 [95% CI 1.66–4.69], $P < 0.001$) and age <3 years at JIA onset (HR 2.8 [95% CI 1.9–4.0], $P < 0.001$) were also significantly associated with risk of uveitis in multivariable analysis. The multivariable model had good power to predict the risk of uveitis (Harrel's C = 0.77).

Table 1. Demographic and clinical data on the JIA patients at enrollment in the ICON-JIA study*

	Total sample (n = 954)†	Sample excluding patients with uveitis before enrollment in the ICON-JIA study (n = 898)‡
Female	641 (67.2)	601 (66.9)
Age at symptom onset, mean ± SD years	7.1 ± 4.6	7.3 ± 4.7
Time from symptom onset to diagnosis, median (IQR) months	3.0 (1.0–7.0)	3.0 (1.0–7.0)
Time from diagnosis to enrollment, median (IQR) months	1.6 (0.4–4.4)	1.5 (0.4–4.2)
JIA category		
Systemic arthritis	35 (3.7)	35 (3.9)
Oligoarthritis	445 (46.7)	410 (45.7)
Psoriatic arthritis	39 (4.1)	38 (4.2)
Enthesitis-related arthritis	100 (10.5)	94 (10.5)
RF-positive polyarthritis	15 (1.6)	15 (1.7)
RF-negative polyarthritis	252 (26.4)	242 (26.9)
Undifferentiated arthritis	68 (7.1)	64 (7.1)
cJADAS-10, mean ± SD	9.8 ± 6.2	9.9 ± 6.3
Inactive disease	56 (6.1)	51 (5.9)
Minimal disease activity	24 (2.6)	22 (2.6)
Moderate disease activity	173 (18.9)	164 (19.0)
High disease activity	664 (72.4)	626 (72.5)
ANA positive§	517 (54.2)	469 (52.2)
RF positive§	31 (3.3)	31 (3.5)
HLA–B27 positive§	146 (15.3)	139 (15.5)
ESR, mean ± SD mm/hour¶	22.8 ± 21.7	22.7 ± 21.9
S100A12, mean ± SD ng/ml#	337.5 ± 806.8	347.8 ± 833.0
Uveitis	133 (13.9)	77 (8.6)

* Except where indicated otherwise, values are the number (%). JIA = juvenile idiopathic arthritis; ICON-JIA = Inception Cohort of Newly diagnosed patients with Juvenile Idiopathic Arthritis; IQR = interquartile range; cJADAS-10 = 10-joint clinical Juvenile Arthritis Disease Activity Score.

† Sample for the analysis of "classic" risk factors.

‡ Sample for the analysis of clinical parameters and biomarkers for the risk of uveitis during follow-up.

§ Percentages refer to the total numbers of 954 and 898 patients in the total sample and the sample excluding patients with uveitis before enrollment, respectively. Test results were missing for antinuclear antibody (ANA) positivity (44 patients [4.6% of all patients]), rheumatoid factor (RF) positivity (177 patients [18.6% of all patients]), and HLA–B27 positivity (234 patients [24.5% of all patients]).

¶ Erythrocyte sedimentation rate (ESR) was reported in 794 and 744 patients, respectively.

Measured in 529 and 494 patients in the total sample and the sample excluding patients with uveitis before enrollment, respectively.

Impact of treatment on uveitis onset. The influence of treatment on the risk of uveitis was analyzed in 898 patients (the sample excluded patients with uveitis onset before enrollment in the ICON-JIA study [see Table 1]). Treatment of arthritis with MTX significantly reduced the risk of subsequent uveitis onset (HR 0.16 [95% CI 0.11–0.24], $P < 0.001$). This effect was also statistically significant after adjustment for established uveitis risk factors (HR 0.14 [95% CI 0.09–0.21], $P < 0.001$).

Table 2. Risk of incident uveitis from onset of first JIA symptoms in the Inception Cohort of Newly diagnosed patients with Juvenile Idiopathic Arthritis study (n = 954)*

	Patients without uveitis at follow-up (n = 821)	Patients with uveitis at follow-up (n = 133)	Incidence of uveitis at follow-up (n = 133)†	Univariate analysis			Multivariable analysis§	
				HR (95% CI)	*P*	C‡	HR (95% CI)	*P*
Female	542 (66.0)	99 (74.4)	99 (15.4)	1.50 (1.01–2.23)	0.048	0.55	0.97 (0.64–1.45)	0.865
Age at JIA symptom onset, mean ± SD years	7.7 ± 4.6	3.8 ± 3.0	–	0.79 (0.74–0.84)	<0.001	0.75	0.82 (0.78–0.88)	<0.001
JIA category								
Oligoarthritis	360 (43.9)	85 (63.9)	85 (19.1)	2.16 (1.51–3.10)¶	<0.001	0.59	1.36 (0.94–1.96)¶	0.104
RF-negative polyarthritis	219 (26.7)	33 (24.8)	33 (13.1)					
RF-positive polyarthritis	15 (1.8)	0 (0.0)	0 (0.0)					
Psoriatic arthritis	37 (4.5)	2 (1.5)	2 (5.1)					
Enthesitis-related arthritis	92 (11.2)	8 (6.0)	8 (8.0)					
Systemic arthritis	35 (4.3)	0 (0.0)	0 (0.0)					
Undifferentiated arthritis	63 (7.7)	5 (3.8)	5 (7.4)					
ANA positive, no. (% tested)	404 (49.2)	113 (85.0)	113 (21.9)	5.00 (3.03–8.23)	<0.001	0.66	2.79 (1.66–4.69)	<0.001
RF positive, no. (% tested)	31 (3.8)	0 (0.0)	0 (0.0)	–	–	–	–	–
HLA–B27 positive, no. (% tested)	135 (16.4)	11 (8.3)	11 (7.5)	0.52 (0.28–0.97)	0.040	0.54	0.80 (0.42–1.50)	0.481

* Except where indicated otherwise, values are the number (%). HR = hazard ratio; 95% CI = 95% confidence interval; RF = rheumatoid factor.
† Incidence of uveitis within a group (row percentage).
‡ Harrel's C, a measure to evaluate the predictive power of parameters to predict the risk of uveitis ranging between 0.5 and 1 (0.5 = prediction by chance, 1 = perfect prediction). The multivariable model had good power to predict the risk of uveitis (Harrel's C = 0.77).
§ Predictors in the multivariable model were female sex, age at first symptoms of juvenile idiopathic arthritis (JIA), oligoarthritis (versus all other JIA categories), antinuclear antibody (ANA) positivity, and HLA–B27 positivity.
¶ The reference is all other categories of JIA.

Patients receiving MTX monotherapy (HR 0.18 [95% CI 0.12–0.29], $P < 0.001$; n = 414) or MTX combined with etanercept (HR 0.10 [95% CI 0.04–0.23], $P < 0.001$; n = 170) showed a reduced risk of uveitis onset. This effect might rely mostly on the effect from MTX, as the uveitis risk was not altered with etanercept monotherapy (HR 0.76 [95% CI 0.28–2.07], $P = 0.589$; n = 16). However, the study might have been underpowered for the analysis of

Table 3. Univariate and multivariable analysis of the impact of cJADAS-10, ESR, and S100A12 levels on the incidence of uveitis in the Inception Cohort of Newly diagnosed patients with Juvenile Idiopathic Arthritis study, at enrollment and during follow-up*

	Univariate analysis		Multivariable analysis†	
	HR (95% CI)	*P*	HR (95% CI)	*P*
Parameters at enrollment (visits with available measurements)				
cJADAS-10 (882)‡	1.00 (0.96–1.04)	0.867	1.02 (0.98–1.07)	0.308
Moderate or high disease activity	1.56 (0.57–4.28)	0.390	1.72 (0.62–4.78)	0.301
ESR (770)‡	1.02 (1.01–1.03)	<0.001	1.02 (1.01–1.03)	<0.001
ESR ≥20 mm/hour	2.98 (1.78–5.00)	<0.001	2.36 (1.38–4.02)	0.002
S100A12 (517)‡	1.40 (1.14–1.72)	0.001	1.50 (1.15–1.96)	0.003
S100A12 ≥250 ng/ml	2.66 (1.47–4.82)	0.001	2.10 (1.15–3.85)	0.016
Time-varying parameters at follow-up (visits with available measurements)				
cJADAS-10 (6,104)‡	1.10 (1.05–1.15)	<0.001	1.17 (1.11–1.23)	<0.001
Moderate or high disease activity	3.41 (2.01–5.77)	<0.001	4.30 (2.51–7.37)	<0.001
ESR (4,329)‡	1.03 (1.01–1.04)	<0.001	1.03 (1.01–1.05)	0.001
ESR ≥20 mm/hour	2.57 (1.48–4.46)	0.001	2.44 (1.37–4.36)	0.003
S100A12 (1,901)‡	1.18 (0.81–1.72)	0.379	1.21 (0.81–1.82)	0.351
S100A12 ≥250 ng/ml	1.45 (0.57–3.70)	0.438	1.54 (0.60–3.99)	0.372

* 95% CI = 95% confidence interval.
† Adjusted for age at disease onset, oligoarthritis, antinuclear antibody positivity, and treatment with methotrexate and biologic disease-modifying antirheumatic drugs.
‡ Hazard ratio (HR) for the increase by 1 unit in the 10-joint clinical Juvenile Arthritis Disease Activity Score (cJADAS-10) and the erythrocyte sedimentation rate (ESR), and for the increase by 50 units in the S100A12 level.

etanercept monotherapy. Treatment with adalimumab as monotherapy (n = 17) or in combination with MTX (n = 55) was also associated with a lower risk of uveitis onset (HR 0.09 [95% CI 0.01–0.61], $P = 0.014$; n = 72).

Laboratory and clinical biomarkers as risk factors for uveitis onset. ESRs (in mm/hour) and S100A12 levels (in ng/ml) were available at enrollment for 770 and 517 patients, respectively. A total of 216 patients (42%) with S100A12 measurement at baseline started DMARD treatment prior to the first S100A12 measurement (median duration of 1.5 months between start of DMARD treatment and S100A12 measurement at baseline). During the follow-up period, ESRs and S100A12 levels could be analyzed for 4,329 and 1,901 visits, respectively. Patients without uveitis during the observation period had a mean ± SD ESR of 21.8 ± 21.3 mm/hour at enrollment compared to 32.5 ± 26.4 mm/hour in patients with uveitis manifestations (see Supplementary Figure 2A, available at http://onlinelibrary.wiley.com/doi/10.1002/art.40544/abstract). Similarly, mean ± SD S100A12 levels were 338 ± 849 ng/ml in patients without uveitis at enrollment and 434 ± 681 ng/ml in patients with uveitis at follow-up (see Supplementary Figure 2B). Both ESR and S100A12 were significantly associated with risk of uveitis onset in univariate and multivariable analyses (Table 3). Elevated S100A12 levels (≥250 ng/ml) during the JIA disease course did not show a significant association with the risk of uveitis at follow-up (HR 1.45 [95% CI 0.57–3.70], $P = 0.438$) (Table 3).

Importantly, clinically active arthritis—in fact, moderate or high active disease state as measured by the cJADAS-10—during the follow-up period significantly predicted subsequent uveitis onset (HR 3.41 [95% CI 2.01–5.77], $P < 0.001$). Patients with an elevated ESR (≥20 mm/hour) at the visit before uveitis onset were at higher risk of developing uveitis (HR 2.44 [95% CI 1.37–4.36], $P = 0.003$) (Table 3 and Figure 1), after adjustment for the established risk factors and arthritis treatment. In a multivariable analysis, moderate or high active disease state as measured by the cJADAS-10 and elevated ESRs was also significantly associated with uveitis onset (Table 3).

Identifying children at risk of uveitis onset is especially important for JIA subgroups in which (silent) chronic anterior uveitis may occur, as uveitis may go unnoticed for a longer time period in these children compared to children in other JIA subgroups (e.g., enthesitis-related arthritis [ERA], with acute anterior uveitis). Therefore, we

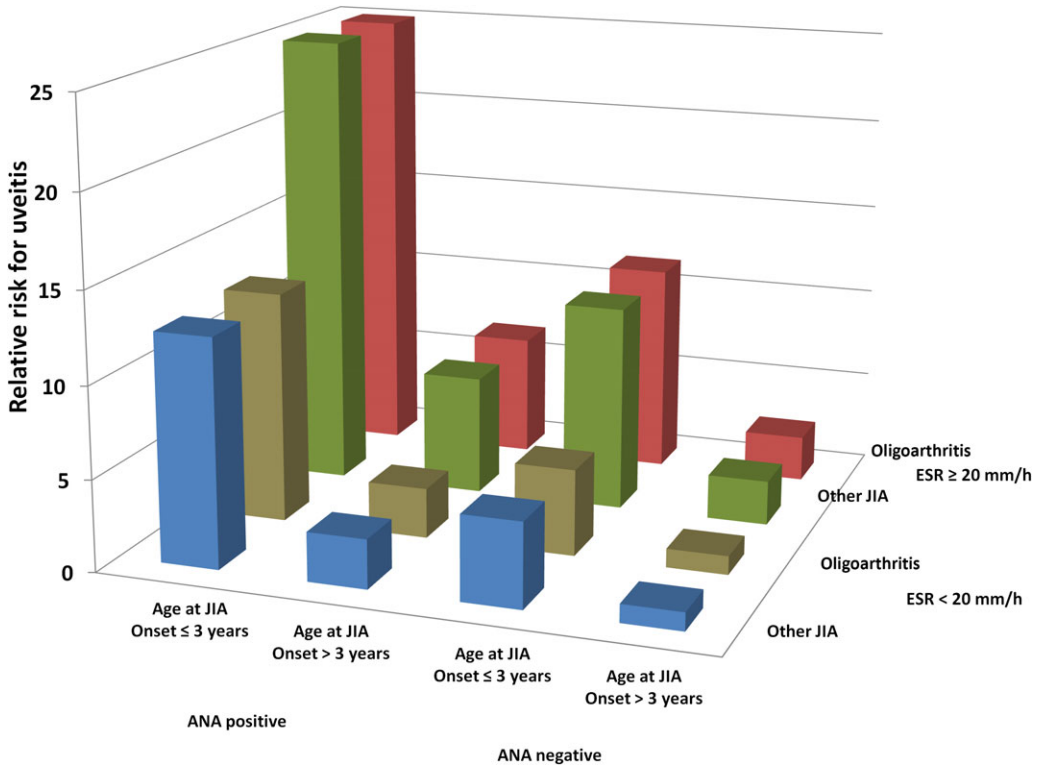

Figure 1. Relative risk of uveitis onset based on age at onset of juvenile idiopathic arthritis (JIA), antinuclear antibody (ANA) positivity, and erythrocyte sedimentation rate (ESR) at follow-up, adjusted for the 10-joint clinical Juvenile Arthritis Disease Activity Score and treatment with methotrexate (MTX) and MTX/biologic disease-modifying antirheumatic drugs.

performed a subgroup analysis for those children who typically may develop chronic anterior uveitis (i.e., oligoarthritis, RF-negative polyarthritis, psoriatic arthritis, and undifferentiated arthritis) (see Supplementary Tables 1 and 2, available at http://onlinelibrary.wiley.com/doi/10.1002/art.40544/abstract). The risk factors for uveitis manifestations (Supplementary Table 1) and the predictive value of ESR and S100A12 (Supplementary Table 2) in this subgroup were similar to those in the whole JIA cohort in the ICON-JIA study, without any remarkable differences (Tables 2 and 3, respectively). The subgroup analysis for children with ERA, who may typically develop acute anterior uveitis instead of chronic anterior uveitis, was underpowered (n = 8 patients with uveitis) due to a low number of uveitis events or even none in the individual categories of the risk factors.

Clinical characteristics at first uveitis documentation. A detailed characterization of uveitis at initial documentation was available for 116 patients (87%), providing information on 162 affected eyes. At first uveitis documentation, bilateral uveitis was seen in 47 patients (40.5%), and an anterior chamber cell grade ≤2+ was found in 92% of patients (0.5+ in 20.7%, 1+ in 27.6%, and 2+ in 28.7% of patients). Uveitis-related complications were present in 28.7% of patients at first uveitis documentation (mainly posterior synechiae in 20.9% of patients and cataracts in 7.8%).

Patients with and those without uveitis-related complications at first uveitis documentation did not differ remarkably with regard to sex, JIA category, ANA positivity, and age at disease onset (Table 4). JIA patients being treated with DMARDs, specifically MTX or biologic DMARDs before uveitis onset, had slightly fewer uveitis-related complications at first uveitis documentation (Table 4). In the exploratory analysis of patients with uveitis onset after ICON-JIA study enrollment, parameters such as the cJADAS-10, ESR, and S100A12 level were analyzed with regard to the presence of secondary complications of uveitis at first documentation of disease (Table 5).

Table 4. Presence of uveitis-related ocular complications at initial uveitis documentation (univariate analyses)*

	No uveitis-related complications (n = 82)	Any uveitis-related complications (n = 33)
Female sex	64 (78.1)	24 (72.7)
Oligoarticular JIA	54 (65.9)	21 (63.6)
ANA positivity	69 (84.2)	30 (90.9)
HLA–B27 positivity	5 (6.1)	3 (9.1)
Age at JIA onset, mean ± SD years	3.4 ± 2.7	4.6 ± 3.3
Age at JIA onset ≤3 years	50 (61.0)	14 (42.4)
JIA disease duration, mean ± SD months	17.4 ± 16.9	6.0 ± 23.1
Uveitis onset after JIA onset	1 (1.2)	3 (9.1)
Previous therapy		
No DMARDs	56 (68.3)	30 (90.9)
Methotrexate	23 (28.1)	3 (9.1)
Etanercept	6 (7.3)	2 (6.1)
Adalimumab	1 (1.2)	0 (0.0)

* Except where indicated otherwise, values are the number (%). JIA = juvenile idiopathic arthritis; ANA = antinuclear antibody; DMARDs = disease-modifying antirheumatic drugs.

Table 5. Presence of uveitis-related ocular complications at initial uveitis documentation for patients with uveitis onset after enrollment in the Inception Cohort of Newly diagnosed patients with Juvenile Idiopathic Arthritis study*

	No uveitis-related complications (n = 54)	Any uveitis-related complications (n = 8)
Parameters at enrollment		
cJADAS-10, mean ± SD	9.57 ± 5.05	9.88 ± 8.00
Moderate or high disease activity	51 (94.4)	7 (87.5)
ESR, mean ± SD mm/hour	32.27 ± 22.72	37.03 ± 27.61
ESR ≥20 mm/hour	37 (68.5)	6 (75.0)
S100A12, mean ± SD ng/ml	497.53 ± 777.64	412.80 ± 131.26
S100A12 ≥250 ng/ml	19 (51.4)	4 (80.0)
Parameters at follow-up		
cJADAS-10, mean ± SD	4.95 ± 4.27	3.00 ± 2.98
Moderate or high disease activity	32 (65.3)	3 (60.0)
ESR, mean ± SD mm/hour	20.57 ± 15.37	13.60 ± 7.79
ESR ≥20 mm/hour	19 (38.0)	1 (20.0)
S100A12, mean ± SD ng/ml	204.15 ± 147.50	81.00 (–)
S100A12 ≥250 ng/ml	6 (31.6)	0 (0.0)

* Except where indicated otherwise, values are the number (%). cJADAS-10 = 10-joint clinical Juvenile Arthritis Disease Activity Score; ESR = erythrocyte sedimentation rate.

DISCUSSION

As uveitis manifestations in patients with JIA are often initially asymptomatic and may lead to irreversible vision impairment, identifying children at risk of uveitis is crucial. Current screening guidelines, based on JIA category, ANA positivity/negativity, age at JIA onset, and JIA disease duration, recommend screening intervals between 3 and 12 months (2,30). Using additional demographic, clinical, and laboratory biomarkers to even better define patients at risk of uveitis onset would be highly desirable. Furthermore, early DMARD treatment might be considered for the high-risk group with high rates of uveitis onset and ocular complications if the number needed to treat as well as a better outcome for such an approach could be justified by confirmed evidence.

In this study cohort, uveitis occurred in 13.9% of children with JIA, which is consistent with previous

publications reporting an overall prevalence of uveitis in JIA of ~9–13% (1,7,31,32); however, higher rates from Nordic countries of up to 20.5% have also been reported (14). In this large, prospective, multicenter study, demographic risk factors, namely, young age at JIA onset, JIA category, and ANA positivity, were significantly associated with the risk of uveitis onset. These findings corroborate the results of previous studies (2,9,14,33). In our study, female sex was found to be a significant risk factor for uveitis in the univariate analysis but not in the multivariable analysis. This corresponds to the results from other cohorts, in which sex was not found to be an independent risk factor (1,2,14,34,35). This may be explained by the predominance of females among those with onset of oligoarticular JIA at young age and by the higher percentage of ANA-positive females (35). A lower risk of uveitis onset within this group of JIA patients with intermediate follow-up duration was found for HLA–B27–positive children; however, this was significant only in the univariate analysis. HLA–B27 positivity in uveitis cases has been described previously, particularly in the ERA subgroup, and uveitis occurrence might increase with longer follow-up duration (2,36).

Children receiving conventional synthetic or biologic DMARDs had a significantly lower risk of uveitis onset in the current study, especially when receiving MTX and/or adalimumab. Preliminary evidence for a protective effect of MTX in JIA was found in a retrospective study by Papadopoulou et al, with uveitis developing in 10.5% of patients receiving MTX compared to 20.2% in those not receiving MTX (odds ratio 0.46, $P = 0.049$) (37), while such a role of immunosuppressive drugs was not clearly confirmed in other studies (14,38). Ravelli et al (39) recently reported an open-label trial comparing intraarticular corticosteroids alone to intraarticular corticosteroids plus MTX in JIA and found no significant difference in new-onset uveitis between patients who received MTX and those who did not ($P = 0.4957$). A protective effect of DMARD treatment has also been suggested in one of our previous studies, in which the uveitis prevalence decreased significantly between 2002 and 2013 from 13% to 11.6% in a national pediatric database, corresponding to an increasing rate of both synthetic (mostly MTX) and biologic DMARD use in the same time period (31). Finally, in another prospective study by our group based on a national database of 3,512 children with JIA in Germany, we found that DMARD treatment significantly reduced the risk of uveitis (for MTX alone, HR 0.63, $P = 0.022$; for tumor necrosis factor inhibitors, HR 0.56, $P < 0.001$; for a combination of the 2 medications, HR 0.10, $P < 0.001$) (9). A maximum of 300 ICON-JIA study patients may also have been included in our previous study, which would represent 8.5% of the patient group examined. The different results for the potential protective effect of MTX on uveitis manifestations might be explained by differences in study populations, study designs (particularly differences in ophthalmologic screening and documentation, for example, frequent prospective uveitis documentation only in the ICON-JIA study specifically focusing on uveitis occurrence and course), follow-up periods, analysis power, and adjustment for other risk factors.

Furthermore, our study gave new insight into the role of clinical activity scores and biomarkers (e.g., ESR and S100A12) as prognostic markers for uveitis in JIA. In 4 previous studies, elevated ESR predicted uveitis manifestations (10–13), while this was only true for the ERA subgroup of JIA in another study from a German cohort (2). It may be speculated that a high ESR correlates with the activity of autoimmune processes in JIA, potentially under the influence of Treg cells (13). Furthermore, the fact that high cJADAS scores indicate a higher risk of uveitis onset supports this theory and also supports previous notions (9). In our study, an ESR ≥20 mm/hour at enrollment indicated a significant risk of uveitis onset (HR 2.36, $P = 0.002$). As ESR is tested routinely in children with JIA, its use as a biomarker could easily be implemented more systematically in clinical practice and also in screening guidelines, as also suggested by Haasnoot et al (13). When analyzing the absolute ESR (instead of a cutoff of ≥20 mm/hour), only a modest HR of 1.02 ($P < 0.001$) was found, which means that for each 1-mm elevation of ESR, the odds for the occurrence of uveitis increase by 2%. Haasnoot et al (13) also found an almost identical ratio (HR 1.016, $P = 0.001$).

Interestingly, S100A12 levels at enrollment predicted uveitis onset. In a pilot study, elevated S100A12 levels were found in the serum and aqueous humor of patients with autoimmune uveitis (23), indicating a promising potential for this biomarker. Previous data support the use of S100A12 and S100A8/9 levels as a disease activity marker for predicting disease relapse and to help make therapeutic decisions in JIA (21,40,41). However, in our study S100A12 levels during the course of JIA disease did not show a significant relationship with the occurrence of uveitis, which might be explained by the influence of antiinflammatory treatment (23) (e.g., DMARDs), the limited number of samples available for S100A12 analysis, and high variations in levels. It must be considered that the HR indicated a positive association of uveitis risk with S100A12 levels during the course of disease, although without statistical significance. This might have been caused by low statistical power due to missing S100A12 measurements (compared to the numbers of available ESR measurements).

The ocular characteristics of eyes with uveitis at study inclusion (n = 116 patients with complete ophthalmological documentation) were similar to those previously reported (2,31,34). Occurrence of ocular complications during the course of JIA-associated uveitis was described in up to 90% of patients (32,42–47). At study inclusion, uveitis-related complications were already found in 28.7% of our patients, compared to 20–64% in previous reports (2,34,48). Such differences may be explained by the introduction of screening programs, the adoption of new JIA treatment regimens in the past few decades, and early and more aggressive treatment, particularly with biologic DMARDs (31). In this regard, the inclusion of patients within 1 year after JIA diagnosis (and not directly after JIA or uveitis onset) has to be considered for our study. Similarly, posterior synechiae and cataracts were the most common ocular complications at first presentation in previous observations (2,34,48). In our study, risk factors for the presence of early ocular uveitis-related complications were young age at disease onset and absence of any DMARD treatment. Interestingly, children treated with MTX, especially, demonstrated a significantly lower occurrence of uveitis-related complications at study inclusion. Such a relationship has also been found in previous studies (31).

The strengths of this study are its prospective multicenter design with a clearly defined inception cohort (inclusion of JIA patients within the first year of JIA diagnosis only) that included a remarkably large number of patients with documented ophthalmologic and pediatric rheumatic conditions based on clearly defined outcome criteria. Allowing the inclusion of children within 1 year and not directly at JIA onset might represent a certain limitation of this study; however, this made it possible to include this large cohort of children. Although the majority of the patients likely developed uveitis during the observation period, the possibility cannot be excluded that more children could develop uveitis after the mean follow-up period of 44.5 months. It must be mentioned that the ICON-JIA study did not explicitly distinguish between insidious (chronic) and acute-onset anterior uveitis. Due to this lack of differentiation in the data collection, we performed a subgroup analysis excluding all patients at risk of acute anterior uveitis (i.e., ERA, systemic arthritis, and RF-positive polyarthritis), and we found no relevant differences compared to the analysis of the whole JIA cohort (see Results).

It would be interesting to know the ANA titer and its influence on uveitis risk. However, the ICON-JIA study is an observational study that does not include the determination of ANAs in a central laboratory. The results of the ANA determinations were only reported by the pediatric rheumatologists, and these were carried out as part of the diagnostic procedure at the routinely assigned local laboratory. The cutoff for a positive titer of ANA may vary among the ICON-JIA study center laboratories. Therefore, only the ANA status (positive, negative, not determined) was recorded and not the ANA titer itself. The cutoff of 250 ng/ml that we used to define elevated S100A12 levels was estimated in our sample. This cutoff has to be confirmed in other cohorts before it may be applicable in general. Missing values in categorical predictor variables were modeled by an additional category. A complete case sensitivity analysis showed that the results from the regression analyses were comparable to the results reported herein. Because of this, the risk of biased estimates may be limited (49). The analysis of uveitis-related complications at first uveitis documentation had an exploratory character because the study was not powered for this analysis.

In conclusion, this prospective study has confirmed demographic risk factors for uveitis in a large, prospective, multicenter setting. Furthermore, it adds knowledge about the predictive value of JIA disease activity scores and laboratory biomarkers (e.g., ESRs and S100A12 levels) for the risk of uveitis manifestations in JIA. Indeed, these parameters are promising tools to better define the group of JIA patients at high risk of uveitis onset. High S100A12 levels and ESRs at JIA onset and high ESRs and high cJADAS-10 scores during follow-up have been found to be significant risk factors for uveitis manifestations.

ACKNOWLEDGMENTS

We thank all other members of the ICON-JIA study group: Tilmann Kallinich (Universitätsmedizin Charité Berlin), Angelika Thon (Medizinische Hochschule Hannover), Jasmin Kümmerle-Deschner (Universität Tübingen), Hans-Iko Huppertz (Prof. Hess-Kinderklinik Bremen), Gerd Horneff (Asklepios Kinderklinik Sankt Augustin), Anton Hospach (Olgahospital Stuttgart), Kirsten Mönkemöller (Kinderkrankenhaus der Stadt Köln), Johannes-Peter Haas (Deutsches Zentrum für Kinder- und Jugendrheumatologie Garmisch-Partenkirchen), Gerd Ganser (St. Joseph-Stift Sendenhorst), Ivan Foeldvari (Kinderrheumatologische Praxis am AK Eilbek Hamburg). We are especially grateful to all patients and their parents for their participation in the ICON-JIA study.

AUTHOR CONTRIBUTIONS

All authors were involved in drafting the article or revising it critically for important intellectual content, and all authors approved the final version to be published. Dr. Tappeiner had full access to all of the data in the study and takes responsibility for the integrity of the data and the accuracy of the data analysis.

Study conception and design. Tappeiner, Klotsche, Sengler, Niewerth, Liedmann, Foell, Minden, Heiligenhaus.

Acquisition of data. Sengler, Niewerth, Liedmann, Lavric, Foell, Minden, Heiligenhaus.

Analysis and interpretation of data. Tappeiner, Klotsche, Walscheid, Foell, Minden, Heiligenhaus.

REFERENCES

1. Carvounis PE, Herman DC, Cha S, Burke JP. Incidence and outcomes of uveitis in juvenile rheumatoid arthritis, a synthesis of the literature. Graefes Arch Clin Exp Ophthalmol 2006;244:281–90.
2. Heiligenhaus A, Niewerth M, Ganser G, Heinz C, Minden K, German Uveitis in Childhood Study Group. Prevalence and complications of uveitis in juvenile idiopathic arthritis in a population-based nation-wide study in Germany: suggested modification of the current screening guidelines. Rheumatology (Oxford) 2007;46:1015–9.
3. Thorne JE, Woreta FA, Dunn JP, Jabs DA. Risk of cataract development among children with juvenile idiopathic arthritis-related uveitis treated with topical corticosteroids. Ophthalmology 2010;117:1436–41.
4. Nguyen QD, Foster CS. Saving the vision of children with juvenile rheumatoid arthritis-associated uveitis. JAMA 1998;280:1133–4.
5. Foster CS, Havrlikova K, Baltatzis S, Christen WG, Merayo-Lloves J. Secondary glaucoma in patients with juvenile rheumatoid arthritis-associated iridocyclitis. Acta Ophthalmol Scand 2000;78:576–9.
6. Saurenmann RK, Levin AV, Feldman BM, Laxer RM, Schneider R, Silverman ED. Risk factors for development of uveitis differ between girls and boys with juvenile idiopathic arthritis. Arthritis Rheum 2010;62:1824–8.
7. Heiligenhaus A, Heinz C, Edelsten C, Kotaniemi K, Minden K. Review for disease of the year: epidemiology of juvenile idiopathic arthritis and its associated uveitis: the probable risk factors. Ocul Immunol Inflamm 2013;21:180–91.
8. Angeles-Han ST, Pelajo CF, Vogler LB, Rouster-Stevens K, Kennedy C, Ponder L, et al. Risk markers of juvenile idiopathic arthritis-associated uveitis in the Childhood Arthritis and Rheumatology Research Alliance (CARRA) Registry. J Rheumatol 2013;40:2088–96.
9. Tappeiner C, Schenck S, Niewerth M, Heiligenhaus A, Minden K, Klotsche J. Impact of antiinflammatory treatment on the onset of uveitis in juvenile idiopathic arthritis: longitudinal analysis from a nationwide pediatric rheumatology database. Arthritis Care Res (Hoboken) 2016;68:46–54.
10. Zulian F, Martini G, Falcini F, Gerloni V, Zannin ME, Pinello L, et al. Early predictors of severe course of uveitis in oligoarticular juvenile idiopathic arthritis. J Rheumatol 2002;29:2446–53.
11. Kotaniemi K, Kotaniemi A, Savolainen A. Uveitis as a marker of active arthritis in 372 patients with juvenile idiopathic seronegative oligoarthritis or polyarthritis. Clin Exp Rheumatol 2002;20: 109–12.
12. Pelegrín L, Casaroli-Marano R, Antón J, García de Vicuña MC, Molina-Prat N, Ignacio Aróstegui J, et al. Predictive value of selected biomarkers, polymorphisms, and clinical features for oligoarticular juvenile idiopathic arthritis-associated uveitis. Ocul Immunol Inflamm 2014;22:208–12.
13. Haasnoot AJ, van Tent-Hoeve M, Wulffraat NM, Schalij-Delfos NE, Los LI, Armbrust W, et al. Erythrocyte sedimentation rate as baseline predictor for the development of uveitis in children with juvenile idiopathic arthritis. Am J Ophthalmol 2015;159:372–7e1.
14. Nordal E, Rypdal V, Christoffersen T, Aalto K, Berntson L, Fasth A, et al. Incidence and predictors of uveitis in juvenile idiopathic arthritis in a Nordic long-term cohort study. Pediatr Rheumatol Online J 2017;15:66.
15. Foell D, Wittkowski H, Roth J. Mechanisms of disease: a "DAMP" view of inflammatory arthritis. Nat Clin Pract Rheumatol 2007;3:382–90.
16. Foell D, Wittkowski H, Vogl T, Roth J. S100 proteins expressed in phagocytes: a novel group of damage-associated molecular pattern molecules. J Leukoc Biol 2007;81:28–37.
17. Wulffraat NM, Haas PJ, Frosch M, De Kleer IM, Vogl T, Brinkman DM, et al. Myeloid related protein 8 and 14 secretion reflects phagocyte activation and correlates with disease activity in juvenile idiopathic arthritis treated with autologous stem cell transplantation. Ann Rheum Dis 2003;62:236–41.
18. Frosch M, Ahlmann M, Vogl T, Wittkowski H, Wulffraat N, Foell D, et al. The myeloid-related proteins 8 and 14 complex, a novel ligand of toll-like receptor 4, and interleukin-1β form a positive feedback mechanism in systemic-onset juvenile idiopathic arthritis. Arthritis Rheum 2009;60:883–91.
19. Wittkowski H, Frosch M, Wulffraat N, Goldbach-Mansky R, Kallinich T, Kuemmerle-Deschner J, et al. S100A12 is a novel molecular marker differentiating systemic-onset juvenile idiopathic arthritis from other causes of fever of unknown origin. Arthritis Rheum 2008;58:3924–31.
20. Gerss J, Roth J, Holzinger D, Ruperto N, Wittkowski H, Frosch M, et al. Phagocyte-specific S100 proteins and high-sensitivity C reactive protein as biomarkers for a risk-adapted treatment to maintain remission in juvenile idiopathic arthritis: a comparative study. Ann Rheum Dis 2012;71:1991–7.
21. Foell D, Wulffraat N, Wedderburn LR, Wittkowski H, Frosch M, Gerss J, et al. Methotrexate withdrawal at 6 vs 12 months in juvenile idiopathic arthritis in remission: a randomized clinical trial. JAMA 2010;303:1266–73.
22. Foell D, Frosch M, Sorg C, Roth J. Phagocyte-specific calcium-binding S100 proteins as clinical laboratory markers of inflammation. Clin Chim Acta 2004;344:37–51.
23. Walscheid K, Heiligenhaus A, Holzinger D, Roth J, Heinz C, Tappeiner C, et al. Elevated S100A8/A9 and S100A12 serum levels reflect intraocular inflammation in juvenile idiopathic arthritis-associated uveitis: results from a pilot study. Invest Ophthalmol Vis Sci 2015;56:7653–60.
24. Petty RE, Southwood TR, Manners P, Baum J, Glass DN, Goldenberg J, et al. International League of Associations for Rheumatology classification of juvenile idiopathic arthritis: second revision, Edmonton, 2001. J Rheumatol 2004;31:390–2.
25. Sengler C, Klotsche J, Niewerth M, Liedmann I, Föll D, Heiligenhaus A, et al. The majority of newly diagnosed patients with juvenile idiopathic arthritis reach an inactive disease state within the first year of specialised care: data from a German inception cohort. RMD Open 2015;1:e000074.
26. Consolaro A, Ravelli A. Defining criteria for disease activity states in juvenile idiopathic arthritis. Rheumatology (Oxford) 2016;55:595–6.
27. Consolaro A, Ruperto N, Bazso A, Pistorio A, Magni-Manzoni S, Filocamo G, et al, for the Paediatric Rheumatology International Trials Organisation. Development and validation of a composite disease activity score for juvenile idiopathic arthritis. Arthritis Rheum 2009;61:658–66.
28. Jabs DA, Nussenblatt RB, Rosenbaum JT, Standardization of Uveitis Nomenclature (SUN) Working Group. Standardization of uveitis nomenclature for reporting clinical data: results of the First International Workshop. Am J Ophthalmol 2005;140:509–16.
29. Klotsche J, Ferger D, Pieper L, Rehm J, Wittchen HU. A novel nonparametric approach for estimating cut-offs in continuous risk indicators with application to diabetes epidemiology. BMC Med Res Methodol 2009;9:63.
30. Cassidy J, Kivlin J, Lindsley C, Nocton J, Section on Rheumatology, Section on Ophthalmology. Ophthalmologic examinations in children with juvenile rheumatoid arthritis. Pediatrics 2006;117:1843–5.
31. Tappeiner C, Klotsche J, Schenck S, Niewerth M, Minden K, Heiligenhaus A. Temporal change in prevalence and complications of uveitis associated with juvenile idiopathic arthritis: data from a cross-sectional analysis of a prospective nationwide study. Clin Exp Rheumatol 2015;33:936–44.
32. Chen CS, Roberton D, Hammerton ME. Juvenile arthritis-associated uveitis: visual outcomes and prognosis. Can J Ophthalmol 2004;39:614–20.
33. Angeles-Han ST, McCracken C, Yeh S, Jenkins K, Stryker D, Rouster-Stevens K, et al. Characteristics of a cohort of children with juvenile idiopathic arthritis and JIA-associated uveitis. Pediatr Rheumatol Online J 2015;13:19.

34. Kotaniemi K, Kautiainen H, Karma A, Aho K. Occurrence of uveitis in recently diagnosed juvenile chronic arthritis: a prospective study. Ophthalmology 2001;108:2071–5.
35. Saurenmann RK, Levin AV, Feldman BM, Rose JB, Laxer RM, Schneider R, et al. Prevalence, risk factors, and outcome of uveitis in juvenile idiopathic arthritis: a long-term followup study. Arthritis Rheum 2007;56:647–57.
36. Zeboulon N, Dougados M, Gossec L. Prevalence and characteristics of uveitis in the spondyloarthropathies: a systematic literature review. Ann Rheum Dis 2008;67:955–9.
37. Papadopoulou C, Kostik M, Böhm M, Nieto-Gonzalez JC, Gonzalez-Fernandez MI, Pistorio A, et al. Methotrexate therapy may prevent the onset of uveitis in juvenile idiopathic arthritis. J Pediatr 2013;163:879–84.
38. Bolt IB, Cannizzaro E, Seger R, Saurenmann RK. Risk factors and longterm outcome of juvenile idiopathic arthritis-associated uveitis in Switzerland. J Rheumatol 2008;35:703–6.
39. Ravelli A, Davì S, Bracciolini G, Pistorio A, Consolaro A, van Dijkhuizen EH, et al. Intra-articular corticosteroids versus intra-articular corticosteroids plus methotrexate in oligoarticular juvenile idiopathic arthritis: a multicentre, prospective, randomised, open-label trial. Lancet 2017;389:909–16.
40. Schulze zur Wiesch A, Foell D, Frosch M, Vogl T, Sorg C, Roth J. Myeloid related proteins MRP8/MRP14 may predict disease flares in juvenile idiopathic arthritis. Clin Exp Rheumatol 2004;22:368–73.
41. Foell D, Frosch M, Schulze zur Wiesch A, Vogl T, Sorg C, Roth J. Methotrexate treatment in juvenile idiopathic arthritis: when is the right time to stop? Ann Rheum Dis 2004;63:206–8.
42. Paroli MP, Speranza S, Marino M, Pirraglia MP, Pivetti-Pezzi P. Prognosis of juvenile rheumatoid arthritis-associated uveitis. Eur J Ophthalmol 2003;13:616–21.
43. Rosenberg KD, Feuer WJ, Davis JL. Ocular complications of pediatric uveitis. Ophthalmology 2004;111:2299–306.
44. Kotaniemi K, Aho K, Kotaniemi A. Uveitis as a cause of visual loss in arthritides and comparable conditions. J Rheumatol 2001; 28:309–12.
45. De Boer J, Wulffraat N, Rothova A. Visual loss in uveitis of childhood. Br J Ophthalmol 2003;87:879–84.
46. Chia A, Lee V, Graham EM, Edelsten C. Factors related to severe uveitis at diagnosis in children with juvenile idiopathic arthritis in a screening program. Am J Ophthalmol 2003;135:757–62.
47. Edelsten C, Reddy MA, Stanford MR, Graham EM. Visual loss associated with pediatric uveitis in English primary and referral centers. Am J Ophthalmol 2003;135:676–80.
48. Woreta F, Thorne JE, Jabs DA, Kedhar SR, Dunn JP. Risk factors for ocular complications and poor visual acuity at presentation among patients with uveitis associated with juvenile idiopathic arthritis. Am J Ophthalmol 2007;143:647–55.
49. Jones MP. Indicator and stratification methods for missing explanatory variables in multiple linear regression. J Am Stat Assoc 2012; 91:222–30.

DOI: 10.1002/art.40530

Clinical Images: Monoclonal gammopathy–associated scleromyxedema presenting as leonine facies

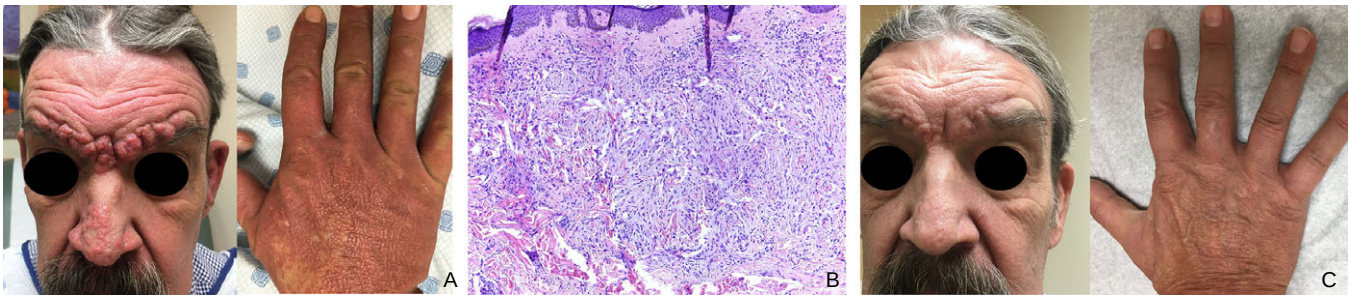

The patient, a 61-year-old man previously in good health, was referred to the scleroderma clinic for a 2-year history of slowly progressive cutaneous eruption involving the dorsal hands, extremities, and central area of the face. Physical examination revealed nodular, erythematous, indurated lesions on the forehead and erythematous papular lesions on the nose with coalescence of firm erythematous papulonodules, resulting in a leonine facies. On the dorsal hands, arms, and legs were numerous, shiny, firm, closely set, slightly translucent papules measuring 1–2 mm with background erythema (**A**). Skin biopsy demonstrated a spindled fibroblastic proliferation in the dermis with increased mucin and variable fibrosis (**B**). The clinical and histologic findings were diagnostic of scleromyxedema. Scleromyxedema is a rare disorder of unknown pathogenesis characterized by a generalized lichenoid papular cutaneous eruption and resulting in diffuse skin induration that may simulate scleroderma. Rarely, larger exophytic nodules, as seen in this patient, may be present. The majority of scleromyxedema cases occur in association with a monoclonal gammopathy. The patient was found to have an IgGλ M protein spike. This patient did not exhibit any CRAB features (hypercalcemia, renal insufficiency, anemia, and bone lesions), and evaluation including hematologic studies culminated in a diagnosis of IgGλ monogammopathy of unclear significance, with plans for ongoing observation. For his scleromyxedema, the patient received intravenous immunoglobulin (IVIG) at doses of up to 2 gm/kg/month (1), with significant improvement in the appearance of lesions after 16 months (**C**). He continues to receive a maintenance dose of 1 gm/kg IVIG every 4 weeks.

Dr. Khanna's work was supported by the NIH (National Institute of Arthritis and Musculoskeletal and Skin Diseases grants K24-AR-063121 and R01-AR-070470).

1. Blum M, Wigley FM, Hummers LK. Scleromyxedema: a case series highlighting long-term outcomes of treatment with intravenous immunoglobulin (IVIG). Medicine (Baltimore) 2008;87:10–20.

Annie Y. Park, MD
Lori Lowe, MD
Dinesh Khanna, MD, MS
University of Michigan
Ann Arbor, MI

ARTHRITIS & RHEUMATOLOGY
Vol. 70, No. 10, October 2018, pp 1695–1698

LETTERS

DOI 10.1002/art.40652

Reduction of CD83 expression on B cells and the genetic basis for rheumatoid arthritis: comment on the article by Thalayasingam et al

To the Editor:

In a recent article in *Arthritis & Rheumatology*, Thalayasingam et al (1) reported that the 6p23 locus, associated with rheumatoid arthritis (RA), has a B cell–specific expression quantitative trait locus (eQTL) effect on CD83. The B cell–specific eQTL effect at this locus is robust and has also been reported by others (2), and it presumably contributes to the pathogenesis of RA by decreasing the expression of CD83 on B cells. We sought to determine the basis for the B cell–specific eQTL effect and to further elucidate the mechanism by which it contributes to RA pathogenesis.

Publicly available epigenomic data showed that rs12529514, the lead single-nucleotide polymorphism (SNP) from RA genome-wide association studies (3), resides near a DNase hypersensitivity site in B cells (4) (Figure 1A). Furthermore, NF-κB induces the expression of CD83 (5), and rs74405933, which is in tight linkage disequilibrium with rs12529514 (r^2 = 1.00 in Asians), alters an NF-κB binding motif. Thus, the B cell–specific eQTL effect may be due to a change in the binding of NF-κB to this locus in B cells.

CD83 regulates the development of murine B cells (5). We therefore hypothesized that CD83 expression might influence the development of human B cells, and we examined the relationship between this haplotype and peripheral blood B cells in healthy subjects from our data set (2,6). Individuals with the RA risk SNP had an increased frequency of CD27−IgD− double-negative B cells (Figure 1B), a subset that is increased in the peripheral blood of RA patients and thought to be pathogenic (6–8). Thus, the rs12529514 risk haplotype, by reducing the expression of CD83 on B cells, may induce changes in B cell differentiation and skew the B cell compartment toward a phenotype similar to that observed in RA.

Supported by Takeda Pharmaceutical.

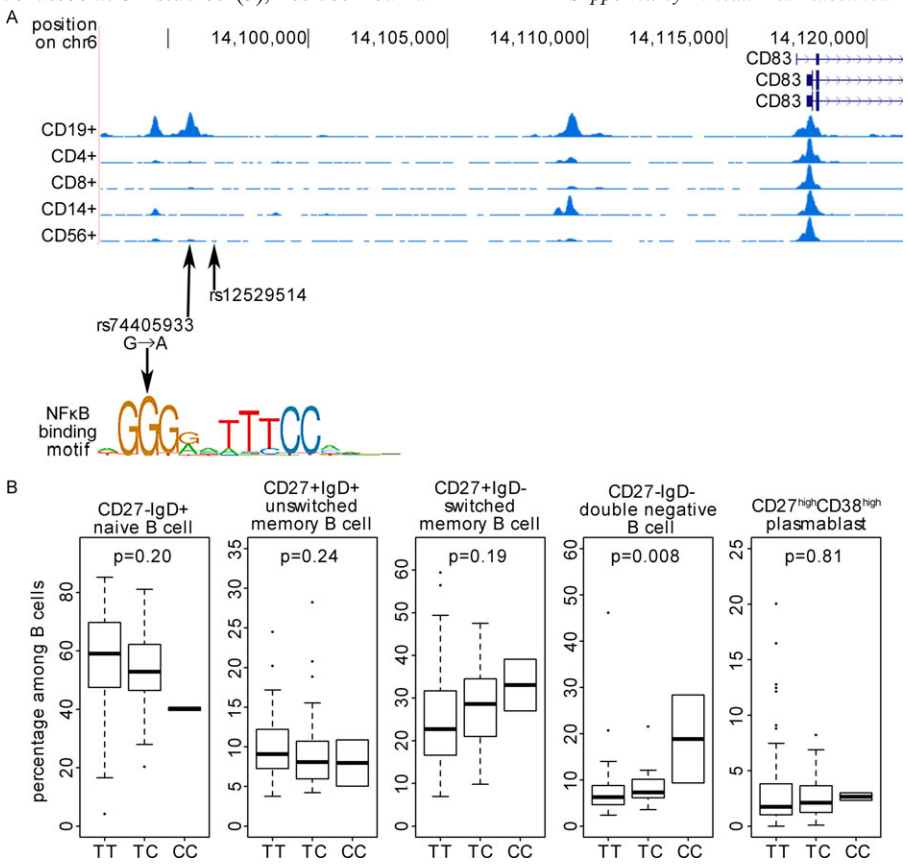

Figure 1. The rs12529514 rheumatoid arthritis risk haplotype and B cells. **A,** Data from the Roadmap Epigenomics Project (4), indicating that rs12529514 resides near a DNase hypersensitivity site in B cells and alters an NF-κB binding site close by. **B,** Flow cytometric analysis of peripheral blood from 106 healthy donors (6). Plots indicate the frequencies of B cell subsets by rs12529514 genotype. Cell subset frequency was normalized by inverse normal transformation, and linear regression was used to assess the effect of rs12529514 genotype on cell subset frequency. Data are presented as box plots, where the boxes represent the interquartile range, the lines within the boxes represent the median, and the lines outside the boxes represent values within 1.5 times the interquartile range. Circles indicate outliers.

Yumi Tsuchida, MD, PhD
Shuji Sumitomo, MD, PhD
Mineto Ota, MD, PhD
Haruka Tsuchiya, MD, PhD
Yasuo Nagafuchi, MD, PhD
Hirofumi Shoda, MD, PhD
Keishi Fujio, MD, PhD
Graduate School of Medicine
University of Tokyo
Tokyo, Japan
Kazuyoshi Ishigaki, MD, PhD
Kensuke Yamaguchi, MD, PhD
Akari Suzuki, PhD
Yuta Kochi, MD, PhD
Kazuhiko Yamamoto, MD, PhD
Center for Integrative Medical Sciences
RIKEN
Yokohama, Japan

1. Thalayasingam N, Nair N, Skelton AJ, Massey J, Anderson AE, Clark AD, et al. CD4+ and B lymphocyte expression quantitative traits at rheumatoid arthritis risk loci in patients with untreated early arthritis: implications for causal gene identification. Arthritis Rheumatol 2018;70:361–70.
2. Ishigaki K, Kochi Y, Suzuki A, Tsuchida Y, Tsuchiya H, Sumitomo S, et al. Polygenic burdens on cell-specific pathways underlie the risk of rheumatoid arthritis. Nat Genet 2017;49:1120–5.
3. Okada Y, Terao C, Ikari K, Kochi Y, Ohmura K, Suzuki A, et al. Meta-analysis identifies nine new loci associated with rheumatoid arthritis in the Japanese population. Nat Genet 2012; 44:511–6.
4. Kundaje A, Meuleman W, Ernst J, Bilenky M, Yen A, Heravi-Moussavi A, et al. Integrative analysis of 111 reference human epigenomes. Nature 2015;518:317–30.
5. Breloer M, Fleischer B. CD83 regulates lymphocyte maturation, activation and homeostasis. Trends Immunol 2008;29:186–94.
6. Nagafuchi Y, Shoda H, Sumitomo S, Nakachi S, Kato R, Tsuchida Y, et al. Immunophenotyping of rheumatoid arthritis reveals a linkage between HLA-DRB1 genotype, CXCR4 expression on memory CD4(+) T cells, and disease activity. Sci Rep 2016;6:29338.
7. Mahmood Z, Muhammad K, Schmalzing M, Roll P, Dorner T, Tony HP. CD27-IgD- memory B cells are modulated by in vivo interleukin-6 receptor (IL-6R) blockade in rheumatoid arthritis. Arthritis Res Ther 2015;17:61.
8. Nakayamada S, Kubo S, Yoshikawa M, Miyazaki Y, Yunoue N, Iwata S, et al. Differential effects of biological DMARDs on peripheral immune cell phenotypes in patients with rheumatoid arthritis. Rheumatology (Oxford) 2018;57:164–74.

DOI 10.1002/art.40548

Mounting evidence indicates that escalating doses of allopurinol are unnecessary for cardiovascular protection: comment on the article by Coburn et al[1]

To the Editor:

We read with interest the recent report by Coburn et al (1) of a methodologically sound propensity score–matched cohort study evaluating the effect of dose escalation of allopurinol on cardiovascular-related and overall mortality. Although the results of that study indicate that increasing doses of allopurinol are associated with a higher risk of mortality, the authors comment that failure to achieve daily doses of ≥600 mg may have contributed to the absence of a protective effect.

In terms of pharmacodynamics, experimental evidence (2) has shown that maximum blockade of xanthine oxidase occurs at relatively low concentrations of oxypurinol (<6 mg/liter or 39.5 μ*M*). These concentrations are much lower than those observed in patients receiving allopurinol at a mean dosage of 300 mg/day (15.2 mg/liter or 100 μ*M*) (2). In addition, high concentrations of oxypurinol (>100–150 μ*M*) have been associated with increased oxidative stress (3). Despite the pooled evidence from experimental studies suggesting that allopurinol can improve parameters of endothelial function, there was no significant association between the dose of allopurinol or the magnitude of decrease in the serum uric acid level and improvement in flow-mediated dilation (4). The recently published results of a randomized controlled trial (RCT) evaluating allopurinol at a dosage of 600 mg/day in patients with cardiac syndrome X failed to show a positive effect of this treatment on endothelial function (5).

In our recent meta-analysis (6), we observed no beneficial effect on CV outcomes with high-dose (600 mg) allopurinol or oxypurinol, especially in heart failure studies, despite a significant reduction (>25%) in uric acid levels in the intervention groups. Interestingly, a recent RCT in patients with chronic heart failure (7) receiving allopurinol at a dosage of 300 mg/day showed significant improvement in clinical, echocardiographic, and laboratory measures of cardiovascular function but no significant reduction (5–7%) in uric acid levels compared with baseline levels and those in the placebo group. Stamp et al (8) compared escalating doses of allopurinol and fixed low doses of allopurinol over 1 year in an RCT, and observed that cardiovascular-related death occurred in 5 of 90 patients in the escalating-dose group compared with 1 of 93 patients in the fixed-dose control group. In the CARES (Cardiovascular Safety of Febuxostat and Allopurinol in Participants With Gout and Cardiovascular Comorbidities) trial (9), febuxostat treatment resulted in a greater reduction in uric acid levels compared with allopurinol but promoted a significant increase in cardiovascular mortality.

Considering the study by Coburn et al (1) and previous evidence, we conclude that escalating doses of allopurinol and control of uric acid using such doses are unnecessary for a cardiovascular protective effect and may be related to adverse cardiovascular outcomes.

Markus Bredemeier, MD, MSc, PhD
Hospital Nossa Senhora da Conceição
Grupo Hospitalar Conceição
Porto Alegre, Brazil

1. Coburn BW, Michaud K, Bergman DA, Mikuls TR. Allopurinol dose escalation and mortality among patients with gout: a national

propensity-matched cohort study. Arthritis Rheumatol 2018;70: 1298–307.
2. Graham S, Day RO, Wong H, McLachlan AJ, Bergendal L, Miners JO, et al. Pharmacodynamics of oxypurinol after administration of allopurinol to healthy subjects. Br J Clin Pharmacol 1996;41:299–304.
3. Stamp LK, Turner R, Khalilova IS, Zhang M, Drake J, Forbes LV, et al. Myeloperoxidase and oxidation of uric acid in gout: implications for the clinical consequences of hyperuricaemia. Rheumatology (Oxford) 2014;53:1958–65.
4. Cicero AF, Pirro M, Watts GF, Mikhailidis DP, Banach M, Sahebkar A. Effects of allopurinol on endothelial function: a systematic review and meta-analysis of randomized placebo-controlled trials. Drugs 2018;78:99–109.
5. Lim TK, Noman A, Choy AM, Khan F, Struthers AD, Lang CC. The APEX trial: effects of allopurinol on exercise capacity, coronary and peripheral endothelial function, and natriuretic peptides in patients with cardiac syndrome X. Cardiovasc Ther 2018;36: e12311.
6. Bredemeier M, Lopes LM, Eisenreich MA, Hickmann S, Bongiorno GK, d'Avila R, et al. Xanthine oxidase inhibitors for prevention of cardiovascular events: a systematic review and meta-analysis of randomized controlled trials. BMC Cardiovasc Disord 2018;18:24.
7. Xiao J, Deng SB, She Q, Li J, Kao GY, Wang JS, et al. Allopurinol ameliorates cardiac function in non-hyperuricaemic patients with chronic heart failure. Eur Rev Med Pharmacol Sci 2016;20: 756–61.
8. Stamp LK, Chapman PT, Barclay ML, Horne A, Frampton C, Tan P, et al. A randomised controlled trial of the efficacy and safety of allopurinol dose escalation to achieve target serum urate in people with gout. Ann Rheum Dis 2017;76:1522–8.
9. White WB, Saag KG, Becker MA, Borer JS, Gorelick PB, Whelton A, et al. Cardiovascular safety of febuxostat or allopurinol in patients with gout. N Engl J Med 2018;378:1200–10.

DOI 10.1002/art.40549

Reply

To the Editor:

We thank Dr. Bredemeier for his comments regarding our study of allopurinol dose escalation and mortality. He presents important evidence to consider in support of an interesting hypothesis that dose escalation of allopurinol may be unnecessary for cardiovascular protection and may actually be related to adverse cardiovascular outcomes. Although we agree that there is evidence suggesting that low doses of allopurinol may be sufficient for cardiovascular protection, we believe that the studies cited highlight a number of areas in which knowledge gaps remain that preclude any definitive conclusions about the effect of dose escalation.

For instance, the mechanistic link between allopurinol treatment and cardiovascular risk is still in the early stages of study. Although higher concentrations of oxypurinol have been associated with increased oxidative stress, the relevant study cited by Dr. Bredemeier was not randomized and did not indicate the allopurinol doses used (1). Without the beneficial insight of a study randomizing patients to high-dose and low-dose allopurinol, it is difficult to determine whether the association between higher oxypurinol concentrations and oxidative stress represents anything more than an epiphenomenon. Assuming that oxypurinol concentrations act as a pathologic culprit, as proposed, it is thus surprising that increasing doses of allopurinol have been demonstrated to yield both cardiovascular and renal protection relative to febuxostat, because oxypurinol is not a byproduct of the latter (2,3). The current evidence, albeit limited, renders additional study in this area of great interest.

We also believe that the current evidence regarding cardiovascular mortality at higher doses of allopurinol is insufficient. Although our nonrandomized study supports Dr. Bredemeier's proposed hypothesis, we are more reserved in our conclusions. The findings from the Bredemeier meta-analysis showing that higher doses of allopurinol were not associated with cardiovascular benefit were primarily driven by a single 24-week study assessing a composite heart failure outcome that included clinical encounters for worsening heart failure and patient's global assessment of heart failure (4,5). Importantly, the study duration, population, and sample size were not designed to assess cardiovascular mortality in patients with gout, which was the significant recently reported finding from the CARES trial (showing an increased risk in gout patients treated with febuxostat relative to those treated with allopurinol) (2). Furthermore, it is uncertain whether the drivers of cardiovascular risk among patients with gout are similar enough to generalize from the broader population among whom high-dose allopurinol has been considered to have beneficial cardiovascular effects.

Brian W. Coburn, PhD
Veterans Affairs Nebraska–Western Iowa Health Care System and University of Nebraska Medical Center
Omaha, NE
Kaleb Michaud, PhD
University of Nebraska Medical Center
Omaha, NE and National Data Bank for Rheumatic Diseases Wichita, KS
Debra A. Bergman, MPH
University of Nebraska Medical Center
Omaha, NE
Ted R. Mikuls, MD, MSPH
Veterans Affairs Nebraska–Western Iowa Health Care System and University of Nebraska Medical Center
Omaha, NE

1. Stamp LK, Turner R, Khalilova IS, Zhang M, Drake J, Forbes LV, et al. Myeloperoxidase and oxidation of uric acid in gout: implications for the clinical consequences of hyperuricaemia. Rheumatology (Oxford) 2014;53:1958–65.
2. White WB, Saag KG, Becker MA, Borer JS, Gorelick PB, Whelton A, et al. Cardiovascular safety of febuxostat or allopurinol in patients with gout. N Engl J Med 2018;378:1200–10.
3. Singh JA, Cleveland JD. Comparative effectiveness of allopurinol versus febuxostat for preventing incident renal disease in older adults: an analysis of Medicare claims data. Ann Rheum Dis 2017; 76:1669–78.

4. Bredemeier M, Lopes LM, Eisenreich MA, Hickmann S, Bongiorno GK, d'Avila R, et al. Xanthine oxidase inhibitors for prevention of cardiovascular events: a systematic review and meta-analysis of randomized controlled trials. BMC Cardiovasc Disord 2018;18:24.
5. Givertz MM, Anstrom KJ, Redfield MM, Deswal A, Haddad H, Butler J, et al. Effects of xanthine oxidase inhibition in hyperuricemic heart failure patients: the xanthine oxidase inhibition for hyperuricemic heart failure patients (EXACT-HF) study. Circulation 2015;131:1763–71.

DOI: 10.1002/art.40543

Clinical Images: Persistent acrocyanosis—a rare manifestation revealing anti–PL-12 syndrome

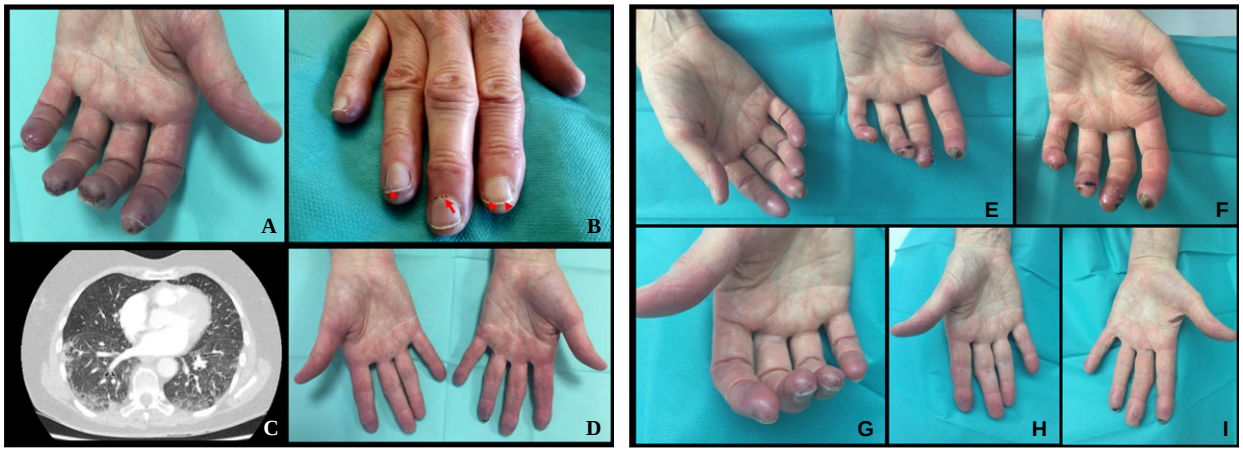

The patient, a 69-year-old woman with asthenia, anorexia, and weight loss of several weeks' duration, was referred for a subacute onset of painful permanent acrocyanosis of the arms and legs without Raynaud's phenomenon. The patient had concomitantly developed grade I/IV dyspnea. Physical examination revealed livedoid acrocyanosis of distal phalanges of the hands (**A**), associated with flame-shaped hemorrhages (**B**) (**arrowheads**) and dilated capillaries at the proximal nailfolds (**B**) (**arrow**), Gottron's sign over the metacarpophalangeal and proximal interphalangeal joints, and a discrete heliotrope rash with a palpable V-shaped rash on the upper chest and forehead. Fine bibasilar crackles were present, and computed tomography showed interstitial lung disease (ILD) (**C**). Immunodot assay revealed anti–PL-12 antibodies. Anti–PL-12 syndrome is usually described as an amyopathic cluster in anti–aminoacyl–transfer RNA synthetase syndrome (ARS). Pulmonary involvement is the most common leading manifestation, with most cases presenting as isolated ILD with dyspnea (1,2). Acute ischemic phenomena are rare in ARS and are generally associated with a history of Raynaud's phenomenon. In our case, the discovery of vascular abnormalities of the arms and legs is what led us to the diagnosis of ARS. Little is known about the pathogenesis of subacute vascular manifestations in ARS. It might be due to several causes of immune-mediated vasculopathy (3). The patient's clinical manifestations initially responded well to high-dose steroid therapy and prostaglandin infusion (**D**), but she experienced a recurrence with cold weather on day 28 (**E** and **F**). The treatment regimen was replaced with intravenous pulse cyclophosphamide and bosentan with a satisfactory outcome by day 63 (**G–I**). In addition to classic dermatologic manifestations, such as Gottron's papules, mechanic hands, or cuticular overgrowth, physicians should note the existence of uncommon acral manifestations, such as ischemic symptoms, that can also indicate ARS and an increased risk of developing necrosis.

Supported by the European Development Fund (project INTERREG V RARENET).

1. Schneider F, Yousem SA, Oddis CV, Aggarwal R. Pulmonary pathologic manifestations of anti-alanyl-tRNA synthetase (anti–PL-12)–related inflammatory myopathy. Arch Pathol Lab Med 2017; 44:51–7.
2. Hervier B, Devilliers H, Stanciu R, Meyer A, Uzunhan Y, Masseau A, et al. Hierarchical cluster and survival analyses of antisynthetase syndrome: phenotype and outcome are correlated with anti-tRNA synthetase antibody specificity. Autoimmun Rev 2012;12:210–7.
3. Pestronk A, Schmidt RE, Choksi R. Vascular pathology in dermatomyositis and anatomic relations to myopathology. Muscle Nerve 2010;42:53–61.

Philippe Mertz, MD
Mathilde Herber, MD
Juliette Jeannel, MD
Hôpitaux Universitaires de Strasbourg and Nouvel Hôpital Civil
Anne-Sophie Korganow, MD, PhD
Aurélien Guffroy, MD
Hôpitaux Universitaires de Strasbourg Nouvel Hôpital Civil UFR Médecine Strasbourg and Université de Strasbourg
Strasbourg, France